



INSTITUTE OF GEOPHYSICS
POLISH ACADEMY OF SCIENCES



PUBLICATIONS
OF THE INSTITUTE OF GEOPHYSICS
POLISH ACADEMY OF SCIENCES

MONOGRAPHIC VOLUME
C-99 (398)

XII IAGA WORKSHOP
ON GEOMAGNETIC OBSERVATORY INSTRUMENTS,
DATA ACQUISITION AND PROCESSING
Belsk, 19-24 June 2006



WARSZAWA 2007

INSTITUTE OF GEOPHYSICS
POLISH ACADEMY OF SCIENCES

PUBLICATIONS
OF THE INSTITUTE OF GEOPHYSICS
POLISH ACADEMY OF SCIENCES

MONOGRAPHIC VOLUME

C-99 (398)

XII IAGA WORKSHOP
ON GEOMAGNETIC OBSERVATORY
INSTRUMENTS,
DATA ACQUISITION AND PROCESSING

Belsk, 19–24 June, 2006

Editor:
Jan REDA

WARSZAWA 2007

Editorial Committee

Roman TEISSEYRE (Editor), Jerzy JANKOWSKI (Deputy Editor),
Janusz BORKOWSKI, Maria JELEŃSKA, Anna DZIEMBOWSKA (Managing Editor)

Editor of Issue

Jan REDA

Editorial Office

Instytut Geofizyki Polskiej Akademii Nauk
ul. Księcia Janusza 64, 01-452 Warszawa, Poland

SUBSCRIPTION

**Subscription orders should be addressed
directly to the Editorial Office.**

**The list of issues to be published in 2007
is on the inside back cover.**

© Copyright by Instytut Geofizyki Polskiej Akademii Nauk, Warszawa 2007

This publication is partly financed by the Polish Committee for Scientific Research

Circulation: 200 copies

ISBN-83-88765-70-1

ISSN-0138-0117

Camera ready copy prepared by:
Dział Informacji i Wydawnictw Naukowych
Instytutu Geofizyki PAN

Printed and bound by:
PPH Remigraf sp. z o.o.
Ratuszowa 11, 03-450 Warszawa

**Proceedings of XII IAGA Workshop
on Geomagnetic Observatory Instruments,
Data Acquisition and Processing**

PREFACE

The XII IAGA Workshop was held on June 19-24, 2006, at Belsk Observatory, Poland. IAGA workshops are cyclic events taking place every two years at various magnetic observatories over the world. The decision about the place and date of the Belsk workshop was undertaken during the 23rd IUGG General Assembly in Sapporo in July 2003.

The Workshop was divided into two parts. The Measurement Session, attended by 60 persons from abroad, was held on June 19-21 at Belsk Observatory. It was followed by the Scientific Session held on June 22-24 at Hotel Wiktorjański in Grójec and Hotel Groman in Sękocin. The Scientific Session was attended by 87 persons from abroad, representing 31 countries from 5 continents. There were also about 15 participants from Poland.

The Measurement Session comprised comparative measurements by DI-flux magnetometers and measurements and tests of proton magnetometers. Twenty-nine DI-flux magnetometers and five proton magnetometers participated in the Session. Along with measurements and tests, there was a training course how to make absolute measurements, led by H.-J. Linthe from Germany and J.-J. Schott from France.

During the Scientific Session, there were 5 invited lectures, 40 regular lectures and 45 poster presentations. There were also two moderated discussions: (1) "Discussion on Virtual observatories and data portals" led by J. Love from the USA, and (2) "Discussion about the form of magnetic yearbooks" led by J. Jankowski from Poland.

The Workshop was made possible owing to the engagement of many persons, in particular those from the International and Local Organizing Committees. We also received support from sponsors. The following institutions and organizations sponsored the Workshop:

- Institute of Geophysics, Polish Academy of Sciences
- Polish Academy of Sciences
- Committee of Geophysics, Polish Academy of Sciences.

- International Union of Geodesy and Geophysics (IUGG)
- International Association of Geomagnetism and Aeronomy (IAGA)
- Space Research Center, Polish Academy of Sciences
- Institute of Geodesy and Cartography

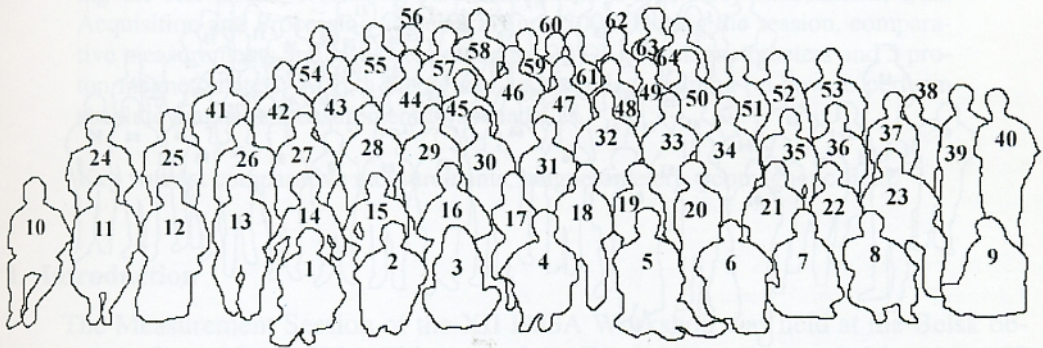
It is to be emphasized that the funds from IAGA and IUGG provided a possibility for many scientists from developing countries, or countries under transformation, to attend the Workshop.

The present Proceedings book contains selected papers presented during the Workshop. The papers were reviewed by the scientific staff of the Earth Magnetism Department of the Institute of Geophysics, Polish Academy of Sciences, and the correspondence with the Authors was made by the Editor. In the next stage, the papers were subject to some technical and, if necessary, language adjustments, by the Editorial Office of the Institute of Geophysics, and finally proof-read by the Authors. We are grateful to Anna Dziembowska, Managing Editor of “Publications of the Institute of Geophysics” for preparing the present Proceedings.

Jan Reda
Editor



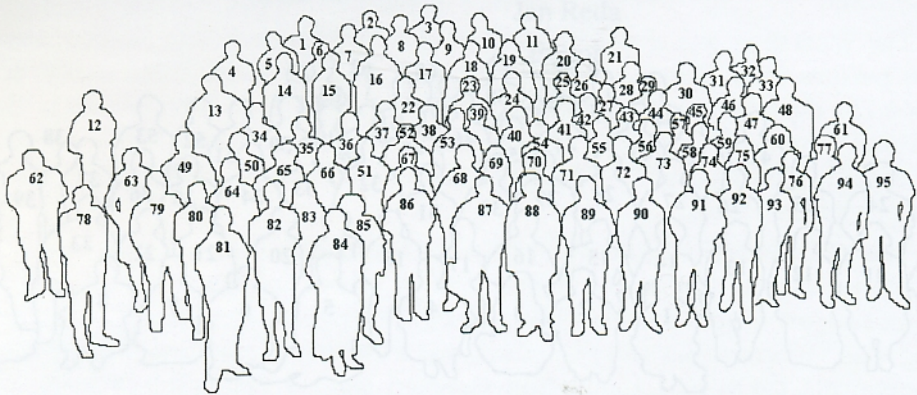
XII IAGA WORKSHOP, 19-24 June 2006, Belsk, Poland



- | | | | | | | | | | |
|----|--------------|----|------------|----|------------|----|------------|----|-------------|
| 1 | H.-U. Auster | 14 | Siekut | 27 | Nowozynski | 40 | Marusenkov | 53 | Yu. Sumaruk |
| 2 | M. Neska | 15 | Hemshorn | 28 | L. Newitt | 41 | Pulz | 54 | Nahayo |
| 3 | A. Neska | 16 | P. Sumaruk | 29 | Hejda | 42 | Schott | 55 | Golkowski |
| 4 | Tomczyk | 17 | M. Newitt | 30 | Horacek | 43 | Linthe | 56 | Truong |
| 5 | Berarducci | 18 | Socias | 31 | Covisa | 44 | Kotze | 57 | Matzka |
| 6 | White | 19 | Anad | 32 | Delipetrov | 45 | Feller | 58 | Calp |
| 7 | Van Loo | 20 | Ac. Covisa | 33 | Pedersen | 46 | Valach | 59 | Raita |
| 8 | Marsal | 21 | Panovska | 34 | Csontos | 47 | Cholakov | 60 | Kultima |
| 9 | J. Marianiuk | 22 | Vaczyova | 35 | Curto | 48 | Srebrov | 61 | Crosthwaite |
| 10 | V. Auster | 23 | Ginzburg | 36 | Di Persio | 49 | Cifuentes | 62 | Pajunpaa |
| 11 | Jaskolska | 24 | Rasson | 37 | Okawa | 50 | Lim | 63 | Heilig |
| 12 | B. Marianiuk | 25 | Reda | 38 | Vujic | 51 | Shirman | 64 | Xin |
| 13 | Yang | 26 | Jankowski | 39 | McKee | 52 | Ernst | | |



XII IAGA WORKSHOP, 19-24 June 2006, Belsk, Poland



| | | | | |
|----------------|---------------|----------------|-----------------|-----------------|
| 1 Shirman | 20 Csontos | 39 Lim | 58 Socias | 77 Yang |
| 2 V. Auster | 21 Matzka | 40 Raita | 59 P. Sumaruk | 78 Vujic |
| 3 Marusenkov | 22 Shevtsov | 41 Iyemori | 60 Sokolova | 79 Vershovskiy |
| 4 Di Persio | 23 Schwarz | 42 Dominici | 61 Feller | 80 Curto |
| 5 Marsal | 24 McKee | 43 Anad | 62 J. Marianiuk | 81 Kowalik |
| 6 Korte | 25 Chulliat | 44 Hegymegi | 63 Newitt | 82 Tomczyk |
| 7 H.-U. Auster | 26 Moran | 45 Ac.Hegymegi | 64 Van Loo | 83 A. Neska |
| 8 Valach | 27 Nahayo | 46 Hejda | 65 Rasson | 84 B. Marianiuk |
| 9 Horacek | 28 Pulz | 47 Hrvoic | 66 Hernandez | 85 Jaskolska |
| 10 Truong | 29 Okawa | 48 Duma | 67 Srebrov | 86 Manda |
| 11 Xin | 30 Delipetrov | 49 Berarducci | 68 Pedersen | 87 Lamali |
| 12 Bakhmutov | 31 Korepanov | 50 Merenyi | 69 Lepidi | 88 Cholakov |
| 13 Ginzburg | 32 Kultima | 51 Cifuentes | 70 Cafarella | 89 Crosthwaite |
| 14 Heilig | 33 Schott | 52 St.-Louis | 71 Reda | 90 Chau |
| 15 Di Mauro | 34 Golkowski | 53 Kotze | 72 Meloni | 91 Migachev |
| 16 Calp | 35 White | 54 De Santis | 73 Kerridge | 92 Tozzi |
| 17 Wesztergom | 36 Love | 55 Pajunpaa | 74 Panovska | 93 Fouassier |
| 18 Turbitt | 37 Linthe | 56 Jankowski | 75 Vaczyova | 94 M. Neska |
| 19 Shanahan | 38 Yumoto | 57 Covisa | 76 Hemshorn | 95 Yu. Sumaruk |

Measurement Session During the XII IAGA Workshop at Belsk

Jan REDA and Mariusz NESKA

Institute of Geophysics, Polish Academy of Sciences
ul. Księcia Janusza 64, 01-452 Warszawa, Poland
e-mail: jreda@igf.edu.pl; nemar@igf.edu.pl

A b s t r a c t

In this paper, we describe the Measurement Session which took place during the XII IAGA Workshop on Geomagnetic Observatory Instruments, Data Acquisition and Processing at Belsk in June 2006. During the session, comparative measurements and tests were made for 29 DI-flux magnetometers and 5 proton magnetometers. Also, a theoretical and practical training on how to perform absolute magnetic measurements was made.

Key words: comparative measurements, magnetometers, geomagnetic field.

1. Introduction

The Measurement Session of the XII IAGA Workshop was held at the Belsk observatory in June 19-21, 2006. This part of the Workshop was attended by about 60 persons. The main issues of the Session were the following:

- comparative measurements of DI-flux magnetometers,
- comparative measurements of proton magnetometers,
- “frequency” tests of proton magnetometers,
- training in absolute measurements performance.

The Measurement Session, and notably the comparison of absolute instruments, was an important part of the XII IAGA Workshop. Similar measurements have been carried out at the former workshops (Rasson 1996, Linthe 1998, Vaczyova and Voros 2001, Loubser 2002, Okada 2005).

The Measurement Session was also a good opportunity for demonstrating the newly developed magnetometers for such measurements: the GAUSS instrument by

the German group from GFZ Potsdam (Auster *et al.* 2007), and AutoDIF by the Belgian group from RMI (Van Loo *et al.* 2007).

The absolute measurements of declination and inclination were made at pillars 1, 2, 4, 6, and 7 in the Absolute House of the Observatory (see Figs. 1 and 2); 29 magnetometers participated in the Session.

The measurements and tests of proton magnetometers involved 5 instruments, and were performed at the pillar in the forest (see the map in Fig. 1).

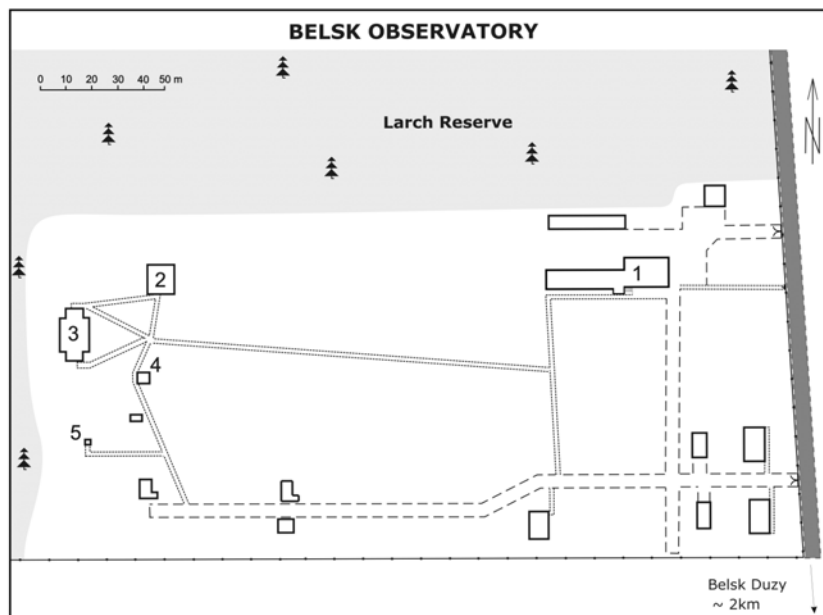


Fig. 1. Plan of the Belsk Observatory. 1 – Main Office, 2 – Variations House, 3 – Absolute House, 4 – Pavilion Altanka, 5 – Pillar in the Forest.

The “frequency” measurements of proton magnetometers were made next to the Pavilion Altanka (see Fig. 1). They were made by means of a special generator borrowed from the Niemegek Observatory. The calibration signal frequency of this generator is based on a signal from the German station DCF, which broadcasts the calibration signal of 77.5 kHz frequency.

Parallel with the measurement and testing of the magnetometers, there was a training session concerning the absolute magnetic measurements. It was led by Hans-Joachim Linthe from GFZ Potsdam (Germany) and Jean-Jacques Schott from E.O.S.T. (France). The session consisted of two parts: lectures and practical training on the measurements with DI-flux magnetometers.

2. DI-Flux Comparison

The DI-flux magnetometers participating in the comparative measurements are listed in Table 1.

Table 1
List of DI-flux instruments and observers

| No | Instrument | Country | Institution | Observer |
|----|--|---------------|---------------------------------------|---------------------|
| 1 | PANDECT/IRM/Zeiss 010B | USA | USGS | Berarducci/White |
| 2 | FGE-G/Mingeo/THEO-010B | China | Lanzhou Institute of Seismology | Changjiang Xin |
| 3 | MAG01H/Zeiss 020B | Bulgaria | Panagjurishte Observatory | Cholakov/Srebrov |
| 4 | PANDECT/IRM/Zeiss 020B | Mexico | UNAM Instituto de Geofisica | Cifuentes/Hernandez |
| 5 | MAG010H/Bartington/THEO-010D | Spain | Toledo Observatory | Covisa |
| 6 | B0610H/Bartington/Zeiss 010B | Australia | Geoscience Australia | Crosthwaite |
| 7 | Fluxgate DMI FGE Model G/MINGEO/Zeiss 010A | Hungary | Tihany Observatory | Csontos |
| 8 | Mag 01H/Bartington/Zeiss 010A | Algeria | CRAAG, Algiers | Anad |
| 9 | MAG 01H/Bartington/Zeiss 010B | Czechy | Geoph. Inst. Czech Acad. Sci., Prague | Horacek |
| 10 | DMI/Zeiss 010A | Finland | Sodankyla Observatory | Kultima/Raita |
| 11 | PANDECT/IRM/Zeiss 010B | Korea (South) | Daezeon Observatory | Lim |
| 12 | MAG 01H/Bartington/Zeiss 010B | Germany | Niemegk Observatory | Linthe |
| 13 | ELSEC 810/Zeiss 015B | Spain | Ebro Observatory | Marsal |
| 14 | PAN-DECT/RMI/Tavistock MK II | Ukraine | Lviv Centre of Inst. of Space Res. | Marusenkov |
| 15 | MAG 01H/Bartington/Zeiss 010B | Germany | Fuerstenfeldbruck Observatory | Matzka/Feller |
| 16 | Bartington/Zeiss 020 | Canada | Natural Resources Canada, Ottawa | Mc Kee/Calp |
| 17 | MAG 01H/Bartington/Zeiss 010B | South Africa | Hermanus Observatory | Nahayo |
| 18 | Fluxgate DMI/Ser.No 00109/Zeiss 010B | Finland | Nurmijarvi Observatory | Pajunpaa |
| 19 | LEMI 203/LCSIR | Macedonia | Fac. of Mining and Geol., Stip | Panovska/Delipetrov |
| 20 | Fluxgate DMI/Zeiss 010B | Denmark | Danish Meteorol. Inst., Copenhagen | Pedersen |
| 21 | PAN-DECT/RMI/Tavistock MK II | Belgium | Dourbes Observatory | Rasson |

Table 1 (continued)

| No | Instrument | Country | Institution | Observer |
|----|--------------------------------------|------------|---|------------------|
| 22 | MAG 01H/Bartington/Mingeo/Zeiss 010B | France | Ecole et Observatoire des Sci. de la Terre / Chambon La Foret Observatory | Schott/Truong |
| 23 | LEMI 203/LCSIR | Kazakhstan | Alma-Ata Observatory | Sokolova |
| 24 | PAN-DECT/RMI/Tavistock MK II | Ukraine | Lviv Observatory | Sumaruk |
| 25 | MAG 01H/Bartington/Mingeo/Zeiss 010A | UK | British Geological Survey | Turbitt/Shanahan |
| 26 | LEMI/LCSIR/3T2KP | Slovakia | Hurbanovo Observatory | Vaczyova/Valach |
| 27 | Mingeo/THEO-010A | Croatia | Department of Geophysics, Zagreb | Vujic |
| 28 | MAG 01H/Bartington/Zeiss 010B | Japan | Kakioka Observatory | Okawa |
| 29 | ELSEC 820/Zeiss 010B | Poland | Belsk Observatory | Belsk Team |

The comparative measurements with DI-flux magnetometers were made in the Absolute House of the Observatory (see Figs. 2 and 3). Measurements were made at pillars 1, 2, 4, 6, and 7. The reduction was made by using the observatory recordings of set I with a PSM magnetometer equipped in Bobrov-type quartz sensors (Jankowski *et al.* 1984). The stability of these magnetometers is of the order of 3nT/year (see Fig. 4). As follows from thorough estimations, the bases of components X, Y, and Z have not changed by more than 0.2 nT throughout the Measurement Session. All the measurements of declination and inclination were related to pillar 2, which is the basic pillar at the Belsk Observatory. The declination and inclination differences relative to pillar 2 have been determined from numerous measurements before the workshop, during it, and afterwards. The differences of D and I in relation to pillar 2 are listed in Table 2.

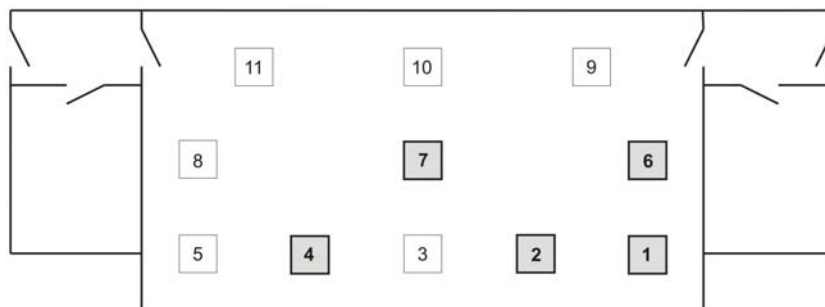


Fig. 2. Plan of the Absolute House.



Fig. 3. Measurements with DI-flux magnetometers.

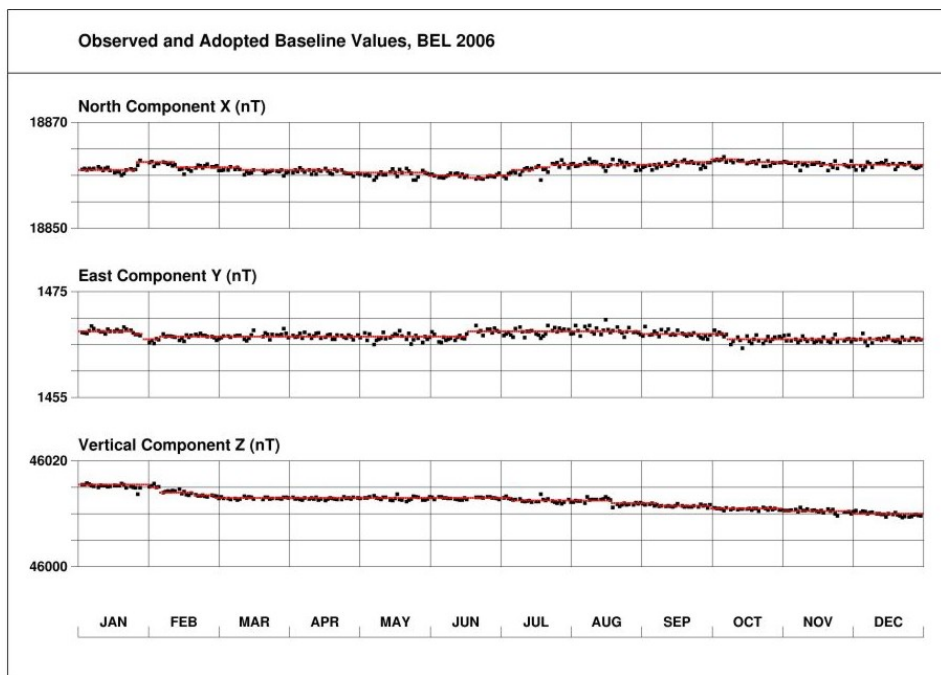


Fig. 4. Base lines of set 1 at Belsk in 2006.

Table 2

Declination and inclination differences, ΔD_p and ΔI_p , for measurement pillars

| | ΔD_p [sec] | ΔI_p [sec] |
|----------------------|--------------------|--------------------|
| Pillar 1 (P1-P2) | -7.3 | -9.3 |
| Pillar 2 (reference) | 0.0 | 0.0 |
| Pillar 4 (P4-P2) | -26.0 | -4.2 |
| Pillar 6 (P6-P2) | 23.3 | -10.3 |
| Pillar 7 (P7-P2) | 20.6 | -1.4 |

As the reference levels for declination and inclination measurements, D_{ref} and I_{ref} , we adopted the mean levels obtained from all the measurements made the Session's participants, excluding the extreme measurements. The so-called historical corrections have not been taken into account. The formulae for calculations were as follows:

$$\Delta D_i = D_i - \Delta D_p - D_{\text{ref}}$$

and

$$\Delta I_i = I_i - \Delta I_p - I_{\text{ref}},$$

where: ΔD_i and ΔI_i – the differences between the inclination/declination measured by the participant and the mean value of all the measurements; D_i and I_i – the inclination/declination measured by the participant and reduced to a specified moment; ΔD_p and ΔI_p – declination/inclination difference for a given measurement pillar; D_{ref} and I_{ref} – mean value of inclination/declination calculated from all measurements made by the Session's participants, excluding the extreme measurements.

The results of comparison of declination and inclination measurements are shown in Tables 3 and 4, respectively; the graphical representation is in Figs. 5 and 6.

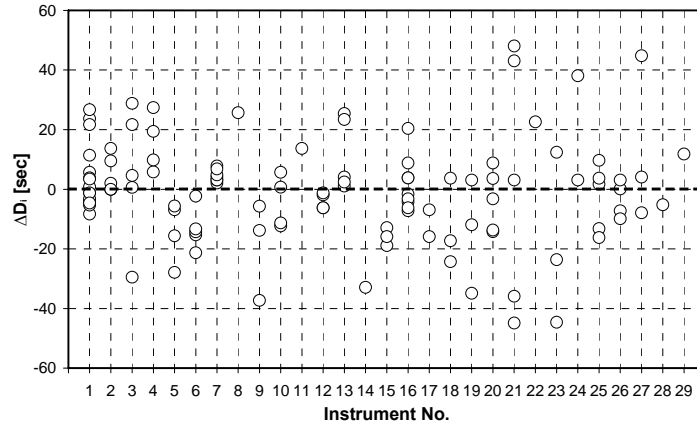


Fig. 5. The differences ΔD_i of the declination measurements.

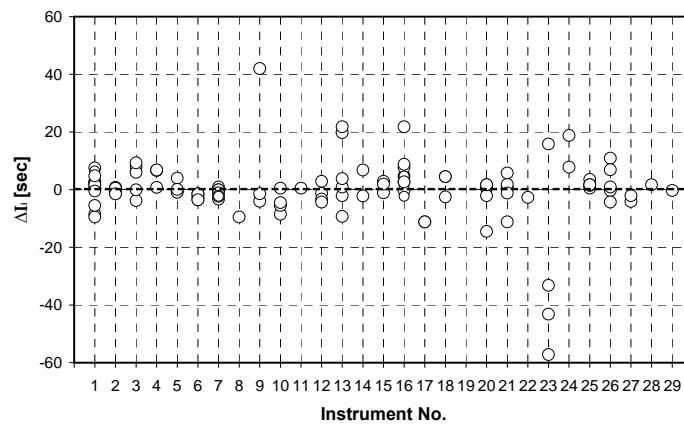


Fig. 6. The differences ΔI_i of the inclination measurements.

Table 3

Results of instrumental differences of declination ΔD_i , in seconds of arc

| No. | 1 | 2 | 3 | 4 | 5 | 6 | 7 | 8 | 9 | Mean | St. Dev |
|-----|----------|----------|----------|-------|-------|------|------|------|------|-------|---------|
| | 10 | 11 | 12 | 13 | 14 | 15 | 16 | 17 | 18 | | |
| 1 | 5.7 | -8.3 | -5.3 | 3.8 | -4.2 | -1.2 | 0.8 | -3.2 | -1.2 | 4.5 | 11.4 |
| | -5.2 | 20.7 | 23.7 | 26.7 | 21.7 | -4.6 | 11.4 | 3.4 | -4.6 | | |
| 2 | 0.1 | 9.5 | 13.7 | 7.2 | 2.0 | | | | | 6.5 | 5.5 |
| 3 | 4.6 | 21.7 | -29.5 | 28.8 | 0.6 | | | | | 5.2 | 22.7 |
| 4 | (-367.9) | 5.8 | 9.8 | 19.4 | 27.4 | | | | | 15.6 | 9.7 |
| 5 | -27.9 | -6.9 | -5.6 | -15.6 | | | | | | -14.0 | 10.3 |
| 6 | -2.3 | -21.3 | -15.3 | -14.3 | -13.3 | | | | | -13.3 | 6.8 |
| 7 | 4.1 | 2.1 | 3.1 | 3.1 | 7.8 | 4.8 | 6.8 | | | 4.6 | 2.0 |
| 8 | 25.7 | | | | | | | | | 25.7 | - |
| 9 | -37.3 | -13.8 | -5.7 | | | | | | | -19.0 | 16.4 |
| 10 | -12.3 | -11.3 | 0.7 | 5.7 | | | | | | -4.3 | 8.9 |
| 11 | 13.7 | | | | | | | | | 13.7 | - |
| 12 | -6.2 | -1.9 | -1.2 | -6.2 | | | | | | -3.9 | 2.7 |
| 13 | (-76.2) | 4.1 | 1.1 | 25.4 | 23.4 | 2.4 | | | | 11.3 | 12.0 |
| 14 | (-133.9) | -32.9 | | | | | | | | -32.9 | - |
| 15 | -18.9 | -12.9 | -15.9 | | | | | | | -15.9 | 3.0 |
| 16 | 3.8 | 8.8 | 3.8 | -4.2 | 20.4 | -1.6 | -7.2 | -3.2 | -6.2 | 1.6 | 8.8 |
| 17 | -6.9 | -15.9 | | | | | | | | -11.4 | 6.4 |
| 18 | 3.7 | -24.3 | -17.3 | | | | | | | -12.6 | 14.6 |
| 19 | -11.9 | 3.1 | -34.9 | | | | | | | -14.5 | 19.1 |
| 20 | -14.2 | -3.2 | -13.7 | 8.8 | 3.6 | | | | | -3.7 | 10.2 |
| 21 | -35.9 | 48.1 | -44.9 | 3.1 | 43.1 | | | | | 2.7 | 43.2 |
| 22 | 22.6 | | | | | | | | | 22.6 | - |
| 23 | -23.6 | (-94.6) | -44.6 | 12.4 | | | | | | -18.6 | 28.8 |
| 24 | 3.1 | 38.1 | | | | | | | | 20.6 | 24.7 |
| 25 | 1.7 | 3.7 | -13.2 | 9.7 | -16.2 | | | | | -2.8 | 11.3 |
| 26 | -7.2 | (-163.2) | (-442.9) | -9.9 | 0.1 | 3.1 | | | | -3.4 | 6.1 |
| 27 | -7.9 | 4.1 | 44.8 | | | | | | | 13.7 | 27.6 |
| 28 | -5.2 | | | | | | | | | -5.2 | - |
| 29 | 11.8 | | | | | | | | | 11.8 | - |

Table 4
Results of instrumental differences of inclination ΔI_i , in seconds of arc

| No. | 1 | 2 | 3 | 4 | 5 | 6 | 7 | 8 | 9 | Mean | St. Dev |
|-----|----------|----------|----------|-------|------|------|------|-----|------|----------|---------|
| | 10 | 11 | 12 | 13 | 14 | 15 | 16 | 17 | 18 | | |
| 1 | -8.5 | -9.5 | -5.5 | 2.7 | 0.7 | 2.7 | -0.3 | 1.7 | -0.3 | 1.5 | 5.0 |
| | 1.7 | 7.5 | 7.5 | 6.5 | -0.5 | 4.8 | 4.8 | 4.8 | 5.8 | | |
| 2 | 0.8 | -1.2 | -1.2 | 0.5 | -1.5 | | | | | -0.5 | 1.0 |
| 3 | -3.8 | 8.0 | 6.0 | 9.3 | -0.1 | | | | | 3.9 | 5.6 |
| 4 | (83.9) | 6.7 | 6.7 | 0.8 | 6.8 | | | | | 5.2 | 3.0 |
| 5 | 4.0 | -0.6 | -0.9 | 0.1 | | | | | | 0.7 | 2.3 |
| 6 | -1.5 | -3.5 | -2.5 | -1.5 | -3.5 | | | | | -2.5 | 1.3 |
| 7 | 0.9 | -0.1 | -0.1 | -1.1 | -3.3 | -2.3 | -2.3 | | | -1.2 | 1.5 |
| 8 | -9.5 | | | | | | | | | -9.5 | - |
| 9 | 42.0 | -4.0 | -1.4 | | | | | | | 12.2 | 25.8 |
| 10 | -8.5 | -5.5 | -4.5 | 0.5 | | | | | | -4.5 | 3.7 |
| 11 | 0.5 | | | | | | | | | 0.5 | - |
| 12 | -1.3 | 2.9 | -3.3 | -4.3 | | | | | | -1.5 | 3.2 |
| 13 | -9.3 | -2.1 | 0.9 | 3.8 | 19.8 | 21.8 | | | | 5.8 | 12.4 |
| 14 | 6.8 | -2.2 | | | | | | | | 2.3 | 6.4 |
| 15 | 2.9 | -1.1 | 1.9 | | | | | | | 1.2 | 2.1 |
| 16 | 4.7 | 2.7 | 7.7 | -0.3 | 8.8 | 21.8 | 4.7 | 2.7 | -2.3 | 5.6 | 7.0 |
| 17 | -11.2 | -11.2 | | | | | | | | -11.2 | 0.0 |
| 18 | -2.5 | 4.5 | 4.5 | | | | | | | 2.2 | 4.0 |
| 19 | (-113.1) | (-138.1) | (-131.1) | | | | | | | (-127.5) | (12.9) |
| 20 | 0.5 | -2.1 | -14.5 | 1.7 | 1.7 | | | | | -2.5 | 6.9 |
| 21 | 0.8 | 1.8 | 5.8 | -11.2 | -1.2 | | | | | -0.8 | 6.3 |
| 22 | -2.7 | | | | | | | | | -2.7 | - |
| 23 | 15.8 | -43.2 | -57.2 | -33.2 | | | | | | -29.5 | 31.7 |
| 24 | 18.8 | 7.8 | | | | | | | | 13.3 | 7.8 |
| 25 | 0.5 | 3.5 | 1.7 | 1.5 | 1.7 | | | | | 1.8 | 1.1 |
| 26 | -0.3 | -4.3 | (-605.1) | 10.9 | 6.9 | 0.9 | | | | 2.8 | 6.7 |
| 27 | -4.1 | -2.1 | (-145.3) | | | | | | | -3.1 | 1.4 |
| 28 | 1.7 | | | | | | | | | 1.7 | - |
| 29 | -0.3 | | | | | | | | | -0.3 | - |

3. Proton Magnetometer Session

Five magnetometers, including three Overhauser GSM-type ones, participated in the Session. The instruments are listed in Table 5; their theoretical resolution is given too.

Table 5
List of the proton magnetometer instruments and observers

| No | Resolution | Instrument | Country | Observatory Institution | Observer |
|----|------------|------------|-----------|--|---------------------|
| 1 | 0.01 nT | GSM-90 | Australia | Geoscience Australia | Peter CROSTHWAITE |
| 2 | 0.01 nT | GSM-19 | Germany | GFZ Potsdam, Adolf Schmidt Geomagnetic Observatory | Hans-Joachim LINTHE |
| 3 | 0.01 nT | GSM-19 | Spain | Ebro Observatory | Santiago MARSAL |
| 4 | 0.1 nT | PMP-7 | Finland | Finnish Meteorological Institute | Kari PAJUNPAA |
| 5 | 0.01 nT | PMP-8 | Poland | Belsk Observatory | Sebastian TOMCZYK |

The Measurement Session of proton magnetometers consisted of the two parts:

- comparative measurements in natural magnetic field of the Earth,
- tests of magnetometers on the basis of standard frequency generator.

Comparative measurements were carried out at the pillar in the forest (see Fig. 1). As the reference level, the results were adopted of measurements made with a Polish PMP-8 magnetometer, which was carefully calibrated according to a new geomagnetic scale a few days before the Workshop. The results of comparative measurements, in tabular and graphic forms, are presented in Table 6 and Fig. 7.

Table 6
Results of instrumental differences of total intensity ΔF

| Inst. No. | Series 1 | | Series 2 | | Mean | |
|-----------|----------|---------------|----------|---------------|---------|---------------|
| | dF | Standard Dev. | dF | Standard Dev. | dF | Standard Dev. |
| 1 | 0.15 | 0.10 | 0.07 | 0.09 | 0.11 | 0.09 |
| 2 | (-3.80) | (0.29) | (-3.93) | (0.18) | (-3.86) | (0.28) |
| 3 | -1.18 | 0.18 | -0.91 | 0.23 | -1.04 | 0.20 |
| 4 | -0.12 | 0.15 | -0.34 | 0.23 | -0.23 | 0.19 |
| 5 | 0.01 | 0.01 | -0.04 | 0.10 | -0.01 | 0.05 |

The magnetometers were tested on the basis of standard frequency generator nearby the Pavilion Altanka (see Figs. 1 and 8); the standard frequency generator was borrowed from the Niemeck Observatory.

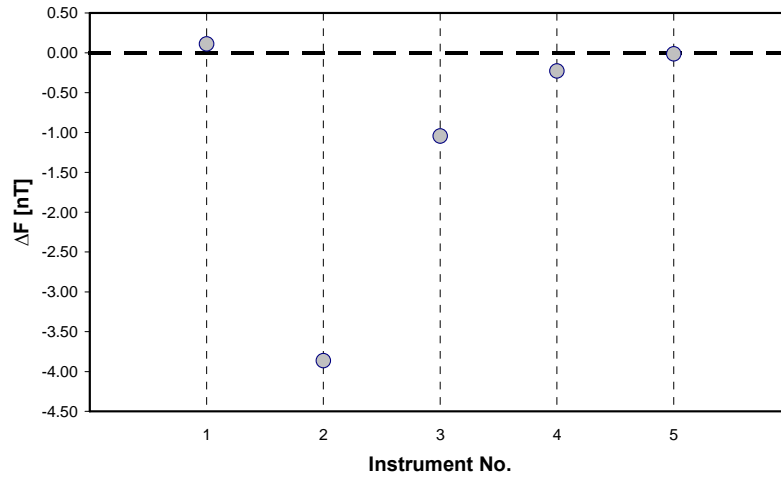


Fig. 7. Result of intercomparison measurements ΔF .



Fig. 8. Testing of proton magnetometers.

In the tests, the use was made of the dependence between the total field F and the precession signal frequency f , as follows:

$$F = 2 \cdot \pi \cdot f / \gamma_p$$

where: γ_p – the gyromagnetic ratio; according to IAGA recommendation of 1992 (Jan-kowski and Sucksdorff 1996) this ratio is $\gamma_p = 2.67515255 \text{ T}^{-1}\text{s}^{-1}$ (the so-called new gyromagnetic ratio).

The results of tests, in tabular and graphical forms, are shown in Table 6 and Fig. 9. In this figure we also mark lines corresponding to the old and new gyromagnetic ratio. Indications of one of the tested proton magnetometers (No. 2) strongly deviated from the rest. It turned out that the instrument had been repaired just before the workshop and has not been properly calibrated.

Table 6
Results of calibration of proton magnetometers

| Inst. No. | 1041.667 Hz | 1250.000 Hz | 1562.500 Hz | 2083.333 Hz | 3125.000 Hz |
|-----------|-------------|-------------|-------------|-------------|-------------|
| | 24465.84 nT | 29359.00 nT | 36698.76 nT | 48931.67 nT | 73397.51 nT |
| 1 | 0.31 | 0.24 | 0.46 | 0.61 | 0.94 |
| 2 | (-1.40) | (-1.71) | (-2.14) | (-2.87) | (-4.33) |
| 3 | -0.05 | 0.00 | -0.06 | -0.09 | -0.13 |
| 4 | -0.06 | 0.00 | 0.00 | 0.07 | 0.11 |
| 5 | -0.04 | -0.07 | -0.08 | -0.09 | -0.16 |

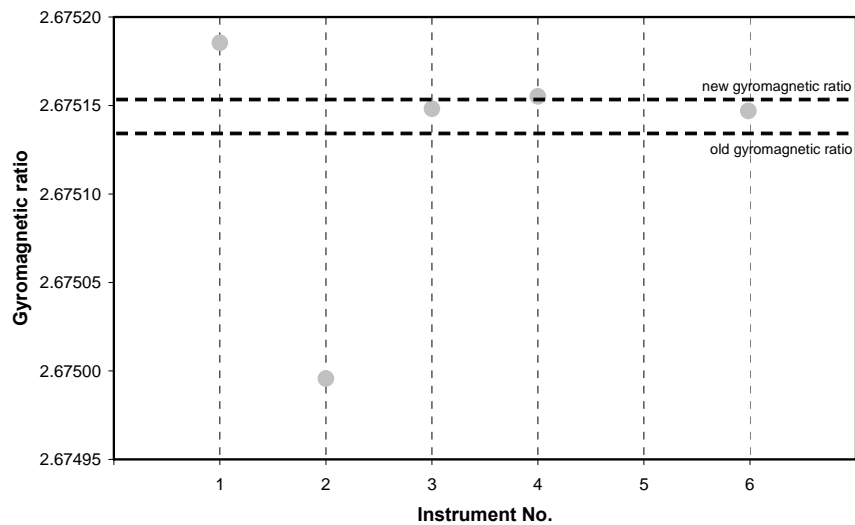


Fig. 9. Distribution of the estimated gyromagnetic ratio.

4. Training Session

The training session related to the absolute measurements consisted of the theoretical and the practical parts. It was led by two experienced observers: Hans-Joachim Linthe from GFZ Potsdam (Germany), and Jean-Jacques Schott from E.O.S.T.

(France). The training consisted of the two parts: theory and practical measurements. The theoretical lectures, including computer presentations, took place in the library of the Observatory. Owing to the nice, sunny weather, it was possible to make the practical training outdoors, next to the pavilion (see Fig. 10).



Fig. 10. Training of DI-flux measurements.

Acknowledgements. The authors and staff of the Belsk Observatory are very grateful to Hans-Joachim Linthe from GFZ Potsdam (Germany) oraz Jean-Jacques Schott from E.O.S.T. (France) for carrying out the theoretical and practical schooling of absolute measurements. We also wish to thank Mr. H.J. Linthe for lending us the DCF generator for proton magnetometer calibration and carrying out the measurements by means of this generator.

References

- Auster, H.U., M. Manda, A. Hemshorn, M. Korte and E. Pulz, 2007, *GAUSS: Geomagnetic Automated System*. **In:** "Proceedings of XII IAGA Workshop on Geomagnetic Observatory Instruments, Data Acquisition and Processing", *Publs. Inst. Geophys. Pol. Acad. Sc. C-99 (398)* (this issue).
- Jankowski, J., and C. Sucksdorff, 1996, *Guide for Magnetic Measurements and Observatory Practice*, IAGA, Warsaw, 1-235.
- Jankowski, J., J. Marianiuk, A. Ruta, C. Sucksdorff and M. Kivinen, 1984, *Long-term stability of a torque balance variometer with photo-electric converters in observatory practice*, *Geophys. Surveys*, **6**, 367-380.
- Linthe, H.-J., 1998, *Results of the comparison measurements and the variometer test recordings during the workshop*. **In:** "Proceedings VIIth IAGA Workshop on Geomag. Obs. Instr. Data Acq. Process.", *Sci. Techn. Rep. STR98/21*, GeoForschungsZentrum Potsdam, 427-443.

- Loubser, L., 2002, *Results of Di-flux and proton magnetometer comparison during the Xth IAGA workshop*. **In:** Proceeding Xth IAGA workshop, Hermanus Mag. Obs., 5-10 (publication on the web site: http://www.hmo.ac.za/XthIAGA_ws.pdf)
- Okada, M., 2005, *Intercomparison and tests of geomagnetic instruments and measurement training at the Kakioka Magnetic Observatory, Japan, in 2004*. **In:** Proceeding of the XIth IAGA WORKSHOP.
- Rasson, J.L., 1996, *Tests and Intercomparisons of geomagnetic instrumentation at the VIth Workshop on Geomagnetic Observatory Instruments, Data Acquisition and Processing*. **In:** "Proceeding VIth Workshop on Geomag. Obs. Instru. Data Acqui. Proc.", Publ. Sci. et Techn. No 003, Inst. Roy. Met. de Belgique Brussels, pp. 16-27.
- Vaczyova, M., and Z. Voros, 2001, *Results of Diflux and proton magnetometer comparison at the IXth IAGA Workshop*. *Contri. Geophys. Inst. Slovak Acad. Sciences*, **31**, 1, 417-426.
- Van Loo, S.A., and J.L. Rasson, 2007, *Presentation of the Prototype of an Automated DIFlux*. **In:** "Proceedings of XII IAGA Workshop on Geomagnetic Observatory Instruments, Data Acquisition and Processing", *Publs. Inst. Geophys. Pol. Acad. Sc.* **C-99 (398)** (this issue).

Accepted April 19, 2007

Past and Present of Polish Geomagnetic Observatories

Jerzy JANKOWSKI and Janusz MARIANIUK

Institute of Geophysics, Polish Academy of Sciences
ul. Księcia Janusza 64, 01-452 Warszawa, Poland
e-mails: jerzy@igf.edu.pl

Abstract

The paper outlines the history of Polish magnetic observatories, beginning from the oldest, presently inactive one, at Świder, to the three observatories operating at present: Belsk, Hel, and Hornsund. We describe changes in the equipment throughout the years, the present instrumentation and accuracies. While discussing the quality of data, of utmost importance is the lack of gaps in the recordings, and the high stability of bases. A specific trait of our observatories is the fact that the instruments they use are mostly of our own make.

Key words: magnetic observatories, PSM variometer, proton magnetometer, recording system.

History

The first Polish geomagnetic observatory was put into operation in 1920 at Świder near Warsaw (see map in Fig. 1). Its founder and many-year director was Professor Stanisław Kalinowski. The observatory was equipped in modern measuring and recording instruments of that time. The absolute magnetic measurements of declination D and horizontal component H were performed with a magnetometer produced by Cambridge Scientific Instruments Co. and a large Sartorius magnetometer; the inclination angle I was measured by an earth inductor produced by Schultz company from Potsdam. The bases of the vertical component Z were calculated from measurements of H and I , in accordance with the generally accepted routine at that time. Three variometers, H , D and Z , and a recorder produced by the firm of Toepfer and Sohn from Potsdam, were installed for continuous magnetic recording. The Świder absolute measurement (wooden) and recording (brick) pavilions of modern design (Figs. 2 and 3) were erected following the example of the observatory at Potsdam.

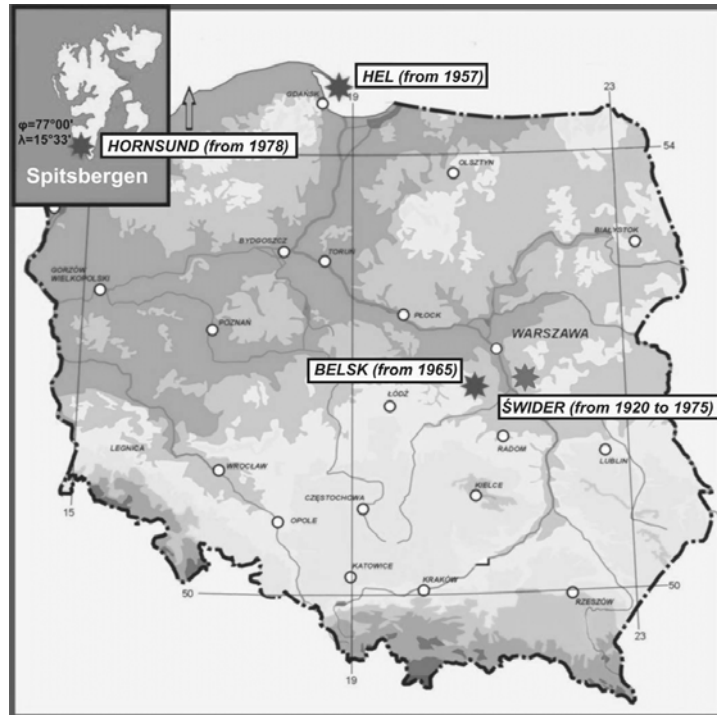


Fig. 1. The location of Polish geomagnetic observatories Belsk, Hel, and Hornsund.



Fig. 2. The Świder Observatory – absolute measurement pavilion.

The Świder observatory operated more-or-less normally (in spite of some errors made at the beginning of its activity) as long as the suburban railroad passing some 1.5 km from the Observatory had not been electrified. This DC powered railroad began to produce strong artificial disturbances in the natural magnetic field, especially the Z component. A next segment of the railroad has been electrified in the post-war period, which further enhanced the artificial noise, as illustrated in Fig. 4.



Fig. 3. The Świder Observatory – recording pavilion.

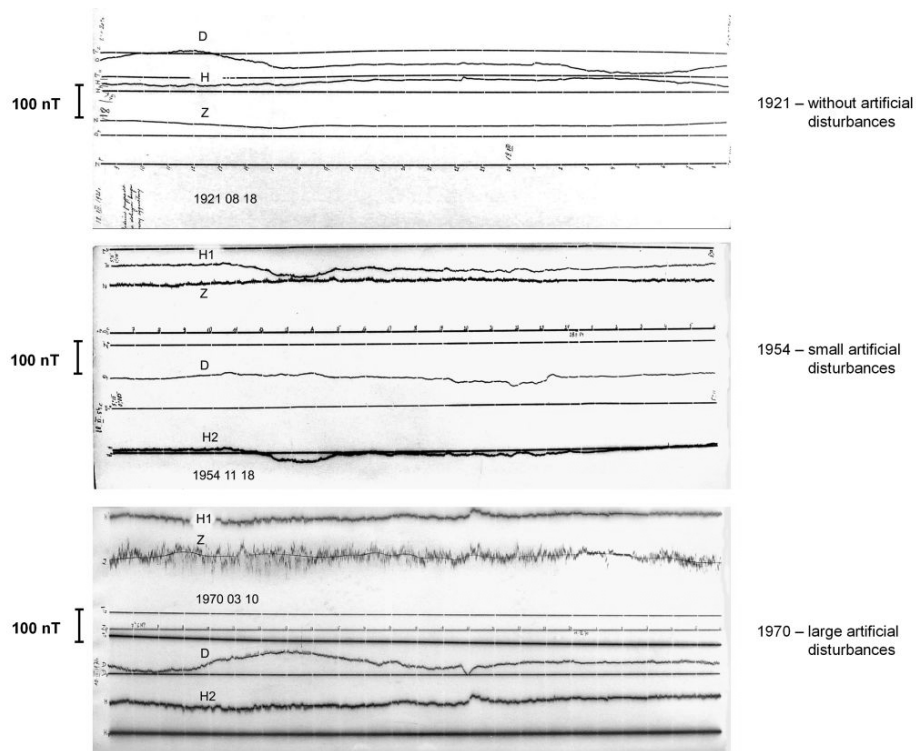


Fig. 4. Artificial noise due to railroad at the Świder observatory (copies of three magnetograms).

The second Polish geomagnetic observatory, established at Hel, began its operation in 1932. Likewise Świder, it was equipped in modern instruments of the time. The absolute measurements of H and D were made with the use of a large Askania theodolite, and those of the magnetic inclination angle I by means of Edelman earth

inductor. Three quartz magnetometers QHM, Nos. 25, 26, and 27, were purchased in Denmark. The magnetic recording was first made by Mascard-system variographs, and since 1934 by a fast-run recorder of La Cour system.

Unfortunately, the Hel observatory was destroyed in 1939 by German army. The pavilions with the instruments were demolished and all the archival data were lost.

In 1929, in the region that then belonged to SW Poland (presently the Ukraine), a magnetic station was put into operation in Daszewo. Since 1932 the works of this station were continued in the newly founded magnetic observatory in Janów by Lwow (presently called Ivanofrankovsk). The observatory is still active, being affiliated to the Ukrainian Academy of Sciences.

After the end of the Second World War, the only observatory that was not destroyed and was able to operate on the territory of Poland was Świder. Unfortunately, because of artificial railroad noise the data produced by this observatory were not very accurate. This was one of the reasons why at the beginning of the 1950s the decision was made to rebuild the Hel observatory and to move the geomagnetic observations from Świder to Belsk. Belsk is located some 45 km south of Warsaw (and some 50 km from Świder) in a typically rural region, with a low level of artificial noise.

The decisions relating to the Belsk and Hel observatories fortunately coincided with the forthcoming III International Geophysical Year. The state authorities declared Poland's participation in this huge international undertaking. Special funds were granted for joining the Geophysical Year project. The Institute of Geophysics (at that time called "Zakład Geofizyki") was able to purchase a rich collection of various instruments for geomagnetic research.

The instruments included three La Cour systems and one Mating Weisenberg system for observatory geomagnetic recordings, and three portable Askania GV3 systems (D, H and Z components) for field recordings. There were bought two large theodolites, Askania and Mating Weisenberg, for absolute measurements of D and H. There were bought two earth inductors for absolute measurements of magnetic inclination angle I, with the aim to equip the Belsk and Hel observatories. There were also bought a dozen or so quartz magnetometers QHM and a few BMZ magnetometers.



Fig. 5. The Hel observatory – recording pavilion.



Fig. 6. The Hel observatory – absolute measurement pavilion.



Fig. 7. The Belsk observatory – recording pavilion.



Fig. 8. The Belsk observatory – absolute measurements pavilion.

The newly purchased instruments provided a very modern, as for those times, instrumentation at the rebuilt Hel observatory and a new observatory at Belsk. In both observatories, the measurement and recording pavilions were constructed in a style that was classical for mid-twentieth century magnetic observatories. The photos are shown

in Figs. 5-8, while the main building of the Belsk observatory is shown in Fig. 9. The reconstructed Hel observatory began its routine operation in 1958, while the Belsk observatory, whose construction took more time, in 1964.



Fig. 9. The Belsk observatory – main building.



Fig. 10. Polish Polar Station Hornsund – recording pavilion.



Fig. 11. The Polish Polar Station Hornsund, Spitsbergen – main building.

In 1989, there was activated a Polish geophysical station located far northerly, in Hornsund fiord, Spitsbergen, The station is in a sense a continuation of the Polish station operating on Bear Island during the II International Geophysical Year. The Hornsund station is mostly focused on observations of events occurring in polar regions. It has two small magnetic pavilions, one being shown in Figs. 10; the main building of the station is shown in Fig. 11.

Evolution of Observation Methods in Polish Magnetic Observatories

The generous purchase of western measurement and recording instruments, associated with the III International Geophysical Year, gave grounds for modern instrumentation of Belsk and Hel observatories. The fast development of new measurement methods over the world forced us to make numerous changes to refine the instruments and methodology of measurement (in spite of the fact that the system of “real socialism” in Poland was not favorable to any progress). The changes introduced are illustrated in Table 1.

Table 1
Main instruments used at Polish geomagnetic observatories in the last 50 years

| BELSK (from 1965) | HEL (from 1957) | HORNSUND (from 1978) |
|---|---|--|
| VARIOMETERS | | |
| 1965 – Mating Wiesenberg variometers (set 1) | 1957 – La Cour basic and storm set | From 1978 Magn. station type PSM + visual recorder |
| 1966 – Bobrov quartz variometers (spare set) | 1966 – Bobrov quartz variometers H, D, Z and F | From 1984 PSM + digital tape recorder type TRC |
| 1978 – Magn. station type PSM + visual recorder | 1985 – Magn. station type PSM + visual recorder | From 1993 PSM + digital recorder DR-02 |
| 1984 – PSM + digital tape recorder type TRC | 1987 – PSM + digital tape recorder TRD (set 1) | From 2001 LEMI 03P + DR-02 (spare set) |
| 1993 – PSM + digital recorder type DR-02 (set 1 and set 2) | 1994 – PSM + digital recorder type DR-02 (set 1 and set 2) | |
| 1995 – records data from proton magnetometer | | |
| ABSOLUTE INSTRUMENTS | | |
| 1966 – proton magnetometers earth inductor, big magnetic theodolit Ascania, magn. QHM and BMZ | 1957 – Magnetic theodolite Mating Weisenberg, earth inductor, magn. QHM and BMZ | From 1978 Proton magnetometer type PMP-4 and quartz magnetometer QHM |
| 1974 – Vector proton magnetometer PMW | 1966 – Proton magnetometers | From 1996 Proton magnetometer type PMP-5 and DI-magnetometer |
| 1993 – DI-flux (Elsec) magnetometer | 1992 – Vector proton magnetometer | |
| 1994 – Proton magnetometer PMP-8 | 1996 – DI-flux magnetometer | |

The real break-through in the methodology of absolute measurements was the introduction of proton magnetometers (constructed in short series at the Institute of Geophysics). Previously, the observatory routine had been to calculate bases of the vertical component Z recordings using the horizontal component H measured in a

classical manner, and the magnetic inclination angle I measured with the Earth's inductor. In moderate geomagnetic latitudes, errors in the Z component determined in this manner were three times greater than those for the H component, so the method was not very accurate. The introduction of proton magnetometers made it possible to calculate Z from the measurements of F and angle I , which much improved the accuracy.

A next important step in the measurement technique development was the designing and implementation of the so-called proton vector magnetometers. In these magnetometers, installed at Belsk and Hel, the measurement sensors were placed within the Braunbeck coils fixed at large non-magnetic theodolites. The use of these magnetometers in observatory practice much simplified the methodology of absolute measurements and the determination of base values of the recordings. The mean random errors of measurements made with this method were some $0.3'$ for magnetic declination, 1.2 nT for the horizontal component H , and 1 nT for the component Z .

A considerable progress was also achieved in the mid-1990s by purchasing three Carl Zeiss Jena non-magnetic theodolites Theo 10B, on which flux-gate magnetometers were installed. Consequently, all three Polish geomagnetic observatories are able to make base determination from absolute measurements of D , I , and F .

In the mid-1960s, continuous magnetic recording systems in Polish observatories were equipped with Bobrov's quartz variometers, of much more stable parameters. At the beginning, these variometers were used in a typical, classical manner for recording of a photo-paper. A next step was the development of the so-called Portable Magnetic Stations PSM. In these stations, the deflection of magnets sensitive to magnetic field changes are converted by the photoelectric converters into electric current changes in a system with a strong negative feed-back. The electric signals from the

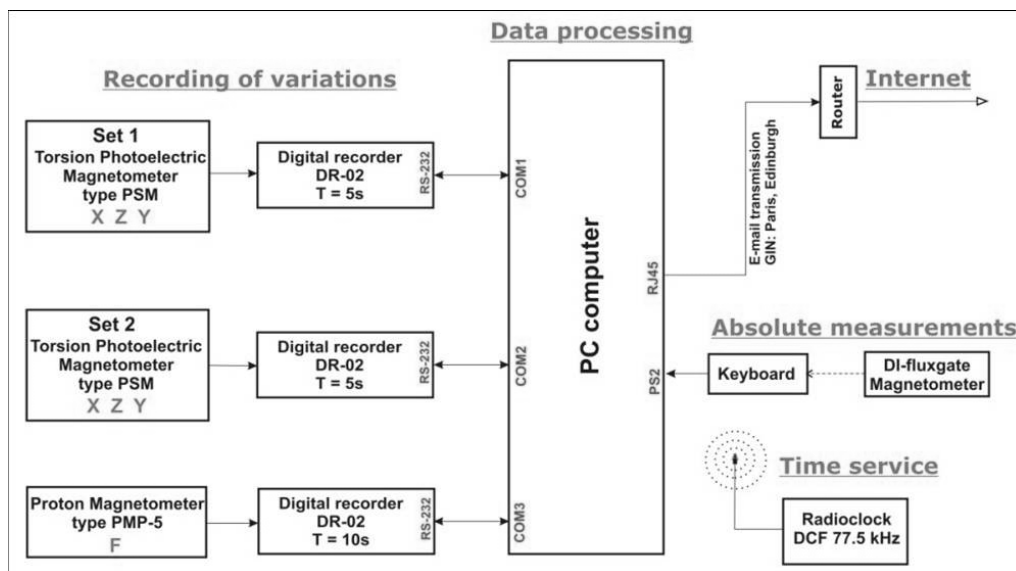


Fig. 12. Scheme of geomagnetic observations at Polish observatories in the framework of INTERMAGNET.

PSM station were first recorded by a three-channel analog pen recorders, and then by digital loggers, whose consecutive, refined models have been designed and constructed at the Belsk observatory.

At present, the instrumentation at all the three Polish magnetic observatories, at Belsk, Hel, and Hornsund, can be regarded as quite up-to-date, satisfying all standard requirements of the INTERMAGNET network. In each of these observatories, the absolute magnetic measurements are made by means of DI-FLUX magnetometers and PMP magnetometers of Polish make. The recordings are carried out by means of PSM stations and 16-bit microprocessor-based digital loggers DR-03. To give an example, we present in Fig. 12 a simplified block diagram of geomagnetic observations at Belsk and Hel. In the Polar observatory at Hornsund, the scheme is similar, except that a small transduced magnetometer has been installed in the spare set 2.

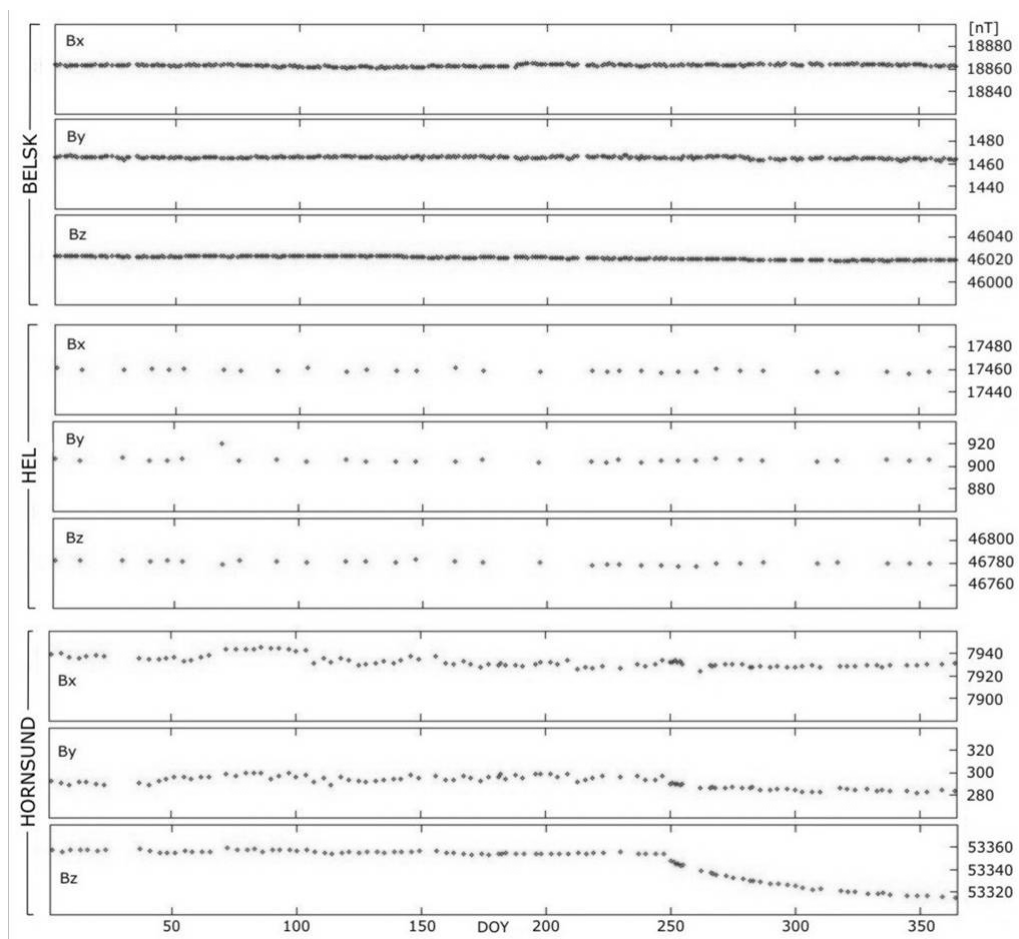


Fig. 13. The 2004 baselines from Belsk, Hel and Hornsund observatories.

Accuracy and Availability of Data

The accuracy of the so-called long-term data produced by the geomagnetic observatories at Belsk and Hel is estimated at about ± 1 nT. The estimates follow from an analysis of the accuracy of absolute base measurements, a comparison of recordings of the two sets, and an analysis of the differences $\Delta F = F - \sqrt{X^2 + Y^2 + Z^2}$, where F stands for the proton magnetometer indications recorded in a continuous manner, and X, Y, and Z are the field component values calculated from recordings of set 1 or 2. The accuracies of basic instruments that are presently used in Polish magnetic observatories are listed in Table 2.

Table 2

Accuracy of the main instruments that are presently used at Polish geomagnetic observatories

| No. | EQUIPMENT | RESOLUTION | ACCURACY | LONG-TERM STABILITY | NOTES |
|-----|--------------------------------------|-----------------------|---------------|---------------------|---|
| 1 | DI-FLUX magnetometers | 0.1 nT | ~ 0.5 nT | ~ 0.5 nT/year | |
| 2 | Proton Magnetometers type PMP-5 | 0.1 nT | ~ 0.5 nT | ~ 0.3 nT/year | |
| 3 | Proton magnetometers type PMP-8 | 0.01 nT | ~ 0.2 nT | ~ 0.3 nT/year | |
| 4 | Photoelectric magnetometers type PSM | ~ 0.01 nT | ~ 0.5 nT | 3..5 nT/year | $Q_t \leq 0.5$ nT/°C (temperature stabilized in recording house) |
| 5 | Digital recorders type DR-03 | 0.025 nT (16 bits) | 0.05 nT | | |

The accuracy of Spitsbergen data is somewhat lower, mostly because of seasonal instability of the pier on which the PSM station variometers are installed at the recording pavilion.

A good measure of the accuracy of observatory data is the stability of bases of the magnetic recordings. To give an example, we present in Fig. 13 the plots of bases at Belsk, Hel, and Hornsund in 2004. The absolute measurements of D, I, and F for base determination are performed 5 times a week at Belsk, few times a month at Hel, and 2-3 times a week at Hornsund.

Of great importance is, in our opinion, the continuity of the collected data, i.e., the lack of gaps in recordings. Two recording sets work permanently at each of the observatories, and the probability of their simultaneous failure is very small. Infrequent gaps in the Belsk and Hel data throughout the last 40 years are listed in Table 3. At the polar observatory Hornsund, where the spare recording set II has not been in operation until the last few years, the gaps are somewhat more numerous, although in some recent years they have not occurred at all.

Table 3

Gaps in the data from the Belsk and Hel observatories in the years 1966-2005

| HEL | | | | | | BELSK | | | | | |
|---|-------|-----|------|-------|-----|---|-------|-----|------|-------|-----|
| Year | Hours | ‰ | Year | Hours | ‰ | Year | Hours | ‰ | Year | Hours | ‰ |
| 1966 | 21 | 2.4 | 1986 | – | – | 1966 | – | – | 1986 | – | – |
| 67 | – | – | 87 | – | – | 67 | – | – | 87 | – | – |
| 68 | – | – | 88 | – | – | 68 | 4 | 0.5 | 88 | – | – |
| 69 | – | – | 89 | – | – | 69 | – | – | 89 | 3 | 0.3 |
| 1970 | – | – | 1990 | – | – | 1970 | – | – | 1990 | – | – |
| 71 | 23 | 2.6 | 91 | – | – | 71 | – | – | 91 | – | – |
| 72 | – | – | 92 | – | – | 72 | – | – | 92 | 2 | 0.2 |
| 73 | – | – | 93 | – | – | 73 | – | – | 93 | – | – |
| 74 | 21 | 2.4 | 94 | – | – | 74 | – | – | 94 | – | – |
| 1975 | – | – | 1995 | – | – | 1975 | – | – | 1995 | – | – |
| 76 | – | – | 96 | – | – | 76 | – | – | 96 | – | – |
| 77 | – | – | 97 | – | – | 77 | – | – | 97 | – | – |
| 78 | – | – | 98 | – | – | 78 | – | – | 98 | – | – |
| 79 | – | – | 99 | 60 | 6.8 | 79 | – | – | 99 | – | – |
| 1980 | – | – | 2000 | – | – | 1980 | – | – | 2000 | – | – |
| 81 | – | – | 01 | – | – | 81 | – | – | 01 | – | – |
| 82 | – | – | 02 | – | – | 82 | – | – | 02 | – | – |
| 83 | – | – | 03 | – | – | 83 | – | – | 03 | – | – |
| 84 | – | – | 04 | – | – | 84 | – | – | 04 | – | – |
| 1985 | – | – | 2005 | – | – | 1985 | – | – | 2005 | – | – |
| HEL 1966..2005, $\Sigma h=125$, ‰=0.36 | | | | | | BELSK 1966..2005, $\Sigma h=9$, ‰=0.03 | | | | | |

The results of geomagnetic observations from Polish observatories are published in a standard form of the so-called magnetic yearbooks (Publications of the Institute of Geophysics, Polish Academy of Sciences). For Belsk and Hel, the yearbooks have been published since 1966, and for Hornsund since 1980. Until 1999 the yearbooks had been presenting the monthly tables of hourly mean values, and since 2000 the tables have been replaced by the daily plots of X, Y, and Z, i.e., size-reduced magnetograms.

The data from Polish observatories have been regularly sent to world data centers (WDC) in Boulder and Copenhagen. In the framework of INTERMAGNET, the one-minute values are everyday transmitted, in an automatic manner, to Paris and Edinburgh; this has been made for the Belsk data since 1984, Hel data since 1988, and Hornsund data since 2002. The archival and current data are also available from the Institute of Geophysics of the Polish Academy Sciences.

Summary

Throughout the last 40 years, we were able establish in Poland three fairly modern magnetic observatories, equipped in relatively up-to-date instruments, mostly of our own make at the Institute of Geophysics. The data produced by these observatories comply with the main accuracy standards, and the continuity of data can be regarded as very good.

At Belsk, the biggest of these three observatories, the routine geomagnetic observations there are accompanied with various works relating to the development of new instruments and measurement methods. The Belsk observatory is also a basis for numerous field surveys carried out by the Institute of Geophysics in Poland and abroad.

Literature

Yearbooks from Polish geomagnetic observatories:

- Results of Geomagnetic Observations, Belsk Geophysical Observatory*, covering the period since 1966 up to the present, published in *Publs. Inst. Geophys. Pol. Acad. Sc.*
- Results of Geomagnetic Observations, Hel Geophysical Observatory*, covering the period since 1966 up to the present, published in *Publs. Inst. Geophys. Pol. Acad. Sc.*
- Results of Geomagnetic Observations, Polish Polar Station Hornsund, Spitsbergen*, covering the period since 1978, published in *Publs. Inst. Geophys. Pol. Acad. Sc.*
- Results of Geomagnetic Observations, Polish Antarctic Station Arctowski*, covering the years 1978 to 1995, published in *Publs. Inst. Geophys. Pol. Acad. Sc.*
- Roczniki Magnetyczne (Annuaire magnetique)*, covering the years 1937-1967. Prace Obserwatorium Geofizycznego im. S. Kalinowskiego w Świdrze.

Other references:

- Czyszek, Z., and W. Czyszek, 1983, *Geophysical Observatory at Hel 1983-82*, *Acta Geophys. Pol.* **31**, 4, 431-444.
- Jankowski, J., and B. Janke, 1963, *O pomiarach za pomocą magnetometru protonowego w Obserwatorium na Helu*, *Acta Geophys. Pol.* **11**, 3, 199-202 (in Polish).
- Jankowski, J., W. Kiełek and W. Romaniuk, 1965, *Tranzystorowy magnetometer protonowy TMP-1*, *Acta Geophys. Pol.* **13**, 1, 57-64 (in Polish).
- Jankowski, J., J. Marianiuk, A. Reda, C. Sucksdorff and M. Kivinen, 1984, *Long-term stability of a torque balance variometer with photoelectronic converter in observatory practice*, *Geophys. Surveys* **6**, 367-380.
- Marianiuk, J., 1977, *Photoelectronic converter for recording the geomagnetic field elements*, *Publs. Inst. Geophys. Pol. Acad. Sc.* **C-4 (114)**, 57-82.
- Ołpińska-Warzechowa K., 1985, *Obserwatorium Geofizyczne im. St. Kalinowskiego w Świdrze*, *Prz. Geof.* **30**, 2, 213-229 (in Polish).

Accepted January 22, 2007

50 Years of History of the Tihany Geophysical Observatory

András CSONTOS, László HEGYMEGI, Balázs HEILIG, Péter KOVÁCS,
László MERÉNYI and Zoltán SZABÓ

Eötvös Loránd Geophysical Institute
Budapest, Kolombusz utca 17-23. H-1145. Hungary
e-mail: csontos@elgi.hu

Abstract

The magnetic observation at Tihany Geophysical Observatory was started more than fifty years ago, in 1955. On the occasion of achieving this historical age, the brief history of the geomagnetic measurements in Hungary and the activities at Tihany Geophysical Observatory is presented. The article gives a retrospective review at the development of the instrumentation, survey campaigns and international connections of the observatory.

1. Historical Review of Hungarian Geomagnetic Observations

The history of systematic geomagnetic recording in Hungary started in 1768 at Nagyszombat University (now Trnava, Slovakia). In 1777, the university moved to Buda, where declination measurements continued with three-times-a-day periodicity until the siege of Buda in 1849, during Hungary's war of independence. Between 1781 and 1792 the observatory was part of the "Societas Meteorologica Palatina" European network.

Organized research of the Earth's magnetic field began with the foundation of the meteorological service in 1851 with the establishment of the Central Institute of Meteorology and Geomagnetism in Vienna, under Karl Kreil (1798-1862), former director of the Prague Observatory. From this date onward, organized investigation of the Earth's magnetic field began under the Habsburg Royalty, in the Austrian Empire. After the Austrian-Hungarian Compromise, however, an independent Hungarian institute was founded in 1870. The founder and first director of the Central Royal Hungarian Meteorological and Geomagnetic Institute was the Austrian Benedictine monk Guido Schenzl (1823-1890), who had already been observing the geomagnetic field in Buda for several years.

The first countrywide geomagnetic surveys in Hungary was carried out by the team of Empire's meteorological institute 1847-1857 (K. Kreil) and later by the independent Hungarian institute 1864-1879 (G. Schenzl), and 1892-1894 (I. Kurländer). Declination was measured using portable magnetic theodolites, inclination was observed with needle inclinometers. Schenzl used a variation needle and strong deflecting magnets to measure the horizontal intensity of the magnetic field. From 1873, the more precise earth inductors were introduced. Figure 1 is a reproduction of one of the maps of this survey.

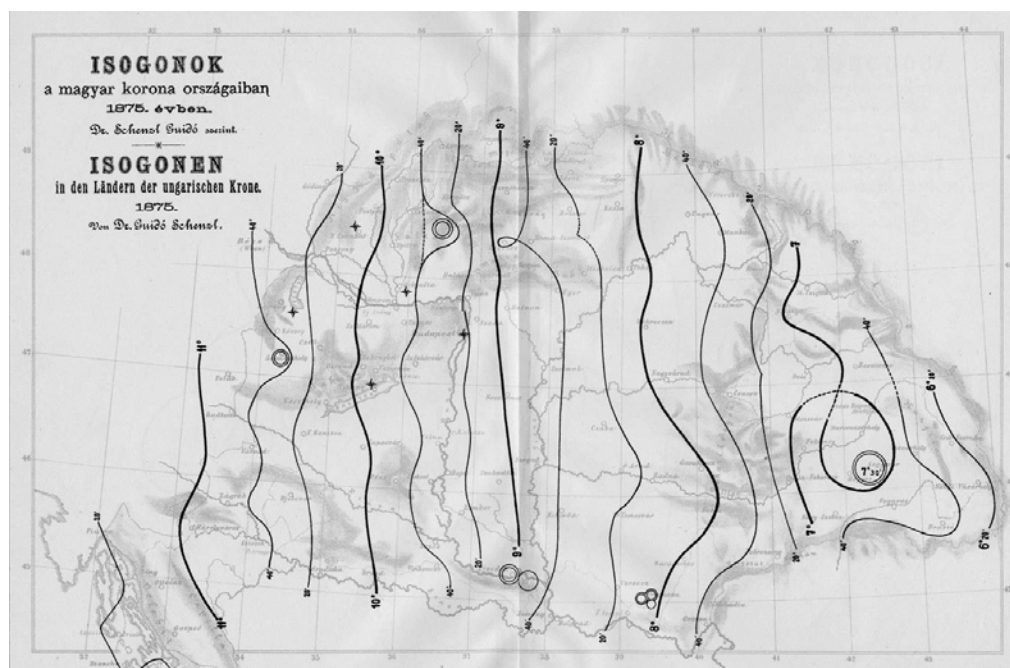


Fig. 1. Guido Schenzl's isogon map of Hungary for the epoch of 1875.0. Locations of historical and present geomagnetic observatories are marked by asterisk (from north to south): Nagyszombat (now Trnava), Ógyalla (now Hurbanovo), Nagycenk, Buda (Budapest), Tihany.

Between 1890 and 1910, the independent Hungarian meteorological institute was headed by Miklós Konkoly Thege (1842-1916). In 1893, in order to avoid the industrial noise of the growing capital, he moved the geomagnetic observations to his personal observatory at Ógyalla (now Hurbanovo, Slovakia), where observations continued. After the First World War the region became part of Czechoslovakia and the observatory's name was changed to Stara Dala. In the period 1938-1945 the territory and the observatory returned to Hungary. After the Second World War the observatory continued its activity under the name Hurbanovo Observatory (Slovakia).

In Hungary, to replace the loss of Ógyalla, a temporary station was built at Budakeszi (near to Budapest) in 1949. In 1950, geomagnetic observations were transferred from the Meteorological Institute to the Eötvös Loránd Geophysical Institute (ELGI). The need for a permanent observatory was strongly felt during the 1949-50 geomagnetic base network measurements. The search for a location free of actual and

possible future industrial disturbance led to the selection of Tihany national park on the peninsula of Lake Balaton (see Fig. 2). The construction work of the observatory started in 1952 and was completed in 1954. The scientific preparation and the project itself, was headed by György Barta (1915-1992), who became later the first leader of the observatory. The observatory has been recording geomagnetic data since 1955. (ELGI Geomagnetism Group, 2006)



Fig. 2. Tihany village on the peninsula in the year 1955. On the left and right sides of the picture, the Abbey, and the office of the observatory can be seen, respectively. From the beginning of the observations in Tihany, the cross of the southern tower of the Abbey is used as a reference mark for the absolute measurements of geomagnetic declination. It can be seen at an angle of precisely $3^{\circ} 59' 10''$ from the observatory's absolute pillar.

In 1961 continuous geomagnetic observation started also in Nagycenk (NCK) Geophysical Observatory, maintained by the Geodetic and Geophysical Research Institute of the Hungarian Academy of Sciences.

2. Instrumentation of Tihany Geophysical Observatory

2.1 *From the analogue instruments to digital techniques*

Tihany Observatory started the continuous recording with analogue photo recorders. The variometer house was constructed in accordance with the needs of classical instruments. To reduce the effect of daily and seasonal temperature variation the rooms are underground and the roof is covered by a thick layer of reeds. The difference between the yearly temperature maximum and minimum is eight degrees centigrade. Between 1954 and 1991, the recording of geomagnetic elements was based on

LaCour instruments (Fig. 3.). In the early '70ies the LaCour variometers were equipped with photoelectric converters and their data recorded digitally. The data were recorded on punched tape. To increase the baseline stability, parallel to LaCour variometers, Bobrov type quartz variometers were installed. The first microprocessor-based recorder, DIMARS (Digital Magnetic Recording System) was developed by ELGI in 1982, for the registration of Bobrov data. The system performed 5 second sampling and the data were recorded on floppy disc in a PC readable format. DIMARS was in use until 1999; it was also employed in several other observatories around the world. Bobrov variometers were changed to LEMI fluxgate magnetometer in 1993. For LEMI a new low power recording system (DIMARK) was developed and built based on PC standard technology between 1999-2000. Data were recorded on a flash memory card from which data download was enabled by remote control via a telephone line. (Annual reports of Tihany Geophysical Observatory 1955-1987).

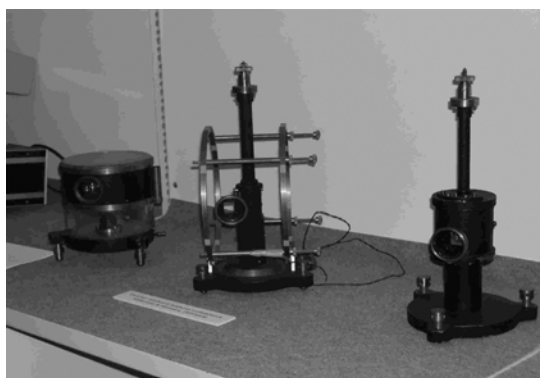


Fig. 3. LaCour instruments.

A new era in the history of Tihany Observatory started when the US-Hungarian Joint Fund (UHJF) accepted a project proposal submitted by ELGI and the US Geological Survey (USGS) to raise the level of the observatory instrumentation to international standards in order to get INTERMAGNET membership. A Meteosat transmitter was installed and regular one-minute data transmission to Geomagnetic Information Node in Edinburgh started. Since 1991 Tihany Observatory's data are annually published on INTERMAGNET's CD-ROM.

Recently, Tihany Observatory's three-component magnetic recording system is based on the FGE magnetometer with suspended sensor, produced by the Danish Meteorological Institute. At our request the magnetometer came equipped with an ADAM 4017 type, 16-bit A/D converter. The system is able to work with a 1-second sampling rate using the DIMARK data acquisition system. In addition, it records the calculated 1-minute mean values required by INTERMAGNET. This data acquisition system is developed by ELGI, and currently used in several observatories of the world.

Parallel to the above, there is a DIDD system working with Overhauser magnetometers of GEM Systems, Canada. DIDD was developed in the framework of an ELGI-USGS-GEM Systems cooperation in the early 1990s with the financial support of UHJF. DIDD system records inclination and declination, as well as total field data

in every 5 seconds. When these data are used as input to a task-oriented DIMARK, it produces real-time XYZF 1-minute means. Thus, DIDD can serve as back-up for our base FGE magnetic recording system. DIDD system is used in about 30 observatories throughout the world.

In 1995, within the framework of a US-Hungarian Joint Fund project, synchronized geomagnetic pulsation observations were started in two pairs of observatories [Boulder–South Park (Colorado, US) and Tihany (Hungary)–Hurbanovo (Slovakia)] to study the near-earth environment processes. Owing to this cooperation a further three-component fluxgate magnetometer (the Canadian NAROD) was installed in the observatory. Currently, it works at a 16 Hz sampling rate to record pulsations in the DC-5Hz frequency range. The resolution of LAWSON LABS' A/D converter is 20 bits and it is synchronized to a GPS unit with ± 0.001 sec accuracy.

2.2 Absolute measurements

The absolute measurements were carried out by QHM and BMZ instruments starting from the foundation of Tihany Observatory. Total field observations were introduced using a home-made proton magnetometer, in 1967. To replace QHM and BMZ instruments an ELSEC-type proton precession magnetometer—complemented by a Helmholtz coil system—was set up in 1979. The first D/I theodolite was purchased and installed in 1983. The first Overhauser magnetometer arrived to Tihany in 1991, thanks to UHJF.

3. Additional Activities of the Observatory

From 1950 onwards, the geomagnetic base network of Hungary has been reobserved every 15 years; this was carried out by György Barta (1949-1950); Etelka Aczél and Róbert Stomfai (1964-1965, see Fig. 4); Tibor Lomniczi and Péter Tóth (1979-1982); Alpár Körmendi and Péter Kovács (1994-95). Since 1965, the institute has also

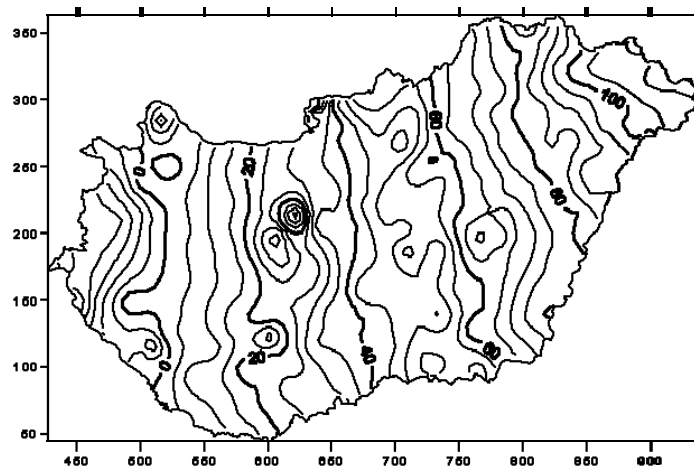


Fig. 4. Isogon lines of declination in Hungary, for the epoch of 1965.0.

maintained a secular network to record secular variations of the magnetic field on 12 to 15 stations of the base network.

In addition to geomagnetic observations the activity of the Observatory included meteorological, earth tide, micro-seismological and geothermal registrations as well as paleomagnetic- and rock-physical parameter measurements from time to time. In co-operation with Eötvös Loránd University (ELTE, Budapest) atmospheric radio noise registrations were carried out for about 20 years and, from 1970 on, whistlers has been observed and recorded in the observatory. Beside the magnetic observations, space research is one of the most important basic activities of the observatory up to this day.

In 1990 the third IAGA Workshop was organized by Tihany Observatory. The personnel of the Observatory is regularly taking part in ELGI's geomagnetic projects. (Körmendi *et al.* 1991)

References

ELGI Geomagnetism Group, 2006, *Tihany Geophysical Observatory 1955-2005*, Eötvös Loránd Geophysical Institute of Hungary, Budapest.

Körmendi, A., *et al.* 1991, *Introduction*, Geophysical Transactions **36**, 3-4, 121-185.

Annual Reports of Tihany Geophysical Observatory 1955-1987.

Accepted February 27, 2007

Keetmanshoop – A New Observatory in Namibia

Hans Joachim LINTHE¹, Pieter KOTZE², Mioara MANDEA³
and Herman THERON²

¹ GeoForschungsZentrum Potsdam – Adolf Schmidt Observatory
Lindenstrasse 7, D-14823 Niemegk Germany
e-mail: linthe@gfz-potsdam.de

² Hermanus Magnetic Observatory
P.O. Box 32, Hermanus, 7200, South Africa
e-mail: pkotze@hmo.ac.za

³ GeoForschungsZentrum Potsdam
Telegrafenberg, D-14473 Potsdam Germany
e-mail: mioara@gfz-potsdam.de

Abstract

One of the most fascinating geophysical studies in southern Africa is to track the evolutionary behaviour of the geomagnetic field. The Keetmanshoop Observatory was installed in 2005 on the premises of the Keetmanshoop Airport as part of a collaboration project between Hermanus Magnetic Observatory (HMO) and GeoForschungsZentrum Potsdam (GFZ). This location was specifically chosen about halfway between Hermanus in the South and Tsumeb in the North in order to correct for disturbance effects from external sources and to refer the repeat station data to a common epoch during field surveys. This newly-established INTERMAGNET-grade observatory will play a key role in the region, as a reference magnetic observatory for field stations within a radius of 600 km located in the large area between the Northern Cape and southern Namibia, a region which has not been adequately covered in the past. In addition it will also serve as an accurate monitor of spatial changes in secular variation across southern Africa.

1. Introduction

In addition to a rapid decrease in the total field intensity over southern Africa, as recorded by the Hermanus Magnetic Observatory since 1941, the orientation of the geomagnetic field in this region is also changing substantially. In the northwest part of

southern Africa the declination of the magnetic field is propagating eastward (Tsumeb) and in the south-east part westward (Hermanus and Hartebeesthoek), causing a spatial gradient over the subcontinent which is presently increasing with time. The spatial structure of the geomagnetic field can therefore not be resolved with only these 3 magnetic observatories. Figure 1 shows the declination and total intensity secular variation of the observatories Hermanus, Hartebeesthoek and Tsumeb.

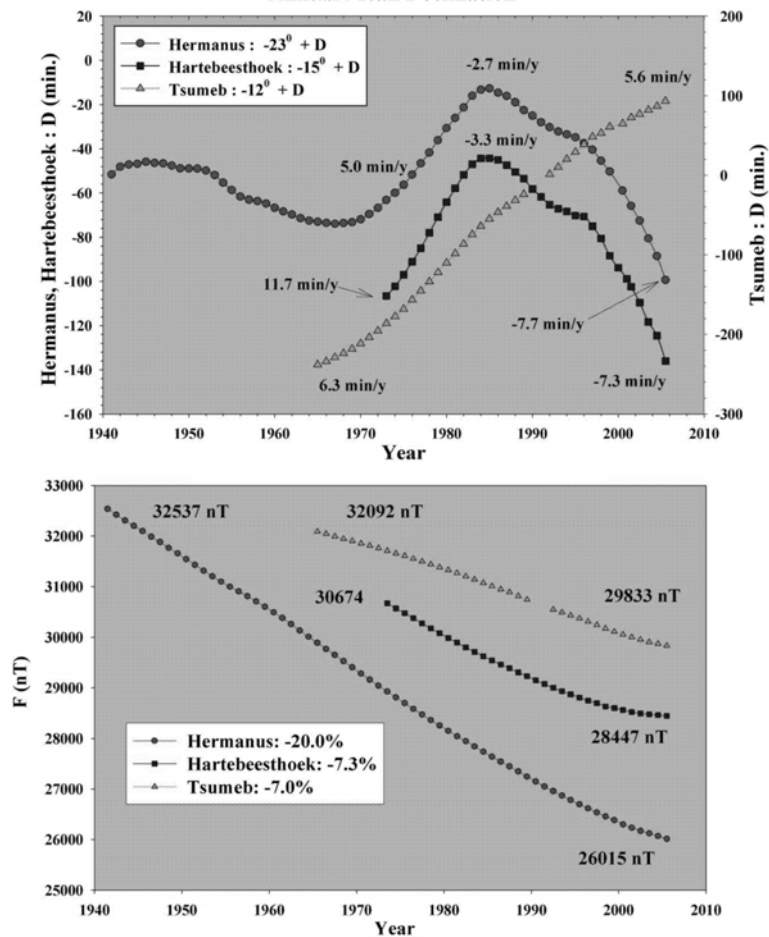


Fig. 1. Declination and total intensity secular variation of the observatories Hermanus, Hartebeesthoek and Tsumeb.

Therefore, the GeoForschungsZentrum (GFZ) and the Hermanus Magnetic Observatory (HMO) have decided to establish a new magnetic observatory at Keetmanshoop in the southern region of Namibia as part of a joint collaborative research project. It will approximately be located halfway between HMO and Tsumeb in a North-South direction, while it will also be approximately on the same latitude as Hartebeesthoek.

The GFZ provided the 3-component fluxgate variometer FGE (Danish Meteorological Institute), 2 Overhauser effect proton magnetometers (model GSM19) and a

DI-flux theodolite (model 3T2KP), equipped with a fluxgate magnetometer model G (DMI). The site was selected on the premises of the Keetmanshoop airport, sufficiently away from man-made magnetic noise, with suitable logistic conditions for the observatory. The instruments are located in a security environment, while airport staff is able to monitor the continuous functioning and perform absolute measurements on a regular basis.

2. Establishment of the New Observatory

In 2005 the GeoForschungsZentrum (GFZ) Potsdam and the Hermanus Magnetic Observatory (HMO), as part of a collaboration project, decided to establish the new geomagnetic observatory in Keetmanshoop, Namibia. At first the Hermanus Magnetic Observatory negotiated with the responsible Namibian governmental agencies and the administration of Keetmanshoop Airport and obtained permission for the establishment and operation of an observatory on its premises.

In order to minimize expenses it was decided not to construct buildings for the measurements and recordings. It was planned to construct a stable pillar for the absolute measurements with a roof for protection against direct sun radiation and wind, while the recording instruments are to be located in a glass-fibre container, buried partially underground, also with a protection roof. Transmission of data to HMO will be done using cellular phone technology. The airport provided a room of the terminal building to place the computer and to store the absolute instruments. Electric power is also supplied by the airport.

First of all, suitable places were searched for the absolute measurement pillar and the variometer container. The airport staff recommended an area of the airport, which will be long-term free of magnetic perturbations, produced by the airport service. A first raw survey was done by means of one of the Overhauser proton magnetometers to find a place free of big total intensity gradients. This proved to be somewhat difficult due to the rather high concentration of magnetic minerals in the soil. Furthermore, the area was covered with a number of big rocks, which showed a very strong magnetic perturbation (the proton magnetometer signal was even saturated close to some of these rocks). Suitable locations were however found for both the absolute measurement pillar and variometer container.

Around the centre of the variometer container more gradient surveys were carried out at 1 m intervals, covering a size of 10×10 m, while those around the absolute measurement pillar was actually 5×5 m. Figure 2 shows the resulting maps of the total intensity gradient sounding.

A contractor carried out the following constructions:

- Absolute measurement pillar construction consisting of an asbestos cement pipe, filled with concrete, on a stable concrete basement;
- Embedding of the variometer container about 1 m deep into the ground with a pillar for the FGE sensor of the same construction as the absolute measurement pillar;

- Construction of wooden protection roofs above the absolute measurement pillar and the variometer container;
- Removal of a number of big rocks to eliminate their influence on the instruments;
- Installation of a sleeve pipe of 550 m length including 7 inspection man-holes for the cables between the variometer container and the computer room; installing of the power supply cable in the pipe;
- Installation of burglar bars and solar shield at windows of the computer room;
- Electrical installation in the computer room;
- Installation of an air conditioner in the computer room.

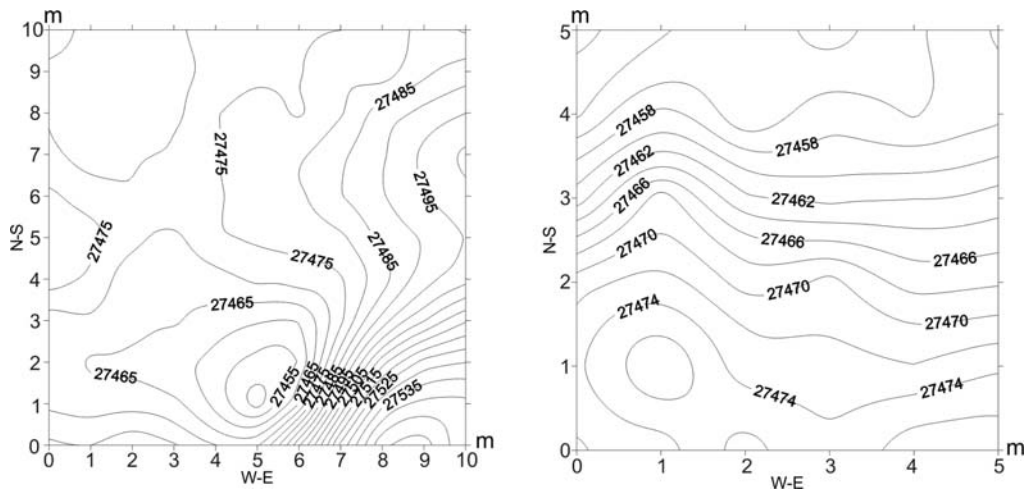


Fig. 2. Total intensity gradient map around the variometer container (left) and the absolute measurement pillar (right), at 2 m elevation both. Isolines in nT.

The constructions were finished by the end of January 2006. Figure 3 shows a sketch of the location.

For the absolute measurements, an azimuth mark was painted on the visible wall of the airport main building. To determine the azimuth value some Sun observations were carried out. HMO did the calculations and determined the azimuth value as $353^{\circ} 38' 30''$. The geographic coordinates of the absolute measurement pillar were determined by means of a GPS receiver as: Latitude = $26^{\circ} 32' 26.1''$ S, Longitude = $18^{\circ} 06' 37.3''$ E, Elevation = 1065 m.

The instruments, the data logger and the optical cable were installed in May 2006 by HMO staff. At the same time 3 airport staff members were trained to carry out absolute measurements. Since that time the recording runs continuously and the absolute measurements are carried out regularly.

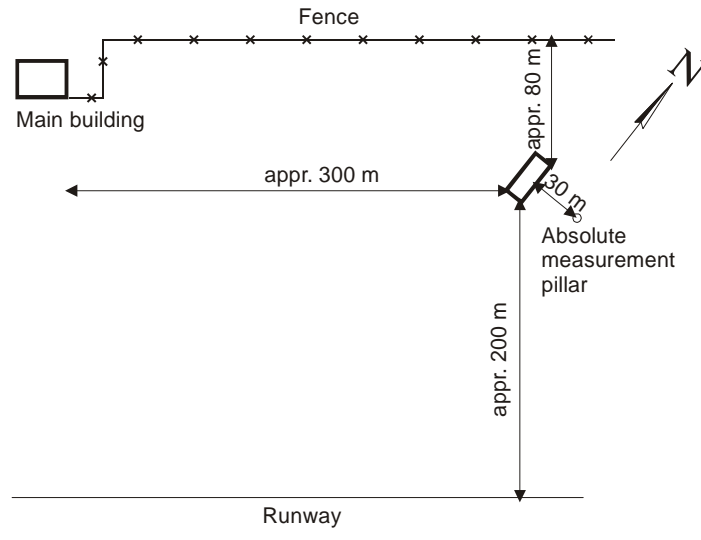


Fig. 3. Sketch of the location.

3. Description of the Data Logger

The data-logging system at the Keetmanshoop Magnetic Observatory is used to control the data-acquisition operations to capture data from the different geomagnetic instruments. This data is stored on Compact Flash media, but is also remotely accessed for further processing. Figure 4 shows the block diagram of the logger system. The system consists of the following:

- Industrial embedded computer;
- Data acquisition modules;
- Cellphone remote communications.

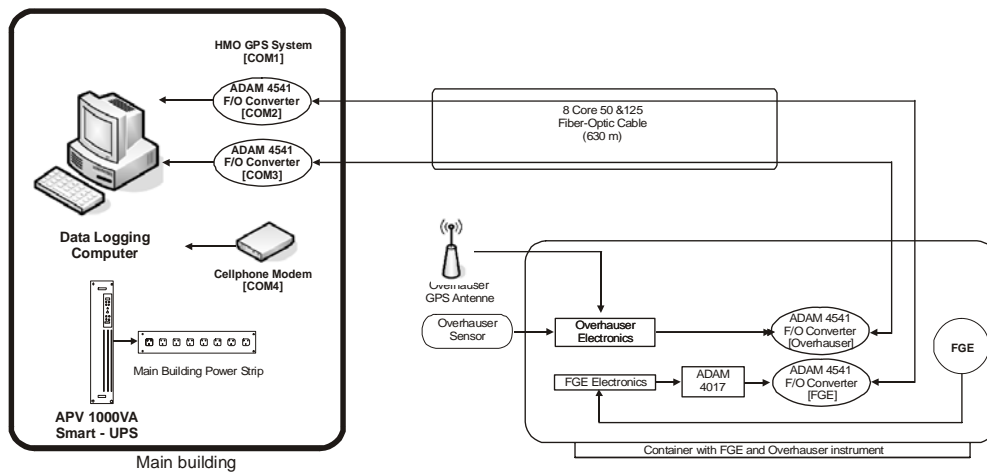


Fig. 4. Block diagram of the data logger.

3.1 Industrial embedded computer

A small industrial embedded computer, iEi Juki Eden 400R, is used as the master controller of all data operations. The operating system is a custom build Linux distribution developed at the HMO, and designed to operate on a Compact Flash card. Additional kernel patches (<http://www.rtai.org>) allow the system to operate as a real-time operating system, while allowing Linux to continue as normal. Specialized software controls the data collection from all the instruments. The HMO-developed GPS system allows accurate sampling of data. Instrument data are stored as well on the Compact Flash card. All data are transmitted daily from Keetmanshoop to the main data server at the Hermanus Magnetic Observatory. A web interface provides the user with the following services:

- Status information on all instruments as well as the HMO GPS system;
- Graphical view of the data from the instruments (24-hour period);
- Data capture screen to input observation data.

3.2 Data acquisition modules

Industry-standard ADAM modules are used for all data conversion. The ADAM 4017 module is used to convert the analogue signal from the fluxgate magnetometer into a digital representation. Due to certain limitations, the digital signals need to be transmitted over a distance of 630 meters. An 8-core fibre optic cable was installed with ADAM 4521 modules to provide reliable communications between the computer and instruments.

3.3 Cellphone remote communications

From past experience it is well known that in Namibian rural areas the local telephone infrastructure is unreliable. As an alternative, cellphone communication was chosen to provide remote connectivity. A previous installation at Tsumeb has proven to be a reliable method for data transfer.

A Wavecom Fastrack cellphone modem is used to interface to the cellphone network. This modem provides a standard modem interface to the computer. A PPP connection is established on a daily basis to transfer data using the FTP protocol.

4. First Measurement Results

To demonstrate the satisfying operation of the variometer and the data logger Fig. 5 shows the recording of 21 May 2006 in comparison to Tsumeb Observatory recording. At the upper part of Fig. 5 the H, D and Z recordings of both observatories are displayed, where an artificial offset was added to Tsumeb data. The lower part shows the differences of both recordings, where Keetmanshoop data were subtracted from Tsumeb values.

Up to now base lines were not determined. The reductions of the absolute measurements are still in preparation.

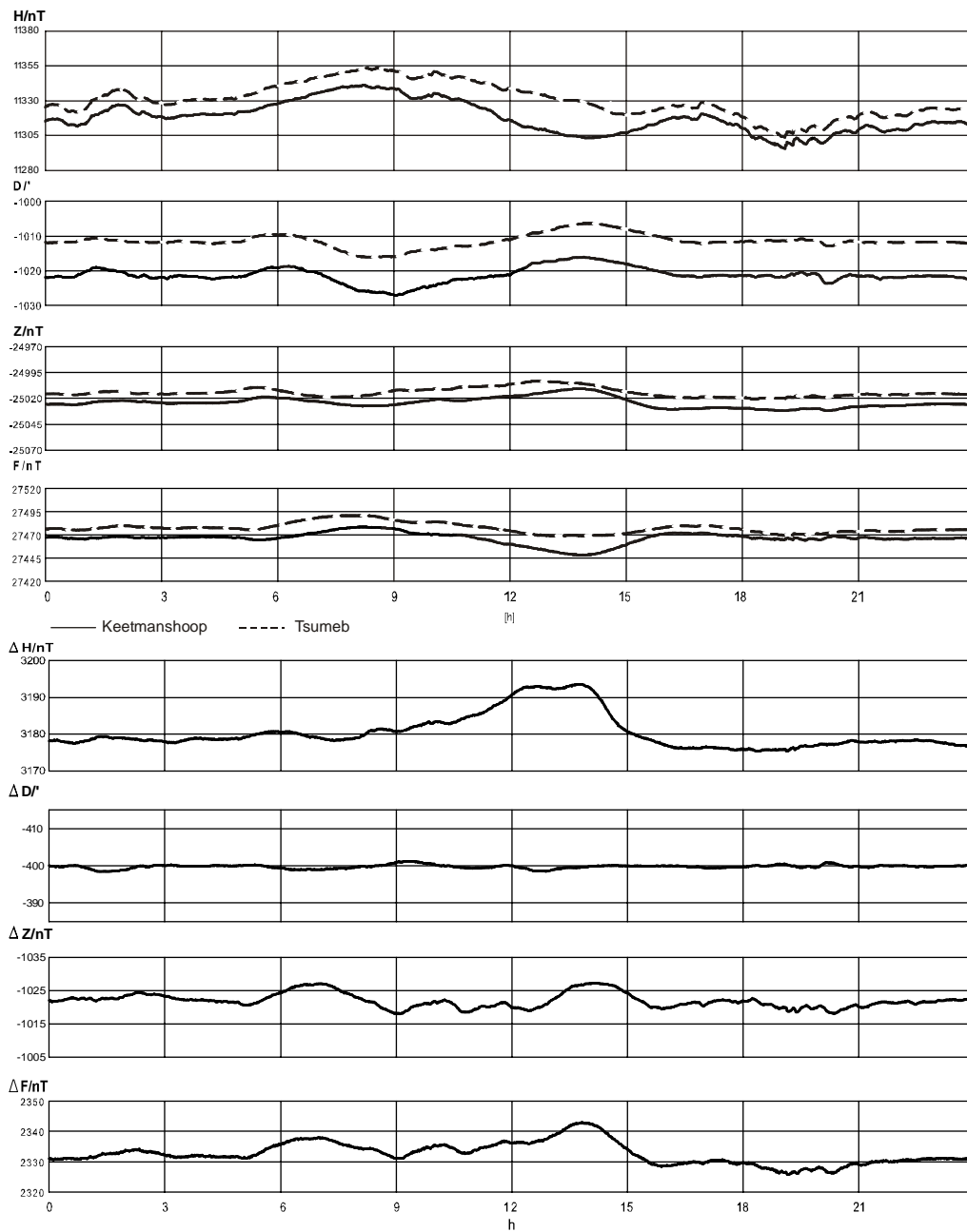


Fig. 5. Recording example in comparison with Tsumeb recording of 21 May 2006.

During several time intervals perturbations of high frequency in the recordings were observed. The origin of this effect could not be explained free of doubt. Eventually mining activities may be the reason. Further soundings are necessary in future.

5. Summary

On the base of a cooperation contract between GeoForschungsZentrum Potsdam and Hermanus Magnetic Observatory a new observatory was established at the Keetmanshoop (Namibia) Airport premises. The instrumentation of this new observatory meets the INTERMAGNET standard. The observatory data are intended to be used for more detailed studies of the magnetic field origin in Southern Africa.

The variometer recordings are working continuously and absolute measurements are carried out regularly. The HMO is mainly responsible for preparation of the observatory data. After resolving of starting problems, for example with strange disturbances, it is planned to apply to get IMO (INTERMAGNET observatory) status.

Acknowledgements. The establishment of the new observatory at Keetmanshoop was made possible through financial support from the Hermanus Magnetic Observatory in South Africa as well as the GeoForschungsZentrum in Potsdam, Germany. The cordial supports of the Namibia Airports Company as well as the Geological Survey of Namibia are greatly appreciated.

Accepted March 7, 2007

Replacement of Gnangara (GNA) with a New Observatory at Gingin

Peter CROSTHWAITE, Peter HOPGOOD and Andrew LEWIS

Geoscience Australia
GPO Box 378, Canberra, ACT 2601 Australia
e-mail: Peter.Crosthwaite@ga.gov.au

A b s t r a c t

Geoscience Australia currently operates 9 geomagnetic observatories on the Australian continent, islands, and the Australian Antarctic Territory. One of these, Gnangara Observatory, is located in the south-west of the Australian continent, on the outskirts of the city of Perth. Along with the recent urban encroachment there have been numerous break-ins, incidents of vandalism, and theft of equipment, often leading to significant data losses and expenses. For these security reasons only, a phased replacement of the Gnangara Observatory by a new observatory at Gingin, 52 km north of Gnangara, is being planned.

1. History of Geomagnetic Observations in South-West Australia

Regular monitoring of the geomagnetic field in the south-west of Australia began when the Carnegie Institution of Washington established an observatory at Watheroo, 162 km north of Gnangara, in 1919. Watheroo was transferred to the Australian Government in 1947. In 1957, the government opened Gnangara, closer to the city of Perth, and after a transition period Watheroo was closed in 1959 (see Figs. 1 and 2).

2. Plans for a New Observatory

Security issues at Gnangara have prompted the search for a site for a new observatory. In recent years, negotiations with the University of Western Australia and the Western Australian Government Department of Conservation and Land Management have been underway to secure a small area of land next to the Australian International Gravity Observatory at Gingin – between Watheroo and Gnangara (116 km south of Watheroo and 52 km north of Gnangara).

Gingin Observatory will comprise

- an Absolute Building containing a single observing pier,
- a buried T-shaped variometer bunker (1 m interior height) capable of housing dual vector variometers with a separation of 7 m, and a scalar variometer,
- an external tripod-observing station,
- and an azimuth pillar.

The building material will be reconstituted limestone. The area is sandy with very low magnetic gradients. The observatory will be networked through the University of Western Australia, and 1-second data will be available in near-real-time as are other Australian observatory data.

Gingin will be instrumented with a Danish Meteorological Institute (DMI) FGE fluxgate-vector-magnetometer and a GEM GSM90 scalar variometer. Absolute instruments will be a DMI fluxgate/Zeiss 020B theodolite magnetometer and a GEM GSM90 scalar magnetometer.

Gnangara will be closed after an overlapping transition period with Gingin.

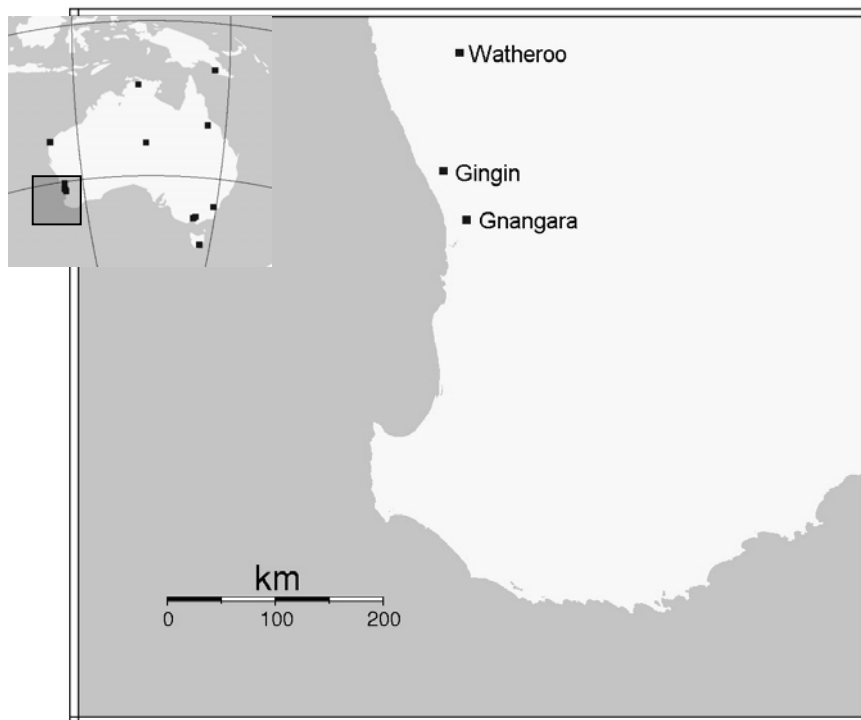


Fig. 1. Location of past, present, and future observatories in south-west Australia.

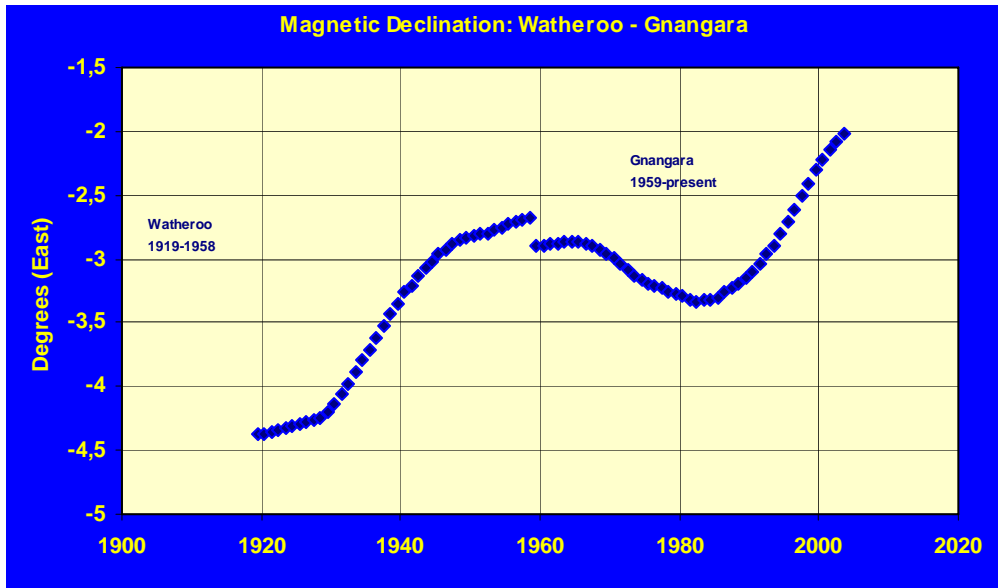


Fig. 2. Declination time-series from south-west Australia.

Accepted February 15, 2007

GAUSS: Geomagnetic Automated System

Hans Ulrich AUSTER¹, Mioara MANDEA², Anne HEMSHORN¹,
Monika KORTE² and Eberhard PULZ²

¹Institut für Geophysik und extraterrestrische Physik, TU Braunschweig
Mendelssohnstrasse 3, 38106 Braunschweig, Germany
e-mail: uli.auster@tu-bs.de

²GeoForschungsZentrum Potsdam
Telegrafenberg, 14473 Potsdam, Germany
e-mail: mioara@gfz-potsdam.de

Abstract

During the XIIth IAGA workshop on geomagnetic observatory instruments in Belsk we presented an instrument measuring the geomagnetic field automatically and absolutely, which was developed by Technical University Braunschweig and GeoForschungsZentrum Potsdam. This paper deals with the instrument basics, the design of the prototype and the measurement results obtained in Belsk. The method is based on the rotation of a three-component fluxgate magnetometer about precisely monitored axes without using a non-magnetic theodolite. This method is particularly qualified for automation because it only requires exact knowledge of the axes orientations. Apart from this, requirements on mechanical precision are moderate.

1. Introduction

Fully automated geomagnetic observatories, which do not require manual operation of any instruments, are necessary to fill the gaps in the global network in remote areas, where access and presence of trained personnel are a problem. Here, we present a device which can perform discrete absolute measurements automatically and thus may replace the DI-flux theodolite in geomagnetic observatories. This does not remedy the need for separate variation and absolute measurements, but all the data can be recorded automatically and transferred to another location for processing. Attempts to automate a DI-theodolite (van Loo and Rasson 2007, this volume) and a proton vector magnetometer (Auster *et al.* 2007, this volume) for discrete absolute measurements are pursued by other groups. Our approach is based on the method of rotating a three-

axis fluxgate magnetometer about a defined axis, in order to determine the field component along that axis (Auster and Auster 2003). The method, outlined in section 2, has been tested with a manually operated prototype instrument for the past 2 years at the Niemegek observatory (Pulz *et al.* 2004). In section 3 we describe the solutions we found for automation of the manual operation steps. Setup in Belsk, steps of data processing as well as measurement results obtained during the workshop are given in Sections 4 and 5.

2. Basics of Applied Method of Absolute Measurement

We take advantage of a new method to determine the absolute magnetic field components by using a three axis fluxgate magnetometer which is turned around a well-defined axis (see Fig. 1). If measurements are taken at three positions the field strength in the direction of the axis can be calculated by Eq. (1).

$$B_{axis-z} \begin{pmatrix} 1 \\ 1 \\ 1 \end{pmatrix} = \begin{bmatrix} B_{mx1} & B_{my1} & B_{mz1} \\ B_{mx2} & B_{my2} & B_{mz2} \\ B_{mx3} & B_{my3} & B_{mz3} \end{bmatrix} \begin{pmatrix} \sin(\varphi) \sin(v) \\ \cos(\varphi) \sin(v) \\ \cos(v) \end{pmatrix} = \mathbf{M}_m \mathbf{n}(\varphi, v). \quad (1)$$

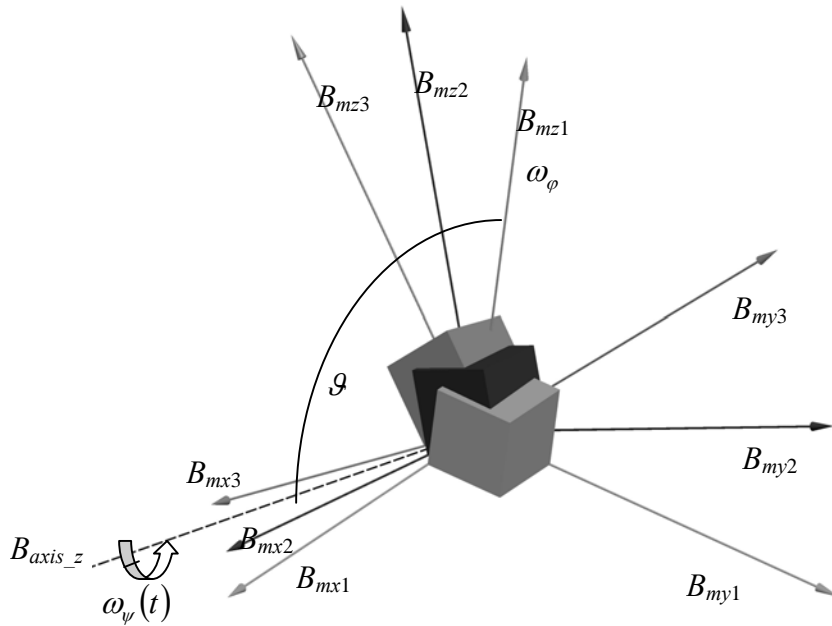


Fig. 1. We have to consider two coordinate systems, the magnetometer system B_m and the reference system B_{axis} which are related by Euler transformation about the angles (φ, θ, ψ) . If the arbitrarily oriented three axes (x, y, z) fluxgate magnetometer is rotated by three angles ψ_1, ψ_2, ψ_3 , the magnetic field B_{axis-z} along the rotation axis can be determined from the values B_{mx1} to B_{mz3} .

Due to the fact that $\mathbf{n}(\varphi, \vartheta)$ is a unity vector, the field magnitude in direction of the rotation axis can be derived by a set of three measurements completely independently from sensor orientation and rotation angle, see Eq. (2).

$$|B_{axis_z}| = Det[\mathbf{B}_m] \left(\begin{array}{l} \left(B_{mx3}(B_{my2} - B_{my1}) + B_{mx2}(B_{my1} - B_{my3}) + B_{mx1}(B_{my3} - B_{my2}) \right)^2 \\ \left(+B_{mx3}(B_{mz2} - B_{mz1}) + B_{mx2}(B_{mz1} - B_{mz3}) + B_{mx1}(B_{mz3} - B_{mz2}) \right)^2 \\ \left(+B_{my3}(B_{mz2} - B_{mz1}) + B_{my2}(B_{mz1} - B_{mz3}) + B_{my1}(B_{mz3} - B_{mz2}) \right)^2 \end{array} \right)^{\frac{1}{2}}. \quad (2)$$

Measurements have to be done for two orientations of the rotation axis in order to measure the field vector completely, if additional scalar absolute intensity data are given. Systematic errors have to be eliminated during the measurement procedure to make the measurement method absolute. A scalar calibration of the fluxgate magnetometer is obtained by comparison of proton magnetometer readings with the field magnitude derived from measurements of the fluxgate magnetometer at various orientations with respect to the Earth field vector. To increase the diversity of sensor orientations with respect to the geomagnetic field for calibration purposes and to increase the redundancy of measurements, the procedure should be repeated after a 90° rotation of the sensor.

An automation of this method is promising because the precision requirements of mechanical operations are low compared to those of the DI flux method. The rotation of the sensor can be done with arbitrary angles because the field determination along the rotation axes is independent from the sensor orientation. Only the directions of the two rotation axes have to be determined precisely in order to allow for an accurate transformation of the data into a geographical reference frame. In the following section we describe in detail the steps of automation.

3. The Automation

The previous, manually operated system is shown in Fig. 2. The three-component magnetometer is situated in a rotatable basket. Four bearing blocks, in which the basket can be rotated, define the two measurement directions. The bearing blocks have to be leveled by means of a level tube, and one set of bearing block have to be aligned to the azimuth mark using a telescope before measurements can be taken. The absolute measurement itself is performed by rotating the basket in both sets of bearing blocks. Magnetometer readings are taken at various rotation angles. At the same time the total field is measured by a scalar magnetometer. The orientation of the three axes fluxgate sensor inside the basket can be altered for calibration of the measurements by unfastening, turning and fastening of the sensor. With data from all the different orientations, the magnetometer can be fully calibrated and the magnetic field in direction of both rotation axes can be calculated.

To automate the measurements, all the manual operation steps have to be performed by motors, as there are

- the rotation around the measurement axis (axis A),
- the turning of the sensor inside the basket (rotation around axis B),
- the change of orientation of the measurement axis (rotation around axis C).

Moreover, the orientation of the measurement axis with respect to the horizontal plane and a geodetic reference frame shall be measured by a laser-optical system.

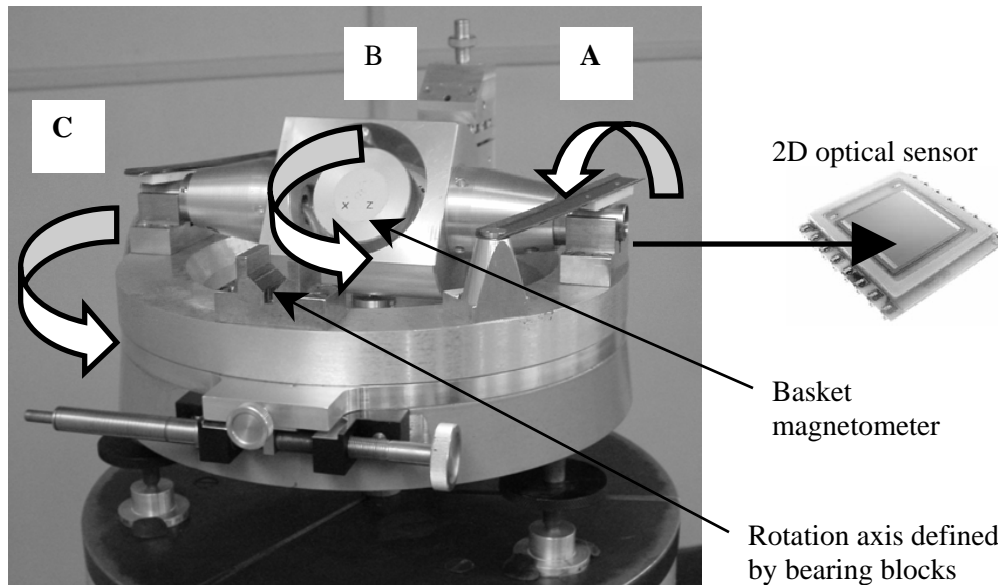


Fig. 2. Instrument which has been operated manually in Niemegek over more than two years. The arrows indicate the three rotations which are necessary to perform the absolute measurement.

All the automated movements have to be achieved without influencing the geomagnetic field. This can be done by non-magnetic motors or by transmission of forces from distant drive units. The only non-magnetic motor solutions we found are based on piezoelectric actuators. Unfortunately the maximum push/pull force of the commercial available piezo motors is with 1N low. Considering gear loss and aging of friction properties a gear reduction of 20 for the sensor rotation (rotation B) and 40 for the basket rotation (rotation A) was realized. The sensor rotation is performed by a gear mechanism inside the basket. To decouple the basket rotation mechanically from the base part an additional weight of 500 g is turned by the piezo motor around the rotation axis of the basket. The weight is accommodated in a distance of 70 mm perpendicular to the rotation axis. The torque is high enough to keep the weight permanently on the bottom side like a ship's keel (see Fig. 4 later in the text). In this way the angular position of the basket can be controlled by rotating the keel versus the rotation axis.

Turning the whole system into a second measurement direction and back requires a rotation around axis C in Fig. 2. Therefore the system is placed on a turn-table. Although the requirement on absolute accuracy of the adjustment of the measurement

axes is relaxed by the measurement range of the optical system, the requirement on stability during one measurement sequence is extremely high. Consequently the table has to be firmly locked in well defined end positions to keep the measurement axis steady during the rotation of sensor and basket. This is achieved by locking the rotating part of the table by means of a ball, which is pressed in a notch of the steady part of the table by a vertically mounted spring. Both, the force to rotate the table and the force to bring the system into and out of the locking mechanism have to be considered for estimating the necessary drive torque. Due to the high torque requirements of the turn-table we investigated pneumatic and hydraulic solutions for this rotation. Our current solution, based on a pneumatic drive unit, is shown in Fig. 3.

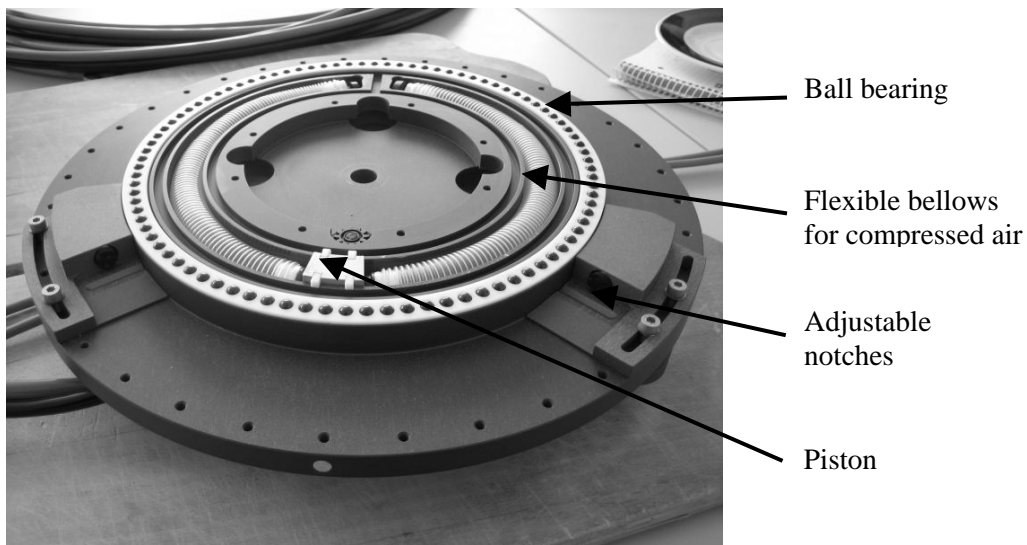


Fig. 3. Steady part of the turn table. The tappet is moved by switching compressed air alternating into the left or right tube. The rotatable part is pushed by the piston into its end positions defined by the notches.

The orientation of the measurement axes has to be known exactly to transform the measured data from the instrument coordinate system into the geographic coordinate system. This can be achieved by a laser beam and optical sensors mounted to known azimuth marks. The optical axis has to be installed inside the rotating basket to determine the direction of the measurement axis. We used a distantly placed laser coupled in by glass fiber. The glass fiber has to be equipped with an optics which focuses the laser beam at the position of the optical sensor. Several 2D optical sensors have been tested for applicability. The dimensions of the optical array should be as large as possible, the data processing simple and the costs reasonable. Finally PSD (Position Sensing Detector) sensors with a sensitive area of 20×20 mm were selected. The measurement axis of the instrument now only has to be oriented within an accuracy given by the dimensions of the optical sensor.

To keep the laser spot within the measured and modeled PSD range we accept a displacement of 10 mm for the adjustment of measurement axis and a deviation of the

laser axis from the rotation axis which results in a circle diameter of also 10 mm. This corresponds to a maximum misalignment error of 2 arcmin in a PSD distance of less than 20 m. Note again that this is the only alignment requirement we have on all three mechanical manipulations.

The geographical reference system, given by the PSD mounting, has to guarantee the full accuracy of 4 arc seconds (0.4 mm in a distance of 20 m). Both, tilting and expansion in vertical direction have to be avoided. With a pillar of two meters height and a temperature gradient of $10^{\circ}\text{C} \pm 20^{\circ}\text{C}$ per year for central Europe we need a pillar material with a linear expansion coefficient of $1 \text{ ppm}/^{\circ}\text{C}$. Fused silica rollers with an thermal expansion coefficient of $0.5 - 0.9 \text{ ppm}/^{\circ}\text{C}$ are selected for the PSD mounting.

A more detailed description of the automation approach is given by Auster *et al.* (2007).

4. Setup in Belsk

Figure 4 shows the turn-table with basket, basket magnetometer and laser optics. A proton magnetometer (see Fig. 5, left) is necessary for calibration and to provide the third vector component. Two PSDs are mounted on pillars in a distance of about 15 m (one is visible in the background of Fig. 5 left). The automatic instrument performs discrete measurements, so this setup has to be complemented by a fluxgate variometer continuously recording the field variations (see Fig. 5, right). All instruments have separate control electronics and a GPS receiver for the exact time signal completes the

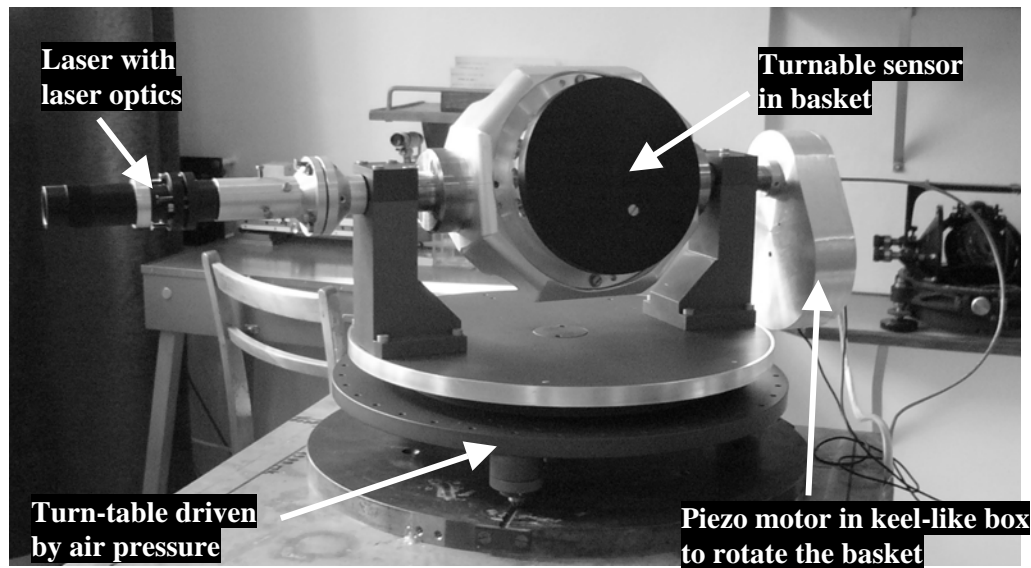


Fig. 4. The automatic absolute instrument with basket, basket magnetometer and laser optics on the turn-table.

setup. To avoid interferences between the single elements, each of them was checked for its magnetic properties. Sources of self-generated magnetic fields are the polarization field of the proton magnetometer, the feedback field of the fluxgate magnetometers and remanent fields of electronics and mechanical parts. The circles in the setup drawing (Fig. 6) indicate the necessary clearance to guarantee disturbances of less than 0.2 nT.

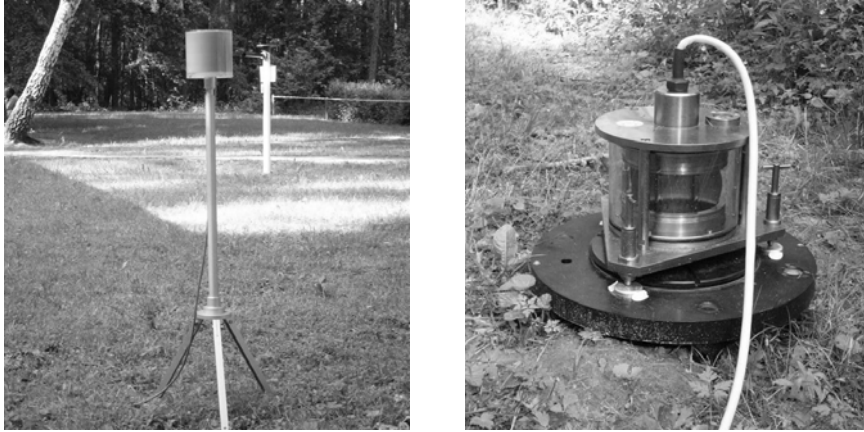


Fig. 5. Proton magnetometer for calibration and determination of third vector component (left panel), three component fluxgate magnetometer for reduction of variation (right panel). The resolution of both magnetometers is 10 pT. Both are provided by Magson GmbH.

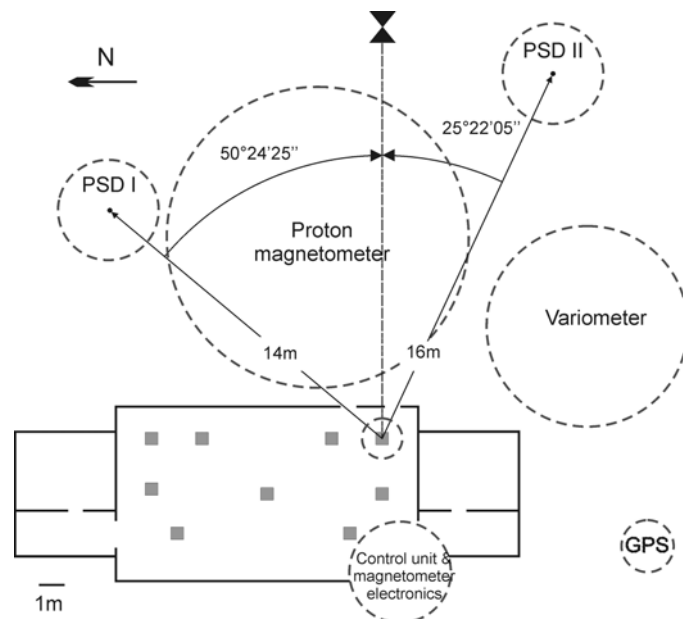


Fig. 6. Setup of all components of the automated observatory in and around the absolute house in Belsk, circles mark the necessary distances around each component to avoid interferences and disturbances.

First, all three rotation parts are brought in their initial positions. To avoid mechanical end stops and to compensate for unequal backwards and forwards velocity of the piezo motor, the sensor and basket rotation are controlled by the magnetic field vector measured by the basket magnetometer. Mean magnetic main field components for the location can be used for orientation control because a rough adjustment is sufficient. The basket is rotated in approximately 60° steps forward and backward in each of the four possible combinations, PSD I & II, sensor orientation I & II. At every stop position, measurements are taken for all three basket magnetometer components and the analogue voltages of the PSD outputs are digitized. The raw data from all 24 values per direction together with simultaneous readings from the additional variometer and proton magnetometer are the basis for the data processing.

The first step of data processing is the calibration of the basket magnetometer. Assuming a linear transfer function between field and magnetometer output, the rotation of the sensor about two axes is sufficient to perform a scalar calibration (Auster *et al.* 2002). The field magnitude on top of the pillar is known from absolute proton magnetometer readings reduced by the previously determined, constant field difference between location of the proton magnetometer sensor and measurement pillar. Thus we can fit each of the magnitudes derived by the basket magnetometer to the true scalar field value. Nine parameters are determined. Measurement results show that the three angles of non-orthogonality are constant within the measurement accuracy of 10^{-6} . The offset stability was better than 0.5 nT during the measurement campaign in Belsk which corresponds to the offset stability of better than 1 nT/year specified in Niemegek before. The scale values depend strongly on the thermal expansion coefficient of copper (about 20 ppm/ $^\circ\text{C}$). These results are in accordance with the properties we expect from a vector compensated fluxgate sensor which was designed for a large temperature range, especially for space applications.

An absolute measurement with the automated system takes up to half an hour, similar to the DI-Flux procedure. Consequently, field variations during this period cannot be neglected and all individual data have to be reduced to the same time, e.g. the beginning of the measurement. Thus, the variometer measurements have to be transformed into the coordinate system of the basket magnetometer, in order to reduce the field measured by the basket magnetometer. The calculation of the field in axis direction can subsequently be repeated by Eq. (1).

Finally, the direction of the measurement axis has to be determined. The crosses in Fig. 7 represent the typical output from the laser beam position (x_i, y_i) on the PSD. The axis direction (x_0, y_0) is determined by the center of a circle fitted to the measurement values. In a distance of 10-15 m (PSD I) a typical displacement error is about 0.05 mm. This corresponds to an angle error of 1 arcsec which is also clearly less than the design goal of 4 arcsec.

5. Results of Belsk Measurement and Outlook

The instrument was operated automatically during the workshop in Belsk. Measurement results compared with the observatory data are plotted in Fig. 8. Measure-

ments (two per hour) were done during the Friday lecture fully automatically. The standard deviation of the difference between the measurements with the automated system and the Belsk observatory data are 1.9 nT in the X-component, 1.3 nT in the Y-component and 0.7 nT in the Z-component.

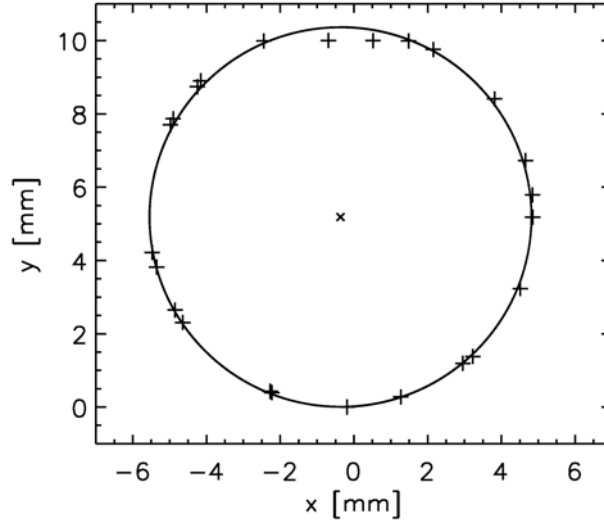


Fig. 7. Laser beam position on the PSD at each measurement of the basket magnetometer (crosses). The measurement axis orientation is determined by fitting a circle to the readings. The center [$x_0 = -0.36$, $y_0 = 5.18$] indicates the axis direction, the radius specifies the misalignment between rotation axis and axis of the laser beam.

These results and the error estimations show that the automated system can provide data well within the accuracy requirements for geomagnetic observatories, and comparable to carefully performed DI-Flux measurements. The automation of absolute measurements has several advantages. Fully automated observatories can be set up at remote locations, where frequent access or the presence of trained personnel can be problematic. The quality of the measurements becomes independent from the qualification of the personnel. Absolute measurements can be performed more frequently, relaxing the requirements on stability of variometers. A very detailed description of instrument development, data processing software and measurements performed in Belsk and Niemegek can be found in Hemshorn (2007).

So far our prototype instrument has been operating fully automatically for short time intervals only. The next step will be to prove the instrument robustness for unattended long term measurements at Niemegek Observatory.

The current instrument design is suitable for use at mid and high latitudes, but not for low latitudes because the measurement axes should be not parallel to the total force. A future task will be to develop a re-designed version of the device for use at low latitudes.

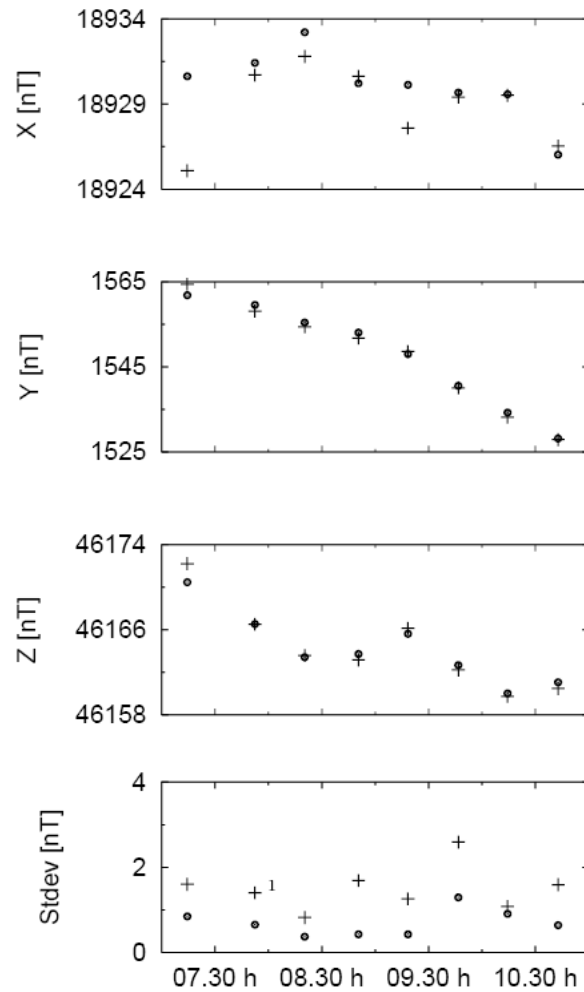


Fig. 8. X, Y and Z components measured by the automated system (dots) and values of Belsk observatory (crosses) are plotted in the upper three panels. In the bottom panel the standard deviation of redundant measurements before (crosses) and after (dots) variation reduction are shown. The values before variation reduction give us an estimate about the field variations during the measurement. After variation reduction the standard deviation provides an uncertainty estimate on the final result.

Acknowledgements. For the design and manufacturing of the mechanics we thank Carsten Müller, Bernd Chares, Markus Thiel, Roland Paul, Jörg Wummel, Bernd Stoll and Katrin Gebauer. For providing the excellent magnetometers and for software development and hardware installation many thanks to Volker Auster, Olaf Hillenmaier, Ronald Kroth, Markus Wiedemann and Edita Georgescu. Finally we wish to thank Anne Neska, Jan Reda and colleagues for support in the Geomagnetic Observatory Belsk.

References:

- Auster, H.U., K.H. Fornacon, E. Georgescu, K.H. Glassmeier and U. Motschmann, 2002, *Calibration of fluxgate magnetometers using relative motion*, Meas. Sci. Technol. **13**, 1124-1131.
- Auster, H.U., and V. Auster, 2003, *A new method for performing an absolute measurement of the geomagnetic field*, Meas. Sci. Technol. **14**, 1013-1017.
- Auster, V., O. Hillenmaier, R. Kroth and M. Wiedemann, 2007, *Advanced Proton Magnetometer Design and its Application for Absolute Measurement*. **In:** "Proceedings of XIIth IAGA workshop on Geomagnetic Observatory Instruments, Data Acquisition and Processing", Pubs. Inst. Geophys. Pol. Acad. Sc. **C-99 (398)** (this issue).
- Auster, H.U., M. Manda, A. Hemshorn, E. Pulz and M. Korte, 2007, *Automation of Absolute Measurement of the Geomagnetic Field*, submitted to Earth Planet Space.
- Hemshorn, A., 2007, *GAUSS: A Geomagnetic Automated System*, Diploma Thesis, Technical University Braunschweig.
- Pulz, E., H.-U. Auster, M. Korte and H.-J. Linthe, 2004, *Experiences with a New Method for the Absolute Component Determination of the Earth's Magnetic Field*, Journal of Electrical Engineering **55**, 10/S, 53-57.
- Van Loo, S.A., and J.L. Rasson, 2007, *Presentation of the prototype of an automatic DI-Flux*. **In:** "Proceedings of XIIth IAGA workshop on Geomagnetic Observatory Instruments, Data Acquisition and Processing", Pubs. Inst. Geophys. Pol. Acad. Sc. **C-99 (398)**, (this issue).

Accepted February 5, 2007

Advanced Proton Magnetometer Design and its Application for Absolute Measurement

Volker AUSTER, Olaf HILLENMAIER, Ronald KROTH
and Markus WIEDEMANN

Magson GmbH,
Carl-Scheele-Strasse 14, 12489 Berlin, Germany
e-mail: office@magson.de

Abstract

A new processor controlled Proton Magnetometer design and its application for an automated absolute measurement will be presented in this paper. The new design is based on an online signal processing of single period measurements of the sensor signal, aiming to improve the resolution and to valuate the signal quality. Applying a cylindrical coil for auxiliary fields, optimized for high homogeneity, a measurement of the geomagnetic field vector can be realized. To demonstrate the need for homogeneous coils, the relation between the homogeneity of the probe volume and the relaxation of the resulting sensor signal will be shown. In order to perform an absolute measurement, the system is equipped with a telescope, aligned along the coil axis and it can be rotated by a motor about its vertical axis. In contrast to conventional methods, the requirements on manual skills of the observer are quite moderate. Furthermore, an option for full automation is provided.

1. Introduction

Methods of measuring components of the Earth magnetic field by using proton magnetometers have been developed between 1950 and 1970. Bias fields of well known direction and intensity were applied to determine field components. In contrast to the "classical" measuring technique, using a suspended magnet as the sensing element, the bias field in this case cannot be generated by permanent magnets, because they produce a very inhomogeneous magnetic field. Thus, special compensated coil systems are used. Examples of well known coil systems, consisting of some pairs of coaxial rings, are named after Helmholtz, Braunbeck, and Fanselau. Design and dimensions of bias coils and proton sensor have to be balanced between contradictive requirements. On the one hand, the proton sensor signal quality increases with the

sensor volume, and on the other hand, it needs a homogeneous bias field over the whole sensor volume. Typical requirements are an accuracy of 0.1 nT and a measurement range of 20-100 μT , allowing a wide range of bias fields. An overview on methods to measure the geomagnetic field by proton vector magnetometers (PVM) is given by De Vuyst (1973). He also described a stationary PVM, consisting of a Helmholtz coil with a diameter of approximately one meter, which can be turned around its vertical and horizontal axis. Due to the fact that PMV measurements are not affected by offset or scaling errors, only the misalignment between coil axis and nominal measurement axis have to be taken into account in order to determine the field vector absolutely. By rotation about the axis of measurement direction, this alignment error can be eliminated.

A similar device, however of smaller dimensions, has been described already by Serson (1962). The bias coil of his PVM consists of two pairs of coaxial rings with equal diameter. The mechanical system was comparable with that of a “classical” magnetic absolute theodolite. Between 1980 and 1990, a PVM with a special cylindrical bias field coil was developed at Niemegek Observatory (1983). The coil has two layers, which are individually compensated up to the sixth order. The proton sensor itself was designed as a double probe in order to suppress electrodynamic noise. To perform a rotation about the vertical axis for the measurement of D and H , the cylindrical coil was mounted on the top of a non-magnetic ZEISS-theodolite 020B (Fig. 1).



Fig. 1. Absolute measurement at repeat station with a PVM mounted on a non-magnetic theodolite.

In the time period mentioned above, this instrument was applied successfully for absolute measurements at repeat stations and for the geomagnetic survey. Recently, further development of this PVM has been carried out by MAGSON GmbH. The proton magnetometer electronics has been redesigned to improve accuracy and to increase the control and data processing capability as described in Section 2. In Sections 3 and 4 the paper describes the development of a new coil system, which combines bias field coil, sample coil and the optical device (telescope or optoelectronic components) for the geodetic adjustment of the PVM as well as the development of a measurement procedure and a mechanical base to perform absolute measurements of D and H with a high degree of automation.

2. New Proton Magnetometer Design

The PM2005 is a new developed classical proton magnetometer with an internal processor for controlling the signal generation and signal processing. The measurement can either be started manually, by a serial command, or by a trigger signal. The measured field value is displayed on an LCD and stored in a data file on a removable flash RAM card. Additional information as signal quality, selected range, sample counter, date, and time are also stored in the data file. The instrument can be combined with a GPS receiver. The GPS information will be used to synchronize the instrument clock and to estimate the earth magnetic field using the integrated IGFR model which will be used as an initial range selection. Furthermore, the instrument provides features that are used in the component measurement application. So a controlled current source to apply bias fields is included.

The main feature of this device is the implementation of an online regression algorithm applied on results of a period measurement of the sensor output signal. Amplitude and length of each period of the proton AC voltage are measured directly. Circuitries like frequency multipliers are removed. For a number of N consecutive periods of the proton AC signal, each period length p_n with $n = 1 \dots N$ is measured. Instead of calculating the arithmetic mean value, the average period length is derived by using a linear regression algorithm. For each period length p_n the accumulated sum

$$s_n = \sum_{i=1}^n p_i, \quad (n = 1 \dots N) \quad (1)$$

is calculated. Assuming equal period lengths ($p_i = p$, ($i = 1 \dots N$)), s_n can be expressed by the linear equation

$$s_n = p \cdot n + q, \quad (2)$$

where the period length p represents the slope and q the offset of the straight, which is equal to 0 for equal period lengths p_i . For real, unequal period lengths p_i , the coefficients p and q can be determined by using the linear regression algorithm:

$$\frac{\partial}{\partial p}, \frac{\partial}{\partial q} \left(\sum_{n=1}^N \left((p \cdot n + q) - \sum_{i=1}^n p_i \right)^2 \right) = 0. \quad (3)$$

Then, the coefficient p represents an average period length of the proton AC signal.

The regression algorithm takes much more care for the relaxation specific of the proton signal and allows a better suppression of disturbing signals (e.g. 50 Hz) compared to arithmetic averaging of period measurements. The noise could be reduced by a factor of two and the instrument becomes more robust against spatial and temporal field gradients. In Fig. 2, a 24 h registration at the Geomagnetic Observatory Niemegk is plotted, comparing PM2005 and a GEM-System Overhauser magnetometer. The noise of the much simpler proton magnetometer sensor is at least in the same order. The noise of both magnetometers, measured during a magnetically quiet period, is about 0.1 nT RMS. Furthermore, the measurement of the signal amplitude makes always an evaluation of the signal quality possible.

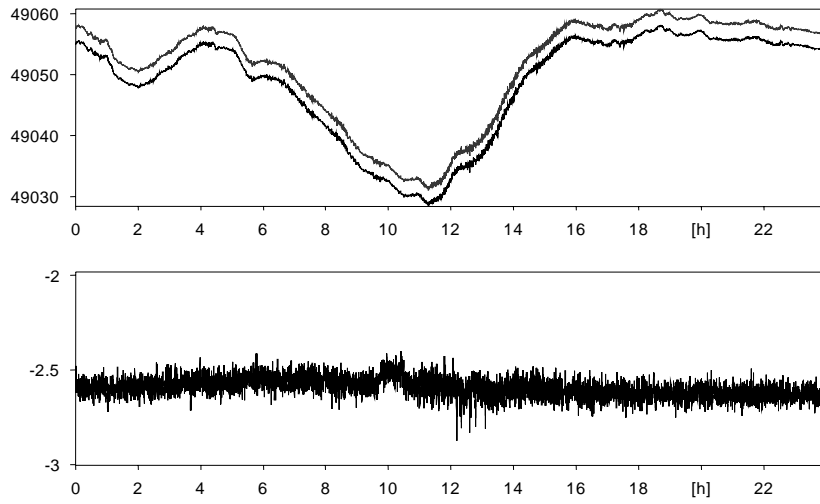


Fig. 2. Comparison of PM2005 (upper recording in upper panel) and GEM-System Overhauser (lower recording in upper panel) and difference between both.

3. Bias Coils

The method of component measurement is based upon the application of bias fields of equal intensity but opposite direction ($+H_b$ and $-H_b$) and measurement of the intensity of the resultant vectors F_+ , F_- , and F_0 (without bias field). The calculated values for the component of the earth magnetic field in the coil axis direction H_a and for the bias field intensity H_b are:

$$H_b = \sqrt{\left(\frac{F_+^2 + F_-^2}{2} - F_0^2\right)}, \quad H_a = \frac{F_+^2 - F_-^2}{4H_b}. \quad (4a, b)$$

The field component in direction of the bias coil axis is independent of bias field intensity, but the inhomogeneity of the bias field over the sensor volume has to be small because the proton sensor signal quality depends on it. To determine the mag-

netic field component absolutely, the direction of the magnetic axis of coil has to be known precisely with respect to a geophysical reference system. Usually coils consisting of several rings (e.g. Helmholtz coils) are used as bias coils. Due to the fact that no access to the proton sensor is necessary, we prefer to apply compensated cylindrical coils which are able to fulfill the requirements on homogeneity and axis alignment much better. The axis of cylindrical coils is well defined because windings are defined by threads which can be inserted precisely by the machine accuracy of a lathe in the carrier material of the coil. Threads with non unique pitches can be used to increase the field homogeneity. To estimate which field gradient ΔH is tolerable, the decay function of the proton magnetometer in dependency on two different angular frequencies ω_1 and ω_2 – related to different field magnitudes – shall be described by the following equation, where T_2 is the relaxation time of the proton signal.

$$A(t) = A_0 e^{-\frac{t}{T_2}} (\sin \omega_1 t + \sin \omega_2 t). \quad (5)$$

Introducing the averaged angular frequency ω and the difference angular frequency Ω which is proportional to the product of field gradient and gyromagnetic ratio γ_H for hydrogen

$$\omega = \frac{\omega_1 + \omega_2}{2}, \quad \Omega = \frac{\omega_1 - \omega_2}{2} = \pi \Delta f = \pi \Delta H \gamma_H, \quad (6a, b)$$

we get the following equation for the proton signal:

$$A(t) = A_0 e^{-\frac{t}{T_2}} \cos(\Omega t) \sin(\omega t) = A e^{-\frac{t}{T_2}} \cos(\pi \Delta H \gamma_H t) \sin(\omega t). \quad (7)$$

In Fig. 3 the proton signal is drawn for field gradients between 0 and 10 nT. Assuming that the frequency measurement is reliable until $A_0/2$, the measurement time decreases from 1 s under undisturbed conditions to 0.3 s in case of a 10 nT field gradient. Thus we need a bias coil which ensures a field gradient of less than 1 nT for typical bias fields of 32,000 nT. This corresponds with a homogeneity requirement of better 3×10^{-5} over the probe volume.

A two cylindrical coils approach for optimizing the field homogeneity leads us to a coil with different pitches at central and outer region. Details about the coil dimensioning can be found in the formulary of the Magson homepage (<http://www.magson.de>). To avoid the influence of the screwing character of winding, a second coaxial and concentric coil, calculated in the same way as the first one, is wound anticlockwise. This double layer design has the advantage, that connector pins are located at the same side which allows a supply via a twisted pair harness. In Fig. 4 the homogeneity of a compensated cylindrical coil is compared with the homogeneity of a Helmholtz coil with identical diameter. The volume of homogeneity better than 10^{-5} of the compensated cylindrical coil exceeds that of the Helmholtz coil at least by a factor of 64 (factor of 4 in each dimension). The homogeneity is good enough up to a distance of 1/3 of the coil radius from the center. Using a cubic probe with an edge length of 4 cm, we need a bias coil with a diameter of 12 cm. An adequate Helmholtz coil has a diameter of half a meter.

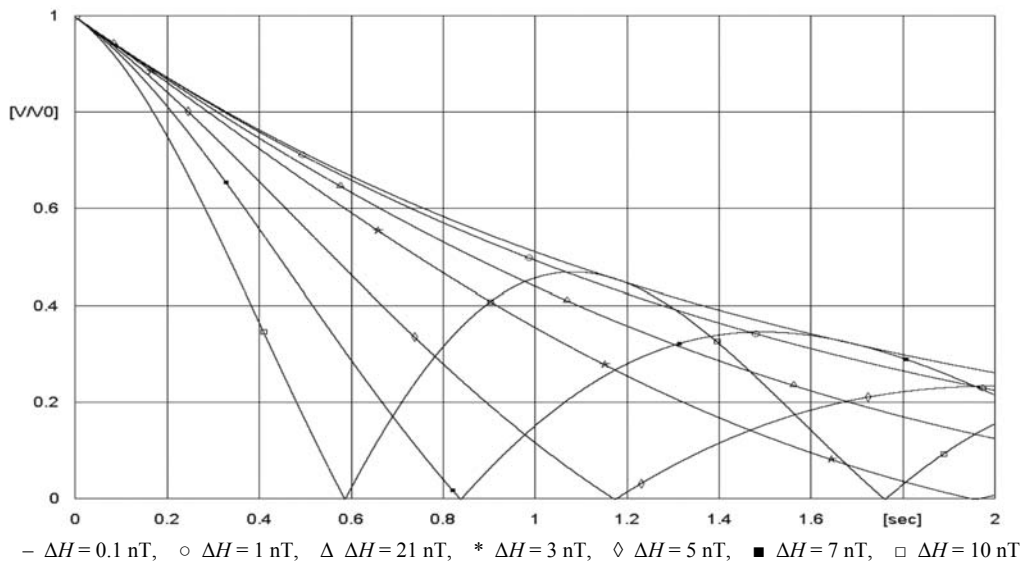


Fig. 3. Relaxation behaviour for field gradients $\Delta H = 0.1 \text{ nT}$, 1 nT , 2 nT , 3 nT , 5 nT , 7 nT and 10 nT over the probe volume. Parameters: $T_2 = 1.5 \text{ s}$ (water sample), $\gamma = 0.042576 \text{ Hz/nT}$.

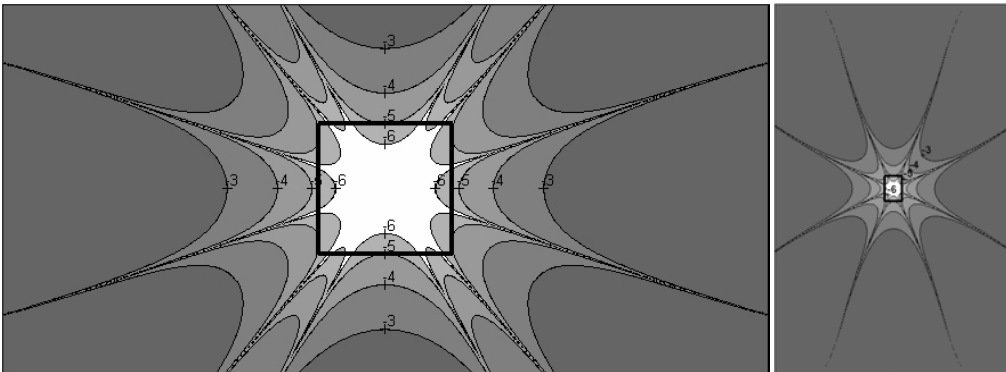


Fig. 4. Relative difference between nominal field and induced field for a compensated cylindrical coil (left side) and a Helmholtz coil (right side). For both coils equal diameters are assumed. The region of homogeneity better than 10^{-5} is marked by squares. The scaling is given in exponents to the base of 10.

4. Usage for Absolute Measurement and Automation Approach

The geographic reference system is defined by the vertical direction and an azimuth mark. To measure an earth magnetic field component correspondingly to this reference system, we accommodate a special proton magnetometer sensor, consisting of four single coils and two samples, which allow integrating a telescope inside our proved compensated cylindrical bias field coil. To determine the deviation of this mechanical axis with respect to the magnetic axis and furthermore to adjust the cross

wires of the telescope, the bias coil can be rotated about its mechanical axis. On one end of the coil a non-magnetic ocular (focal length 10 mm) is placed, on the other end a lens (focal length 230 mm) is located (see Fig. 5). For the automatic version of the PVM the ocular has been replaced by a CCD circuit with a suitable alignment mechanism.

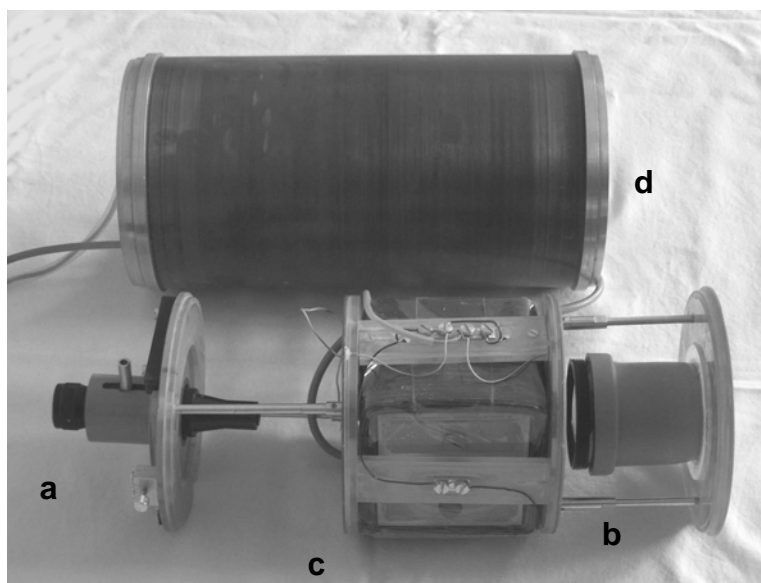


Fig. 5. Disassembled proton magnetometer sensor: Non-magnetic ocular (a), lens (b) and the probe with coils and samples (c) will be mounted inside the bias coil (d).

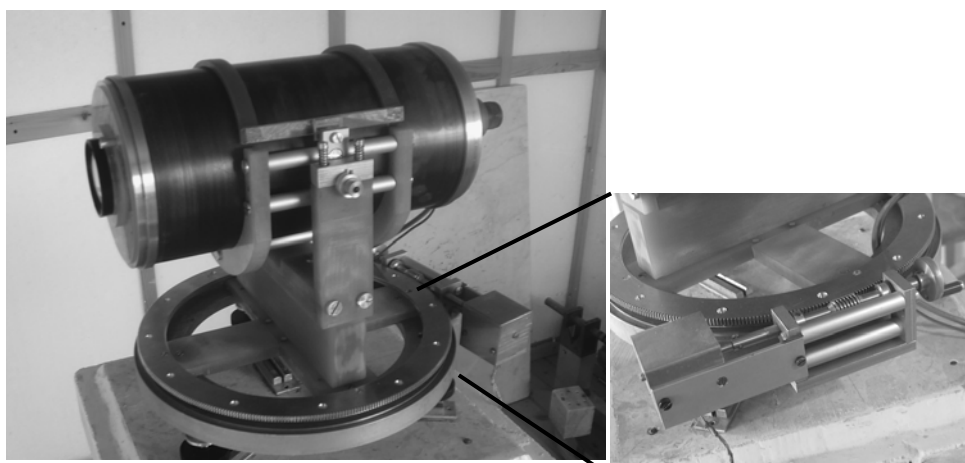


Fig. 6. The prototype of the PVM used for a (semi) automated absolute measurement. The system can be rotated manually by a hand crank or automatically by a step motor.

To measure the field vector completely, the bias coil is mounted on a rotation table with a diameter of 270 mm and a ring gear on its periphery (360 teeth). The alignment error between the rotation axis of the table and the vertical axis is monitored by

an electronic inclinometer. A self blocking drive unit for the rotation table is realized by a worm gear engaging with a ring gear. The rotation table can be rotated either manually or by a step motor. In the manually operated system, the worm gear axle is connected to a hand crank (see Fig. 6). In this case the rotation angle α (versus geographic north) is measured by an incremental counter. The resolution is 500 pulses per revolution of the worm gear axle which corresponds to an accuracy of 0.12 arcmin. The magnetic field at the rotation angle α can be expressed as a function of declination D , horizontal force H , vertical field component Z and the tilt angle versus horizontal plane γ .

$$H(\alpha) = H \cos(\alpha + D) \cos(\gamma) + Z \sin(\gamma). \quad (8)$$

In the first step the system is set either by observer and telescope or automatically by an optoelectronic device into the direction α_0 of a well known target. From this position, n single measurements are started with the angular distance of $\Delta\alpha$.

$$\Delta\alpha = \frac{360^\circ}{n}, \quad \alpha_n = \alpha_0, \alpha_0 + \Delta\alpha, \alpha_0 + 2\Delta\alpha, \dots, \alpha_0 + (n-1)\Delta\alpha. \quad (9)$$

For each measurement direction the proton magnetometer measurement range for positive and negative bias fields can be determined using approximate values for D , H and F and a suitable bias field H_b by the following equation:

$$F_{\pm} = \sqrt{Z^2 + H_b^2 + H^2 \pm 2H_b H \cos(\alpha_n + D)}. \quad (10)$$

$H(\alpha)$ will be calculated by Eq. 4 for all set angles α . After reduction of the variation we perform a harmonic analysis:

$$H(\alpha) = A_0 + A_1 \cos(\alpha) + A_2 \sin(\alpha) \quad (11)$$

with

$$A_0 = \frac{1}{n} \sum_n H(\alpha_n), \quad (12a)$$

$$A_1 = \frac{2}{n} \sum_n H(\alpha_n) \cos(\alpha_n), \quad (12b)$$

$$A_2 = \frac{2}{n} \sum_n H(\alpha_n) \sin(\alpha_n). \quad (12c)$$

Using amplitude and phase we can rewrite Eq. 11:

$$H(\alpha) = A_0 + A \cos(\alpha + \varphi) \quad (13)$$

with

$$A = \sqrt{A_1^2 + A_2^2} \quad \text{and} \quad \varphi = \arctg\left(\frac{A_2}{A_1}\right). \quad (14a, b)$$

Note, that the arctg function is multivalued with $\pm k\pi$ ($k = 0, 1, \dots$).

If we compare the coefficients of Eq. 8 and Eq. 13 now, we get:

$$Z \sin \gamma = A_0, \quad H \cos \gamma = A, \quad D = \varphi. \quad (15a, b, c)$$

With an iteration procedure

$$H_1 = A \left(1 - \frac{A_0^2}{F^2 - A^2} \right)^{-0.5}, \quad H_n = A \left(1 - \frac{A_0^2}{F^2 - H_{n-1}^2} \right)^{-0.5}, \quad (16)$$

we get finally the horizontal force $H = H_n$. For tilt angles less than 20° , $n = 6$ iteration steps are sufficient to suppress the error below a 0.1 nT threshold.

5. Summary and Outlook

A new designed proton magnetometer equipped with a compensated cylindrical bias coil has been used for absolute measurement of the Earth's field components. Advantages of the signal processing based on a regression algorithm, influence of field gradients on the proton magnetometer signal, high homogeneity of the compensated bias coil as well as the algorithm for components determination by rotation of the PVM are presented. Steps of automation are already done and will be object of further developments.

Acknowledgements. Many thanks to our Polish colleagues for the well organized workshop.

References

- De Vuyst, A.P., 1973, *Proton and Proton Vector Magnetometers*, IAGA Scientific Session, Commission I, Kyoto, Institut Royal Meteorologique de Belgique, Miscellanea Serie C, n° 7.
- Serson, P.H., 1962, *Method of Making an Electromagnetic Measurement*, Canadian Patent No.654.552, issued Dec. 25, Class 324-1.
- Auster, V., and R. Winkler, 1985, *Kernresonanzmagnetometrische Einrichtung zur absoluten Messung des erdmagnetischen Feldvektors*, Patentschrift DD 290 119 A7, Berlin, issued Dec. 04.

Accepted February 27, 2007

New Concepts in Geomagnetic Observatories Operation

Jean L. RASSON and Sebastien van LOO

Royal Meteorological Institute of Belgium
Centre de Physique du Globe, DOURBES, B-5670 Viroinval
e-mail: jr@oma.be

A b s t r a c t

Using the IAGA definition of a geomagnetic observatory and a wish list from geomagnetic data users, we look into new ways to fulfill these requirements using the new developments in absolute and variometric instrumentation. We try to project how future observatories will look like, especially considering the new automatic instruments which will soon be forthcoming.

1. Introduction

When looking for innovative ideas for Geomagnetic Observatories (GO), it is of course useful to ask the question: what is wanted from magnetic observatories? Part of the answer is to be delivered by the GO's data users and another part is to be found in the IAGA definition of a GO: "A Geomagnetic Observatory is a place where the geomagnetic vector has been observed for an extended period of time".

"Extended" in this context means at least one year, so that annual means of three independent components of the geomagnetic vector can be computed. Therefore one of the most important requirements for a GO is its ability to operate in the long term. Whereas this goal has been attained in many GO's, others have had trouble in maintaining the observations over an extended portion of time. It is therefore a logical way to go to investigate how this long life can be attained.

The IAGA mention of "place" in the GO definition has its importance too: it is to be chosen so that the GO's are evenly distributed on the globe. Some innovative concepts to solve this problem should be found based on new automated equipment and a rational approach in the collaboration with host countries where observatories are in need.

Additionally, it is clear that the user wants observations of good quality, without gaps in the time series. How can we innovatively attack the problem?

Last and independently of the IAGA definition, there is nowadays a user base interested in data sampled faster, up to 1/s.

2. User Driven new Geomagnetic Observatory Concepts

INTERMAGNET decided in 2003 at its Dourbes meeting to create a new recording standard based on a 1 second means data acquisition. The first requirements for such a geomagnetic data acquisition system were compiled during an INTERMAGNET survey investigating the needs of the scientific community using geomagnetic time series data (Love 2006). They are given in Table 1.

From the survey it appears that a timing accuracy of 0.01 s is required, so that a GPS or equivalent timing method must be used. The amplitude and phase response of the magnetometer must be carefully shaped and checked. The resolution should be not less than 0.01 nT. This list of requirements probably means that 1-minute means INTERMAGNET data acquisition systems cannot fit them: 16 bits ADC's have simply not the dynamic range. On the other hand, the 0.01 nT noise applies not only to the instrumentation but also to the site noise. This means that the deployment of 1 s INTERMAGNET systems is worth the effort only in GO sporting very low noise magnetic characteristics.

Some new prototype instruments are being developed right now for a sampling at 1 Hz. See the article "New INTERMAGNET Fluxgate Magnetometer" by Korepanov *et al.* in this issue for the first realization of a fast sampling variometer according to standards set by INTERMAGNET.

Table 1
1-second INTERMAGNET standards: results of survey

| User | Data Resol [nT] | Data Accuracy | Filter Preferences | Time Accuracy | Time Position |
|-------------|-----------------|---------------|--------------------|---------------|--------------------|
| Chulliat | 0.001 | NA | Gaussian digital | 0.001 s | Centered on UT sec |
| Engebretson | 0.1 | NA | | 0.1 s | Centered on UT sec |
| Fraser | 0.1 | NA | Uniform phase | GPS | No preference |
| McPherron | 0.01 | | Good phase | 0.001 s | |
| Hughes | 0.01-0.003 | NA | Digital is ideal | 0.05 s | Centered on UT sec |
| Moldwin | 0.1 | NA | | 0.001 s | Centered on UT sec |
| Masahito | > 0.1 | | | 0.1-0.01 s | |
| Waterman | 0.01 | NA | Digital | 0.1-0.05 s | Centered on UT sec |
| Consensus | 0.01 | NA | Digital | 0.01 s | Centered on UT sec |

3. Data Quality

But fast data acquisition is not the only way for innovation. The quality of the recorded data is a primary concern for the observer and user. Good data is obtained

through the agency of various factors like: low noise as produced by the instrument or the site environment, adequately monitored baseline changes, accurate timing, the absence of gaps in the time series, the absence of spikes, etc. Another item concerning data quality is global coverage. An observatory which fills a gap in the global coverage is improving the representation one can make of the geomagnetic field and is therefore decreasing the “noise” in the field picture. A good time series should also be available in the long term. Finally, nowadays good data also means that it should be rapidly and easily accessible.

4. New Concepts for Improving Observatories and Their Data

New concepts must try to find ways to improve:

- The global distribution of GO’s by looking into possibilities to provide more observatories where they are scarce: in developing countries and oceanic areas
- Promotion of long term operations by making GO’s more affordable. Therefore we must look into ways to provide operation with low cost in manpower, maintenance and processing. The setup of GO’s with low sensitivity to cultural and industrial development and well protected against vandalism will also enhance the durability of a GO.

4.1 Global distribution: Focus on developing countries (DC)

It is important to realize that DC’s often provide very low noise sites (important for fast sampled data). Therefore, helping DC’s to improve and install geomagnetic observatories often leads to win-win situations: the target country will have good data, leading to better services to the socio-economic community (safe navigation using magnetic compass), while the worldwide scientific community will benefit from better global coverage and lower noise data. Training of observatory staff may also contribute to a reduction in the digital divide.

Experience and past failures have shown the importance of receiving full collaboration from the on site staff, and that careful planning is a must, even if it is sometimes difficult. As a rule we should try to maximize the use of existing infrastructure, especially real estate. In order to provide the normally expensive observatory equipment, older equipment, accurate but deemed obsolete can be refurbished, recalibrated and usefully redeployed without large funding. In general, there is no need to automate too much the observation procedures, as staff are often numerous.

4.2 Global distribution: Need for automatic observatories

As one of the main concerns is the installation of new observatories where they are missing, it will be necessary to automate GO’s so as to: permit operation in hardly accessible places, to reduce costs and to improve accuracy where qualified human observers are not forthcoming.

5. Different Approaches for Obtaining Automation of Observatories

5.1 *Precise variometer set-up*

Setting-up of a very precise variometer is an obvious approach to automate. An absolute measurement (non-automated) close to this variometer will determine once and for all (or very infrequently) its baselines and orientation.

By “very precise” we mean that the scale factor is known at the 0.1% or better level and that the orthogonality is OK or can be corrected for. We mean also that it is stable so that the long term drift is nil or linear, that it is temperature-insensitive and that the variometer is maintained in a fixed orientation (stable pillars). Last, the variometer should be installed in a clean geomagnetic environment.

There is a flaw however: there is no way to check if the baseline and orientation remains constant otherwise than by doing an absolute measurement.

An automatic observatory along these lines could be successful for careful installations of precise full-field variometers for which a correction matrix is known in a well protected environment and with baseline checks every year.

5.2 *Automate DIflux*

The idea is to robotize the full absolute measurement protocol: automate DIflux and Modulus measurements. A nearby variometer runs in parallel, also in automatic mode. Modulus automatic measurements are already a reality. DIflux measurements are hard to implement in an automatic way because of the following difficult tasks:

- realize nonmagnetic robotic action for moving the fluxgate over 360° around both vertical and horizontal axes as well as fine positioning in any orientation,
- realize non-magnetic digital angle measurement,
- realize automatic target sightings or equivalent.

Early attempts to automate the DIflux in our lab started in the late 1980'ies with the design of several prototypes: The first proto used a motorized custom theodolite with digital encoders and with removable telescope. This early device allowed to validate the idea and to establish that a basic accuracy at the 3 second of arc level or better was possible. A second prototype was built in the 1990'ies: it was a modified nonmagnetic Ruska theodolite with digital encoders but was not motorized. This device was demonstrated in the Uppsala IAGA assembly in 1997 and participated in the geomagnetic instrument intercomparison workshop in Huancayo, Peru (Veliz Castillo and Rasson 1998). Both those instruments allowed the Automatic DIflux concept to mature and the motto became: keep it simple! Therefore, the following concepts were introduced:

- Realization that the telescope can be removed altogether;
- Use laser instead of telescope. Magnetic parts in laser would have no effect on accuracy (Gilbert and Rasson 1998);
- Alternatively, a sunshot can be performed also in automatic mode using a simple sensitive optical device using a split photoelectric cell. This does

away with the need for a far away target. Using this automatic device and a reduction using UT1 instead of UTC allows an accuracy of the azimuth determination by sunshot at the level of 1 second of arc or better;

- Use of piezoelectric motors (with high quality ceramic bearings). They have no noticeable magnetic signature in the idle or rotating state. Moreover, they have an high holding torque when idle;
- The rotating load is so small that the motor bearings double as theodolite axis bearings;
- Dual encoders at 180° ensure high angular accuracy.

In the early 2000'ies, work on a third prototype was initiated along those new concepts. A working model has been presented in this workshop in the absolute house of Belsk observatory. Please refer to the paper "Presentation of the Prototype of an Automated DIFlux" by van Loo and Rasson in this volume for technical details on this device.

6. Designing the Future Geomagnetic Observatories

6.1 *Future GO's should be built to last*

The future design of magnetic observatories, as they are to last for the longest possible time, should therefore take into account:

- avoidance of cultural noise, present and future:
 - Direct field perturbations like those caused by magnetic objects (cars on nearby road, effect of magnets in appliances),
 - Ground current effects. DC ground currents are able to travel on long distances and the effects are extremely difficult to foresee and to protect against. They are surely associated with railway lines, faulty mains connections and power stations.
- Limited funding available. The interruption of the GO funding is a frequent reason for stopping the operation of an observatory. Therefore, low operation costs are a basic way to maintain long term funding.
- Possibility of vandalism, robbery. As the future GO may very well be an unattended estate, the possibilities of these kinds of unpleasant actions are very likely. Many observatories have been broken into in the past, and the effects are almost always catastrophic: damage or destruction of the geomagnetic instruments, buildings left with open access. The cost and time and data loss is often huge as replacement of the equipment is difficult: the repair team often lives in another continent.

Some ways to discourage vandalism are:

- Make the GO difficult to access and to break into.
- Make it look very dull, uninteresting and worthless.

6.2 So how will they look like?

We try to foresee how the future GO will look in our opinion. The traditional separation between variometric and absolute instruments will be upheld. Continuously recording XYZ Variometer and PPM will be deployed in an “install and forget” approach. An automatic Diflux will be operating as a companion.

The traditional threesome of observatory buildings will be replaced by a single column like building (see Fig. 1) featuring small chambers where the automatic equipment is set-up. The top is equipped with a radome wherein the automatic Diflux is installed. This provides convenient access for the Diflux to the sunrays as it sits above the treetop level. The lower part of the column has a small room for the data acquisition, power and communications equipment. The height for the structure is tentatively set at 30 m. This kind of facility, which could be made of nonmagnetically armed concrete, should be affordable. A piece of land not bigger than 40×40 m should be sufficient to host it.

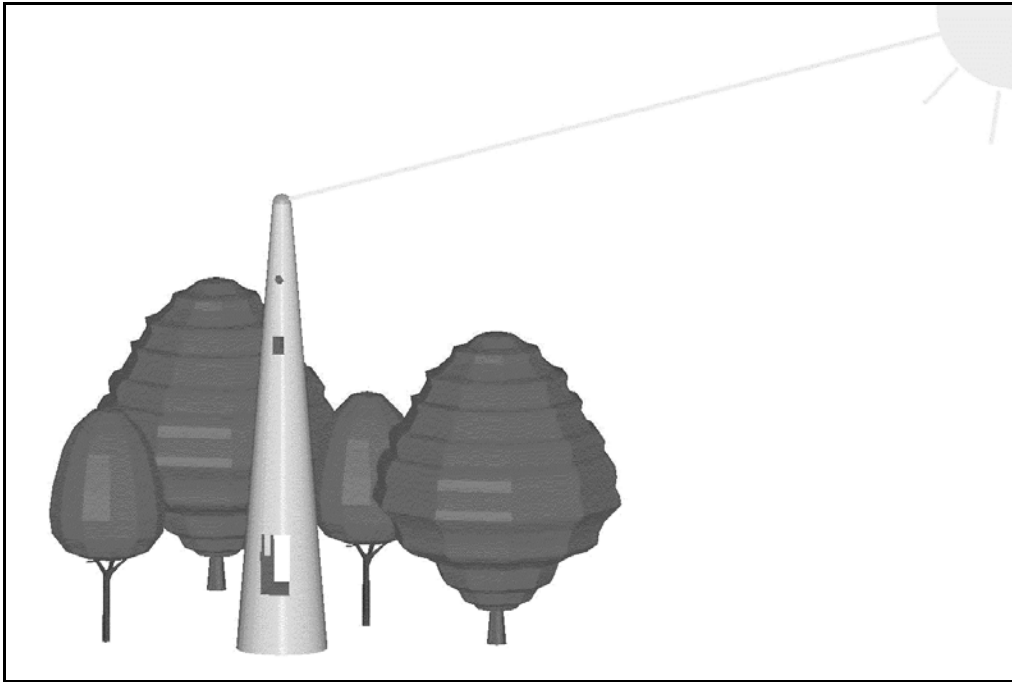


Fig. 1. How could a future geomagnetic observatory look like? This picture shows several concepts for an unattended GO: An automatic Diflux is installed on top of the pillar like structure and gets its orientation from sightings on the sun. Directly below a PPM and an XYZ variometer are operating in an “install and forget” configuration. The elevated position protects against unauthorized access, allows unobstructed reception of the sunrays and may attenuate perturbations originating in ground currents.

For finding the North Geographic reference direction it will use a sunshot with GPS timing (corrected to UT1 for accuracy) instead of usual target. The elevated posi-

tion will also render the measurements less susceptible to contamination by cultural noise. It will moreover render unauthorized access difficult preventing vandalism and break-in. The high pillar structure will be equipped with continuous 2 axis tilt monitoring. Data access will be via web interface.

6.3 How will sea-bottom magnetic observatories look like?

One notable difference with a surface observatory is the inability to use astronomical or GNSS fixes to get the True North and time: At 4000 m water depth an observer cannot use sunshots or GPS because the salt water column will let no electromagnetic waves through. Therefore the only way we know of to find True North is to use a so-called gyroscopic North Seeker. Here a gyroscopic device sensing the Earth's rotation and oriented by the pull of gravity will have its rapid rotation axis precess around the True North direction. Existing commercial North seekers are reasonably non-magnetic and have a North pointing accuracy of about 20 second of arc if suitable precautions are taken and enough observation time is allowed for.

Therefore sea-bottom GO's must be completely automatic, they will use automatic Diflux combined with a North Seeker (gyrotheodolite). There is also the possibility to merge the Diflux and DI variometer by having two orthogonal fluxgate operating on the Diflux (Chave *et al.* 1995).

7. Conclusions

New concepts for magnetic observatories will allow improved world coverage of the observations by:

- Rational approach to instrumentation, management and funding in Developing Countries,
- Introduction of fully automated observations where necessary by way of:
 - Automated Diflux and other equipments,
 - Ultra stable variometers in well protected environments.

Automation of Declination/Inclination measurement brings a new concept in magnetic observatories and will solve the challenge of sea-floor magnetic observatories.

User driven development of fast data acquisition leads to renew the concepts for fast sampling variometers.

References

Chave, A.D., A.W. Green, R.L. Evans, J.H. Filloux, L.K. Law, R.A. Pettit, J.L. Rasson, A. Schultz, F.N. Spiess, P. Tarits, N. Tivey and S.P. Webb, 1995, *Report of a Workshop on Technical Approaches to Construction of a Seafloor Geomagnetic Observatory*, Technical Report WHOI-95-12, Woods Hole Oceanographic Institution, Woods Hole, USA.

- Gilbert, D., and J.L. Rasson, 1998, *Effect on Diflux Measuring Accuracy due to a Magnet located on it*. Proceedings of the VIIIth Workshop on Geomagnetic Observatory Instruments, Data Acquisition and Processing, Scientific Technical Report STR98/21, Geo-ForschungsZentrum Potsdam, 168-171.
- Korepanov, V., *et al.*, 2007, *New INTERMAGNET Fluxgate Magnetometer*, *Publs. Inst. Geophys. Pol. Acad. Sc. C-99* (398) (this issue).
- Love, J.J., 2006, *1-Second Operational Standard for Intermagnet*, private communication.
- Van Loo, A., and J.L. Rasson, 2007, *Presentation of the Prototype of an Automated Diflux*, *Publs. Inst. Geophys. Pol. Acad. Sc. C-99* (398) (this issue).
- Veliz Castillo, O., and J.L. Rasson, 1998, *Results of Diflux Intercomparisons at the 3th Escuela Latino-Americana de Geomagnetismo in Huancayo, Peru*, *Revista Geofisica* **48**, 41-50.

Accepted February 27, 2007

Presentation of the Prototype of an Automated DIFlux

Sébastien A. VAN LOO and Jean L. RASSON

Royal Meteorological Institute of Belgium
Centre de Physique du Globe, B-5670 Dourbes, Belgium
e-mail: sebvl@oma.be

A b s t r a c t

Recently, we developed the first prototype of an automated DIFlux. This instrument performs absolute measurements of the geomagnetic field orientation (declination and inclination), without requiring the intervention of a human operator, nor maintenance. New possibilities are offered to the geomagnetic surface observatories, which may be completely automated in the near future. This may be particularly important for measurements in locations that are difficult to access, such as remote areas and the seafloor, hence improving the distribution of observations on the Earth's surface. Obviously, the instrument itself should not disturb the field to be measured. In this context, automation is a big challenge because several key elements, like the sensors, the motors, the angular encoders and the electronic circuits, contain generally ferromagnetic elements and conduct electrical currents, which may disturb the observations. Solutions to carry out the operations of sensor rotation, precise electronic reading of the angles and automatic orientation in the reference frame (determined by the local horizontal plane and geographic North) without disturbing the magnetic field will be exposed.

1. Introduction

At present, scientists do not have a physical model able to predict with sufficient precision the evolution of the geomagnetic field. The only way of determining it is to measure it. So the geomagnetic field is well-known only in the vicinity of the magnetic observatories. At the most inaccessible places, like the seafloor, high altitudes, and deserted areas, data is lacking, except for interpolations.

As a vector quantity, the complete definition of the magnetic field of the Earth, in a single point at a certain epoch requires evaluation of its absolute value (total field F) and its direction (declination D and inclination I). The first is commonly measured absolutely and automatically with a proton magnetometer. The variations of the field

direction are generally recorded automatically too, but its absolute determination must still be carried out manually, using a DIFlux magnetometer (Rasson 2005). If this last instrument could be automated, it would finally become possible to establish completely autonomous magnetic observatories, working without need for an operator nor maintenance. A total and uniform coverage of the planet would become feasible then (Chave *et al.* 1995).

That encouraged us in the 1990's to set up the AutoDIF project, the first phase of which will be completed in January 2008 (Rasson 1996, van Loo *et al.* 2006). The first phase is devoted to the development of a new totally automatic and absolute measurement instrument of the orientation of the geomagnetic field. Initially the reference to geographic North will be done similarly as in the traditional surface observatories, sighting a remote target of known azimuth. In the second phase, we will work on the automation of a gyroscopic North-seeker, in order to make the instrument more compact. The detailed specifications of our AutoDIF project are presented in Table 1.

Table 1
Specification of the automatic declination-inclination magnetometer AutoDIF

| | Errors in declination | Errors in inclination | Azimuth reference | Dedication |
|---------|-----------------------|-----------------------|--|---|
| Phase 1 | < 6 arcsec | < 6 arcsec | Automatic pointing of a distant target | Surface observatories |
| Phase 2 | < 20 arcsec | < 6 arcsec | Automatic gyroscopic North-seeker | Stations where the available volume is limited (seafloor) |

The realisation of such an instrument, being at the same time accurate, non magnetic and automatic, represents a serious challenge because several key elements, like the motors, the angular encoders and the electronic circuits, contain generally ferromagnetic elements and convey electrical currents which may disturb the natural field. We propose solutions in the following.

We start by briefly exposing how a fluxgate sensor can be used to determine the orientation of the ambient magnetic field. Then, we present a support to position the sensor in the field, consisting of a non magnetic theodolite, an accurate system of angle reading and piezoelectric motors, which do not disturb the field. Solutions are also proposed to determine the orientation of the measurement reference frame compared to the absolute reference frame of the Earth, defined by geographic North and the local horizontal plane. Finally, we evoke in a few words the data-processing and acquisition devices. These components of the AutoDIF instrument are shown in Fig. 1.

2. Detection of the Orientation of the Magnetic Field

To detect the orientation of the ambient magnetic field, we use a fluxgate sensor, like the one used in the traditional DIFlux manual. We refer the reader for the details

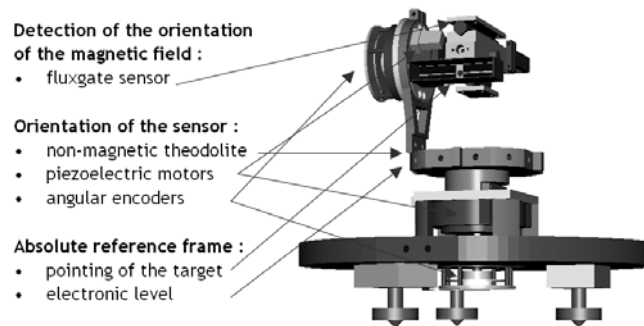


Fig. 1. Disposition of the fundamental devices of the AutoDIF.

of the working principle of a fluxgate sensor to the paper by Primdahl (1979). Let us simply remember that the fluxgate produces a signal, which is proportional to the component of magnetic field parallel to its axis (in fact it realises the scalar product of the magnetic field and the axis of the probe vectors).

The so called zero measurement method consists in seeking the positions of the probe, which produces a null signal, the field to be measured being then exactly perpendicular to the fluxgate axis. Thus the magnetic declination is measured after putting the fluxgate horizontally by turning it around a vertical axis. The inclination is obtained after placing the fluxgate in the magnetic meridian plane, rotating it around a horizontal axis.

3. Orientation of the Sensor

3.1 *Non magnetic theodolite*

In order to be able to orient the sensor in all the possible directions, the fluxgate probe is mounted on a theodolite. As shown in Fig. 2, in spherical coordinates, the orientation of the sensor is entirely determined by the angle ϕ around the vertical axis (reading on the horizontal circle) and the angle θ around the horizontal axis (reading on the vertical circle).

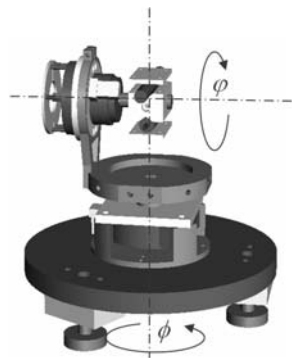


Fig. 2. Orientation of the fluxgate in space using a theodolite.

The evolution of the theodolite prototypes that we realised, which of course were built of non magnetic materials, is displayed on Fig. 3.

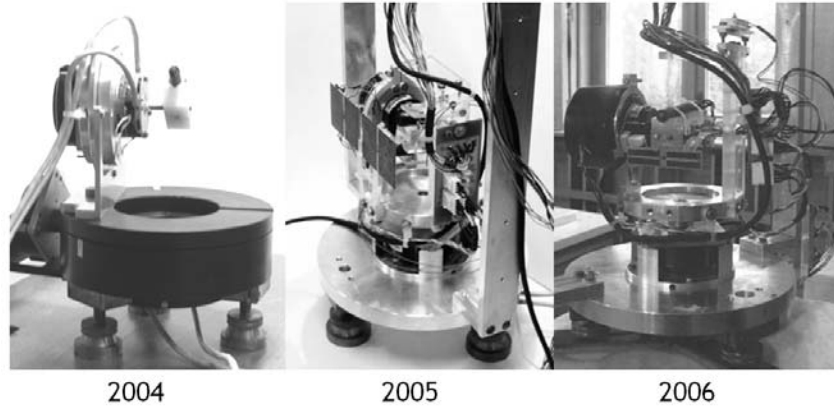


Fig. 3. Evolution of the AutoDIF prototypes during the last three years.

In order to eliminate the mechanical errors related to the manufacture of the theodolite, the values of the declination and inclination are calculated after averaging the measurements taken in the four possible positions, presented in Table 2.

Table 2

Different sensor positions allowing the measurement of the declination and the inclination

| Measurement | Position of the sensor compared to the horizontal axis | Position of the vertical circle compared to the vertical axis |
|-------------|--|---|
| Declination | above | in the North |
| | under | in the North |
| | under | in the South |
| | above | in the South |
| Inclination | above | in the West |
| | under | in the West |
| | under | in the East |
| | above | in the East |

3.2 Angular encoders

The electronic sensing of angles is ensured using optical angular encoders. One system is set up for each of the two principal axes of the theodolite.

A graduated disk, fixed on the relevant axis, rotates between a light source and a detection system (Fig. 4). Gratings, with the same period as the graduated disk, are placed behind the light source in order to amplify the signal obtained by optical Moiré

effect. These gratings are shifted a quarter of a period in order to obtain two sinusoidal signals. The disk is also equipped with an additional track, producing only one reference pulse per rotation.

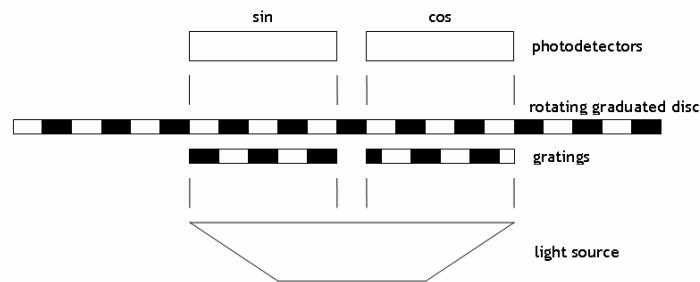


Fig. 4. General diagram of an optical encoder.

Since we use disks with 2500 graduations, a resolution of 0.0360° is obtained simply by counting the periods (using a quadrature x4 counter). As the two sinusoidal signals are in phase quadrature (Fig. 5), calculating the arctangent of the signals leads to continuous evaluation of the angles at a precision of about 1 arcsec, depending mainly on the accuracy and quality of the encoders, the electronic disturbances, and the mechanical alignment of the system. The reference pulse is used to make this incremental encoder absolute.

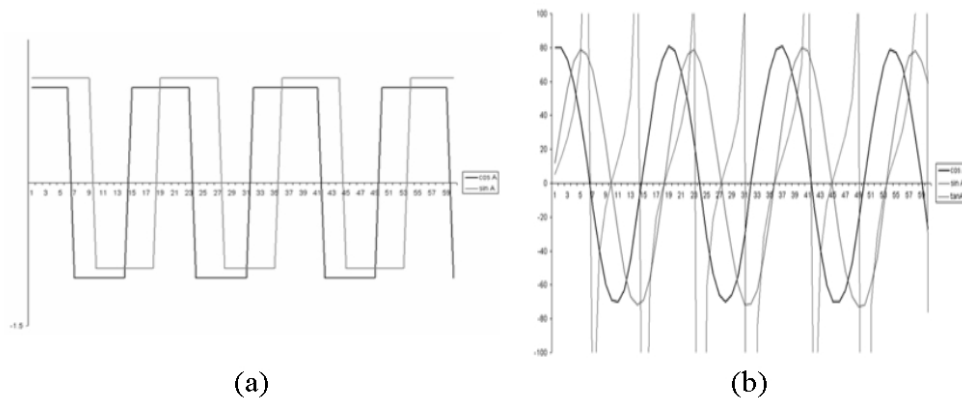


Fig. 5. Electric signals allowing (a) the period count and (b) the continuous sensing of the angle by interpolation between the period increments.

It can be understood easily that the precision of the angle reading is conditioned by the quality of the electronic signals. The errors related to the encoder and electronics quality, like amplitude modulation and undesired offset are corrected in real-time by a digital processing algorithm.

Errors related to mechanical misalignment of the encoder compared to the rotation axis are corrected putting two encoders around the same disk, at more or less 180° (Fig. 6). In this case the average of the two measured angles produces a result free from eccentricity errors.

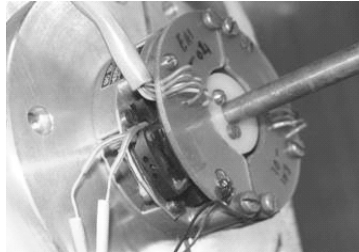


Fig. 6. Two encoders placed around the horizontal axis.

Encoders that are available on the market are generally not magnetically clean. Moreover it is impossible to arrange two of them side by side symmetrical on the same disk. So some parts, essentially the detector board, have to be replaced by specially designed circuits, as illustrated on Fig. 7.

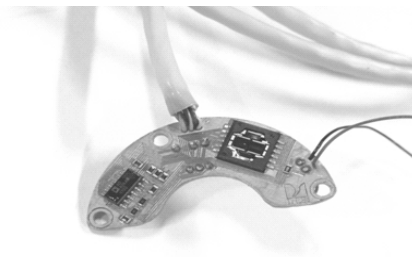


Fig. 7. Example of a detector board for the angular encoder including a ready-made IC as detector and a linear amplifier.

3.3 Piezoelectric motors

Considering the fluxgate probe, the non-magnetic theodolite and the angular encoders, we have all the components of a digital DIFlux theodolite, but not robotised yet. The rotations around the two axes of the theodolite are achieved by piezoelectric motors, which are commercially available in totally non-magnetic versions.

The principle of operation of such a motor is based on the generation of a deformation wave which is propagated on the surface of an annular piezoelectric crystal, constituting the fixed part of the motor (the stator). The rotation of the mobile shaft is obtained by pressing its base against the stator, where it is pulled by the movement of the deformation wave (see Fig. 8). This traveling wave is obtained by stimulating the crystal with two high voltage signals (300 Vpp), one cosine and one sine, at a frequency of about 40 kHz. In this way, power is applied by a small, non-disturbing AC current.

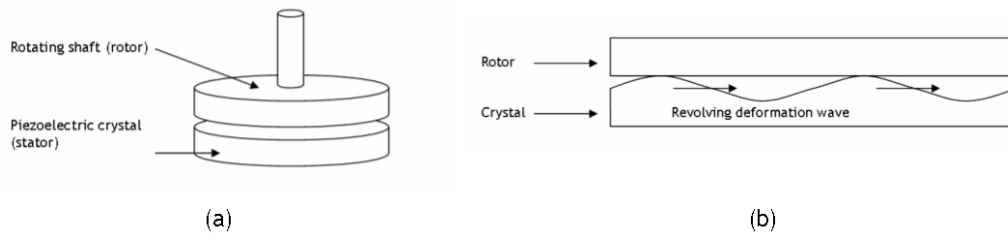


Fig. 8. (a) General diagram of a rotary piezoelectric motor, (b) Detail of the interface between rotor and stator.

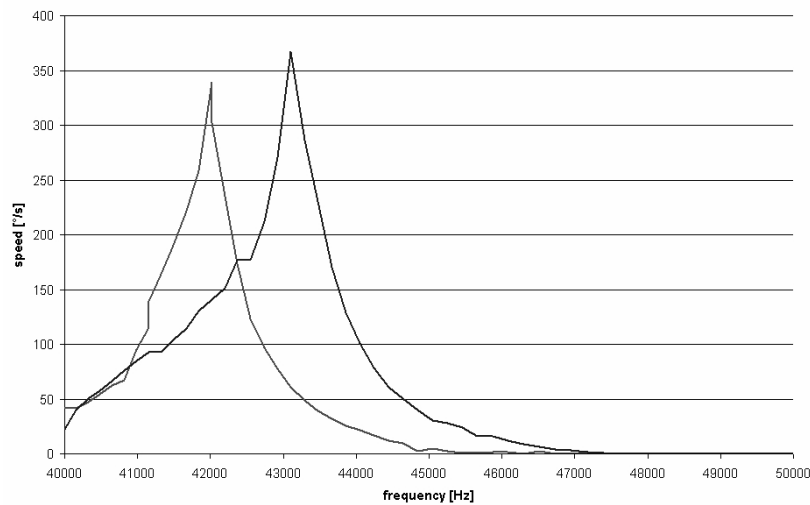


Fig. 9. Rotation speed of a Shinsei USR60 piezoelectric motor in the two directions of rotation.

For example, when a position has to be reached with great precision, or in order to avoid brutal starts and stops, the rotation speed has to be controlled very finely. As shown in Fig. 9, speed can be modulated using the excitation frequency of the crystal. But since the behaviour of the motors varies largely, depending on their temperature, their wear and even on the direction of rotation, the frequency has to be corrected continuously, especially for very slow motion, using the angular encoders data as a feedback signal.

Under these conditions, the shafts of the motors are appropriate to be used directly as axes for the theodolite, with no need for a transmission, or reduction system.

4. Orientation of the Instrument in an Absolute Reference Frame

As presented above, the instrument is able to measure the orientation of the magnetic field related to its own reference frame. In order to qualify the instrument as absolute, it remains to determine the orientation of the instrument compared to the absolute reference frame of the Earth, which we can define by the local horizontal plane and the direction of geographic North.

4.1 Electronic level

The electronic level provides a reference to the horizontal. It is built in the same manner as a traditional bubble level, but is filled with a liquid containing an electrolyte, which has the properties of a three-terminals variable resistor, varying according to the position of the bubble (Fig. 10).

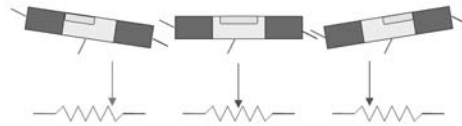


Fig. 10. The electronic level presented in analogy with a three-terminals variable resistor.

The horizontality is then accurately measured using a Wheatstone bridge, and the angles around the horizontal axis (read on the vertical circle) can be corrected by software easily.

4.2 Electronic target

In the first phase of the project, the orientation of the instrument compared to geographic North is obtained by pointing a distant target with known azimuth, as is usually done in magnetic observatories (Fig. 11).



Fig. 11. (a) The corner cube reflector used as a target, (b) The photocells receiving the light reflected from the reflector.

A laser diode module is installed in place of the telescope. It points a corner cube reflector, which is centred at a point with precisely known azimuth (actually the visual target). According to properties of the corner cube reflector, the incident light ray is reflected 180° , but translated by a distance e depending on the angle α between the incident ray and the line which connects the centre of the corner cube to the vertical axis of the theodolite (Fig. 12). Two solar cells are disposed around the laser in order to evaluate the translation of the reflected ray. The difference of light falling on the two solar cells is directly related to the pointing of the centre of this electronic target: when the reflected ray returns precisely in the middle, the laser points exactly the centre of the target.

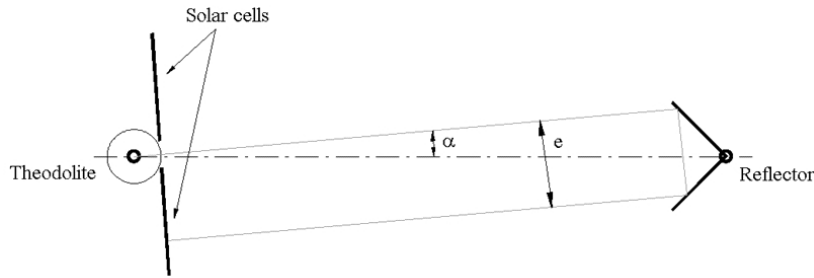


Fig. 12. Geometrical optics with the corner cube reflector.

The laser diode module that is used as light source is a little magnetic. But its effect on the final magnetic measurements results is eliminated because it accompanies the fluxgate sensor in the four positions taken for declination and inclination. In order to reduce mechanical errors of the theodolite, the target is also sighted in two positions (probe up and probe down). The goal of the second phase of the project is to replace this system by an automatic gyroscope. This certainly will make it possible to work in a more confined volume.

5. Data Processing and Remote Control

The signals produced by all the electronic acquisition systems (reading of angle, fluxgate, level, pointing of target) are collected by a microcontroller using analog to digital converters. They are then processed and instructions are sent to the motor drivers, in order to carry out the desired operations. The data storage, the time synchronisation, and the user interface are ensured by a computer, connected to the microcontroller via USB bus. Figure 13 shows the user interface, as displayed on the host computer.

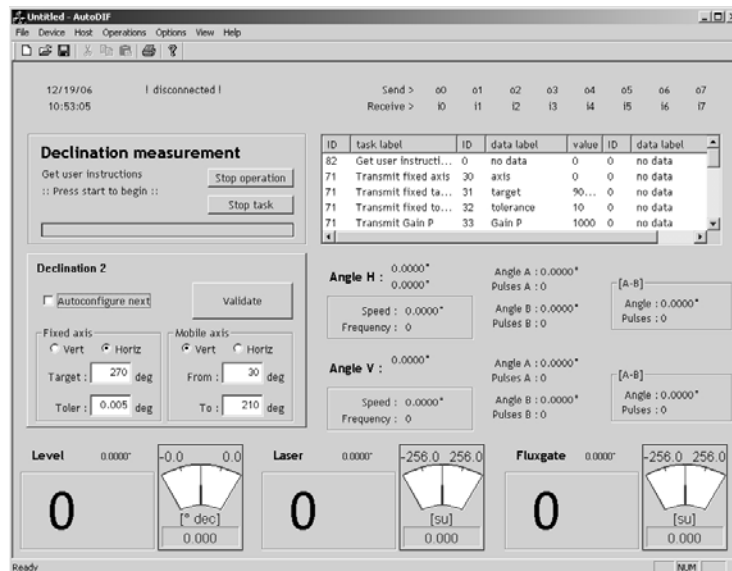


Fig. 13. Screenshot illustrating the AutoDIF user interface.

6. Conclusion

Presently, our instrument performs absolute measurements of the orientation of the geomagnetic field vector automatically, using the manual DIFlux measurement protocol. But a human operator is no longer needed.

Our first prototype, entering the qualification phase, is presently in service in the magnetic observatory of the Centre de Physique du Globe de l'IRM in Dourbes. The first results are evaluated daily and seem encouraging.

References

- Chave, A.D., A.W. Green, R.L. Evans, J.H. Fillioux, L.K. Law, R.A. Petit, J.L. Rasson, A. Shultz, F.N. Spiess, P. Tarits, N. Tivey and S.P. Webb, 1995, *Report of a Workshop on Technical Approaches to Construction of a Seafloor Geomagnetic Observatory*, Technical Report WHOI-95-12, Woods Hole Oceanographic Institution, Woods Hole, USA.
- Primdahl, F., 1979, *The fluxgate magnetometer*, J. Phys, E: Sci. Instrum. **12**, 241-253.
- Rasson, J.L., 1996, *Progress in the design of an automatic DIFlux*. **In:** Proceedings of the VIth Workshop on Geomagnetic Observatory instruments, Data Acquisition and Processing, J.L. Rasson Ed., Publ. Sci. et Tech. No 003, Institut Royal Meteorologique de Belgique, Brussels, 190-194.
- Rasson, J.L., 2005, *About Absolute Geomagnetic Measurements in the Observatory and in the Field*, Publication Scientifique et Technique No 040, Institut Royal Meteorologique de Belgique, 43p.
- van Loo, S.A., and J.L. Rasson, 2006, *Development of an Automatic Declination-Inclination Magnetometer*. **In:** J.L. Rasson and T. Delipetrov (eds.), "Geomagnetics for Aeronautical Safety", NATO Science Series, 177-186

Accepted February 8, 2007

Underwater Magnetometer MG-01/2003 for Geomagnetic Offshore Soundings

Janusz MARIANIUK, Waldemar JÓŹWIAK, Anne NESKA and Mariusz NESKA

Institute of Geophysics of the Polish Academy of Sciences
01-452 Warszawa, ul. Ks. Janusza 64, Poland
e-mail: belsk@igf.edu.pl

A b s t r a c t

A magnetometer constructed to carry out geomagnetic variation measurements on the sea bottom is described. The main difference between onshore and offshore variation measurements is – beside requirements concerning protection against the underwater environment – the fact that an offshore instrument cannot be placed according to the geomagnetic (or geographic, respectively) coordinate system. It has to be aligned “virtually” instead, by means of additional clinometer records after the real measurement. The software performing this is described here as well. The instrument has been applied successfully in the Baltic Sea several times. The data achieved thereby fits very nicely in the well-investigated onshore surrounding and efficiently helps to understand the structure of electric conductivity in the subsurface of this region.

1. Design of the Magnetometer

The bottom magnetometer MG-01/2003 was designed and built at Belsk Observatory in 2003 (Marianiuk 2005).

The set of instruments is installed within a tight capsule, resistant to high pressure and marine water, made of non-magnetic materials (see Fig. 1). The bottom magnetometer employs a suitably adjusted transduction magnetometer LEMI8G produced by the Lviv Centre of the Institute of Space Research, National Academy of Sciences of the Ukraine (Korepanov *et al.* 1998). The magnetometer consists of a three-component sensor for the measurement of three mutually perpendicular magnetic field components (see Fig. 2), and an electronic console with a microprocessor. The housing with the console contains also a 20-bit, 5-channel digital recorder with an 8 MB data storage memory. In the upper part of the capsule, there is installed a double electronic clinometer purchased from the American company Applied Geomechanics. The

N and E axes of the clinometer exactly coincide with the X and Y axes of the magnetometer. In the lower part of the capsule, two 12V/25Ah batteries are fixed. They ensure a continuous operation of the instrument for about 12 days. See Fig. 3 for a schematic overview of the magnetometer's design and Table 1 for its basic parameters.



Fig. 1. The bottom magnetometer MG-01/2003 in its capsule.



Fig. 2. The LEMI magnetometer in the interior of the capsule.

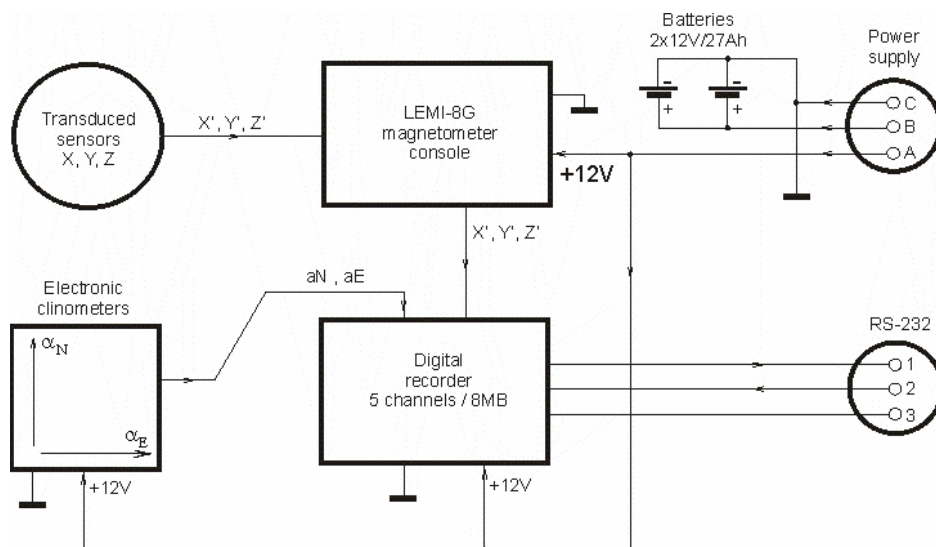


Fig. 3. Simplified block scheme of the bottom magnetometer MG-01/2003.

Table 1

Basic parameters of the bottom magnetometer MG-01/2003

| | |
|----------------------------------|----------------------|
| Measurement range: | $\pm 65\,000$ nT |
| Accuracy of measurement: | ± 1 nT |
| Resolution of measurement: | ± 10 pT |
| Transmission band: | 1 Hz ... DC |
| Internal memory (Compact Flash): | 8 MB |
| Capacity of memory: | $416 * 10^3$ samples |
| Sampling interval: | 1 ... 255 s |
| Measurement range of tiltmeters: | $\pm 50^\circ$ |
| Resolution of tiltmeters: | $\pm 0.01^\circ$ |
| Power supply: | 120 mA/12 V |
| Mass of entire magnetometer: | 106 kg |
| Maximum depth of immersion: | ~ 1000 m |

2. Algorithm of Operation

Once the magnetometer sinks in the water reservoir, the orientation and inclination of the instrument are random, and instead of the real components we record components in an arbitrary system of coordinates X' , Y' and Z' . Along with the magnetic components, indications of the electronic clinometers, α_X and α_Y , are recorded.

From the recorded “inclined” magnetic components and the indications of the electronic levels, it is possible to calculate the real, “upright”, magnetic components H , D , and Z (or X , Y and Z , if we know the approximate value of magnetic declination in the study area), which are needed to calculate the results of geomagnetic sounding.

To explain the procedure, let us use an analogy to the investigations on land. While making the land geomagnetic survey, we first install a magnetometer sensor on a stable stand, and then perform the following two operations:

1. In accordance to the indications of bubble levels, we level the magnetometer sensor with an accuracy to a few angular minutes.
2. Having made the leveling, we turn the sensor about the vertical axis so as to obtain the maximum indications on the X channel and minimum (i.e., nearly zero) on the Y channel. Then, the X axis of the magnetometer coincides with the magnetic north direction and the horizontal component H , and the Z axis is directed vertically.

A similar procedure is made on the data read from the bottom magnetometer by the LEMI3TRD software developed by Dr. Krzysztof Nowożyński (Nowożyński 2005). In the first stage, the program makes a virtual leveling of the instrument on the basis of electronic levels' data; in the second stage it virtually rotates the magnetometer's sensor (cf. Fig. 4).

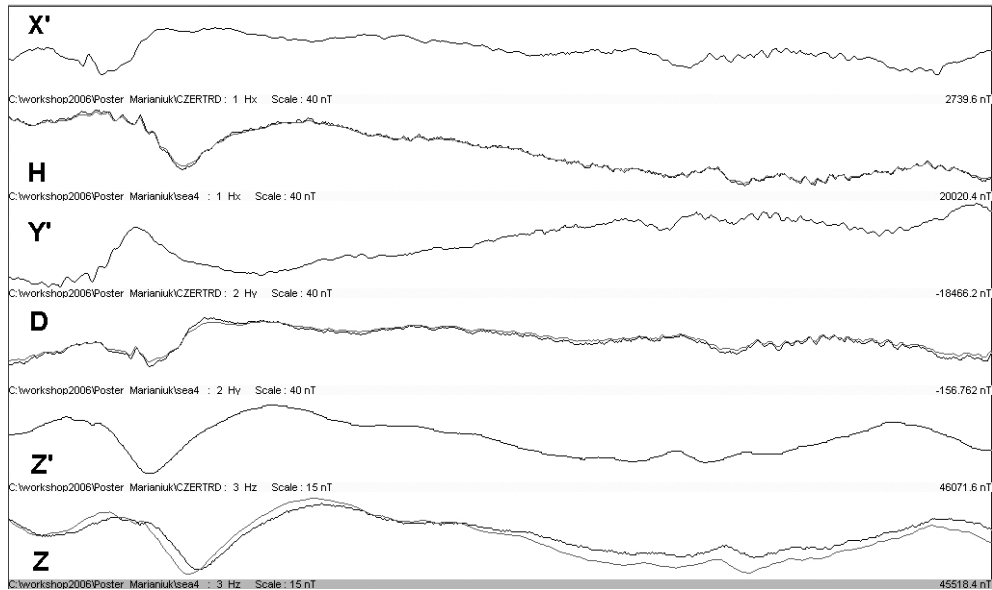


Fig. 4. The 85 min time series measured by the bottom magnetometer MG-01/2003 between Rügen and Bornholm Islands (cf. Fig. 5). X' , Y' , Z' are raw data in the coordinate system according to the magnetometer's orientation. H , D , Z indicate components after rotation in the geomagnetic system. For comparison there are displayed data of Rügen site as gray lines. The scale of the y axis is 40 nT for the horizontal and 15 nT for the vertical components.

The magnetometer possesses two tight interfaces at the capsule. One interface is used for adjusting the magnetometer's measurement parameters and for reading out of the recorded data. The other one enables a charging of the batteries in the interior of the magnetometer. When the magnetometer is taken back from the water, the data recorded is read out and virtually corrected for its orientation by means of the program LEMI3TRD. As a result, one gets data files in TRD format which is the default for further processing of geomagnetic and magnetotelluric field data at the Institute of Geophysics PAS.

3. Soundings in the Baltic Sea

After construction of the magnetometer, a number of tests have been carried out to check whether the new device and the associated software work properly. First experiments were carried out in the measurement houses and in the fire-rescue pool of the observatory. Subsequent field measurements took place in the large, deep Lake Rajgradzkie in North-East Poland.

In 2005, there were made two geomagnetic soundings in the Baltic Sea (Jóźwiak *et al.* 2005). These offshore soundings were accompanied by a number of onshore sites close to the Polish coast and on the islands Bornholm, Usedom, and Rügen. Their locations are displayed in Fig. 5.

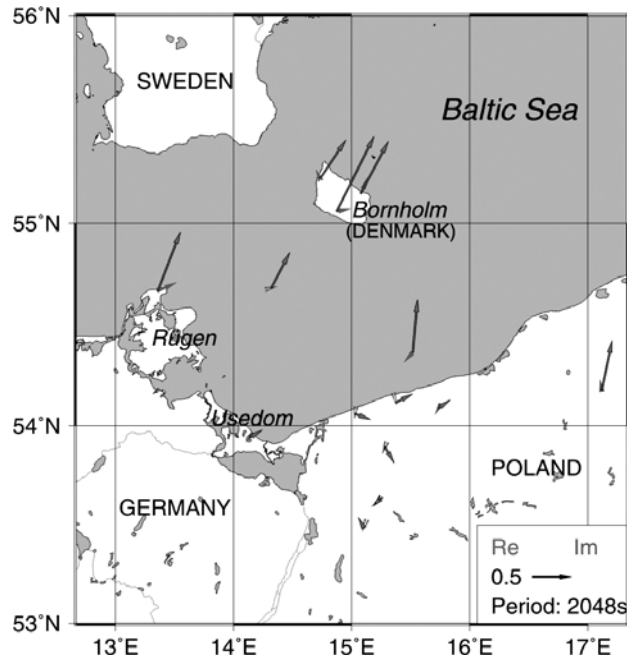


Fig. 5. 2005 measurement area with induction arrows.

The measurements were a complete success. Figure 4 shows time series before and after rotation in the proper coordinate system. A comparison of the corrected time series with data from a land site underlines the similarity, i.e. reasonability, of the offshore measurements (same figure). The geomagnetic transfer function obtained from the time series data are of the same quality as the onshore ones. Figure 6 shows induction arrows over period for the offshore sounding between Bornholm and Rügen.

The induction arrows and perturbation vectors of both offshore sites fit very well into the picture drawn by the surrounding onshore sites, as Figs. 5 (induction arrows) and 7 (perturbation vectors excited by magnetic component X at Niemegk Observatory) show. Moreover, they make that picture more detailed and exact. It can be concluded from it that an anomaly of electric conductivity, which is even better conducting than the sediments of the North German-Polish Basin to the South, strikes there in the east-west direction along the Baltic coast.

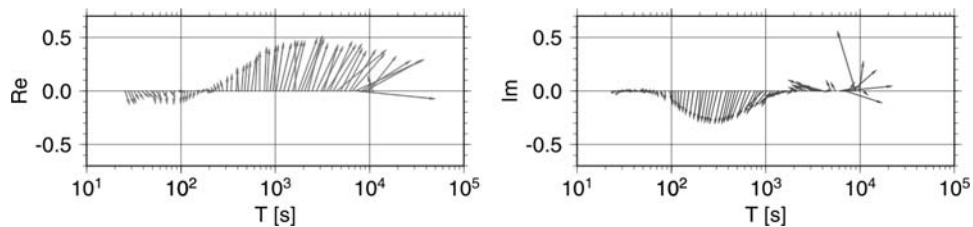


Fig. 6. Induction arrows (real and imaginary) of offshore site between Rügen and Bornholm Islands. The smoothness of the transfer function up to several 1000 seconds indicates a good data quality.

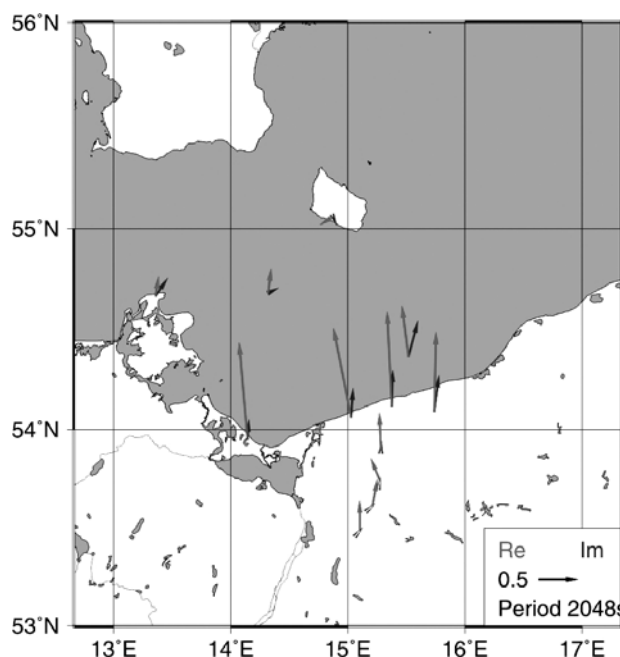


Fig. 7. Perturbation vectors describing the anomalous horizontal field with respect to X component measured simultaneously at Niemegk Observatory. The huge north components along the Baltic coast indicate an anomalous, EW striking current system in this region, possibly due to graphite in the old suture between Baltica and Avalonia.

Acknowledgements. This work was supported by KBN grants 2 P04D 02527 and 8 T12B 029 21.

References

- Józwiak, W., and A. Neska, 2005, *Electromagnetic sounding in SW Baltic region: Significant induction anomaly indicated by Perturbation Vectors*, *Publs. Inst. Geophys. Pol. Acad. Sc. C-95* (386), 97-105.
- Korepanow, V., A. Best, B. Bondaruk, H.-J. Linthe, J. Marianiuk, K. Pajunpaa, L. Rakhlin and J. Reda, 1998, *Experience of Observatory Practice with LEMI-004 Magnetometers*, *Revista Geofisica* **48**, 31-40.
- Marianiuk, J., 2005, *Magnetometer MG-01/2003 for geomagnetic sounding at a water reservoir bottom*, *Publs. Inst. Geophys. Pol. Acad. Sc. C-92* (379), 119-130.
- Nowożyński, K., 2005, *Tilt-correction algorithm for vector magnetometers*, *Publs. Inst. Geophys. Pol. Acad. Sc. C-92* (379), 131-135.

Accepted February 13, 2007

Schumann Resonance Observation in Polish Polar Station at Spitsbergen and Central Geophysical Observatory in Belsk

M. NESKA¹, G. SÁTORI², J. SZENDRŐI², J. MARIANIUK¹,
K. NOWOŻYŃSKI¹ and S. TOMCZYK¹

¹Institute of Geophysics of the Polish Academy of Sciences
ul. Ks. Janusza 64, 01-452 Warszawa, Poland
e-mail: nemar@igf.edu.pl

²Geodetic and Geophysical Research Institute of the Hungarian Academy of Sciences
H-9400 Sopron, Csatkai u. 6-8., Hungary
e-mail: satori@ggki.hu

Abstract

Two sets of Schumann resonance apparatus, each consisting of an electric ball antenna and two induction magnetometers, have been constructed in Belsk Observatory in 2003 and 2004. The apparatus have been installed in the Polish Polar Station in Hornsund at Spitsbergen as well as in Belsk Observatory. The vertical electric (E_z) and the horizontal magnetic (B_x , B_y) components have been measured in Hornsund and Belsk since September 2004 and February 2005, respectively. The sampling rate amounts to 100 Hz. The parameters of the magnetic and electric sensors make it possible to register four Schumann resonance modes (8, 14, 20 and 26 Hz). The observation results are presented.

Schumann resonances (SR) are the electromagnetic eigenfrequencies of the Earth-ionosphere cavity (Fig. 1). They were first predicted and discussed by W.O. Schumann (1952). The excitation source of Schumann resonances is the world thunderstorm activity. Resonances can be observed at around 8 Hz, 14 Hz, 20 Hz, etc. The first measurements and spectral analysis which confirmed the existence of such resonances were performed by Balser *et al.* (1960).

The observation of Schumann resonances can provide valuable information about the world thunderstorm activity, the properties of the upper dissipative boundary layer of the Earth-ionosphere cavity, and climatic changes. A large number of research projects shows influences of the SR signal on human health (blood pressure, melatonin level, cardiac and neurological disease).

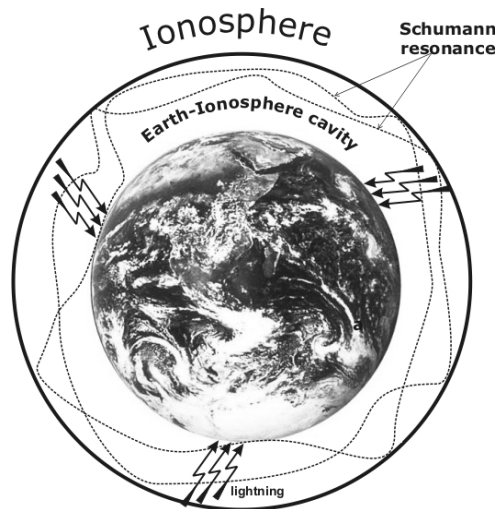


Fig. 1. Earth-ionosphere cavity.

In the Schumann resonance band we can find three major types of natural ELF radio noise (Ogawa *et al.* 1966): Extremely Low Frequencies (ELF) background, ELF flashes and ELF bursts. Figure 2 shows typical waveforms of these three Schumann resonance signals.

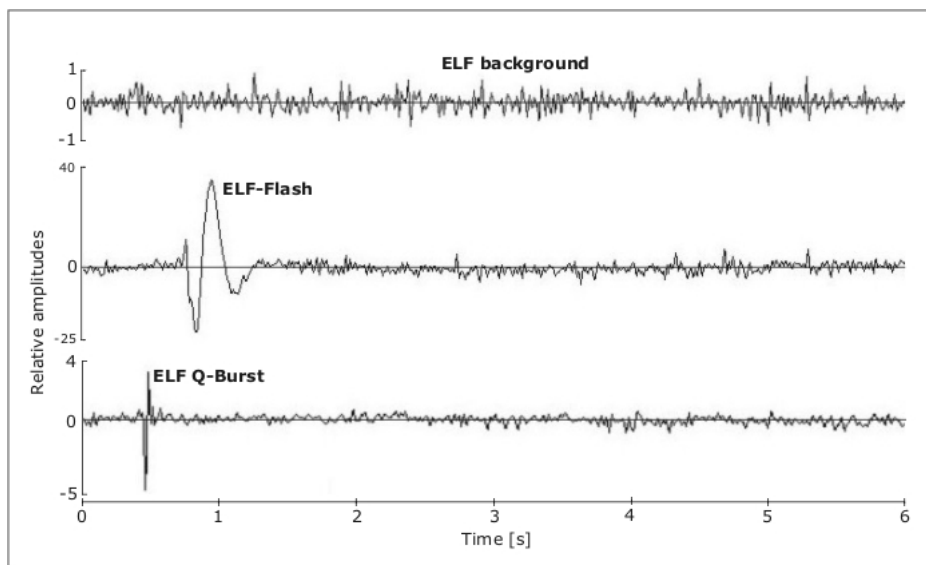


Fig. 2. Typical signal forms (Bx component measured in Belsk).

Two sets of Schumann resonance apparatus, with electric ball antennas (Fig. 3) and induction magnetometers (Fig. 4) were constructed in Belsk Observatory in 2003 and 2004. The SR apparatus were installed at the Polish Polar Station at Spitsbergen

(77.0°N, 15.5°E) and in Belsk Observatory (51.8°N, 20.8°E) in the frame of a Hungarian-Polish project. The project was supported by NATO Collaborative Linkage Grant (EST.CLG.980431). The locations of Polish Schumann resonance stations are shown in Fig. 5. The vertical electric (E_z) and the horizontal magnetic (B_x , B_y) components have been measured in Hornsund and Belsk since September 2004 and February 2005, respectively.



Fig. 3. Electric antenna.



Fig. 4. Induction coils.

A schematic diagram of the SR recording system is shown in Fig. 6. The magnetic sensors are buried half a meter deep in the subsurface. The electric ball antenna is put on a ceramics-made insulating pillar of two meter height. The preamplifiers are placed at the bottom of the electric antenna and inside of the induction coils. The pre-amplified SR signals are passed to the input of electronic console where they are filtered and afterwards amplified. The amplified signals are fed to the input of the 16-bit analogue-digital converter, then passed to the PC computer via parallel interface and saved on a hard drive.

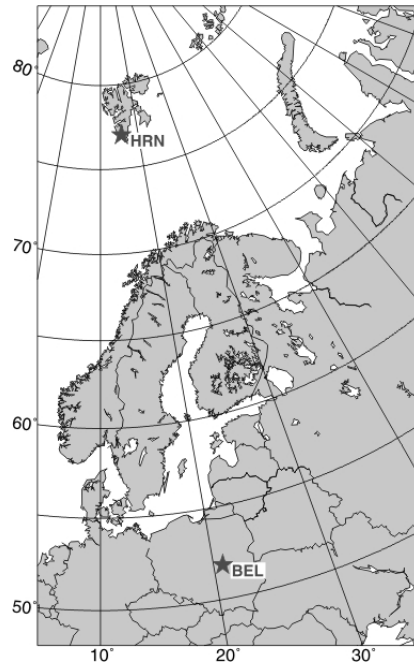


Fig. 5. Locations of Polish Schumann resonance stations: BEL – Belsk Observatory (Poland), HRN – Polish Polar Station in Hornsund (Spitsbergen, Norway).

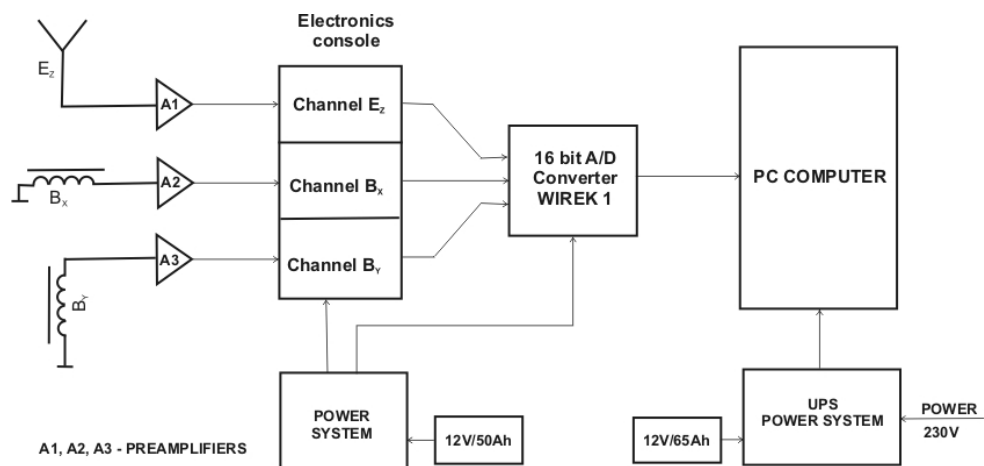


Fig. 6. Schematic diagram of the SR recording system at Spitsbergen and Belsk.

The sampling rate amounts to 100 Hz. The parameters of the magnetic and electric sensors make it possible to register four Schumann resonance modes (8, 14, 20 and 26 Hz). Examples of time series and power spectrum density (B_x , B_y and E_z components) recorded in the Schumann resonance frequency range in Belsk Observatory are shown in Figs. 7 and 8.

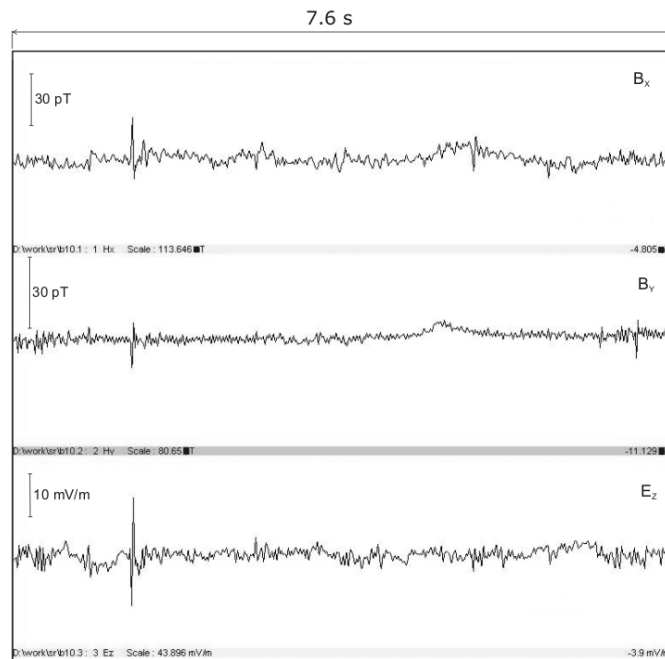


Fig. 7. Time series recorded in the Schumann resonance frequency range in Belsk Observatory (September 18, 2005).

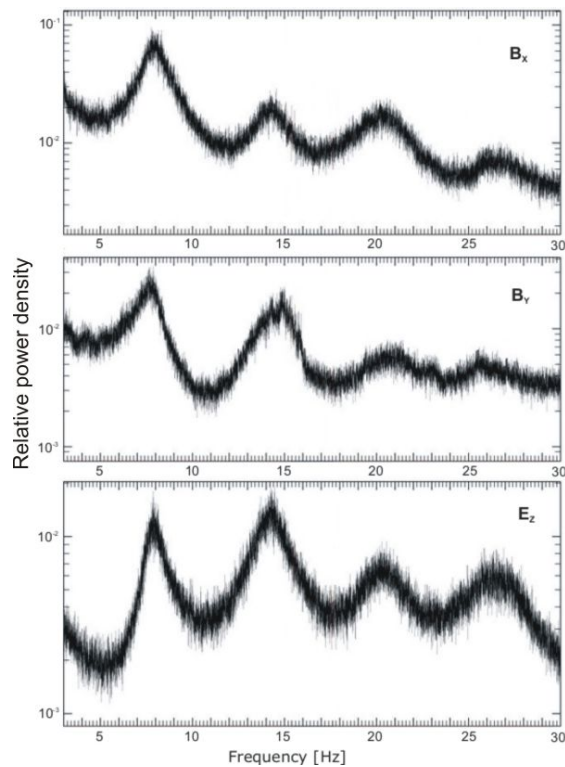


Fig. 8. Spectrum of B_x , B_y , and E_z components (Belsk, September 18, 2005) with four Schumann resonance modes.

Figure 9 presents the mean daily relative amplitude variations in October 2005. The amplitude maxima clearly show the activity of the large thunderstorm regions during the day. The complex demodulation by (Sátori *et al.* 1996) as a spectral technique has been used for determination of peak-frequencies and the corresponding amplitudes of the first three Schumann resonance modes.

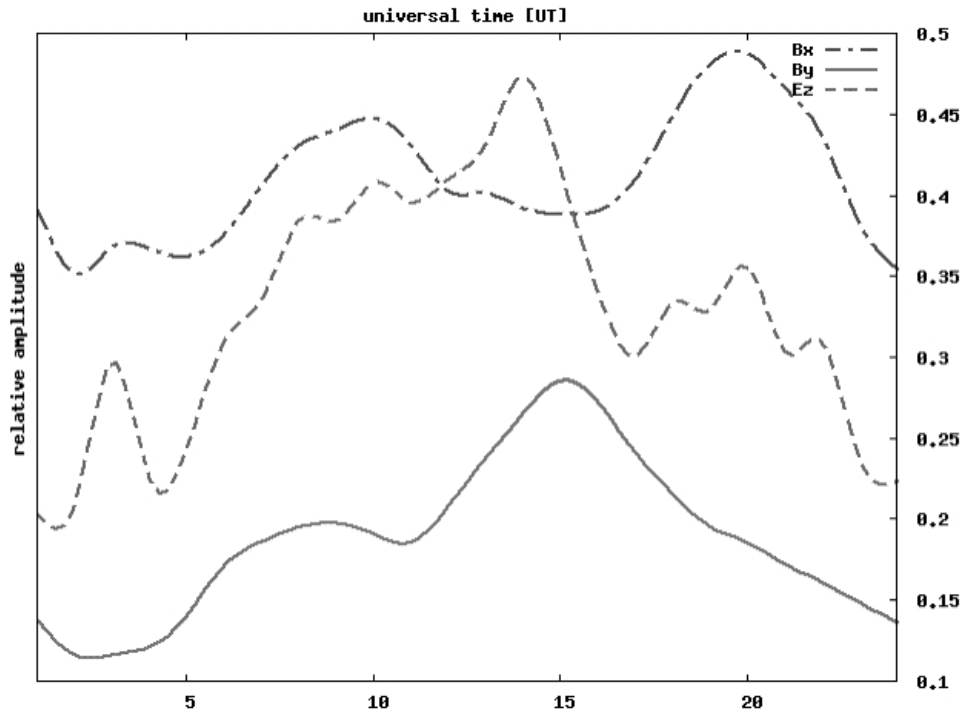


Fig. 9. Mean daily variations of relative amplitudes for the first Schumann resonance mode - Bx, By, and Ez components (Belsk, October 2005).

References

- Balsler, M., and C.A. Wagner, 1960, *Observation of Earth-ionosphere cavity resonances*, *Nature* **188**, 638-641.
- Ogawa, T., Y. Tanaka, T. Miura and M. Yasuhara, 1966, *Observation of natural ELF electromagnetic noises by using the ball antennas*, *J. Geomagn. Geoelectr.* **18**, 443-454.
- Sátori, G., J. Szendroi and J. Vero, 1996, *Monitoring Schumann resonances – I. Methodology*, *J. Atmos. Terr. Phys.* **58**, 1475-1482.
- Schumann, W.O., 1952, *Über die strahlungslosen Eigenschwingungen einer leitenden Kugel, die von einer Luftschicht und einer Ionosphärenhülle umgeben ist*, *Zeitschrift für Naturforschung* **7a**, 149-154.

Accepted February 12, 2007

A New Model of Telluric Amplifier for Magnetotelluric Soundings

Sebastian TOMCZYK

Institute of Geophysics of the Polish Academy of Sciences
ul. Ks. Janusza 64, 01-452 Warsaw, Poland
e-mail: stomczyk@igf.edu.pl

A b s t r a c t

In 2005, a new series of two-channel telluric amplifiers has been designed and constructed at Belsk Observatory. This model named TWG-0501 is designed mainly for magnetotelluric field measurements. These amplifiers basing on microprocessors provide a number of new functions, e.g., automatic compensation for the constant part of input voltage and remote setting of working parameters by means of a RS-232 interface and a local computer network. The range of input voltage is ± 100 mV and that of output voltage ± 10 V for this device. More details are presented in this article.

A two-channel telluric amplifier has been constructed for investigation of telluric currents. Such currents are induced in the upper layers of the Earth's crust by natural geomagnetic field variations. Table 1 shows basic parameters of this amplifier and Fig. 1 its photo. A telluric amplifier serves for amplification of weak incoming signals from the sensors (electrodes) buried in the soil. The device contains two independent differential amplifiers placed in a common casing. This enables a synchronous recording of the electric field of two pairs of electrodes that are usually directed perpendicularly, N-S and E-W. We can see an example of such a registration in Fig. 2.

The amplifier can be used with any electrodes, if their contact resistance to the soil is lower than $10\text{ k}\Omega$ and their polarization voltage lower than ~ 250 mV. In practice, the length of the telluric lines can take values from several meters to few hundred meters. Figure 3 shows such an electrode.

Table 1
Basic parameters of Telluric Amplifier model TWG-0501

| Nr | Parameter | Unit | Value | Remark |
|----|-------------------------------|----------------------------|-----------------|-----------------------|
| 1 | Gain per channel | V/V | $100 \pm 0.2\%$ | for DC |
| 2 | Average noise ($G = 1$) | μV | < 1 | |
| 3 | Damping of in-phase signals | dB | 95 | for $f < 0.02$ |
| 4 | Input resistance | $\text{M}\Omega$ | > 100 | for DC |
| 5 | Output resistance | Ω | 70 | for DC |
| 6 | Maximum input signal | mV | ± 250 | |
| 7 | Maximum output signal | V | ± 10 | |
| 8 | Thermal coefficient | $\text{mV}/^\circ\text{K}$ | < 1 | |
| 9 | Signal transfer band | Hz | 0 – 0.25 | |
| 10 | Output voltage of thermograph | V | $0 \pm 0.5\%$ | for 0°C |
| 11 | Thermograph scale value | $^\circ\text{K}/\text{V}$ | $10 \pm 0.5\%$ | |
| 12 | Current consumption | A | 0.15 | for 13.0 V |



Fig. 1. Telluric amplifier model TWG-0501.

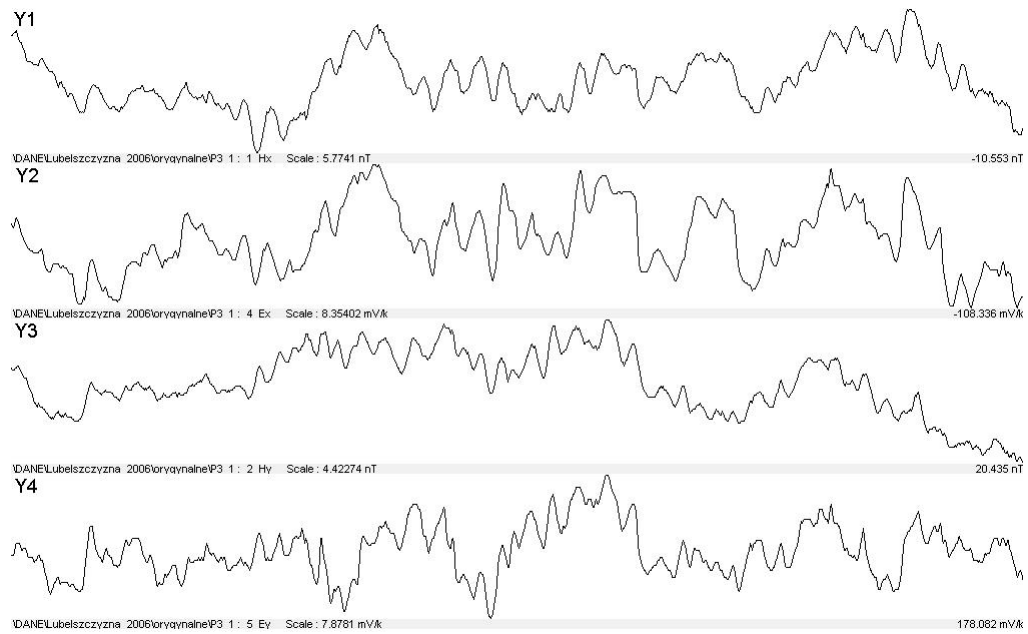


Fig. 2. Example of registration. X axis – 1000 sec. Y1 axis – Hx 5.77 nT; Y2 axis – Ex 1.67 mV/km. Y3 axis – Hy 4.42 nT; Y4 axis – Ey 1.71 mV/km.



Fig. 3. Electrode.

The amplifier has been designed for usage together with transduced magnetometers LEMI-003P, which are produced in Lviv (Ukraine). This set of devices is applied to magnetotelluric field measurements. The DC low-pass filters in both devices are practically the same, which allows to avoid the necessity of introducing the instrument's characteristics for the person who is processing the collected data.

For magnetotelluric field soundings there is usually applied a telluric length of about 100 m. With regard to thermal coefficients, the electrodes are buried to a depth of minimum 70 cm. Since the electrodes work well only in moist ground, it is necessary to place ca. 10 kg of a mixture of technical bentonite with water in every electrode hole. Bentonite is very hygroscopic (it absorbs water from its surrounding), so it preserves the moisture of the electrodes and improves stability of their potential. When installing the electrodes, one has to pay special attention to the state of the insulation of telluric cables too. Every (even the smallest) damage causes a contact between the conductor and the soil (even through plants) and therefore worsens the quality of telluric registrations.

The resistance of the conductor's insulation to the ground should be at least 100 times as big as the transition resistance between electrode and ground, i.e. not less than 0.5-1 M Ω .

The amplifier is equipped with a controlling system for telluric lines. In case of an interrupted line, there appears a signaling "OFF LINE". Furthermore, it is possible to measure the resistance of the line in the range of 0.1-50 k Ω . This measurement is carried out by means of AC of 20 Hz. Thereby a polarization of the electrodes is avoided.

The input circuits of the amplifier are protected against over-voltages, which can be inducted between electrodes and telluric lines during atmospheric discharges. The protecting system consists of diodes and varistors and is able to hedge the amplifier against short-term over-voltages of amplitudes up to 1000 V. Figure 4 shows a block diagram of the telluric amplifier.

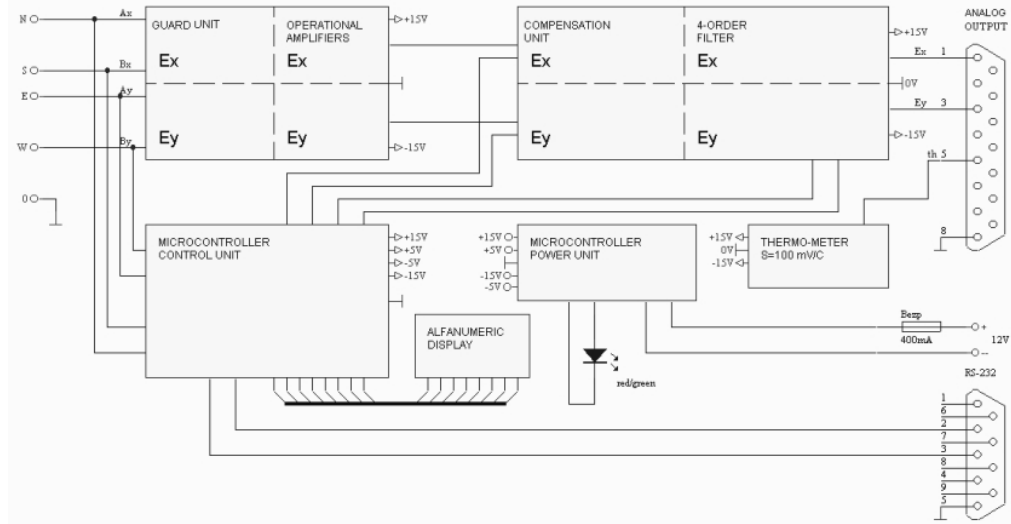


Fig. 4. Block diagram of telluric amplifier TWG-0501.

The filters are of 4-th order of Sallen Key with a cut-off frequency of 4 s. The filters of both channels possess very similar parameters. We show their characteristics in Figs. 5 and 6.

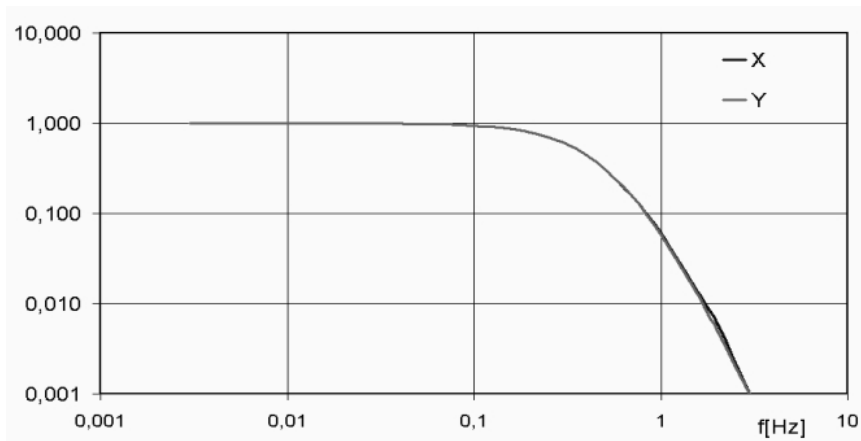


Fig. 5. Amplitude characteristic of the amplifier.

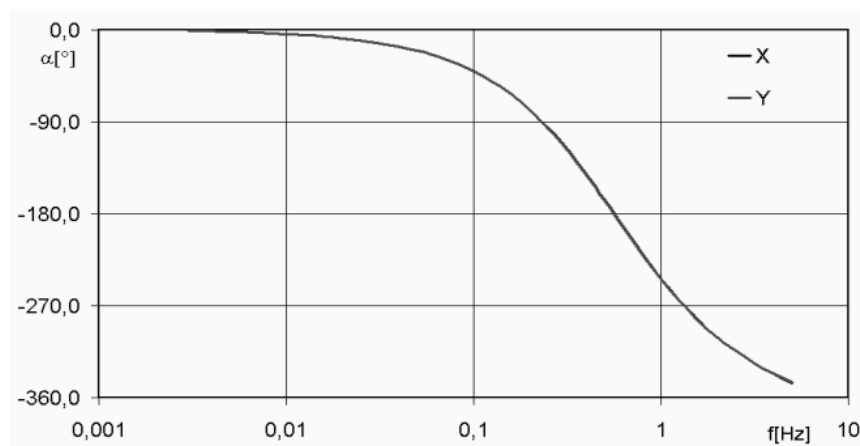


Fig. 6. Phase characteristic of the amplifier.

The amplifier possesses a detailed setup, where all working parameters can be adjusted. An additional digital calibration based on given memorized voltage and resistance patterns provides a fast correction of parameters even under field conditions by means of a simple calibrator. A remote control is enabled by means of a RS-232 port and standard terminal programs.

Due to this, no special software is necessary for a remote control of the amplifier. The software "Hyper terminal" for Windows, "Minicom" for Linux or "Mirror" for DOS is sufficient. A control of the amplifier by means of a local network "LAN" is also possible. See Fig. 7 for an example of control of such a kind.

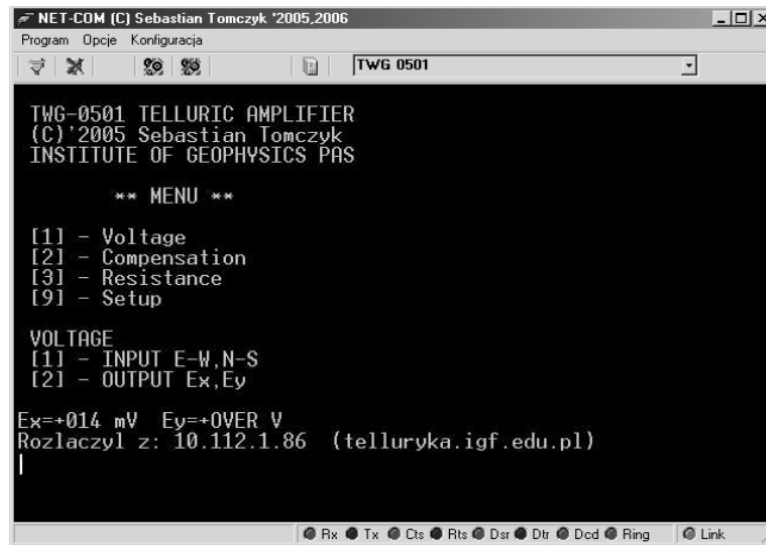


Fig. 7. Operation of the amplifier.

Conclusions

The presented telluric amplifier proved to be the best one in practical applications, especially for field measurements. The automatic compensation for the constant value improves the data quality, and the remote control enables to check the telluric lines in case of difficult access to the place of measurement.

Accepted February 7, 2007

Project of Absolute Three-Component Vector Magnetometer Based on Quantum Scalar Sensor

Anton VERSHOVSKIY

Ioffe Phys.-Tech. Institute
26, Polytechnicheskaya, St.-Petersburg, 194021 Russia
e-mail: antver@mail.ru

A b s t r a c t

A project of vector magnetometer of new kind based on optically pumped quantum M_x -sensor placed in symmetrical magnetic coils system is proposed and mathematically proved. The device uses a new method of the fast precision measurement of three Earth magnetic field (EMF) vector components providing absolute accuracy of the order of 0.1 nT at 0.1 s sampling rate. Absoluteness here implies that the process of measurement changes the measured parameter, i.e., field component value, no more than by the value determined by the sensitivity of scalar sensor. The short-term resolution of the method is determined by the M_x -sensor sensitivity.

1. Introduction

There are different systems using for measuring magnetic field vector a scalar sensor placed into the coil system, (i.e., Fairweather 1972). Particularly, it is well known that any component of magnetic field can be measured by measuring the field scalar value – provided that two orthogonal components are compensated down to zero with a special magnetic coils system. This method does not require high compensation accuracy, since according to vector addition rules the contribution of small residual orthogonal component is to high extent suppressed in the presence of a big non-compensated component.

However it is difficult to build a real three-component device based on this method because the compensation of any field component requires relatively strong compensating magnetic field; therefore, procedures of measuring of three field components by this method must be separated in space or in time. Besides, a very fast scalar magnetometer is needed in order to follow field jumps arising when switching from one component measurement to another.

The main point of the method proposed here lies in creation of a system of compensating fields around the sensor, harmonically changing in such a way that the total field vector in the sensor would rotate, keeping its length, around the initial field direction and during each rotation cycle would pass through three different points, two components of the field in each compensated with high accuracy and third component not compensated at all so it can be measured.

As a scalar device we propose cesium or potassium optically pumped magnetometer registering oscillating signal of transverse magnetization of the atoms in the cell – so-called quantum M_x -magnetometer, characterized with high accuracy and speed.

The suggested method is applicable to wide field range, though its application for precise measuring of EMF components is most obvious, because of EMF high homogeneity and relatively small variations.

The mathematical model of the magnetometer based on these principles was built and the behavior of the device was modeled numerically. Numerical modeling shows that using standard Cs sensor with 20 nT resonance linewidth one can achieve about 0.015 nT r.m.s. sensitivity in each field component at 0.1 s sampling rate, accompanied by 0.1 nT absolute accuracy – provided that coil constants do not vary by more than 100 ppm and coil axes directions do not vary by more than 0.6°.

2. Description of the Method

The scalar quantum sensor is supposed to be placed in the center of a symmetric three-component system of magnetic coils. The system is oriented so that both the principal diagonal of the cube inscribed into the system of coils and the symmetry axis of the sensor are directed along the Earth magnetic field \mathbf{H}_0 . The coordinate system we choose is rigidly bound to the axes of the coil system, so all three components of the Earth magnetic field vector in this coordinate system are initially equal in magnitude: $H_X = H_Y = H_Z = |\mathbf{H}_0| / \sqrt{3} = H_0$.

The field H_{ACi} in each coil ($i = X, Y, Z$, the subscripts AC indicate oscillating values) is initially chosen to provide complete compensation for the relevant component of the Earth magnetic field \mathbf{H}_i . In practice, the initial choice of the fields and the orientation of the coil system are implemented using a priori information about the measured field vector. After that, all the components are being automatically compensated using a system of feedback loops.

When the compensating fields are turned on simultaneously in all three coils, the total field at the sensor vanishes. Switching the field of the i -th coil off ($i = X, Y, Z$) leads to the appearance of the corresponding uncompensated i -th component which can be measured by the sensor. The accuracy of the measurement, in this case, is by a few orders of magnitude higher than the accuracy of compensation for the orthogonal components of the field, because the contribution ΔH of the uncompensated orthogonal component ΔH_i is proportional to $1 - \cos(\alpha)$, where α is a small angle ($\alpha \sim \Delta H_i / H_i$).

Taking as an example the measurement of the X-component, let us estimate the requirements to the accuracy of the transverse component compensation. Let us as-

sume that the module of the measured field equals 50000 nT, so the mean value of any field component $|\mathbf{H}_i| = |\mathbf{H}_0|/\sqrt{3} \approx 28867$ nT, and the error introduced into the measurement of the X-component due to inaccuracy in compensation for the Z-component should not exceed $\Delta H_x = 0.1$ nT. Therefore, the maximum value of the field in the Z-component is $\Delta H_z = H_i \cdot \sin[\arccos(1 - \Delta H_x / H_x)]$; in the presence of two components that are simultaneously not completely compensated, $\Delta H_y = \Delta H_z = 54$ nT. In other words, the relative error of the transverse component compensation may reach $1.8 \cdot 10^{-3}$. It means that the coil system may be manufactured using any material that provides constancy of geometrical shape of the system (orthogonality of the coils) with no special requirements to the size stability of the coil system.

A cycle of such measurements over $i = X, Y, Z$ will provide full information about all three components of the field. This information, in turn, is used to adjust the values of the compensating fields $H_{ACX}, H_{ACY}, H_{ACZ}$ in the coils X, Y, Z by means of three feedback loops.

The next step consists in changing from discrete measurements of the field to continuous or quasi-continuous measurements: we make the field rotate continuously or quasi-continuously (discretely, with a small step) in such a way that three points on the rotating vector hodograph meet the above conditions $H_{ACi} = 0$ ($i = X, Y, Z$). The total magnetic field vector, in this case, is always tilted by 35.2° with respect to the axis of optical pumping of the M_x -magnetometer. Thus, one may provide continuity of locking the resonance, and real measurements are made in three points of the rotation circle. It is important that the measurement of the component H_i is performed, as before, at the moment when the corresponding compensating field H_{ACi} is turned off, and only the compensating fields orthogonal to H_i are on. In this way, the absolute measurements of the field components are realized.

3. Discussion

Let us discuss the main drawbacks of this method and possible ways of their elimination:

1. The requirements to orthogonality of the coils are rather severe, namely, the limitation of the error by the value 0.1 nT leads to the requirement on orthogonality of the coil axes on the level of $3 \cdot 10^{-6}$ or $0.6''$ which can be hardly achieved. Therefore, the non-orthogonality of the coils in the system should be measured periodically and should be compensated electronically. Then the estimate of $0.6''$ will refer to variation of the angles between the coils of the system. The procedure of calibration of the systems characterized by a no ideal orthogonality of the axes is described in (Merayo 2000).

2. The inertness of the magnetic coils and of the sensor will lead to a delay in the measurement of the magnetic field and, as a consequence, to a shift of the points on the circle in which the measurements are made. Negative effect of this delay is rather small, but if the system is required to be fast, the most efficient way to suppress the effect of this delay is to create conditions when the direction of the magnetic field constantly coincides with the principal axis of the system.

3. The constancy of the module of the magnetic field upon its rotation holds only for small angular deviations of the measured magnetic field from the axis of the coil system. For large angular deviations of the field, the rate of variation of the field module upon its rotation increases which may reduce the accuracy of the measurements. Two last drawbacks may be eliminated by continuous compensation for the field variations using (a) slow compensating fields H_{DCi} of the coils – in this case, the method partly loses its absoluteness, or (b) using a mechanical servo-system. This last method does not affect the absoluteness of the measurements, but is much more complicated.

In both cases, the additional slow feedback systems provide constancy of the total magnetic field module in all points of the rotation circle. The closely lying points of the circle become equivalent; this fact strongly mollifies the requirements to the accuracy of choosing the points on the circle and makes it possible to pass from measuring the magnetic field in three points on the circle to measuring on the whole circle detecting vector signal from this measurement.

4. The rotation of the magnetic field at a frequency of ω around the axis of the M_x -sensor is known to cause a shift of the measured field strength by the value $\pm\omega/\gamma$ (where γ is the gyromagnetic ratio) depending on the rotation direction (the so-called gyroscopic effect). However, since the rotation rate is known, this effect can be easily taken into account without the loss of the accuracy of the measurements.

4. Numerical Simulation

We have numerically tested two models: (1) with the measurements in three points of the circle and (2) with synchronous detection of the signal over whole circle as mentioned above. Both models were examined: (A) with no system of compensation for the field variations and (B) with the systems of compensation. It was assumed that the compensation for the field variations and the field modulation are performed using the same coils.

We simulated the systems with a potassium sensor with the resonance line width $\Gamma = 1$ nT, as well as the systems with a cesium sensor ($\Gamma = 20$ nT) characterized by the intrinsic short-term sensitivity $\sigma_{0.1s} = 10$ pT r.m.s. As expected, the use of the sensor with a broad resonance line, at the expense of reduced sensitivity, provided advantages both in the width of the frequency locking range and in the field tracking speed.

Our test showed the best results when using model 2B (signal detection over the whole modulation period and with the field variation compensation) with Cesium sensor; it has shown the following values of the parameters:

- absolute accuracy $|\delta H_i| = 0.1$ nT;
- response time $\tau = 0.1$ s;
- short-term (0.1 s) sensitivity in the field components $\sigma_i = 0.015$ nT r.m.s.;
- the range of tracking of the field variations $|\Delta H_{i\max}| > 1000$ nT;
- the maximum allowable variation of the angle between coils $|\Delta\beta| = 0.6^\circ$;
- the maximum allowable drift of the magnetic coil system: $|\Delta k_{i\max}| = 115$ ppm.

When using a mechanical servo-system instead of electronic system of compensation for the field variations, the admissible drift of the magnetic coil system may reach ± 1350 ppm.

5. Conclusion

The numerical tests of the new method show that, using an optically pumped M_x -magnetometer and a three-component symmetric magnetic coils system, it is possible to simultaneously measure all three components of the Earth magnetic field with an absolute accuracy of ± 0.1 nT short-term (0.1 s) and sensitivity of 0.015 nT r.m.s at 0.1 s time.

Acknowledgments. Author is grateful to E.B. Alexandrov and A.S. Pazgalev for helpful discussions of the idea.

References

- Fairweather, A.J., and M.J. Usher, 1972, *A vector rubidium magnetometer*, J. of Physics E: Scient. Instr. **5**, 986-990.
- Merayo, J.M.G., *et al.*, 2000, *Scalar calibration of vector magnetometers*, Meas. Sci. Technol. **11**, 120-132.

Accepted January 29, 2007

Fast 3-Component Variometer Based on a Cesium Sensor

A. VERSHOVSKIY¹, M. BALABAS², A. IVANOV², V. KULYASOV²,
A. PAZGALEV¹ and E. ALEXANDROV¹

¹Ioffe Phys.-Tech. Institute
26, Polytechnicheskaya, St.-Petersburg, 194021 Russia
e-mail: antver@mail.ru

²S.I.Vavilov State Optical Institute
14 Birzhevaya, St.-Petersburg, Russia
e-mail: mbalabas@yandex.ru

Abstract

New compact and fast three-component variometer measuring the total terrestrial magnetic field intensity in 20÷65 μT range and two transverse components in $\pm 1 \mu\text{T}$ range is presented. The reproducibility of the field components measurements is 0.15 nT, the noise-limited sensitivity is 0.01 nT r.m.s. or 0.25" at 0.1 s sample rate.

1. Introduction

In this paper, we present a vector magnetometer-variometer intended for simultaneous measurement of the total terrestrial magnetic field intensity in 20÷65 μT range and two transverse components in $\pm 1 \mu\text{T}$ range with a rate of up to ten measurements per second. The device is an implementation of the idea of a vector magnetometer based on a scalar sensor placed in a variable magnetic field (Fairweather 1972). The main features distinguishing the variometer from predecessors are the use of an optically pumped M_x -sensor (Alexandrov *et al.* 1996) and a continuous fast rotation of the transverse magnetic field. The same concept underlies the potassium magnetometer-variometer described in (Alexandrov *et al.* 2004). The idea is to place a fast quantum magnetometer at the center of a highly stable magnetic coils system producing magnetic field rotating around the geomagnetic field vector. As long as the magnetic coils system is aligned along geomagnetic field, the field detected by the sensor does not contain fast modulation; the situation changes if geomagnetic field deflects from the coils system axis – the field detected by the scalar sensor becomes modulated. If the modulation amplitude is not too big, the M_x -sensor is capable of following it. From the

amplitude and phase of modulation the information about value and direction of the field deflection can be extracted; this information is used for creating fields compensating the field deflection.

2. Operation of the Device

Our variometer consists of a Cs magnetic sensor and a quartz coils system that are integrated into a 23×23×23 cm case mounted on a tilted quartz support, as well as of a pumping lamp and a microprocessor-controlled electronic unit positioned at a 2-3 m distance from the sensor.

The coil system is a combination of a precision solenoid with the axis directed along the geomagnetic field vector and two coils producing mutually orthogonal fields in the plane perpendicular to the solenoid axis. The coils are excited by a sinusoidal current with frequency f (several tens or hundreds of hertz) so that their current phases are shifted by 90° relative to each other. As a result, the coils produce a field rotating with frequency f in the plane perpendicular to the geomagnetic field. A direct current passing through the solenoid induces a magnetic field compensating for $\sim 95\%$ of the geomagnetic field. When all three currents are switched on simultaneously, the vector of a magnetic field formed at the center of the system precesses about the geomagnetic field with an apex angle of about 45° .

The frequency of magnetic resonance detected by M_x -sensor depends on the magnetic field in the coil system, which, in turn, depends on remaining longitudinal magnetic field and the amplitude of the rotating transverse field. The magnetic resonance frequency remains constant if the external field is stable and the ring system axis is perfectly aligned with the field.

When the geomagnetic field transverse components change, the precession axis of the net magnetic field vector at the center of the system is deflected from the geomagnetic field vector. This leads to the modulation of the field magnitude at frequency f . A digital feedback system tracking the resonance frequency directly detects this modulation, and produces two orthogonal fields that completely compensate for these transverse components. The direct currents in the transverse coils become a measure of variation of the geomagnetic field transverse components. The longitudinal component of the compensated geomagnetic field can be found from the magnitude of the resultant field vector, solenoid current and the rotating component amplitude.

The 95% compensation of longitudinal magnetic field mentioned above allows one to increase approximately 10 times the angle between the rotating magnetic vector and the axis of rotation and to raise correspondingly the transverse sensitivity of the device.

Cesium was chosen as an appropriate working substance for the M_x -sensor because of a small quadratic splitting of magnetic lines into sub-levels. In magnetic field H , the resonance band of Cs appears as a set of equidistant lines spaced at $26.6 \text{ Hz} \cdot H^2$, where H is measured in gauss. In applied small magnetic field of 0.07 G, the spacing is about 0.13 Hz, which is much smaller than the width of each of the lines. Thus, all the lines actually merge into an intense and nearly symmetric resonance. This ensures

a low systematic error in measuring the field longitudinal component. On the other hand, relatively big linewidth of cesium resonance (comparing to potassium) provides faster sensor response.

3. Experiment

The variometer was tested in both a magnetic shield and a magnetic field stabilizer. All the measurements were carried at a temperature kept at $(22\pm 2)^\circ\text{C}$.

The test results show that, when the parameters are adjusted to a maximal variation sensitivity, the geomagnetic field transverse components allowing the capture of the magnetic resonance signal do not exceed ± 100 nT, otherwise the signal frequency modulation becomes too strong for M_x -sensor to follow the resonance frequency. The initial range of capture was extended ± 750 nT by complicating the capture algorithm. As soon as the device is locked, the maximal variation of transverse field components is ± 1000 nT.

The effective time constant T in the transverse (x and y) channels varies from 0.03 to 1 s depending on the amplification factor in the feedback loops. In subsequent experiments, the parameters were taken such that T fell into the range between 0.1 and 0.15 s. It was shown that the standard deviation of the variometer intrinsic noise in the transverse channels lies within 0.010 nT for measurement time of 0.1 s.

We also analyzed the start-to-start reproducibility of the variometer: the deviation did not exceed ± 0.15 nT. Admittedly, the long-term stability was not investigated to the full extent. To reach a stability within ± 0.1 nT in the z channel requires further exploration and minimization of drifts.

An automatic procedure of calibration of the constants of the x , y , and z coils, as well as of their cross-constants was developed and implemented in the device algorithm.

4. Conclusion

The vector magnetometer-variometer presented in this paper can be used as an instrument for geophysical observatories; it is characterized by a combination of high transverse sensitivity, data reproducibility, and speed.

Acknowledgments. Authors thank V. Shifrin and E. Choporova for the help in testing the device at the magnetic station of the Institute of Metrology (VNIIM).

References

- Alexandrov, E.B., M.V. Balabas, A.S. Pazgalev, A.K. Vershovskii and N.N. Yakobson, 1996, *Double-resonance atomic magnetometers: from gas discharge to laser pumping*, Laser Physics **6**, 244-251.

- Alexandrov, E.B., M.V. Balabas, V.N. Kulyasov, A.E. Ivanov, A.S. Pazgalev, J.L. Rasson, A.K. Vershovski and N.N. Yakobson, 2004, *Three-component variometer based on a scalar potassium sensor*, Meas. Sci. Technol. **15**, 918-922.
- Fairweather, A.J., and M.J. Usher, 1972, *A vector rubidium magnetometer*, J. Physics E: Scient. Instr. **5**, 986-990.

Accepted January 29, 2007

Extending Magnetic Observations to Seafloor: the Case of GEOSTAR and ORION Missions in the Adriatic and Tyrrhenian Seas

Angelo DE SANTIS^{1,2}, Domenico DI MAURO¹, Lili CAFARELLA¹,
Paolo PALANGIO¹, Laura BERANZOLI¹, Paolo FAVALI^{1,3} and Sergio VITALE²

¹ Istituto Nazionale di Geofisica e Vulcanologia
Via di Vigna Murata 605, 00143 Roma, Italy
e-mail: desantisag@ingv.it

² Università "G.D'Annunzio"
Via dei Vestini 30, 66013 Chieti Scalo, Italy

³ Università degli Studi "La Sapienza", Roma, Italy

Abstract

GEOSTAR (1 and 2) and ORION-GEOSTAR 3 seafloor missions have been performed in the frame of a European project whose main objective is the deep-sea investigation by means of an automatic multidisciplinary observatory. During the three GEOSTAR missions it has been possible to acquire scalar and vector magnetic data, useful to improve global and regional geomagnetic reference models and to define sub-surface electric conductivity structure. In this work, after a brief description on the calibration and orientation of acquired data, we propose some estimations of the electrical conductivity of the lithosphere beneath the three different measurement sites.

1. Introduction

The external part of the Earth's Magnetic Field (shortly EMF) generates electromagnetic (EM) waves that penetrate in the Earth's interior down to the crust and the mantle. Using magnetovariational (MV) techniques (such as the Geomagnetic Deep Sounding, GDS), which record induction magnetic fields from such sources over an appropriate magnetometric array, it is possible to find some geoelectric properties that characterise sub-surface structures.

During the recent years it has also been possible to adapt such "inland" techniques directly to the seafloor observations. GEOSTAR (*GEophysical and Oceano-*

graphic Station for Abyssal Research) missions belong to a large European program, directed by the Istituto Nazionale di Geofisica e Vulcanologia (INGV), that has as the main target the deep-sea submarine investigation, for long periods, with an automatic multidisciplinary station with the characteristics as close as possible to those of an observatory, in relation with the extremely harsh environmental conditions of working. In Europe, GEOSTAR project is unique and it has been implemented since 1995 in two successive phases (GEOSTAR and GEOSTAR-2), and then integrated in 2002-2005 by the ORION-GEOSTAR-3 (*Ocean Research by Integrated Observation Network*) project with the purpose to develop a network of seafloor observatories, validated in the bathyal plain of the Tyrrhenian Sea (Marsili Basin). Some information about this and other seafloor projects can be found in a recent review (Favali and Beranzoli 2006).

The organisation of this paper is the following: after this introduction, next section will introduce the seafloor observations, then we will focus on GEOSTAR and ORION missions, with particular attention to magnetic instruments and acquired magnetic data. The fourth section will describe some of the MV techniques used to estimate the mean conductivity of the lithosphere under the three sites of seafloor measurements, as indicated in the fifth section. Conclusions will summarise some of the main results, and will anticipate some of the future developments.

2. Seafloor Observations

For a complete geomagnetic field analysis, it would be necessary to make EMF measurements on the whole Earth's surface and above. Land recordings alone are not sufficient for this purpose and, since the Earth's surface is covered by oceans and seas for about 2/3, to record the geomagnetic field as much completely as possible, it is necessary that we take measurements also in areas covered by seas, for instance on the seafloors.

Seafloor magnetic measurements are much more difficult than inland measurements. Main problems could arise from the increase of pressure with depth (about 0.1 atm/m), instruments corrosion (especially for long periods of running, such as more than a few months), difficulties on vector instruments orientation according to the geographical directions NS-EW and production of EM field due to dynamo action of the sea water motion (mean conductivity $\sigma_w \approx 3-6$ S/m) within the EMF, which is added to the typical field otherwise recorded by the magnetometers. On the contrary, some clear advantages are evident, such as the temperature stability in time (change of temperature can influence magnetometer quality), the improvement of the planetary distribution of the magnetic data, the screening effect of the water column from some external EM fields and the expected high magnetic S/N ratio.

3. GEOSTAR and ORION Missions

During GEOSTAR, GEOSTAR-2 and ORION-GEOSTAR-3 missions it has been possible to monitor the solid Earth's processes (such as seismicity, geomagnetic and gravity fields) and physical, geochemical and biological processes with impact on

global changes (e.g., geo-hazards, carbon's cycle, origin of life, climatic oceanography). In terms of EMF observations, the project has given significant contribution for: (1) the feasibility for the realisation of an equal distribution of observatories in all the world to improve the reliability of global and regional magnetic field models; (2) the study on temporal variations of the magnetic field from short to long periods (seconds to years); (3) the investigation of the conductivity structures within the Earth by means of MV techniques; (4) the study of the EMF radial variation in correspondence with *Oersted* (1999 – present) and *CHAMP* (2000 – present) satellite missions. Table 1 summarises the main information about the three GEOSTAR missions. Figure 1 shows the locations of the deployments and in Table 2 there are some more information about acquired magnetic data.

Table 1
The three GEOSTAR missions
(see also Favali *et al.* 2006)

| Projects | Project years | Location of main seafloor mission | Depth (m) | Period of acquisition |
|-----------------|---------------|-----------------------------------|-----------|------------------------------------|
| GEOSTAR | 1995-1998 | Adriatic Sea, Offshore Ravenna | -42 | Aug.-Sep. 1998 (21 days) |
| GEOSTAR-2 | 1999-2001 | Tyrrhenian Sea, Ustica | -1950 | Sept. 2000 – Apr. 2001 (205 days) |
| ORION-GEOSTAR-3 | 2002-2005 | Tyrrhenian Sea, seamount Marsili | -3320 | Nov. 2003 – May 2005(*) (477 days) |

(*) This mission was subdivided in two sub-missions:
1st Part: from 14/12/03 to 26/04/04; 2nd Part: from 14/06/04 to 23/05/05.

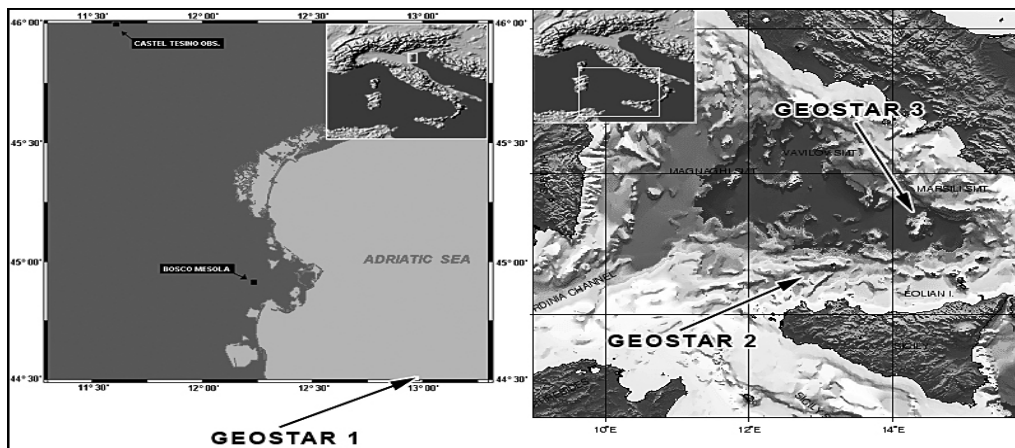


Fig. 1. Locations of the deployments for the three GEOSTAR seafloor missions.

Table 2
Magnetic data acquired during the three GEOSTAR seafloor missions
(see also De Santis *et al.* 2006)

| Seafloor mission | Instrument | Percentage of acquired data |
|--|---|-------------------------------------|
| GEOSTAR | Vector horizontal suspended magnetometer (X, Y) | almost 100% |
| | Scalar magnetometer (F) | almost 100% |
| GEOSTAR-2 | Vector suspended magnetometer (X, Y, Z) | almost 100% |
| | Scalar magnetometer (F) | around 8% (*) |
| ORION-GEOSTAR-3 | Vector suspended magnetometer (X, Y, Z) | 0% (1st Part) (**), 100% (2nd Part) |
| | Scalar magnetometer (F) | 100% (1st Part), 42% (2nd Part) |
| (*) An electronic device failure reduced the sampling rate from 1 value/minute to only 1 value every 12 minutes. (**) A mechanical damage of the vector magnetometer during deployment prevented from having X, Y, Z measurements in the 1st part of mission. | | |

3.1 GEOSTAR schematic principle of operation

GEOSTAR module consists of two modules, the mobile docker vehicle (called MODUS – MOBILE Docker for Underwater Sciences) and the bottom station (Fig. 2). MODUS is used for the bottom station positioning/recovering, system check and bidirectional communication between ship and bottom station, when it is connected to the vehicle. The bottom station hosts: power supply, all the acquiring instruments, acquisition and control system, and communications devices.

A scalar magnetometer and a vector magnetometer are placed at the ends of two booms at two opposite corners of the bottom station which are taken vertical during the deployment. Once on the seafloor, the bottom station extends its arms, in this way the magnetometers are more distant from GEOSTAR main frame to reduce EM disturbances as much as possible. Finally, MODUS is disconnected from the station and recovered by the ship. Table 3 lists the main features of magnetometers. Recorded data are stored both in on-site hard-disks and in particular capsules, named *messengers*, which are periodically released by the station to reach the sea surface (GEOSTAR-2 configuration). There are also available other communication systems: a bidirectional acoustic transmission system between ship and bottom station, and another in which a surface buoy serves as radio/satellite bridge communications between the underwater observatory and inland station (see e.g. Favali *et al.* 2006).

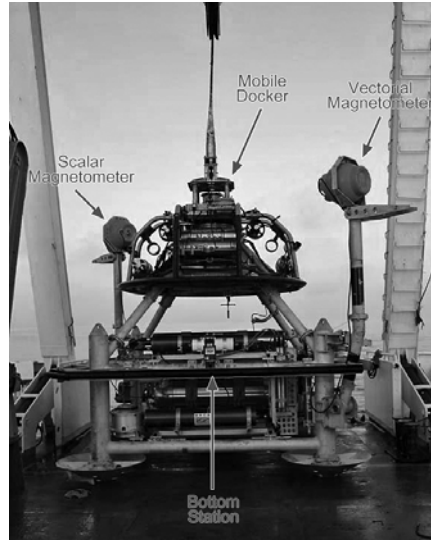


Fig. 2. GEOSTAR module (bottom station with MODUS on its top) in GEOSTAR-2 configuration on the deck of R/V Urania before deployment (Favali *et al.* 2006).

Table 3

Main features of magnetometers

| Instrument type | Resolution | Power consumption | Absolute accuracy | Sampling rate |
|--|------------|-------------------|-------------------|---------------|
| Three axial suspended fluxgate magnetometer, designed and built by INGV Labs (*) | 0.1 nT | 2 W | 5-10 nT | 6 values/min |
| Scalar magnetometer (Overhouser effect) adapted GEM System | 0.1 nT | 1 W | 1 nT | 1 value/min |

(*) During GEOSTAR a two horizontal component magnetometer was used with similar characteristics of the three axial fluxgate

3.2 Magnetometer calibration and GEOSTAR frame orientation

The recorded data cannot be directly used for analysis and a calibration was necessary to remove the magnetic signature of the whole GEOSTAR system. Also the GEOSTAR frame had to be mathematically re-oriented in relation with geomagnetic North (De Santis *et al.* 2006).

The compensation value has been obtained by the relation that links the reference MF (taken from L'Aquila Observatory, Italy) with the recorded GEOSTAR MF (\mathbf{B}_{GS}), together with permanent (\mathbf{B}_{perm}) and induced fields, due to the GEOSTAR structure:

$$\vec{B}_{ref} = \vec{B}_{GS} - \vec{B}_{perm} - \delta \cdot \vec{B}_{GS}, \quad (1)$$

where δ is a 3×3 constant coefficients matrix which characterizes the induced field (found negligible). So for the permanent contribution of the field, the following values have been estimated: $B_{x_{perm}} = 1075.4 \pm 0.8$ nT, $B_{y_{perm}} = 448.2 \pm 3.0$ nT, $B_{z_{perm}} = 1077.6 \pm 1.0$ nT. Also the scalar magnetometer needed a systematic correction of -295 nT on its recordings.

A rough estimation of the GEOSTAR frame orientation with respect to geographical north was made during every release of the bottom station with the integrated compass 3D-ACM (three-component Acoustic Current Meter). Nevertheless, a more accurate evaluation of the GEOSTAR frame orientation was estimated comparing magnetic data (particularly the horizontal components X and Y of the EMF) recorded by GEOSTAR with the analogous data from Gibilmanna, L'Aquila and Ustica ground stations, the latter station specifically installed during the GEOSTAR-2 mission. Such comparison was resolved with a least squares regression obtaining an orientation angle of around -120° for GEOSTAR 2 and -242° for GEOSTAR 3. For GEOSTAR it was not retained necessary to effect such operation.

4. MV Techniques

Among the MV techniques, GDS (*Geomagnetic Deep Sounding*) provides information about the lateral contrasts of electrical conductivity in the Crust and in the upper mantle. From the knowledge of the geomagnetic Cartesian components, it is possible to estimate by least squares regression the transfer functions, $A(f)$ and $B(f)$, that relate the vertical component Z with the horizontal ones, X and Y , in the frequency domain:

$$Z(f) = A(f) X(f) + B(f) Y(f). \quad (2)$$

From the transfer functions it is then possible to determine the induction arrows. They represent pseudo-vector entities that undergo a distorted MF near the interface among two different conductivity media. Module and phase, real and imaginary parts of induction arrows can be expressed as:

$$\begin{aligned} V_r(f) &= \sqrt{[\operatorname{Re} A(f)]^2 + [\operatorname{Re} B(f)]^2}, & \Theta_i(f) &= \operatorname{arctg} \frac{\operatorname{Im} B(f)}{\operatorname{Im} A(f)} \\ V_i(f) &= \sqrt{[\operatorname{Im} A(f)]^2 + [\operatorname{Im} B(f)]^2}, & \Theta_r(f) &= \operatorname{arctg} \frac{\operatorname{Re} B(f)}{\operatorname{Re} A(f)} \end{aligned}$$

where V_r , V_i = real and imaginary modules of the induction arrows, respectively; Θ_r , Θ_i = real and imaginary phases of the induction arrows, respectively. In the Wiese convention (with phases as indicated above) the induction arrows point towards the less conductive medium (Wiese 1962), while in the Parkinson convention (adding 180° to the phases indicated above) the induction arrows point to the higher conductive medium (Parkinson 1962).

An important parameter to consider in the MV techniques is the skin depth. For an EM variation of period T (in minutes) in a medium of conductivity σ (in S/m), the

skin depth δ (in km) is the propagation distance over which EM waves are attenuated by a factor $1/e$, we can write:

$$\delta = 3.9 (T/\sigma)^{1/2}. \quad (3)$$

Ionospheric fields act as polarising fields, and the usable periods in the sea are between $5 \text{ h} > T > 3 \text{ min}$, this because variations with smaller periods are screened while those with greater periods do not satisfy the condition $k^2 < 2\pi\mu\sigma/T$ (k = spatial wavenumber, μ = magnetic permeability). Moreover, it is necessary also to consider the induced fields by sea currents and tides, the latter with typical periods $T = 1$ and $T = 1/2$ day. If we consider the inclusive zone among the sea surface and the seafloor, we can observe that the external part of the EMF generates, above the surface, a time variable electric current and, in turn, this produces an induced current system in the seawater in association with a magnetic field; the complex EM system will induce another MF also beneath the seafloor (Fig. 3). For this reason, in order to reduce seawater motion effects on our transfer functions estimations, we can consider our analysis to be valid only when $R(f) = H_1(f)/H_0(f) < 1$ (e.g., Palshin *et al.* 1995), where: H_0 and H_1 are the EMF horizontal components recorded at the surface and on the seafloor respectively (Fig. 3). In this way the transfer functions that are considered effective are only those corresponding with the frequencies where the EM signal provides $R < 1$.

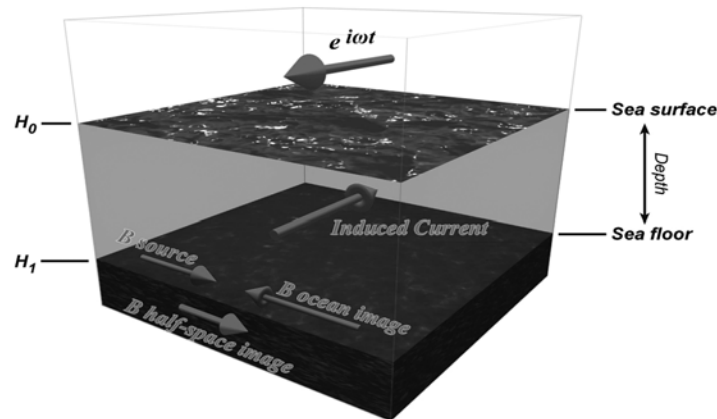


Fig. 3. EM fields system in sea environment (adapted from Jegen 1997).

5. Preliminary Estimations of the Mean Lithospheric Conductivity

Using the technique exposed above, it has been possible to obtain the induction arrows relative to the three different missions (not shown here; Vitale 2006). A reasonable assumption is that the EM lithospheric depth corresponds to the skin depth associated with the period showing the main clear contrast of direction in the induction arrows. Under this simple hypothesis, and imposing the lithospheric depths as obtained by seismological studies (Calcagnile and Panza 1981) for the three sites of

GEOSTAR deployments, it is possible to find the following mean conductivities as derived from equation (3) when considering periods T and skin depths δ : 10^{-2} S/m with $T = 17-20$ min and $\delta \approx 80$ km for the Adriatic Sea, 10^{-1} S/m with $T = 4-5$ min and $\delta \approx 40$ km for GEOSTAR-2 and around 1 S/m with $T = 15$ min and $\delta \approx 20$ km for ORION-GEOSTAR-3, respectively. Figure 4 shows a lithosphere depth map estimated from seismic studies and the corresponding lithospheric depths under the three GEOSTAR missions.

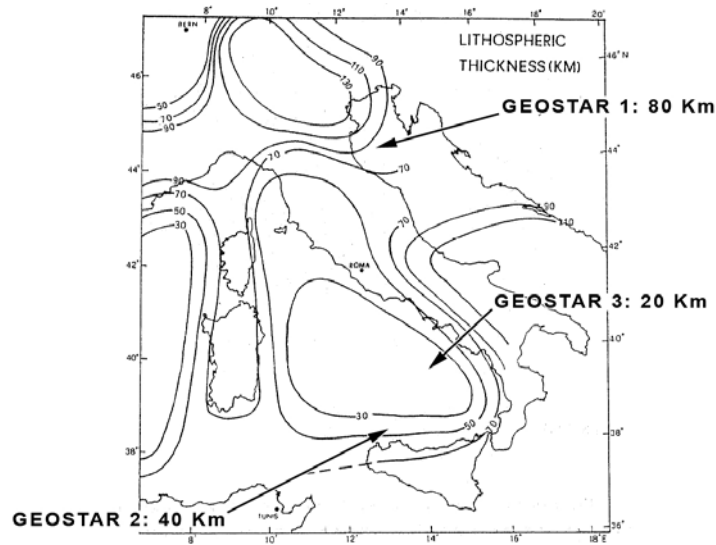


Fig. 4. Lithospheric depth map (Calcagnile and Panza 1981) with specific lithosphere depth values for the three GEOSTAR missions.

6. Conclusions

The seafloor GEOSTAR, GEOSTAR-2 and ORION-GEOSTAR-3 missions have provided an important magnetic dataset, useful both to the possible definition of conductivity structures underneath the seafloor, and to improving the geomagnetic models. We have shown that, with simple arguments, it is possible to estimate the mean lithosphere electrical conductivity under the three points of GEOSTAR deployment obtaining decreasing values of conductivities from the first site to the most recent one. Of course, more analyses will be needed, both in time and frequency domain, to uncover more details and properties of the Tyrrhenian and Adriatic crust and mantle, and possibly to independently estimate the lithospheric depth together with the corresponding electrical conductivity. Future analysis will include forward and inversion modeling of the acquired data during the three seafloor missions.

Acknowledgments. The GEOSTAR and ORION projects were funded by the EC under the Marine Science and Technology Programme. We thank all the people who were involved directly or indirectly in both projects.

References

- Calcagnile, G., and G.F. Panza, 1981, *The main characteristics of the lithosphere-asthenosphere system in Italy and surrounding regions*, Pure Appl. Geophys. **119**, 865-879.
- De Santis, A., D. Di Mauro, L. Cafarella, R. D'Anna, L.R. Gaya-Piquè, P. Palangio, G. Romeo and R. Tozzi, 2006, *Deep seafloor magnetic observations under GEOSTAR project*, Annals of Geophysics **49**, 2/3, 681-693.
- Favali, P., and L. Beranzoli, 2006, *Seafloor Observatory Science: a review*, Annals of Geophysics **49**, 2/3, 515-567.
- Favali, P., L. Beranzoli, G. D'Anna, F. Gasparoni, J. Marvaldi, G. Clauss, H.W. Gerber, M. Nicot, M.P. Marani, F. Gamberi, C. Millot and E.R. Flueh, 2006, *A fleet of multi-parameter observatories for geophysical and environmental monitoring at seafloor*, Annals of Geophysics **49**, 2/3, 659-680.
- Jegen, M.D., 1997, *Electrical properties of the mantle upwelling zone beneath a mid ocean ridge, an application of vertical gradient sounding*, [Thesis] University of Toronto, 178 pp.
- Palshin, N.A., Yu.M. Abramov, A. De Santis, A. Meloni, A.M. Poray Koshits, V.S. Shneyer and L.M. Abramova, 1995, *Magnetovariational gradient sounding the Tyrrhenian Basin*, Physics of the Solid Earth **31**, 4, 352-355.
- Parkinson, W.D., 1962, *The influence of continents and oceans on geomagnetic variations*, Geophys. J. Roy. Astron. Soc. **6**, 4, 441-449.
- Wiese, H., 1962, *Geomagnetische Tiefentellurik, II, Die Streichrichtung der Untergrundstrukturen des elektrischen Widerstandes, erschlossen aus geomagnetischen Variationen*, Geofis. Pura Appl. **52**, 83-103.
- Vitale, S., 2006, *Studi magnetovariazionali per l'indagine sulle proprietà geoelettriche del fondale marino del Tirreno meridionale (Magnetovariational studies of geoelectric properties of Southern Tyrrhenian seafloor)*, [Thesis] Università "G. D'Annunzio", Chieti, 190 pp.

Accepted February 12, 2007

Comparison of Observatory Data in Quasi-Real Time

Krzysztof NOWOŻYŃSKI and Jan REDA

Institute of Geophysics, Polish Academy of Sciences
ul. Księcia Janusza 64, 01-452 Warszawa, Poland
e-mails: kn@igf.edu.pl, jreda@igf.edu.pl

Abstract

The quality of magnetic observations depends on such factors as: parameters of the recording instruments, and mainly their stability; the accuracy with which the so-called bases are being determined; the precision with which the sensors are positioned and the accuracy of scale values determination.

Every observatory has its own procedures for verifying these parameters. In this paper we present a method of data verification based on: (a) comparison of data calculated from vector magnetometer records with the proton magnetometer records, (b) comparison with data recorded at other observatories.

We present Internet software enabling a comparison between any two observatories. It is possible to compare current data (Reported or Adjusted) as well as Definitive data. The address of Web page for making the comparison is the following: <http://rtbel.igf.edu.pl>

Key words: INTERMAGNET, geomagnetic observations.

1. Introduction

Magnetologists working at geophysical observatories make much effort to improve the quality of geomagnetic field observations. The refinement of observation methods concerns both the geomagnetic field recording and the absolute measurements, decisive for monitoring the so-called secular variations.

The main factors affecting the quality of geomagnetic observations are the following:

- accuracy of determination of the so-called bases of recordings and their stability,
- accuracy of determination of the so-called scale values of the recordings,

- accuracy of positioning of the orientation of sensors,
- effect of thermal changes on the geomagnetic field recording,
- level of regional and local noise.

The experience of magnetologists shows that one of the most efficient ways of improving the quality of data is the widely understood comparison. The comparison may refer to measuring instruments, as for instance comparison of instruments for absolute measurements at IAGA workshops (Jankowski and Sucksdorff 1996). Another example is a comparison of momentary values at 02 h and 11 h, performed through several tens of years by many European observatories. It seems that the era of Internet offers quite new possibilities for performing comparison of geomagnetic observations.

2. Comparisons Between Observatories with the Use of Web Application

Comparisons of magnetic observations at adjacent, not very distant observatories may be of great importance for refining the quality of observations. We may expect the comparison of recordings to be helpful for detecting some faults that may happen, such as:

- changes in “magnetic levels” of a given observatory, resulting from erroneous determination of base levels,
- errors in the determination of scale values of the recording,
- errors or mistakes in the setting of clocks of the magnetic field recording instruments.

These were the reasons that motivated us, at the Institute of Geophysics, to develop a software enabling a comparison between the observatories belonging to the INTERMAGNET. The first version, created in 1997, provided a possibility of comparing only the two Polish observatories, Belsk (BEL) and Hel (HLP). This application has remained operative up now (<http://www.igf.edu.pl/mag/index.poland.html>, author: Michał Jankowski), and the experience with its use is very good. Basing on this experience, we created a new version, with much greater abilities, available at <http://rtbel.igf.edu.pl/>.

The internet page <http://rtbel.igf.edu.pl/> serves for graphical representation of observatory data collected in the framework of the INTERMAGNET project. Available are the archival data in the final version for all the observatories as well as the current data from those observatories that decided to submit the data in the IMFV1.22 format to the address imc@igf.edu.pl.

The new application makes it possible to compare any two observatories belonging to the INTERMAGNET. Of course, it is most sensible to compare adjacent observatories. The INTERMAGNET data can be visualized as one-day data or for 30-day period. There is an option to choose which components, X, Y, Z, or F, are to be visualized. The page enables us to see data from one or two observatories simultaneously. In addition, there is a possibility to display the K indices determined by the observato-

ries, as well as the K indices calculated by the ASm method (Nowożyński *et al.* 1991) or the energy indices E (Reda and Jankowski 2004).

The main part of the Web application welcoming window is shown in Fig. 1. A comparison of magnetograms from two nearby observatories is shown in Fig. 2.

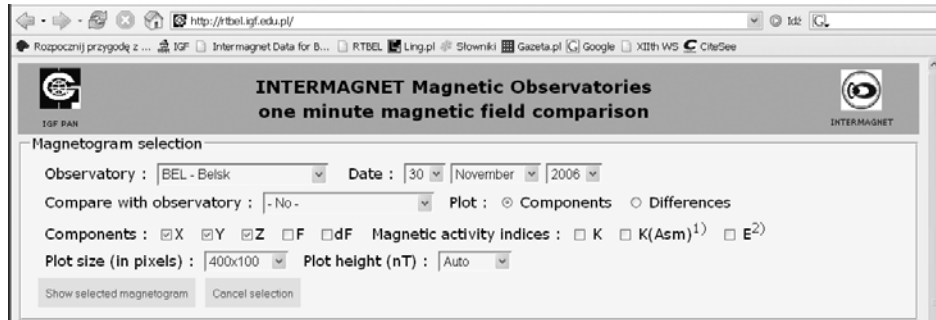


Fig. 1. The main Web application menu.

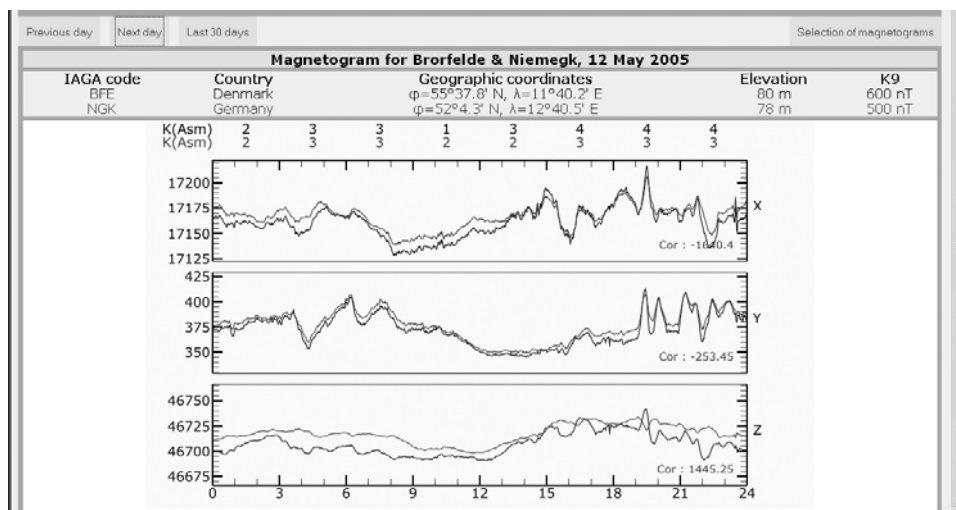


Fig. 2. An example of comparison of magnetograms from two adjacent observatories.

Figure 3 presents 30-day plot of components X, Y, and Z from two adjacent observatories. In this case, the Web application helped us detect a jump-like change in the Y component (by about 50 nT) in one of the observatories. The change was caused by erroneous determination of the smoothed base level. We purposefully deleted the names of the observatories, since our aim is to demonstrate the abilities of the Web application, not to publicize the observational errors.

The continuous recording of total field F has been performed in more and more observatories. Such a recording is optional for the INTERMAGNET observatories (St-Louis *et al.* 2004). A comparison of the total field calculated from the vector magne-

tometer, F_v , with that directly recorded by the scalar magnetometer, F_s , may be very important. Such comparisons are possible with the help of the Web application discussed here, as shown in Fig. 4. The figure displays 24-hour F_v - F_s curves from two observatories: curves (a) and (b). In this case, the application detected a very local, internal observatory disturbances in one of the observatories (curve (b)), that were easy to eliminate.

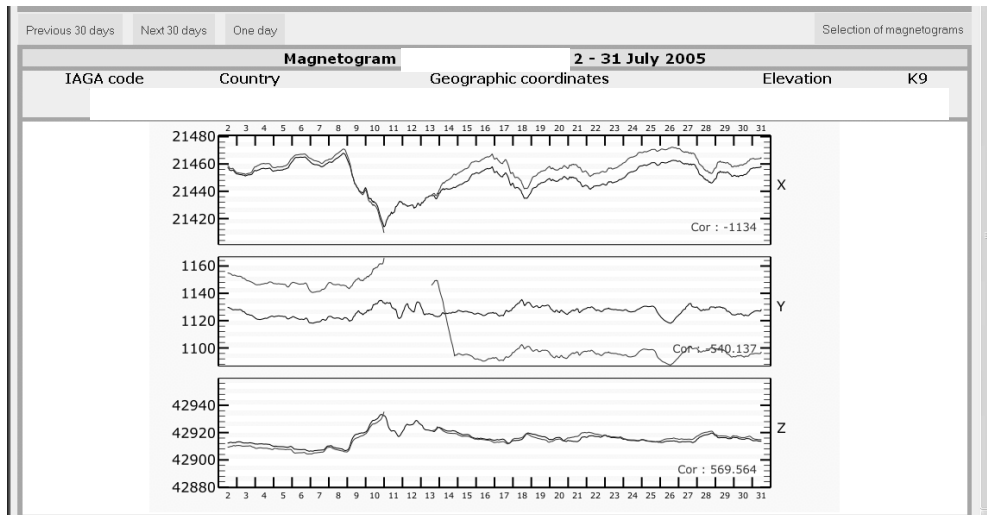


Fig. 3. An example of 30-day comparison of data from two adjacent observatories.

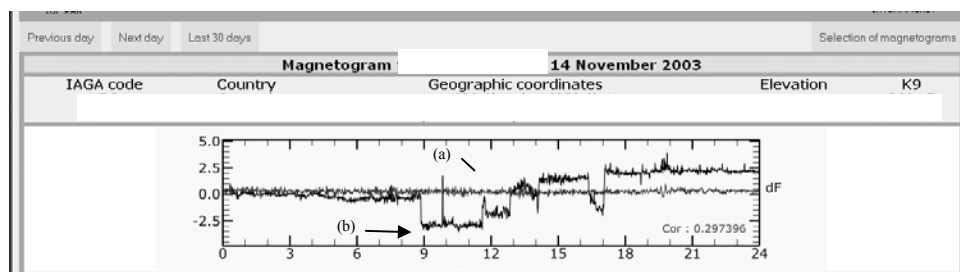


Fig. 4. Plots of differences F_v - F_s for two observatories.

3. Summary

The Web application described here has worked for over a year. It proved to be very useful for verifying the Definitive data before their final compilation on CD-ROM 2005. The authors encourage the personnel of the INTERMAGNET observatories to use this application for Reported and Adjusted data. The only thing to be done in order to use this software for such data is to send the magnetic data in the IMFV1.22 format to the address imc@igf.edu.pl. The Web application is available from the page <http://rtbel.igf.edu.pl/>.

References

- Jankowski, J., and C. Sucksdorff, 1996, *Guide for magnetic measurements and observatory practice*, IAGA, Warszawa, Poland, 235pp.
- Nowożyński, K., T. Ernst and J. Jankowski, 1991, *Adaptive smoothing method for computer derivation of K-indices*, *Geophys. J. Int.* **104**, 85-93.
- Reda, J., and J. Jankowski, 2004, *Three hour activity index based on power spectra estimation*, *Geophys. J. Int.* **157**, 141-146.
- St-Louis, B.J. (editor), 2004, *INTERMAGNET Technical Reference Manual*, version 4.2, 92pp.

Accepted February 8, 2007

The New BCMT Magnetic Database

Danielle FOUASSIER and Arnaud CHULLIAT

Équipe de Géomagnétisme, Institut de Physique du Globe de Paris
4, place Jussieu – 75252 Paris cedex 05 – France
e-mails: fouassie@ipgp.jussieu.fr; chulliat@ipgp.jussieu.fr

Abstract

The “Bureau Central de Magnétisme Terrestre” (BCMT) is a French organization in charge of the processing and distribution of magnetic data from 16 observatories (AAE, AMS, BNG, BOX, CLF, CZT, DRV, KOU, LZH, MBO, PAF, PHU, PPT, QSB, TAM, TAN), including those run in cooperation with foreign countries. The goal of this project is to carefully check all BCMT data and make them available on a public website in IAGA-2002 format. Data include hourly, daily, monthly and annual means as well as minute values when available. This task is quite simple for data dating from the INTERMAGNET era data, since occasional errors and discontinuities are known and well documented on CD-ROMs. However, some difficulties arise for older data, such as: missing or hard-to-find information on sampling rate, instruments and centering of hourly values; discrepancies between data in numerical format, data printed in year-books and data currently available in World Data Centers; spikes; undocumented data corrections. Such problems are occasional, but ought to be consistently tackled prior to scientific usage of old magnetic data.

1. Introduction

Long data series from magnetic observatories are widely used to investigate long-term variations of both the internal and external fields. Series of observatory monthly and annual means have revealed the occurrence of so-called geomagnetic jerks (Courtillot *et al.* 1978), originating within the Earth’s liquid core. In recent years, there has been a renewed interest in the long-term evolution of rapid variations of external origin (e.g., Le Mouél *et al.* 2004, Chulliat *et al.* 2005). This evolution can partly be attributed to the coupling between the main field and electrical currents in the ionosphere and magnetosphere.

Unfortunately, the number of magnetic observatories quickly decreases when going back in time. Few observatories throughout the world have data series extending for more than 50 years. Old magnetic observatory data are rare and therefore should be made available to all users. They should also be carefully checked, because the quality of instruments and data processing necessarily varied over time. Although a tedious task, checking old data is less expensive and time-consuming than building a new observatory and operating it for several decades.

The “Bureau Central de Magnétisme Terrestre” (BCMT), founded in 1921, coordinates the management of French magnetic observatories from different institutions (IPGP, EOST and IRD). It is currently in charge of the processing and distribution of magnetic data from seven French observatories (AMS, CLF, CZT, DRV, KOU, PAF, PPT) and nine observatories installed and run in cooperation with foreign institutions (AAE, BNG, BOX, LZH, MBO, PHU, QSB, TAM, TAN) (Fig. 1). All observatories belong to the INTERMAGNET network.

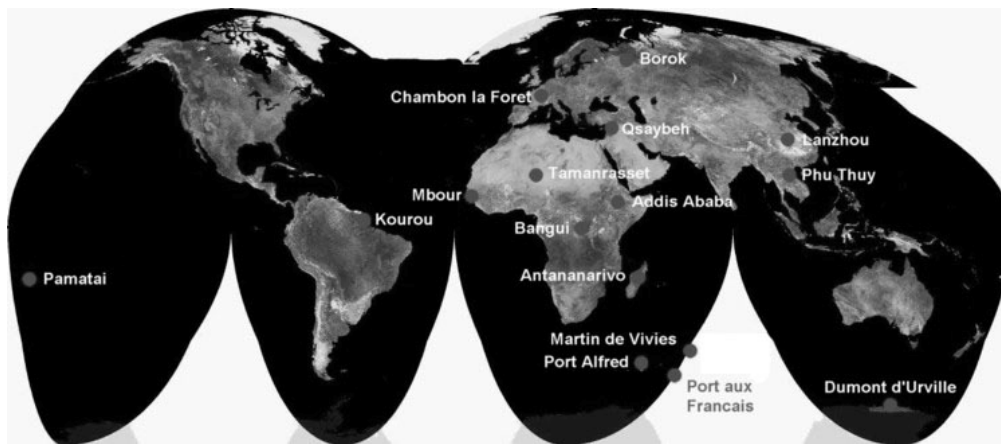


Fig. 1. Magnetic observatories having their data processed and distributed by the BCMT.

As shown in Fig. 2, several BCMT data series are very long. The combined PSM-VLJ-CLF series is exceptionally long, with a total length of 123 years in 2006. Four observatories (BNG, DRV, MBO and PAF) have series longer than 50 years. Also it should be noted that several foreign observatories (AAE, BOX, LZH, PHU, TAM and TAN) joined BCMT after their opening, thus having longer series in reality than indicated in Fig. 2.

A few years ago, a reevaluation of data discontinuities (jumps) in all BCMT observatories was undertaken. Reassessed jump values and associated documentation were recently published in the BCMT yearbook (Bitterly *et al.* 2005; an English translation of that paper will be published in 2007). Thanks to this effort, monthly means and annual means series of enhanced quality are now available for internal field studies.

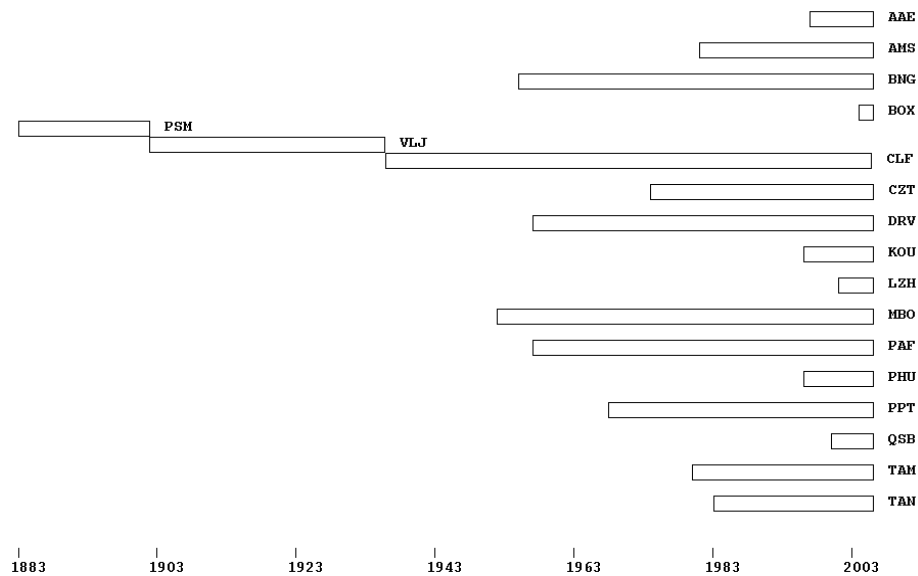


Fig. 2. Lengths of the BCMT data series.

The present project aims at completing the overall verification of old BCMT data, focusing on hourly values which are of interest for external field studies. All historical BCMT data will then be made available on a public website in IAGA-2002 format and sent to WDCs.

2. Database Structure

We chose to store minute values as well as hourly, daily and monthly means in IAGA-2002 format. As a general rule, data files contain the recorded components of the field (for example HDZF or XYZF), not the recalculated ones. In particular, the field modulus (F component) is the one recorded by an independent scalar magnetometer (when available), not the one calculated from the vector components. However, there are two exceptions:

- Minute values from the INTERMAGNET era are always given in XYZ.
- The F component of annual means is always recalculated from the vector components, in order to be consistent with INTERMAGNET file format.

The IAGA-2002 format includes a detailed header with precise information on sensor orientation, sampling rate and data interval type. This information is not so easy to find in old yearbooks (at least for some observatories), which lead us to do extensive research in BCMT archives; in a few cases, this information is missing. Taking advantage of the IAGA-2002 expendable header, we also added comments describing how means were calculated.

Annual means are stored using the INTERMAGNET file format. Jump values are not integrated but listed within the data series, at round dates (for example, a jump occurring between 1982 and 1983 is dated 1983.0). Footnotes documenting jumps are added whenever possible.

3. Data Checking

Checking old magnetic data is not a straightforward task. Past observers have done an impressive job by manipulating complicated instruments and manually processing a very large quantity of analog data. As their measurement and processing methods are not in use anymore, we should be extremely cautious when modifying old data. Therefore our motto during this project was: understand as much as possible, change as less as possible.

We systematically analyzed hourly values from all BCMT data series, and occasionally analyzed minute values. The checking method involved several tests complementing each other:

- Visual control from graphics (spikes, jumps, etc);
- Control of data listings;
- Inter-comparison of BCMT digital data and yearbooks;
- Inter-comparison of BCMT digital data and WDC data.

It is assumed that the most reliable data source is the yearbooks, since digital data were obtained by digitalizing yearbooks and WDC data were sent by BCMT. However, we found several anomalies in yearbooks. Some of them were corrected in digital data at an unknown date, without any note in subsequent yearbooks; some others were corrected by WDC staff.

Very different sorts of problems were found in hourly values, with various degrees of seriousness. Typical problems can be categorized as follows:

- Errors in old yearbooks (where hourly values are listed):
 - Misprint values
 - Spikes
 - Incorrect data block (one month of BNG declination having an offset of about 5')
- Errors originating in the digitalization of old yearbooks:
 - Wrong coding at data capture (lasting up to several days)
 - Incorrect data rejection (for example, at CLF on 12 October 1927 and 11 September 1930)
- Errors originating in the post-processing of digital data (means, etc):
 - Unnoticed effects of software bugs

- Loss of one data block
- Shifted date stamps (for example in a bissextile year)
- Hourly means computed from too small a number of minute values or spiked minute values
- Corrected errors in yearbooks left uncorrected in digital data

An example of isolated digitalization error is shown in Fig. 3. In that case, the data in the yearbook is $4^{\circ}58.8'$, while that in the computer is $4^{\circ}38.8'$. A more spectacular example is shown in Fig. 4, where wrong data capture lasted for a month. The reason for this is unknown.

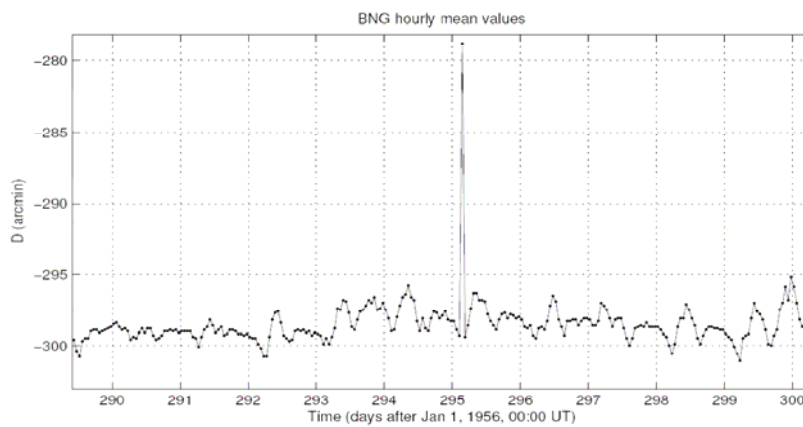


Fig. 3. Example of an isolated digitalization error in BNG data (D component, October 1956).

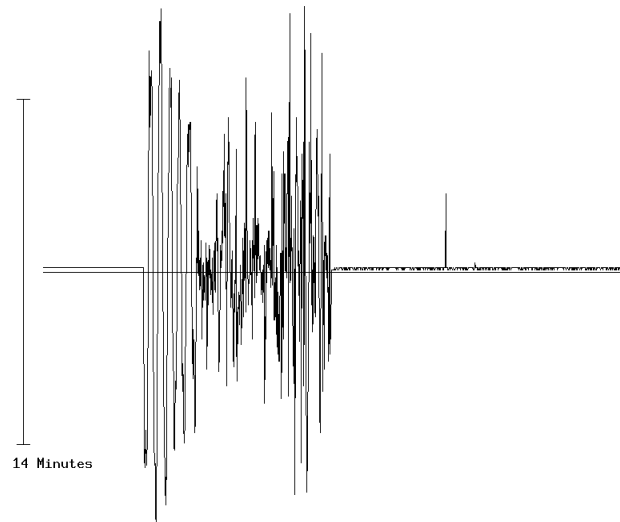


Fig. 4. Example of digitalization errors lasting several weeks in CLF data. The figure shows the difference between the original D component and the corrected one, from 1/6/1960 to 31/7/1960.

Once they have been detected, digitalization errors can be readily corrected by coming back to the original yearbooks. This is not the case for instrumental spikes, such as the ones shown in Fig. 5. For most spikes, it was decided to remove the data without interpolating. When minute values are available, spikes in hourly means usually come from spikes in minute values and can be corrected by removing the wrong minute values.

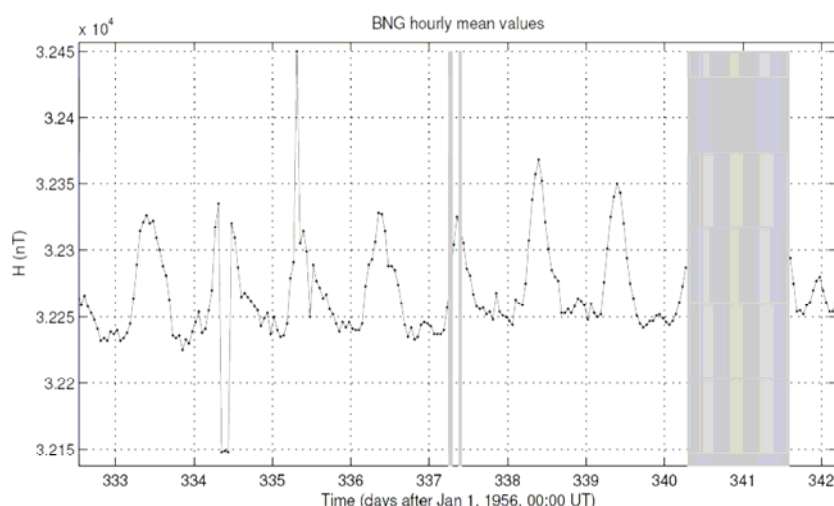


Fig. 5. Example of spikes in BNG data (December 1956).

4. Conclusion

The database is now technically ready and the data checking has been completed in all observatories, except for hourly values at PSM (1883-1900) and VLJ (1901-1922) which still need to be digitalized. In the coming months, the database will be made publicly available on the BCMT website (<http://obsmag.ipgp.jussieu.fr>) and all BCMT data will be updated in WDCs.

It has been a tedious work to construct this database and to check all data. However, significant data errors have been corrected and useful data information previously scattered in different archives is now available to users within the IAGA-2002 format.

References

- Bitterly, M., A. Chulliat, D. Fouassier, J.-L. Le Mouél, M. Manda and J.J. Schott, 2005, *Analyse des séries de données obtenues dans les observatoires du BCMT depuis leur création*, in: *Observations Magnétiques – Magnetic results 2002*, Bulletin n°21, BCMT, Paris.

- Chulliat, A., E. Blanter, J.-L. Le Mouél and M. Shnirman, 2005, *On the seasonal asymmetry of the diurnal and semidiurnal geomagnetic variations*, J. Geophys. R. **110**, A05301, doi:10.1029/2004JA010551.
- Courtilot, V., J. Ducruix and J.-L. Le Mouél, 1978, *Sur une accélération récente de la variation séculaire du champ magnétique terrestre*, C.R. Acad. Sci. D **287**, 1095-1098.
- Le Mouél, J.-L., E. Blanter, A. Chulliat and M. Shnirman, 2004, *On the semiannual and annual variations of geomagnetic activity and components*, Ann. Geophys. **22**, 3583-3588.

Accepted February 26, 2007

The Hourly Mean Computation Problem Revisited

Jean-Jacques SCHOTT¹ and Hans Joachim LINTHE²

¹Ecole et Observatoire des Sciences de la Terre
5 rue Descartes, F-67084 Strasbourg Cedex France
e-mail: JeanJacques.Schott@eost.u-strasbg.fr

²GeoForschungsZentrum – Adolf Schmidt Observatory
Lindenstrasse 7, D-14823 Niemegk Germany
e-mail: linthe@gfz-potsdam.de

Abstract

The computation of hourly means based upon one minute values raises the question of the influence of gaps on the mean values. The issue is revisited in this paper from a statistical point of view. In a first step, relevant statistics for gap and data distribution within hourly intervals are built up using actual time series. Then, the statistics are applied to full one minute field values in order to evaluate the dispersion of the hourly means due to the gap and data statistical distribution. The data from PAF observatory (Port-Aux-Français, Kerguelen Island) in the range 1999 to 2003 is used for illustration.

1. Introduction

Hourly means have been used for a long time in external field modeling, for instance diurnal variation modeling. In recent years, they have become increasingly interesting in internal field or internal plus external field modeling (i.e., Sabaka *et al.* 2002). However, a long standing problem has come up with the hourly mean computation, namely the tolerable length of gap within an hourly interval. This issue has become particularly acute since the advent of digital recording. Few references on this problem are available. The most recent paper was published by Manda (2002). It was motivated by a question addressed by L. Loubser (Hermanus observatory) to the community of observers. Among the answers, the one given by De Santis could be considered a starting point for the present study: “In my opinion, for most typical kinds of quiet and moderate magnetic activity, it would be probably better to have one data every three (i.e. 33% data only) instead of having just the first half of the whole period but nothing of the remaining (i.e. 50 % data).” This opinion strongly suggests a statistical approach of the issue.

2. Elaboration of Hourly Mean Statistics

An overview of the data and gaps distribution is readily provided by the scrutiny of one minute time series over a selected time span. Figure 1, left, shows the histograms built up using the X, Y, Z (in geographical reference frame) and F components from PAF observatory over the years 1999-2003. In order to obtain representative distributions, we should select time intervals free of major changes in the instrumentation and/or data processing methods, etc. The distribution of data segments is equivalently the distribution of time elapsed between two successive failures. This strongly suggests a Weibull distribution (Gibra 1973) designed to model electronic component life time, and therefore relevant to model the failures arising in data acquisition equipments. On the other hand, the distribution of gaps is close to a mere exponential distribution. This depends on a variety of parameters as a result of the way the observatory is operated.

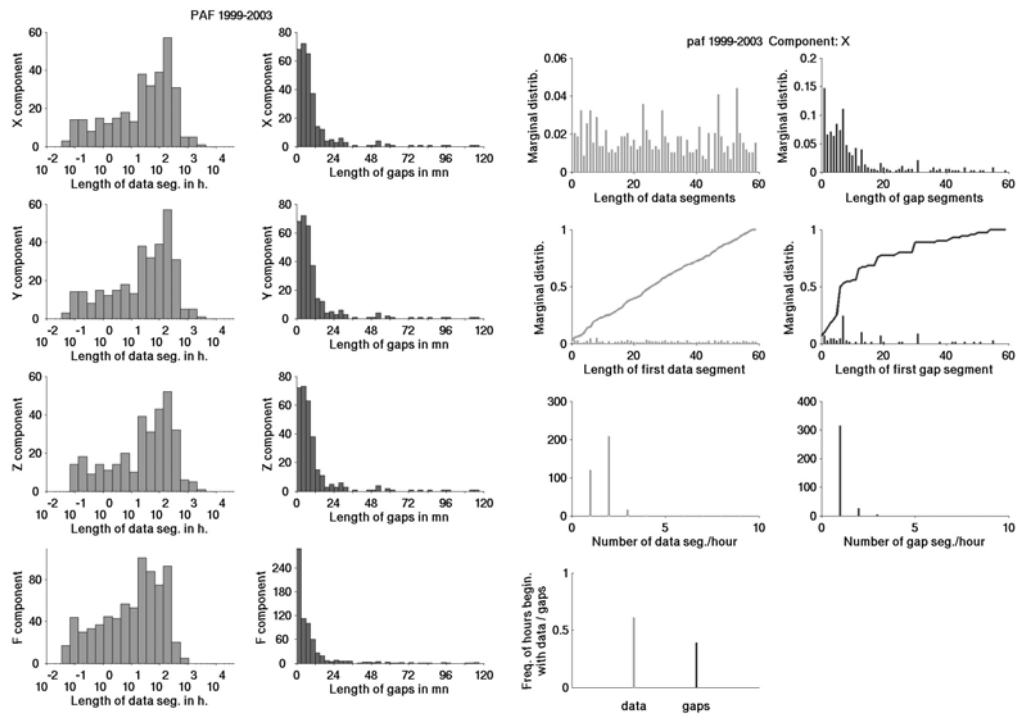


Fig. 1. Left: distribution of the length of data segments (left) and gap segments (right) for PAF observatory during the years 1999-2003. The horizontal scale is logarithmic for the data and linear for the gaps. Right: statistics regarding the distribution of data segments and gap segments within hourly intervals. See text for explanations.

Regarding hourly mean computation, the relevant basic information is the hourly intervals containing both data and gaps. A large number of situations may be imagined. Elementary combinatorial analysis demonstrates that there are about 1.15×10^{18} possibilities. However, all of them are not realistic. It is more advisable to base the

statistics upon real distributions. In any case, the data/gap, denoted T_{dg} in the sequel, or gap/data transitions, denoted T_{gd} , are the considered random variables.

Therefore, the first step is, in a given series of minute values, to select the hourly intervals containing both data and gaps. Indeed, for obvious reasons, intervals without gaps or data can be discarded. Preliminary statistics may be performed on the distribution of T_{dg} and T_{gd} . Figure 1, right, shows some distributions of interest. Upper left: distribution of length of data segments; upper right: distribution of length of gap segments; second row left: length of the first data segment in the hourly interval (histogram and cumulative function); second row right: length of the first gap segment (histogram and cumulative function); third row left: number of data segments per hour; third row right: number of gap segments per hour; bottom: frequency of segments beginning with data (light gray), respectively gaps (dark gray). In the example of PAF observatory, the length of data segment is roughly uniform, whereas the length of gap segments clearly is not. The third row illustrates the fact that not all theoretical distributions are realistic: for instance, the number of failures per hour hardly overruns three.

Having obtained a set of hourly intervals, whose distribution of data and gaps is typical for a given observatory and period of time, the next step consists in computing the estimated hourly means based upon this set, on one hand, on full records of one minute values on the other hand. The estimated hourly means are random variables whose distribution depends on the maximum tolerated gap length and the shape of the field variation, as already noticed by Manda (2002). The shape itself depends on the magnetic activity and the location of the observatory, mainly its geomagnetic latitude. The hourly means being regarded as random variables, their distribution may be represented on histograms and characterized by usual statistical parameters like their standard deviation, percentiles (less sensitive to outliers).

3. Examples

3.1 Hourly mean distribution for a quiet day

Figure 2 shows an example of the hourly mean distribution obtained for PAF observatory based upon the distribution of data and gaps segments computed using the method outlined in the previous section, on one hand, and the daily records for 3 February 2001, on the other hand. Left part of Fig. 2 displays the distribution of the hourly mean for hour 7 U.T. (the hours are numbered from 0 to 23) and shows the increase of dispersion due to the increase of gap length. The lower drawing displays the daily variation of the selected component, in this case the component along geographic east. The field variation during hour 7 is thickened.

The head “at most n minutes missing” means that all distributions of data and gap sequences with less than $n+1$ missing values are taken into account. Therefore, the number of suitable cases increases with the tolerated gap length. std stands for standard deviation and the 95% figure is the width of the interval containing 95% hourly means. Under a Gaussian assumption, it would be twice the standard deviation. It can be noticed that this is roughly the case, although a Gaussian assumption is not required

in this study. Half of the 95% interval may also be interpreted as a confidence interval at the 95% confidence level. Right part of Fig. 2 is like the left part apart from the maximum tolerated length of gap being fixed and its influence checked across the day using 6 selected hours highlighted on the lower drawing. Thus, the figure illustrates the influence of the shape of the field variation. Although the magnetic activity is very small (e.g. K indexes on Fig. 3), a moderate variation of the hourly mean scattering may be noticed. It is clearly correlated with the slope of the hourly variation. Hour 7 selected previously has the largest slope and, hence, the largest dispersion.

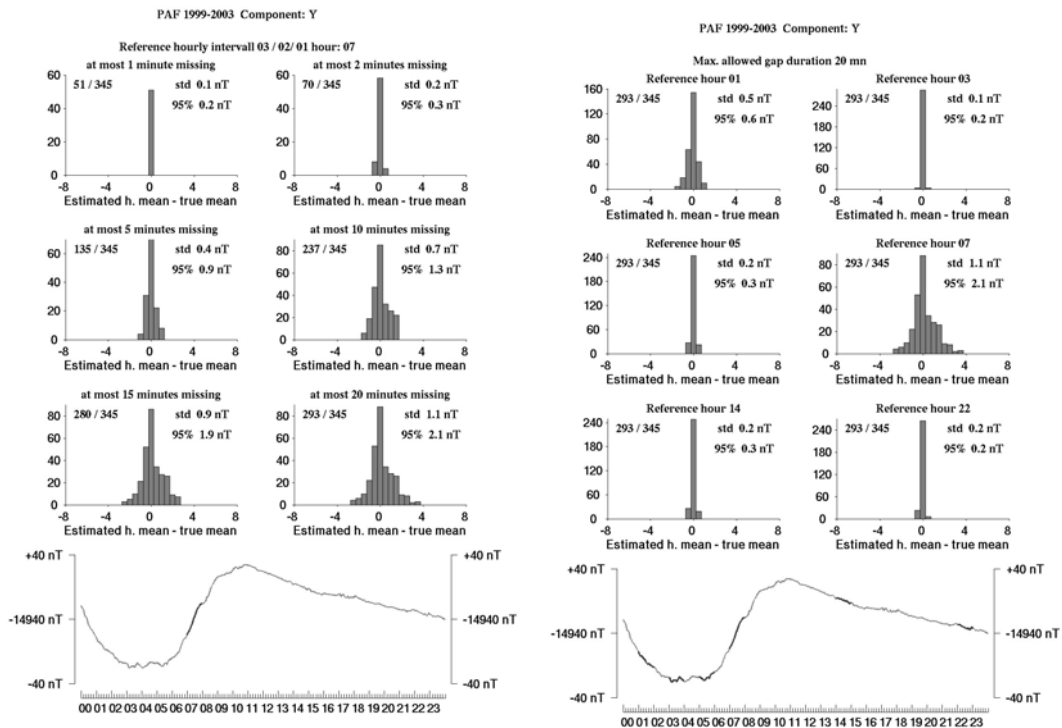


Fig. 2. Left: distribution of estimated hourly means around the true mean for various maximum gap lengths, the hourly interval being fixed. Right: similar to left with a fixed maximum length of gap and various hourly intervals throughout the day. See text for further explanations.

The head “at most n minutes missing” means that all distributions of data and gap sequences with less than n+1 missing values are taken into account. Therefore, the number of suitable cases increases with the tolerated gap length. std stands for standard deviation and the 95% figure is the width of the interval containing 95% hourly means. Under a Gaussian assumption, it would be twice the standard deviation. It can be noticed that this is roughly the case, although a Gaussian assumption is not required in this study. Half of the 95% interval may also be interpreted as a confidence interval at the 95% confidence level. Right part of Fig. 2 is like the left part apart from the maximum tolerated length of gap being fixed and its influence checked across the day using 6 selected hours highlighted on the lower drawing. Thus, the figure illustrates

the influence of the shape of the field variation. Although the magnetic activity is very small (e.g. K indexes on Fig. 3), a moderate variation of the hourly mean scattering may be noticed. It is clearly correlated with the slope of the hourly variation. Hour 7 selected previously has the largest slope and, hence, the largest dispersion.

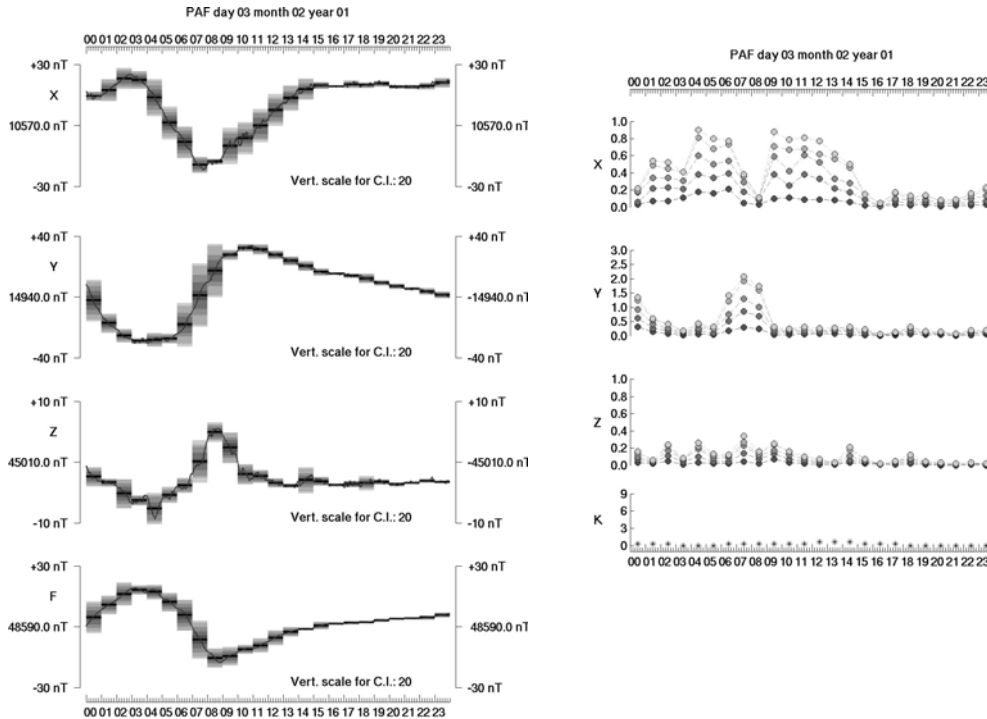


Fig. 3. Left: Confidence intervals for the 24 hourly means and tolerated gap lengths 2, 5, 10, 15, 20 minutes. Colours vary from dark grey to light grey accordingly. Vertical scale of the c.i. magnified 20 times. Right: width of the confidence interval versus hour of the day, for the same maximum tolerated gaps as on the left figure. Bottom: K indexes for the day.

Figure 3, left, displays the confidence intervals for the 24 hourly means and tolerated gap lengths 2, 5, 10, 15, 20 minutes. The confidence intervals are pictured as rectangles colored from dark grey (2 minute gaps) to light grey (20 minute gaps). For the sake of clarity, the confidence intervals are magnified 20 times with respect to the vertical scale. Again, we see the clear correlation between the slope of the hourly variation and the width of the confidence interval. Figure 3, right, summarizes the confidence interval widths (note that the vertical scales are variable), for every hour and the same five selected gap lengths as on the left. The lower drawing shows the variation of the K indexes over the day. There is no correlation between the width of the confidence intervals and K, all the lesser as the K index is a logarithmic scale not designed for characterizing quiet day variations. Once again, the diurnal variation of the confidence interval is correlated with the slope of the field diurnal variation, which could be modeled with a Sq model (Malin and Gupta 1977, for instance).

3.2 Hourly mean distribution for a disturbed day

On the other end of the field disturbance scale, Figs. 4-5 illustrate the effect of strong disturbances on the computation of hourly means. The selected day is within the so-called Halloween storm. Figure 4 makes evident the dramatic increase of the hourly mean scattering. Note the large variation of the horizontal scale, either according to the tolerated gap length or to the shape of the hourly variation. In addition, the figure reveals the poor sampling of these very scattered distributions, despite the long time series analysed. Figure 5, left, is similar to Fig. 3, left, except for the vertical magnification of the confidence intervals, reduced to 10 times the field vertical scale. It shows also that even during strongly disturbed days, some hourly means are moderately scattered. Finally, Fig. 5, right, equivalent to Fig. 3, right, summarizes the daily variation of the confidence intervals and shows again that the correlation with the K indexes is rather poor in this case. The lack of correlation may be explained by the fact that during strong magnetic storms, PAF behaves like an auroral observatory due to the northwards expansion of the auroral oval. This fact is supported by the clear correlation observed, on the other hand, with the auroral indexes (Fig. 6).

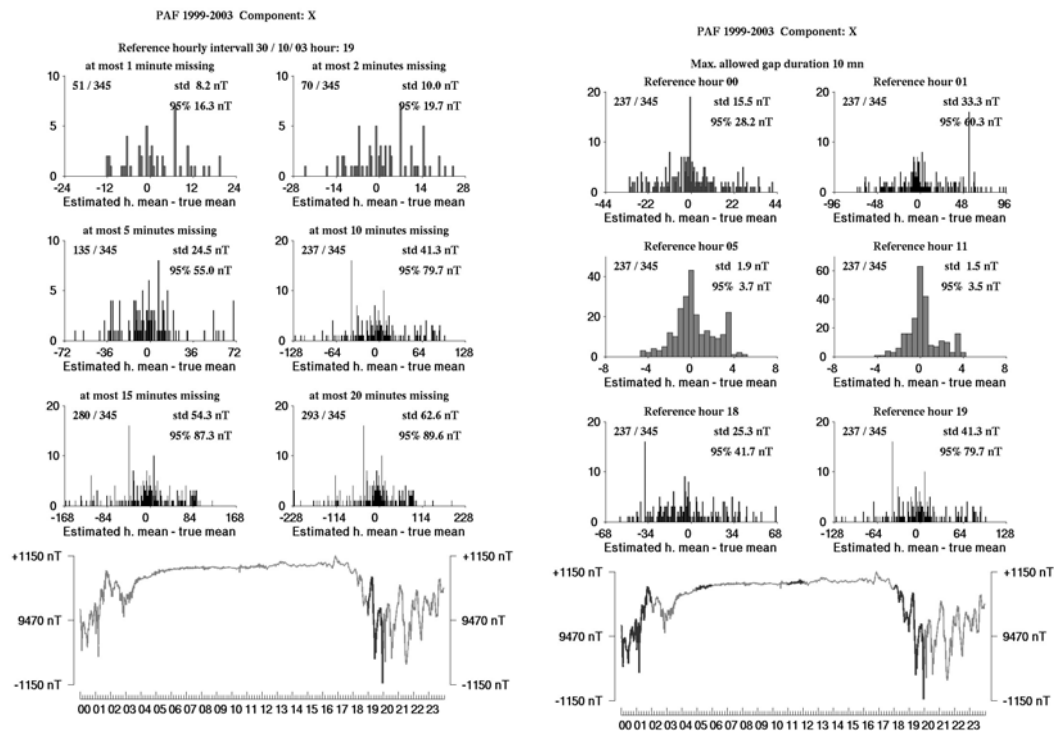


Fig. 4. Same as Fig. 2 for a disturbed day, apart from the test hour selection.

4. Discussion and Further Developments

One motivation for this study was the hope that a simple policy for computing the hourly means or not, according to the number of data missing, could be suggested.

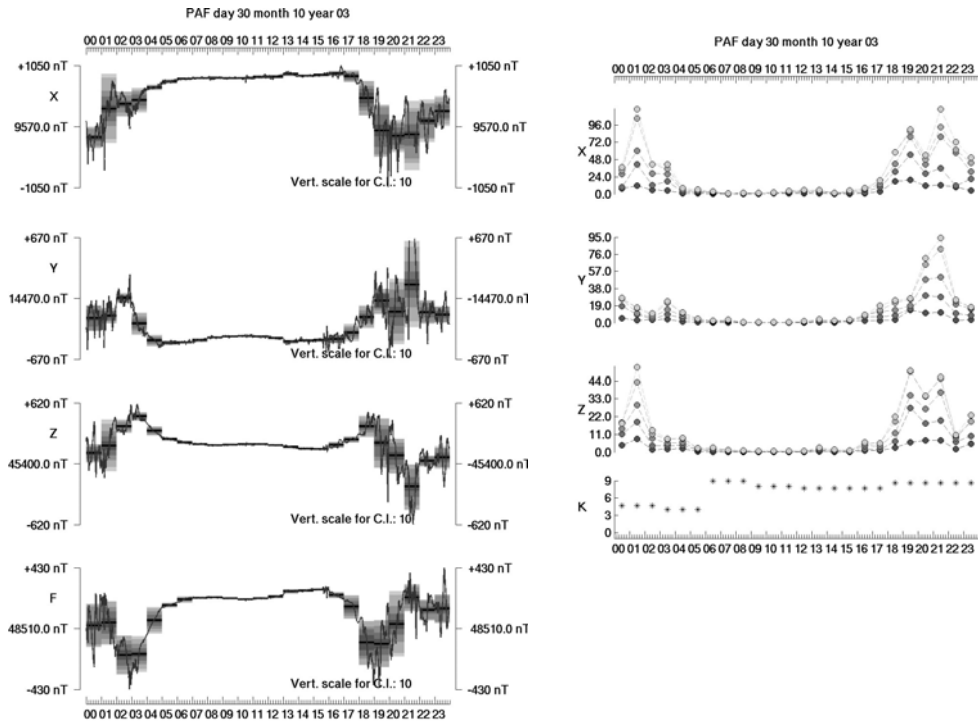


Fig. 5. Similar to Fig. 3 for the disturbed day used as an example in Fig. 4. On the left, vertical scale for the confidence intervals magnified 10 times.

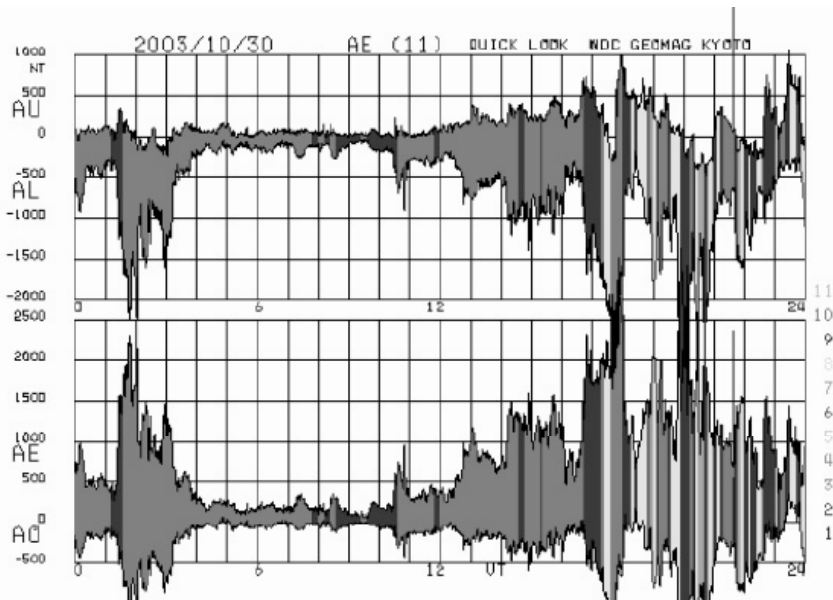


Fig. 6. Quick look auroral indexes for the 30 October 2003 (downloaded from web site swdwww.kigi.kyoto-u.ac.jp). To be compared to the daily variation of the confidence intervals in Fig. 5.

This goal clearly could not be reached, due to the large number of parameters involved. These parameters include the statistical distribution of data and gaps, which is peculiar to each observatory, the location of the observatory, the level of magnetic disturbance. The comparison of Figs. 5 and 6 suggests that appropriate magnetic indexes could be a relevant parameter for taking into account the magnetic activity, above some level of disturbance. On the other end of the disturbance scale, Sq models might be helpful to play an equivalent role. Anyway, assuming that the distribution of data and gaps, and of course the location of a specific observatory, would be known, the upper threshold for missing data, with respect to an upper limit of error assigned to the hourly means, should be a function of an hourly parameter reflecting the shape of the field variation. In addition, this parameter would depend on the component, that is would be a 3 or 4 dimension vector.

On the other hand, this study draws the attention on the fact that the hourly mean based upon an incomplete set of data is only an estimate of the true, unknown value. It can therefore be treated as a random variable, whose properties may be investigated with the method outlined above. In particular, a confidence interval may be associated to each hourly mean. In order to compute it, either a typical record (without gaps) or an appropriate parameter, fairly accurately correlated with the confidence interval in order to provide a reasonable estimation for it, has to be available. To this end, the analysis of a fairly large number of suitably distributed observatories and levels of disturbance would have to be performed.

Yet, the statistical analysis presented herein is rather elementary from at least two points of view. First, as can be seen in Fig. 4, the distribution of hourly means, based upon actual sequences of data and gaps, is poorly sampled, due to the rather small size of the set of hours containing gaps. This is probably (and hopefully) the case for most observatories. This observation calls for the search of a method which could generate hourly sequences of gaps and data having the same statistical properties than the actual ones. We have attempted to do it using a Markov chain process based upon transition probability matrices data/gap and gap/data constructed with real data. The result is not really satisfying because the transition probability matrices themselves are poorly sampled. In an attempt to build up smooth versions of them, we have adjusted the empirical transition probability functions by theoretical distributions, namely a mixture of positive binomial and negative binomial distributions (Gibra 1973). The result is better, but not significantly. Thus, further investigations have to be carried out, although we believe that they should not change significantly the confidence interval estimates.

A completely different way to explore would be to implement statistical methods dealing with missing data (Little and Rubin 1987). The idea behind this concept is to find a way of replacing the missing data without altering the estimates of the parameters looked for – in the present case, merely the mean value. For instance, the field variation in every incomplete hourly interval could be modeled by some parametric function (polynomials, sine functions, etc.) whose parameters would be estimated from the available data by some least-squares or likelihood method, according to schemes referred to in the statistical literature (see for instance Little and Rubin 1987,

for references). This way of computing hourly means would perhaps not completely make meaningless the question of the tolerable length of gap, but would certainly make less critical the choice of the threshold.

5. Conclusion

The influence of missing data on the hourly means of the magnetic field components has been investigated from a statistical point of view based upon actual distributions of gaps and data peculiar to a specific observatory. The study confirms and amplifies conclusions already drawn by Manda (2002), namely that the error involved depends, beside the length of gap, on the shape of the field variations and the level of the magnetic disturbance. These features, in turn, depend on the position of the observatory. The influence of the magnetic disturbance upon the confidence interval might be quantified with the help of an appropriate magnetic activity index. However, overall, the problem of fixing a limit to the tolerable length of gap in an hourly set of data is probably ill-posed. One way of circumventing the difficulty would be to rely on statistical methods dealing properly with missing data.

References

- Gibra, I.N., 1973, *Probability and Statistical Inference for Scientists and Engineers*, Prentice-Hall, London, 596 pp.
- Little, R.J.A., and D.B. Rubin, 1987, *Statistical Analysis with Missing Data*, John Wiley & Sons, New York, 278 pp.
- Malin, S.R.C., and J.C. Gupta, 1977, *The Sq current system during the International Geophysical Year*, Geophys. J.R. astr. Soc. **49**, 515-529.
- Manda, M., 2002, 60, 59, 58, ... *How many minutes for a reliable hourly mean?*, Proceedings Xth IAGA Workshop, Hermanus 112-120.
- Sabaka, T.J., N. Olsen and R.A. Langel, 2002, *A comprehensive model of the quiet-time, near-Earth magnetic field: phase 3*, Geophys. J. Int. **151**, 32-68.

Accepted February 14, 2007

Intercalibration of dIdD and Fluxgate Magnetometers

Balázs HEILIG

Eötvös Loránd Geophysical Institute, Tihany Geophysical Observatory
Kossuth u. 91, H-8237 Tihany, Hungary
e-mail: heilig@elgi.hu

Abstract

Fluxgate magnetometers are the most frequently used vector magnetometers in current observatory practice. However, at more and more sites, alternative solutions, e.g. dIdD magnetometers are also applied to record the geomagnetic variation. In this paper we demonstrate the advantage of the simultaneous use of a fluxgate and a dIdD by introducing a cross-calibration between these instruments. The calibration of a fluxgate is a process to determine 9 parameters including 3 scale factors, 3 offset values, 3 orthogonality parameters. As follows from the dIdD principles, the dIdD is void from offset and scale factor errors. Therefore, to calibrate the dIdD one has to determine one single orthogonality error; the other orthogonality conditions are satisfied automatically since the 3rd dIdD axis is defined mathematically as perpendicular to the two physical axes of the instrument. Furthermore, the intercalibration can yield information on relative orientation errors, i.e. the orientation of one instrument can be determined relative to a well-oriented reference instrument.

1. Introduction

Fluxgate magnetometers are the most frequently used vector magnetometers in current observatory practice. However, at more and more sites, alternative solutions, e.g. dIdD magnetometers are also applied to record the components of the geomagnetic variation. Three component fluxgate variometers have 12 parameters to be determined during a calibration process: 3 scale values, 3 offsets, 3 orthogonality errors and 3 orientation errors (see Table 1). At the same time, the dIdD has only 4 parameters needed to be calibrated: the orthogonality of the two coil-system (ε_{DI}), and the 3 orientation angles (I_0 , D_0 and ε_0). The dIdD can have neither scale value, nor offset problems since the vectors of the magnetic field components in the arbitrary reference frame of this instrument are derived from absolute, total field readings. Thus, the dIdD can be considered as an absolute instrument, but, unfortunately, only in its own refer-

ence frame. The problem of calibration of the dIdD equals to finding its (maybe non-orthogonal) reference frame.

We demonstrate here a process to calibrate the dIdD against a reference fluxgate magnetometer supposed to be sufficiently oriented. The dIdD calibrated according to the method described below can be used as a vector variometer (not as an absolute instrument). Moreover, the scale values of the reference magnetometers can be determined during the same procedure.

2. Computation of the dIdD Components (The dIdD Reference Frame)

First let us suppose that the dIdD is perfectly aligned and oriented, i.e. its I and D coil axes are orthogonal, the D coil axis is horizontal and both axes are perpendicular to the magnetic field vector. The third axis, let us call it the S (sensor) axis, is defined mathematically to be perpendicular to both coil axes, so taking into account our assumptions it is parallel to the magnetic field. Moreover, the S axis is directed parallel to the field, while the D coil axis is directed toward magnetic east, and the I coil is directed so that the S-D-I axes form a right-handed system. This S-D-I system is referred to as the dIdD reference frame in this paper. The same notation will be used also for an arbitrary orientation of the instrument, the dIdD reference frame is always defined physically by the orientation of the coils (Schott and Pankratz 2001).

The dIdD components in an arbitrary dIdD reference frame can be computed as (Schott *et al.* 2001):

$$B_i = \frac{I_+^2 - I_-^2}{4A_i}, \quad (1)$$

$$B_d = \frac{D_+^2 - D_-^2}{4A_d}, \quad (2)$$

$$B_s = \sqrt{F^2 - B_i^2 - B_d^2}, \quad (3)$$

$$A_i = \sqrt{(I_+^2 + I_-^2 - 2F^2)/2}, \quad (4)$$

$$A_d = \sqrt{(D_+^2 + D_-^2 - 2F^2)/2}, \quad (5)$$

where F (total field), I_+ (deflected parallel to the I axis), I_- (deflected antiparallel to the I axis), D_+ (deflected parallel to the D axis), D_- (deflected antiparallel to the D axis) are the five readings of a dIdD sequence, A_i and A_d are the deflection fields generated by the I- and D-coils, respectively, B_i , B_d , and B_s are the dIdD vector components along the I, D, and S axes. Here we supposed that the opposite deflection fields applied in the same coil have the same magnitude, and that the field variation is negligible during the measurement sequence. Current dIdD models are based on the GSM-19 Overhauser magnetometer model of the Gem Systems and able to take a whole measurement cycle during a few seconds.

3. Transformation from the dIdD to the XYZ Reference Frame

Unlike the usual treatment we do not use the approximative formulae to calculate dD and dI (e.g. Pankratz *et al.* 1999). The transformation of the data from the dIdD reference frame to the XYZ reference frame is achieved by correcting the orthogonality error and implementing a 3D rotation represented here as three consecutive rotations around the S, D and I axes, respectively.

1. The orthogonality error ε_{ID} , that is taken positive if the angle between the I and D axes is less than 90° , can be removed e.g. by the following formulae:

$$B_{ic} = B_i, \quad (6)$$

$$B_{dc} = \frac{B_d - B_i \sin(\varepsilon_{ID})}{\cos(\varepsilon_{ID})}, \quad (7)$$

$$B_{sc} = \sqrt{B_i^2 + B_d^2 + B_s^2 - B_{ic}^2 - B_{dc}^2}, \quad (8)$$

where B_{ic} , B_{dc} and B_{sc} stand for the corrected components. This transformation sets the D axis perpendicular to the I axis.

2. In the next step the orthogonal reference frame is rotated by ε_0 about the S axis in a clockwise direction when looking towards the origin. This step corresponds the leveling of the D coil. The matrix of rotation is:

$$\overline{\overline{E}}_0 = \begin{pmatrix} 1 & 0 & 0 \\ 0 & \cos(\varepsilon_0) & -\sin(\varepsilon_0) \\ 0 & \sin(\varepsilon_0) & \cos(\varepsilon_0) \end{pmatrix}. \quad (9)$$

3. A further rotation by I_0 about the D-axis, in a counterclockwise direction when looking towards the origin, brings the I axis horizontal. The resulting reference frame corresponds to an HDZ system:

$$\overline{\overline{I}}_0 = \begin{pmatrix} \cos(I_0) & 0 & -\sin(I_0) \\ 0 & 1 & 0 \\ \sin(I_0) & 0 & \cos(I_0) \end{pmatrix}. \quad (10)$$

4. Finally a rotation by D_0 about the I axis, in a clockwise direction when looking towards the origin, transforms the HDZ system to a geographic XYZ system.

$$\overline{\overline{D}}_0 = \begin{pmatrix} \cos(D_0) & -\sin(D_0) & 0 \\ \sin(D_0) & \cos(D_0) & 0 \\ 0 & 0 & 1 \end{pmatrix}. \quad (11)$$

The 3D rotation can be written in the form:

$$\vec{B}_{xyz} = \overline{\overline{D}}_0 \left(\overline{\overline{I}}_0 (\overline{\overline{E}}_0 \cdot \vec{B}_{sdi_corr}) \right), \quad (12)$$

where B_{sdi_corr} denotes the components in the orthogonalized coordinate system, i.e. (B_{sc}, B_{dc}, B_{ic}) , and B_{xyz} stands for the XYZ representation of the field vector.

4. Calculation of D_0 and I_0 from a Single Absolute Measurement

Supposing the orthogonality of the coil axes ($\varepsilon_{ID} = 0$), the transformation can be unfolded from Eq. (12) as:

$$X = B_{sc} \cos D_0 \cos I_0 - B_{dc} (\cos D_0 \sin I_0 \sin \varepsilon_0 + \sin D_0 \cos \varepsilon_0) - B_{ic} (\cos D_0 \sin I_0 \cos \varepsilon_0 - \sin D_0 \sin \varepsilon_0), \quad (13)$$

$$Y = B_{sc} \sin D_0 \cos I_0 - B_{dc} (\sin D_0 \sin I_0 \sin \varepsilon_0 - \cos D_0 \cos \varepsilon_0) - B_{ic} (\sin D_0 \sin I_0 \cos \varepsilon_0 + \cos D_0 \sin \varepsilon_0), \quad (14)$$

$$Z = B_{sc} \sin I_0 + B_{dc} \cos I_0 \sin \varepsilon_0 + B_{ic} \cos I_0 \cos \varepsilon_0. \quad (15)$$

If we know the absolute values of the field components for a certain time and also the simultaneous SDI components measured by the dIdD, then using numerical methods we can determine the three orientation angles, ε_0 , D_0 , and I_0 from Eqs. (13)-(15).

If we go further supposing that the D axis is horizontal ($\varepsilon_0 = 0$), D_0 and I_0 can be expressed in closed form:

$$\cos I_0 = \frac{ZB_i + \sqrt{B_s^2 (B_s^2 + B_i^2 - Z^2)}}{B_i^2 + B_s^2}, \quad (16)$$

$$\cos D_0 = \frac{XW + \sqrt{X^2 W^2 - (W^2 + B_d^2)(X^2 - B_d^2)}}{W^2 + B_d^2}, \quad (17)$$

$$\text{where} \quad W = B_s \cos I_0 - B_i \sin I_0. \quad (18)$$

This method yields a simple alternative way to estimate the dIdD reference frame, with the same assumptions, of the solution proposed by Schott and Pankratz (2001).

5. The Intercalibration Process

Equations (16)-(18) are valid only when two assumptions are fulfilled: the D-axis is horizontal and the two coils are orthogonal. The intercalibration process described below is an example for a procedure that is suitable for determining the missing error values as well. The calibration process benefits from the natural variation of the geomagnetic field. The method is based on minimizing the fluctuation in the component differences between the dIdD to be calibrated and the reference vector magnetometer.

The difference of the corresponding vector components, e.g. $X_1 - X_2$ of two properly aligned and oriented (i.e. calibrated) variometers, apart from some noise, gives a

time independent, constant value. Variometers with different orientations, however, give fluctuating component differences. Minimizing the fluctuations in all components simultaneously while changing the calibration parameters one can estimate the mutual orientation, the relative scale values and/or the relative misalignment errors of the two instruments. Finally, as an additional information we can calculate the baseline differences between the calibrated and the reference instrument.

The intercalibration of a dIdD and a fluxgate instrument is especially advantageous. Since all the scale values of the dIdD equal 1 (Table 1), the relative scale values to be determined will be the actual scale values of the fluxgate instrument. An important consequence of the mathematical definition of the S axis of the dIdD is that this instrument has only one possible orthogonality error, namely the misalignment of the mutual position of the two coils, ε_{ID} . Assuming that the reference triaxial fluxgate sensors are orthogonal and that these sensors are orientated perfectly in the geographic XYZ frame, the calibration will give an estimation of the orthogonality error and the three orientation angles of the dIdD. The baseline differences between the two instruments in this case will be an estimation of the actual fluxgate baselines.

Table 1
Comparison of dIdD and fluxgate calibration parameters

| Calibration parameters | Fluxgate | dIdD | Absolute vector magnetometer |
|------------------------|-----------------|---------------------------|------------------------------|
| Scale values | c_x, c_y, c_z | 1, 1, 1 | 1, 1, 1 |
| Baseline | X_b, Y_b, Z_b | 0, 0, 0 | 0, 0, 0 |
| Orthogonality errors | 3 angles | 0, 0, ε_{ID} | 0, 0, 0 |
| Orientation | 3 angles | ε_0, D_0, I_0 | 0, 0, 0 |

In practice, there does not exist any perfect reference magnetometer. Both the sensor misalignment and orientation errors can reach tens of arc minutes. However, we can still want to determine the 4 dIdD calibration parameters needed to convert the dIdD data into the reference frame of the fluxgate magnetometer, e.g. when we intend to fill data gaps of the primary recording system with data derived from the measurements of a poorly oriented dIdD.

During the optimization process a minimum is searched for the sum of the *rms* values (R) of the three detrended difference signals:

$$R = \sum_{i=x,y,z} rms \left[filter \left(B_i^{didd}(t) - B_i^{fg}(t) \right) \right], \quad (19)$$

where

$$B_i^{didd}(t) = \overline{D_0} \left[\overline{I_0} \left(\overline{E_0} \cdot \overline{B}_{sdi_corr}(t) \right) \right]_i, \quad i = x, y, z. \quad (20)$$

The 7 free parameters are: I_0 , D_0 , ε_0 , ε_{DI} for the dIdD, and c_x , c_y , c_z , for the fluxgate. Before calculating the rms values, two filters had been applied to the difference signals: a highpass filter to exclude the slow trends connected to temperature variations of the fluxgate magnetometer, and a lowpass filter to remove the ‘high’ frequency instrument noise. The computation was implemented on a daily basis using a Quasi-Newton method in Matlab’s Optimization Toolbox (function *fminunc*). The starting values of I_0 and D_0 were calculated from Eqs. (16)-(18). All other initial angle parameters were set to zero and all scale values to 1.

In the example given below we used the DMI FGE fluxgate, the primary variometer of the Tihany Observatory as a reference instrument to find the orientation of a first generation (i.e. not suspended model with a coil system 3 dm in diameter) dIdD that was installed in February 2000. During the installation process the D axis was set horizontal within 10 arc minutes, and also the orthogonality of the coils was adjusted with the same precision. The initial values of $I_0 = 63.398^\circ$ and $D_0 = 2.401^\circ$ were derived from a set of absolute measurements. Since then the raw XYZ components of the dIdD have been recorded, i.e. for the calculation of components not the actual but the initial orientation parameters were used. However, during the passed years the dIdD pretty changed its position. Using the method presented here we implemented the intercalibration procedure for all (available) days in 2003.

In Fig. 1 a and b the component differences between dIdD and FGE before and after the calibration process are shown for August 23. It can be seen that the rather large amplitude fluctuations in the raw differences almost completely disappeared after the calibration ($R_{min} = 0.18$ nT). The accuracy of the parameter estimation mainly depends on the overall noise level in the data, more exactly on the signal-to-noise ratio in the difference time series. For example supposing a variation of 30 or 300 nT and a 0.3 nT noise level, an 1% or 0.1% relative accuracy can be achieved, respectively. The effect of noise can be somewhat decreased by filtering the data, or averaging the results for several days.

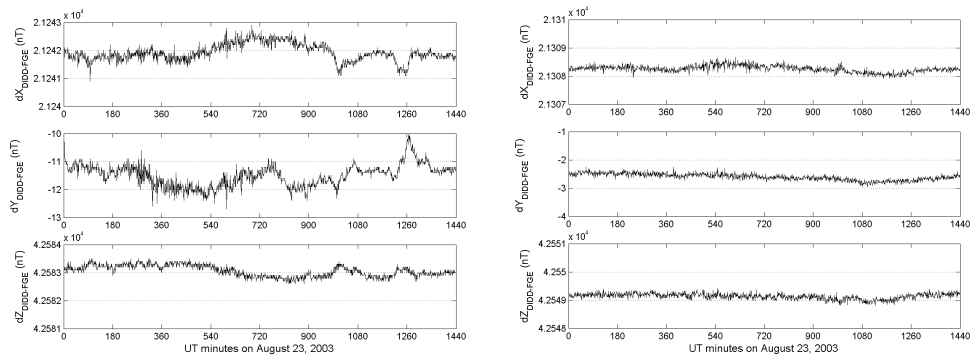


Fig. 1. The component differences between dIdD and FGE during one day (a) before, and (b) after the calibration process.

In Fig. 2 the deviations of the estimated dIdD calibration parameters from their yearly means are plotted for the whole year. The yearly mean values (\pm standard

deviations) calculated for all days (when R_{min} was less than 0.3 nT) are: $I_0 = 63.276^\circ \pm 0.099^\circ$, $D_0 = 2.717^\circ \pm 0.209^\circ$, $\varepsilon_0 = -0.664^\circ \pm 0.234^\circ$, $\varepsilon_{DI} = -0.101^\circ \pm 0.146^\circ$, $c_x = 0.9983 \pm 0.0015$, $c_y = 0.9989 \pm 0.0016$, $c_z = 0.9976 \pm 0.0070$. We note here that according to the calibration certificate of the FGE instrument all the misalignments of fluxgate sensors are less than 1 mrad. With the help of the resulting 4 transformation parameters, the dIdD SID data can be converted to an approximate XYZ system applying Eqs. (6)-(11), in addition the FGE baseline can also be estimated. Of course the converted dIdD components will not point in the true XYZ directions since the reference FGE was obviously not perfectly oriented and not completely void from orthogonality errors. Even so, the baseline calculation for e. g. November 12 resulted values very close to the true adopted baselines ($X_b = 21292$ nT, $Y_b = -4$ nT, $Z_b = 42564$ nT, the difference from the adopted baselines are 38 nT, 4 nT and 10 nT, respectively). It means that the FGE was installed carefully and served as a really good reference.

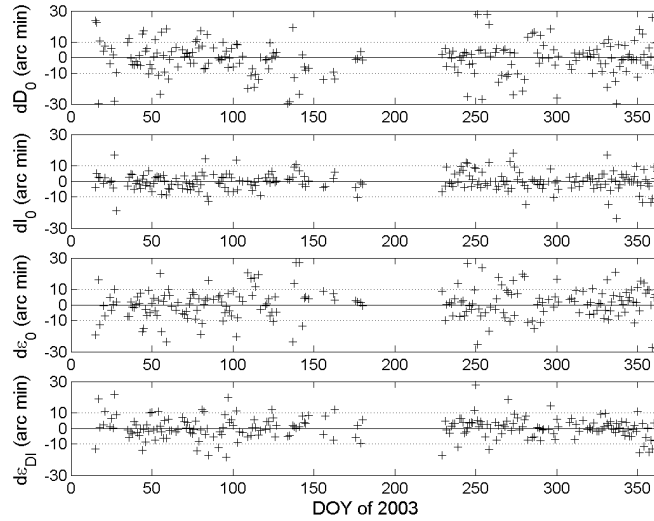


Fig. 2. The deviation of the estimated dIdD calibration parameters from their yearly means.

Here our intention was to implement a relative calibration between the dIdD and the main recording system of the observatory to be able to fill incidental data gaps. For this purpose we did not need a perfect calibration, we could be satisfied with a ‘good enough’ solution, when the component difference fluctuations do not surpass the instrument noise level. The real dIdD orientation can be found in a similar way. In that case instead of using a reference variometer, a sufficiently long series of absolute measurements is needed as a reference.

6. Summary

In this paper a method was presented for the determination of the orientation of a dIdD instrument, as well as its orthogonality error. The process is based on minimiz-

ing the fluctuation of the component differences between the calibrated and the reference instruments. The accuracy of this method at mid-latitudes is at the order of a few mrad, but even better can be achieved by averaging the estimations for 10-20 days. The accuracy level is limited by the S/N of the difference signals.

Acknowledgments. I thank my colleagues: A. Csontos, L. Hegymegi, L. Merényi, L. Szabados (ELGI, Hungary), L. Pankratz, E. Sauter (USGS Geomagnetism Group) and I. Hrvoic (Gem Systems) for their contribution to the dIdD project. I also thank J.J. Schott for the helpful discussions we had several years ago when he stayed at the Tihany observatory working on dIdD related problems. This work was supported by the Hungarian Scientific Research Fund (NI 61013).

References

- Pankratz, L.W., E.A. Sauter, A. Körmendi and L. Hegymegi, 1999, *The US-Hungarian Delta I – Delta D (dIdD) Quasi-absolute Spherical Coil System. Its history, evolution and future*, Geophysical Transactions **42**, 195-202.
- Schott, J.J., and P. Leroy, 2001, *Orientation of the dIdD magnetometer*, Contributions to Geophysics and Geodesy **31**, 43-50.
- Schott J.J., V. Boulard, A. Péres, J.M. Cantin and J. Bitterly, 2001, *Magnetic component measurement with the dIdD*, Contributions to Geophysics and Geodesy **31**, 35-42.

Accepted February 21, 2007

On the Various Published Formulas to Determine Sensor Offset and Sensor Misalignment for the DI-flux

Jürgen MATZKA^{1,2} and Truls Lynne HANSEN³

¹ now at: Danish Meteorological Institute
Lyngbyvej 100, DK-2100 Copenhagen, Denmark
e-mail: jmz@dmi.dk

² previously at: Geophysical Observatory Fürstenfeldbruck, University Munich
Ludwigshöhe 8, D-82256 Fürstenfeldbruck, Germany

³ Tromsø Geophysical Observatory, University of Tromsø
N-9037 Tromsø, Norway
e-mail: Truls.Hansen@tgo.uit.no

A b s t r a c t

An inconsistency regarding the calculation of sensor offset and sensor misalignment for the fluxgate theodolite in the IAGA Guide for Magnetic Measurements and Observatory Practice (Jankowski and Sucksdorff 1996) is discussed and resolved by comparison of the given formulas and examples with the original literature (Kring Lauridsen 1985) and experimental data. An erroneous sign is found on page 99 in formula (5.7) for inclination collimation and formula (5.8) for sensor offset calculated from the declination measurement. Jankowski and Sucksdorff (1996) have the same formulas as Kring Lauridsen (1985), but a different sequence of theodolite positions for the declination measurement led to a confusion of input variables and consequently to the erroneous signs. An electronic version of Kring Lauridsen (1985) is now available on request.

1. Introduction

The absolute measurement of declination D by a fluxgate theodolite (DI-flux) as described by Kring Lauridsen (1985) and on page 87 to page 100 in Jankowski and Sucksdorff (1996) is not affected by the sensor offset of the fluxgate and the misalignment of the fluxgate sensor with the optical axis of the telescope, provided that the sensor offset and the misalignment are small and remain constant during the measurement. In the following, the reference to Kring Lauridsen (1985) will be abbreviated

by KL and Jankowski and Sucksdorff (1996) by JS. The sensor offset S_0 is defined as the (small) fluxgate reading in zero field (KL, formula 5). The horizontal misalignment or declination collimation δ is the (small) angle between the sensor axis and the plane defined by the optical axis X' and the downward pointing axis Z' of the horizontal circle. For a north-pointing telescope, $\delta > 0$ if the sensor axis is misaligned towards a northeasterly/southwesterly direction. The vertical misalignment or inclination collimation ε is the (small) angle between the optical axis and the plane defined by the sensor axis and Y' , which is the axis of the vertical circle. For a north-pointing telescope, $\varepsilon > 0$ for a sensor axis dipping to north (KL, formula 2). All three parameters are now referred to as theodolite parameters. When calculated from a declination measurement, they will be referred to as $S_{0,D}$, δ_D and ε_D . Likewise, the inclination measurement as described in KL and JS allows to calculate the sensor offset $S_{0,I}$ and the inclination collimation ε_I . The declination collimation δ cannot be calculated from the inclination measurement described in KL and JS.

For measurements of declination and inclination with the DI-flux we noticed opposite signs for $S_{0,D}$ and $S_{0,I}$ as well as for ε_D and ε_I when using the procedures and formulas given in JS. A further complication arose from the fact that this inconsistency apparently does not affect the example for a declination and an inclination measurement given there. For obvious reasons, this problem didn't receive much attention in the past. Firstly, the number of geomagnetic observatories that calculate theodolite parameters seems to be limited, and most of these base their calculation on the original publication by KL (leading to consistent results, see below). Secondly, theodolite parameters are usually adjusted to be close to zero and the discrepancy in sign can then be disguised by the noise level of the measurement. Thirdly, the main purpose of routinely calculating the theodolite parameters, namely to control their stability from one measurement to the other, is not adversely affected by an erroneous sign. It is nevertheless of advantage to know the correct signs of the misalignment angles, e.g. during any procedure of adjusting a sensor on a telescope. Whereas the IAGA guidebook (JS) is an important and valuable contemporary reference for geomagnetic observatory work and widely in use, the original publication by KL has been out of print, making it difficult for interested persons to work out the differences in theodolite parameters for KL and JS. In the following, the above described inconsistency is discussed and resolved. Additionally, an electronic copy of KL is available on request.

2. Results

2.1 *Experimental results*

Figure 1 shows sensor offset $S_{0,D}$ and $S_{0,I}$ and inclination collimation ε_D and ε_I for six DI-flux measurements at the Geophysical Observatory Fürstfeldbruck (FUR). The theodolite is a Zeiss 10B and no particular care was taken to adjust the sensor axis to the optical axis. The absolute measurements were conducted with the zero-method and according to the procedure described in JS (their Tables 5.1, 5.2 on pages 90 to 93). The theodolite parameters were calculated according to JS (their formulas 5.6 to

5.10 on pages 99, 100). It is obvious from Fig. 1 (left panel) that both $S_{0,D}$ and $S_{0,I}$ as well as ε_D and ε_I are of opposite sign. The sensor offset S_0 is additionally dependent on temperature (right panel). We note that the change in ε_D and ε_I between measurements no. 3 and no. 4 in Fig. 4 is large compared to the variation of ε_D and ε_I usually observed from one absolute measurement to the next at FUR and that this coincides with an intentional transfer of the DI-flux from one pillar to another.

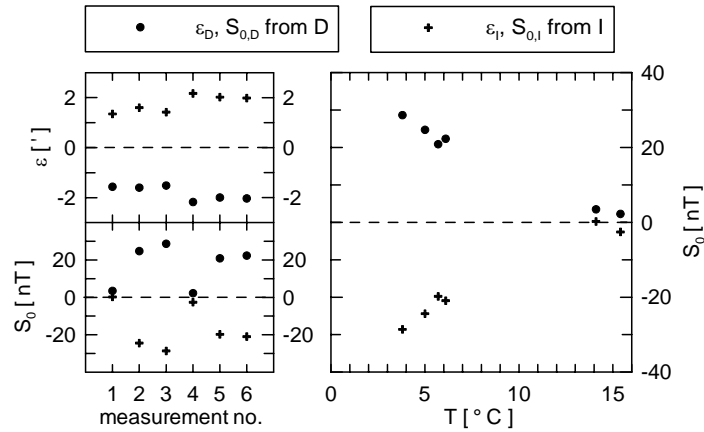


Fig. 1. Theodolite parameters inclination collimation ε_D and ε_I and sensor offset $S_{0,D}$ and $S_{0,I}$ determined according to JS for six DI-flux measurements at FUR (left panel). The strong variability of the sensor offset S_0 is controlled by temperature (right panel).

The sign for all theodolite parameters for the experimental data from Fig. 1 and the example calculated in JS (their Tables 5.1, 5.2) is given in the upper part of Table 1. For both data sets, the theodolite parameters were calculated according to the procedure outlined in JS and in KL. Within both data sets, the calculation after JS and after KL gives the same sign only for the parameters $S_{0,I}$, δ_D and ε_I . The experimental data from Fig. 1 gives consistent results for $S_{0,D}$ and $S_{0,I}$ as well as for ε_D and ε_I when calculated after KL, but opposite signs when calculated after JS. The data from JS (their Tables 5.1, 5.2) behaves exactly vice versa.

An experiment was performed, where the fluxgate sensor housing was deliberately misaligned by comparatively large angles. The tangents of the angles were determined with a ruler. Following the definition of the signs of the angles by KL as outlined in our introduction, the angles were approximately $\delta = +2.3^\circ$ and $\varepsilon = +1.6^\circ$. This substantial misalignment was chosen to be larger than any additional misalignment between the sensor axis and the sensor housing to make sure that the sign of the misalignment is well defined. The resulting theodolite parameters determined according to the procedures of JS and KL are shown in the lower left part of Table 1. Firstly, we recognise that the signs of individual parameters do show the same relationship between the result after JS and the result after KL as we already observed for the experimental data of Fig. 1. From that, a simplified scheme can be derived for the two experimental data sets. In this scheme, all theodolite parameters calculated after KL

are set to be +1 and the parameters for JS are set +1 when the sign is the same as after KL, or -1 when the sign is opposite to KL. This derived scheme is shown in the lower right part of Table 2. Secondly, δ_D , ε_D and ε_I calculated after KL and δ_D and ε_I calculated after JS are in agreement with the deliberate misalignment. However, ε_D calculated after JS gives the opposite sign.

Table 1
Sign of theodolite parameters

| | Experimental data from Figure 1, this paper | | Example data from JS, their Table 5.1, 5.2 | |
|---------------------------------|--|-------------------------------|---|-------------------------------|
| Theodolite parameters ... | ... calculated after JS | ... calculated after KL | ... calculated after JS | ... calculated after KL |
| $S_{0,D}$ | + | - | - | + |
| $S_{0,I}$ | - | - | - | - |
| δ_D | - | - | + | + |
| ε_D | - | + | + | - |
| ε_I | + | + | + | + |
| | Experimental data with $\delta \sim +2.3^\circ$ and $\varepsilon \sim +1.6^\circ$ | | Experimental data, derived scheme | |
| Theodolite parameters ... | ... calculated after JS | ... calculated after KL | ... calculated after JS | ... calculated after KL |
| $S_{0,D}$ | 13 nT | -13 nT | -1 | +1 |
| $S_{0,I}$ | -8 nT | -8 nT | +1 | +1 |
| δ_D | 1.8° | 1.8° | +1 | +1 |
| ε_D | -1.4° | +1.4° | -1 | +1 |
| ε_I | +1.4° | +1.4° | +1 | +1 |

2.2 Comparison of formulas

The publication by KL was checked for possible errors in sign by one of us (TLH) without being able to find one. In the following, we will neglect any terms arising from temporal variations, or from the residual or close-to-zero-technique, or from imperfect telescope leveling. Then, the structures of the formulas given by JS are identical to those in KL, e.g. compare the formula for δ_D in JS (their formula 5.6) with the one in KL (his formula 13, his Table 1). A difficulty in comparing the formulas is that the circle readings for the DI-flux measurements are labeled sequentially with an index running from 1 to 4 both in KL (e.g. as $\varphi_1, \varphi_2, \varphi_3, \varphi_4$ in his formula 13) and in JS (e.g. as A'_1, A'_2, A'_3, A'_4 , in their formulas 5.6 to 5.8). The index from 1 to 4 refers to

one of four theodolite positions during either the declination or the inclination measurement.

Let us consider the 1. reading of the declination measurement, for which in JS the telescope is defined to be pointing to the west and the sensor is up, i.e. on top of the telescope (their Table 5.1). In KL, the first reading is done in a position where the telescope is not pointing to the west but pointing to the east and the sensor is up. Note that this information is not immediately obvious in KL, because the orientation of the alidade there is indicated by the position of the vertical circle, not of the telescope. The positions of the theodolite in KL can also be reconstructed from the scheme on his page 4, where clearly the 1. position is obtained by rotating the telescope by approximately $\pi/2 + D$ from north towards east. In Table 2 the sequence of all four positions for both the declination and inclination measurement after KL and JS are compared.

Table 2

Various sequences of the four positions for DI-flux measurements

| Position no: Sequence: | 1 | 2 | 3 | 4 |
|---------------------------|----------------------------|-----------|-----------|-----------|
| Declination after JS | telescope: W sensor: up | E up | W down | E down |
| Declination after KL | telescope: E sensor: up | W up | E down | W down |
| Inclination JS and KL | telescope: N sensor: up | S down | N down | S up |

3. Discussion

The internal consistency of the theodolite parameters calculated after KL and the internal inconsistency in sign for $S_{0,D}$ and $S_{0,I}$ as well as ε_D and ε_I calculated after JS already suggests some error in sign for the method described in JS (Table 1, upper left part). The validity of the calculation of ε_D , ε_I and δ_D after KL is independently confirmed by experimental results from a fluxgate with known misalignment (Table 1, lower left part). Also, the validity for δ_D and ε_I and the error in sign for ε_D calculated after JS are confirmed. Employing the experimentally derived scheme (Table 1, lower right part) suggests (but doesn't prove) that $S_{0,D}$ after JS is subject to an error in sign and that $S_{0,I}$ after JS is correct.

A comparison of the procedures and formulas shows that there is no difference for the inclination measurement between KL and JS. However, for the declination measurement the first and the second as well as the third and the fourth position are interchanged in JS compared to KL (Table 2). The circle readings of the first and second position as well as for the third and fourth reading are contributing to the formulas of $S_{0,D}$ and ε_D with different sign and the observed interchange of the positions leads to the opposite sign for this parameters (e.g. formula 5.7 and 5.8 on page 99. in JS).

However, in the formula for the calculation of δ_D (e.g. formula 5.6 on page 99 in JS), the readings of the third and second position as well as the for the third and fourth position are contributing with the same sign, and the observed interchange does not change the sign here.

In contrast to all experimental data that we have gathered, the measurement example shown and calculated in JS is in itself consistent. Also, it gives inconsistent signs for the theodolite parameters when calculated after KL (Table 1, upper right panel). Since the problem in JS is an interchange of measurement position which is not taken into account in their formulas, the actual values cited in their example must also have experienced an interchange in one way or another.

4. Conclusion

The experimental results and the comparison of the formulas in JS and KL lead to the conclusion, that either the sequence of positions as laid down in JS (their Table 5.1, starting with telescope pointing west and sensor up) has to be changed to the sequence described by KL (starting with telescope pointing east, sensor up) to fit the formulas 5.7 and 5.8 on page 99 in JS, or that the sign for $S_{0,D}$ and ϵ_D in formulas 5.7. and 5.8 on page 99 in JS has to be changed to fit the sequence described in Table 5.1 in JS. In order to make available new copies of KL, we have produced an electronic version that is available on request.

Acknowledgements. JM would like to thank Ole Rasmussen for initially sending him a copy of KL and time series of theodolite parameters. Martin Feller is thanked for many FUR absolute measurements.

References

- Jankowski, J., and C. Sucksdorff, 1996, *Guide for Magnetic Measurements and Observatory Practice*, International Association of Geomagnetism and Aeronomy, Warsaw, 235 pp.
- Kring Lauridsen, E., 1985, *Experience with the DI-fluxgate magnetometer inclusive theory of the instrument and comparison with other methods*, Geophysical Papers R-71, Danish Meteorological Institute, Copenhagen, 30 pp.

Accepted February 13, 2007

An Assessment of the BGS $\delta D\delta I$ Vector Magnetometer

Santiago MARSAL, J. Miquel TORTA and John C. RIDDICK

Observatori de l'Ebre, CSIC – Universitat Ramon Llull
Horta Alta, 38. 43520 Roquetes, Spain

e-mails: smarsal@obsebre.es; jmtorta@obsebre.es; john_riddick@hotmail.com

Abstract

Assuming optimal conditions, the $\delta D\delta I$ vector magnetometer can be considered as a semi-absolute instrument. In this paper, the real situation and its differences with the ideal one are critically examined and regarded as potential sources of error. The analysis is applied to the equipment designed by the British Geological Survey (BGS) in the late 1980s, and the given figures are provided from the instrument in use at the Livingston Island Geomagnetic Observatory (LIV). Improved versions have been developed since then, being based on generally the same principles of measurement; thus, most of the results shown can be adapted to the new generation of magnetometers of this type.

1. Introduction

The automatic BGS $\delta D\delta I$ vector magnetometer (Riddick *et al.* 1995) consists of two mutually perpendicular pairs of Helmholtz coils and a proton magnetometer mounted at their center for total field measurements, F . Two bias currents are alternatively applied to each pair of coils in opposite senses, generating additional magnetic fields in the proton magnetometer, which allow the measurement of variations in magnetic Declination (from the D pair), δD , and Inclination (from the I pair), δI . This device was initially conceived as a semi-absolute instrument (Alldredge 1960, or Alldredge and Saldukas 1964). Following this assumption, the origin of the angular variations, D_0 and I_0 , requires to be established once by making absolute measurements; after that, D and I are computed from $D_0 + \delta D$ and $I_0 + \delta I$, respectively. For this equipment to operate as a semi-absolute observatory instrument, a series of requirements are necessary, the most important of which are presented below:

- Stability of the pier where the instrument is deployed;
- Both D coils are parallel and contained in a vertical plane;
- The D and I pairs are perfectly, mutually perpendicular;

- The coils polarization is identical in both (direct and inverse) directions;
- Geometrical stability (e.g., no temperature or humidity effects);
- The proton magnetometer is located at the centre of both pairs and its dimensions are small as compared with the coils.

If these requisites are fulfilled, it can be shown that Eqs. (1) and (2) hold:

$$D = D_0 + \delta D = D_0 + \arcsin\left(\frac{f(D)}{\cos I}\right), \quad (1)$$

$$I = I_0 + \delta I = \arcsin\left(\sin I_0 \sqrt{1 - f(I)^2 - f(D)^2} + f(I) \cos I_0\right), \quad (2)$$

where:

$$f(x) \equiv \frac{F_{x+}^2 - F_{x-}^2}{4FA_x}, \quad x = D, I \quad (3)$$

$$A_x = \sqrt{\frac{F_{x+}^2 + F_{x-}^2}{2} - F^2} \quad (4)$$

and $F_{x\pm}$ is the magnetic field intensity generated by the direct (+) and inverse (-) polarization of the corresponding coils. In practice, A_x is approximately the mean value of the direct and inverse fields, $A_{x\pm}$, generated by the coils along their respective axes, while $F_{x\pm}$ result from the vector addition of $A_{x\pm}$ and the natural magnetic field.

2. The Real Case

In this section we analyze the errors produced in a real situation, as operationally not all of the above mentioned requirements can be met.

2.1 Approximations

Developing Eqs. (1) and (2) up to second order we get:

$$D = D_0 + \delta D \cong D_0 + \frac{180^\circ}{\pi} \frac{f(D)}{\cos I} \cong D_0 + \frac{180^\circ}{\pi} \frac{f(D)}{\cos I_0} (1 + f(I) \tan I_0), \quad (5)$$

$$I = I_0 + \delta I \cong I_0 + \frac{180^\circ}{\pi} f(I) - \frac{90^\circ f^2(D)}{\pi} \tan I_0, \quad (6)$$

where D and I (and related angles) are expressed in degrees.

In the observatory practice, Eq. (5) is normally used integrally, while the first-order approximation is used for Eq. (6). The term neglected in this equation can be written as follows:

$$\frac{90^\circ f^2(D)}{\pi} \tan I_0 \cong \frac{\pi}{360^\circ} \sin I_0 \cos I_0 \delta D^2. \quad (7)$$

The error generated as a result of omitting this term depends on the change in Declination, δD , which can easily exceed 1° during periods of high magnetic disturbance. These field changes can lead to an error of the order of 15 arc-seconds at mid-latitude observatories. We can even consider that the absolute value of δD is increasing with time in a given observatory as a result of the secular variation; in consequence, if the instrument is not re-oriented from time to time in order to reduce δD , the error generated by neglecting the last term of Eq. (6) can reach the order of 0.1 arc-minutes per year at locations of a high secular variation. This error can be overcome by simply using the second-order expression, thus avoiding the annoying necessity of re-orientating the coils.

2.2 Accuracy and time resolution

The maximum theoretical accuracy can be determined by assuming that the only limitation of the instrument is due to the proton magnetometer precision, acting in a random manner for the different measurements of the field vectors made during a cycle of measurements, i.e., F_{D+} , F_{D-} and F for D ; F_{I+} , F_{I-} and F for I . Hence, the associated statistical error is propagated as a sum of squares for both, D :

$$\begin{aligned}\delta(\delta D) &= \sqrt{\left(\frac{\partial(\delta D)}{\partial F_{D+}} \delta F_{D+}\right)^2 + \left(\frac{\partial(\delta D)}{\partial F_{D-}} \delta F_{D-}\right)^2 + \left(\frac{\partial(\delta D)}{\partial F} \delta F\right)^2} \\ &= \frac{180^\circ}{\pi} \frac{\delta F}{\cos I_0} \sqrt{\frac{1}{2A_D^2} + \frac{1}{2F^2}}\end{aligned}\quad (8)$$

and I (where the terms A_D and $\cos I_0$ from Eq. (8) are to be substituted with A_I and 1, respectively). With a series of assumptions, and considering that the accuracy of the proton magnetometer is $\delta F = 0.2$ nT in its full range, an accuracy between 1 and 5 arc-seconds can be obtained for most of the mid-latitude observatories for both angular elements. In practice, accuracy will also depend on the stability of the current applied to the coils in both senses, $A_{x\pm}$.

The time resolution is limited by the length of time it takes to make a complete set of measurements. The time required for total field measurements depends upon the proton magnetometer type in use; additionally, both F_{x+} and F_{x-} need a certain time to establish a stable current in the coils. At LIV, the complete cycle (F_1 , F_{I+} , F_{I-} , F_2 , F_{D+} , F_{D-}) takes for 28 s; this slow sampling impedes the detection of rapid magnetic variations. The new generation of $\delta D \delta I$ magnetometers has reduced the cycle duration in order to increase the sampling rate and meet INTERMAGNET requirements (see www.intermagnet.org/im_manual.pdf).

2.3 Instrument orientation and imperfect orthogonality of the coils

Poor instrument orientation is another factor that limits its accuracy. This misorientation can be described by three successive rotations defined by the angles Φ , ψ and θ around the three coordinate axes. If D_0 and I_0 are the Declination and Inclination of the D and I coils respectively, let Φ be the difference between the real value of D_0 and

its assumed value, ψ the difference between the assumed value for I_0 and the corresponding real value, and θ the angle between the vertical plane and the plane defined by the D coils (θ is positive when the D coils are turned anti-clockwise when looking from the North side). It can be demonstrated that Eqs. (1) and (2) are modified as follows as a result of this general rotation:

$$D = D_0 + \varphi + \arcsin\left(\frac{f(D) - \sin\theta \sin I}{\cos\theta \cos I}\right), \quad (9)$$

$$I = \arcsin\left[\sin(I_0 - \psi) \cos\theta \sqrt{1 - f(I)^2 - f(D)^2} + f(D) \sin\theta + f(I) \cos\theta \cos(I_0 - \psi)\right]. \quad (10)$$

It should be noted that angles Φ and ψ are corrected with the D and I base lines, respectively, but not θ . Hence, it is very important to align the D coils in a vertical plane when the instrument is deployed for the first time. In order to avoid this effect, the new generations of $\delta D \delta I$ include suspended coils (Hegymegi 2004). The above expressions can also be used to characterize tilting of the pier; in this case, we have to consider the possibility that Φ , ψ and θ are time-dependent.

The imperfect orthogonality of the D and I pairs of coils can also be analyzed. Let σ be the angle between the plane defined by the D coils and the line orthogonal to the I coils (σ is positive when the I coils are turned anti-clockwise when looking from the North side). It can be shown that Eq. (9) still holds, whilst a term $\sigma f(D)$ is to be added to the second-order development of Eq. (10).

2.4 Errors due to current instabilities. Despiking

A fundamental requirement for the correct measurement of the D and I variations is that both deflecting fields, A_{x+} and A_{x-} , are of equal magnitude. Let us call it ‘‘hypothesis of symmetrical polarization’’. If this hypothesis is not fulfilled, an erroneous measurement will be produced, resulting in a spike in the data. The fundamental problem arises from our ignorance of the separated values A_{x+} and A_{x-} . The technique we propose following is aimed at detecting spikes from the $\delta D \delta I$ data. It consists of searching for asymmetrical polarizations. In practice, the current stability varies, as it can be observed from Fig. 1, where a temperature dependence is clearly shown. Nevertheless, this effect is not in general appreciated during the short time a single measurement cycle lasts.

Similar reasonings apply to both Declination and Inclination; hence, let us consider only Inclination. From geometrical considerations, and with the above mentioned approximations, it is easy to compute δI for both the direct and inverse polarizations:

$$\delta I_+ = \frac{180^\circ}{\pi} \left(\frac{F_{I_+}^2 - F - A_{I_+}^2}{2FA_{I_+}} \right), \quad (11)$$

$$\delta I_- = -\frac{180^\circ}{\pi} \left(\frac{F_{I_-}^2 - F - A_{I_-}^2}{2FA_{I_-}} \right). \quad (12)$$

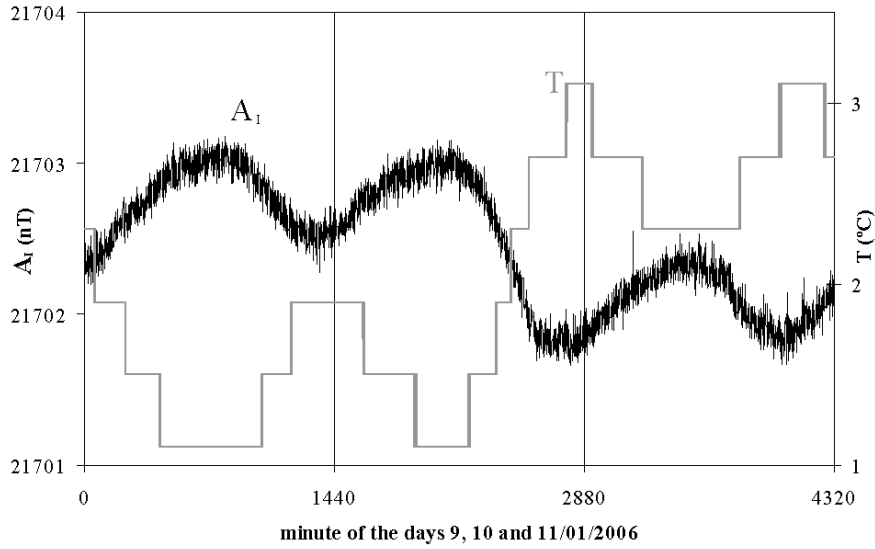


Fig. 1. The field intensity A_I (Eq. 4, black line in the figure) generated by the bias currents in the I coils at LIV is negatively correlated with temperature (grey line).

Additionally, if we make $A_{I+} = A_{I-} \equiv A_I$ and $\delta I_+ = \delta I_- \equiv \delta I$, we obtain Eq. (4) for A_I and the first-order approximation of Eq. (6) for δI , i.e., $180^\circ/\pi \cdot f(I)$. By similitude with Eqs. (11) and (12), let us now introduce the following two observables:

$$\delta I'_+ = \frac{180^\circ}{\pi} \left(\frac{F_{I+}^2 - F - \langle A_I \rangle^2}{2F \langle A_I \rangle} \right), \quad (13)$$

$$\delta I'_- = -\frac{180^\circ}{\pi} \left(\frac{F_{I-}^2 - F - \langle A_I \rangle^2}{2F \langle A_I \rangle} \right), \quad (14)$$

where $\langle A_I \rangle$ stands for the “normal” or mean value of the polarization intensity, and it can be computed in several ways, as for example:

$$\langle A_I \rangle = \frac{1}{60} \sum_{\substack{m'=m-30 \\ (m' \neq m)}}^{m+30} A_{I,m'}, \quad (15)$$

i.e., the mean of A_I computed as Eq. (6) one hour around the minute of interest, m , excluding the value corresponding to this minute. If an anomaly is present in the minute m , e.g., only in the direct (+) polarization, it will be revealed in the $\delta I'_+$ observable (Eq. 13) due uniquely to the anomalous value of F_{I+} , since $\langle A_I \rangle$ is independent of minute m ; on the contrary, if the inverse polarization (and hence F_{I-}) is normal, $\delta I'_-$ (Eq. 14) will have the correct value. Therefore, a plot of $\delta I'_+$ and $\delta I'_-$ against time in the same graph will help to identify spikes in the $\delta D \delta I$ record. If both values coincide

within the instrument accuracy (see subsection 2.2), there is no reason to suspect of the value obtained for δI ; otherwise, the measurement may be in error. The discrepancy between the δI values obtained from both polarizations will become more evident if their difference is plotted, giving rise to a new observable: $disI \equiv (\delta I'_+ - \delta I'_-)/2$. In fact, this observable allows us to easily detect anomalous polarizations, since it can be shown that (for minute m) $disI_m \approx 180^\circ/\pi \cdot (A_{I,m} - \langle A_I \rangle)/F$, but it does not provide any information on the actual accomplishment of the “symmetry hypothesis”, which is the only valid criterion to reject any data. In order to do this, $ErrI$ observable is additionally defined, whose expression for minute m is as follows:

$$ErrI_m = \frac{\left| \delta I'_{+(m)} - \frac{\delta I'_{+(m+1)} + \delta I'_{+(m-1)}}{2} \right| + \left| \delta I'_{-(m)} - \frac{\delta I'_{-(m+1)} + \delta I'_{-(m-1)}}{2} \right|}{2}. \quad (16)$$

This observable helps to evaluate the symmetry degree of both polarizations, in such a way that a spike in both $disI$ and $ErrI$ -vs.-time plots in a given minute is a clear indication that the corresponding I value should be rejected. Similar expressions and procedures are valid for Declination, where a factor $\cos I_0$ is to be added in the denominator of Eqs. (11)–(14). As a real example, a spike is observed in the plot of the $ErrD$ observable (Fig. 2, data from LIV observatory) after being detected in $disD$. If these tests had not been applied, this erroneous value would have passed unnoticed.

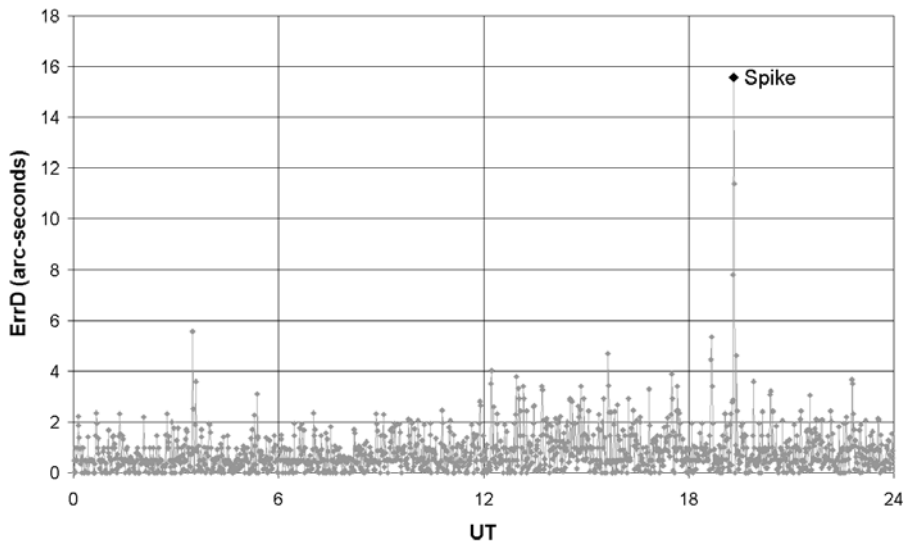


Fig. 2. A spike in Declination is corroborated by applying the $ErrD$ observable. The value is clearly outside both the surrounding data samples and the instrument accuracy.

A simpler technique can be applied to detect spikes in total intensity, F . In this case, the observable $disF$ can similarly be defined as $(F_1 - F_2)/2$, where both F_1 and F_2 are directly provided by the $\delta D \delta I$. This observable is also recommended to be com-

puted for every minute and plotted against time providing a visual detection of erroneous values. Again, if the $disF$ value for a given minute is clearly larger than both the proton magnetometer resolution and the natural magnetic disturbance for the surrounding minutes, it is a clear candidate for rejection.

2.5 Other errors

From Eq. (8) it can be concluded that the theoretical accuracy of the measurements is improved by increasing the magnetic fields induced by the coils (A_D and A_I). On the other hand, too great an applied field would produce an excessive gradient in the proton magnetometer sensor, resulting in a poor signal quality; therefore, an optimal value must be found. The finite dimensions of the coils, along with the possibility of the proton magnetometer not being exactly in the centre of both pairs of coils would also give rise to an increase in the magnetic gradient across the proton sensor. To avoid this, the BGS designed 80 cm diameter Helmholtz coils, generating a field A_x of circa 60% of the natural intensity, F . In this case, the gradient is such that a theoretical difference of a few tens of nT is produced between the centre and the extreme of the proton sensor (depending on its size). Other solutions to the gradient problems are the use of cylindrical windings, or the so-called spherical coils.

A significant temperature and humidity variation could result in a change in the $\delta D\delta I$ configuration. For this reason, the thermal expansion coefficient of the material supporting the coils, as well as its water absorption capability must be low. For instance, the instrument in use at LIV has a theoretical surface thermal expansion coefficient of $1.9 \times 10^{-5} \text{ K}^{-1}$, which implies no more than 0.2 mm yearly variation in the lineal dimensions.

3. Conclusions

The BGS $\delta D\delta I$ has proved to be a reliable system, presenting some advantages with respect to other magnetometers, such as low temperature dependence and acceptable short-term stability. Other effects, such as long-term pier instabilities or distortion of the coils alignment can introduce additional errors if the measurements are not regularly corrected by absolute observations, this being the fundamental problem of some remote observatories and especially LIV, where absolute measurements can only be carried out for three months per year.

In examining the overall accuracy of the $\delta D\delta I$ system we conclude that the main limiting factors have been found to be the ability of the coil current generator to reliably generate identical positive and negative bias currents, along with the temporal resolution being reduced by the long time period required to make a complete set of measurements.

References

- Allredge, L.R., 1960, *A Proposed Automatic Standard Magnetic Observatory*, J. Geophys. Res. **65**, 11.
- Allredge, L.R., and I. Saldukas, 1964, *An automatic Standard Magnetic Observatory*, J. Geophys. Res. **69**, 10.
- Hegymegi, L., 2004, *New Suspended dIdD Magnetometer for Observatory (and Field?) Use*, Proceedings of the XIth IAGA Workshop, 28-33, Kakioka.
- Riddick, J.C., C.W. Turbitt and J. McDonald, 1995, *The BGS Proton Magnetometer ($\delta D/\delta I$) Observatory System Mark II. Installation Guide and Technical Manual*, British Geological Survey Technical Report WM/95/32. BGS Geomagnetism Series, Edinburgh.

Accepted January 29, 2007

Quality Assurance Project for the Magnetic Calibration and Test Laboratory of the Nurmijärvi Geophysical Observatory

Kari PAJUNPÄÄ, Maria GENZER, Pentti POSIO,
Heikki NEVANLINNA and Walter SCHMIDT

Finnish Meteorological Institute, Nurmijärvi Geophysical Observatory
FIN-05100 Röykkä, Finland
e-mail: kari.pajunpaa@fmi.fi

Abstract

The magnetic calibration and test laboratory of the Nurmijärvi Geophysical Observatory is aimed for magnetometer and compass calibrations, for magnetic cleanliness measurements and for compass swing base measurements at airfields. The increased importance of space and aviation industry has given rise to the development of the quality system for the calibrations and tests. The European standard EN ISO/IEC 17025:2000 states the demands for the quality system. This standard has been followed both for technical and management requirements. We will describe main technical parameters and competence of the laboratory. Traceability to the international standards is fulfilled and comparisons with other laboratories have been made.

1. General Information

Since its beginning in 1951, the Nurmijärvi Geophysical Observatory is part of the Finnish Meteorological Institute. During the first decades, the Geophysics Department of the institute had a remarkable science program in geomagnetism and the observatory had a key role in this study. Gradually the role of space physics increased in the department and in 2004 the name of department was changed to Space Research Division. Still today observation of the magnetic field variations over the whole of Finland is one of the corner stones of the Space Research Division. The Nurmijärvi observatory has searched for other activities to preserve also basic magnetic observations. In this respect the need of the society for magnetic observations and magnetic measurements has become important. These include declination information for maps, measurements at airfields and calibrations of sight compasses. Internationally, there has

been a need for satellite and ground based magnetometer calibrations (Pajunpää *et al.* 1997) and magnetic cleanliness measurements for satellite components. Excluding the map declination measurements, the observatory has combined the calibrations and tests under the name “Nurmijärvi Magnetic Calibration and Test Laboratory” (NuMCTL).

A project was initiated at the end of 2003 to build a quality system for the laboratory and to get an accreditation for the facility. The aim of the project was to improve the reliability of the measurements and the quality of all functions. An application for the accreditation was given to the Finnish Accreditation Services (FINAS) in October 2006.

2. Building up the Quality System

The quality system was built for the NuMCTL in 2004-2005. The standard ISO/IEC 17025:2005 (CEN/CENELEC 2005) specifies the requirements for the competence to carry out tests and calibrations and was the basis for the work. A quality manual and method guides for all test and calibration methods were published. The work was guided by a steering committee that had meetings almost every month.

3. Traceability of the Measured Quantities

The measured quantities need to be traced to the international standard values (SI). In all the tests and calibrations the key values are the direction of the magnetic field and the scalar magnetic induction. Therefore, the standard magnetic observatory instruments, a DI-theodolite and a proton magnetometer, play a central role in the tracing of the measured quantities. In the magnetometer calibration the DI-theodolite is used to measure the magnetic directions in the calibration coil system, and the proton magnetometer is used to measure the coil constants. The DI-theodolite and the proton magnetometer are also used for magnetic anomaly and declination measurements on the airfields during compass swing base measurements and for absolute measurements in the absolute house of the observatory. The compass calibration is based on the known declination in the absolute house.

The traceability of the DI-theodolite is based purely on the comparison measurements at IAGA workshops and in the Nordic Comparison meetings. The proton magnetometer is also compared in the IAGA workshops but another calibration for the instrument is performed by a calibrated frequency standard. In the table below are the comparison results for the Zeiss Jena THEO 010B with a DMI fluxgate and for a PMP-7 proton precession magnetometer. The PMP-7 was here corrected for its old gyro constant. Table 1 shows the difference of the NuMCTL from the average result of the international observatory community. The calibrated 2 kHz frequency standard of the NuMCTL has given for the PMP-7 at constant temperature an error of less than ± 0.1 nT during several years.

In the magnetometer calibration the electric current measurement is the essential parameter affecting the accuracy. However the absolute accuracy of the current is not

important as it is taken care of in the coil constant determination. Critical is the stability of the current measurement. Therefore, the current measurement system based on three 1-ohm resistors is calibrated with an external reference resistor. Especially the temperature dependence of the resistors needs to be determined.

Table 1

Comparison results for the DI-theodolite and PMP-7 of the Nurmijärvi observatory

| Workshop year | Dourbes 1994 | Niemegk 1996 | Hurbanovo 2000 | Kakioka 2004 | Uppsala 2005 |
|---------------|--------------|--------------|----------------|--------------|--------------|
| Delta D | < 10" | < 5" | < 5" | < 10" | < 5" |
| Delta I | < 5" | < 5" | < 10" | < 5" | < 5" |
| F | < 0.5nT | | < 0.2nT | < 0.2nT | |

4. Estimation of Uncertainty

Estimation of the uncertainty of the measurements is based on the publication EA-4/02 of the European Co-operation for Accreditation (EAL Committee 2 1999). Standard uncertainties of all input quantities were estimated and an uncertainty budget

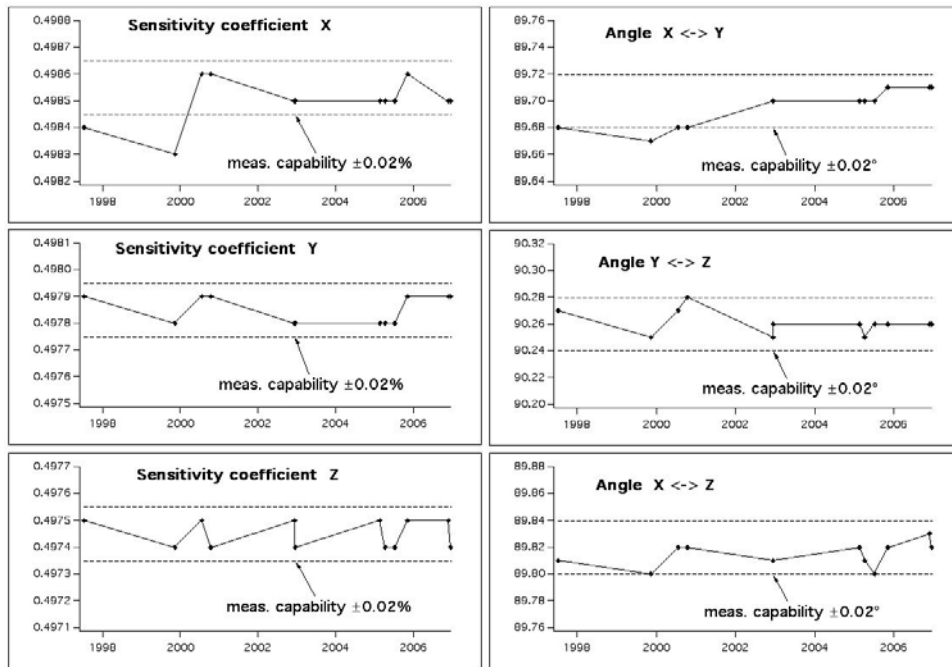


Fig. 1. Sensitivity coefficients (left) in the units [nT/mV] and angles between sensors (right) in the units [degrees] of the LEMI-004 magnetometer as determined with the calibration system during the years 1997-2006 (horizontal axis). The standard uncertainty limits are presented as the dashed lines.

was built for the calibration quantities. In Fig. 1 the standard uncertainty limits (dashed lines) are presented for the low noise LEMI-004 magnetometer (Korepanov *et al.* 1996). The aim of the picture is to present the combined stability of the magnetometer and of the calibration system.

5. Measurement Capability

In Table 2 we present the best measurement capability of the NuMCTL. These extended (coverage factor $k = 2$) standard uncertainty values were determined in the uncertainty estimation. The assigned values correspond to coverage probabilities of approximately 95%. In the case of magnetometer calibration, the uncertainty depends also on the calibrated magnetometer. The result of an instrument with poor resolution and accuracy is associated with larger numbers of uncertainty.

Table 2
Measurement capability with extended ($k = 2$) standard uncertainty

| | |
|---|---------------------------|
| Magnetometer calibration | |
| Angles between orthogonal components of a magnetometer | $\pm 0.02^\circ$ |
| Angles between magnetic and mechanical axes of a magnetometer | $\pm 0.03^\circ$ |
| Transformation coefficients of a magnetometer | $\pm 0.02\%$ |
| Offsets of a magnetometer | ± 1 nT |
| Temperature drift of a magnetometer | ± 0.03 nT/ $^\circ$ C |
| Compass calibration | |
| Error of a sight compass | $\pm 0.5^\circ$ |
| Magnetic cleanliness measurement | |
| Magnetic dipole moment | $\pm 5\%$ |
| Direction of magnetic dipole | $\pm 5^\circ$ |
| Centre of magnetic dipole | ± 5 cm |
| Compass swing base measurement | |
| Relative magnetic declination | $\pm 0.02^\circ$ |
| Absolute magnetic declination | $\pm 0.03^\circ$ |

6. Discussion

The NuMCTL provides means and equipment for accurate calibration of three-component magnetometers for satellite and ground based observations. Sight compasses are calibrated for aviation companies and authorities and compass swing bases at airfields are explored for magnetic anomalies and determined for declination. Additionally the laboratory makes magnetic cleanliness measurements for satellite instruments.

A quality system has been built for the laboratory and an application for accreditation has been left for most part of NuMCTL activities.

References

- CEN/CENELEC, 2005, EN ISO/IEC 17025:2005 – *General requirements for the competence of testing and calibration laboratories*, CEN National Members and CENELEC Members, 61 pp.
- EAL Committee 2, 1999, EA-4/02 – *Expression of the uncertainty of measurement in calibration*, EAL Task Force, 79 pp.
- Korepanov, V., B. Bondaruk, R. Berkman, L. Rakhlin, L. Hegymegi and A. Kormendi, 1996, *Fluxgate magnetometer design*. **In:** Proceedings of the VI Workshop on Geomagnetic Observatory Instruments, Data Acquisition and Processing, 18-24 September, 1994, Dourbes, Belgium, 28-31.
- Pajunpää, K., V. Korepanov and E. Klimovich, 1997, *Calibration system for vector DC magnetometers*. **In:** Proceedings of the XIV IMEKO World Congress, 1-6 June, 1997, Tampere, Finland, IVA, 97-102.

Accepted February 12, 2007

Temperature Tests on Modern Magnetometers

András CSONTOS, László HEGYMEGI and Balázs HEILIG

Eötvös Loránd Geophysical Institute
Budapest, Kolombusz utca 17-23. H-1145. Hungary
e-mail: csontos@elgi.hu

Abstract

Geomagnetic observatory and field work needs very accurate measurements. The precision of the measurements is affected by several factors but one of the most important is the temperature change. That is why every observatory tries to provide stable temperature environment for recording instruments. The temperature correction is an important part of data reduction. The manufacturers use different ways to reduce the temperature effect on instruments. Having a lot of trouble working on this problem we decided to build a nonmagnetic temperature test hut in Tihany Observatory. In this hut we have tested temperature sensitivity of different types of magnetometers. In this paper we present some of our results.

1. Introduction

The temperature sensitivity is one of the most important parameters affecting the long-term stability of magnetometers used in observatory and field practice. To improve the precision, temperature stable environment and calculated corrections are applied in most observatories. This solution can be effective within a certain limit in an observatory, but generally unusable at repeat station measurements. In order to improve the precision, we decided to study the characteristics of the temperature effect on different magnetometers. Having more detailed information on these processes, one can construct more ideal circumstances his measurements. On the other hand, this study can lead us to the main sources of disturbing effects and gives us hope to eliminate or at least to reduce them.

Individual instruments, because of constructional differences can have different “weak points”, where the big part of the instability comes from. Usually one or more of the following factors is responsible for the effect:

- a) Mechanical deformation of the sensor holder;
- b) Electrical parts of the magnetometer are sensitive to temperature changes;
- c) The inhomogeneous compensation field of the fluxgate sensor (Bitterly *et al.* 1988);
- d) Thermal change of susceptibility;
- e) Transient effects.

Improvement can be achieved in different ways and the main directions are the following:

- a) Appropriate choice of material for parts of the magnetometer;
- b) Ensure mechanical stability for the sensor (e.g. Rasmussen 1991);
- c) Real-time data correction using independent measurements (for example temperature or tilt meters) (Korepanov *et al.* 2004);
- d) Using methods theoretically free from temperature effect.

These steps are not independent of each other. Several manufacturers apply more of them at the same instrument, but the results are different. Having a lot of trouble working on this problem, we decided to build a nonmagnetic temperature test hut in Tihany Geophysical Observatory. The goal of this project was to study the most important source of temperature effect on magnetometers by using high amplitude thermal change and comparison of different types of modern magnetometers in practically similar conditions. The tested instruments are most common in observatories and they represent four different ways in the production of high precision magnetometers.

To separate the temperature effect on the sensor from the effect on the electronics, during the tests we put only the sensor units into the heat chamber. The electronic unit of the instrument was in nearly constant ambient temperature. In this way our results show the behavior of the sensor's scale factor and offset.

We suppose that the temperature change has some effect on the pier too but because all the instruments (except DMI FGE) were tested on the same pier and with identical temperature conditions, this effect was neglected. On the other hand, from the point of view of a user, an integrated effect is interesting if he wants to use his instrument not only in the observatory but also in the field during magnetic repeat station measurements.

2. Background

It is not a usual task in the observatory activity to build a nonmagnetic temperature test hut but it was relatively easy to realise it in Tihany Geophysical Observatory, because one of our building was practically a double isolated pavilion. After reinforcing the thermal isolation we installed the programmable heating and cooling system. We applied infrared lamps for heating and as far as possible nonmagnetic air conditioner device for cooling. All the unnecessary iron parts of the air conditioner device were removed, and others were changed to iron-free material. The distance between the compressor and the hut is 11 meters. To control the temperature in the hut we built an electronics. Using this unit the amplitude, the period and the wave form (sinusoidal

or triangle) of the temperature change was possible. We used to set maximum $1.5^{\circ}\text{C}/\text{hour}$ temperature change, because this value is realistic during the field work. The maximum range of temperature change was 50°C . After the first experiments we experienced magnetic influence caused by the Seebeck-effect during the cooling period caused by two different metals in the heat sink. After to change it for aluminium the effect disappeared.

In this paper we present the test of the Narod triaxial ring-core fluxgate magnetometer, Danish Meteorological Institute FGE fluxgate magnetometer, LEMI-17 triaxial fluxgate magnetometer and the suspended DIDD system. All the tested and reference instruments are oriented (or in case of DIDD system transformed) to XYZ coordinate system. The main reference instruments were the DMI FGE magnetometer. This instrument is installed in the new variation house of the observatory in temperature stabilised environment to $\pm 0.2^{\circ}\text{C}$. During the test of DMI FGE, the reference instrument was the DIDD system of the observatory. This system is installed in the old variation house. This building is a cellar, that is why the temperature change was practically zero during the test. The data collection system was the DIMARK, except during the test of LEMI-17 magnetometer. It had his own data acquisition system.

3. Test Results for the Different Magnetometers

3.1 Test of LEMI-17 fluxgate magnetometer

This instrument was manufactured with a built-in thermometer and tilt meter. The device automatically corrects the recorded value with the measured temperature- and tilt effect. We used its self collected temperature values for our computation too. Figure 1 shows the behavior of the difference curve between the tested and reference instrument during seven days. At the first look we can notice that there is a phase shift between the temperature and difference curves. We calculated the correlation factor between the two quantities fusing different delays to determine its maximum value. In this case maximum values are at X: -314 minutes; Y: 614 minutes; Z: 1004 minutes. A possible explanation of these delays can be that we measured the temperature not at the place of the source of the temperature effect. The next step was the computation of temperature coefficient from the delay corrected values and calculation of the residual values after temperature correction. The results without and with delay correction are different (see Fig. 2.) but the residual values show that in spite of the systematic calculation the corrected values are not free from thermal shock effect. The consequence of this result: The observer should ensure temperature stable environment for the instrument, because a part of the temperature effects can not be corrected. The temperature coefficients are: X = $0.5 \text{ nT}/^{\circ}\text{C}$, Y = $-0.33 \text{ nT}/^{\circ}\text{C}$, and Z = $0.19 \text{ nT}/^{\circ}\text{C}$. The maximal residuals are about 2 nT .

3.2 Test of Narod ring-core triaxial fluxgate magnetometer

The instrument for easy transportation was placed in a plastic box. The sensor has an 80 meter long cable. This device does not have any built-in thermometer, that is why we used an external temperature sensor. For temperature variation effect on the instrument, see Fig. 3.

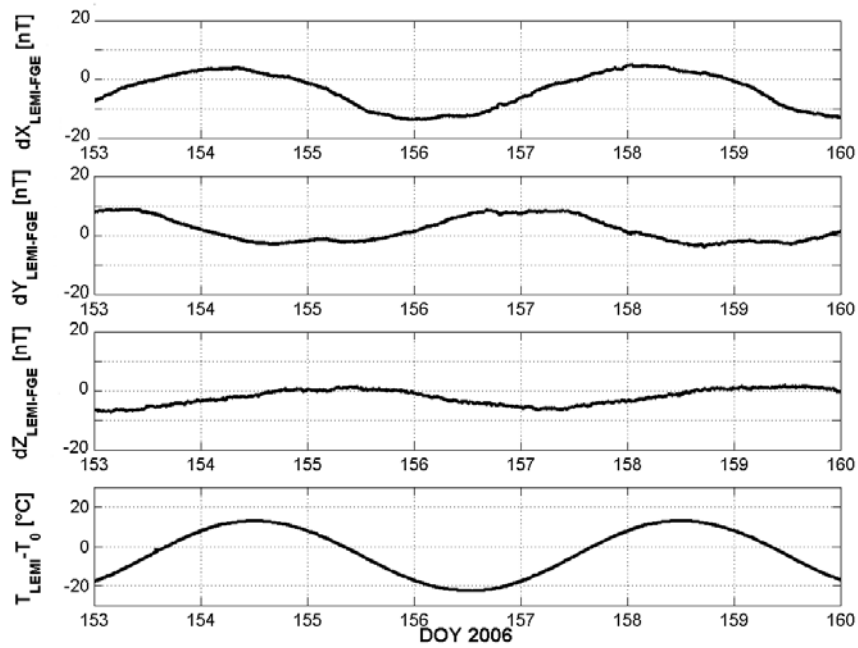


Fig. 1. Variation of the difference value between the LEMI-17 and the reference system.

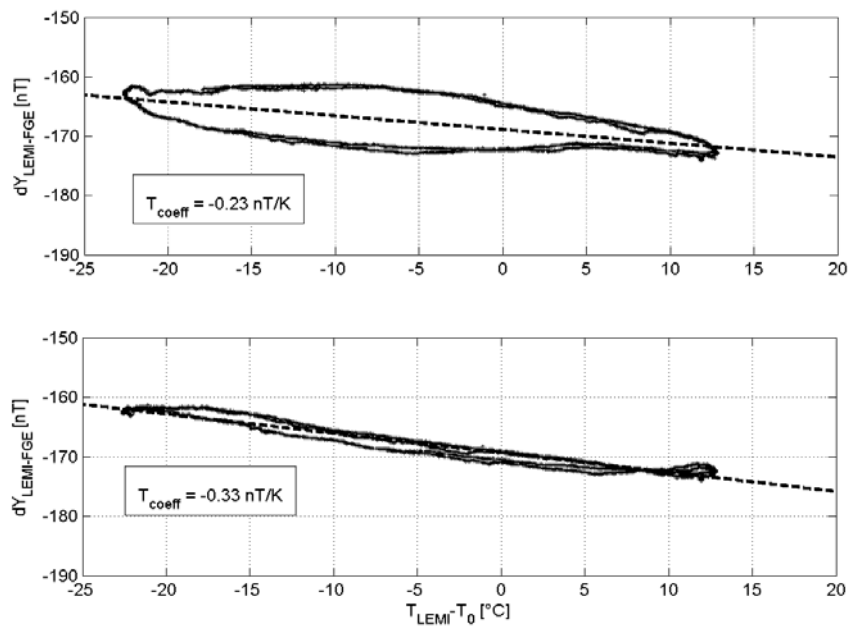


Fig. 2. Calculated temperature coefficient without (upper) and with delay correction (lower).

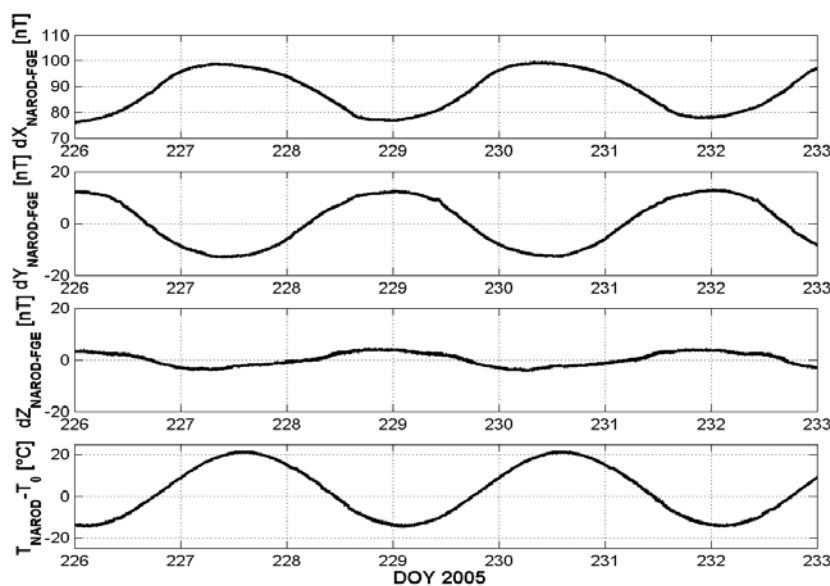


Fig. 3. Behaviour of the Narod magnetometer during the period of temperature test.

The calculations are the same like in case of LEMI. The delays are: $X = -133$ minutes, $Y = -182$ minutes, and $Z = -247$ minutes. The temperature coefficients are: $X = 0.64$ nT/°C, $Y = -0.73$ nT/°C, and $Z = 0.21$ nT/°C. The maximal residuals are about 2 nT.

3.3 Test of DMI FGE magnetometer

The tested DMI FGE magnetometer is the main recording system of the observatory. That is why we did not test it in the temperature hut. During the extremely cool winter, the temperature in the new variation house of the observatory was not stable. This circumstance gave us the possibility to determine the temperature coefficient of the suspended device. We may consider this measurement as a control experiment. Figure 4 shows the behavior of the difference value between the tested and reference instruments and the temperature of the sensor measured by the built-in thermometer.

The range and the speed of the temperature variation are more attenuated in this experiment. The results of the calculation are similar to the above described fluxgate magnetometers. The delays are: $X = 380$ minutes, $Y = 146$ minutes, and $Z = \text{na.}$ The temperature coefficients are: $X = 0.28$ nT/°C, $Y = -0.58$ nT/°C, and $Z = -0.08$ nT/°C. The maximal residuals are about 1 nT.

3.4 Test of DIDD magnetometer

The suspended mini DIDD system was tested in the temperature hut too. This vector magnetometer is based on Overhauser effect (see Hegymegi *et al.* 2004 for more details). The temperature is measured by an external temperature sensor. Figure 5 shows the difference curves between the DIDD and the reference instrument after correction with phase shift and the calculated thermal coefficients.

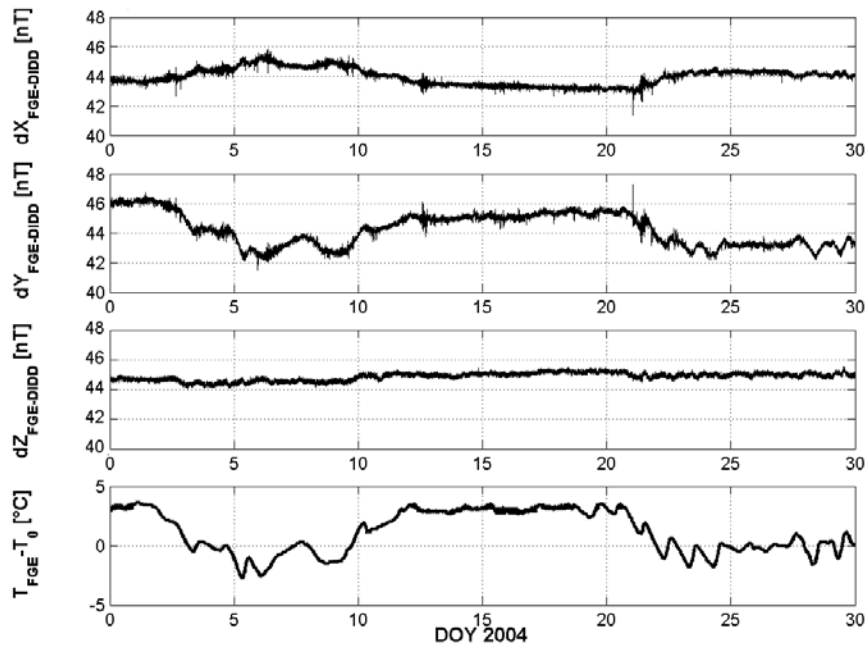


Fig. 4. Behaviour of the DMI FGE magnetometer during the extremely cool winter.

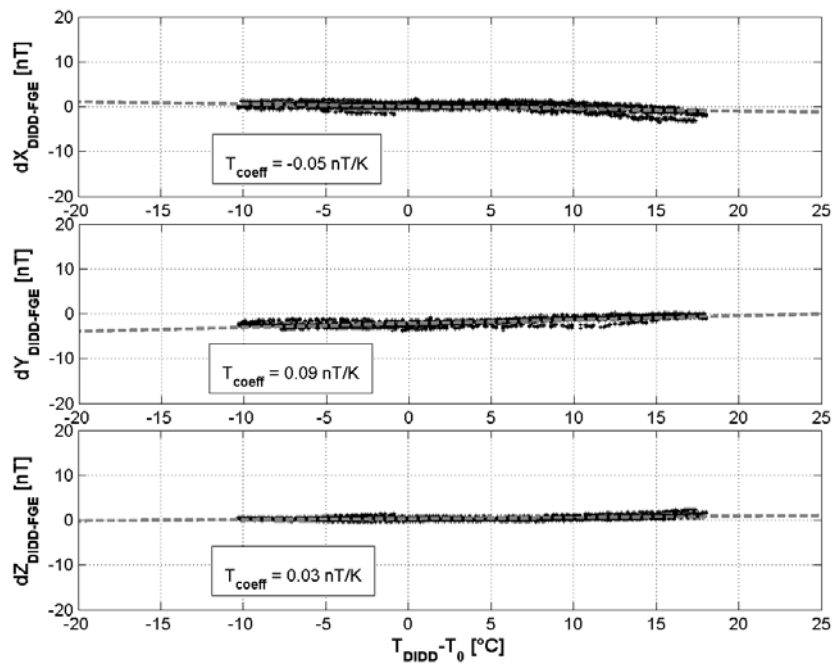


Fig. 5. Measured differences between the DIDD and reference instrument and calculated thermal coefficients.

The delays are: $X = 85$ minutes, $Y = 265$ minutes, and $Z = -14$ minutes. The temperature coefficients are: $X = -0.05$ nT/°C, $Y = 0.09$ nT/°C, and $Z = 0.03$ nT/°C. The maximal residuals are about 1.5 nT.

4. Conclusions

It is possible to determine the temperature coefficient for every instrument quite precisely using the above method. If there is temperature measurement in an observatory, the calculation of thermal coefficients can be carried out. There is remarkable phase shift between the temperature change and the response by the instrument. This delay does not seem to be a linear function of the amplitude of temperature variation but its determination is important if we want to make temperature correction with low residual errors. The possibility of temperature correction is limited to 1-2 nT. That is why the use of a temperature stabilized environment is the best way to reach very accurate measurement. The difference is high between the temperature sensitivity of different modern instruments. It is a general observation that suspension improves very much the temperature stability of a component magnetometer.

Acknowledgments. Authors would like to express their thanks to Valery Korepanov and the team of Lviv Centre of Institute of Space Research for the useful discussions and their help during the test of LEMI-17 device.

References

- Bitterly, J., *et al.*, 1988, *Digital recording of variation in the Earth's magnetic field in French observatories: description of equipment and results for the period 1972-86*. **In:** Proceedings of the International Workshop on Magnetic Observatory Instruments, Ottawa, pp. 75-83.
- Hegymegi, L., *et al.*, 2004, *New suspended dIdD Magnetometer for Observatory (and Field?) Use*. **In:** Proceedings of XIth IAGA Workshop on Geomagnetic Observatory Instruments, Data Acquisition and Processing, Kakioka, pp. 28-33.
- Korepanov, V., *et al.*, 2004, *Anti-tilt sensor construction efficiency study*. **In:** Proceedings of XIth IAGA workshop on Geomagnetic Observatory Instruments, Data Acquisition and Processing, Kakioka, pp. 34-35.
- Rasmussen, O., 1991, *Tilt-compensation of fluxgate magnetometers*, *Geophys. Trans.* **36**, 3-4, 261-271.

Accepted February 27, 2007

Temperature Influence over Magnetic Declination Measurements

Iliya CHOLAKOV and Bozhidar SREBROV

Geophysical Institute, Bulgarian Academy of Sciences
“Acad. G. Bonchev” str., block 3, 1113 Sofia, Bulgaria
e-mails: srebrov@geophys.bas.bg; geomagpag@abv.bg

A b s t r a c t

An investigation of temperature influence over magnetic declination measurements in geomagnetic observatory Panagyurishte is made. The examined period is from 1991 to 2005. A good correlation between the declination base values and the seasonal temperature variation is shown.

1. Introduction

The study of secular geomagnetic field variations is associated with the accumulation of long series of highly accurate, stable, and reliable observatory data. The data acquisition is going through two stages – registration, mainly digital and analog, and absolute measurements of the geomagnetic field elements. The application of modern measurement equipment enables to obtain observatory data of high precision of about 1 nT. Data stability for a long time period is an important requirement.

Data published by many authors (Rasmussen and Lauridsen 1990, Lauridsen 1991, Petiau 1996, Jankowski and Suckdorff 1996, Schulze 1998, Beblo 1998, Bitterly *et al.* 2001, Curto and Sanclement 2001) show that with existing high requirements for data precision, the following factors are important: temperature, humidity, variation difference between the points of registration and measurement, batter of the pillars, hydrological processes taking place under the variation and absolute houses.

Results of temperature influence on the absolute declination value are presented in the paper. A time period of 15 years (1991-2005) is taken. Since 1999 a seasonal temperature trend on the basic declination line is observed.

2. Observatory Activity

Measurements of the geomagnetic elements D, H, Z, and F have been carried out in Panagyurishte observatory (PAG) during the period 1991-2005 with two series of

Bobrov-type quartz variometers, with standard velocity of 20 mm/h and record sensibility of about 2 nT/mm. The variometers are installed in two rooms in the variometric house, and their walls are thermally insulated with air gaps (Fig. 1). This creates a good room's temperature stability. The annual room temperature change is about 4-5°C while the outside temperature varies in the range of 50°C. The absolute declination measurements are carried out in the absolute house on the pillar № 1 (Fig. 1). This pillar and the other five ones are concrete octahedrons of 2 m height and 25 cm face. Their stability is guaranteed by a common concrete basement of the dimensions: 4 m width, 6 m length, and 1.2 m thickness. Pillar №1 is basic for providing absolute measurements in the observatory. The normal magnetic theodolite "Matting und Wiesenberg - 164" is fixed on it. Besides declination measurements, the horizontal intensity by Gauss-Lamont methods is also measured. Two observers take measurements three times monthly, and the mean value is calculated. During the winter months the temperature in the absolute house is kept at about 19-20°C.

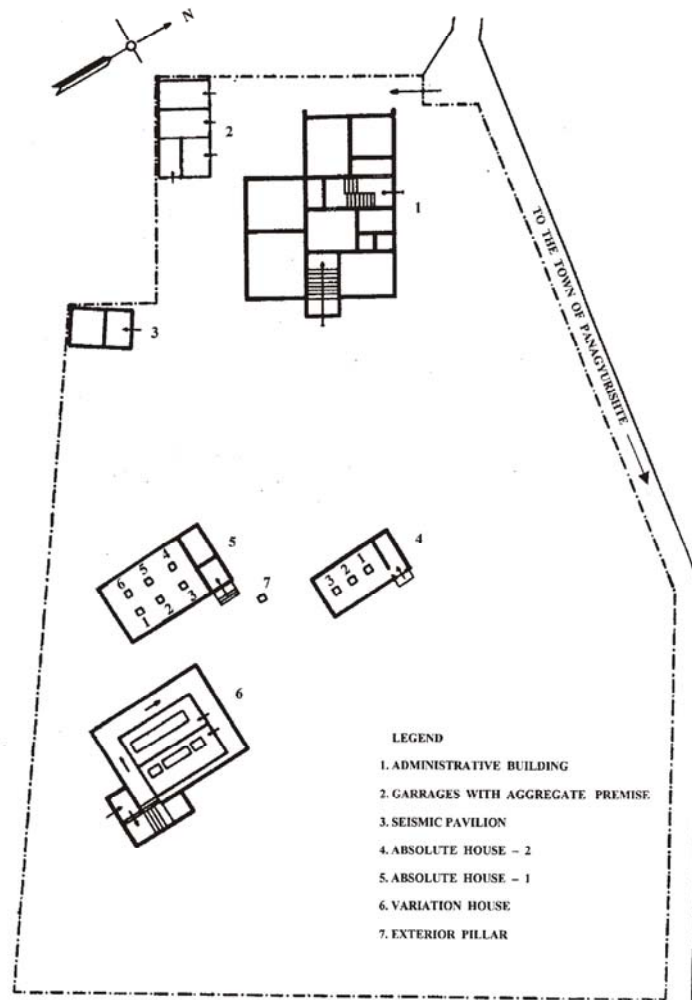


Fig. 1. Plan of Geomagnetic Observatory Panagyurishte.

3. Seasonal Trend Study of the Base Declination Line

In 1999 a significant part of the trees surrounding the absolute house were removed which influenced the solar radiation regime of the house. Till that year the base declination line stability has been very high (about 0.1 – 0.25 min. annually) which is in the range of measurement accuracy. For example, in 1992, temperature data in the absolute house varied by about 4-5 °C annually (from 19°C in the cold months up to 24°C in hot months, Fig. 2).

Since 1999 an increase in summer temperatures registered in absolute house has been observed and the temperature variation amplitude reached 7-8°C.

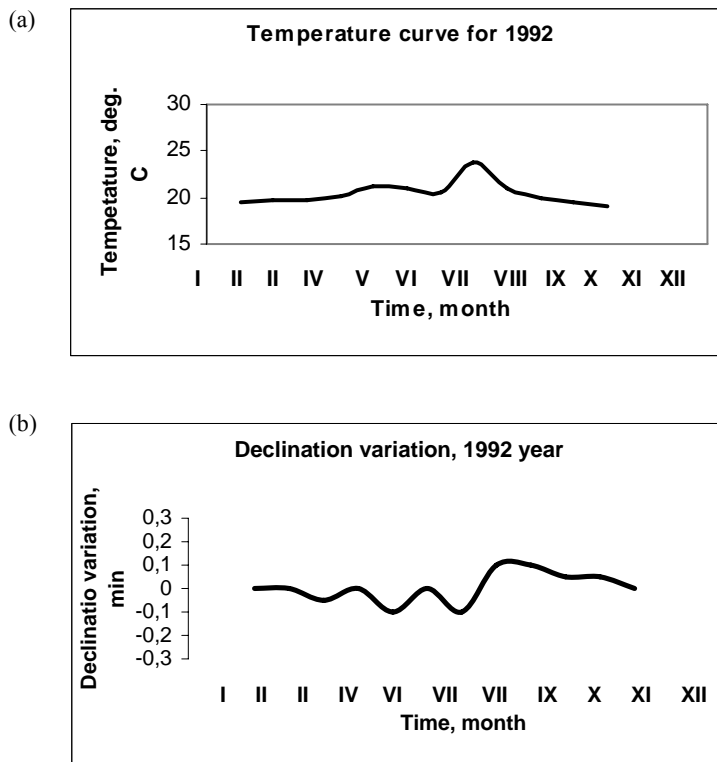


Fig. 2. Temperature and declination variations in the absolute house, 1992.

An annual trend of base declination values which correlates with the annual temperature trend has been established. Two temperature and declination graphs for 2003 are presented in Fig. 3. The seasonal base line declination and temperature trend for the whole 15 years period are shown in Fig. 4. The base line amplitude reaches up to 0.5 – 0.6 min. An analysis of possible reasons has been made. According to it, the most probable factors for the annual base declination line trend is the volumetric deformation of the pillar which serves as theodolite basement. This can be also seen in Fig. 4, where the base line declination maxima are slightly shifted from the temperature maxima. This is caused by the high thermal capacity of the pillar as its volume is very large.

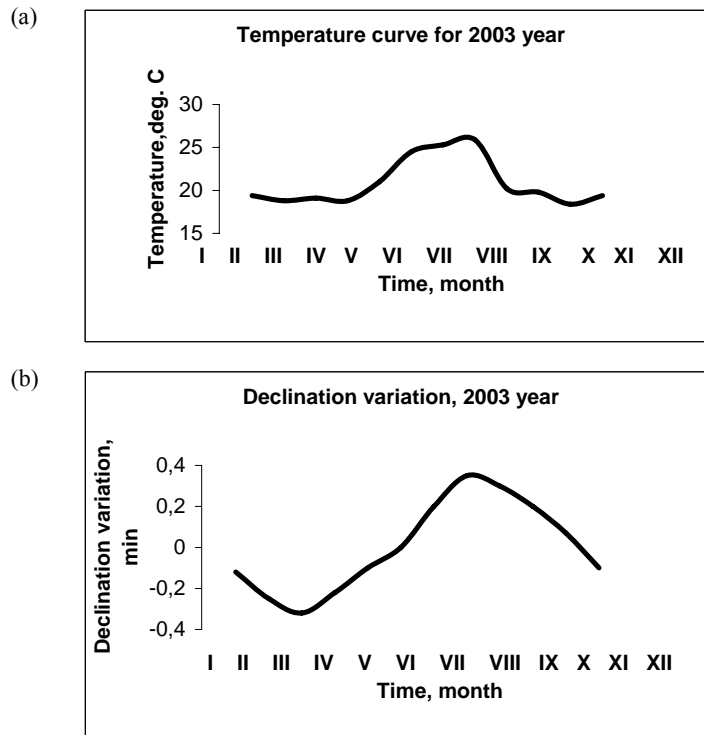


Fig. 3. Temperature and declination variations in the absolute house, 2003.

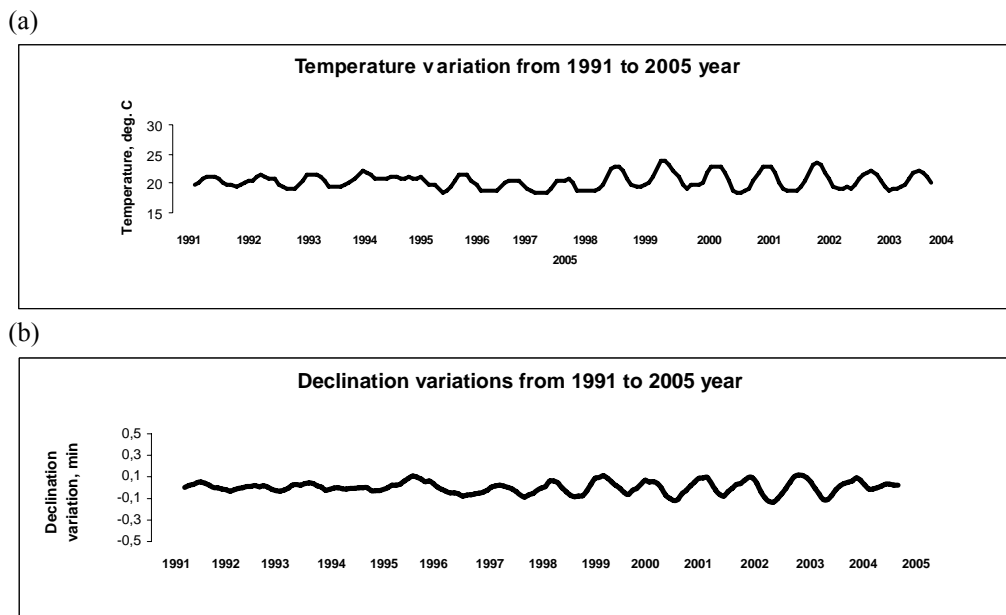


Fig. 4. Temperature and declination variations in the absolute house, 1991-2005.

References

- Bitterly, J., M. Bitterly and M. Manda, 2001, *Study of baseline values over long-time period at Chambon la Foret observatory*, Contrib. Geophysics and Geodesy **31**, 1, Geoph. Institute, Slovak Academy of Sciences.
- Beblo, M., 1998, *Some remarks on absolute measurements (in FUR)*. **In:** VII IAGA Workshop on Geomagnetic Observatory Instruments, Data Acquisition and Processing, Adolf Schmidt-Observatory for Geomagnetism Niemegek, September 8-15, 1996, 98/21.
- Curto, J.J., and E Sanclement, 2001, *Levelling Error corrections to D-Measurements in DI-flux magnetometers*, Contrib. Geophysics and Geology **31**, 1, 111-117, Geoph. Institute, Slovak Academy of Sciences.
- Jankowski, J., and C. Sucksdorff, 1996, *Guide for Magnetic Measurements and Observatory Practice*, International Association of Geomagnetism and Aeronomy, Warsaw, 235 pp.
- Lauridsen, E.K., 1991, *Review of Accuracy and Sources of error in Geomagnetic Measurements*, Münchner Geophysikalische Mitteilungen, München, Heft 5, 69-97.
- Petiau, G., 1996, *Temperature and tilt correction on Chambon la Forêt observatory magnetometers*. **In:** Proc. VI Workshop on Geomagnetic Observatory Instruments, Data Acquisition and Processing, J.L. Rassin (ed.), Publication scientifique et technique N° 003, édité par l'Institut Royal Meteorologique de Belgique, 209-214.
- Rasmussen, O., and K. Lauridsen, 1990, *Improving baseline drift in fluxgate magnetometers caused by foundation movements, using band suspended fluxgate sensors*, Phys. Earth Planet. Int. **59**, 78-81.
- Schulz, G., 1998, *Long-term experience with digital variometer systems of different generations at Wingst observatory*. **In:** VII IAGA Workshop on Geomagnetic Observatory Instruments, Data Acquisition and Processing, Adolf Schmidt-Observatory for Geomagnetism Niemegek, September 8-15, 1996, str. 98/21.

Accepted February 7, 2007

Development of Artificial Geomagnetic Disturbances Monitoring System

T. OKAWA, T. TOKUMOTO, S. NAKAJIMA, T. OWADA, T. TOYA,
F. MUROMATSU, N. KUMASAKA and T. KOIKE

Kakioka Magnetic Observatory, Japan Meteorological Agency
595 Kakioka, Ishioka, Ibaraki, 315-0116, Japan
e-mails: t_okawa@met.kishou.go.jp; tokumoto@met.kishou.go.jp

Abstract

The performance of geomagnetic field measuring instruments is quite good now. However, our life styles are changing with urbanization, and sometimes this has a bad influence on the environment of observations. Vehicles which run near an observation point are especially troublesome, making it difficult to keep the progress of data quality. We aimed to build a system to monitor artificial disturbances, to be completed in 2006. Using this system, we expect to obtain more accurate analytical results.

1. Introduction

A fundamental algorithm which estimates artificial geomagnetic disturbances by several geomagnetic measurement devices has been developed last year. Meanwhile, artificial geomagnetic disturbances caused by magnetic bodies, such as automobiles or buildings, can be virtually considered as one magnetic dipole moment. So, a real-time artificial geomagnetic disturbance monitoring system can be constructed combining real-time magnetic data recording systems, such as the Automatic Observation System of Kakioka Magnetic Observatory. The monitoring system analyzes the position and magnitude of the magnetic moment, and gives useful information whether geomagnetic disturbances exist or not.

However, it is more difficult to analyze a momentarily changing magnetic moment by varying geomagnetic disturbances caused by a moving automobile. We have a plan to add an equipment which locates the automobile's passing at a fixed point in this system. It also seems important to review what is the most efficient arrangement of a restricted number of observation instruments. This system will make us look for-

ward to get more accurate analytical results. This system is going to be built in 2006. We will outline it below.

2. Estimate of Disturbance Quantity and Arrangement of Survey Points

The arrangement of survey points is important in order to get a disturbance source efficiently with a limited number of magnetometers. In the past, a lot of disturbances occurred from automobiles which run at the road in the observatory east side. For example, the estimated quantity of the influence in each survey point in such a case is shown in Fig. 1. The track where the car passes to the south from the north is shown by the black thick line on the map. In this case, it is barely possible to detect it in point F3, and is very difficult in point F4.

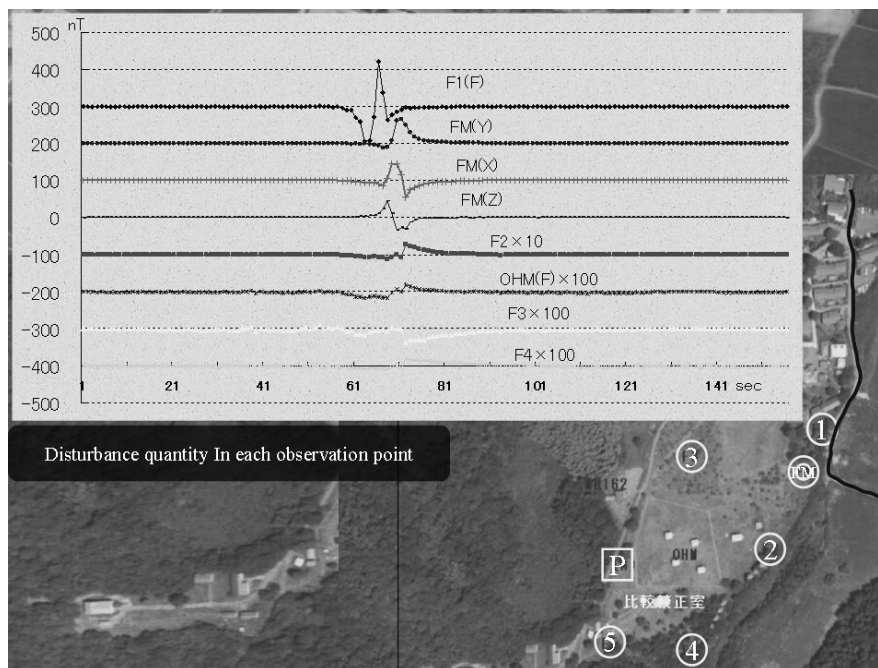


Fig. 1. Disturbance quantity in each observation point.

As a result, we considered the following factors as decisive in the arrangement:

- The disturbance quantity is larger than the measuring noise level.
- The disturbance period is expected to be longer than several seconds.
- The change is expected to appear at more than one component or point.
- The change appears clearly in each component of the fluxgate magnetometer.
- The disturbance area is not as wide as the vehicle.

This year we were mainly concerned with detection of the disturbance sources around the southeastern area of the observatory.

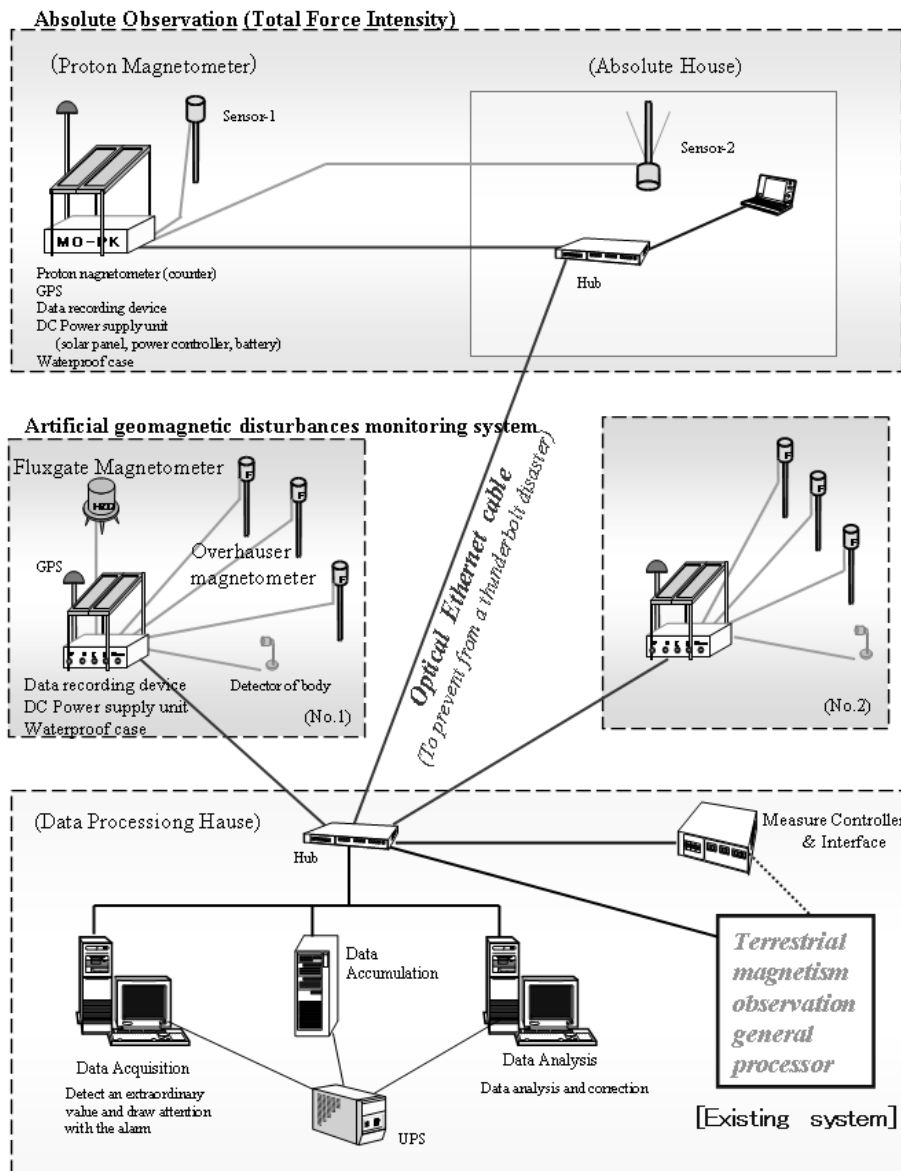
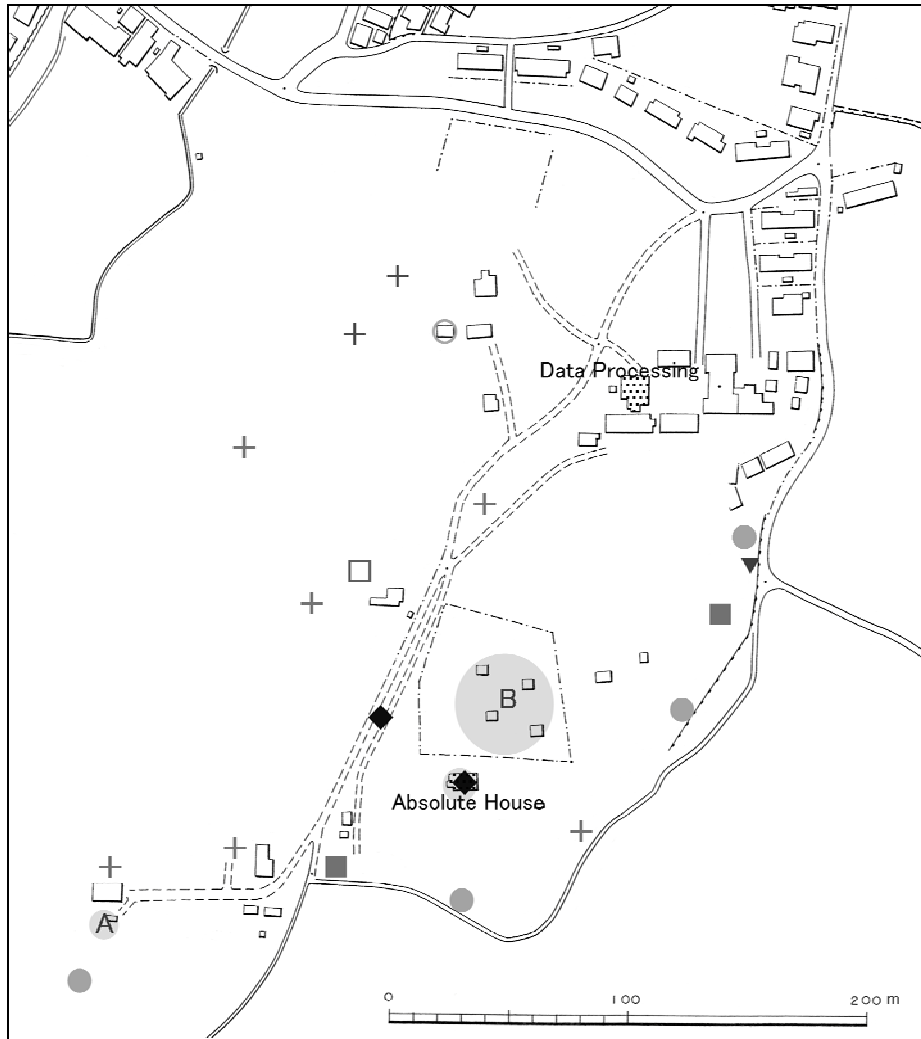


Fig. 2. The equipment composition.

3. Equipment

The system is composed of the following equipment (Fig. 2):

- Proton magnetometers: 2 sets.
- Fluxgate magnetometers (X, Y, Z): 2 sets. This includes an inclinometer of the sensor X, Y and a thermometer (sensor and amplifier circuit).
- Overhauser magnetometers (F): 4 sets (It is possible to extend it to 6 sets).



| Sign | Magnetometer | Component. | Resolution | Sampling |
|------|--------------------------------|------------|------------|----------|
| A | Fluxgate magnetometer | H Z D | 0.01nT | 1s |
| B | Overhauser magnetometer | F H Z D | 0.01nT | 1s |
| ◆ | Proton precession magnetometer | F | 0.01nT | 5s-60s |
| ● | Overhauser magnetometer | F | 0.01nT | 1s |
| ■ | Fluxgate magnetometer | H Z D | 0.01nT | 1s |
| ▼ | Moving object detection device | On/off | | 1s |
| ○ | Overhauser magnetometer | F | 0.01nT | 1s |
| □ | Fluxgate magnetometer | H Z D | 0.01nT | 1s |
| + | Repeat observation point | F | 0.1nT | 1s |

Fig. 3. Arrangement of observation points.

- Moving object detection device: 1 set (It is possible to extend it to 2 sets). The detector of bodies uses supersonic wave Doppler method. Provided that the neighborhood residents' privacy is not violated, it is possible to think about changing to a CCD camcorder in the future.
- Data recording and control interface devices: 2 sets. This includes a backup storage (Compact Flash Memory card).
- Power supply (solar panel and battery, deep cycle type): 3sets.
- Optical Ethernet cable (LAN).
- GPS.

The arrangement of observation points is shown in Fig. 3. To prevent a disaster by thunderbolts, the instruments are driven by a solar battery DC power supply. Also, for similar reasons, each signal is exchanged by LAN which uses optical Ethernet cables.

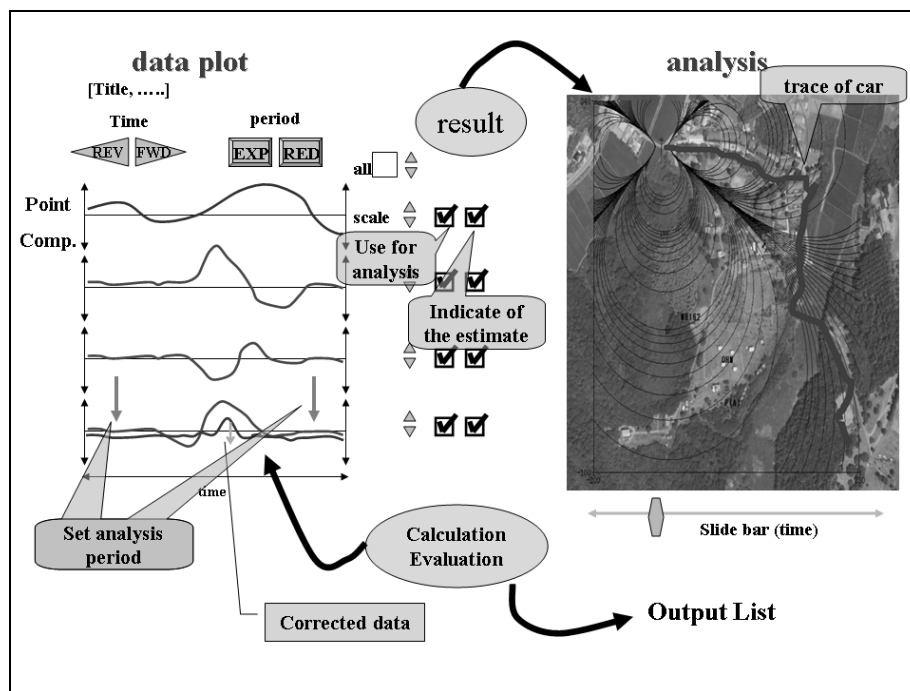


Fig. 4. Analysis process.

4. Monitoring and Analysis

The system has the following purposes:

- Watching whether the regular observation point receives an artificial disturbance or not.
- Alarm of the artificial disturbance occurrence by a real-time process.

- Analysis of size and position of the magnetic dipole moment of a source.
- Correction of the regular observed value.

The process of analysis gives a big load to the computer. Therefore, as a pre-treatment of the analysis, it is realistic to make a judgement using a comparison between survey data and some reference data. Next, the interactive process is calculated and the quality of the regular observed value is improved (Fig. 4).

Such high quality terrestrial magnetism observations may be useful in the study of volcanism, seismic activity prediction, the study of magnetosphere disturbances related to solar activity, and so on.

Accepted March 2, 2007

Intercomparison of Momentary Values: an Application to Check the Reliability of Ebre Observatory Data

Santiago MARSAL and J. José CURTO

Observatori de l'Ebre, CSIC – Universitat Ramon Llull
Horta Alta, 38. 43520 Roquetes, Spain
e-mails: smarsal@obsebre.es; jjcurto@obsebre.es

A b s t r a c t

Intercomparison of momentary values from observatories across Europe has been used as a test of reliability for the magnetic stations of this area, as well as for the whole net. One of the techniques used, based on the standard deviation of the mutual differences of monthly mean values, has permitted to obtain a measure of quality of the Ebre Observatory (EBR) magnetic elements for the period 1997-2001. The results nearly coincide with those obtained for the most significant observatories of the network, pointing out a good performance of EBR observatory.

1. Introduction

During the 1950s a few central European observatories agreed to exchange their respective data for intercomparison purposes. Data from the different stations were collected by Wingst Observatory (WNG), and a series of procedures was applied to establish the quality of their records, as well as the quality of the network itself (several applications of the comparisons are shown in Schulz and Beblo 1996). Particularly, these procedures were based on the momentary values (MV) comparison, i.e., the observatories' magnetic field values (H, D, Z and F) of the ten selected quietest days of each month taken at 02:00 UT, which is supposed to coincide with the period least disturbed by S_q on central European longitudes. Along the time, the number of participating observatories progressively increased, and in the quinquennium 1997-2001 a total of 26 observatories presented their data, Ebre Observatory (EBR) being one of them. Some preliminary results are presented here for EBR, specifically those resulting from the application of linear regressions to the standard deviation of the mutual differences of the MV monthly means, once detrended by the secular variation (SV).

2. Procedure and Objectives

Once the 5-year data from the participating observatories have been collected, Wingst Observatory is in charge of selecting and averaging the ten MVs of each month. A list of monthly mean values is therefore obtained for each observatory. Direct comparison of these values is not adequate, since they are affected by the “constant” trends associated to the SV; hence, a detrending is applied by means of first order regression models estimated from five epoch values for each magnetic element, virtually eliminating in this way the internal magnetic field influence. The resulting values are now equally distributed around a mean that we can artificially set as zero. In an ideal situation, and supposing identical external field conditions for each observatory, as well as identical crustal response to the external fields, the obtained values should coincide. Just in order to minimize the external field differences among the observatories, the momentary values are taken from the quietest days at 02 UT. Nevertheless, in a real situation several departures from these ideal assumptions are observed, and in consequence, the detrended monthly means of the participating stations do not coincide, especially in case of:

- defective absolute instruments
- incorrect adjustments
- magnetic impurities in the immediate vicinity of the pier
- electromagnetic interferences

(see Schulz and Gentz 1998). As well, this technique is not only sensible to instrumental pathologies or noise, but also to unavoidable natural phenomena, as:

- latitudinal effects, like the ring or the field aligned currents (FACs)
- longitudinal differences of the participating observatories
- differential induced magnetic fields
- annual and lunar variation.

In order to evaluate the natural or artificial origin of such residual differences among observatories, it is reasonable to assume that, if they have a natural origin, similar variations should correspond to close locations. On the contrary, if the difference is due to an instrumental problem, no rules of vicinity apply. Therefore, the following step to evaluate a given observatory, in this case EBR, consists of computing the standard deviation of the differences of the detrended monthly mean values between EBR and each one of the remaining stations, and afterwards representing them against their relative location, either distance, longitude or latitude differences with respect to EBR. The standard deviations are denoted as $\sigma_Y^{XXX-EBR}$, where Y stands for the magnetic element (D, H, Z and F) and XXX for the station concerned. A linear regression is then fitted, being the axis intercept the value of interest, which intuitively corresponds to the standard deviation predicted by the net at the point the concerned station (EBR in this case) is located; obviously, the ideal value for the axis intercept is zero, and its absolute actual value constitutes a quality factor for the concerned magnetic element measured at that observatory. In general, large intercepts should be interpreted as poor coherency of the observatory or malfunction of the sensors. Never-

theless, as pointed out by Schulz and Gentz (1998), care should be taken in this interpretation, because intercept values may be strongly affected by the quality of nearby stations and their location within the network, in such a way that the technique is less reliable for extremely located observatories, as EBR.

3. Results and Evaluation

In Fig. 1 the standard deviation of the detrended monthly mean differences among EBR and the different observatories of the network are represented as a function of distance, latitude and longitude for D, H, Z and F. As mentioned, the meaningful parameter is the axis intercept, but also the correlation coefficient R (or equivalently R^2), which provides information on the degree of dependency of the standard deviations with respect to the variable used in each case to represent the relative observatory locations. In view of the plots, at least two traits are discerned:

- In all cases longitude with respect to EBR is the worst variable (i.e., R is low) to predict the standard deviation values, as expected if an appropriate choice of the quietest days has been made; nevertheless, significant dependencies with longitude are still found for both, σ_D and σ_H , which indicates that residual longitudinal effects are still present, probably due to the network extension.
- In all cases the relation between standard deviations and latitude are highly significant (i.e., given the number of experimental points, R denotes a very good correlation between both variables; see Taylor 1982). This fact denotes the influence of the abovementioned latitudinal effects as ring currents, ionospheric currents associated to the FAC's system or differential annual magnetic variation among southern and northern observatories, separated by more than 20° .

Let us now evaluate the EBR behavior. If this is to be done, a unique value for the axis intercept is to be given, either that coming from distance, latitude, or longitude. To do it, we have decided to choose the variable with the most significant correlation in each case, i.e., distance for both D and H and latitude for both Z and F.

$$\sigma_D (\text{DIST} = 0) = -0.10 \pm 0.14 \text{ arc-min}; \quad R = 0.77,$$

$$\sigma_H (\text{DIST} = 0) = 0.6 \pm 0.6 \text{ nT}; \quad R = 0.57,$$

$$\sigma_Z (\text{LAT} = \text{LAT}_{\text{EBR}}) = 1.1 \pm 0.7 \text{ nT}; \quad R = 0.40,$$

$$\sigma_F (\text{LAT} = \text{LAT}_{\text{EBR}}) = 0.8 \pm 0.6 \text{ nT}; \quad R = 0.83,$$

where the reported uncertainties correspond to the standard deviation of the observatory values with respect to the regression lines. It is worth mentioning that the ideal zero is inside the uncertainty for D and H, while it is outside for both F and especially for Z. A different concept is the uncertainty associated to the axis intercept value, which is 0.04 arcmin for D, 0.2 nT for both H and F, and 0.1 nT for Z. If distance is taken as the independent variable for Z and F, $\sigma_Z (\text{DIST} = 0) = 0.8 \pm 0.7 \text{ nT}$ and $\sigma_F (\text{DIST} = 0) = 0.8 \pm 0.9 \text{ nT}$.

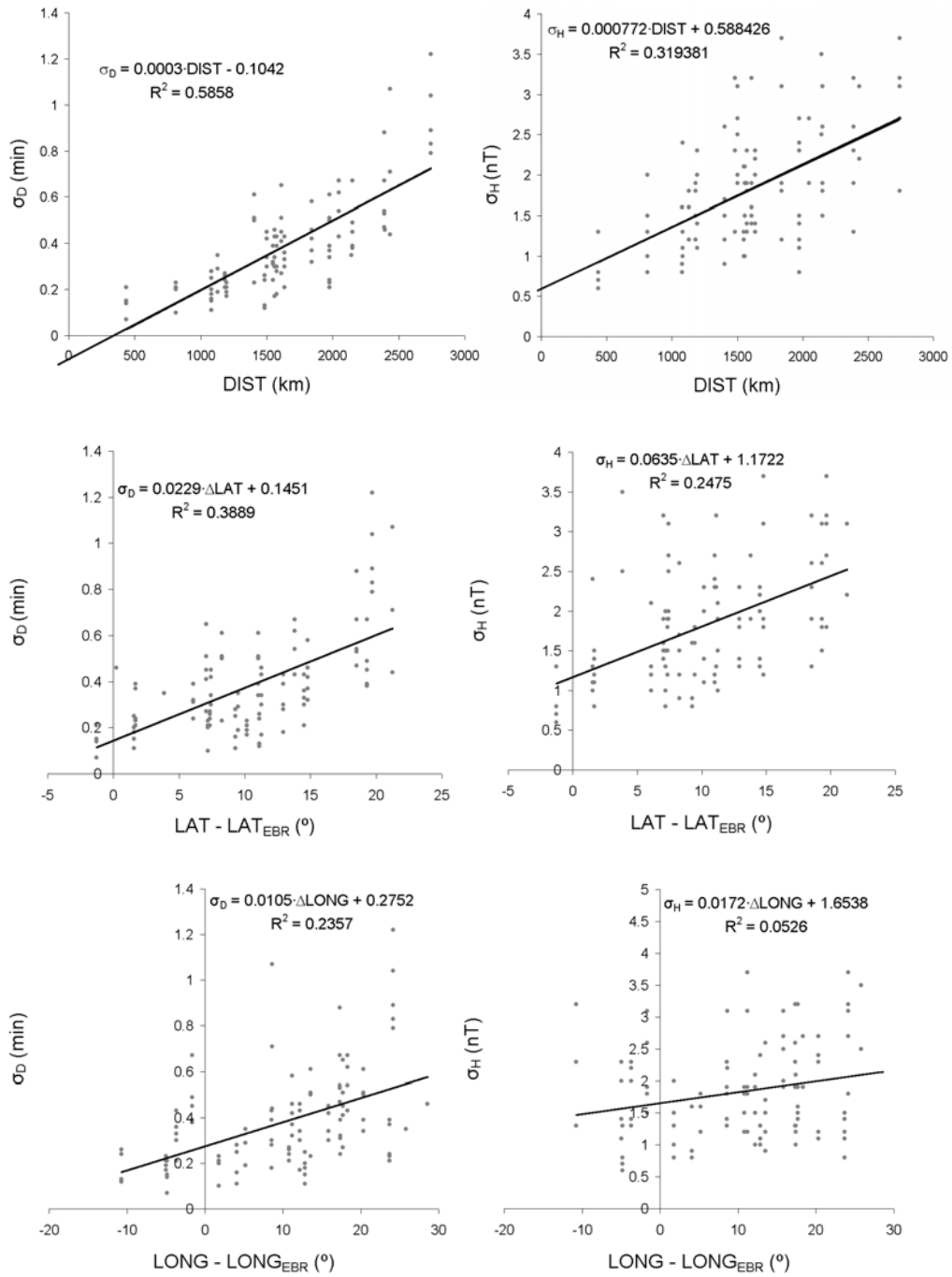


Fig. 1. Standard deviations σ_D (left) and σ_H (right) against distance, latitude and longitude with respect to Ebre.

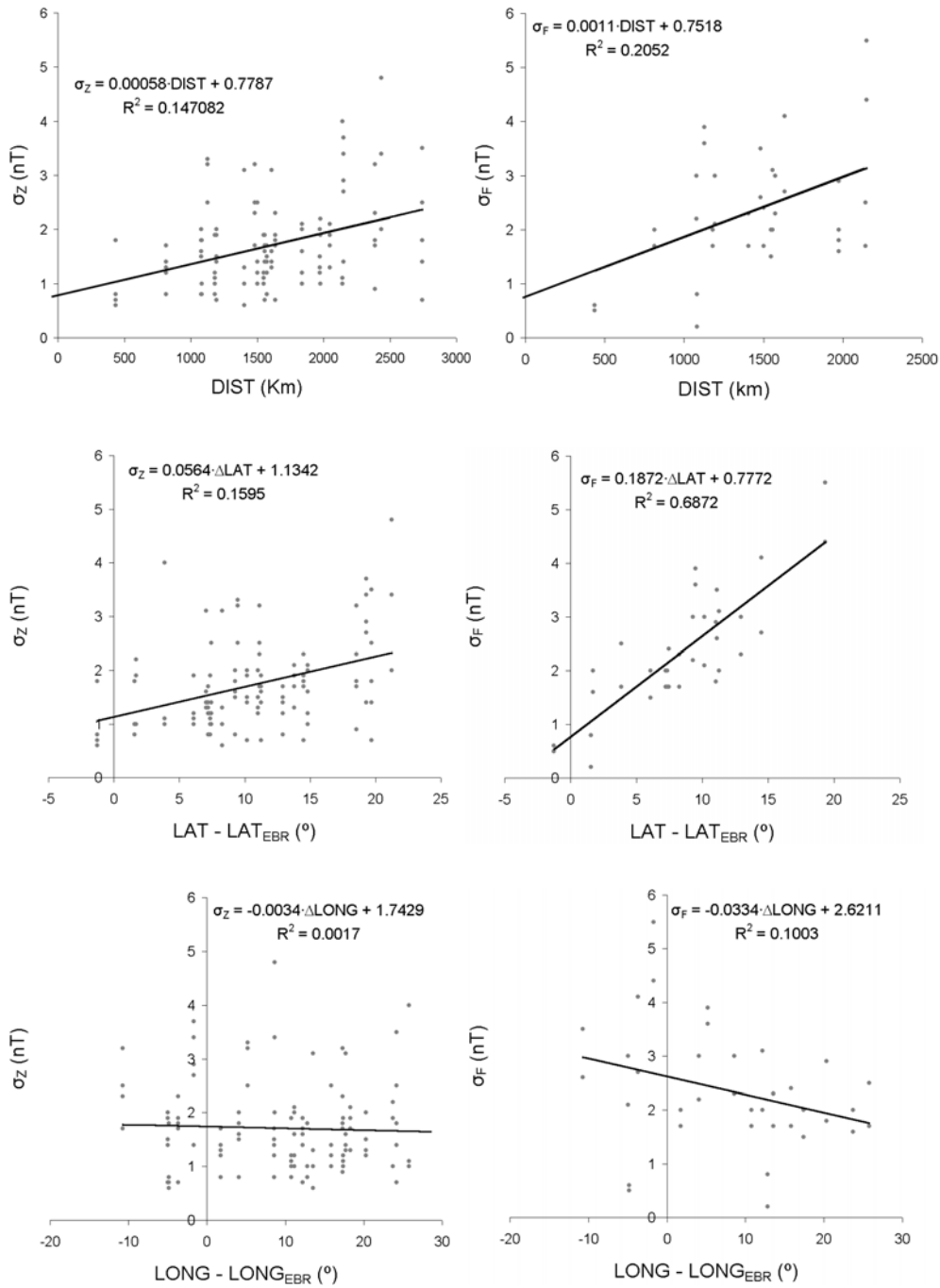


Fig. 1. (cont.) Standard deviations σ_Z (left) and σ_F (right) against distance, latitude, and longitude with respect to Ebre.

In order to check the repeatability of the axis intercept values, and in view that longitude and latitude are not sufficient to describe separately the standard deviation behavior by themselves, we have fitted a bi-dimensional function to the standard deviation, of the form $\sigma_Y(\Delta\text{LONG}, \Delta\text{LAT}) = A + B \cdot \Delta\text{LONG} + C \cdot \Delta\text{LAT}$. The results for the axis intercepts are now the following:

$$\begin{aligned} \sigma_D(\text{LONG} = \text{LONG}_{\text{EBR}}, \text{LAT} = \text{LAT}_{\text{EBR}}) &= 0.03 \text{ arc-min}; & R &= 0.80 \\ \sigma_H(\text{LONG} = \text{LONG}_{\text{EBR}}, \text{LAT} = \text{LAT}_{\text{EBR}}) &= 0.6 \text{ nT}; & R &= 0.55 \\ \sigma_Z(\text{LONG} = \text{LONG}_{\text{EBR}}, \text{LAT} = \text{LAT}_{\text{EBR}}) &= 1.2 \text{ nT}; & R &= 0.40 \\ \sigma_F(\text{LONG} = \text{LONG}_{\text{EBR}}, \text{LAT} = \text{LAT}_{\text{EBR}}) &= 0.8 \text{ nT}; & R &= 0.83 \end{aligned}$$

Except for D, the axis intercept values, as well as the quality of the adjustments (expressed by means of the correlation coefficients), are approximately the same, showing a good agreement between the discrete techniques used.

Finally, a comparison between mean values of the Ebre intercepts for this quinquennium with the intercepts of the whole network for the preceding years is shown in Fig. 2. The solid line represents approximately the upper limit of this measure of coherence. Data from the network were obtained by Schulz and Gentz (1998).

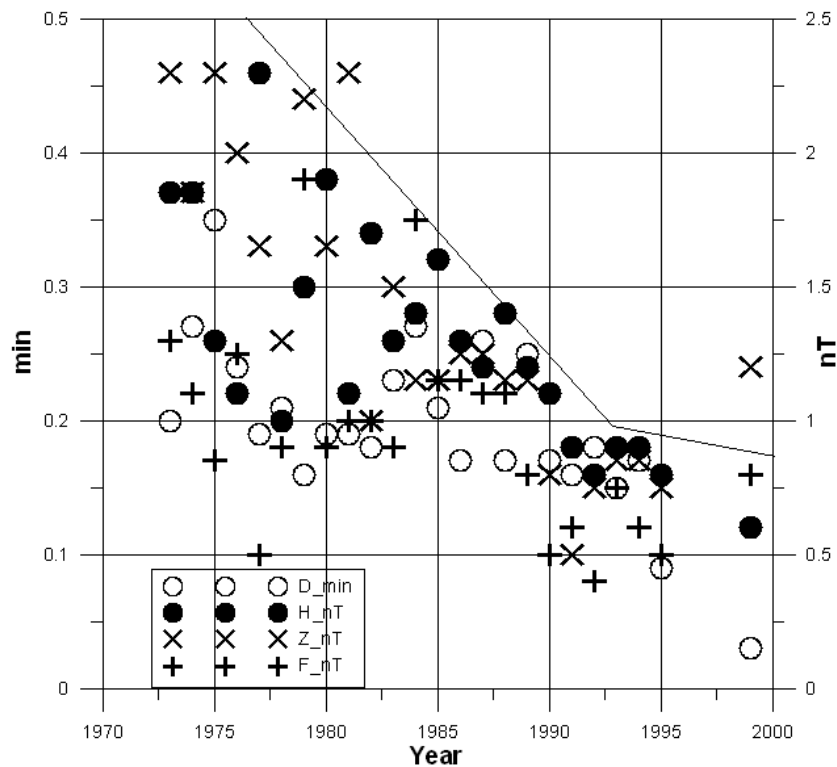


Fig. 2. Temporal evolution of the mean values of the intercepts for the whole network (1973-1995). Mean values for Ebre (obtained from the bi-dimensional fit) for the period 1997-2001 are displayed centred at 1999.

4. Conclusions

Ebre results for the quinquennium 1997-2001 are in general in perfect concordance with those of the whole network, even considering its extreme location.

Investigation is in progress in order to explain the slight departure of the Z axis intercept for Ebre, which could be explained by means of inductive effects due to the earth conductivity, rather than malfunction of the observatory standards.

The net has been improving its performance along the time. Intercomparison between observatory and international standards, with use of QHM magnetometers in the seventies and the generalized use of D/I fluxgate theodolites in the eighties (Bitterly 1990), contributed to this improvement.

Acknowledgments. The authors thank Dr. G. Schulz and Dr. H. J. Linthe for their effort to provide these lists of quiet days and to compile data from the observatories.

References

- Bitterly, J., 1990, *Declinometre-Inclinometre a Vanne de Flux*, Institut de Physique du Globe, Strasbourg.
- Schulz, G., and M. Beblo, 1996, *Monitoring Geomagnetic Standards by the comparison of Momentary Values between European observatories in the past, present and future*, VIth IAGA Workshop on Geomagnetic Observatory Instruments, Data Acquisition and Processing, Dourbes.
- Schulz, G., and I. Gentz, 1998, *Results of the momentary value comparison between European observatories - A summary of the last two decades*, VIIth IAGA Workshop on Geomagnetic Observatory Instruments, Data Acquisition and Processing, Niemegek.
- Taylor, J.R., 1982, *An Introduction to Error Analysis, the Study of Uncertainties in Physical Measurements*, University Science Books, Oxford Univ. Press, Oxford, 270 pp.

Accepted February 14, 2007

Survey of Magnetic Observatory Charging Practices

Larry NEWITT

Canadian Hazards Information Service, Natural Resources Canada
7 Observatory Crescent, Ottawa, Canada K1A 0Y3

Abstract

A survey of institutes operating magnetic observatories reveals that many are dependent or somewhat dependent on revenue received for data and services. Although policies vary from institute to institute, the practice of charging for data applies only to commercial users. Other services for which charges are normally applied include calibration services, instrument development and specialized surveys. Although most institutes are not dependent on revenue for their core activities, they rely on revenue to finance many non-essential operations.

1. Introduction

Magnetic observatory data have many direct and indirect commercial applications in addition to the traditional scientific use. Many observatories also offer a range of related services to clients. The decision to charge for data and/or services rests with the individual observatory or institute. Nevertheless, it is useful for an observatory to set its pricing policy with some knowledge of what others are doing. At the INTERMAGNET meeting held in 2005 I was asked to conduct a survey of magnetic observatories or the institutes that operate them to determine current pricing practices. The results of the survey were presented at the 2006 INTERMAGNET meeting, which was held in Warsaw immediately after the XII IAGA Workshop on Geomagnetic Observatory Instruments, Data Acquisition and Processing.

2. Survey Questionnaire

The questionnaire was sent to all observatories or institutes on the "worldobs" mailing list. The list has 177 entries and is believed to include almost all operating observatories, of which there are approximately 155. The recipients were asked to respond to the following questions:

(1) Do you charge for magnetic observatory data, products or services?

- (a) never
- (b) sometimes
- (c) always

(2) Does your charging policy have to conform to a broader institutional or government policy?

- (a) yes
- (b) no
- (c) partially

If you do not charge for data you can stop now; otherwise, carry on.

(3) For which of the following do you charge?

- (a) definitive observatory minute data
- (b) provisional minute data
- (c) provisional fast sample (1-sec, 5-sec)
- (d) real-time data
- (e) compass calibrations
- (f) magnetometer calibrations
- (g) instrument repair and development
- (h) special magnetic surveys
- (i) magnetic charts and models
- (j) magnetic and space weather forecasts
- (k) other

(4) Please list the charges for each item ticked in the previous question.

(5) Is your observatory dependent on revenue to cover operating costs?

- (a) highly dependent
- (b) somewhat dependent
- (c) not dependent

Usable responses were received from 23 institutes responsible for 88 observatories in 19 countries.

3. Survey Results

The major results of the survey are given in the following tables. They exclude three responses that could not be used. Two were returned blank. The third gave contradictory responses, claiming that the institute never charged but that it was highly dependent on revenue.

Table 1 shows that very few observatories charge for all products and services all the time. In the majority of cases the observatory or institute does not have complete freedom to set prices but must work within guidelines imposed at a higher level.

Table 1
Responses to question 1 and question 2

| | Charge | | | Conform to policy | | | |
|---------------|--------|-----------|-------|-------------------|-----------|----|---------|
| | Always | Sometimes | Never | Yes | Partially | No | Unknown |
| Countries | 2 | 13 | 6 | 7 | 6 | 6 | 2 |
| Institutes | 2 | 15 | 6 | 7 | 6 | 8 | 2 |
| Observatories | 5 | 61 | 22 | 33 | 24 | 18 | 13 |

Table 2
Responses to question 3 and question 4

| Product | Number of institutes | Charges (US\$) |
|-----------------------------------|----------------------|---|
| Def. 1-min data | 7 | Typically \$100 to \$200 per day with discounts for large requests. May be as little as \$15 per day or as much as \$40,000 per year. For directional drilling, charges may be on a per borehole basis. No charges to academic users. |
| Prov 1-min data | 8 | |
| Prov 1-sec 5-sec data | 6 | |
| Real-time data | 7 | |
| Compass calibrations | 9 | Typically \$200 to \$300. May be as low as \$150 or as high as \$3500. Some institutes charge an hourly rate (\$60 to \$130); sometimes charges are job specific. |
| Magnetometer calibrations | 10 | |
| Instrument repair and development | 6 | Very dependent on the specific job. Charges range from \$400 to \$60000. |
| Special magnetic surveys | 12 | Typically \$1000 per day plus expenses. Some institutes charge an equipment rental fee (~\$500). |
| Magnetic charts and models | 10 | Quite variable; may depend on client usage. Small requests may be charged a per value (e.g. \$15) or per file (e.g. \$500) fee. Service may be provided on an annual basis (\$1000 to \$10000) |
| Forecasts | 1 | \$1000 per year |
| Others | 2 | e.g., consultations, training |

Table 2 lists the number of institutes that charge for the different data products. Comments added to the questionnaire indicate that when an institute says that it charges for a product or service this does not mean that it charges every client every time. Institutes seldom charge academic users, for example. Charges may be waived for small requests.

The final question dealt with the dependency of the institute on the revenue it generated. The results are given in Table 3.

Table 3
Response to question 5

| Number of observatories | | |
|-------------------------|--------------------|---------------|
| Highly dependent | Somewhat dependent | Not dependent |
| 3 | 9 | 11 |

Written comments were supplied by approximately one third of the respondents. These greatly aided the interpretation of the survey results.

4. Discussion

It became apparent when reading the responses that the questionnaire should have included a definition of the word “revenue”. Typically an institute that operates observatories receives its core funding from its host organization, such as a government department. However, some institutes supply services to other government departments; this often involves a transfer of funds from the client department to the institute. I do not consider this to be revenue; it is just a case of core funding coming from multiple sources.

Charging practices vary greatly from institute to institute. However, virtually all institutes have adopted a policy of not charging for data that is to be used only for research purposes. Practices regarding the charging of commercial users of data also differ. Some institutes charge what the market will bear. At the other extreme is the attitude that companies are tax payers and they should “...not to pay two times (sic). It will be different if they ask for something specific, but standard products are free of charge...” Variable pricing is also common. Users of large volumes of data will often receive a reduction in the unit price. Very small requests are sometimes answered free of charge since it is too much trouble to invoice the client.

Charges for services such as calibrations, instrument development and repair, and surveys are also highly variable. Some institutes charge a flat rate; others work on an hourly rate; others choose one or the other depending on the nature of the job. Some institutes waive the charges for work done for other government agencies.

Although ten institutes claim to charge for providing declination values from reference field models, most of these institutes do not produce models themselves. Presumably they are providing value-added service by eliminating the need for the client to become familiar with the software. A couple of the institutes that actually produce models consider that the models constitute only one part of a much broader service that they provide to clients.

Only one respondent charged for forecasts. The attitude among most institutes that provide forecasts was expressed by one respondent as follows: “...made the decision not to charge for forecasts because of the danger of having ...to try to justify the charge against forecast failures.” However, some institutes conduct research related to space weather for which they receive revenue.

Finally, although only three institutes said that they were highly dependent on revenue, nine said they were somewhat dependent. The revenue provides a buffer against unforeseen expenses and enables the institute to engage in activities outside the set of core activities for which they are funded.

Accepted February 15, 2007

A New Geomagnetic Field Model for Southern Africa Based on 2005 Ground Survey Data

Pieter B. KOTZÉ¹, M. MANDEA² and M. KORTE²

¹Hermanus Magnetic Observatory, Hermanus, South Africa
e-mail: pkotze@hmo.ac.za

²GeoForschungsZentrum, Potsdam, Germany

Abstract

Geomagnetic field observations over southern Africa, including countries like South Africa, Namibia, and Botswana, were conducted during October and November 2005 as part of a collaborative project, called COMPASS (COMprehensive Magnetic Processes under the African Southern Sub-continent) between the Hermanus Magnetic Observatory (HMO) in South Africa and the GeoForschungsZentrum Potsdam (GFZ) in Germany.

For this purpose some 40 repeat stations were identified, separated by distances ranging from 300 till 400 km. These stations form part of a network of 75 repeat stations, established by the HMO during the last 60 years, and visited at regular intervals of 5 years till 2000. Due to the rapid secular variation change over this area, it was decided to conduct annual surveys at a reduced number of repeat stations. Therefore, between 2000 and 2004 surveys were conducted at a total of 12 stations on an annual basis. This did however not allow for good spatial resolution, hence the increased number of stations in 2005. For the field survey of 2005 the stations were also selected to form two independent sets of 20 beacons each, enabling one to visit these at alternative years respectively. During this campaign 2 teams, consisting of both HMO and GFZ observers, using similar DI Flux theodolites and fluxgate variometers, gathered geomagnetic field data over southern Africa.

Results obtained from this field survey, together with information from the 3 continuously recording magnetic observatories in southern Africa at Hermanus, Hartebeesthoek and Tsumeb, have been used to model the main geomagnetic field, employing a polynomial approach.

1. Introduction

The magnetic field, produced in the core by a self-consistent dynamo mechanism and also known as the “main field”, has a magnitude of approximately 60,000 nT in

the polar regions, and decreases to values less than 20,000 nT in the South Atlantic Anomaly region. Observations of the geomagnetic field started in the nineteenth century and today approximately 150 observatories around the globe are recording the field on a time scale of 1 minute and shorter. These observations are crucial in understanding the underlying mechanisms responsible for the generation of the core field, but in particular the long time series are vital to understand the evolutionary behaviour of the field in various parts of the world.

In order to better understand the mechanisms underlying the generation of the Earth's magnetic field, it is desirable to have as long a record as possible of the evolution of the field. The evolution of declination (the angle between the geographic and magnetic north directions) and inclination (the angle of the magnetic field with respect of the horizontal direction) of the magnetic field have been measured over many centuries (Alexandrescu *et al.* 1996, Manda 2000). In southern Africa, the Hermanus Magnetic Observatory (HMO) has been executing geomagnetic repeat surveys on a routine basis for nearly 50 years. These surveys normally include countries such as South Africa, Namibia, Zimbabwe and Botswana and have been conducted at regular intervals of 5 years till 2000 at almost 70 positions. However, due to the rapid change of the geomagnetic field in this region, it was decided to conduct field surveys on an annual basis, but at a few selected repeat stations. It was therefore decided to visit 10 selected repeat stations at annual intervals for 2003 and 2004. The experience gained from these surveys has shown that the limited number of stations over the Southern African region is insufficient to accurately model the secular variation due to the increasing temporal and spatial gradients. A better spatial resolution, however, demanded an increase in the density of the repeat stations. In 2005 a total of 40 stations were selected for a survey campaign. At 34 stations it was possible to obtain good quality results (Fig. 1).

Results obtained during this field survey were used to derive mathematical models of the main geomagnetic field components measured using polynomials that can be expressed as a function of latitude and longitude. In this publication we present modelling results for declination (D), horizontal component (H), vertical component (Z), as well as total field (F).

2. Data Collection and Field Surveys

Continuous recording of geomagnetic field variations is conducted at Hermanus (34° 25.5' S, 19° 13.5' E), Hartebeesthoek (25° 52.9' S, 27° 42.4' E) and Tsumeb (19° 12' S, 17° 35' E). All these observatories comply with INTERMAGNET standards. The primary instrument for recording of magnetic field variations is the FGE fluxgate magnetometer, manufactured by the Danish Meteorological Institute in Copenhagen, Denmark. This instrument is based on three-axis linear-core fluxgate technology, optimised for long-term stability and records the components H, D and Z. An Overhauser-type magnetometer further provides absolute total field information, while baselines for the other components are obtained using a DI Flux theodolite.

For field survey purposes, field stations are marked by concrete beacons, ensuring that all observation points are exactly reoccupied during surveys. Most measure-

ments are taken on a standard 1.2 m pillar, while in a few cases observers had to use a tripod mounted above a clearly marked shorter beacon. The field survey of 2005 was separated into three different sectors. At first a survey was done by only HMO field surveyors, then 2 independent teams, each consisting of a staff member from HMO and GFZ, conducted a simultaneous field survey in southern Africa. The repeat stations visited during the 2005 field survey campaign can be seen in Fig. 1. The positions with circles were found not suitable for field survey measurements. Mostly it was a case that the region was no more magnetically quiet, or that the observation pillar was destroyed due to urban expansion projects. A DI fluxgate magnetometer was used as primary instrument during field surveys to obtain values of D and I, while an Overhauser magnetometer delivered values of total field intensity (F). Corrections for diurnal variation and other disturbing effects were made by comparing field station observations with magnetic data recorded on site with a LEMI suspended tri-axis fluxgate instrument. This proved to be a vast improvement by using magnetic observatories, sometimes a distance of more than 300 km away (see Korte *et al.* 2007, this volume).

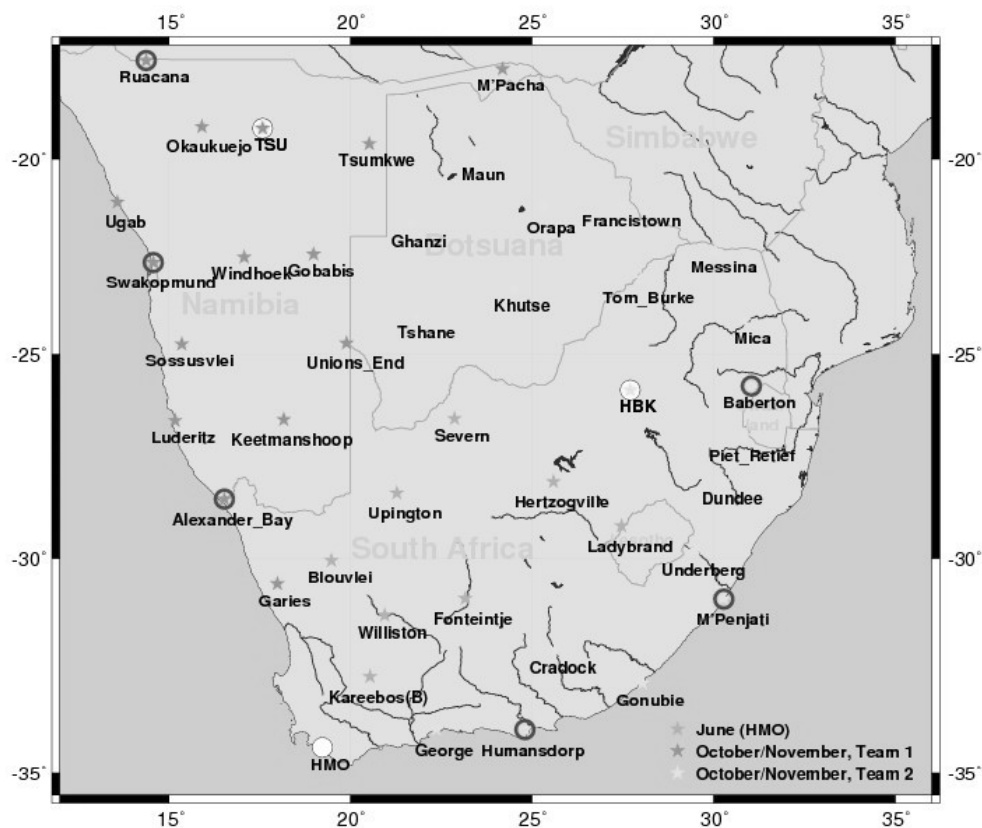


Fig. 1. Map of distribution of repeat stations over the Southern African region, showing the locations visited by the different field survey teams.

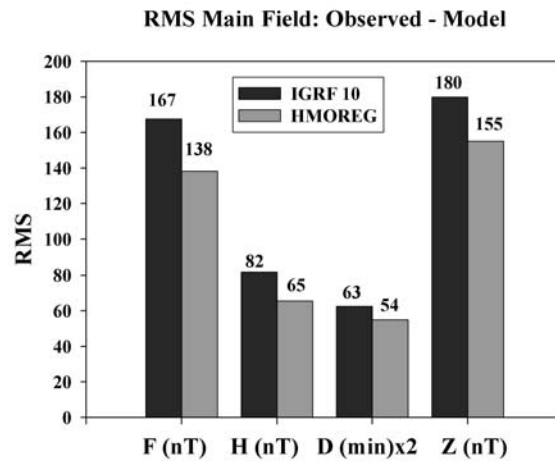


Fig. 2. Comparison of RMS differences between the IGRF10 global field model, the regional model for southern Africa, HMOREG, and field survey measurements. Declination D is scaled up by a factor of 2 in order to match the scale of the bar chart.

3. Regional Geomagnetic Field Modelling over Southern Africa

Over the past few years since 2000, satellite data have been used extensively to model the main field over southern Africa, especially to obtain information over areas not accessible by ground survey teams, like the surrounding ocean areas. Models derived in this way proved to be superior in resolution as well as accuracy to global field models when compared with ground observations (Kotzé 2001). On the other hand, however, ground magnetic field measurements have been exclusively used to derive secular variation models for southern Africa (Kotzé 2003). The field survey conducted in 2005 enabled a polynomial-based main field regional model, called HMOREG. A statistical comparison between these models and IGRF 10 for each field component can be seen in Fig. 2. The models derived for each individual component were based on third degree polynomials as a function of latitude and longitude, with 10 statistically significant coefficients for each magnetic field component modelled:

$$\text{Comp} = A + BX^3 + CYX^2 + DXY^2 + EY^3 + FX^2 + GXY + HY^2 + IX + JY$$

where: $X = 26 - \text{Latitude}$; $Y = 24 - \text{Longitude}$; Comp = Main field component (F, H, D, Z); A–J = coefficients derived from field survey data using least squares fit.

As observatory data, in general, are more accurate than repeat survey data, because of better baseline control and because seasonal and other short-term variations are more effectively removed by using annual means, we introduced weighing factors for both observatory and repeat station secular variation data in a ratio 1:0.7 in the least-squares solution. This ratio was determined by minimizing the RMS difference between model fits and survey data. There were 96 vector differences from 32 repeat stations and 9 vector differences from the 3 observatories, providing a total of 105 data values for the present time interval. A regional main field model for epoch 2005.5 was

subsequently derived. The least-squares routine used to fit the data was the stepwise regression procedure described by Efraymson (1960), which has the ability of both entering and removing variables at given levels of statistical significance.

Results obtained by modeling the field survey observations as obtained during the 2005 field survey of southern Africa can be seen in Figs. 3, 4, and 5. A third degree polynomial was used to model the geomagnetic field data.

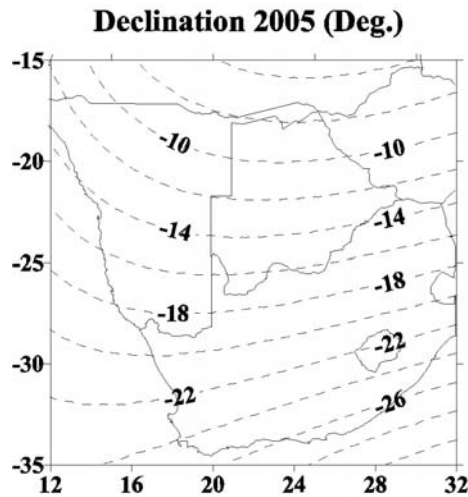


Fig. 3. A contour plot showing the declination for southern Africa as determined by a third degree polynomial fit to field survey data of 2005.

4. Conclusions

The dynamic variation of the magnetic field as observed in southern Africa (Kotzé 2003) necessitates a dense array of suitable ground-based observations for this region with field surveys conducted at regular intervals, preferably on an annual basis.

Results obtained by modelling the declination for 2005 over southern Africa revealed an extremely steep spatial gradient, ranging from almost 26 degrees west of true north in the southern part, to almost 10 degrees west of true north in the northern part. This can clearly be seen in Fig. 3. In comparison to previous field surveys, this pattern is indicative of a growing gradient in the orientation of the geomagnetic field of southern Africa in a north-west to south-eastern direction. The pattern displayed by the horizontal field component H in Fig. 4, clearly indicates that the sub-continent is under the influence of a strong spatial gradient, ranging from 11,000 nT in the south-west to 15,000 nT in the north-western part of the region. This weak H -component in the south-western part of southern Africa can be ascribed to the influence of the South Atlantic Anomaly. As a result, the X -component is anomalously small (Jackson *et al.* 2000). This behaviour is confirmed by the observed pattern for F as displayed in Fig. 5, showing a large spatial gradient from north to south. In the south-western part of the sub-continent the total field is almost 26,000 nT, whereas over the northern part of the region the field is almost 30,000 nT.

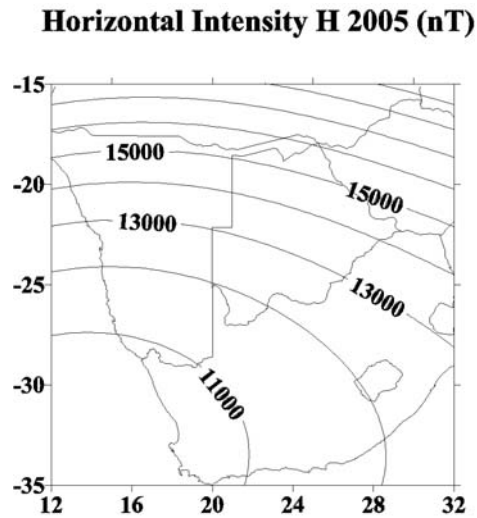


Fig. 4. A contour plot showing the characteristics of the horizontal field component H as modelled by a third degree polynomial using 2005 field survey data.

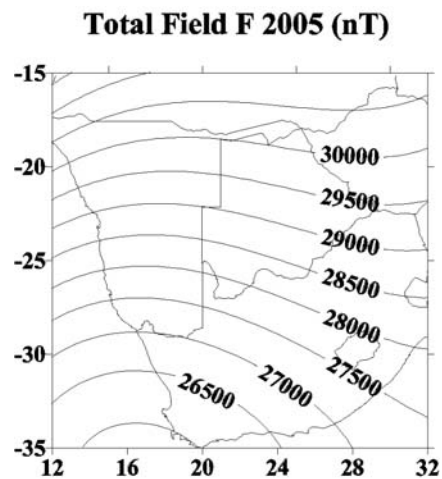


Fig. 5. A contour plot exhibiting the spatial characteristics of the total field F after modelling the field survey measurements of 2005 by means of a third degree polynomial.

Since the first magnetic field measurements started in the nineteenth century, a continuous decrease of the Earth's magnetic dipole moment has been observed. The change in the field strength is, however, not evenly distributed over the globe. In particular, the most rapid decrease of the core field is observed in the Southern Atlantic region. In this regard southern Africa provides an ideal opportunity to study these geomagnetic field changes, as shown in the field survey done in 2005. Since the establishment of the Hermanus Magnetic Observatory in South Africa in 1941, the total field intensity has decreased by 20%, which is greater than decreases observed at any other magnetic observatory.

More interestingly, the growth and position changing of patches of the reverse flux under South African region, from 1840 onwards, can be responsible for changes in dipole moment. Recently, Gubbins *et al.* (2006) showed, by separating contributions of the two hemispheres in the change of axial dipole (g_1^0), that most of the dipole intensity diminishing has come from the Southern Hemisphere. The recent satellite-based models, like CHAOS (Olsen *et al.* 2006), confirm the behaviour of reverse flux patches below southern Africa. These reverse flux patches are likely linked to the expulsion of toroidal flux, which seems to be during the last recent decades, in an active period of expulsion through the core surface.

Moreover, it has been shown recently (Dormy and Mandaia 2005) that patches of intense secular variation appear in the South Atlantic hemisphere. It is therefore of the utmost importance to conduct field surveys similar to this one in 2005 in order to obtain data for the compilation of models of fluid flow at the top of the Earth's core which seem to play a key role in the present behaviour of the geomagnetic field of southern Africa.

The IGRF 10 global field model and the newly-derived polynomial models based on the field survey data of 2005 were statistically compared for each component with the survey measurements. Based on root-mean-square differences, for certain components the improvement obtained is almost 20%, as shown in Fig. 2. However, even better improvements (more than 30%) can be obtained when using spherical cap modelling techniques to model satellite data over southern Africa (Kotzé *et al.* 2001). As a next step we intend to integrate satellite magnetic field measurements with ground observations and then use spherical cap modelling to obtain a geomagnetic field model for this region.

Acknowledgements. This work was made possible through financial support from the Hermanus Magnetic Observatory in South Africa as well as the GeoForschungsZentrum Potsdam, Germany. Support was given by the Geological Survey of Namibia during the field surveys as well as the running of the magnetic observatory in Tsumeb, while the logistical support provided by Geological Survey of Botswana to carry out repeat station measurements is highly appreciated. We particularly acknowledge the active participation of Tiyapo Ngwisanyi in the 2005 survey in Botswana.

References

- Alexandrescu, M., D. Gibert, D. Hulot, J-L. Le Mouél and G. Saracco, 1996, *Worldwide wavelet analysis of geomagnetic jerks*, J. Geophys. Res. 101, 21975-21994.
- Dormy, E., and M. Mandaia, 2005, *Tracking geomagnetic impulses down to the core-mantle boundary*, Earth Planet. Sci. Lett. 237, 300-309.
- Efroymson, M.A., 1960, *Multiple regression analysis*. **In:** A. Ralston and H.S. Wilf (eds.), "Mathematical Methods for Digital Computers", John Wiley, New York, 191-203.
- Gubbins, D., A. Jones and C. Finlay, 2006, *Fall in Earth's magnetic field is erratic*, Science **312**, 5775, 900-902, DOI: 10.1126/science.1124855.

- Jackson, A., Jonkers, A. & M. Walker, 2000, *Four Centuries of Geomagnetic Secular Variation from Historical Records*, Phil. Trans. R. Soc. Lond. **358**, 957-990.
- Korte, M., P. Kotzé, M. Manda, M. Fredow, E. Nahayo and B. Pretorius, 2007, *Towards better observation of the geomagnetic field in repeat station networks*, Proceedings, XIIth IAGA Workshop on Geomagnetic Observatory Instruments, Data Acquisition and Processing.
- Kotzé, P.B., 2001, *Spherical cap modelling of Ørsted magnetic field vectors over southern Africa*, Earth Planets Space **53**, 357-361.
- Kotzé, P.B., 2003, *The time-varying geomagnetic field of Southern Africa*, Earth Planets Space **55**, 111-116.
- Manda, M., 2000, *French magnetic observation and the theory at the time of DE MAGNETE*, In: W. Schroder (ed.), "Geomagnetism Research past and present", IAGA, Bremen-Roennebeck, 73-80.
- Olsen, N., H. Lühr, T. Sabaka, M. Manda, M. Rother, L. Tøffner-Clausen and S. Choi, 2006, *CHAOS – A Model of Earth's Magnetic Field derived from CHAMP, Ørsted, and SAC-C magnetic satellite data*, Geophys. J. Int. (accepted for publication).

Accepted February 12, 2007

Systematic Magnetic Observations in Italy

Antonio MELONI, Lili CAFARELLA, Paola DE MICHELIS, Angelo DE SANTIS,
Domenico DI MAURO, Guido DOMINICI, Stefania LEPIDI, Paolo PALANGIO,
Roberta TOZZI and Achille ZIRIZZOTTI

Istituto Nazionale di Geofisica e Vulcanologia
Via di Vigna Murata 605, Roma, Italy
e-mail: meloni@ingv.it

Abstract

Istituto Nazionale di Geofisica e Vulcanologia (INGV) is responsible for systematic magnetic observations in Italy made in observatories and repeat stations. At present, two regularly working geomagnetic observatories cover central and northern Italy: L'Aquila (the main Italian observatory since 1958) and Castello Tesino (since 1964). A new observatory is, at the moment, being installed in the southern Mediterranean (near Sicily) at Lampedusa Island. Once this installation is successfully completed, the three observatories will be able to provide a full coverage of the whole Italian latitudinal extension.

A network of magnetic repeat stations is regularly distributed across Italy and measurements in some locations have been made for more than a century. Since the end of the 1970's, INGV has been developing a modern repeat station network used for the compilation of the Italian magnetic maps. The most recent survey was made between 2004 and 2005 using L'Aquila Observatory as reference.

1. Introduction

The history of geomagnetic measurements in Italy dates back to 1640 when the Fathers Borri and Martini made the first magnetic survey by measuring the values of declination at 21 sites, but it was only in 1880 that the idea of funding an Italian geomagnetic observatory was first proposed. Before the foundation of L'Aquila geomagnetic observatory in 1958 for the International Geophysical Year by *Istituto Nazionale di Geofisica e Vulcanologia (INGV)*, the Italian national research institute devoted to the study of geophysics, the geomagnetic field in Italy was measured at the observatory of Pola (1880-1925), in the Istria Peninsula (now Croatia), and then at the observatory of Castellaccio (1932-1962), near Genova, maintained by *Istituto Idrografico*

della Marina. Therefore, an almost complete time series starting in 1880 is available for the horizontal component H and declination D (see Cafarella *et al.* 1992). Now, nearly at the fiftieth anniversary of L'Aquila observatory, INGV is in charge of systematic magnetic field observations in Italy. This task is accomplished by both running geomagnetic observatories and by periodically measuring the field at several repeat stations. At present, there are two geomagnetic observatories regularly running on the Italian territory: L'Aquila (central Italy) and Castello Tesino (northern Italy). In the near future the observatories will become three with the addition of the forthcoming observatory of Lampedusa Island in the southern Mediterranean, that is being tested at this time. In order to give a complete overview of the geomagnetic field observation activities the next two sections illustrate, respectively, the main features of each observatory and the Italian magnetic network in some detail; the last section summarises some future development of our observation activities and equipments.

2. The Italian Geomagnetic Observatories

As already mentioned, the three geomagnetic observatories (for simplicity we will refer to Lampedusa as if it were a real running observatory), extend latitudinally as shown in Fig. 1. At present only L'Aquila (IAGA code AQU) complies with the standards for Intermagnet observatories. We plan also to have Castello Tesino (IAGA code CTS) and Lampedusa (LMP) to follow the strict standards required for the observatories of the Intermagnet network also in matter of absolute measurements, so that they could provide data to the whole geomagnetic community regularly. This could happen, for instance, when procedures for automatic absolute measurements will be available. In fact, at this time Castello Tesino and Lampedusa are not manned and only occasionally absolute measurements are made by visiting staff. Each of the three observatories has pillars for absolute measurements and more than an azimuth mark is available. Absolute values of declination and inclination are measured by means of a standard magnetic theodolite (DI-flux). An idea of the short and long term time variability of the geomagnetic field in Italy can be given by Fig. 2: the left panel summarises the daily variations recorded at the three sites of L'Aquila, Castello Tesino and Lampedusa during a quiet day, the right panels show the secular variation recorded at L'Aquila and Castello Tesino for H , D , Z and F .

2.1 L'Aquila geomagnetic observatory

L'Aquila geomagnetic observatory (geographical latitude and longitude $42^{\circ}23'$ N and $13^{\circ}19'$ E; altitude 682 m a.s.l.; corrected geomagnetic latitude $36^{\circ}19'$ N at 2006.0) is the main Italian magnetic observatory since 1958. The observatory consists of four amagnetic buildings. Two of these are devoted to host variometers and to perform absolute measurements while the others are for laboratories and general service buildings. Differently from Castello Tesino and Lampedusa observatories, L'Aquila is manned and absolute measurements are performed several times a week by on-site personnel.

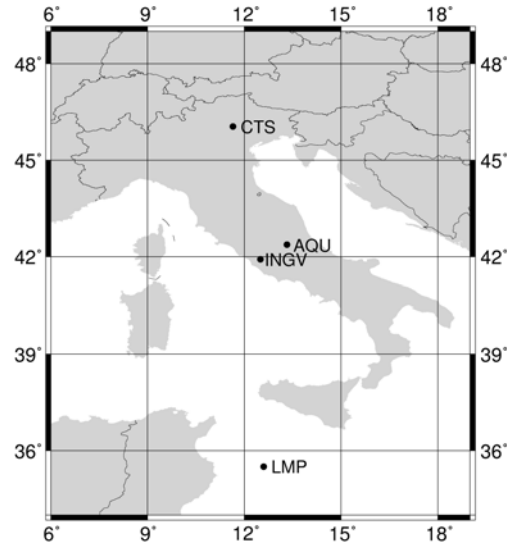


Fig. 1. Location of the head office of INGV in Rome, and of the geomagnetic observatories: Castello Tesino (IAGA code CTS), L'Aquila (IAGA code AQU) and Lampedusa (LMP).

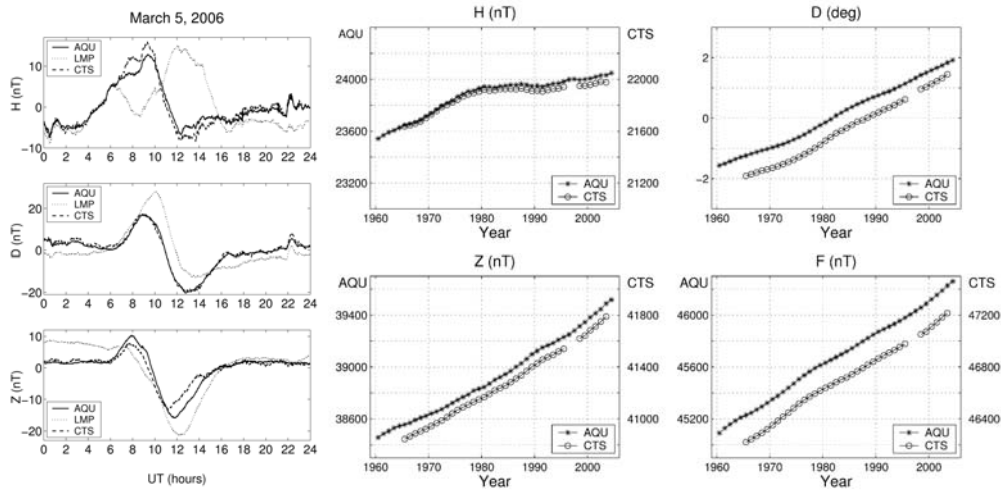


Fig. 2. Left panel: a comparison among the daily variations of the three Italian observatories during a magnetically quiet day. Right panels: secular variation for L'Aquila and Castello Tesino observatories.

Variation measurements of H , D and Z are made by means of three independent systems contemporarily running: two three-axial fluxgate magnetometers (one with toroidal and the other with linear sensors) and a two-axial fluxgate magnetometer for the measurement of D and I , all supported by a proton magnetometer for the measurement of total intensity F . Measurements of H , D , Z and F are also made by a proton precession vector magnetometer with a resolution of 0.1 nT. All these measuring systems have a sampling rate of 1 sec. An accurate time mark of the measurements is

guaranteed by the use of GPS on all systems. Besides the traditional monitoring of the geomagnetic field, at L'Aquila other observations are performed such as pulsation recording, radiometer measurements in the ULF, ELF and VLF bands, magnetotelluric field measurements and telluric self potential measurements. The observatory provides magnetic variation data for the study of the distribution and morphology of pulsations, magnetic storms and all short period transient magnetic variations. L'Aquila staff also provides for the operation and maintenance of a magnetic network for the detection of magnetic field changes due to tectonomagnetic effects. The network is located in Central Italy, it consists of four magnetic stations for long term measurement of total magnetic field, by means of proton precession magnetometers.

As already mentioned, L'Aquila observatory has been participating to the Intermagnet network since 1999. For this purpose a dedicated three-axial fluxgate magnetometer acquisition system has been realized at INGV. It has an excellent long-term stability and a good sensitivity. The core of the coils is a torus made of Vitrovax 60/25 that is an amorphous material with a glass structure.

On the web site of INGV real time L'Aquila magnetograms, real time automated K indices estimated with the FMI (Finnish Meteorological Institute) method (Pirjola *et al.* 1990, Sucksdorff *et al.* 1991), manually calculated K indices and annual means are available (<http://www.ingv.it/geomag/laquila.htm>). Besides this online data publication, since 1960 the yearbook of this observatory, compiled with data from the proton precession vector magnetometer, has been regularly published.

2.2 *Castello Tesino geomagnetic observatory*

The observatory of Castello Tesino is located in North-eastern Italy (geographical coordinates 46°03' N, 11°39' E, altitude 1175 m a.s.l.; corrected geomagnetic latitude 40°50' N at 2006.0) and since 1964 it has been working almost continuously. It was designed to run automatically and to be remotely checked from the INGV head office in Rome. The observatory consists of three amagnetic stone buildings: one is for absolute measurements, one for the automatic digital systems (personal computers, instruments and sensors) and the last is a general services building (UPS, LAN devices as hubs and routers).

The variations of H , D and Z components are measured by two independent systems consisting of two three-axial fluxgate magnetometers and stored on two different personal computers. One system consists of a fluxgate magnetometer LEMI-008i (resolution of 0.1 nT) built at Lviv Centre of the Institute of Space Research (Ukraine) connected to a personal computer that allows real time data downloading. This is possible due to its connection to the INGV LAN by means of a high speed connection. The second system comprises a vector magnetometer built at INGV laboratories connected to another personal computer; data coming from this second system are downloaded daily via modem. This magnetometer will be soon substituted with the more modern meteomagnetic station LEMI-017. Total field intensity is monitored by means of an Overhauser magnetometer (GEM-GSM19). All the sensors (the two fluxgate and the Overhauser magnetometer sensors) are located in a room equipped with a non magnetic heater connected to a thermostat. The two acquisition systems store both

1-minute and 1-second sampled data into daily files. To guarantee a precise time mark of the measurements, each computer is equipped with a GPS providing real UT. One minute sampled data coming from both systems can be viewed through the INGV internet pages (<http://www.ingv.it/geomag/ctesino.htm>) where daily magnetograms are available.

At present, at the observatory also a fluxgate magnetometer property of the Space Research Institute of the Austrian Academy of Sciences (in the framework of the CHIMAG network, see <http://saturn.iwf.oeaw.ac.at/iwfmag/chimag/>) is hosted. These data, together with those from the other instruments of the network, are used to study magnetic field line resonances.

2.3 Lampedusa geomagnetic station

On Lampedusa Island – south of Sicily – a geomagnetic observatory is now being installed (geographical latitude and longitude 35°31' N and 12°32' E; altitude 35 m a.s.l.; corrected geomagnetic latitude 27°25' N at 2006.0). Until now, it has undergone a series of different tests implying also changes in the magnetic instruments or in the acquisition systems in order to find the optimal configuration. These tests have begun at the end of 2005 when the first instruments were installed; the observatory will probably start running in its final configuration in 2007.

The observatory consists of a small stone building with a wooden roof containing all the automatic digital systems. The sensors are buried in thermally isolated boxes just outside the building. At present the observatory is equipped with an Overhauser magnetometer for the total intensity of the field (GEM System, Canada) and a vectorial flux-gate magnetometer (EDA FM100/B, Canada) for the variations of H , D and Z . When properly operating, this new observatory will be the most southern European observatory and, together with L'Aquila and Castello Tesino, will allow peculiar mid-latitude magnetic studies like for example the study of the local drift of the ionospheric focus currents (responsible for the daily variation). Moreover, it is located inside a protected natural reserve with the advantage of a very low electromagnetic noise level. From a practical point of view, the disadvantage of this location is the absence of any kind of service (electric supply and telephone line). Consequently electric power is now supplied by four solar photovoltaic panels and the instruments are connected to a special acquisition unit able to store data and to provide communication and file transmission via GSM connection.

3. The Italian magnetic repeat station network

Since the end of 1970's, INGV has systematically made magnetic field measurements in Italy with the main purpose of elaborating magnetic cartography. These measurements are repeated at intervals of five years at a number of repeat stations which constitute the Italian Magnetic Network. To maintain the degree of detail needed to take into account the shape of the Italian peninsula and islands, the first order network is made of 110 main points distributed on a regular grid with an average spacing of about 58 km. Repeat stations, regularly distributed over the Italian territory

and integrated by geomagnetic observatories, allow the determination of the spatial structure and the time variation of the Earth's magnetic field over Italy.

The most recent survey took approximately one year (September 2004 – November 2005) and was reduced to 2005.0 using the observatory of L'Aquila as reference; the corresponding magnetic maps are in press. The number of repeat stations is 133 including the two observatories, thus reaching a station density of about one station on 2800 km². The number has grown since in the same period magnetic measurements were made also outside Italy, in collaboration with other research institutes or universities. In particular in Albania measurements were made on 11 repeat stations (in collaboration with the National Academy of the Sciences of Albania and with the Tirana University) and in Corsica on 3 repeat stations (in agreement with the *Institut de Physique du Globe de Paris – IGP*). All these measurements have been included in the elaboration of cartography, as well as of secular variation and normal fields, thus contributing to a better definition of the magnetic field spatial and temporal variation in the Ionian and Tyrrhenian areas. The left panel of Fig. 3 shows the location of the main points of the first order magnetic Italian network, the right panel shows the magnetic inclination map for epoch 2005.0.

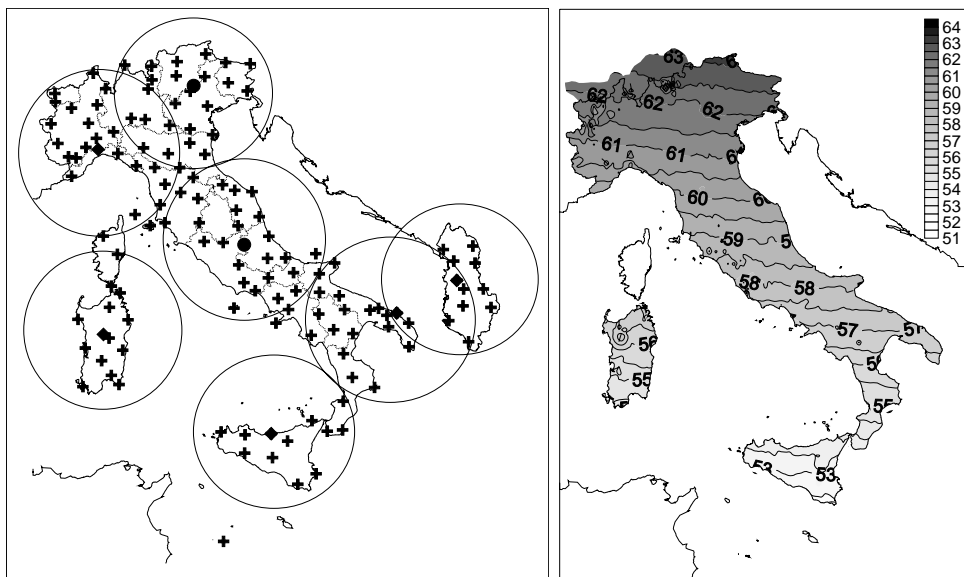


Fig. 3. Left panel: repeat stations (crosses); observatories (circles); temporary stations (diamonds). The circumferences specify the coverage for the estimation of rapid time variation of the geomagnetic field and are centred on observatories and temporary stations. Right panel: magnetic inclination I (in degrees) over Italy for epoch 2005.0.

An edition of three magnetic maps to the scale 1/1,500,000 (one map for each element: F , H and Z) was published at 1979.0. At the same date also a magnetic anomaly map of total field was published (Molina *et al.* 1994). The 1979.0 survey was updated in collaboration with IGM (*Istituto Geografico Militare*) and also declination

was remeasured at all repeat stations, bringing to a four magnetic maps collection (F , H , Z and D) to the scale 1/2000000 (Arca *et al.* 1988). In the following years the regular updating of the magnetic measurements was made by INGV only for scientific purposes without the involvement of IGM for the compilation of the corresponding new magnetic maps (Meloni *et al.* 1994, De Santis *et al.* 1997). New maps were available at 2000.0 (Coticchia *et al.* 2001) and the maps from the last survey referred to 2005.0 will appear soon.

4. The Future of Magnetic Measurements in Italy

Geomagnetic observatories record continuously and over long term the time variation of the Earth's magnetic field and maintain the accurate absolute standard of the measurements. Reaching the highest possible accuracy is an important goal in geomagnetic measurements since phenomena such as secular variation and impulses in the secular variation have amplitudes of few nanoteslas. Moreover, only magnetic observatory data can allow a comprehensive modelling of the geomagnetic field, not only from a mathematical standpoint but also on a physical basis, necessary to distinguish and physically represent all sources of the measured geomagnetic field correctly.

Activities planned for the near future will be devoted to improvements in instruments and operations in both observatories and networks. For what concerns observatories activities they will involve in particular the displacement of the instruments of Castello Tesino observatory in a new building about a hundred meters far from the present one and, of course, the completion of the installation of Lampedusa observatory.

The Intermagnet standard is now the excellence for geomagnetic observatories. In Italy this is so far achieved only at L'Aquila. We have the reasonable expectation to upgrade progressively also the other two structures of Castello Tesino and Lampedusa to this standard.

What concerns the magnetic repeat station activities and the consequent normal field (an analytical expression of second order degree polynomial type, in latitude and longitude) computation and maps production for the Italian region, we expect to reasonably proceed with the five years survey, in time with IGRF new generations. Moreover, developments in this activity will also follow the new coordination of European networks recently created, MAGNET (acronym of Magnetic Network in Europe), to which Italy has adhered putting its results in common with other European nations.

References

- Arca, S., O. Battelli, G. Dominici, A. Marchetta and A. Meloni, 1988, *Italian Magnetic Network at 1985.0*, Bollettino di Geodesia e Scienze Affini **4**, 339-350.
- Cafarella, L., A. De Santis and A. Meloni, 1992, *Secular variation in Italy from geomagnetic field historical measurements*, Physics of the Earth and Planetary Interiors **73**, 206-221.

- Coticchia, A., A. De Santis, A. Di Ponzio, G. Dominici, A. Meloni, M. Pierozzi and M. Sperti, 2001, *Italian Magnetic Network and geomagnetic field maps of Italy at year 2000.0*, Bollettino di Geodesia e Scienze Affini **IV**, 261-291.
- De Santis, A., M. Chiappini, G. Dominici and A. Meloni, 1997, *Regional geomagnetic field modeling : the contribution of the Istituto Nazionale di Geofisica*, Annali di Geofisica **40**, 1161-1169.
- Meloni, A., O. Battelli, A. De Santis and G. Dominici, 1994, *The 1990.0 magnetic repeat station survey and normal reference fields for Italy*, Annali di Geofisica **37**, 5, 949-967.
- Molina, F., E. Armando, R. Balia, O. Battelli, E. Bozzo, G. Budetta, G. Caneva, M. Ciminale, N. De Florentis, A. De Santis, G. Dominici, M. Donnalioia, A. Elena, V. Iliceto, R. Lanza, M. Loddo, A. Meloni, E. Pinna, G. Santarato and R. Zambrano, 1994, *Geomagnetic survey of Italy at 1979.0, repeat station network and magnetic maps*, Technical Report of Istituto Nazionale di Geofisica, N. 554.
- Pirjola, R., J. Ryno and C. Sucksdorff, 1990, *Computer production of K-indices by a simple method based on linear elimination*. In: K. Kauristie, C. Sucksdorff and H. Nevanlinna (eds.), Proceedings of International Workshop on Observatory Data Acquisition and Processing, 136-146, Geophysical Publications N°15, Finnish Meteorological Institute, Helsinki.
- Sucksdorff, C., R. Pirjola and L. Häkkinen, 1991, *Computer production of K-values based on linear elimination*, Geophysical Transactions **36**, 333-345.

Accepted February 21, 2007

The Newest Measurements of the Total Magnetic Field Strength in Croatia

A. MARKI, G. VERBANAC, E. VUJIĆ and V. VUJNOVIĆ

Geophysical Institute A. Mohorovičić, University of Zagreb, Faculty of Science
Ulica kralja Zvonimira 8, HR-10000 Zagreb, Republic of Croatia
e-mail: eugvujic@gfz.hr,

A b s t r a c t

In autumn 2003 we made a ground survey of total magnetic field strength in a part of Croatia from river Drava north to river Sava and Pokuplje, between the lines Zagreb–Koprivnica in the west, and Hrvatska Kostajnica–Virovitica in the east. During summer 2004 measurements were extended to the north-western part of Croatia (Hrvatsko Zagorje and Žumberak), and also to 100 km south from Zagreb (Banovina). Also, measurements during 2005 were performed in the region from river Kupa on south and river Drava on north. A total of 56 positions were surveyed in a net with spacing of 15-20 km. For data reduction, the total field strengths were recorded at the geomagnetic observatories Tihany and Fuerstfeldbruck. Isodynames were obtained for the observed region at epoch 2004.5. Basic purpose of our measurements is to find roughly the position for the Geomagnetic Observatory.

1. Locations of Measurements

Figure 1 shows the locations of ground survey measurements (crosses) and positions of the larger towns in the study region of Croatia (circles).

2. Base Stations

Figure 2 shows the dependence of the standard deviation of the absolute values of the differences between the moving average of base measurements and base measurements, on distances from Zagreb (capital), with Kp index as parameter. Base stations (Overhauser effect proton magnetometer) were installed in the vicinity (70-150 m away) of the site for ground survey. During the least active days we wanted to see how this standard deviation depends on the distance from Zagreb, because this city is the source of great magnetic disturbances, including leakage electrical currents from the electric tramway net. We conclude that the locations at distances greater than 35 km from Zagreb can be considered as possible sites for the Geomagnetic Observatory.

In these places, the calculated standard deviation generally falls below 0.05 nT. This standard deviation depends also on soil composition of the measurement site (lateral and vertical electrical conductivity inhomogeneities), size of the moving window, part of the day when measurements are performed, etc.

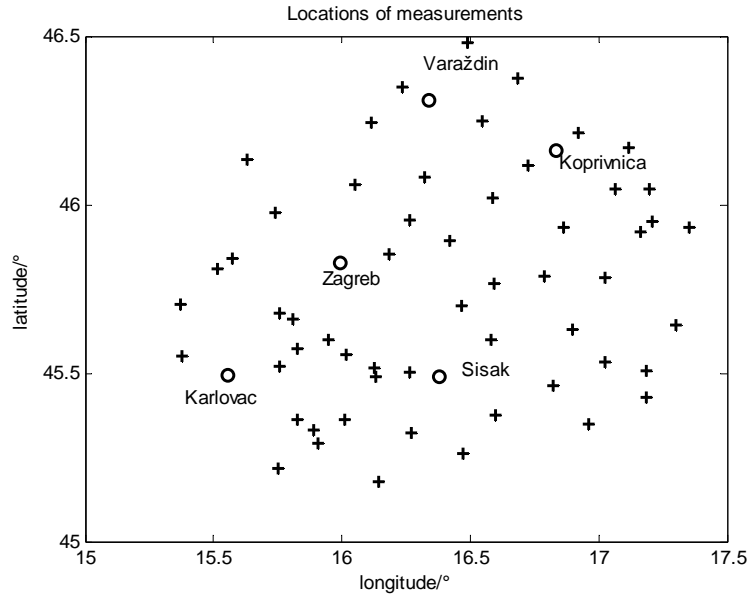


Fig. 1. Location of ground survey measurement sites (crosses) in Croatia.

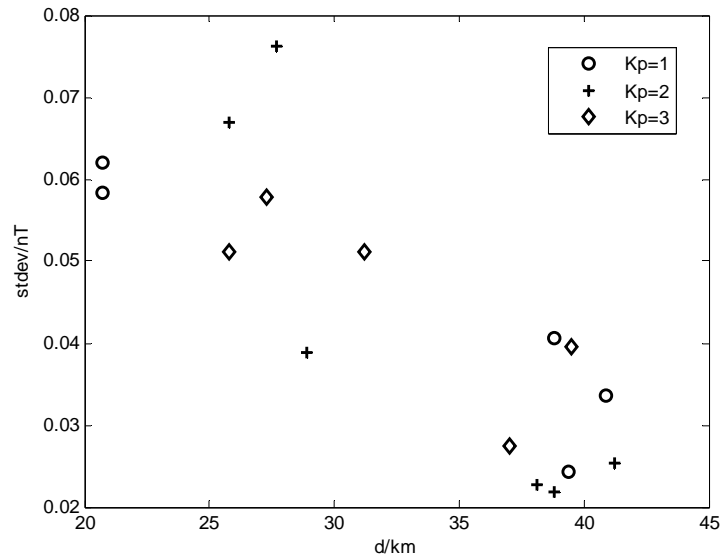


Fig. 2. Standard deviations of the absolute values of differences between the moving average of base measurements and the base measurements vs. distance from Zagreb.

Figure 3 shows two magnetograms obtained with Overhauser effect proton magnetometers with the sampling rate of 3^{-1} Hz, at two different locations during the same day. Stojdraga ($\varphi = 45^{\circ} 50.416'$, $\lambda = 15^{\circ} 34.342'$) is located about 10 km away from the railway station Dobova in Slovenia, and the Slovenian Railway network uses direct electrical current. At that station, leakage electrical currents flow in the ground which produce magnetic field perturbations, and this effects can be seen on magnetogram. Great peaks on magnetogram correspond to the time moments when trains have left the station (checked with the train schedule). Pisarovina ($\varphi = 45^{\circ} 33.407'$, $\lambda = 16^{\circ} 1.210'$) is located about 38 km away from Dobova, and at that location we did not observe the effects of additional magnetic fields.

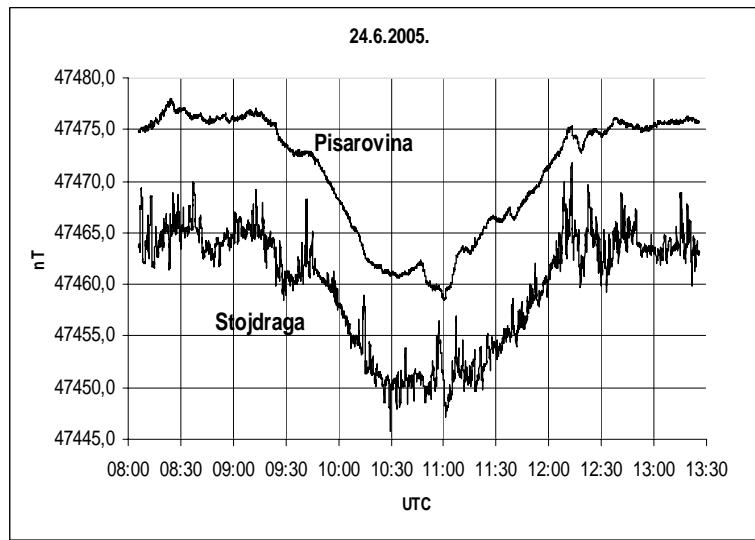


Fig. 3. Magnetograms obtained at two stations.

3. Data Reduction

The data obtained with Overhauser effect proton magnetometers using mobile or walking mode options are reduced to the epoch 2004.5, because for that epoch both the observatories, Fuerstenfeldbruck and Tihany, have definite values of annual means. Data from observatories are collected from Intermagnet web site or by private communications. We have used one minute average values of the total field for data reduction. The following expression was used:

$$F_l^{2004.5} = F_{obs}^{2004.5} + F_l^t - F_{obs}^t,$$

where $F_l^{2004.5}$ is the mean value at epoch 2004.5 at the location, $F_{obs}^{2004.5}$ is the mean value at epoch 2004.5 at the observatory, F_l^t is the value of the total field at the moment t at the location and F_{obs}^t is the value of the total field at the same moment (hour and minute) at the given observatory. The given expression was used independently

for each of the individual measurements at the location, and we then averaged all reduced values to obtain just one value at each location. So far we have not used weighted factors, and instead of that we obtained values at each location using two observatories and then comparing them.

Figure 4 shows difference of the reduced total fields at each location between values obtained with FUR and THY Observatory. These differences are not greater than 10 nT. The maximal distance of locations from the FUR Observatory is about 554 km and the minimal distance is about 400 km. From the THY Observatory the maximal distance is about 250 km and the minimal distance is about 100 km. We used 47942 nT as the mean value at 2004.5 for the FUR Observatory and 47957 nT for the THY Observatory at the same epoch. The number of locations which are used for the reduction with FUR Observatory are 56, and the number of locations for the THY Observatory are 43. If we take only locations where Kp index was not greater than 3, we have 39 locations for reduction with FUR, and 28 locations for data reduction with THY.

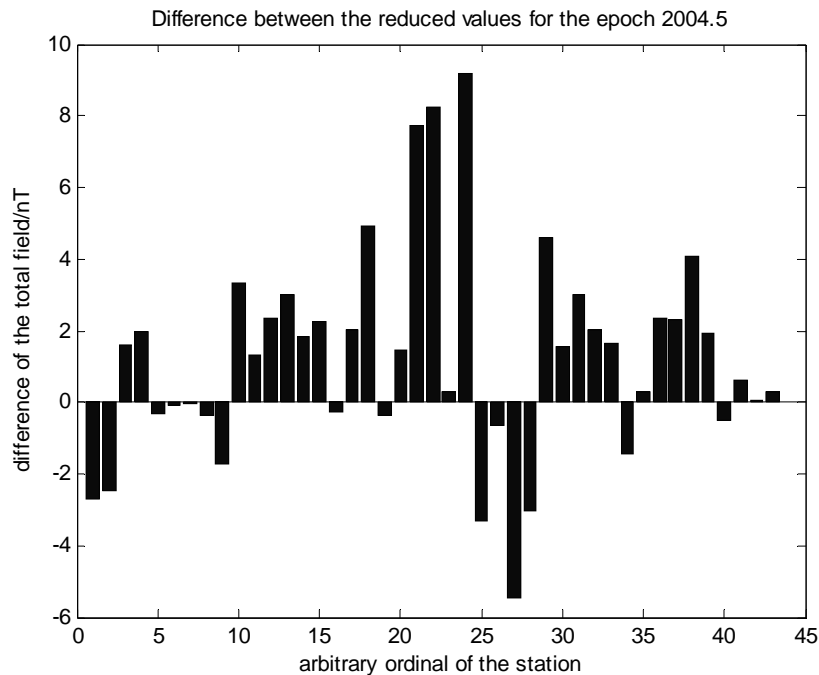


Fig. 4. Differences of the reduced fields at each location between observatories FUR and THY.

Figure 5 shows dependence of the absolute value of the difference of two obtained reduced fields on Kp index. Each mark corresponds to one location. One can suppose that this difference is independent of geomagnetic activity.

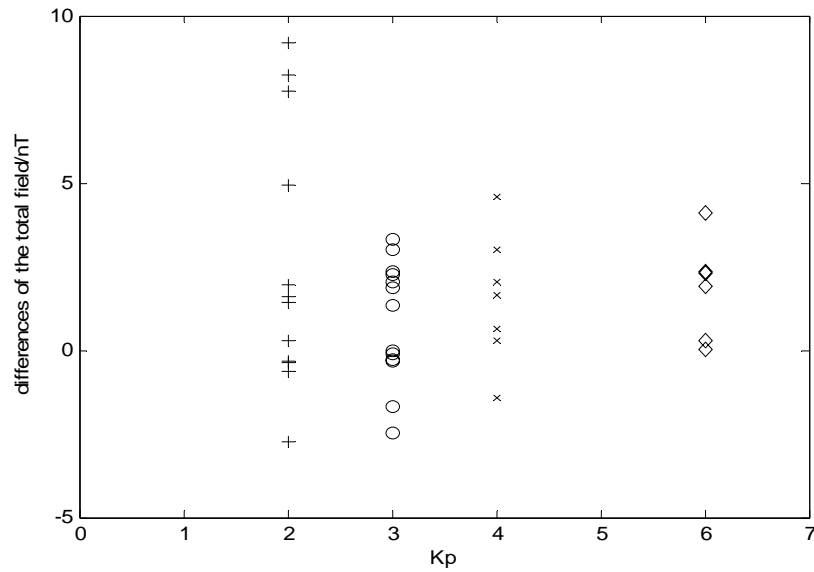


Fig. 5. The absolute values of the difference of two reduced fields vs. index Kp.

Figures 6 and 7 display the absolute value of the difference between values obtained from observatories and IGRF10 Model at 2004.5 for given locations, respectively. In the case of the reduction with FUR Observatory, the maximal difference is 84.7 nT, and the minimal is 0.3 nT. In the second case, the minimal difference is 3.3 nT, and the maximal is 85 nT. Some of the locations are the same in both cases, and numbers of locations is different because of data availability.

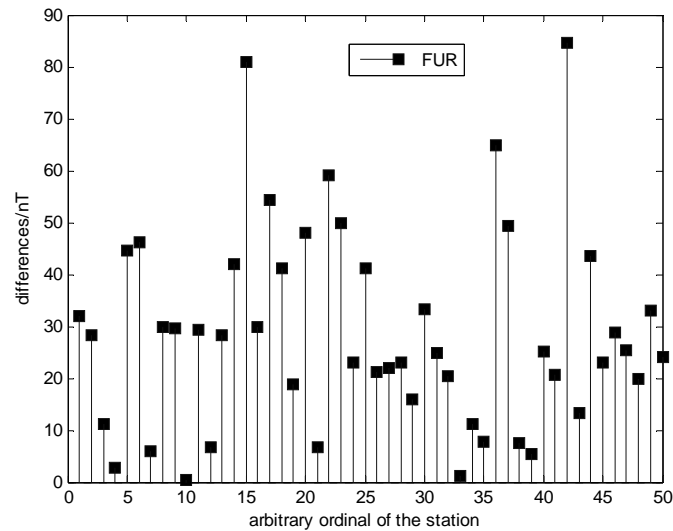


Fig. 6. The absolute values of differences between observatory data and IGRF10 Model for the FUR observatory.

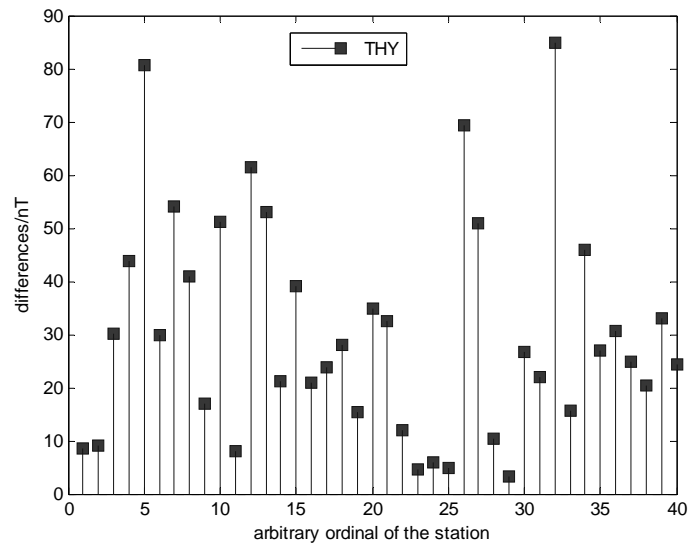


Fig. 7. The absolute values of differences between observatory data and IGRF10 Model for the THY observatory.

Figure 8 shows the time difference in years between the epoch 2004.5 and epoch of measurement at each location, in the case of FUR Observatory.

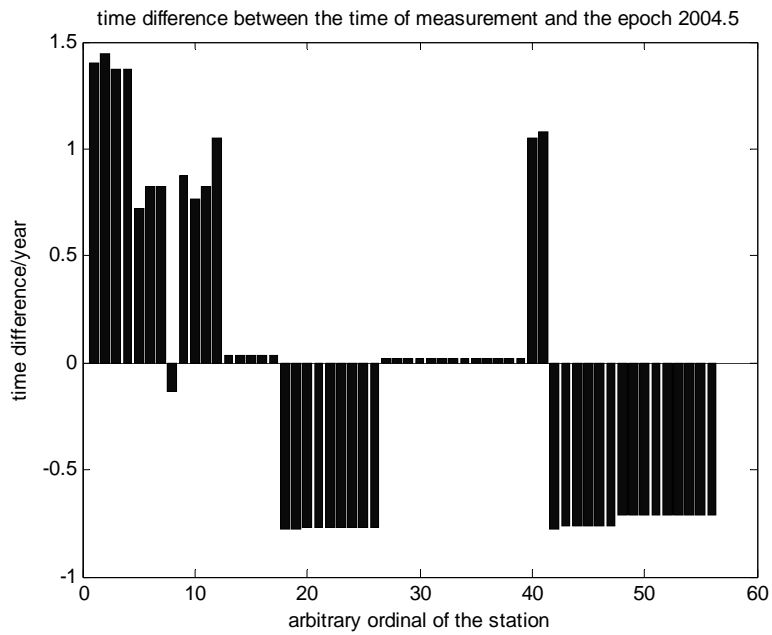


Fig. 8. Time differences between epoch 2004.5 and epoch of measurement.

4. Preliminary Isodynames

On the basis of reduced values at given epoch, one can make a map of isodynames at that epoch. These maps are shown on next four figures. Figures 9 and 10 represent isodynames at epoch 2004.5 in the cases where FUR and THY Observatory

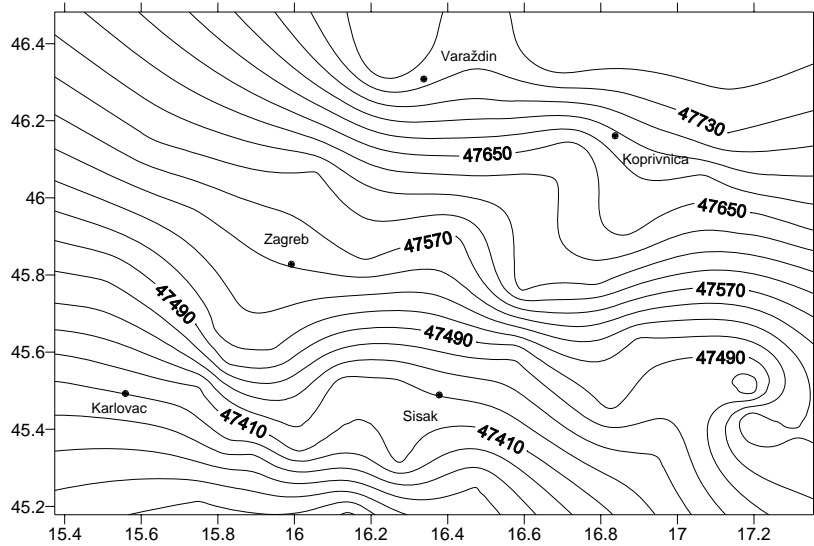


Fig. 9. Data reduction with FUR Observatory.

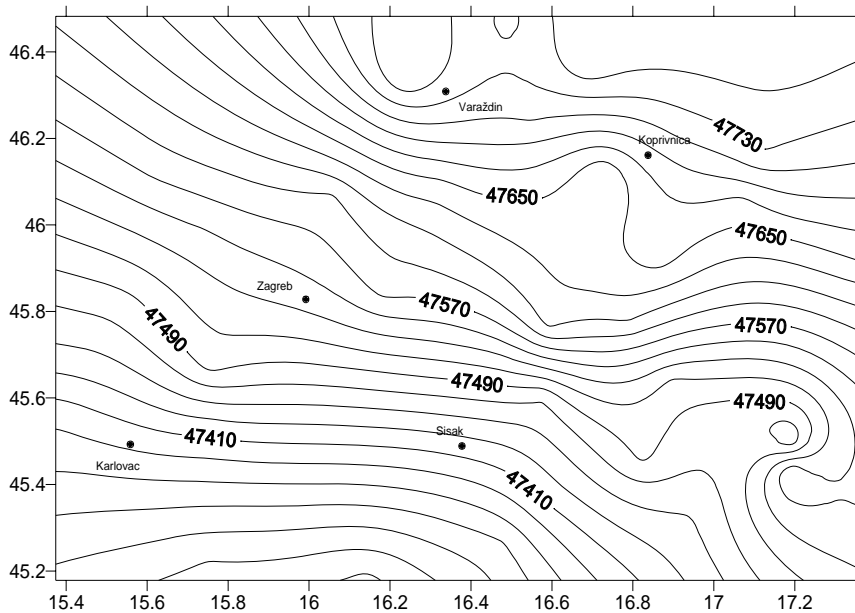


Fig. 10. Data reduction with THY Observatory.

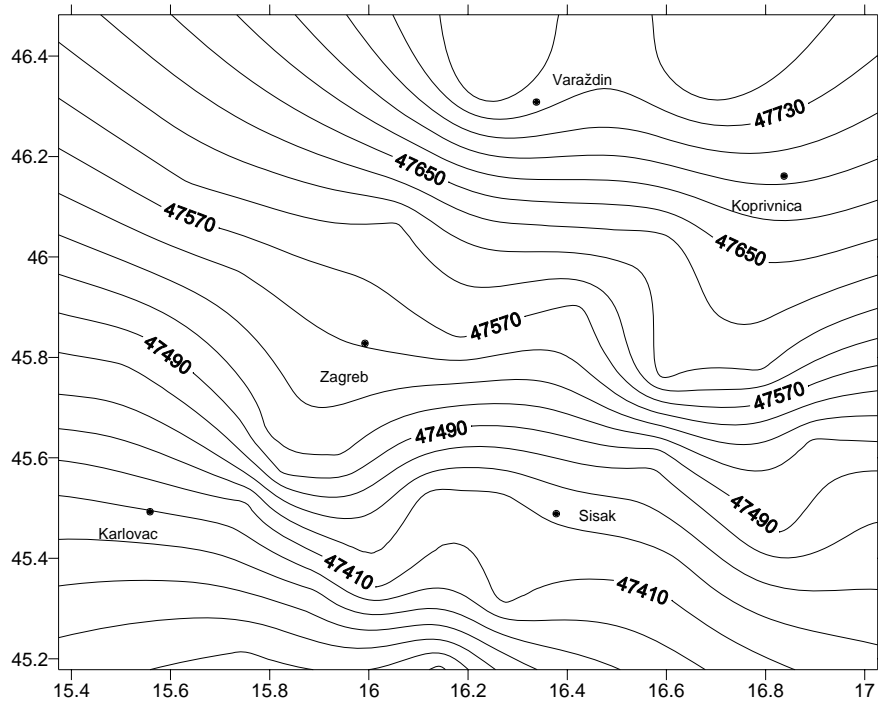


Fig. 11. Data reduction with FUR Observatory (locations with $K_p \leq 3$).

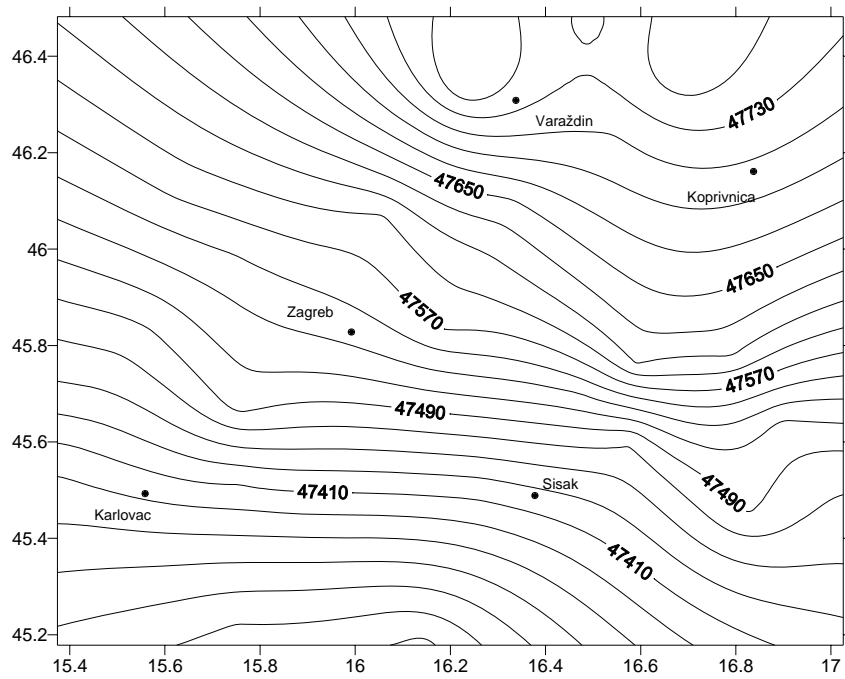


Fig. 12. Data reduction with THY Observatory (locations with $K_p \leq 3$).

are used for data reduction, respectively. Major anomalies (some of them known from historical measurements) can be seen. These are: near village Lepavina in the vicinity of town Koprivnica, Petrova and Zrinska Gora (mountains) south of towns Karlovac and Sisak, and region between Moslavačka and Zrinska Gora (mountains) in southeast part of the investigated region. One of the possible locations for Geomagnetic Observatory can lie on isodiname northwest of town Sisak, on line Zagreb-Sisak, at least 38 km away from Zagreb.

Figures 11 and 12 represent isodynamos of the total field where the maps are obtained with the reduced values for locations when Kp index was not greater than 3. The major difference is in the southeast part of the region.

5. Conclusion

Basic purpose of our ground survey measurements was to see roughly the position of the Geomagnetic Observatory. Our intention is to find the place not more than 60 km away south from Zagreb and to avoid natural and artificial anomalies and disturbances. After that we have to investigate selected area with several grids of measurements (on different spatial scales) to obtain the horizontal and vertical gradients of the total field and also perform measurements that include electrical and electromagnetic methods to obtain the picture of lateral and vertical conductivity inhomogeneities of soil at the site of Observatory. We also need more sophisticated methods of data reduction because of the absence of an observatory and data of secular variation in Croatia.

Acknowledgements. We thank Msc. Heilig Balazs and Msc. Andras Csontos from Tihany Observatory, Dr. Juergen Matzka from Fuerstenfeldbruck Observatory and Dr. Magdalena Vaczyova from Hurbanovo Observatory, who kindly gave us the data that we asked for. The majority of data are collected from the Intermagnet web site.

References

- De Santis, A., M. Chiappini, G. Dominici and A. Meloni, 1997, *Regional geomagnetic field modelling: the contribution of the Istituto Nazionale di Geofisica*, *Annal. Geophys.* **40**, 5, 1161-1169.
- Jankowski, J., and C. Sucksdorff, 1996, *Guide for magnetic measurements and observatory practice*, International Association of Geomagnetism and Aeronomy, Warszawa, 237 pp.
- Korte, M., and M. Fredow, 2004, *Magnetic repeat station survey of Germany 1999/2000*, Scientific Technical Report, GFZ Potsdam, 23 pp.
- Kovacs, P., and A. Kormendi, 1999, *Geomagnetic repeat station survey in Hungary during 1994-1995 and the secular variation of the field between 1950 and 1995*, *Geophysical Transactions* **42** (3-4), 107-132.

- Newitt, L.R., C.E. Barton and J. Bitterly, 1996, *Guide for magnetic repeat station surveys*, International Association of Geomagnetism and Aeronomy, Warszawa, 113 pp.
- Schulz, G., M. Beblo, A. Best, A. Volker and M. Gropius, 1997, *Definitive Results of the Geomagnetic Repeat Station Survey of Germany: Normal Field Model and Anomalies*, Dt. Hydrogr. Z. **49** (1), 21-33.
- Vaczyova, M., 1999, *Distribution of the Earth's magnetic field on the territory of Slovakia for the 1995.5 epoch*, Contributions to Geophysics and Geodesy **29** (4), 269-284.
- Vujnović, V., G. Verbanac, J. Orešković, A. Marki, K. Marić, I. Lisac and M. Ivandić, 2004, *Results of the preliminary geomagnetic field strength measurements in the northern part of middle Croatia*, Geofizika **21**, 69-87.
- Yanagihara, K., 1977, *Magnetic field Disturbance Produced by Electric Railway*, Geophys. Mag. **38**, 1, 17-34.
- http://www.intermagnet.org/apps/dl_data_def_e.php

Accepted January 22, 2007

Correlation Between IGRF2000 Model and Measured Geomagnetic Data on the Territory of the Republic of Macedonia from 2003 and 2004 Measurements

Sanja PANOVSKA, Todor DELIPETROV, Blagoj DELIPETREV
and Marjan DELIPETREV

Faculty of Mining and Geology, Department of Geology and Geophysics
Goce Delcev No. 89, 2000 Stip, Republic of Macedonia
e-mail: panovskasanja@yahoo.com

A b s t r a c t

On the basis of the measurements carried out in 2003 and 2004 on the network of repeat stations in the Republic of Macedonia, correlation between IGRF and the 2003 model as well as the 2004 model and analysis between the models were made. It should be taken into consideration that the difference in altitude among repeat stations (15 points) is about 1300 m (Galicica is at the highest elevation above sea level, of 1691 m, and Nikolic at the lowest, of 300 m). During data processing, correction for altitude was not made, and measured data were corrected with the data from neighboring observatories Panaguirishte (Bulgaria), Tihany (Hungary) and Aquila (Italy). The paper presents correlations between IGRF model and 2003 and 2004 model for all components of geomagnetic field. The time changes for 2003 and 2004 were also calculated.

1. Introduction

Analyses of the geomagnetic field were done using the measurements carried out in 2003 and 2004 on the territory of the Republic of Macedonia, on the grid of repeat stations of 2003 (Rasson and Delipetrev 2004). The value of elements of the geomagnetic field was calculated according to IGRF 2000 on the grid of repeat stations and the additional points outside the boundaries of the country. The isolines on the map represent the values of IGRF model. The isolines in other maps also indicate the differences with measured values. Resume is given on the first measurements performed in 2002 in Mts. Galicica, Ponikva and Plackovica. An analysis of time variations of the geomagnetic field in the repeat stations was also carried out.

The analyses of the gradient of measured data in 2004 reduced to the epoch 2004.5 on the territory of the country indicates that (Delipetrov 2003):

- The values of declination generally increase towards the east with mean gradient of some 0.002 °/km.
- The values of total intensity increase towards the north with mean gradient of some 2.5 nT/km.
- Horizontal component indicates increases of values towards the south with mean gradient of some 5.1 nT/km.
- The angle of inclination increases towards the north with mean gradient of some 0.009 °/km.
- The values of the northern component of the geomagnetic field increase towards the south with mean gradient of some 5.1 nT/km.
- The values of the eastern component increase generally towards the east with mean gradient of some 0.8 nT/km.
- Vertical component indicates an increase towards the north with mean gradient of some 6.1 nT/km.

2. International Geomagnetic Reference Field – 2000

The IGRF is a series of mathematical models describing the Earth's main field and its secular variation (IAGA Division V, Working Group 8). Each model comprises a set of spherical harmonic coefficients (called Gauss coefficients), g_n^m , h_n^m , in a truncated series expansion of a geomagnetic potential function of internal origin:

$$V = a \sum_{n=1}^N \sum_{m=0}^n \left(\frac{a}{r} \right)^{n+1} \left(g_n^m \cos m\varphi + h_n^m \sin m\varphi \right) P_n^m(\cos \theta) \quad (1)$$

where a is the mean radius of the Earth (6371.2 km) and r , φ , θ are the geocentric spherical coordinates (r is the distance from the centre of the Earth, φ is the longitude eastward from Greenwich and θ is the colatitude (90° minus the latitude)). The $P_n^m(\cos \varphi)$ are Schmidt quasi-normalized associated Legendre functions of degree n and order m ($n \geq 1$ and $m \leq n$). The maximum spherical harmonic degree of the expansion is N . Coefficients for dates between the 5-year epochs are obtained by linear interpolation of the corresponding coefficients for the neighboring epochs. The IGRF coefficients and the computer programs for synthesizing the field components are available from many web pages throughout the world.

2.1 IGRF model for 2004.5 for the territory of the Republic of Macedonia

IGRF model was used to calculate all components of the geomagnetic field of the Republic of Macedonia (D, I, F, H, X, Y, Z). Then, data were extrapolated to cover the whole territory of Macedonia in which the Surfer program was applied. Kriging was used as a grid method (Surfer Help). The result is isolines maps of all components of

geomagnetic field that can be used in many applications. Figures 1-4 represent the maps of isolines of IGRF model for 2004.5 epoch. The calculator used to calculate IGRF elements of the geomagnetic field for the epoch 2004.5 is Geomagix of USGS available at the web site:

<http://geomag.usgs.gov/geomag/geomagAWT.html>

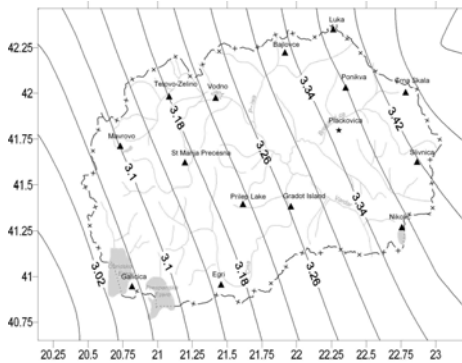


Fig. 1. Map of declination (D) from the IGRF 2000 model for epoch 2004.5.

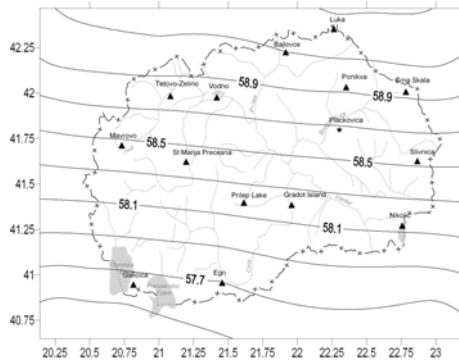


Fig. 2. Map of inclination (I) from the IGRF 2000 model for epoch 2004.5.

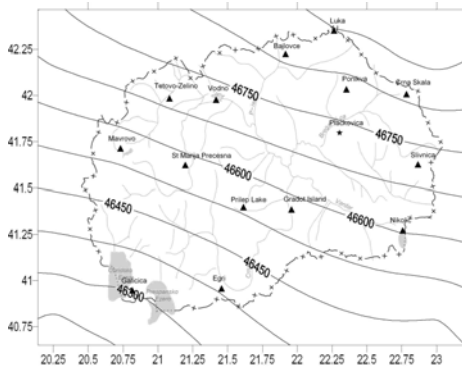


Fig. 3. Map of total intensity (T) from the IGRF 2000 model for epoch 2004.5.

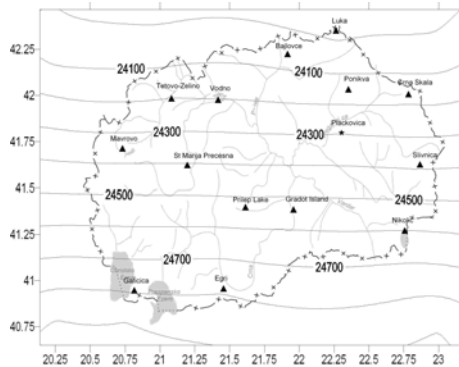


Fig. 4. Map of the horizontal component (H) from the IGRF 2000 model for epoch 2004.5.

3. The Differences Between IGRF Model and Measured Results

Comparisons between mean annual values and calculated IGRF values were carried out on 15 repeat stations in 2003 and 2004. The values are calculated based on IGRF 2000 model for the epoch 2003.5 and 2004.5. The model IGRF values were removed from the annual mean values to get the residual ΔD , ΔI , ΔF , ΔH , ΔX , ΔY and ΔZ values. Table 2 gives the range of the differences. Maps for the differences of the

components of the geomagnetic field between the compared models are shown in the following figures (Figs. 5-8):

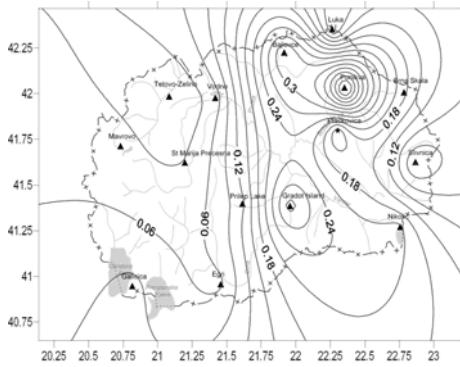


Fig. 5. Map of differences between measured values of declination and the IGRF 2000 model values for epoch 2004.5.

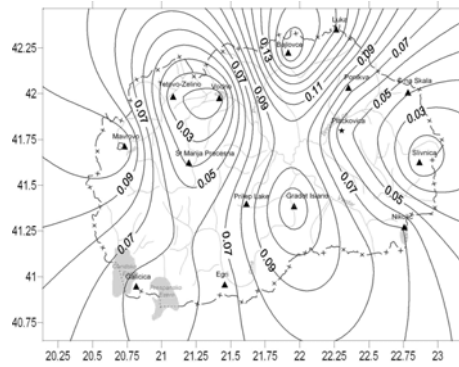


Fig. 6. Map of differences between measured values of inclination and the IGRF 2000 model values for epoch 2004.5.

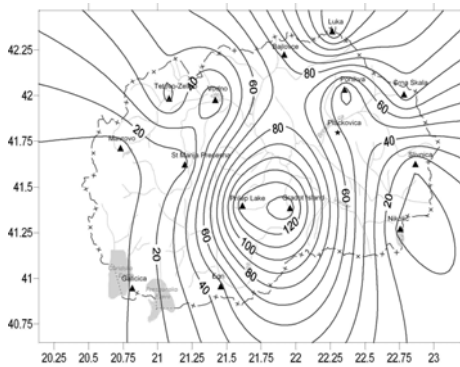


Fig. 7. Map of differences between measured values of total intensity and the IGRF 2000 model values for epoch 2004.5.

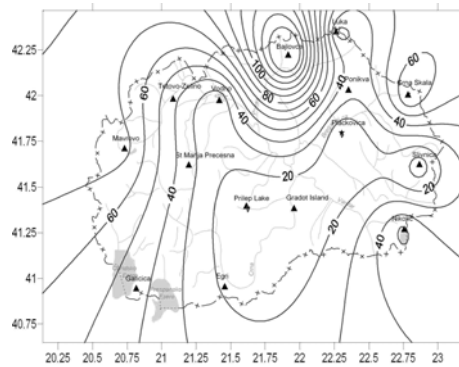


Fig. 8. Map of differences between measured values of the horizontal component and the IGRF 2000 model values for epoch 2004.5.

4. The Differences Between 2003 and 2004

The analyses of measurements carried out in 2003 and 2004 were done after reduction of data from neighboring geomagnetic observatories in Aquila, Tihany and Panaguirishte. Figures 9-12 give maps of isolines of measured values of all components of geomagnetic field for 2003.5 and 2004.5 with dashed and full lines, respectively. The isolines of the two models are drawn with the same values in order to indicate the time evolution. Table 3 shows the intervals in which differences range be-

tween measured values of all components of geomagnetic field for epoch 2003.5 and 2004.5. The isolines of declination the northern and eastern component have clear tendency towards East, whereas other components indicate small variation.

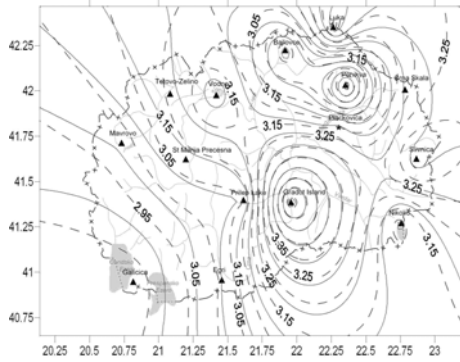


Fig. 9. Map of values of declination of the geomagnetic field, epoch 2003.5 (dashed lines) and 2004.5 (full lines).

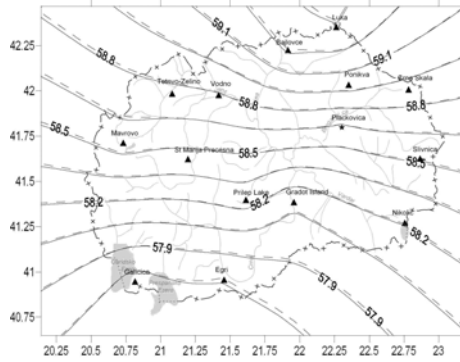


Fig. 10. Map of values of inclination of the geomagnetic field, epoch 2003.5 (dashed lines) and 2004.5 (full lines).

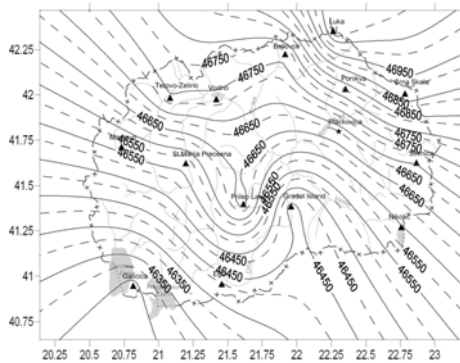


Fig. 11. Map of values of total intensity of the geomagnetic field, epoch 2003.5 (dashed lines) and 2004.5 (full lines).

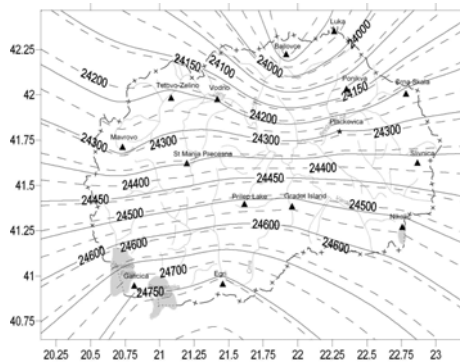


Fig. 12. Map of values of horizontal component of the geomagnetic field, epoch 2003.5 (dashed lines) and 2004.5 (full lines).

5. Analyses of 2002-2004 Measured Values

The following figures (Fig. 13) show time variation of magnetic declination, inclination and total vector for three repeat stations (Galicica, Plackovica and Ponikva) in Macedonia. Data from three neighboring geomagnetic observatories (Aquila, Tihany and Panaguirishte) are used to reduce measurements to a given epoch, 2002.5, 2003.5 and 2004.5. The diagrams indicate regular variation of intensity of total vector

and inclination, for values of some 30 nT/year and some $0.02^\circ/\text{year}$, respectively. Declination indicates higher and irregular variation, particularly for the Ponikva repeat station. This nature of variation requires longer period of observation.

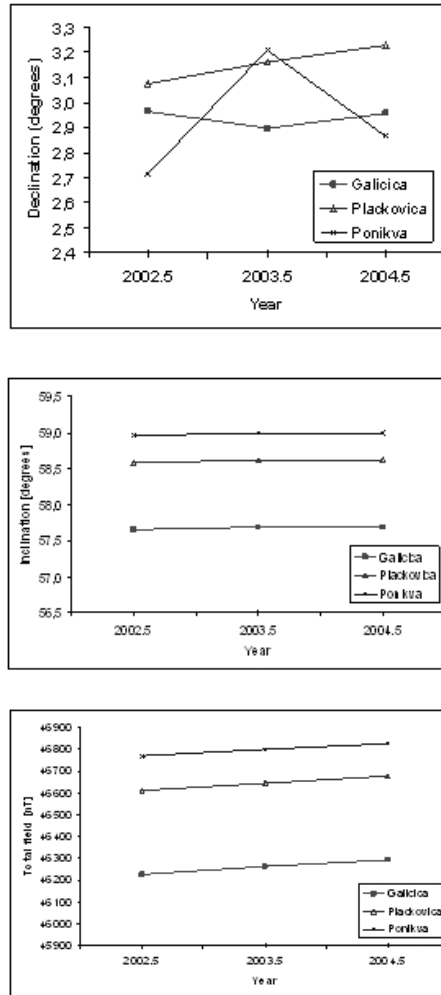


Fig. 13. Time variation of declination, inclination and total intensity for repeat stations Galicica, Plackovica and Ponikva.

6. Conclusion

Comparison of the analyses between measured results and those of IGRF model shows that the results of repeat stations vary in the intervals listed in Table 1. The correlation of results between measurements in 2003 and 2004 indicates the following variation listed in Table 2.

Table 1.

Max. and min. differences between measured values and IGRF values of repeat stations

| |
|--|
| $0.006^{\circ} < \Delta D_{2004.5-IGRF} < 0.512^{\circ}$ |
| $0.011^{\circ} < \Delta I_{2004.5-IGRF} < 0.172^{\circ}$ |
| $5.9 \text{ nT} < \Delta F_{2004.5-IGRF} < 139.7 \text{ nT}$ |
| $2.1 \text{ nT} < \Delta H_{2004.5-IGRF} < 162.7 \text{ nT}$ |
| $1.5 \text{ nT} < \Delta X_{2004.5-IGRF} < 154.7 \text{ nT}$ |
| $4.7 \text{ nT} < \Delta Y_{2004.5-IGRF} < 217.1 \text{ nT}$ |
| $1.5 \text{ nT} < \Delta Z_{2004.5-IGRF} < 178 \text{ nT}$ |

Table 2.

Max. and min. differences between measured values 2003.5 and 2004.5 of repeat stations

| |
|--|
| $0.041^{\circ} < \Delta D_{2004.5-2003.5} < 0.093^{\circ}$ |
| $0.0001^{\circ} < \Delta I_{2004.5-2003.5} < 0.021^{\circ}$ |
| $21.3 \text{ nT} < \Delta F_{2004.5-2003.5} < 34.9 \text{ nT}$ |
| $3.1 \text{ nT} < \Delta H_{2004.5-2003.5} < 17.5 \text{ nT}$ |
| $1.4 \text{ nT} < \Delta X_{2004.5-2003.5} < 15.7 \text{ nT}$ |
| $18.1 \text{ nT} < \Delta Y_{2004.5-2003.5} < 40.5 \text{ nT}$ |
| $19.7 \text{ nT} < \Delta Z_{2004.5-2003.5} < 38.3 \text{ nT}$ |

References

- Delipetrov, T., 2003, *Basics of Geophysics*, Faculty of Mining and Geology, Stip, Republic of Macedonia.
- International Association of Geomagnetism and Aeronomy (IAGA), Division V, Working Group 8.
- Rasson, L.J., and M. Delipetrov, 2004, *Magnetic Repeat Station Network Description*, Dourbes, Belgium.
- Surfer Help: Kriging, www.goldensoftware.com

Accepted January 22, 2007

Geomagnetic Data of the Republic of Macedonia Obtained in 2004

Marjan DELIPETREV, Todor DELIPETROV, Blagoj DELIPETREV
and Sanja PANOVSKA

Faculty of Mining and Geology, Department of Geology and Geophysics
Goce Delcev No. 89, 2000 Stip, Republic of Macedonia
e-mail: marjan@rgf.ukim.edu.mk

Abstract

During 2004, measurements of the geomagnetic field were carried out on the existing network of repeat stations (15 points) of the Republic of Macedonia. The equipment used was from the Royal Observatory, Dourbes, consisting of: 1 Diflux/GPS receiver type FLM3/A serial 001, 1 Proton magnetometer Geometrics G816 (electronics + sensor) serial 1579, 1 Geodetic Tripod and 1 Monocular digital compass KVH Data scope II pn#01-0162 Serial 02070033 and the equipment from the Faculty of Mining and Geology, Stip: 1 Diflux type LEMI 203 (from Tempus JEP Project “Geomagnetic measurements and quality standards”) and proton magnetometers Bison and Geometrics. The territory of the Republic of Macedonia is relatively small, but from the point of view of its geology it is very complex and differentiated. The relief consists of high mountain massifs of up to 2700 m separated by blocks of subsidence and depressions. The field measurements included observation of the total vector of the geomagnetic field F , declination D , and inclination I . All parameters of the geomagnetic field of the Republic of Macedonia were calculated based on the measurements. Based on the results of the elements of the geomagnetic field and observations carried out in 2004, it can be determined that: the total vector F varies about 800 nT, the inclination I varies less than 2 degrees, and the declination D is less than 1 degree.

1. Introduction

Modern geomagnetic measurements in the Republic of Macedonia started in 2002. They were carried out by the Department of Geology and Geophysics at the Faculty of Mining and Geology in Stip in cooperation with the Royal Meteorological Institute – Geomagnetic Observatory in Dourbes, Belgium. A grid of 15 repeat sta-

tions was formed and a site for the future Geomagnetic Observatory in the country was selected.

Within the Tempus Project IB_JEP-17071-2002 “Geomagnetic measurements and quality standards”, during the period from 2003 to 2004, training was carried out for 8 persons (4 for geomagnetic measurements) in the Dourbes Observatory as well as practical measurements in the territory of the Republic of Macedonia. The Tempus Project made it possible for a large number of engineers to learn the issues related to geomagnetic investigations.

In 2002, observing of several repeat stations was carried out in the Republic of Macedonia in order to define the site for the future Geomagnetic Observatory. The repeat stations in Mts. Galicica, Ponikva and Plackovica were studied several times. The analyses of the physical and other parameters indicated that the most appropriate location for the construction of the future Observatory is Mt. Plackovica.

In 2003 a complete survey on 15 repeat stations on Macedonia was performed. The same was done in 2004.

2. Measurements in Macedonia in 2004

In August 2004, measurements of D, I, and F were carried out on the grid of repeat stations (Rasson and Delipetrev, 2004). The names and the geographic coordinates of the 15 repeat stations are given in Table 1, and Fig. 1 shows the map of repeat stations. Measured and calculated components of the geomagnetic field in 2004 and standard deviations are given in Table 2 and Table 3, respectively. Figures 2-5 show maps resulting from these measurements.

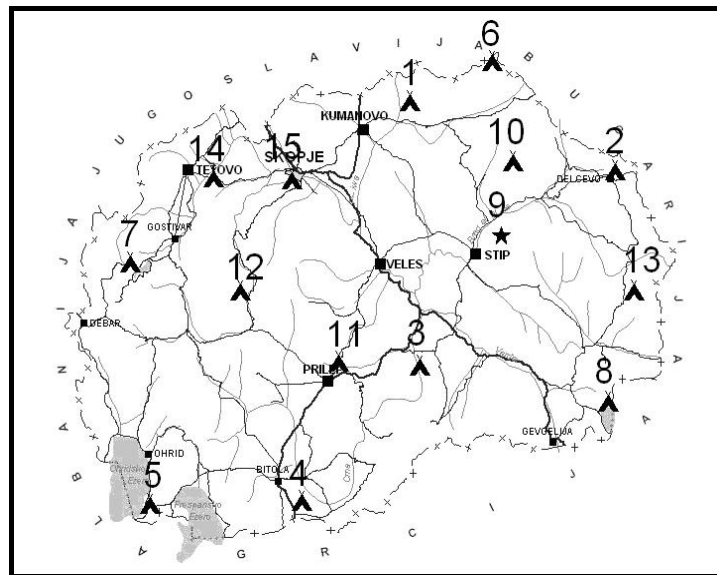


Fig. 1. Map of repeat stations in the Republic of Macedonia.

Table 1
Geographic coordinates of repeat stations

| Repeat station | Geographic latitude | Geographic longitude | Altitude |
|---------------------|---------------------|----------------------|----------|
| Bajlovce | 42° 13' 16" | 21° 55' 17" | 592 m |
| Crna Skala | 41° 59' 41" | 22° 47' 28" | 833 m |
| Gradot Island | 41° 23' 15" | 21° 57' 06" | 317 m |
| Egri | 40° 57' 56" | 21° 26' 54" | 626 m |
| Galicica | 40° 57' 23" | 20° 48' 51" | 1684 m |
| Luke | 42° 20' 39" | 22° 16' 29" | 1180 m |
| Mavrovo | 41° 42' 58" | 20° 43' 38" | 1418 m |
| Nikolic | 41° 15' 54" | 22° 44' 36" | 300 m |
| Plackovica | 41° 47' 41" | 22° 18' 13" | 677 m |
| Ponikva | 42° 01' 35" | 22° 21' 29" | 1618 m |
| Prilep lake | 41° 24' 11" | 21° 36' 32" | 870 m |
| Sv. Marija Precesna | 41° 37' 38" | 21° 11' 36" | 837 m |
| Slivnica | 41° 36' 54" | 22° 51' 46" | 1252 m |
| Tetovo-Zelino | 41° 59' 09" | 21° 04' 46" | 522 m |
| Vodno | 41° 58' 40" | 21° 24' 57" | 569 m |

Table 2
Measured and calculated parameters of the geomagnetic field in 2004

| Repeat Station | D (°) | I (°) | F (nT) | H (nT) | X (nT) | Y (nT) | Z (nT) |
|----------------|-------|--------|---------|---------|---------|--------|---------|
| BAI | 2.997 | 59.269 | 46758.4 | 23893.9 | 23861.3 | 1249.1 | 40192.4 |
| CRN | 3.260 | 58.883 | 46920.4 | 24247.8 | 24208.5 | 1378.9 | 40169.2 |
| EGR | 3.097 | 57.765 | 46430.1 | 24765.7 | 24729.5 | 1338.1 | 39273.6 |
| GAL | 2.955 | 57.694 | 46291.2 | 24740.2 | 24707.3 | 1275.3 | 39125.4 |
| GRA | 3.576 | 58.083 | 46438.4 | 24551.3 | 24503.5 | 1531.3 | 39417.7 |
| LKA | 3.337 | 59.390 | 47036.7 | 23950.4 | 23909.8 | 1394.3 | 40482.4 |
| MVR | 3.058 | 58.577 | 46561.4 | 24275.2 | 24240.6 | 1294.9 | 39732.7 |
| NIK | 3.146 | 58.203 | 46594.8 | 24551.2 | 24514.2 | 1347.3 | 39601.9 |
| PLC | 3.229 | 58.619 | 46679.2 | 24307.0 | 24268.4 | 1369.2 | 39851.3 |
| PON | 2.868 | 58.994 | 46825.7 | 24121.1 | 24090.9 | 1206.7 | 40135.0 |
| PRP | 3.101 | 58.277 | 46665.8 | 24537.7 | 24501.7 | 1327.5 | 39693.8 |

Table 2 (continuation)

| Repeat Station | D (°) | I (°) | F (nT) | H (nT) | X (nT) | Y (nT) | Z (nT) |
|----------------|-------|--------|---------|---------|---------|--------|---------|
| SLI | 3.442 | 58.509 | 46696.9 | 24392.8 | 24348.8 | 1464.5 | 39819.5 |
| SMP | 3.137 | 58.443 | 46562.2 | 24368.2 | 24331.7 | 1333.4 | 39676.5 |
| TET | 3.186 | 58.762 | 46747.1 | 24242.8 | 24205.3 | 1347.4 | 39969.7 |
| VOD | 3.274 | 58.787 | 46740.1 | 24221.5 | 24181.9 | 1383.5 | 39974.5 |

Table 3

Standard deviation

| Repeat Station | | | Standard deviation | | |
|----------------|------|---------------|--------------------|-------|--------|
| No. | Code | Locality | D (°) | I (°) | F (nT) |
| 1. | BAI | BAILOVCE | 0.008 | 0.003 | 2.129 |
| 2. | CRN | CRNA SKALA | 0.015 | 0.006 | 2.696 |
| 3. | EGR | EGRI | 0.011 | 0.002 | 3.257 |
| 4. | GAL | GALICICA | 0.004 | 0.001 | 2.110 |
| 5. | GRA | GRADOT island | 0.018 | 0.004 | 0.918 |
| 6. | LKA | LUKA | 0.011 | 0.002 | 5.794 |
| 7. | MVR | MAVROVO | 0.008 | 0.004 | 0.558 |
| 8. | NIK | NIKOLIC | 0.007 | 0.000 | 2.204 |
| 9. | PLC | PLACKOVICA | 0.007 | 0.003 | 3.754 |
| 10. | PON | PONIKVA | 0.003 | 0.006 | 2.709 |
| 11. | PRP | PRILEP lake | 0.008 | 0.003 | 2.858 |
| 12. | SLI | SLIVNICA | 0.002 | 0.008 | 1.472 |
| 13. | SMP | ST MARIA PRE | 0.010 | 0.004 | 2.956 |
| 14. | TET | TETOVO | 0.001 | 0.002 | 0.401 |
| 15. | VOD | VODNO | 0.011 | 0.002 | 4.386 |

3. Geomagnetic Observatory in the Republic Macedonia in Mt. Plackovica

The Republic of Macedonia does not possess an operating Geomagnetic Observatory. It is important to say that over the past years the Faculty of Mining and Geology worked on a project for establishing a geomagnetic observatory with a net of repeat stations (Delipetrov 1991). The location for the Geomagnetic Observatory was

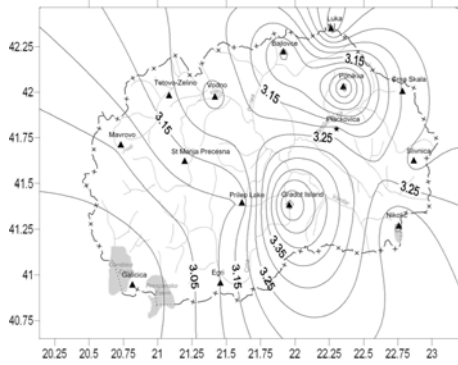


Fig. 2. Map of measured values of declination (in deg) of the geomagnetic field, epoch 2004.5.

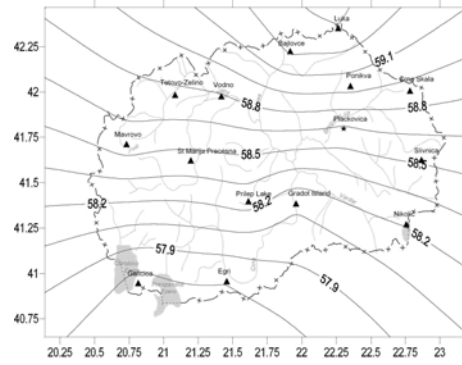


Fig. 3. Map of measured values of inclination (in deg) of the geomagnetic field, epoch 2004.5.

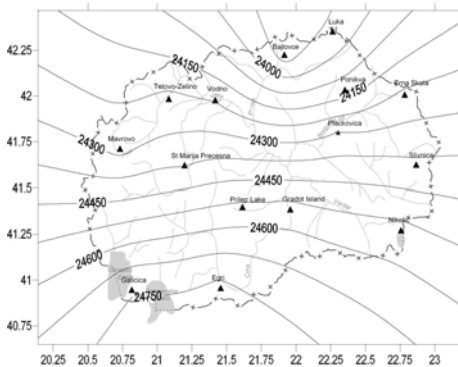


Fig. 4. Map of measured values of horizontal intensity (in nT) of the geomagnetic field, epoch 2004.5.

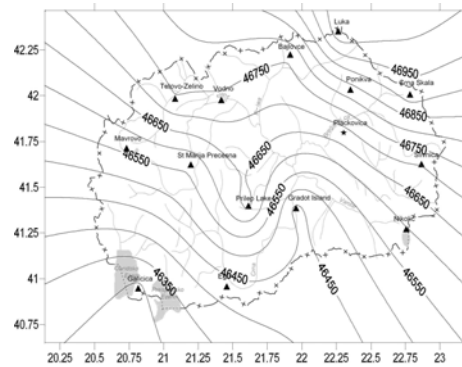


Fig. 5. Map of measured values of total intensity (in nT) of the geomagnetic field, epoch 2004.5.

decided after measurements carried out on the repeat stations network. A detailed geomagnetic map of the terrain was also compiled. Owing to the fact that the population in the area is not dense and the stable gradient of the geomagnetic field, excellent conditions for the operation of the Observatory are provided (Fig. 6).

The implementation of Tempus project under the title “Geomagnetic measurements and quality standards” during the period 2003-2006 intensified the activities for establishing the Geomagnetic Observatory. The following equipment was purchased within the project: Theodolite Zeiss 010 A, Theodolite LEMI 203, and Variometer LEMI 008.

The equipment will be used in the Geomagnetic Observatory and in measurements of the repeat stations network. The equipment is of the highest quality and in accordance with INTERMAGNET standards.



Fig. 6. Satellite image of the terrain of the Geomagnetic Observatory Plackovica.

Parallel to the measurements of the geomagnetic field on the repeat stations network, the following services for the Geomagnetic Observatory at Plackovica (Fig. 7) were completed:

1. The construction site for the Observatory was acquired, the size being 10 hectares. The land was given by the Government of the Republic of Macedonia,
2. A proposal plan for the construction of the Geomagnetic Observatory was developed (Velkovska, 2005), (see Fig. 8),
3. Technical facilities for the staff in the Geomagnetic Observatory (offices, living facilities, sanitation) were constructed,
4. Power supply was installed to the existing facilities,
5. An access road was constructed to the facilities of the Geomagnetic Observatory.

4. Conclusion

Measurements carried out in 2004 on the existing network of repeat stations have been presented in maps (Figs. 2-5). Each component varies within the intervals listed in Table 4.

The Observatory in Plackovica provides good accommodation conditions for the personnel, and currently we are in the stage of constructing absolute and variometer huts.



Fig. 7. Geomagnetic Observatory, Plackovica – implementation carried out so far.

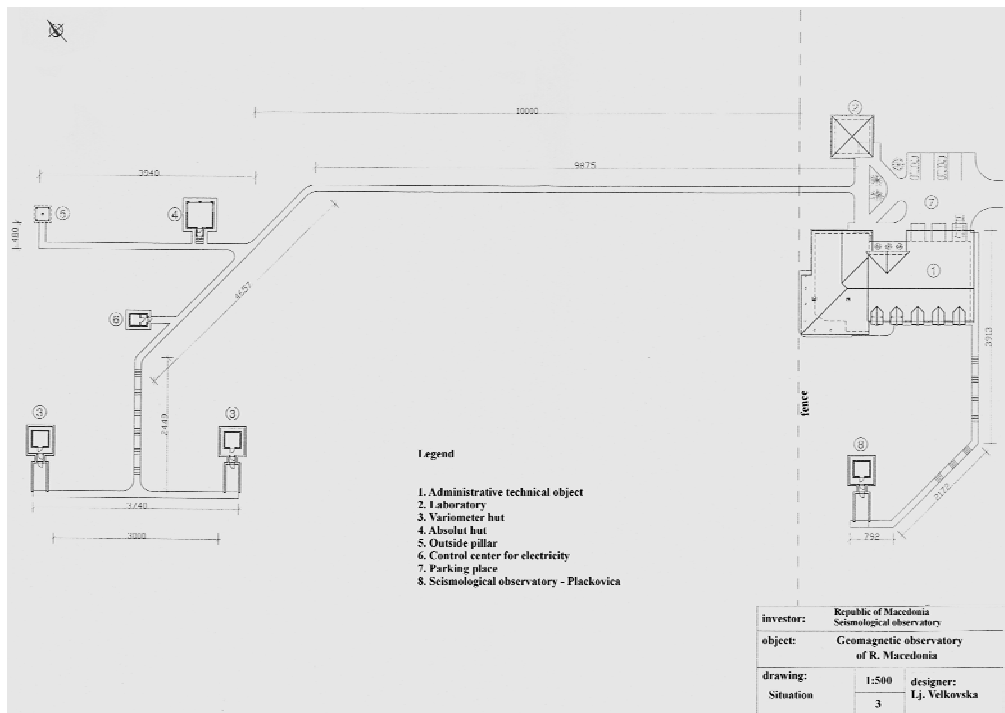


Fig. 8. Schematic plan of the Geomagnetic Observatory Plackovica.

Table 4

Maximum and minimum values of repeat stations

| |
|---|
| $2,868^{\circ} < D < 3,576^{\circ}$ |
| $57,694^{\circ} < I < 59,390^{\circ}$ |
| $46291,2 \text{ nT} < F < 47036,7 \text{ nT}$ |
| $23893,9 \text{ nT} < H < 24765,7 \text{ nT}$ |
| $23861,3 \text{ nT} < X < 24729,5 \text{ nT}$ |
| $1206,7 \text{ nT} < Y < 1531,3 \text{ nT}$ |
| $39125,4 \text{ nT} < Z < 40482,4 \text{ nT}$ |

References

- Delipetrov, T., 1991, Report: “*Establishing geomagnetic observatory in the Republic of Macedonia according to INTERMAGNET standards*”, Stip, R. Macedonia.
- Rasson, L.J., and M. Delipetrov, 2004, *Magnetic Repeat Station Network Description*, Dourbes, Belgium.
- Velkovska, Lj., 2005, *Proposal project for geomagnetic observatory in the Republic of Macedonia, Skopje*, Republic of Macedonia.

Accepted January 22, 2007

Repeat Station Data Reduction Using the CM4 Model

Zedidia ANDRIAMBAHOAKA¹, Jean-Jacques SCHOTT²
and Flavien RANAIVONOMENJANAHARY¹

¹ Institut et Observatoire de Géophysique d'Ambohidempona
BP 3843 Antananarivo Madagascar
e-mails: zedidia_and@yahoo.fr; fnranai@univ-antananarivo.mg

² Ecole et Observatoire des Sciences de la Terre
5 rue Descartes, F-67084 Strasbourg Cedex France
e-mail: JeanJacques.Schott@eost.u-strasbg.fr

Abstract

As an alternative to the commonly used method for the reduction of repeat station data, we have tested the relevance of the CM4 model for removing the external field. The dense network of observatories in Western Europe offers a good opportunity for this study. The prospect, however, is to elaborate a method which could be applied to the repeat station network of Madagascar, where only one observatory is available and the distance to the remotest repeat station is about 800 km.

1. Introduction

This study aims at improving the method of data reduction of repeat stations with application to the network of Madagascar. With the help of a nearby reference observatory, the classical method (Newitt *et al.* 1996) is based on the assumption that the transient variations of the magnetic field are identical at both the repeat station and the observatory. Under this assumption, the annual mean of the field at the repeat station S , centered on the date t of the measurement, is derived from the annual mean at the observatory O for the same time span by the equation:

$$\bar{\bar{B}}(S,t) = \bar{\bar{B}}(O,t) + (\bar{B}(S,t) - \bar{B}(O,t)) \quad (1)$$

The overhead bar stands for mean values, in this case, annual means. The error involved in the assumption of transient variation uniformity is difficult to assess. In addition, bearing in mind that a repeat station network is mainly devoted to internal field surveying, this simple method of reduction does not completely eliminate the external

field. Indeed, it is well known that annual means are still contaminated by long term external contributions which may be significant (i.e., Gavoret *et al.* 1986).

In an attempt to circumvent the drawbacks of the standard method, we have tried to model the external contributions by means of the comprehensive CM4 model (Sabaka *et al.* 2002, 2004) and to find out a formulae which could express the external field at any repeat station in an area around the reference observatory.

2. External Field Modeling

2.1 Preliminary

In order to validate the method, we have taken advantage of the dense observatory network in Europe. We have selected a set of observatories where data are available for the period 1993-2004. The observatory of Budkov (BDV), which is located in a more or less central position, has been chosen as reference observatory. The observatories THY, CLF, FUR, NCK, HRB, NGK, SUA play the role of repeat stations (Fig. 1a). Figure 1b displays an estimate of the error inherent to the classical method of reduction. The error is defined as the r.m.s. of $G(O,t) - G(S,t)$, after removal of the secular variation (fitted by a parabolic function of time). G stands for X, Y, or Z hourly means, O is the reference observatory, and S is one of the observatories of the set mentioned above. X, Y and Z are the field components in the geographical reference frame. As expected, the error increases with the distance to the reference observatory. In this example, it is about $5 \cdot 10^{-3}$ nT/km for X, $4 \cdot 10^{-3}$ nT/km for Y and $4 \cdot 10^{-3}$ nT/km for Z. (As a matter of comparison, the distance between TAN and the farthest repeat station of the network of Madagascar is about 800 km).

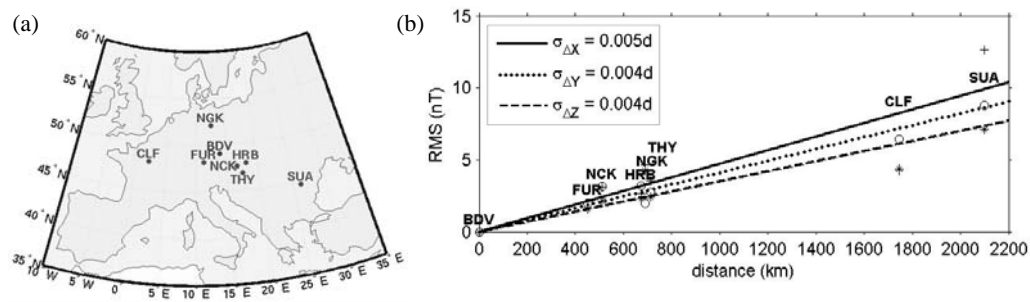


Fig. 1. (a) Location of the reference observatory (BDV) and the set of observatories used as repeat stations. (b) R.m.s. misfit of the hourly means (second term of right-hand side of Eq. 1) as a function of distance to the reference observatory, for the field components X (crosses), Y (circles), Z (stars), respectively.

2.2 Problem setting

The modeling outlined below deals with hourly means, in order to be consistent with the CM4 modeling. Figure 2 shows that, in the case of TAN observatory in par-

ticular, the CM4 model yields only a first approximation. In order to improve the modeling, we have to add second order terms. At the reference observatory, we suggest to model the field by the following equation:

$$\begin{aligned} \vec{B}(O, h) = & \vec{B}_{i,CM4}(O, h) + \vec{b}_i(O) + \delta\vec{B}_i(O, h) + \vec{B}_{e,CM4}(O, h) + \dots \\ & \vec{b}_e(O, h) + \delta\vec{B}_{e,CM4}(O, h), \end{aligned} \quad (2)$$

where $\mathbf{B}(O, h)$ is the field measured at the reference observatory O (internal plus external); $\mathbf{B}_{i,CM4}(O, h)$ is the internal field given by the CM4 model at O ; $\mathbf{b}_i(O)$ is the bias field (various estimates of these bias fields have been published, i.e. Manda and Langlais, 2002; however, for the sake of consistency, the bias fields computed by CM4 have been adopted); $\delta\mathbf{B}_i(O, h)$ is the secular variation not modelled by CM4; $\mathbf{B}_{e,CM4}(O, h)$ is the external field given by CM4; $\mathbf{b}_e(O, h)$ is the long-term external field not modelled by CM4; $\delta\mathbf{B}_{e,CM4}(O, h)$ is the short-term external field not modelled by CM4.

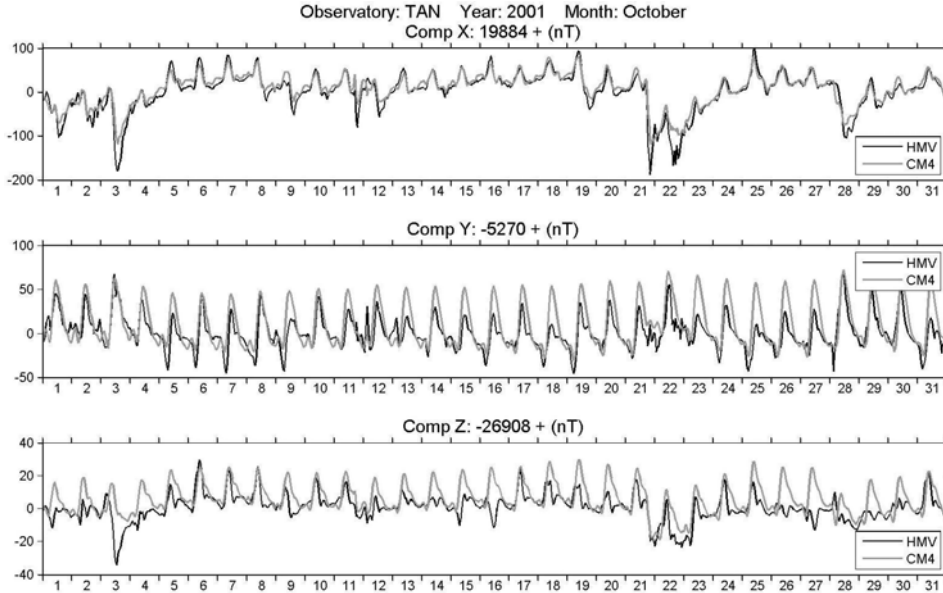


Fig. 2. Comparison of the hourly mean values (HMV) for TAN observatory and the modeling provided by the CM4 model for the month October 2001.

Let us define the residual field $\rho(O, h)$ by:

$$\begin{aligned} \vec{\rho}(O, h) = & \delta\vec{B}_i(O, h) + \vec{b}_e(O, h) + \delta\vec{B}_{e,CM4}(O, h) \\ = & \vec{B}(O, h) - \vec{B}_{i,CM4}(O, h) - \vec{B}_{e,CM4}(O, h) - \vec{b}_i(O), \end{aligned} \quad (3)$$

where h stands for the time expressed in hours.

With respect to the aim of this study, terms $\mathbf{b}_e(O, h)$ and $\delta\mathbf{B}_{e,CM4}(O, h)$ are our main concern. In particular, we would like to construct $\delta\mathbf{B}_{e,CM4}(O, h)$ in such a way

that it is a stationary signal with annual zero mean. Figure 3 shows the distribution of $\rho(O, h)$ for the year 2001. Although the distribution may not be symmetrical (i.e. its mode different from its mean), the mean turns out to be the most robust measure of location. As $\delta\mathbf{B}_i(O, h)$ and $\mathbf{b}_e(O, h)$ vary smoothly with time, the distribution reflects mainly the statistical properties of $\delta\mathbf{B}_{e,CM4}(O, h)$.

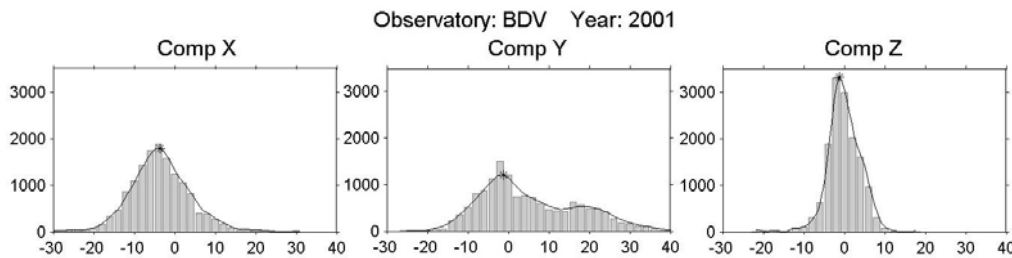


Fig. 3. Distribution of the hourly residual ρ in nT (Eq. 3) for each component and for the year 2001.

2.3 Residual secular variation and long-term external variations

Let $\bar{\rho}(O, h)$ be the running mean value of $\rho(O, h)$ over one year centered on h . Following Gavoret *et al.* (1986) we model the long term external variations using night time values in order to exclude most of the solar daily variation contribution. This selection is clearly equally valid for the identification of $\delta\mathbf{B}_i$. With the constraint $\delta\bar{\mathbf{B}}_{e,CM4}(O, h) = 0$, Eq. 3 leads to:

$$\bar{\rho}(O, h) = \delta\bar{\mathbf{B}}_i(O, h) + \bar{\mathbf{b}}_e(O, h). \quad (4)$$

Figure 4b shows for each component X, Y, Z, the variation of $\bar{\rho}(O, h)$ over the period 1994-2004.

We have now to model $\delta\bar{\mathbf{B}}_i(O, h)$ and $\bar{\mathbf{b}}_e(O, h)$. In the *CM4* model, the secular variation is modelled with a set of *B*-splines constructed with equispaced knots at 2.5 year intervals. Over the time span 1993-2004, it may equally well modelled with orthogonal polynomials. Thus, the *CM4* internal field may be represented by:

$$\vec{B}_{i,CM4}(O, t) = \sum_{k=0}^{K-1} \vec{a}_k P_k(t). \quad (5)$$

The coefficients \mathbf{a}_k may be computed by a simple least-squares regression using the true *CM4* internal field as data. The regression yields estimates of \mathbf{a}_k as well as a covariance matrix.

$\delta\mathbf{B}_i(O, h)$ may be considered as a perturbation of $\mathbf{B}_{i,CM4}(O, h)$ likewise modelled with orthogonal polynomials restricted to low degrees. Accordingly, $\delta\bar{\mathbf{B}}_i(O, h)$ will be modelled with orthogonal polynomials. Their a priori coefficients \vec{a}_k^0 as well as a covariance matrix may be derived from the corresponding parameters of $\delta\mathbf{B}_i(O, h)$.

According to Gavoret *et al.* (1986), we tentatively model $\bar{b}_e(O, h)$ (which, according to its definition, is close to $\mathbf{b}_e(O, h)$) as a function of time proportional to some index of geomagnetic activity or solar-terrestrial conditions. It turns out that the Wolf numbers are the most appropriate. Finally, $\bar{\rho}(O, h)$ is modelled by the equation:

$$\bar{\rho}(O, h) = \bar{\alpha}\bar{R}(h) + \sum_{k=0}^{K'-1} \bar{a}_k P_k(h) \quad (6)$$

where $\bar{R}(h)$ is interpolated from its smooth monthly values by interpolating splines.

The parameters $\bar{\alpha}$ and \bar{a}_k are estimated by stochastic inversion. Figure 4b shows the model of $\bar{\rho}(O, h)$ computed according to Eq. (6).

2.4 Residual short-term external field

Having modelled $\delta\mathbf{B}_e(O, h)$ and $\mathbf{b}_e(O, h)$, we may return to Eq. (2), where the last unknown term is $\delta\mathbf{B}_{e,CM4}(O, h)$. $\delta\mathbf{B}_{e,CM4}(O, h)$ is assumed to be a small perturbation of the *CM4* external field model. Of the a priori parameters involved in the *CM4* modelling (conductivity model, solar flux $F_{10.7}$, Dst index), it turns out that the most easy to handle is Dst. Figure 4a shows that it is possible to fit exactly $\delta\mathbf{b}_{e,CM4}(O, h)$ by

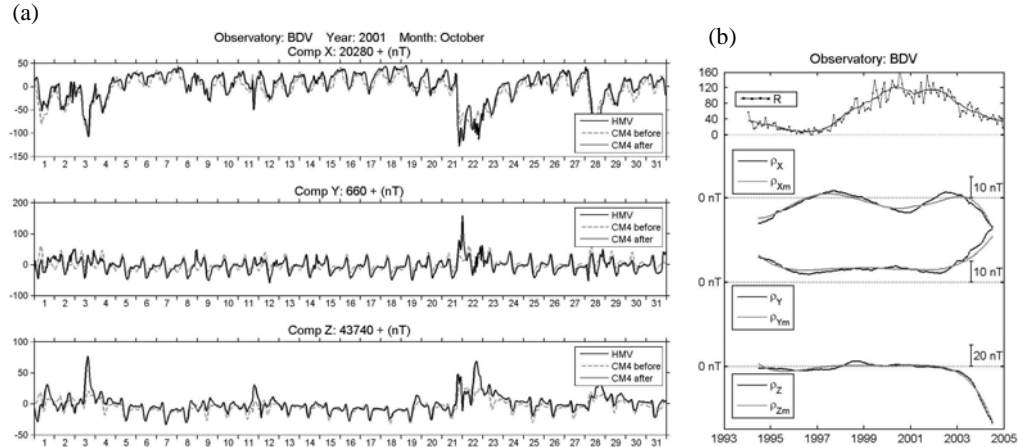


Fig. 4. (a) Example of exact modeling of $\delta\mathbf{B}_{e,CM4}(O, h)$ (Eq. 8) using hourly perturbations of the Dst index as adjustment parameter. Hourly mean data are for BDV observatory, in October 2001. See text for further explanation; (b) Black curves: variation of the running yearly mean value of ρ (Eq. 4) for each component X, Y, Z over the time span 1994-2004. Grey curves: modeling of ρ using Eq. (6).

a slight change δD_{st} of D_{st} (of course, δD_{st} has no longer the meaning of a geomagnetic index). On Fig. 4a, the adjusted curves cannot be distinguished from the actual ones. According to its definition, the field $\delta\mathbf{B}_{e,CM4}$ has a zero annual running mean. Let us recall that in the *CM4* model, D_{st} parameterizes only the dipolar term of the magnetospheric field.

Having computed, at the reference observatory, the perturbation δD_{st} required to obtain the best fit of $\delta \mathbf{B}_{e,CM4}(O, h)$, it is obvious to compute the same field $\delta \mathbf{B}_{e,CM4}(S, h)$ at any station S by the incorporation of δD_{st} into the $CM4$ external field model. Finally, our model for the external field is:

$$\vec{B}_e(S, h) = \vec{B}_{e,CM4}(S, h) + \delta \vec{B}_{e,CM4}(S, h) + \vec{b}_e(S, h). \quad (7)$$

The last step is the computation of $\mathbf{b}_e(S, h)$, which, at the moment, is only known at the reference observatory. We may assume that $\mathbf{b}_e(S, h)$ is the gradient of a time varying external magnetic potential. $\mathbf{b}_e(S, h)$ being known at only one point, only the dipolar term can be resolved unambiguously. Thus, we derive $\vec{b}_e(S, h)$ from the equation

$$\vec{b}_e(S, h) = -\overline{grad} \left[\frac{r}{a} (g_{e,1}^0(h) \cos \theta + g_{e,1}^1(h) \sin \theta \cos \varphi + h_{e,1}^1(h) \sin \theta \sin \varphi) \right]. \quad (8)$$

The Gauss coefficients $g_{e,1}^0$, $g_{e,1}^1$, $h_{e,1}^1$ may be easily derived from $\mathbf{B}_e(O, h)$ by standard computations taking into account the reference frame change from geodetic to geocentric.

3. Example and Discussion

Equation (7) yields the proposed formulae for the removal of the external field at any repeat station S . It is valid only within some area around the reference observatory. We may check its validity by comparison with the standard method. Figure 5a shows, for the year 2001, the ‘‘internal’’ field computed at CLF by means of the reduction equation:

$$\vec{B}_i(S, h) = \vec{B}(S, h) - \vec{B}_e(S, h) \quad (9)$$

where $\mathbf{B}_e(S, h)$ is computed with Eq. (7) as compared to $\mathbf{B}_i(S, h)$ computed with Eq. (1). The noisy pattern accounts for the imperfect removal of the external contribution. We observe an improvement on component Y only. The most conspicuous result is the nearly 20 nT difference in the X and Z components. This difference is not constant in time as shown in Fig. 5b where the monthly mean of the difference is displayed. Figure 6 is similar to Fig. 1a. It shows that the r.m.s. of the dispersion around a parabolic fit is nearly the same as for the standard method.

Despite the rather modest improvement in the scattering of the ‘‘internal’’ field, Fig. 5 shows, to our mind, an important, although well-known result: the annual mean rather imperfectly represents the internal field because it is still significantly contaminated by field of external origin. The $CM4$ -based modeling differs from the classical reduction of external field by a fluctuating non zero field. The fluctuations may account for the persistence of a long-term external component (Gavoret *et al.* 1986).

Improvements of this modeling which is a first order perturbation of the $CM4$ model can be easily imagined mainly along two lines. The first one would be to allow slight changes of the Gauss coefficients for the ionospheric field (Sabaka *et al.* 2002). around their $CM4$ values. The second would be to consider small changes of the conductivity model, which is valid essentially for Europe, in order to make the induced

part of the ionospheric field more flexible. Both improvements would require a deep scrutiny of the $CM4$ model. In a recent paper, Olsen *et al.* (2005) suggest to split up the D_{st} index into an external and internal part. Although this new parameterization partly overlaps our empirical perturbation δD_{st} , it could balance or constrain changes of the ionospheric field. Improvements should also take into account the spatial distribution of the field $\mathbf{b}_e(S, h)$. The dipolar approximation is prescribed by the field being known at the reference observatory only. Although we believe that its geometry is simple, a worldwide analysis of observatory data could perhaps help to refine its description.

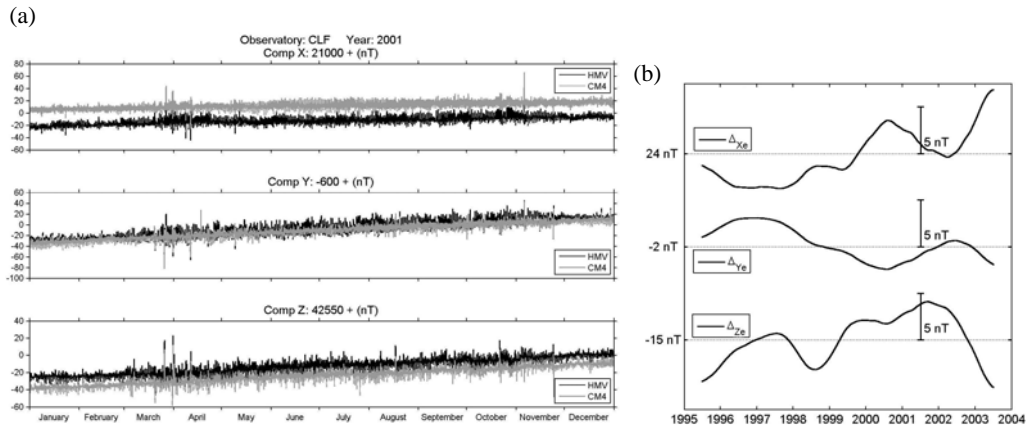


Fig. 5. (a) “Internal” field computed at CLF using Eq. (9) (curves labelled $CM4$) compared to the estimate given by Eq. (1) (curves labelled HMV); (b) Monthly mean of the difference ($CM4$ modeling) – (HMV modeling) over the interval 1995-2004. The curves show that the difference is a function of time.

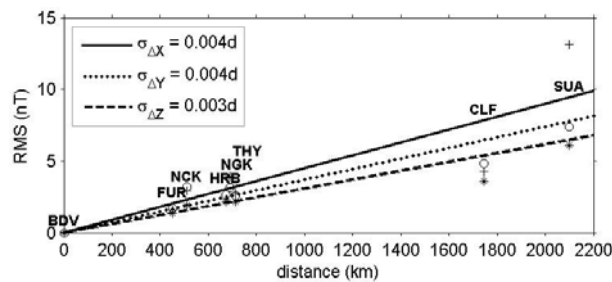


Fig. 6. R.m.s. misfit of the hourly means modelled by Eq. (9) as a function of distance to the reference observatory, for the field components X, Y, Z respectively. Same legend as Fig. 1 which it has to be compared to.

The last step, not considered here, would be to model field variation on the one-minute scale, which is more appropriate for the reduction of repeat station data. However, this step in the reduction process would be less critical either if the survey would

be carried out outside the main part of the daily variation, and during quiet days, or if the field variations would be recorded for a short time with a portable variometer.

4. Conclusions

The first order *CM4* model complemented by some second order terms derived from the analysis of the magnetic field variation at the reference observatory provides a promising tool for data reduction at the repeat stations. On one hand, with the second order modeling carried out in this study, its accuracy is only similar to the one of the standard method using a reference observatory. But, on the other hand, improvements of the external field modeling may be imagined, and may benefit from improvements of the *CM4* model or the like. The most conspicuous result is the mean difference between the “internal” field yielded by this method and the “internal” field (i.e. the annual mean) given by the standard method. The validation of the former with respect to the latter requires, however, further investigations. Finally, we have not tried to further reduce the field of the “repeat” stations to a common epoch. This should not be a serious drawback as regional modeling, like global modeling, can easily take into account measurements performed at different times.

References

- Gavoret, J., D. Gibert, M. Menvielle and J.L. Le Mouel, 1986, *Long-term variations of the external and internal components of the Earth's magnetic field*, Jour. Geophys. Res. **91**, B5, 4787-4796.
- Mandea, M., and B. Langlais, 2002, *Observatory crustal magnetic biases during MAGSAT and Oersted satellite missions*, Geophys. Res. Lett. **29**, 10.1029 2001 GLO13693.
- Newitt, L.R., C.E. Barton and J. Bitterly, 1996, *Guide for magnetic repeat station surveys*, IAGA ed., Working Group V-8, 114pp.
- Olsen, N., T.J. Sabaka and F. Lowes, 2005, *New parameterization of external and induced fields in geomagnetic field modeling, and a candidate model for IGRF 2005*, Earth Planets Space **57**, 1141-1149.
- Sabaka, T.J., N. Olsen and R.A. Langel, 2002, *A comprehensive model of the quiet-time, near-Earth magnetic field: phase 3*, Geophys. J. Int. **151**, 32-68.
- Sabaka, T.J., N. Olsen and M.E. Purucker, 2004, *Extending comprehensive models of the Earth's magnetic field with Oersted and CHAMP data*, Geophys. J. Int. **159**, 521-547.

Accepted January 22, 2007

Report on Activities and Plans of MagNetE – the Group for European Repeat Station Surveys

Gerald DUMA

Central Institute for Meteorology and Geodynamics
Hohe Warte 38, A-1190 Vienna, Austria
e-mail: gerald.duma@zamg.ac.at

In February 2003, scientists from 20 European countries followed an invitation to join a novel initiative: the first workshop on European Geomagnetic Repeat Stations, to be held at the Adolf Schmidt-Observatory for Geomagnetism in Niemegk, Germany. The objective of this workshop was to coordinate the effort of more homogeneous surveys in Europe. So far, geomagnetic measurement campaigns in many countries were performed not as a concerted action but differed with respect to the survey time, the interval of repeat measurements, the station density and measurement techniques. In order to perform detailed studies on the European geomagnetic field and its variations and to compile geomagnetic maps on a wider scale, with high accuracy, it was required to homogenize the measurements.

The 2003 workshop resulted in very detailed recommendations for European Magnetic Repeat Station Surveys, aiming at the goal to acquire geomagnetic data of highest possible quality for research purposes. Another outcome of the workshop was to start repeat measurements already in 2004 according to the concept of a common European Survey and to provide a first homogeneous geomagnetic data set at an European scale.

During the IUGG Meeting 2003 in Sapporo, Japan, the new initiative of coordinated European surveys was also well recognized by the IAGA, Division V, leading to IAGA Resolution #4.

The interest in this scientific topic is shared by most of the national geomagnetic institutions in European countries. The second workshop on repeat surveys, this time hosted by the Institute of Geodesy and Cartography in Warsaw, was conducted with an even higher number of participants of 20 countries, in April 2005. Again, reports

on recent measurement activities in their countries were given by the participants and many scientific details were addressed concerning the most appropriate strategy to acquire good repeat measurement results. Another important task was how to make repeat station data available to the scientific community. The option to extend the existing data base at the WDC Edinburgh seemed acceptable to many participants. It was also discussed, that error estimates should be given for any data at the WDC, and possibly an additional classification scheme for the quality of repeat station data should be introduced.

During the workshop 2005 it was also decided to entitle the initiative of common European surveys and data acquisition by the acronym MagNetE – Magnetic Network in Europe – also reminding of William Gilberts famous 17th century latin book “De Magnete”. Finally, the representative of Romania kindly offered to host the next MagNetE workshop in 2007.

Accepted February 9, 2007

On Separation of the Secular Variations of Different Origins

Yuri SUMARUK

Institute of Geophysics NASU
Lviv Magnetic Observatory, Ukraine
e-mail: sumar@mail.lviv.ua

Abstract

Secular variations (SV) are a complex phenomenon in time and space. The main origin of SV is inside the Earth. But SVs are complicated by external sources such as variations due to the magnetospheric and ionospheric currents and also by currents induced in the crust. There is an anticorrelation between the time changes of SVs and geomagnetic activity. Especially, one can see it on short period (one year) SV changes of the horizontal component of the geomagnetic field ($\Delta SV(H)$). If we express geomagnetic activity by means of some geomagnetic index, as, e.g., K_p , we can derive a linear regression equation between $\Delta SV(H)$ and $\Delta \Sigma K_p$, where $\Delta \Sigma K_p$ is the difference between mean yearly values of K_p . Usually the correlation coefficient between these values does not exceed 0.4-0.6. The sensitivity of $\Delta SV(H)$ to $\Delta \Sigma K_p$ for individual observatories varies. For European observatories the highest sensitivity exists for the Surlari magnetic observatory.

By subtracting $\Delta SV(H)$ dependent on $\Delta \Sigma K_p$ from $\Delta SV(H)$, we obtain $\Delta SV_1(H)$ independent of magnetic activity. The resulting $SV_1(H)$ at observatories of the northern hemisphere of the Earth appear to be in accordance with a quasi-sinusoidal law. The period of the quasi-sinusoids is about 78-80 years. The mean-per-cycle Wolf numbers of solar activity show the same changes. This means that by subtracting these long period variation from $\Delta SV_1(H)$, we can find out the SV variation independent of the geomagnetic and solar activity ($\Delta SV_2(H)$).

It is interesting to note that the zero isoline of such $\Delta SV_2(H)$ passes through regions of intense tectonic activity.

Key words: secular variations, external sources.

The separation of external sources of SV allows to use the remainder for investigations of the Earth's interior. The most informative component of the geomagnetic field with regard to changes of external sources is H.

We have derived the differences between mean year values of H (SV(H)) (Golovkov *et al.* 1983, Golovkov *et al.* 1984-1989, Golovkov and Dimant 1990) for nine European magnetic observatories (COI, VAL, CLF, STO, HAD, NGK, SUA, WIT, LVV) and also five Asian observatories (SVD, IRT, YSS, MGD, VLA) for almost 100 years. To investigate the dependence SV(H) on magnetic activity, the second differences ($\Delta SV(H)$) between SV(H) of successive years were calculated. As measure for magnetic activity changes there has been chosen $\Delta \Sigma K_p$, i.e. differences between successive mean yearly values of ΣK_p (ΣK_p is the daily sum of K_p). The correlation coefficient between $\Delta SV(H)$ and ΣK_p has been derived for every individual observatory. Usually the correlation coefficients did not exceed 0.4-0.6, their dispersion being 0.13. The sensitivities of $\Delta SV(H)$ to $\Delta \Sigma K_p$ for different observatories vary. The highest sensitivity exists for Surlari magnetic observatory.

Figure 1 shows the dependence of $\Delta SV(H)$ on $\Delta \Sigma K_p$ for mean European and mean Asian observatories. Two straight lines reflect the regression equations which connected $\Delta SV(H)$ and $\Delta \Sigma K_p$ according to the correlation coefficients.

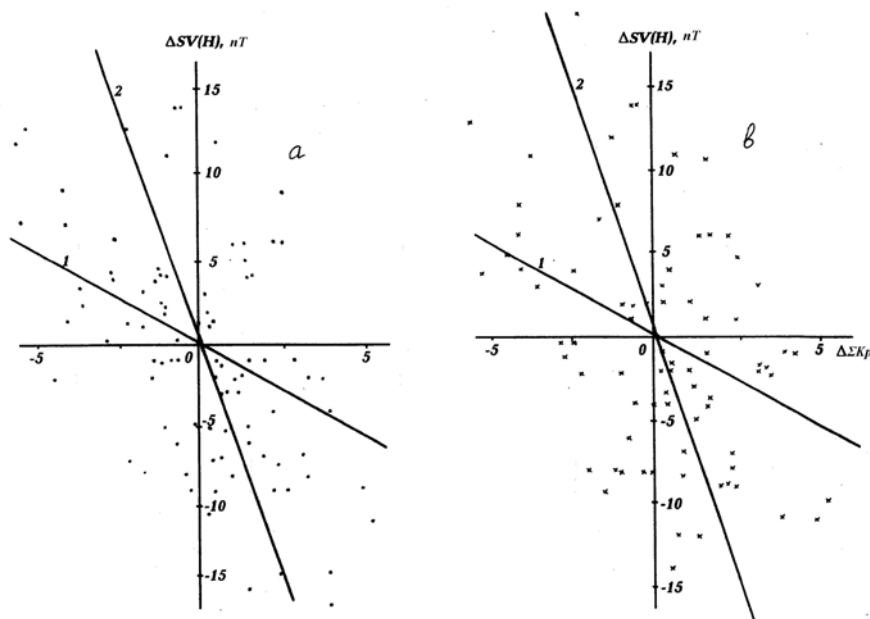


Fig. 1. Dependence of $\Delta SV(H)$ on $\Delta \Sigma K_p$ for European (a) and Asian (b) observatories.

Figure 2 represents the same dependence of $\Delta SV(H)$ on $\Delta \Sigma K_p$ for magnetic observatory Tangerang ($\varphi = -06.17^0$; $\lambda = 106.63^0$). This observatory has a long series of observations and is placed near the zero line of SV(H). The correlation coefficient between $\Delta SV(H)$ and $\Delta \Sigma K_p$ is $r = -0.61 \pm 0.08$ and the sensitivity of $\Delta SV(H)$ to changes $\Delta \Sigma K_p$ is almost one order of magnitude higher than for European or Asian observatories.

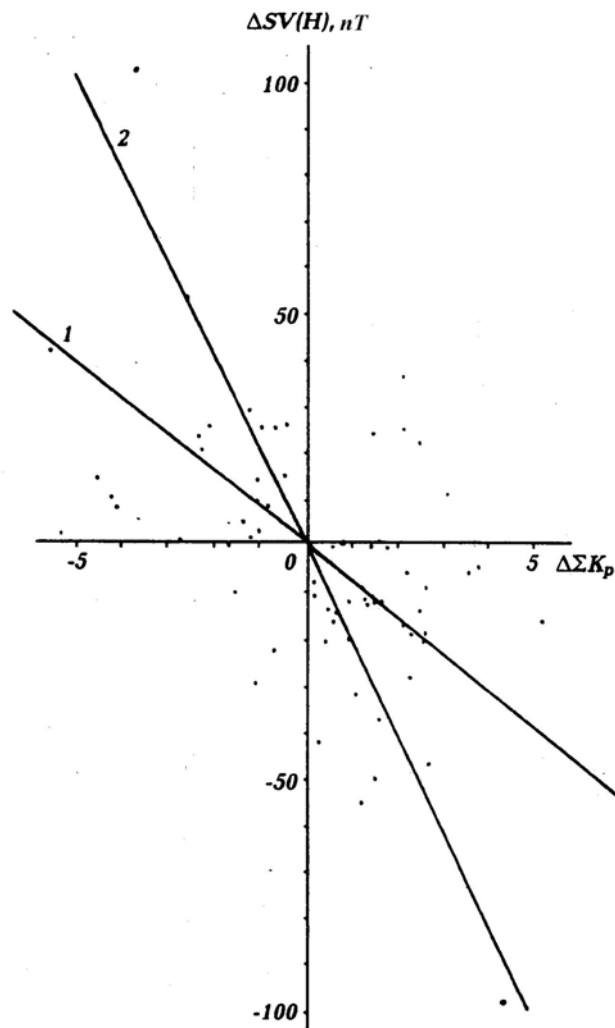


Fig. 2. Dependence of $\Delta SV(H)$ on $\Delta \Sigma K_p$ for Tangerang magnetic observatory.

Figure 3 presents sensitivities of the SV European observatories to the changes of magnetic activity. The sensitivity increases from eastern to western observatories. The dotted curves are isolines of sensitivity.

Table 1 shows correlation coefficients and linear regression equations between $\Delta SV(H)$ and $\Delta \Sigma K_p$. The right column is the sensitivity of $\Delta SV(H)$ to changes $\Delta \Sigma K_p$. Thus it is possible to calculate a correction to $SV(H)$ due to the changes of magnetic activity. By subtracting $\Delta SV(H)$ from $SV(H)$ we obtain $SV_1(H)$ independent of magnetic activity.

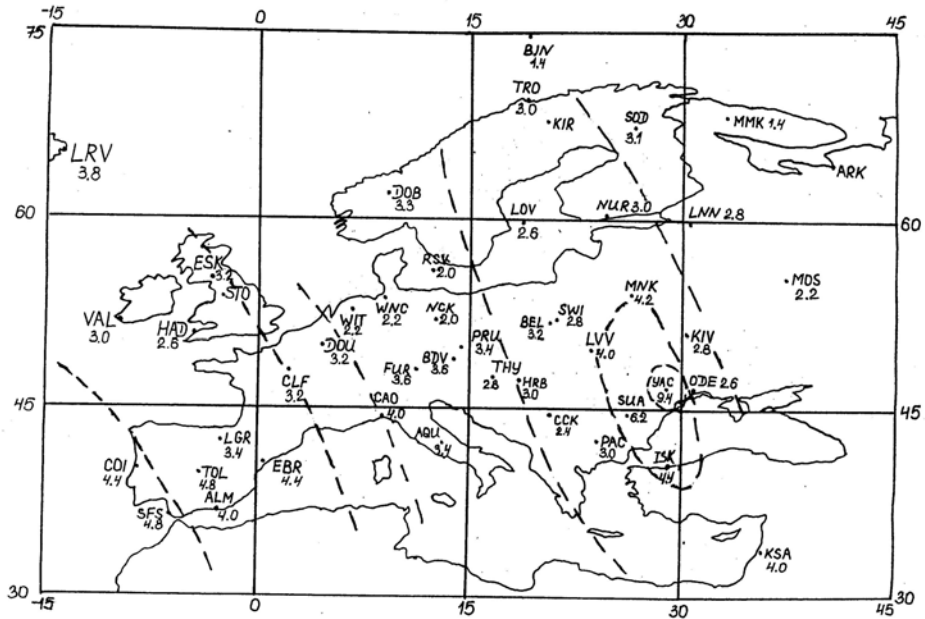


Fig. 3. Sensitivity of European observatories to changes of magnetic activity.

Table 1

Correlation coefficients and regression equations between $\Delta SV(H)$ and $\Delta \Sigma K_p$

| Observatory | r_1 | σ_1 | $\Delta SV(H)$ | r_2 | σ_2 | $\Delta \Sigma K_p$ | ε |
|---------------|-------|------------|--|-------|------------|-----------------------------------|---------------|
| European row | -0.51 | 0.08 | $(-1.44 \pm 0.22)^* \Delta \Sigma K_p$ | -0.50 | 0.08 | $(-0.17 \pm 0.03)^* \Delta SV(H)$ | 2.6 |
| Asian row | -0.40 | 0.10 | $(-1.14 \pm 0.20)^* \Delta \Sigma K_p$ | -0.36 | 0.10 | $(-0.13 \pm 0.03)^* \Delta SV(H)$ | 2.5 |
| Tangerang | -0.60 | 0.08 | $(-7.68 \pm 1.02)^* \Delta \Sigma K_p$ | -0.61 | 0.08 | $(-0.05 \pm 0.01)^* \Delta SV(H)$ | 11.6 |
| Frederickburg | -0.40 | 0.11 | $(-1.20 \pm 0.30)^* \Delta \Sigma K_p$ | -0.37 | 0.11 | $(-0.12 \pm 0.04)^* \Delta SV(H)$ | 2.8 |
| Tucson | -0.60 | 0.08 | $(-2.00 \pm 0.30)^* \Delta \Sigma K_p$ | -0.55 | 0.13 | $(-0.16 \pm 0.04)^* \Delta SV(H)$ | 3.2 |

Figure 4 shows these corrected $SV_1(H)$ for two observatories WIT (middle) and IRT (bottom). The upper curve shows the mean yearly Wolf numbers for 13-20 solar cycles. Mean-per-cycle Wolf numbers and $SV_1(H)$ are shown by horizontal thick lines. Wittweeen and Irkutsk observatories were chosen because the difference of their lon-

gitudes amounts to 98° and because they have long series of data. The vertical dotted lines connect the maxima-per-cycles Wolf numbers with crossing points between mean $SV_1(H)$ values and the curve of $SV_1(H)$. As one may see, the points divide the curve $SV_1(H)$ in two parts. The first part corresponds to the rising phase of the Wolf numbers and the second one to its decreasing phase. At most cycles, the increasing (decreasing) phase coincides with a decreasing (increasing) of $SV_1(H)$, which is also a reversal dependence. The phenomenon may be explained in the same way as above for short period variations.

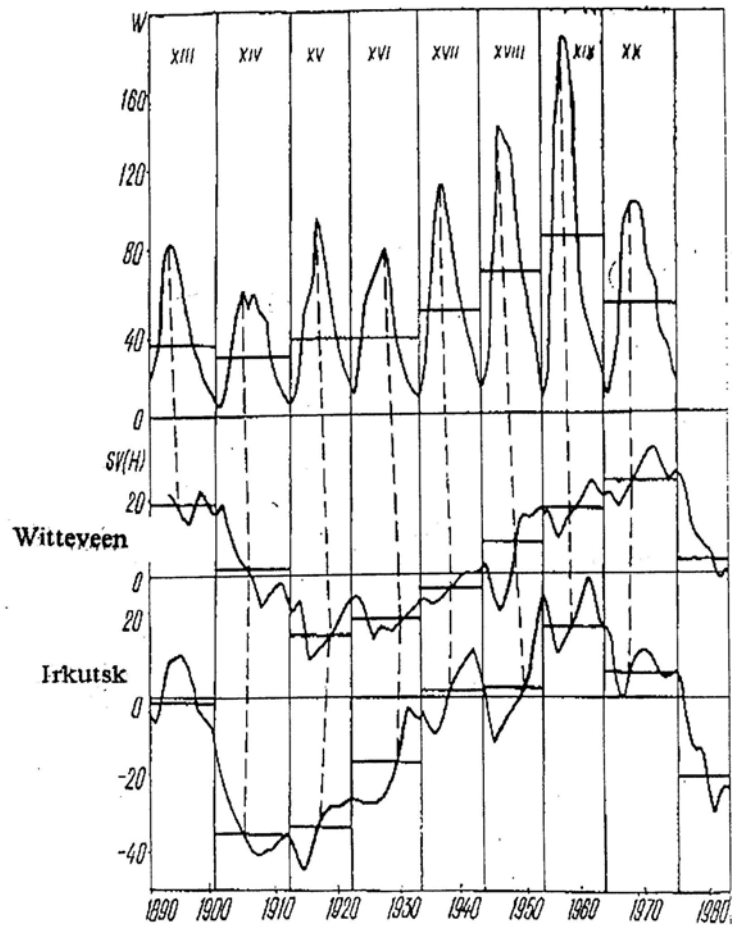


Fig. 4. Corrected $SV_1(H)$ for Witteveen and Irkutsk. See text for details.

To exclude these variations, the mean-per-cycle values were calculated. The resulting values $\Delta SV_2(H)$ at all observatories of the northern hemisphere of the Earth appear to be in accordance with a quasi-sinusoidal law. The period of the quasi-sinusoid is about 78-80 years. The mean-per-cycle Wolf numbers of solar activity show the same changes.

It may be supposed that these events correlate. The main problem is to choose the zero level of the variations. At all observatories the variations should coincide in phase. By means of such an assumption we have received dates of sign changes of the sinusoids at every observatory. An example of such a determination is shown in Fig. 5 for several observatories. The zero transition of the $\Delta SV_2(H)$ variations of the 78-80 year period were observed at approximately 1902-1905, 1947-1949, and 1980-1982 (in Fig. 5 shown by vertical lines). In Fig. 5 corrections were not introduced on short-period SV variations. The horizontal dotted lines show the value of the $\Delta SV_2(H)$ variations independent of external sources.

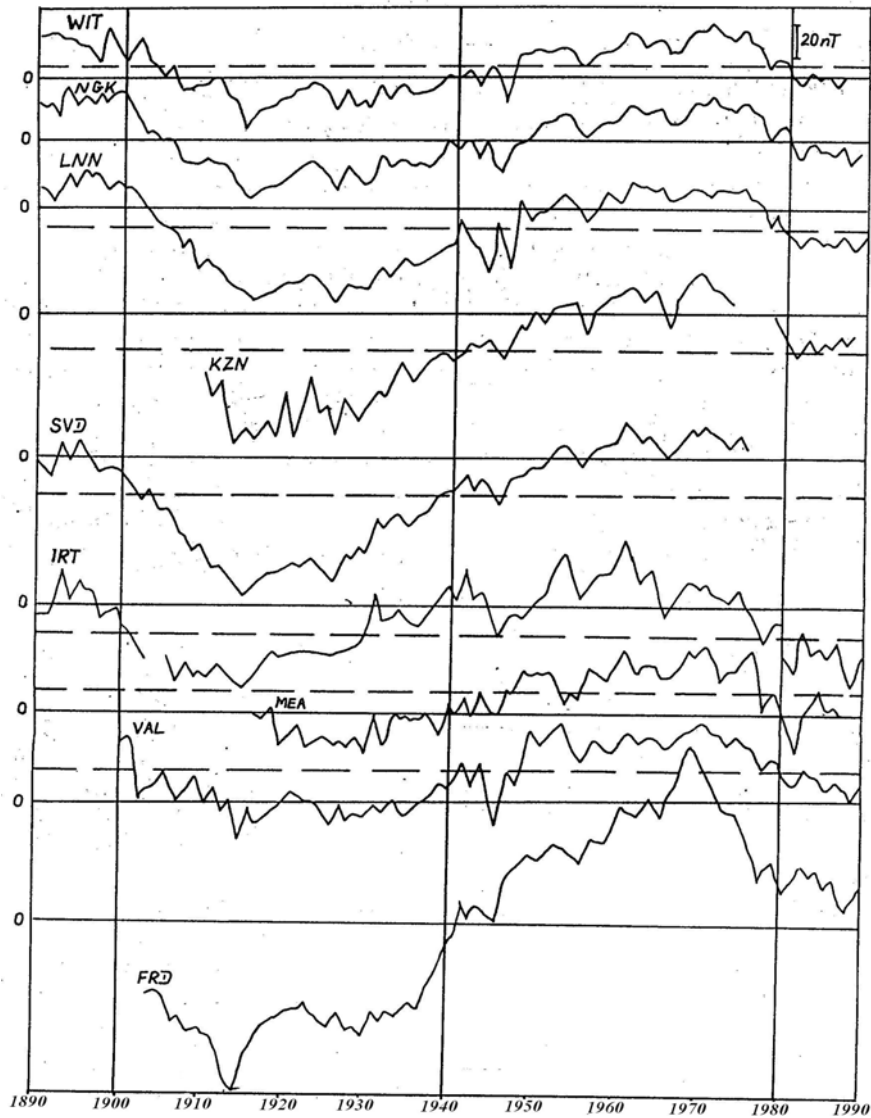


Fig. 5. $\Delta SV_2(H)$ variations at observatories of the northern hemisphere.

Figure 6 shows zero isolines of $\Delta SV_2(H)$ variations. Figures near names of observatories signify the value of $\Delta SV_2(H)$. Zero isolines pass through regions of intense tectonic activity, and they surround regions of positive $\Delta SV_2(H)$ at middle latitudes of the Earth's northern hemisphere.

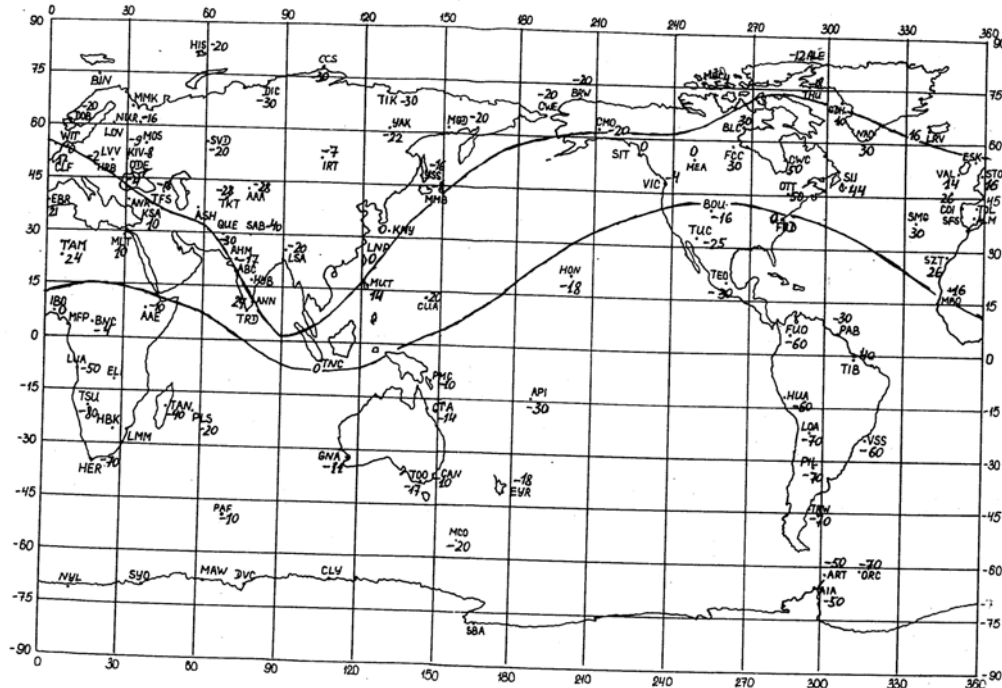


Fig. 6. Zero isolines of $\Delta SV_2(H)$ variations.

Conclusions

An attempt was made to investigate the contribution of external origins to $SV(H)$ changes. $SV(H)$ changes of external origins consist of short and long period variations. There is an anticorrelation between short period (one year) $\Delta SV(H)$ and geomagnetic activity expressed by $\Delta \Sigma K_p$ indices.

The changes of $\Delta SV(H)$ per unit $\Delta \Sigma K_p$ vary for individual observatories. Long period (78-80 years) variations of $SV(H)$ and the same variations of the Wolf number show consistent changes.

A spatial distribution of secular variations due to internal origins has been found when the parts of $SV(H)$ due to external origins (its dependence on ΣK_p and Wolf numbers) were subtracted.

References

- Golovkov, V.P., G.I. Kolomijtseva, L.P. Konyashchenko and G.M. Semyonova, 1983, *The summary of the annual mean values of magnetic elements at world magnetic observatories*, ISSUE XVI, IZMIRAN, Moscow, 342 p.
- Golovkov, V.P., E.M. Dimant and G.I. Kolomijtseva, 1984-1989, *Summary of the annual mean values of magnetic elements at the world magnetic observatories*, ISSUE XVII-XXII, IZMIRAN, Moscow.
- Golovkov, V.P., and E.M. Dimant, 1990, *Summary of the annual mean values of magnetic elements at the world magnetic observatories net*, ISSUE XXIII, IZMIRAN, Moscow, 50 p.

Accepted February 22, 2007

Experimental Modeling of Impact Effects on the Magnetic Susceptibility of Geological Materials

Atmane LAMALI¹, Pierre ROCHETTE², Jérôme GATTACCECA²
and Michel BOUSTIE³

¹ Centre de Recherche en Astronomie, Astrophysique et Géophysique (CRAAG), Algérie
CRAAG BP 63 Bouzaréah 16340 Algiers, Algeria
e-mail: atmane_lamali@yahoo.fr

² CEREGE (CNRS/Université Aix-Marseille 3), France
BP 80, 13545 Aix-en-Provence Cedex 4, France
e-mails: rochette@cerege.fr; gattacceca@cerege.fr

³ Laboratoire de Combustion et de Détonique (UPR CNRS 9028) ENSMA Poitiers, France
ENSMA, 1 Av. Clément Ader, 86961 Futuroscope France
e-mail: boustie@lcd.ensma.fr

A b s t r a c t

It is known that magnetic susceptibility of ferromagnetic materials changes if mechanical stress is applied. Various magneto-mechanic interactions can contribute to this variation. Elsewhere, it has been recognized, physically, that magnetostriction and magnetic hysteresis are intrinsically coupled phenomena. This study examined the hysteresis loops of shocked geological materials with different magnetic mineralogy. We calculated the differential magnetic susceptibility from hysteresis loops obtained from rock specimens after they were impacted using high-order explosives (penthrite). Maximum pressure is about 20 GPa. The experimental setup and procedure are described and a large number of the obtained experimental results are presented and discussed.

1. Introduction

The physical mechanism of the driven shock effect on magnetic properties of rocks is still not very well understood. Magnetic susceptibility is one of the most important of these magnetic properties within a given magnetic mineralogy. On the other hand, a number of authors found experimental evidence that shock pressures on the

order of only 1 GPa or less can remove magnetic remanence, while even a few MPa can reduce it (Hargraves and Perkins 1969, Pohl *et al.* 1975, Cisowski and Fuller 1978, Pohl *et al.* 1981).

The studies carried out on the pressure effect on magnetic susceptibility are rather scanty. If we intend to determine the bulk susceptibility under pressure conditions, the measurements can only be performed using a special equipment involving pressure cells (Kapicka *et al.* 2003). Similarly, other experimental processes and systems were developed to measure reversible magnetic susceptibility under high pressures (Gilder *et al.* 2002). Such measurements find also their interest in the investigation of magnetic properties modification of the ribbons with tape recording under stress of hauling and efforts exerted by the read heads (Hug *et al.* 1994, Radwan 2002).

Previous studies show that impact structures (meteoritic craters or nuclear explosion sites) are characterized by a reduction in magnetic susceptibility (Pilkington *et al.* 1992, Ugalde *et al.* 2003). Additionally, the studied magnetic properties (susceptibility, NRM intensity and Koenigsberger ratio) of the rocks sampled outside the Lappajärvi impact structure are very different from the targeted rock (Pesonen *et al.* 1992). Hence, the effects of shock waves on the intrinsic magnetic properties are frequent phenomena in geological or industrial materials. Furthermore, the interpretation of the paleomagnetic signals of most meteorites depends on these phenomena. Similarly, the remagnetization patterns associated with impact basins on Mars, the Moon or asteroids cannot be interpreted with certainty if one neglects this aspect (Rochette *et al.* 2001, Halekas *et al.* 2002, Hood *et al.* 2003, Rochette *et al.* 2003, Hart *et al.* 200, and Kletetschka *et al.* 2004).

In order to highlight the laboratory pressure-induced changes in magnetic susceptibility, we calculated the differential magnetic susceptibility from hysteresis loops obtained from rocks impacted using high-order explosives (penthrite). The shock wave is modeled numerically with maximum pressure reaching 20 GPa. In this paper, the assumptions on the variation of magnetic susceptibility under pressure were presented by referring to the previous works on the physical theory of magnetostriction. An expression for the magnetostriction is derived from minimization of the internal energy with respect to strains, which is necessary for mechanical equilibrium, after domain wall motion or wall bowing.

2. Main Theory

When exposed to an external field (H), a ferromagnetic substance acquires a magnetic moment (M), which varies nonlinearly until saturation. The value of M depends on whether H is increasing or decreasing: the curve $M(H)$ defines a hysteresis loop whose derivative dM/dH is the differential susceptibility (X_{diff}). In other words, X_{diff} changes as a function of H whose integral Eq. (1) defines a hysteresis loop

$$M(H) = C + \int_{H_0}^H H_{diff}(H) dH . \quad (1)$$

The initial susceptibility is measured in a low AC or DC field (< 1 mT) and is defined as the ratio M/H . The initial susceptibility is due to reversible displacements of mobile domain walls in multidomain (MD) particles or moment rotation in single-domain (SD) particles. In the latter case, low fields are not very effective in rotating SD moments. Therefore, susceptibilities in SD and pseudo-single-domain (PSD) grains are usually lower than that of MD grains. However, what is actually measured in the laboratory is the apparent susceptibility, χ_o , not the intrinsic susceptibility, χ_i . The difference is due to the effects of self-demagnetization. One should remind that inside a grain, the applied field, H , is modified by the demagnetizing field resulting from surface charges (Dunlop and Özdemir 1997, Hunt *et al.* 1995, and references therein).

3. Experimental Procedure

Experimental procedures were described in Lamali *et al.* (2005) and are summarized briefly here. The blocks of rocks are arranged in a rubber container filled with sand and gravel. A stick of explosive is stuck vertically on the flat surface of the sample. The blocks are oriented according to the local field declination with an average angle of 90° regarding to the direction of their natural remanent magnetization (NRM), in order to distinguish the overprint magnetization acquired during the shock. The container is maintained closed by a heavy wood cover. With the aim of targeting well the part that is most affected by the shock wave propagation, we carried out an in-depth millimeter-length sampling around the point of impact using the diamond wire saw. We obtained ten (10) specimens for each block of impacted rock which corresponds to “3 cm” in depth from the impacted area. The specimens have parallelepiped shape with a volume of $4 \times 4 \times 3$ mm³. With this geometric form, we are sure that the total magnetization intensity of each specimen largely exceeds the background noise of the cryogenic magnetometer and is directly measurable with the vibrating sample magnetometer (VSM). Before all measurements, each specimen was weighed. The same sampling procedure is followed for non-impacted rock.

In order to determine the shock effect on different magnetic mineralogy, we chose four types of rocks (microdiorite, basalt, rhyolite and schist). Thermomagnetic curves carried out with KLY2 suggest the presence of magnetite in microdiorite, titanomagnetite in basalt, hematite in rhyolite and pyrrhotite in schist. A number of rock-magnetic experiments (NRM analysis, hysteresis, anisotropy of magnetic susceptibility) have also been carried out for all impacted and non impacted specimens (Lamali *et al.* 2005).

4. Results and Interpretation

In this paper, we focused on the hysteresis loops measurement where the differential magnetic susceptibility is calculated according to equation Eq. (1). On the other hand, we showed (Lamali *et al.* 2005) that measured magnetic susceptibilities for all impacted specimens and their magnetic anisotropy factor are strongly modified by the

shock wave in the first centimeter of the impact point. Furthermore, we also showed that shock wave imparted a magnetic foliation with a minimum susceptibility axis parallel to the direction of impact. On the other hand, the unshocked specimens have homogeneous magnetic susceptibilities and hysteresis parameters (see Table 1, showing remanence, coercivity, saturation, and other parameters). We show in Figs. 1-3 the obtained curves of the differential magnetic susceptibility from hysteresis loops, respectively, for the shocked basalt, microdiorite and schist samples. Unfortunately, we could not represent the curves relating to the rhyolite specimens while the measured magnetic signal by the VSM apparatus is too noisy. It is often the case when the major carrier of magnetization in the sample is the hematite.

Table 1

Hysteresis parameters of shocked and unshocked materials
(For each parameter, the number of measured specimens is $n = 10$)

| Hysteresis parameters | Basalt | | Microdiorite | | Schist | |
|---|----------------------------|----------------------------|----------------------------|----------------------------|----------------------------|---------------------------|
| | Unshocked | shocked | Unshocked | shocked | Unshocked | shocked |
| Mr (Am ² kg ⁻¹) | 9.78±0.67 10 ⁻² | 1.08±0.16 10 ⁻¹ | 2.38±0.20 10 ⁻² | 5.35±4.98 10 ⁻² | 4.48±2.90 10 ⁻² | 7.20±4.5 10 ⁻² |
| Ms (Am ² kg ⁻¹) | 6.22±0.46 10 ⁻¹ | 6.41±0.21 10 ⁻¹ | 1.28±0.14 10 ⁻¹ | 1.84±0.26 | 9.14±6.02 10 ⁻² | 1.43±0.9 10 ⁻¹ |
| Mr/Ms | 1.57±0.03 10 ⁻¹ | 0.17±0.03 | 1.39±0.07 10 ⁻² | 0.03±0.03 | 4.99±0.28 10 ⁻¹ | 0.51±0.03 |
| Bc (mT) | 5.19±0.16 | 5.05±0.89 | 1.86±0.08 | 4.05±4.12 | 23.8±5.9 | 26.79±12.16 |
| Bcr (mT) | 18.4±1.1 | 16.20±1.81 | 19.1±0.7 | 20.5±5.82 | 31.3±11.7 | 32.59±15.38 |
| Bcr/Bc | 3.54±0.14 | 3.24±0.17 | 10.3±0.4 | 7.34±2.76 | 1.29±0.12 | 1.21±0.06 |

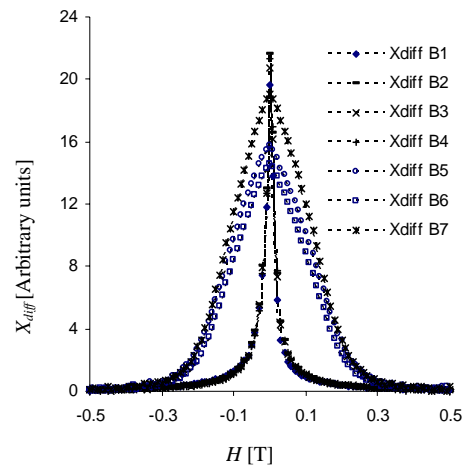


Fig. 1. Microdiorite X_{diff} curves (E1 to E7: distance from impact).

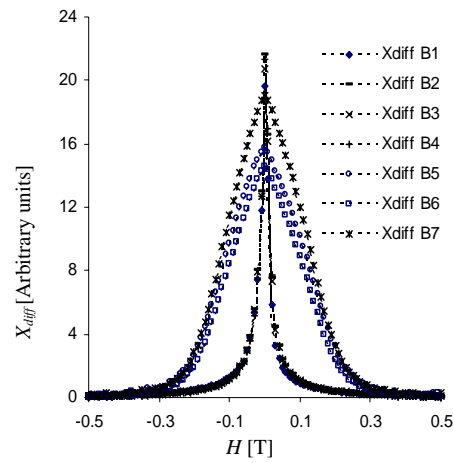


Fig. 2. Basalt X_{diff} curves (B1 to B7: distance from impact).

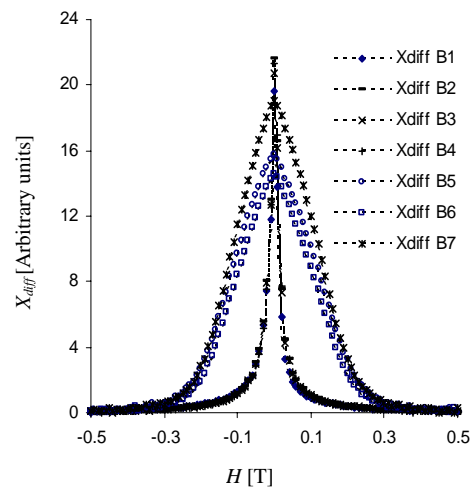


Fig. 3. Schist X_{diff} curves (S1 to S7 distance from impact).

Pressure-induced changes in magnetic parameters have been studied on a large set of rock samples. The modification of these parameters is noticeable in the rock with ferrimagnetic minerals. We examined here the changes in the differential magnetic susceptibility parameter. We observe in Figs. 1-3 that this parameter is strongly affected by the shock wave in the first centimeter of the all impacted rocks. Here we focus on the major peak. This peak grows as the pressure decreased from its maximum at first relevant shocked specimens. For impacted microdiorite specimens, these peaks reach a pronounced minimum at the first few steps of shock wave propagation (Fig. 1). Otherwise, at this stage of propagation, the impacted basalt specimens

present a considerable peak with a delimited narrow area (Fig. 2) and this confirms that the coercivity was strongly affected. These observations concern microdiorite and basalt, with magnetite and titanomagnetite bearing mineralogy, respectively, rather than pyrrhotite present in schist where the peaks show a chaotic evolution towards the shock wave propagation (Fig. 3). The presence of pyrrhotite under its two crystallographic phases (monoclinic and hexagonal) in schist specimens may be the cause of this behavior. We can deduce that the magnetic mineralogy behaves differently under pressure.

We can put forward several hypotheses which could explain these pressure-induced changes referring to previous works. The shock wave affects differently the intrinsic magnetic properties, owing to differences in mineralogical composition, texture, porosity, grain size and alteration degree (Pesonen *et al.* 1992). Previous studies show that magnetostriction coefficients in magnetite increase with increasing titanium concentration which makes titanomagnetite more stress-sensitive than pure magnetite, where the bulk volume decreases 1% to 2% [GPa], and closer atomic distances should result in heightened superexchanging interaction and thus influence the magnetostriction (Gilder *et al.* 2002, 2004 and references therein). Referring to the micromagnetism theory, it is known that the number of dislocation increases with stress which acts to reduce domain size, inhibit wall motion and/or physically create single or subvolumes that take on single domain properties (Gilder *et al.* 2005). Additionally, under great deformations, the important density of fixed dislocations and their strongly heterogeneous walls distribution anchor and curve the principal walls very easily (Hug *et al.* 1994). Intergrown phases and local stress field around may serve, in addition to lattice defects, as a strong pinning sites for domain walls and also magnetic interactions may not be negligible (Kapicka *et al.* 2003). In conclusion, the decrease of mean susceptibility under uniaxial stress is related to the decreased mobility of the domain walls or to qualitatively different behavior of the changes of directional susceptibilities of orientations different with respect to the applied stress (Kapicka 1990, 1992).

Finally, it is noteworthy that these observed pressure-induced changes are irreversible and not annealed for temperature up to 580°C. Similar irreversible changes in magnetic properties have been observed in magnetite under hydrostatic pressures up to 6 GPa (Gilder *et al.* 2004) and in hematite powder subjected to shocks between 8-27 GPa (Williamson *et al.* 1986).

5. Conclusions

Laboratory pressure treatment results indicate that the intrinsic magnetic properties (hysteresis, susceptibility) of the magnetite-, titanomagnetite- and pyrrhotite-bearing rocks are permanently modified by a shock wave generating a peak pressure greater than a few GPa. Many factors cited above may be responsible for these modifications. We recommend additional laboratory measurements which are ineluctable to investigate the real origin of these pressure-induced changes.

Acknowledgments. This study is a detailed interpretation of the hysteresis loops obtained during my training in rock magnetism laboratory at CEREGE (University Aix-Marseille 3 and CNRS), in order to obtain the master2 research diploma under the direction of Pr. Pierre Rochette. We acknowledge Fabienne Vadeboin at CEREGE who kindly contributed to carry out all our measurements.

References

- Cisowski, S.M., and M. Fuller, 1978, *The effects of shock on magnetism of terrestrial rocks*, J. Geophys. Res. **83**, 3441-3458.
- Dunlop, D.J., and Ö. Özdemir, 1997, *Rock magnetism*, Cambridge Univ. Press, Cambridge, 573 p.
- Gattacceca, J., M. Boustie, B.P. Weiss, P. Rochette, E. Lima, L.E. Fong and F. Baudenbacher, *Investigating impact demagnetization through laser impacts and SQUID microscopy*, Geology (in press).
- Gilder, S., and M. LeGoff, 2005, *Pressure dependence on the magnetic properties of titanomagnetite using the reversible susceptibility method*. In: J.H. Chen, Y.B. Wang, T.S. Duffy, G.Y. Shen and L. Dobrzhinetskaya (eds.), "Advances in High-Pressure Technology for Geophysical Applications", Elsevier, Chapter **15**, 315-335.
- Gilder, S., M. LeGoff, J.C. Chervin and J. Peyronneau, 2004, *Magnetic properties of single and multi-domain magnetite under pressures from 0 to 6 GPa*, Geophysical Research Letters **31**, L10612, doi:10.1029/2004GL019844.
- Gilder, S., M. LeGoff, J. Peyronneau and J.C. Chervin, 2002, *Novel high pressure magnetic measurements with application to magnetite*, Geophysical Research Letters **29**, 10.1029/2001GL014227.
- Halekas, J.S., D.L. Mitchell, R.P. Lin, L.L. Hood, M.H. Acuña and A.B. Binder, 2002, *Demagnetization signatures of lunar impact craters*, Geophys. Res. Let. **29**, doi: 10.1029/2001GL013924.
- Hargraves, R.B., and W.E. Perkins, 1969, *Investigations of the effect of shock on natural remanent magnetism*, Journal of Geophysical Research **74**, 2576-2589.
- Hart, R.J., S.H. Connell, M. Cloete, L. Mare, M. Drury, and M. Tredoux, 2000, *Super magnetic' rocks generated by shock metamorphism from the centre of the Vredefort impact structure*, South African Journal of Geology **103**, 151-155.
- Hood, L., N.C. Richmon, E. Pierazo and P. Rochette, 2003, *Distribution of crustal magnetic fields on Mars: shock effect of basin-forming impacts*, Geophys. Res. Let. **30**, 10.1029/2002GL016657.
- Hug, E., M. Kant and M. Clavel, 1994, *Influence de l'écroissage sur les propriétés magnétiques d'alliages Fe-3%Si non orientés*, Journal de Physique III **4**, 7, 1267-1284.
- Hunt, C.P., B.M Moskowitz and S.K Banerjee, 1995, *Magnetic properties of rocks and minerals*. In: T.J. Ahrens (ed.), "Rock physics and phase relations", AGU, Washington DC, 189-204.

- Kapicka, A., V. Hoffmann and E. Petrovsky, 2003, *Pressure instability of magnetic susceptibility of pyrrhotite bearing rocks from the KTB borehole*, *Studia Geophysica Et Geodaetica* **47**, 2, 381-39.
- Kapicka, A., 1992, *Magnetic susceptibility under hydrostatic pressure of synthetic magnetite samples*, *Physics of the Earth and Planetary Interiors* **70**, 248-252.
- Kapicka, A., 1990, *Variations in mean susceptibility of rocks under hydrostatic and non-hydrostatic pressure*, *Physics of the Earth and Planetary Interiors* **63**, 78-84.
- Kletetschka, G., J.E.P. Connerney, N.F. Ness and M.H. Acuna, 2004, *Pressure effects on Martian crustal magnetization near large impact basins*, *Meteoritics & Planet. Sci.* **39**, 11, 1839-1848.
- Lamali, A., J. Gattacceca, P. Rochette and M. Boustie, 2005, *Magnetic effects of explosive driven shocks on geological materials*, AGU San Francisco Dec. 2005.
- Pesonen, L.J., N. Marcos and F. Pipping, 1992, *Palaeomagnetism of the Lappajärvi impact structure, western Finland*, *Tectonophysics* **216**, 1-2, 123-142.
- Pilkington, M., and R.A.F. Grieve, 1992, *The geophysical signature of terrestrial impact craters*, *Reviews of Geophysics* **30**, 161-181.
- Pohl, J., U. Bleil and U. Hornemann, 1975, *Shock magnetization and demagnetization of basalt by transient stress up to 10 kbar*, *J. Geophys.* **41**, 23-41.
- Pohl, J., and A. Eckstaller, 1981, *The Effect of Shock on Remanence in Multi-Domain Iron Grains and Implications for Palaeointensity Measurements*, *Lunar and Planetary Science* **XII**, 851-853.
- Radwan, M.M., 2002, *Magnetostriction Properties of $Fe_{40}Ni_{38}B_{18}Mo_4$ Amorphous Alloy*, *Egypt. J. Sol.* **25**, 1.
- Rochette, P., J.P. Lorand, G. Fillion and V. Sautter, 2001, *Pyrrhotite and the remanent magnetization of SNC meteorites: A changing perspective on Martian magnetism*, *Earth Planet Sci. Lett.* **190**, 1-12.
- Rochette, P., G. Fillion, R. Ballou, F. Brunet, B. Oulladiaf and L. Hood, 2003, *High pressure magnetic transition in pyrrhotite and impact demagnetization on Mars*, *Geophys. Res. Lett.* **30(13)**, 1683, doi:10.1029/2003GL017359.
- Ugalde, H.A., N. Artemieva and B. Milkereit, 2003, *Numerical Modelling and Petrophysical Constraints the Magnetic Signature of Impact Structures*, Expanded Abstracts, 3rd International Conference in Large Meteorite Impacts, Noerdlingen, Germany, Abstract 4017.
- Williamson, D.L., E.L. Venturini, R.A. Graham and B. Morosin, 1986, *Morin transition of shock-modified hematite*, *Phys. Rev. B* **34**, 1899-1907.

Accepted March 22, 2007

World Monthly Means Database Project

Arnaud CHULLIAT and Kader TELALI

Équipe de Géomagnétisme, Institut de Physique du Globe de Paris
4, place Jussieu – 75252 Paris cedex 05 – France
e-mails: chulliat@ipgp.jussieu.fr; telali@ipgp.jussieu.fr

Abstract

Observatory monthly means are widely used for studying geomagnetic secular variation. They provide a better time resolution than annual means and are well suited for investigating the so-called geomagnetic jerks. While annual and hourly means have been compiled for a long time within the WDC system, no such tradition exists for monthly means. This project aims at filling the gap by building a publicly available monthly means database. It is also motivated by the need to resolve occasional inconsistencies between annual and hourly means present in WDCs. To begin with, we computed monthly means for all INTERMAGNET observatories from WDC hourly means. We stored them in a data format providing information on data discontinuities (“jumps”), as well as data components, quality and sources. Then we assessed the quality of the data by systematically comparing them with WDC annual means and with predictions of the CM4 geomagnetic model (Sabaka *et al.* 2004). Although most of the data are valid, some serious discrepancies arise, requiring that some observatories correct their data.

1. Introduction

Observatory monthly means are used for modeling the geomagnetic secular variation (e.g., Wardinski and Holme 2006), generated by fluid flows at the top of the Earth’s core (e.g., Chulliat and Hulot 2000). Averaging over one month is a powerful and easy-to-implement way to remove most magnetic variations of external origin, while keeping variations of internal origin. More rapid variations of internal origin are filtered out by the lowly conducting mantle. Annual means are also used for studying the secular variation, but they do not provide enough time resolution for investigating sudden changes of the core field variation trend, called geomagnetic jerks (e.g., Mandea *et al.* 2000).

There are various public archives of old magnetic observatory data throughout the world (see the list in Table 1). Unfortunately, none of them compiles observatory monthly means.

Table 1
Public archives of old observatory data

| Data type | WDC |
|---------------|--------------------------|
| Annual means | Edinburgh (BGS) |
| Monthly means | None |
| Hourly means | Copenhagen (DMI)*, Kyoto |
| Minute values | Copenhagen (DMI)*, Kyoto |
| Second values | Kyoto |

*As of April 2007, the Geomagnetic Data Master Catalogue previously hosted by DMI has been transferred to the WDC in Edinburgh.

One could think of simply computing monthly means from hourly means whenever they are needed. However, it is not such an easy task to compute consistent monthly means series from WDC data. One is faced with two difficulties:

1. Data discontinuities, or “jumps”, are treated differently in the various public archives. For example, jumps are not integrated yet documented in the Edinburgh WDC, while they are neither documented nor integrated (in general) in the Copenhagen WDC.
2. There are occasional inconsistencies between data from different WDCs. Possible reasons are that data were not simultaneously sent by observatories to each WDC, or that data were not updated in all WDCs after a revision.

Several monthly means databases have been built by individual researchers in recent years. Some years ago, Mioara Mandea built such a database and made it publicly available (Alexandrescu 1998). However, this database was not always consistent with data in WDCs. As data discontinuities were integrated without being documented, it was more difficult to track down the origin of inconsistencies.

Here we propose a new method for archiving monthly means, to apply this method to INTERMAGNET observatories and systematically check the consistency of the obtained monthly means series. This is the first step toward a new, publicly available monthly means database.

2. Data Format

The IAGA-2002 format is not convenient for our purpose because it forces each year of data to be stored in a different file. Moreover, some of the information in the IAGA-2002 header is not relevant to monthly means (for example digital sampling rate) while some potentially more useful information (for example data quality) cannot be included in data records.

Thus, we designed a new, specific file format for archiving monthly means, with the following properties (see Fig. 1):

- Usual information on observatory is given in a IAGA-2002 like 5-line header.
- Information on data discontinuities is provided in the rest of the header.
- Information on observed elements, data quality and the origin of the data is provided in data records using codes (L, M and R) similar to those used by the Edinburgh WDC to store observatory annual means.
- All data for a given observatory are stored in the same file (except when the name of the observatory changes) with time counted in decimal years.

```

Station Name           Chambon La Foret
IAGA Code              CLF
Geodetic Latitude [deg] 48.017
Geodetic Longitude [deg] 2.266
Elevation [m]          145
# This data file is part of the IGP monthly means database.
# Data last verified by the observatory: December 2006
# Conditions of use: these data are for scientific/academic use.
# NOTES:
# 1936 Site differences Val Joyeux - Chambon
# 1957 New proton magnetometer
# 1968 Theodolite and absolute pier change
# 1983 Absolute pier change
TIME      X      Y      Z L M R
1936      -387   -96    278 9 9 1
1936.042  19724  -3323  41342 2 1 1
1936.124  19733  -3317  41351 2 1 1
1936.206  19739  -3313  41344 2 1 1
1936.290  19733  -3305  41355 2 1 1

```

Fig. 1. Header of the CLF monthly means data file in the proposed format.

3. Database Construction

To begin with, we restricted ourselves to INTERMAGNET observatories, as a first step toward a larger database. For each INTERMAGNET observatory, monthly means were calculated as far back in time as possible from hourly values retrieved from the WDC in Copenhagen, or directly from our own recently revised digital archive in case of French observatories. Information on data discontinuities was obtained from the WDC in Edinburgh, as well as information on observed elements and data quality (whenever available).

4. Checking Method

Three tests were systematically applied to each monthly means series:

1. Internal consistency of the series was checked by visual inspection of various plots. Particular attention was paid to data discontinuities.
2. Consistency between the series and that of annual means was checked by re-

calculating annual means from the monthly means. Although this is clearly not the best method to compute annual means (which should be computed from daily means), the error associated with the unequal number of days in each month is negligible for the purpose of the checking.

3. Consistency between the series and those at other observatories was checked by comparing it with the secular variation predicted by the CM4 model (Sabaka et al. 2004) from 1960 to present time. It is expected that the CM4 misfit becomes larger at an anomalous observatory provided it is not too far from other non-anomalous observatories.

5. Results of the Tests

Most tested monthly means series have no problem. However, about 10% of them fail at one test at least. It is not the purpose of this paper to list problematic observatories, since most problems should be easily corrected in the near future. Here we want to show how very simple consistency tests can be useful for improving the overall quality of data stored in public archives. Therefore, the following examples should be seen as illustrations only.

Figure 2 shows two examples of anomalies in monthly means series. The first one is an artificial offset of about 120 nT in monthly means from January to October 1984, coming from a corresponding offset in hourly values retrieved from the Copenhagen WDC. Error of that kind can be easily corrected by coming back to the original raw data. The second example of anomaly is a series of oscillations of amplitude 100-200 nT between 1950 and 1960. The cause of this observation is unknown, but it is suspicious since it is not observed in neighboring observatories.

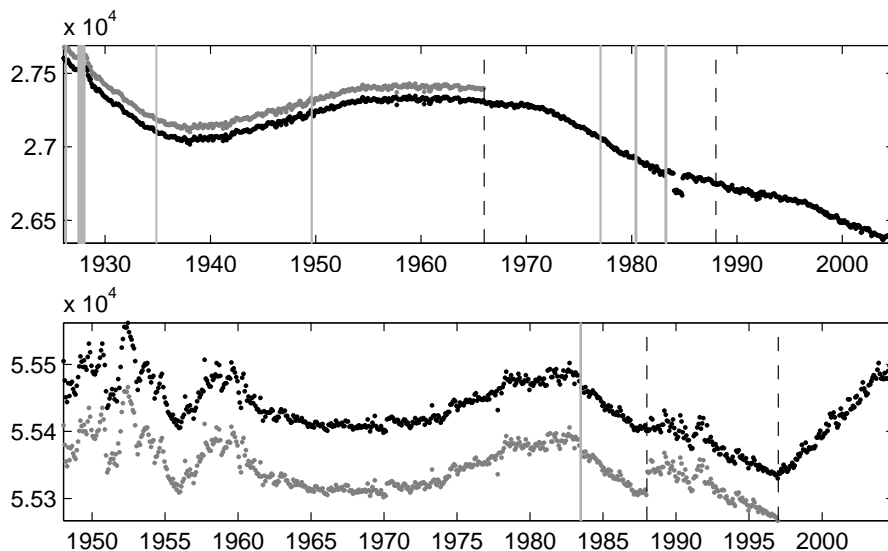


Fig. 2. Two examples of anomalies in monthly means series. The grey (resp. black) dots represent monthly means before (resp. after) integrating jumps. Jumps are indicated by vertical dashed lines. Grey rectangles show data gaps. Vertical scale in nT.

Figure 3 shows two examples of inconsistencies between monthly means (calculated from hourly values retrieved from the Copenhagen WDC) and annual means (retrieved from the Edinburgh WDC). In the first example, the 1973 jump has been integrated in annual means instead of being simply documented there. There is also an undeclared jump in 1967. Although an approximate correction of these errors is possible, a precise determination of the jump values would require having access to the original observatory data. In the second example, there is an undeclared, uncorrected jump in the annual means in 1977, which has been corrected in the hourly values (hence the absence of jump in the monthly means series).

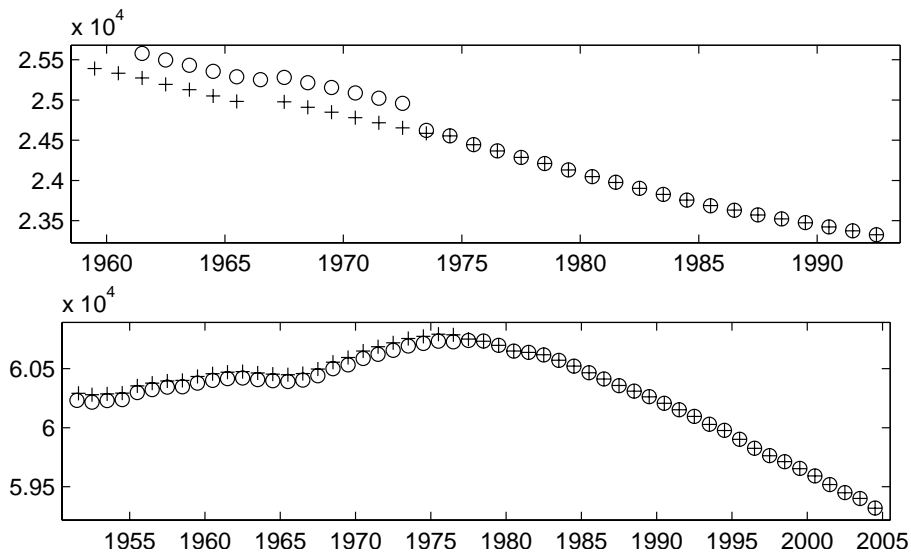


Fig. 3. Two examples of inconsistencies between monthly means and annual means. Crosses represent annual means from the Edinburgh WDC; circles represent annual means calculated from monthly means. The values are after correction of jumps. Vertical scale in nT.

Although not represented here, systematic comparison of monthly means and annual means series also reveal inconsistencies between data time spans. Quite frequently, there is at least one year with an annual mean available but without hourly value. The opposite also occurs, but less frequently.

Additional anomalies can be detected by comparing monthly means and field values predicted by the CM4 model. One such anomaly is shown in Fig. 4: there is a decreasing difference between CM4 and the monthly means of the considered observatory from 1970 to 1980. As several other observatories are located within a few thousand kilometers from this observatory, and the spatial scale of the detectable core field at the Earth's surface is about 3000 km, the core field predicted by CM4 is well constrained in the area of this observatory. Therefore, the difference between CM4 and the observatory monthly means indicates some anomaly of unknown origin in the observatory data.

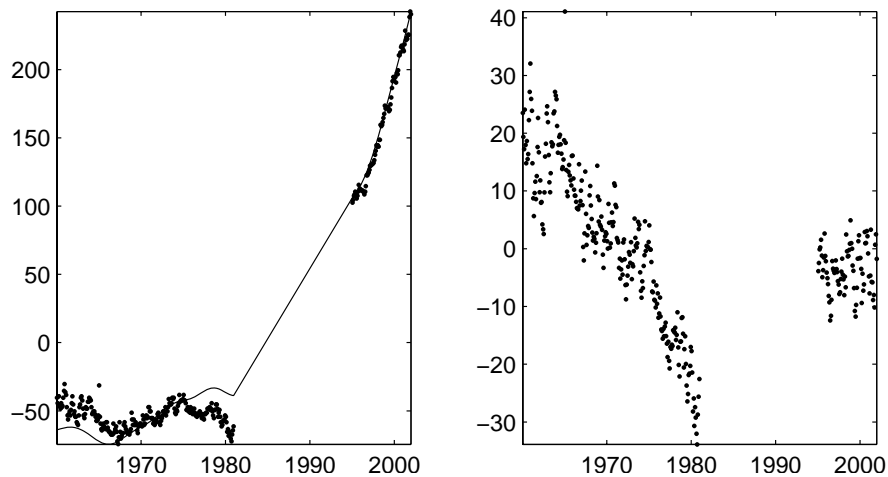


Fig. 4. An example of inconsistency between monthly means and the CM4 model. Left side graph: monthly means (dots) versus values predicted by CM4 (core field part, corrected for crustal bias) at the observatory location (line). Right-side graph: differences between the two. Vertical scale in nT.

6. Conclusion

We computed monthly means for all INTERMAGNET observatories from hourly values retrieved from the Copenhagen WDC, and archived them using a specifically designed file format. Like annual means archived at the Edinburgh WDC, we did not integrate data discontinuities but instead documented them in the header of the file.

After performing systematic tests, we found that about 10% of the monthly means series have inconsistencies, either internal or with respect to the annual means archived in Edinburgh or the CM4 model. Some of the inconsistencies can easily be corrected by the user or the relevant WDC, while others require that some observatories investigate their old original data.

The work presented here is a first step toward a new, publicly available monthly means database. The success of this project depends on the willingness of world observatories to send their old data and to investigate potential discrepancies.

Acknowledgments. This project originated from a conversation with Nils Olsen, who is greatly acknowledged for several suggestions along this work. We thank Mioara Manda for providing us with her monthly means database and for helpful discussions. We also thank Susan MacMillan for providing us with the complete BGS annual means database.

References

- Alexandrescu, M., 1998, *Database of Geomagnetic Observatory Monthly Means Seeks Contributors*, Eos AGU **79**, 345.
- Chulliat, A., and G. Hulot, 2000, *Local computation of the geostrophic pressure at the top of the core*, Phys. Earth planet. Inter. **117**, 309-328.
- Mandea, M., E. Bellanger and J.-L. Le Mouél, 2000, *A geomagnetic jerk for the end of the 20th century*, Earth Planet. Sci. Lett. **183**, 369-373.
- Sabaka, T.J., N. Olsen and M.E. Purucker, 2004, *Extending comprehensive models of the Earth's magnetic field with Ørsted and CHAMP data*, Geophys. J. Int. **159**, 521-547.
- Wardinski, I., and R. Holme, 2006, *A time-dependent model of the Earth's magnetic field and its secular variation for the period 1980-2000*, J. Geophys. Res. **111**, B12101, doi:10.1029/2006JB004401.

Accepted February 12, 2007

Worldwide Observatory Hourly Means from 1995 to 2003: Investigation of Their Quality

Monika KORTE¹, Mioara MANDEA¹ and Nils OLSEN²

¹ GeoForschungsZentrum Potsdam
Telegrafenberg, 14473 Potsdam, Germany
e-mails: monika@gfz-potsdam.de; mioara@gfz-potsdam.de

² Danish National Space Center
Juliane Maries Vej 30, 2100 Copenhagen, Denmark
e-mail: nio@spacecenter.dk

Abstract

We examined the hourly mean values from worldwide geomagnetic observatories as available from the World Data Center C1, Copenhagen, for erroneous or problematic data. A number of outliers and jumps were found, as well as instabilities in baseline control. It is impossible to correct all these data without checking the original values at the individual observatories again. We provide a table of identified problems to alert both users and the data owners about them and encourage each observatory to correct their data where possible.

1. Introduction

Geomagnetic observatory data are used for a multitude of different purposes, from main field and secular variation studies to investigations of external magnetic field variations and mantle conductivity. With digital data recording the availability of high resolution geomagnetic time series has increased (Fig. 1). These data are an important complementation of the recent high resolution magnetic data obtained by satellites like Ørsted and CHAMP. Hourly mean values (HMs) and one minute values are common data products from geomagnetic observatories (Jankowski and Sucksdorff 1996, St.-Louis 2004). The data are delivered to World Data Centers (WDC), where they are stored and freely available for scientific purposes. However, erroneous data can find their way into the databases. Sources of error are plentiful: Errors simply might occur in data transfer or importation to the database. Measurement errors happen and uncorrected values might be delivered to a WDC by mistake. Moreover, raw

observatory data consist of variation measurements and baseline determinations, which have to be combined to the final absolute time series. Producing good final data requires both skill in the absolute measurements to determine the baseline and care in processing the data. Even slight mistakes in either of these steps can lead to poor baseline control, which can result in artificial variations in the time series.

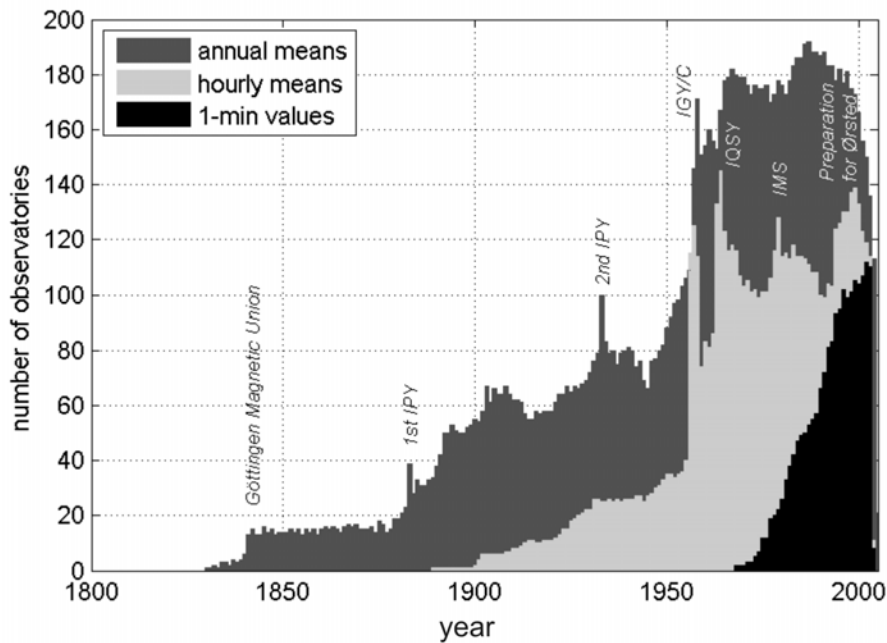


Fig. 1. Number of geomagnetic observatories providing annual means, hourly means and 1-min values, as a function of time. International campaigns, like the *Göttingen Magnetic Union*, the 1st and 2nd *International Polar Year (IPY)*, the *International Geophysical Year (IGY)*, the *International Quiet Solar Year (IQSY)*, the *International Magnetospheric Study (IMS)* and the preparation of the *Ørsted* satellite mission have stimulated observatory data processing and encouraged the opening of new observatories.

HMV's are well suited to detect most problems in high resolution observatory data and are widely used in scientific studies (e.g. Balasis and Egbert 2006, Le Mouel *et al.* 2005, Sabaka *et al.* 2004, Macmillan and Thomson 2003, to name just a few recent publications). We started a project to check all the available HMVs for outliers, jumps (i.e. uncorrected sudden baseline level changes), baseline drifts and other obvious problems. With approximately 150 observatories worldwide, this is a huge task. We first concentrated on the time from 1995 to 2003. Many observatories had changed to digital recording by 1995, and the number of available data (reported to the WDC) increased significantly then, during preparation for the *Ørsted* satellite mission. 2003 was the last epoch for which a reasonable number of global data was available at the time when the work was done. Here, we first describe the dataset and our main method of quality check. We mention further methods which we tested and which also can be useful to detect problematic data. We summarise the results of our work and

show some examples of detected problems. The full list together with figures is available online at http://www.gfz-potsdam.de/pb2/pb23/COM/comparison_obs.html.

For several reasons it is beyond the scope of our work to actually correct the data. First, we are not authorised to manipulate other observatories' data. Second, in many cases a correction is not straightforward. Except for some cases where individual outliers could be removed or corrected by interpolation or where the magnitude of a clear jump might be estimated, it will be necessary to go back to original data sources to figure out the source of the problems. Doing this for all observatories is beyond our capacity. Third, if baseline problems result from insufficient or inaccurate absolute measurements, it will unfortunately very likely be impossible to correct for them. Our basic intention is to alert data producers and users to problematic data. Given the importance of high quality geomagnetic observatory time series we urge all the original data holders to make efforts to correct erroneous data and update the WDC archives.

2. Checking Data Quality by Comparison

The data we used are the annual HMV files that were available at WDC C1 Copenhagen (<http://dmiweb.dmi.dk/fsweb/projects/wdcc1/>) in March 2005. The data were checked by intercomparison, i.e. the annual data series from each observatory were visually compared to those of at least two neighbouring observatories. We implemented a method to plot the north (X), east (Y) and vertical (Z) components of two observatories together with the differences. Examples are shown in Fig. 2 to 4. All these figures show real observatory data, but the stations have been made anonymous because similar features as shown here can be seen in data series from several other observatories, too.

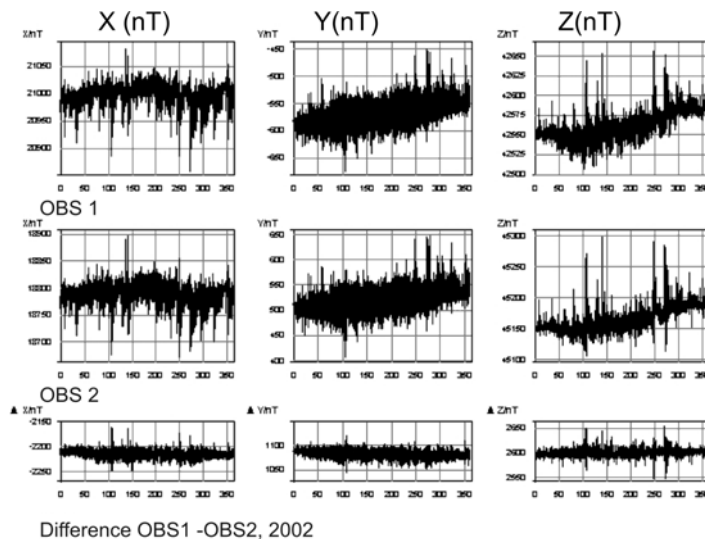


Fig. 2. Comparison of hourly mean values from two observatories. Example for a distance of a few hundred km and no detected data problems.

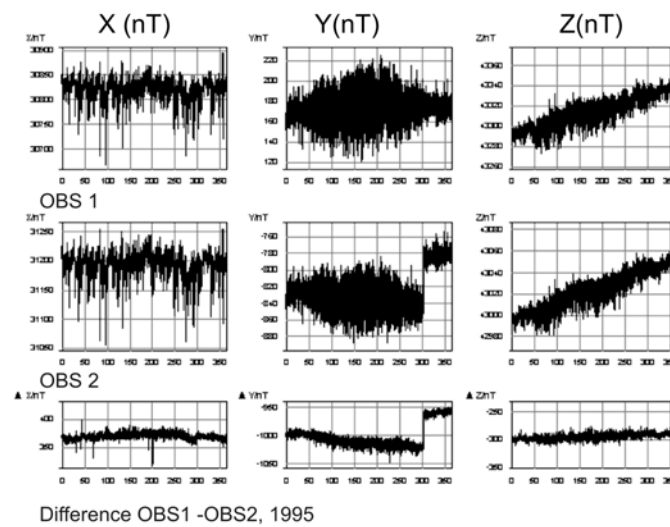


Fig. 3. Comparison of hourly mean values from two observatories where a baseline jump is clearly seen in Y and less clearly in X at about day 300 of the year.

In the differences, we expect to see constant offsets due to core and lithospheric field morphology, slow deviations due to differences in local secular variation, and high-frequency scatter due to differences in external and induced field contributions. Differences in secular variation and external fields depend on the distance between stations, and at times of higher levels of geomagnetic activity the differences in external and induced variations are more pronounced. These features can be seen in Fig. 2, where two observatories about 800 km apart are compared for a year when no data problems have been detected.

Spikes above the general high-frequency variation level which occur during magnetically quiet to moderately disturbed times, sudden jumps or strong variations on time-scales of a few weeks to months in the differences, on the other hand, can indicate data errors and problems in baseline control. Fig. 3 shows an example where a baseline jump is obvious in Y at about day 300 of the year. In Y the jump even is obvious in the individual data series from the second observatory. Fig. 4 shows an example where several problems are detected. This demonstrates how the comparison to two other observatories, respectively, helps to determine in which of the data series the problem occurs. In the first comparison between OBS1 and OBS2 a baseline drift in X and Z, something that looks like a kind of technical disturbance, a probable jump in Y and some outliers are marked. In the second comparison between OBS3 and OBS2, most of the problems are seen again except for two of the outlier spikes. Consequently, all problems seen in both comparisons must result in the data series common to both, in this case OBS2, and the other two outliers must originate in the OBS1 time series (which can be subsequently confirmed by a comparison of OBS1 to another observatory). In order to determine more exactly the day of the year where the problem occurred, we zoomed in on the plots. Thus we obtained a list of identified problems.

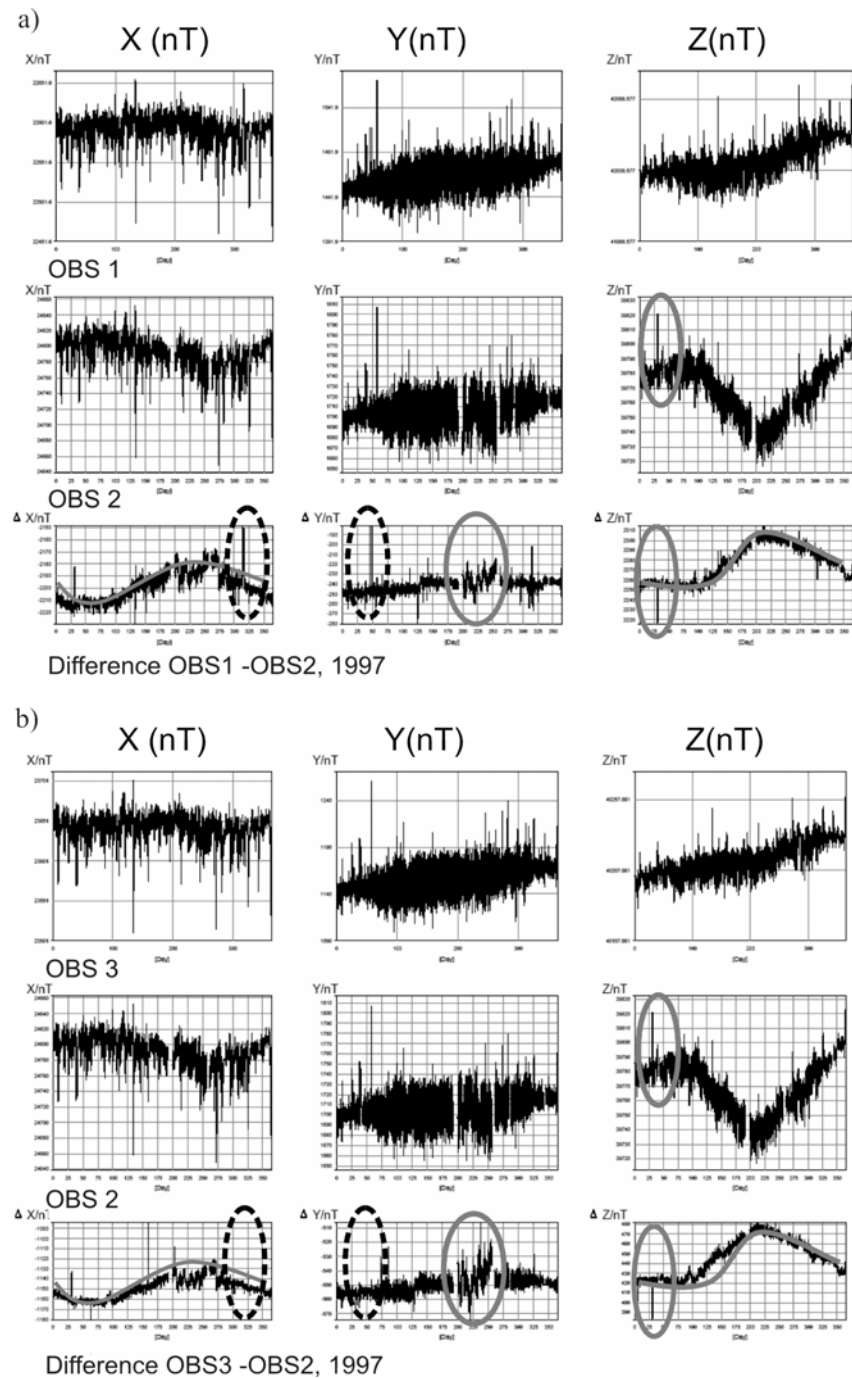


Fig. 4. An example demonstrating a number of different data problems. a) Comparison between OBS1 and OBS2, b) between OBS3 and OBS2. The problems in gray originate in the OBS2 data series, the ones marked by a dashed line originate in the OBS1 data series.

3. Further Methods

We tested two further methods of observatory data quality check, which can be performed for individual observatories without the need for direct intercomparison with others. The first is to check the mean daily variation of the components per year. It is useful to identify problems in reporting the data, particularly if data are reported with the wrong sign or in local time (LT) instead of universal time (UT). Fig. 5 shows two examples. In Fig. 5a the variations in X and Y look different at YAK than at other

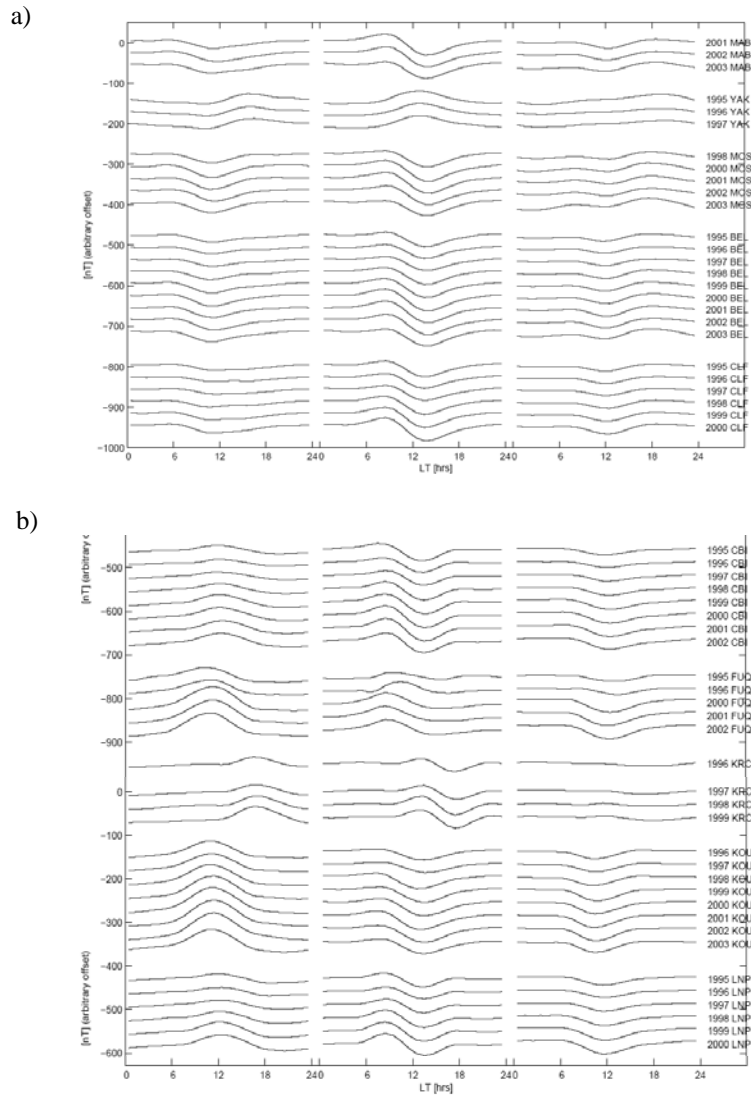


Fig. 5. Mean daily variation per year and observatory for the X, Y and Z (left to right) components. Observatories are ordered by geomagnetic latitude. Differences from the general patterns in YAK (a) and KRC (b) suggest an error in declination sign and reported time, respectively (see text).

observatories of similar geomagnetic latitude. It seems that declination recordings have been considered with the wrong sign in the determination of the X and Y component data throughout all the years. In Fig. 5b it seems that the KRC data are reported in local time instead of UT. If these data are shifted by the LT–UT difference, the mean daily variations agree much better with those of other observatories at comparable geomagnetic latitudes. Only few problems of this kind were detected. Apart from the examples shown in Fig. 5, we found that the data from observatory TTB seem to be reported in local time and in PEG this might be true for 1999.

The second alternative method is to compare the observatory data to predictions of the global CM4 model (Sabaka et al. 2002, 2004). This model, covering the time span from 1960 to 2002, describes not only the geomagnetic core field and secular variation, but includes the long-wavelength lithospheric field and quiet time external fields. Modulated by the Dst index as a measure for magnetospheric activity and the F10.7 solar irradiance index, the CM4 model can also represent the variations due to external field activity to a certain degree. The geomagnetic activity is not fully described by the model, and comparisons between CM4 predictions and observatory recordings at any location look similar to comparisons between neighbouring observatories. By studying the differences jumps, outliers or baseline variations become apparent in the same way as in the comparison to another observatory. An example where a potential baseline instability is detected is shown in Fig. 6. We did not yet apply this method to all the observatory data, but we are considering to include this comparison in our future work within this project.

4. Results and Conclusions

The hourly means data series from 1995 to 2003 from geomagnetic observatories around the world, available at WDC C1 Copenhagen, have been checked for problematic data mainly by intercomparison of neighbouring stations. A number of problems have been identified, ranging from outliers in the data and jumps in the time series to continuous baseline variations. There are in fact only few observatories where we did not detect any questionable data within the 8 years that we studied. The long list of identified problems is not included in this report, but is published on a website together with plots of the intercomparisons. It can be found at http://www.gfz-potsdam.de/pb2/pb23/COM/comparison_obs.html.

It should be kept in mind, that problems are identified easily when observatories are not too far from another and lie at low to mid latitudes. At high latitudes, where geomagnetic external variations are strong, only very severe outliers or jumps can be detected with any of the methods we tested. Jumps or outliers of only a few nT are not detectable within the strong and highly inhomogeneous variations. The same is true for very remote observatories when the method of observatory intercomparison is used.

Erroneous outliers might simply be rejected from the time series, but to correct for jumps and baseline variations it is advisable to consult the original data and check whether some real assessment of the problem can be made instead of only an estimation of the problem. Therefore it is beyond our capacity to offer corrections for the

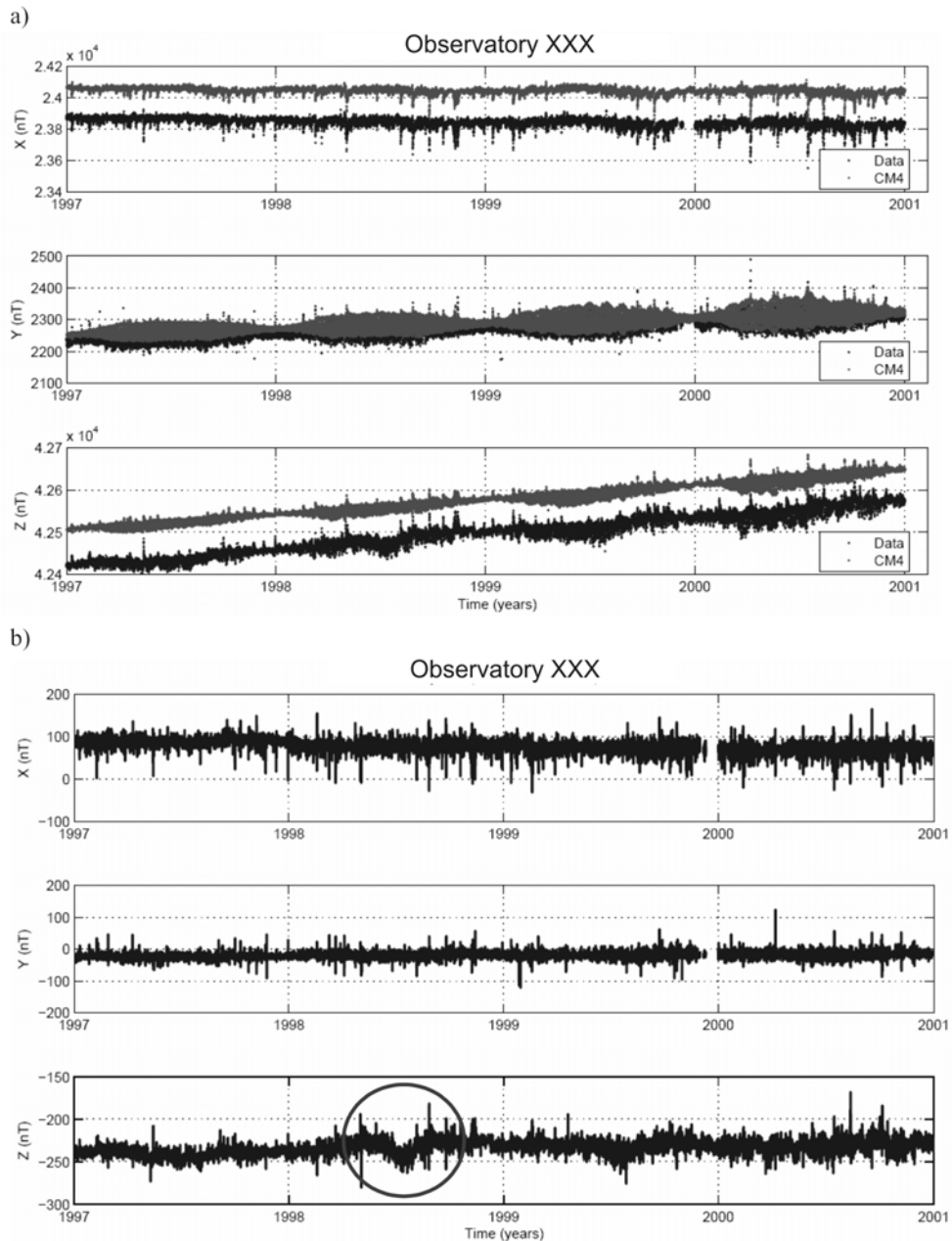


Fig. 6. a) Comparison of measured data and CM4 model predictions for the X, Y and Z component of an observatory for 4 years, b) Differences between data and model predictions. An unusual variation in the Z component in 1998 hints at a baseline problem.

identified problems. The intention of this work is to alert any users to existing problems in individual data series, but leave it to them how to handle them – whether to reject data or estimate a correction. Our main goal is to bring existing problems in the data series stored at the WDC to the attention of the producers and owners of the data,

i.e. the individual observatories. We encourage them to make every effort to correct their data and update the WDC database. The long data series of high resolution observatory data still hold significant potential for research, but it is important that the data are of high quality. Meanwhile we learned that efforts are going on in France, the USA, China and India to check and improve their observatories data series.

So far we focussed on the time interval 1995 to 2003, for which many observatories have been recording the data in digital form. We will continue this project and next we will focus on the preceding time interval, from 1957 to 1994.

Acknowledgments. We thank all the geomagnetic observatories around the world that deliver their data to the World Data Centers, thus making the data easily available for all kinds of scientific studies. This work would not have been possible without preparatory data visualisation and comparison by Hans-Joachim Linthe, Jürgen Haseloff, Jutta Schulz, Katrin Tornow and Anneleen Glodek at Niemegek observatory.

References

- Balasis, G., and G.D. Egbert, 2006, *Empirical orthogonal function analysis of magnetic observatory data: Further evidence for non-axisymmetric magnetospheric sources for satellite induction studies*, Geophys. Res. Let. **33**, L11311, doi:10.1029/2006GL025721.
- Jankowski, J., and C. Sucksdorff, 1996, *IAGA Guide for Magnetic Measurements and Observatory Practice*, International Association of Geomagnetism and Aeronomy, 232pp.
- Le Mouel, J.-L., V. Kossobokov and V. Courtillot, 2005, *On long-term variations of simple geomagnetic indices and slow changes in magnetospheric currents: The emergence of anthropogenic global warming after 1990?*, Earth Planet. Sci. Let. **232**, 237-286.
- Macmillan, S., and A. Thomson, 2003, *An examination of observatory biases during the Mag-sat and Ørsted missions*, Phys. Earth Planet. Int. **135**, 97-105.
- Sabaka, T., N. Olsen and R.A. Langel, 2002, *A comprehensive model of the quiet-time, near-Earth magnetic field: phase 3*, Geophys. J. Int. **151**, 32-68.
- Sabaka, T., N. Olsen and M.E. Purucker, 2004, *Extending comprehensive models of the Earth's magnetic field with Ørsted and CHAMP data*, Geophys. J. Int. **159**, 521-547.
- St.-Louis, B., 2004, *INTERMAGNET Technical Reference Manual*, INTERMAGNET.

Accepted February 12, 2007

Panagjurishte Observatory Upgrade for INTERMAGNET

Hans Joachim LINTHE¹, Iliya CHOLAKOV² and Mioara MANDEA³

¹ GeoForschungsZentrum Potsdam – Adolf Schmidt Observatory
Lindenstrasse 7, D-14823 Niemegk Germany
e-mail: linthe@gfz-potsdam.de

² Geophysical Institute Sofia of the Bulgarian Academy of Sciences
Geomagnetic Observatory, BG4500 Panagjurishte, Bulgaria
e-mail: geomagpag@abv.bg

³ GeoForschungsZentrum Potsdam
Telegrafenberg, D-14473 Potsdam Germany
e-mail: mioara@gfz-potsdam.de

A b s t r a c t

Panagjurishte Geomagnetic Observatory was installed in 1937. From that time, this observatory runs continuously, the used instruments being a classical set made by Mating & Wiesenberg, Potsdam. A long collaboration exists then between Panagjurishte Observatory and Adolf Schmidt Geomagnetic Observatory Niemegk. In 2005 the GeoForschungsZentrum (GFZ) Potsdam and the Geophysical Institute Sofia of the Bulgarian Academy of Sciences (GIBAS) agreed in a cooperative programme, the aim being to upgrade the Panagjurishte Observatory with modern instruments in order to qualify it as an IMO. The GFZ provided a DI-flux theodolite, a vector and a scalar variometer and the data logger. The GIBAS purchased 2 computers, an uninterruptible power supply unit, network components and the internet connection. A Polish proton magnetometer is still in use. The arrangement of the instruments, comparisons of the classical and the modern system and the first results of absolute measurement reductions are presented.

1. Introduction

The Geophysical Institute Sofia of the Bulgarian Academy of Sciences (GIBAS) operates Panagjurishte Geomagnetic Observatory, which was opened on 7 November 1937 (Cholakov 1998). Its geographical location is at 42°30.9' latitude, 24°10.6' longitude and 556 m elevation. The observatory operates since the beginning continuously

a classical set of magnetometers made by Mating & Wiesenberg, Potsdam. Beginning with Panagjurishte Observatory establishment, both observatories, Panagjurishte and Niemeck, cooperate closely. This collaboration is expressed in regular comparison measurements of both observatories. Table 1 shows the results of comparisons. Sixteen measurements were carried out during 40 years more or less regularly.

Table 1

Comparison measurement results of Panagjurishte and Niemeck observatories

| Year of Meas. | Obs. host | Operators | PAG – NGK | | | |
|---------------|-----------|------------------------------|-----------------|------------------|------------------|------------------|
| | | | ΔD ' | ΔH nT | ΔZ nT | ΔF nT |
| 1963 | NGK | K. Kostov | +0,42 | 0,0 | 0,0 | – |
| 1964 | PAG | A. Grafe, W. Zander | –1,30 | +3,2 | –1,0 | – |
| 1966 | NGK | K. Kostov | –0,43 | +2,2 | – | – |
| 1967 | PAG | A. Grafe, W. Zander | –0,02 | +0,3 | –5,6 | – |
| 1969 | NGK | K. Kostov | +0,7 | –0,8 | –1,5 | –3,0 |
| 1971 | PAG | K. Lengning, W. Zander | –0,80 | +0,5 | –2,0 | –1,8 |
| 1974 | NGK | K. Kostov | 0,0 | –0,4 | +0,8 | –0,3 |
| 1975 | PAG | K. Lengning, W. Zander | –0,48 | +1,3 | +0,3 | +0,4 |
| 1976 | NGK | K. Kostov | –0,04 | –1,2 | – | –0,1 |
| 1978 | NGK | K. Kostov | +0,06 | –1,1 | 0,0 | –0,3 |
| 1980 | NGK | K. Kostov, I. Butchvarov | –0,02 | +0,2 | – | –0,4 |
| 1984 | PAG | E. Ritter, W. Zander | +0,11 | +1,2 | – | +0,7 |
| 1986 | NGK | I. Cholakov, Ch. Georgiev | +0,18 | +0,1 | – | +0,3 |
| 1987 | PAG | E. Ritter | –0,86 | –2,2 | – | – |
| 1992 | CLF | I. Cholakov | +0,1 | –3,3 | +2,0 | +0,7 |
| 2003 | NGK | I. Cholakov, B. Srebrov | +0,23 | –2,6 | +1,0 | +0,16 |

Panagjurishte observatory owns the following classical instruments:

- Magnetic theodolite Mating & Wiesenberg for D and H (Gauß/Lammont);
- Oscillation box Mating & Wiesenberg for H;

- Earth inductor Mating & Wiesenberg for I;
- Two quartz variometers sets type "Bobrov" with photographic recording for H, D, Z and F.

Panagjurishte Observatory purchased the following proton magnetometers: an ELSEC 592/J in 1969, a PMP-2A in 1975, and a PMP-5A in 1989 from Central Geophysical Observatory Belsk of the Institute of Geophysics of the Polish Academy of Sciences, Warsaw. All observatory data were obtained on the base of this set of instruments until 2005. Figure 1 shows the ground plan of the observatory.

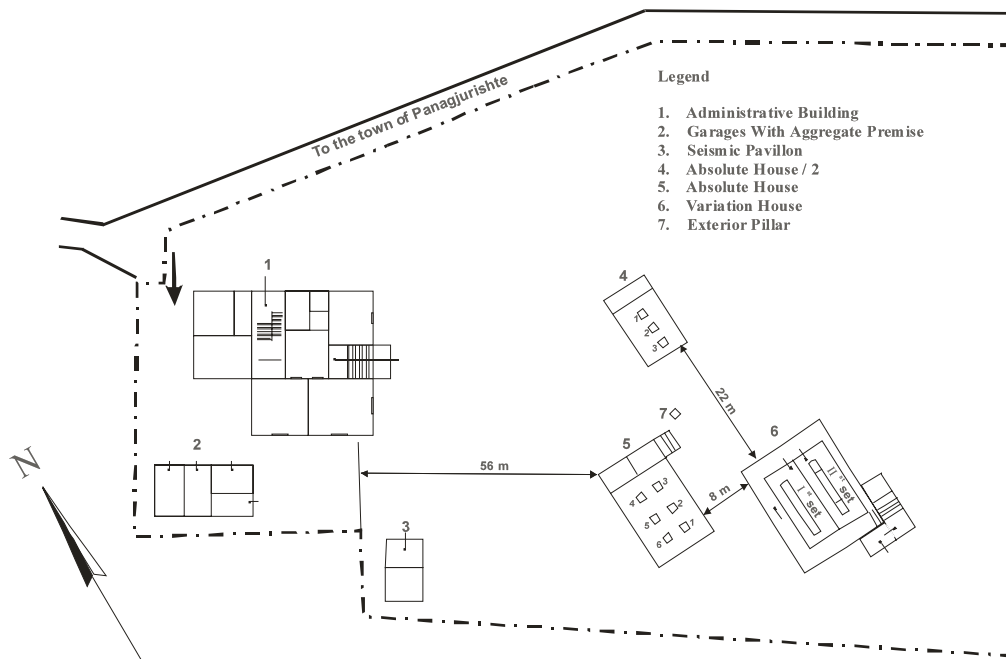


Fig. 1. Ground plan of Panagjurishte Observatory.

2. Instruments Upgrade

In 2005 the GeoForschungsZentrum Potsdam and the Geophysical Institute Sofia of the Bulgarian Academy of Sciences agreed in a contract on the upgrade of Panagjurishte Observatory to join the observatory to INTERMAGNET. The contributions of both partners are listed in Table 2.

The DI-flux, consisting of a Zeiss THEO 020B and a Bartington fluxgate MAG 01H was placed on pillar No. 5 in the absolute house. The azimuth value exists for this pillar. The observatory staff was trained to carry out the D and I absolute measurements by means of the instrument. They were also instructed to reduce the measurements by means of EXCEL tables, which were also provided by GFZ Potsdam.

The three-axial variometer MAGSON and the sensor of the Overhauser proton magnetometer GSM-90 were placed in the variometer house in the West room. The

data logger MAGDALOG (Linthe, 2004) was installed in the electronic box of the MAGSON (primary part) and in the main building (secondary part). The connecting glass fiber cable (RS232 connection) and the power supply cable were placed into a pipe, which connects in the underground both the buildings. A switching board, which carries the electronic box of the Overhauser proton magnetometer GSM-90, transformers, optical transmitters and further components, has been mounted in the entrance room of the variometer house.

Table 2
Contributions of the partners to the observatory upgrade

| GeoForschungsZentrum Potsdam | Panagjurishte Observatory of the IGP BAS |
|---|---|
| THEO 020B (Zeiss), MAG 01H (Bartington) | Computers and components |
| Three-axial fluxgate variometer MAGSON | Internet connection |
| Overhauser proton magnetometer GSM-90 | Network components |
| Data logger MAGDALOG | Operation system and network administration |
| Glass fibre cable and components | Installation |
| Staff training | |

Two computers were placed in the main building of the observatory: a DOS PC for running the secondary software of the data logger MAGDALOG and a Linux PC as central file server. Both PCs are connected by means of a LAN. A Windows PC is also connected to the LAN for any manual routine data processing. The LAN has connection to Internet for data transmission. The DOS PC, the Linux PC, the MAGDALG data logger, the MAGSON variometer and the GSM90 proton magnetometer are powered by an uninterruptible power supply unit (UPS) with a capacity of about 30 minutes.

The time base of the logger is a special GPS unit, which receives the satellite signal and sends the time information in DCF77 code (German radio clock signal) to the logger. Because of that, the normal logger software can be used to synchronize the primary PC clock. The GPS unit has been mounted on the roof of the main building. The time code is sent by one core of the glass fiber cable to the primary data logger in the variometer house. Lightning protection components were mounted at both ends of the power supply cable and into the cable of the GPS unit.

The installation of the instruments, data loggers and computers was carried out on 20-28 June 2005. Two people from Niemeck Observatory, several employees from the Geophysical Institute Sofia and the whole Panagjurishte staff were included. Also during this time interval, Panagjurishte staff was instructed to use the DI-flux, to reduce the absolute measurements and to handle the recording system.

The absolute measurements by means of the DI-flux theodolite are carried out weekly. The corresponding total intensity readings are taken from the GSM90 Over-

hauser proton magnetometer recordings taking into account the difference between the location of the GSM90 sensor and the measurement pillar No. 5. The pillar difference is checked regularly by means of measurements taken by the proton magnetometer PMP-5A at pillar No. 5, which are compared with the GSM90 recordings.

During the summers 2005 and 2006 very heavy thunderstorms happened in Bulgaria. Though lightning protection measures, the UPS was destroyed by very heavy lightnings and so the recording was out of work during the time intervals July-October 2005 and June-October 2006. Finally a suitable lightning protection system was installed to avoid such problems in future. Absolute measurements by means of the DI-flux were carried out even during summer time. The readings were reduced with the classical recordings.

In November 2006 a second recording system was installed again on the base of the cooperation contract. The GIBAS was able to purchase a suspended three-axial fluxgate variometer FGE manufactured by the Danish Meteorological Institute Copenhagen. The GIBAS further provided a DOS PC and the GFZ Potsdam installed a second data logger MAGDALOG. It is intended to complete the recording system by an Overhauser proton magnetometer GSM90.

3. First Measurement Results

At present, 18 months of absolute measurements by means of the DI-flux theodolite and nearly one year of continuous MAGSON recordings are available. The obtained base lines are very satisfying. Figure 2 shows the reduced absolute measurements and the adopted base lines for the recorded elements H, D and Z. The reduced measurements by means of the classical instrument set are drawn as rectangles. Those of the DI-flux in combination with the Overhauser proton magnetometer GSM90 (taking into consideration the pillar difference) are depicted as triangles. The classical measurements were reduced using the Bobrov type photographic recording variometers. The DI-flux measurements were reduced by means of the MAGSON recordings. The dashed lines represent the adopted base lines obtained from the reduced absolute measurements by means of the Mating & Wiesenberg and PMP-5A instrument set. The solid lines are the base lines adopted from the reduced absolute measurements by means of the DI-flux theodolite on pillar No. 5 and the GSM90 Overhauser proton magnetometer. The total intensity difference between pillar No. 5 and the GSM90 was determined to:

$$\Delta F_{\text{GSM90-P5}} = F_{\text{GSM90}} - F_{\text{P5}} = -38.6 \text{ nT} . \quad (1)$$

The proton magnetometer PMP-5A has an instrumental offset against an Overhauser proton magnetometer GSM19 (owned by GFZ Potsdam) of:

$$\Delta F_{\text{PMP5A-GSM90}} = F_{\text{PMP5A}} - F_{\text{GSM90}} = 1.0 \text{ nT} . \quad (2)$$

The other proton magnetometer PMP-2A was also tested. It does not have any offset against the Overhauser proton magnetometer GSM19. The instrumental offset is taken into consideration, when the difference between pillar No. 5 and the GSM90 is checked by measurements taken by means of the proton magnetometer PMP-5A.

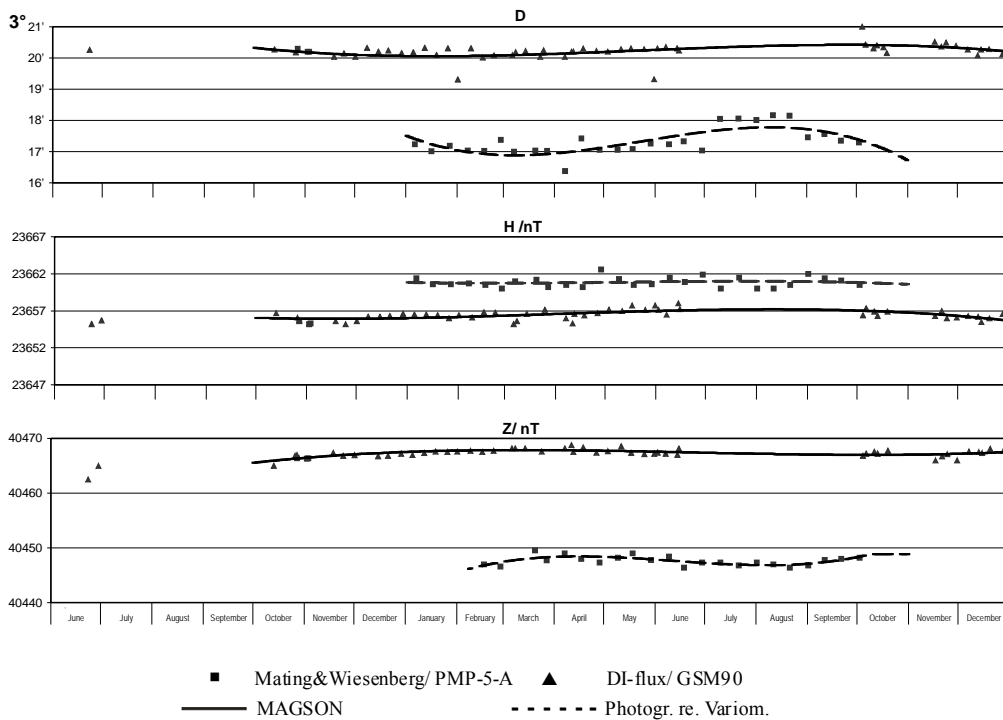


Fig. 2. Absolute measurement results and adopted base lines for the classical and the new instrument set.

The final observatory data, obtained by means of the new instrument set, show clearly offsets in the magnetic elements against the data from the classical instrument set. First estimations determined the offsets to:

$$\Delta H = H_{MW} - H_{DIflux} \approx -6.3 \text{ nT}, \quad (3)$$

$$\Delta D = D_{MW} - D_{DIflux} \approx -0.1', \quad (4)$$

$$\Delta Z = Z_{MW} - Z_{DIflux} \approx +4.2 \text{ nT}, \quad (5)$$

with MW: Element level of the classical instrument set;

DIflux: Element level of the “new” instrument set.

They are caused by several influences. The first reason is that there are pillar differences in the absolute house. The pillar differences are well determined. They are listed in Table 3. The differences of the special magnetic elements can be found in the single lines. The columns are ordered after the pillars.

The pillar differences alone do not explain the offset levels. The classical measurements are taken at 3 different pillars (declination and horizontal intensity by means of the Mating & Wiesenberg theodolite at pillar No. 1, horizontal intensity by means of the oscillation box at pillar No. 2, inclination by means of the earth inductor at pil-

lar No. 6, and total intensity by means of the proton magnetometer PMP-5A as well at pillar No. 6). The DI-flux measurements are taken at pillar No. 5. The second reason is obviously a systematic error in the absolute determination of the horizontal intensity by means of the classical magnetic theodolite and the oscillation box. This fact was also found when Niemeck Observatory changed from the classical instrument set to the DI-flux and proton magnetometer (Best *et al.* 1997).

Table 3

Pillar differences in Panagjurishte absolute house

| Element | P ₁ -P ₅ | P ₆ -P ₅ | P ₁ -P ₆ |
|------------|--------------------------------|--------------------------------|--------------------------------|
| ΔD | -0.4 ' , | - | - |
| ΔH | -0.3 nT | - | - |
| ΔZ | -0.4 nT | -2.1 nT | +1.7 nT |
| ΔF | - | -0.3 nT | +0.4 nT |

After the final data processing the Panagjurishte level offset between the classical and the new system will be stated with the annual mean values as a jump in the level of the observatory with the beginning of the year 2007.

4. Summary

With the instrumental upgrade of Panagjurishte Observatory, a long tradition of international cooperation has been continued. So one long-term geomagnetic observatory more obtained INTERMAGNET standard. On the base of the cooperation contract both the partners contributed to this success. GFZ will continue the support for Panagjurishte Observatory by further upgrades of the software and in the preparation of the final observatory data. The status of an IMO (INTERMAGNET observatory) has been applied.

References

- Best, A., and H.-J. Linthe, 1997, Ergebnisse der Beobachtungen am Adolf-Schmidt-Observatorium für Geomagnetismus in Niemeck im Jahre 1996, Jahrbuch 1996 des Adolf-Schmidt-Observatoriums Niemeck, Potsdam.
- Cholakov, I., 1998, *60 Years Geomagnetic Observatory Panagyurishte*. VIIth IAGA Workshop on Geomagnetic Observatory Instruments, Data Acquisition and Processing, September 8-15, 1996, Adolf Schmidt – Observatory for Geomagnetism Niemeck, STR 98/21, Potsdam, pp. 17-24.
- Linthe, H.-J., 2004, *MAGDALOG – Data logger for magnetic observatories*. Proceedings of the XIth IAGA Workshop on Geomagnetic Observatory Instruments, Data Acquisition and Processing, November 9-17, 2004, Kakioka and Tsukuba, Japan, pp. 90-94.

Accepted March 7, 2007

New INTERMAGNET Fluxgate Magnetometer

V. KOREPANOV¹, YE. KLYMOVYCH¹, O. KUZNETSOV¹, A. PRISTAY¹,
A. MARUSENKOV¹ and J. RASSON²

¹Lviv Centre of Institute of Space Research NAS and NSA of Ukraine
e-mail: marand@isr.lviv.ua

²Institut Royal Meteorologique, Centre de Physique du Globe
B-5670 Dourbes Belgium
e-mail: jr@oma.be

Abstract

The peculiarities of a candidate INTERMAGNET compatible 1-second magnetometer design are considered and analyzed. A new magnetometer functional diagram, which combines analogue and digital processing, is proposed. The first results of the magnetometer prototype tests are presented and discussed.

1. Introduction

The major part of ground-based magnetometer systems provides digital data as 1-minute means today. They cover, therefore, a spectrum narrower than that provided by the 20 mm/h photographic recordings of the past. This is somewhat in contradiction with the needs of present scientific applications, which require having broadband data, i.e. data with increasingly fast temporal resolution.

To address this shortcoming, INTERMAGNET decided at its Dourbes meeting in 2003 to create a new recording standard based on a 1 second means data acquisition. The first requirements for such a geomagnetic data acquisition system were compiled during an INTERMAGNET survey investigating the needs of the scientific community using geomagnetic time series data (Love 2005). The main consensus of the survey is as follows: geomagnetic data acquired at 1 Hz sampling should have 0.01 nT resolution at least, be filtered by a digital filter and be centered onto the UTC second within 0.01 s.

This large increase in the operational frequency range met some important difficulties, the most serious of which are discussed and addressed below.

2. Requirements to the New 1 s INTERMAGNET Magnetometer

Presently, with even relatively noisy instruments, e.g. with 100 pT/sqrt(Hz) @ 1 Hz, the noise level does not prevent to reach a signal-noise ratio better than 1 in the full operational frequency range when averaging for 1-minute data.

The necessity to measure quicker magnetic fluctuations requires using instruments with much lower noise level – 1 pT/sqrt(Hz) @ 1 Hz and below. As a rule the induction sensors are used for these purposes. But some progress in design of flux-gate sensors gives us expectation to use it also for measurement of magnetic fluctuations within the so called “dead band” at 0.1–1 Hz frequency. So, the new 1-second INTERMAGNET compatible magnetometer should provide an extremely low noise level as compared to other flux-gate instruments.

The decrease of the noise level and preserving the same upper limits of the measured fluctuations automatically require bigger dynamic range of the instrument. The coarse calculations show that even using the internationally accepted 10 pT resolution and the range of measurement ± 5000 nT, the necessary dynamic range is equal to 120 dB. For providing such value, at least a 20-bit ADC should be used.

The other problem which arises is to provide a sufficient level of immunity to manmade (industrial) noise, especially as produced by power lines. Really, in comparison with the 1-minute magnetometer the 1-second one is sixty times closer to 50/60 Hz mains harmonics and the probability of aliasing to the passband is much higher. Moreover, against a background of the lower noise of the instrument the mains interference will be more considerable. The quite realistic estimation of the level of magnetic fields produced by power lines is $A_{50} = (1 - 100)$ nT_{rms}. In order to estimate the necessary suppression factor K of this type of noise two criteria could be used: spectral density cleanliness and wideband signal-noise ratio. In both cases the 50 Hz products could be compared with the magnetometer noise as well as with the geomagnetic variations. Let us approximate spectral density of geomagnetic fluctuations b_g and magnetometer noises b_n by the following expressions:

$$b_g = b_{g0} \cdot \frac{f_0^3}{f \cdot (f + f_1)^2}, \quad (1)$$

$$b_n = b_{n0} \cdot \left(1 + \frac{f_{n0}}{f} \right), \quad (2)$$

where b_{g0} = geomagnetic fluctuations spectral density value at frequency f_0 ; f_1 = corner frequency of the geomagnetic variations (below this frequency the slope of the spectrum decreases to 3 dB/octave); b_{n0} = the magnetometer noise spectral density value at the so-called plateau; f_{n0} = corner frequency, below which magnetometer noises increase.

The wideband signal-noise ratio criterion in the given frequency band can be described by the expression:

$$\frac{B}{A_{50}/K} \geq 1 \Rightarrow K \geq \frac{A_{50}}{B}, \quad (3)$$

where B = level of the signal in the band from f_{\min} to f_{\max} . The spectral density cleanliness criterion is given by the expression:

$$\frac{\sqrt{b(f)}}{A_{50}/(K \cdot f_{\min}^{1/2})} \geq 1 \Rightarrow K \geq \frac{A_{50}}{\sqrt{b(f)} \cdot f_{\min}}. \quad (4)$$

The estimations of the suppression factor were calculated taking into account the following values of the parameters: $f_{n0} = f_0 = 1$ Hz; $\sqrt{b_{n0}} = \sqrt{b_{g0}} = 1$ pT·Hz^{-1/2}; $f_{\max} = 0.5$ Hz; $f_1 = 0.0002$ Hz; $A_{50} = 1$ nT. They are presented in Table 1. From this table it follows that the necessary suppression factor of 50-Hz signal could reach 120 dB and more.

Table 1
Estimations of the necessary 50-Hz suppression factor

| f_{\min} , Hz | SNR | | Spectral density cleanliness | |
|--------------------|-------------------------|------------------------------|------------------------------|------------------------------|
| | K1, dB (Magn. noise) | K2, dB (Geomagn. variat.) | K3, dB (Magn. noise) | K4, dB (Geomagn. variat.) |
| 10^{-1} | 131 | 99 | 60 ... 65 | 0 ... 61 |
| 10^{-2} | 123 | 53 | 60 ... 75 | 0 ... 71 |
| 10^{-3} | 119 | 9 | 60 ... 85 | 0 ... 81 |
| 10^{-4} | 116 | 0 | 60 ... 95 | 2 ... 91 |
| 10^{-5} | 114 | 0 | 60 ... 105 | 20 ... 101 |
| 10^{-6} | 112 | 0 | 60 ... 115 | 40 ... 111 |

3. The particularities of the magnetometer design

So, the new magnetometer should provide fast frequency response on the one hand, and deep suppression of the mains harmonics on the other hand. In order to fulfil these mutually contradictory requirements we propose the following magnetometer structure (Fig. 1).

The frequency response of the magnetometer itself corresponds to a first order low pass filter. For suppressing 50/60 Hz interferences, the output signal of the magnetometer is fed to an analogue second-order notch filter, which is connected to the input ADC. Optionally an anti-aliasing low-pass filter could be added at the ADC input. ADC output data is going through the linear phase digital low-pass filter and the flow of 10 Hz data is formed. These data enter the PC, where further operations are performed. By applying a 10-Hz data Gaussian low-pass digital filter similar to the INTERMAGNET 1-minute one, the final 1-second data are produced and recorded.

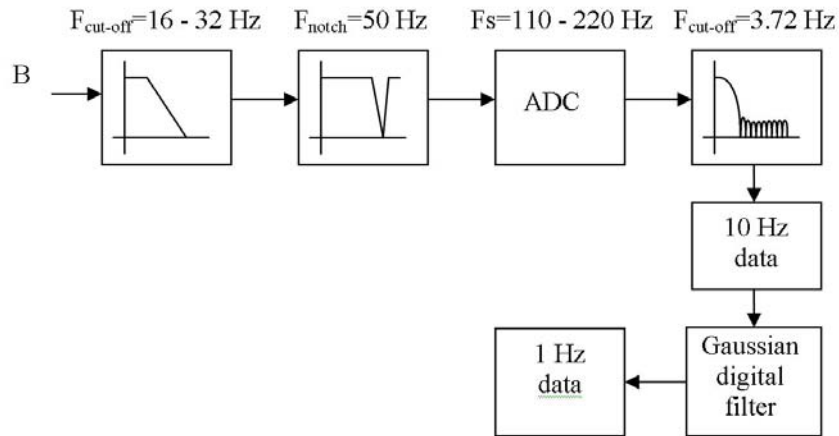


Fig. 1. The new INTERMAGNET compatible magnetometer functional diagram.

The cut-off frequency of the magnetometer analogue channel is selected in the band between 16-32 Hz, which allows preserving the condition of a small (5-10 ms) and linear phase delay in the frequency band from DC to 10 Hz. Such a value of the cut-off frequency simultaneously provides practically negligible attenuation of the measured signals at frequencies below 1 Hz.

The Q-factor of the 50 Hz notch-filter should be relatively high in order to minimize phase delay and amplitude attenuation in the operational frequency range. The calculations show that using a second-order notch-filter with $Q > 10$, the additional phase delay will be no more than 0.4 ms at frequencies up to 10 Hz, and the passband amplitude attenuation may be neglected.

The low-pass digital filter was chosen taking into account the following considerations: linear phase delay, maximal bandpass flatness, zero of amplitude-frequency response at the frequencies 10, 50 and 60 Hz, deep suppression of the signal above 10 Hz. All these requirements are successfully fulfilled by the finite-impulse response filter based on the so-called flat-topped window, which is presented in Fig. 2.

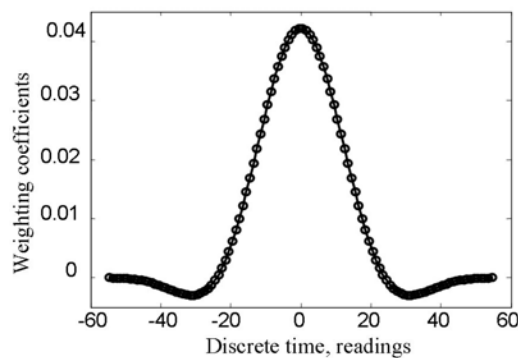


Fig. 2. The flat-topped time window.

The frequency and phase response of the digital filter at sampling frequency $F_s = 220$ Hz are presented in Fig. 3. As it is clearly seen, the filter frequency response has multiple zeros at every multiple of 2 Hz starting from 10 Hz and the maximal level of the minor lobes is less than -81 dB. The cut-off frequency at level -3 dB is equal to 3.72 Hz and the gain errors at the frequencies of 0.5 and 1 Hz are equal to $+0.03$ and -0.103% , correspondingly. The relatively big phase delay is highly linear and stable due to the quartz-stabilized ADC sampling frequency and can easily be corrected for by shifting the data time scale by the corresponding value of 256 ms. The parameters of the magnetometer frequency response are presented in Table 2.

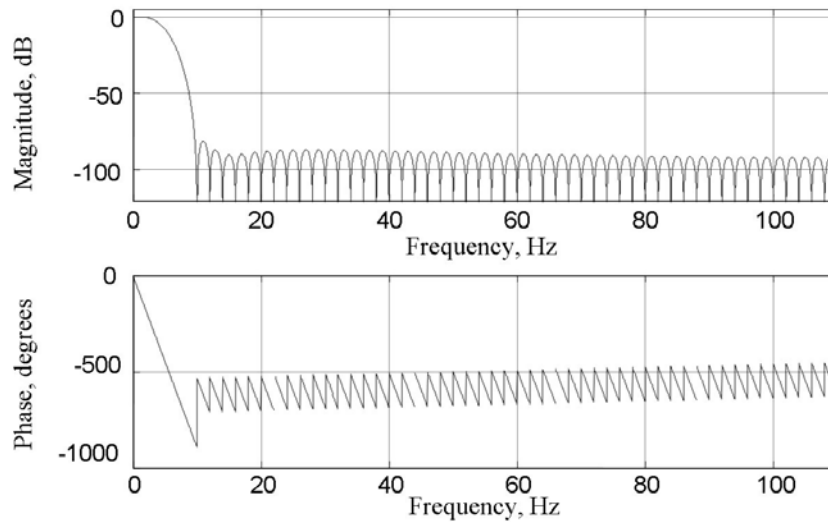


Fig. 3. The frequency response of the digital filter.

Table 2

Total frequency response

| Frequency | 0.001 | 0.1 | 0.5 | 1.0 |
|-------------|----------------|---------------|---------------|---------------|
| Attenuation | 0.0% | 0.0004% | -0.002% | -0.23% |
| Phase | -0.093° | -9.22° | -46.1° | -92.2° |
| Delay | 256.12 ms | 256.12 ms | 256.12 ms | 256.12 ms |

4. The Results of Tests of New Magnetometer Prototype

The first attempt to realize the proposed functional diagram of the magnetometer was carried out. The prototype was constructed using a magnetometer based on the traditional analogue design and an existing data acquisition system (CAM-unit), which is produced by LC ISR for collecting data from search coil sensors (LC ISR, 2005).

The CAM-unit contains three GPS synchronised 24-bits ADC's, which provide simultaneous analogue-to-digital conversions of all three magnetometer output channels with a sampling frequency of $F_s = 256$ Hz. These data were transferred to the PC, where the on-line digital filtration procedure was performed. The filtered data is then decimated to 16 Hz and stored in the PC hard disk. The functional diagram of the prototype sufficiently corresponds to what is described above (see Fig. 1). To this end, an existing 4-order low-pass filter embedded into the CAM-unit was left in operation. The cut-off frequency of this filter is to 100 Hz which still gave about 6.5 ms of an additional phase delay for signals in the passband.

The prototype was tested at the Dourbes Geomagnetic Observatory of the Royal Meteorological Institute of Belgium. The results of the tests are described below. The frequency and phase response of the analogue part of the instrument (measured at the test point just at ADC input) is presented in Fig. 4.

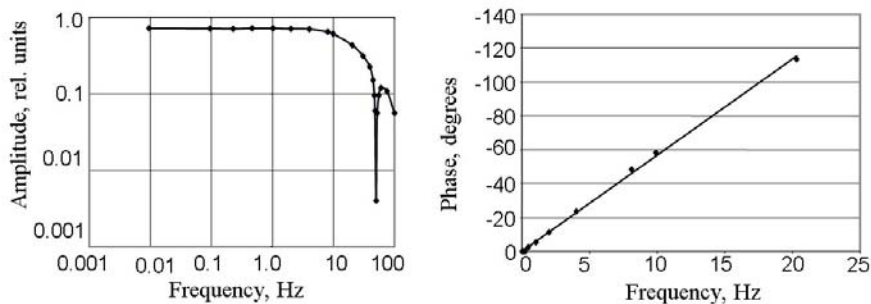


Fig. 4. The frequency and phase response of the analogue channels of the prototype.

The scale factors, range and linearity of the transfer function and noise measurements were carried out using the special facility – the K^{39} full field stabilizer (Fig. 5a), which produces a given magnetic field with high stability and low noise level. It was found that the measurement range of the instrument is equal to ± 3000 nT and linearity of the transfer function is better than 100 ppm for all magnetometer components. The tested magnetometer noise of Z-component in the stabilized field of 44000 nT is presented in Fig. 5b. The standard deviation during a 1-minute record is 0.013 nT. The noise spectra calculated using long time records are presented in Fig. 6. The noise level measured in the full field stabilizer is close to the one measured in the magnetic shield at LC ISR. Some small difference could be explained by the extra noise of stabilizer products at frequencies 0.2 Hz, 0.4 Hz, 0.8 Hz etc.

Such a low noise prototype allowed us to measure geomagnetic variations starting from 0.3 Hz and below, which is in good agreement with Nyquist bandwidth of 1-second sampled data. The executed analysis showed that this design concept allows us still to raise temporal resolution of such a magnetometer till 0.1 second while maintaining the severe INTERMAGNET requirements as to phase shift and filtration parameters. The only improvement which is still necessary is to lower the magnetometer noise below 1 pT.

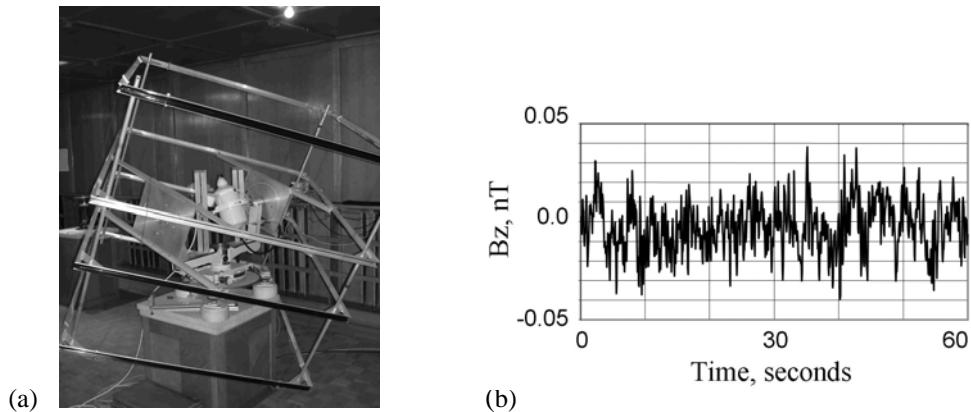


Fig. 5. The K^{39} full field stabilizer and the prototype noise in the stabilized 44000 nT field.

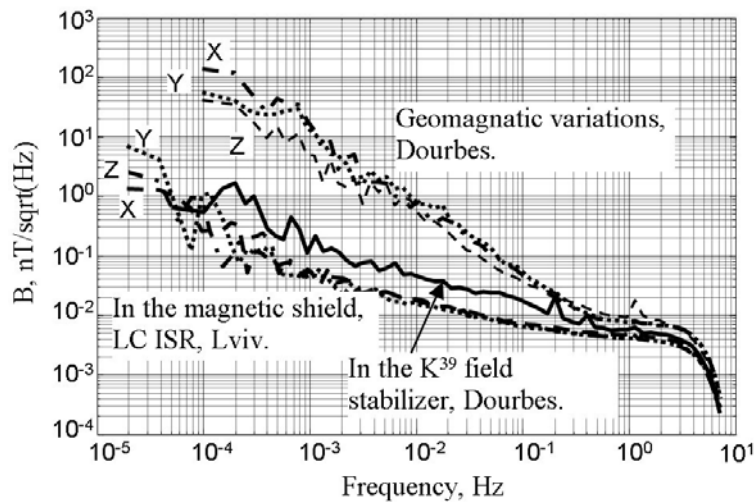


Fig. 6. The spectra of the magnetometer prototype noise and of the geomagnetic variations.

5. Conclusion

The particularities for a candidate INTERMAGNET 1-second magnetometer are considered and analyzed. In order to fulfil the conflicting requirements for its frequency response, a new magnetometer functional diagram, which combines analogue and digital filters, is proposed. Using this approach a prototype was designed, built and successfully tested. The results of the tests demonstrate the possibility to satisfy the specifications regarding the timing accuracy (< 0.01 s error), data resolution (< 0.01 nT) and noise level. The proposed magnetometer could even be used at a 0.1-second sampling, if the minimization of flux-gate sensors noise is provided to the required level. However, it was also shown that the digital filter realized for the magnetometer prototype using an external PC with a corresponding executable is unreliable because of possible errors in the data transmission channel, computer and magnetome-

ter. For the next step it is planned to implement the proposed filtration algorithm into the magnetometer hardware using an high-speed microprocessor. The parameters of such magnetometer and results of its tests will be presented to the observatory community within one year.

References

- Love, J.J., 2005, *1-Second Operational Standard for Intermagnet, Minutes of the OPSCOM/EXCON INTERMAGNET meeting, Mexico 2005*, unpublished.
- LC ISR, 2005, *Satellite synchronized ULF induction magnetometer set*, <http://www.isr.lviv.ua/LEMI30.htm>, 133 kB.

Accepted February 29, 2007

Magnetic Observatories in the 21st Century: an Endangered Species?

David KERRIDGE

British Geological Survey
Murchison House, West Mains Road,
Edinburgh, EH9 3LA, Scotland, UK
e-mail: djk@bgs.ac.uk

Abstract

Magnetic observatories have a long history of producing data that has led to many scientific discoveries. However, a long history is no guarantee of a long future and it is important to keep under review the factors that influence the support given to magnetic observatory operations. The data that observatories produce must be seen to be relevant to current and future scientific research, and also to 'real-world' applications. By understanding local and international demands for data, in terms of quality, resolution and availability, observatories can tailor their operations, choosing appropriate instrumentation and methods for data acquisition processing and distribution. The INTERMAGNET programme has attempted to address several of these issues.

1. Introduction

Because of the utility of the magnetic compass for navigation and curiosity about the magnetic properties of the Earth, geomagnetic field measurements have been made and recorded for more than 400 years. The main spatial and temporal variations of the geomagnetic field, including correlations with auroral sightings and solar activity, were discovered by the middle of the 19th century. Systematic observations of the geomagnetic field at multiple locations, the start of the development of a global magnetic observatory network, began with the establishment, by Gauss, of the Göttingen Magnetic Union in 1834. Further impetus to the development of the network was given by the International Polar Years, and particularly by the International Geophysical Year, which ran from July 1957 to December 1958. More recently, the INTERMAGNET programme has helped to accelerate the modernisation of observatories and coordinate activities across the international network.

Although early observations established a good deal of the phenomenology of the geomagnetic field, scientific understanding remains incomplete, and there is strong interest in geomagnetism and solar-terrestrial interactions today. The broad scientific objective is to develop understanding of the sources and processes, internal and external to the Earth's surface, which generate the magnetic fields that combine to produce the overall field observable at any point in space and time. Data help to constrain theories, and magnetic observatories are a source of such data.

The role and importance of synoptic measurements to solar-terrestrial physics was the subject of a study commissioned by the Royal Society of London (1992), the findings of which were also reported by Willis *et al.* (1994). (The term 'synoptic data' was defined as data acquired in a consistent fashion over a long period of time, generally at several sites, providing a general survey of conditions.) The Royal Society study, which considered the role of magnetic observatories, cited the underpinning value of synoptic data to fundamental research, the relevance to studies of global change, the potential for new discoveries, and practical applications, as benefits of long-term monitoring. The general scientific requirements for a global geomagnetic observatory network were discussed in a report to the US Geodynamics Committee (Heiztler *et al.* 1994), and by Langel *et al.* (1995) who emphasized the requirements for geomagnetic main field modelling.

A decade on from these studies it is worth re-examining the role of magnetic observatories. Recent satellite missions have re-invigorated scientific research into geomagnetism and it is a reasonable expectation that there will be near-continuous observations made by satellites in the future. This raises the question of whether satellites can replace some observatory functions. Also, the funding environment for scientific research has changed. The relevance of research to societal concerns such as health, wealth and safety are factors currently influencing funding decisions in directed research programmes. Does observatory science contribute to the understanding of what are now commonly considered to be priority issues?

2. The Core Field

A strong motivation in running magnetic observatories is to monitor the evolution of the Earth's main magnetic field, originating in the fluid outer core. The importance of long-term observations in support of this endeavour is illustrated in Fig. 1 where (irregular) declination measurements at a number of locations in the vicinity of London, and regular measurements at the observatories in Greenwich (1842-1925), Abinger (1926-1956) and Hartland (1957-2005) are plotted together. (Simple site differences between the observatories have been applied to approximately reduce the data to Greenwich.) The plot shows that, over the last 425 years, magnetic declination has varied between extremes of around 11°E and 25°W in London.

Long data series, such as those in Fig. 1, are important in characterizing the scales of temporal variations in the core-generated field, which are termed secular changes. The typical time scale is years to centuries, and the typical magnitude is 10-100 nT y⁻¹. These parameters help to define the observational requirements for magnetic observatories: they should run for many years, achieve measurement accuracy in

all components of the field vector of around 1 nT, and maintain the long-term stability needed to resolve the typical secular change signal.

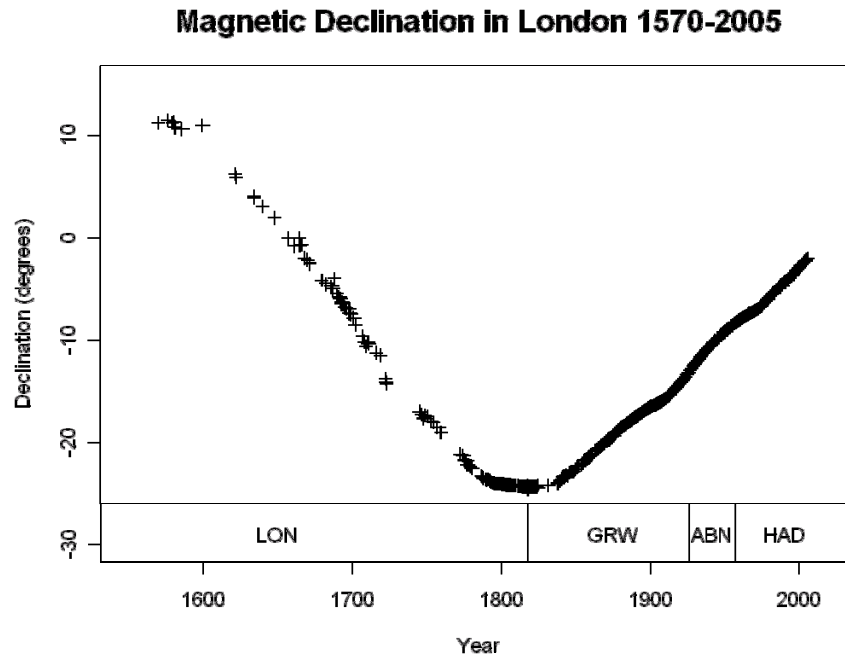


Fig. 1. A composite plot of magnetic declination measurements from sites around London (LON), and Greenwich (GRW), Abinger (ABN) and Hartland (HAD) magnetic observatories.

Put into a more mathematical form, the geomagnetic field \mathbf{B} at position \mathbf{r} and at time t may be expressed relative to its state at time t_0 in the form of a Taylor series:

$$\mathbf{B}(\mathbf{r}, t) = \mathbf{B}(\mathbf{r}, t_0) + \frac{\partial \mathbf{B}(\mathbf{r}, t_0)}{\partial t} (t - t_0) + \frac{\partial^2 \mathbf{B}(\mathbf{r}, t_0)}{\partial t^2} \frac{(t - t_0)^2}{2} + \dots \quad (1)$$

The first term on the right hand side of the equation is the ‘snapshot’ of the main field at time t_0 , the time rate of change of the main field in the second term is the geomagnetic secular variation and the second time derivative of the field is the secular acceleration. The accuracy of this approximation depends on the time interval $(t - t_0)$ and on the spectrum of the time variations of the field.

Considering Eq. (1), and the typical time scales of secular changes, it is reasonable to approximate the main field snapshot at an observatory location by an annual mean value and estimate the secular variation by differencing annual means. Most global geomagnetic field models have the form of Eq. (1), using spherical harmonic functions to describe the spatial variation of the main field and the secular variation. An example is the 10th generation International Geomagnetic Reference Field (IGRF), with a nominal lifetime of five years (Macmillan and Maus 2005).

In fact, there are features of secular change on rather shorter timescales that are not immediately apparent in plots such as Fig. 1. In Fig. 2 the first differences of the declination data shown in Fig. 1, for 1900 onwards are plotted. (No correction for the spatial gradient in secular variation between London and Hartland has been made.) There are several abrupt changes in the slope of the secular variation curve for declination, the majority in recent decades. The existence of such ‘geomagnetic jerks’ was first recognised by Courtillot *et al.* (1978) and Malin *et al.* (1983), who noted the step change in secular acceleration at 1969/70.

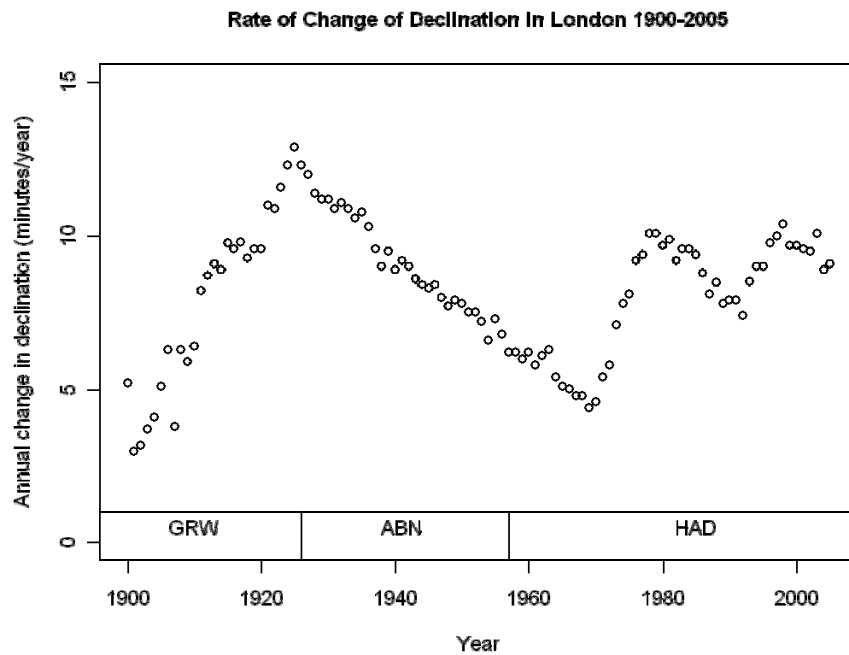


Fig. 2. Secular variation of declination in London estimated using data from Greenwich (GRW), Abinger (ABN) and Hartland (HAD) magnetic observatories.

The main field and secular variation provide a means of probing the pattern of fluid motions at the core surface, yielding an estimate of a typical velocity of about 10 km y^{-1} (e.g. Gubbins 1982, Whaler 1982). The observation of jerks has provoked questions concerning the nature of the core dynamo and the electrical conductivity of the mantle, and intriguing correlations have been found with decadal changes in the length of the day, linking geomagnetic observations to exchange of angular momentum between the mantle and the core (e.g. Holme and de Viron 2005).

3. External Fields

With the adoption of continuous recording instruments at magnetic observatories, studies of the patterns of short-term changes in the geomagnetic field and their geographical distribution became possible. Cycles in geomagnetic field behaviour such as

the annual and solar cycle modulations of the solar quiet time variations, the 27-day recurrence pattern in magnetic disturbances, and the semi-annual variation in the frequency of magnetic storms, emerged. Our current understanding of the electric current systems in the ionosphere and magnetosphere, and the magnetic fields they create, has resulted from various types of measurement on the ground and, (crucially for mapping the magnetosphere) in space, and data from magnetic observatories have played a part.

In recent years, long-term changes in the nature of short-term effects of external origin have come to light. The source of these effects is solar forcing, whether by means of electromagnetic radiation or interactions of the main geomagnetic field with the solar wind. If the Earth as the 'receiver' is not changing in its response, the changes most likely reflect changes in the behaviour of the Sun. Figure 3 shows the annual number of magnetic storms per year since 1868, with the count based on the *aa* index, together with sunspot number. The upward trend in magnetic activity during the 20th century is evident, and Clilverd et al. (1998, 2002) ascribe this to changes in solar activity. Lockwood (1999) explained the effect in terms of changes in the solar coronal magnetic field, with a consequent effect on total solar irradiance. If this theory is correct, then there are implications for the natural component of climate change. Courtillot et al. (2007) have reviewed the evidence for a connection between geomagnetism and climate change provided by a number of recent analyses of long series of geomagnetic and solar data (see references therein).

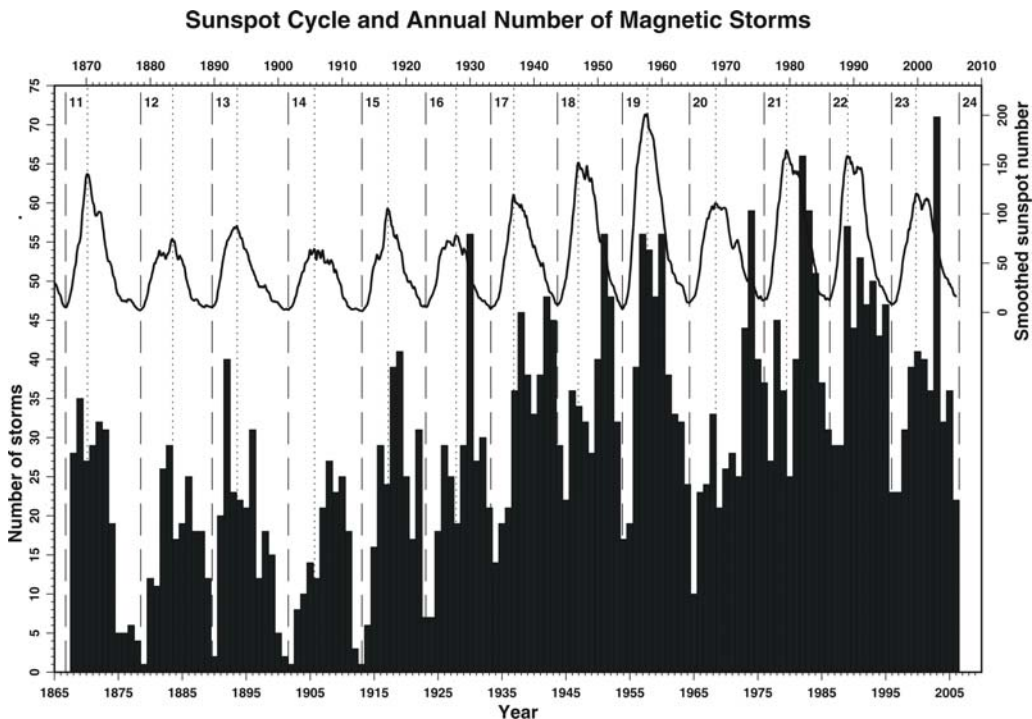


Fig. 3. Changes in magnetic storm activity (histogram) and sunspot numbers (line) 1868-2006.

4. Modern Applications of Magnetic Observatory Data

One of the early motivations for establishing magnetic observatories was to provide data for navigation. Modern developments, especially the availability of GPS to all sectors, including low-cost receivers for the general public, have relegated the magnetic compass to the status of a back-up device for many activities. An important application running counter to this general trend is the use of the geomagnetic field as a directional reference for production drilling in the hydrocarbons industry (Russell *et al.* 1995). The reference geomagnetic field data at a drilling site are usually computed using a global geomagnetic field model. In some instances, data from nearby observatories are used to monitor the state of disturbance of the field, especially where near-real-time access to the data is possible (Reay *et al.* 2005).

When the geomagnetic field is disturbed, the accuracy of magnetic navigation decreases and the level of hazard posed to a range of technologies increases. The reality of the risk posed to electrical distribution networks during magnetic storms was made clear by the well-known event of March 1989 when Quebec lost its electricity supply because of Geomagnetically Induced Currents (GIC) flowing into the power distribution system. It is a real possibility that the likelihood of similar events will increase in the future as grid systems become more interconnected. Magnetic observatories provide data on the inducing magnetic fields and, in combination with knowledge of the Earth's conductivity structure, these data can be used to model the GIC flowing in an electrical grid system and provide data to support decision-making by grid operators (e.g. Thomson *et al.* 2005).

There are many more examples of applications that make use of magnetic observatory data. For instance, observatories act as national standards bodies in many countries, offer calibration facilities and act as reference stations for magnetic surveys. Other applications, such as launch planning and management of low Earth orbit (LEO) satellites, rely on solar and magnetic activity indices for atmospheric density modelling (e.g. Mugglesi and Kerridge 1991).

5. INTERMAGNET (www.intermagnet.org)

INTERMAGNET aims to create a global near-real-time geomagnetic monitoring system by co-ordinating the activities of the worldwide network of national observatories. By the end of 2006, 100 magnetic observatories, more than half of the total number of observatories in operation worldwide, were participating. INTERMAGNET has improved observatory operations and improved access to high-quality near-real-time globally-distributed magnetic observatory data for the international scientific research community. These achievements have resulted from a range of activities including: definition of target standards for observatory operations; provision of technical advice and assistance to raise standards; establishment of Geomagnetic Information Nodes (GINs) to collect data; web delivery of data; publication of an annual CD-ROM of definitive data from participating observatories with independent quality control; co-operation with other organisations including the World Data Centres and the International Association of Geomagnetism and Aeronomy (IAGA) on matters such as data

formats; and, 'horizon scanning' to ensure that observatories are prepared to meet future scientific needs and that relevant technological developments are recognised. Examples of current challenges are automation of absolute measurements of the geomagnetic field vector, and meeting the demand for high time resolution data from the space physics community.

6. Conclusions

Magnetic observatories have contributed to many important scientific discoveries because they have produced long series of continuous, high quality measurements at low-noise sites, and significant new results based on observatory data continue to be published. Because of important discoveries in climate-related fields such as ozone depletion over Antarctica (Farman *et al.* 1985) and global dimming deduced from evaporation pan measurements (e.g. Stanhill and Cohen 2001), there is an increasing appreciation of the benefits of long-term monitoring to acquire data on the state of the planet. This increased appreciation is apparent in the establishment of GEO, dedicated to developing a Global Earth Observation System of Systems (GEOSS). GEO will coordinate the operations of various types of monitoring systems, improving interoperability and access to data and information. GEO began as an initiative of the space sector in Earth Observation, but now embraces ground-based observations. INTERMAGNET intends to provide the link from geomagnetism to GEOSS.

The Ørsted and CHAMP satellite missions, launched in February 1999 and July 2000, respectively, have produced excellent magnetic survey data and opened up new possibilities for geomagnetic field research. The success of these missions in generating new knowledge and understanding has been influential in making the case for the SWARM constellation of three satellites to be launched in 2010 by the European Space Agency. In some respects this success can be seen as a threat to observatory operations; for example, studies investigating whether secular variation can be determined from satellite data have been carried out (e.g. Mandaia and Olsen 2006). Provision of secular variation data is the traditional role of magnetic observatories. In practice, for a variety of purposes – discrimination between different magnetic field sources is one example – there are advantages to be gained by combining observatory and satellite data; the two data types are complementary.

Magnetic observatories continue to meet the expectations of synoptic monitoring as described in the 1992 Royal Society report in all respects. The challenge to future operations is to respond effectively to the needs of interest groups in science, government and the private sector. There is good reason for optimism because of the strong relevance of observatory data to the needs of these groups.

Acknowledgments. This paper is published with the permission of the Executive Director, British Geological Survey (NERC).

References

- Clilverd, M.A., T.D.G Clark, E. Clarke and H. Rishbeth, 1998. *Increased magnetic storm activity from 1868 to 1995*, J. Atmos. Solar-Terr. Phys. **60**, 10, 1047-1056.
- Clilverd, M.A., T.D.G Clark, E. Clarke, H. Rishbeth and T. Ulrich, 2002. *The causes of long-term change in the aa index*, J. Geophys. Res. **107** (A12), 1441.
- Courtilot, V., J. Ducruix and J.-L. Le Mouél, 1978, *Sur une accélération récente de la variation séculaire du champ magnétique terrestre*, C. R. Acad. Sci. Paris, 287, Série D, 1095-1098.
- Courtilot V., Y. Gallet, J.-L. Le Mouél, F. Fluteau and A. Genevey, 2007, *Are there connections between the Earth's magnetic field and climate?*, Earth Planet. Sc. Lett. **253**, 3-4, 328-339.
- Farman, J.C., B.G. Gardiner and J.D. Shanklin, 1985, *Large losses of total ozone in Antarctica reveal seasonal ClOx/NOx interaction*, Nature **315**, 207-210.
- Gubbins, D., 1982, *Finding core motions from magnetic observations*, Phil. Trans. R. Soc. Lond. A **306**, 1492, 247-254.
- Heirtzler, J., J. Booker, A. Chave, A.W. Green, R. Langel and N.W. Peddie, 1994, *An enhanced geomagnetic observatory network*. Report to the US Geodynamics Committee, National Research Council, 67pp.
- Holme R., and O. de Viron, 2005, *Geomagnetic jerks and a high-resolution length-of-day profile for core studies*, Geophys. J. Int. **160**, 2, 435-439.
- Langel, R.A., R.T. Baldwin and A.W. Green, 1995, *Toward an improved distribution of magnetic observatories for modeling of the main geomagnetic field and its temporal change*, J. Geomag. Geoelectr. **47**, 475-508.
- Lockwood, M., R. Stamper and M.N. Wild, 1999, *A doubling of the Sun's coronal magnetic field during the last 100 years*, Nature **399**, 437.
- Macmillan, S., and S. Maus, 2005, *International Geomagnetic Reference Field – the tenth generation*, Earth Planets Space **57**, 1135-1140.
- Malin, S.R.C., B.M. Hodder and D.R. Barraclough, 1983, *Geomagnetic variation: a jerk in 1970*. In: 75th Anniversary Volume of Ebro Observatory, 239-256, Ebro Obs., Taragona, Spain.
- Mandea, M., and N. Olsen, 2006, *A new approach to directly determine the secular variation from magnetic satellite observations*, Geophys. Res. Lett. **33**, L15306, doi:10.1029/2006GL026616.
- Mugellesi, R., and D.J. Kerridge, 1991, *Prediction of solar and geomagnetic activity for low-flying spacecraft*, ESA Journal 15, 123-131.
- Reay, S.J., W. Allen, O. Baillie, J. Bowe, E. Clarke, V. Lesur and S. Macmillan, 2005, *Space weather effects on drilling accuracy in the North Sea*, Annales Geophysicae **23**, 3081-3088.
- Royal Society, 1992, *Synoptic data for solar-terrestrial physics – the United Kingdom contribution to long-term monitoring*, The Royal Society, London, 58pp.
- Russell, J.P., G.M. Shiells and D.J. Kerridge, 1995, *Reduction of well-bore uncertainty through application of a new geomagnetic in-field referencing technique*. Proceedings of the SPE Annual Technical Conference, Dallas, 22-25 October, 1995, SPE 30452, 16 pp.

- Stanhill, G., and S. Cohen, 2001, *Global dimming*, *Agricultural and Forest Meteorology* **107**, 255-278.
- Thomson, A.W.P., A.J. McKay, E. Clarke and S.J. Reay, 2005, *Surface electric fields and geomagnetically induced currents in the Scottish Power grid during the 30 October 2003 geomagnetic storm*, *Space Weather* **3**, S11002, doi:10.1029/2005SW000156.
- Whaler, K., 1982, *Geomagnetic secular variation and fluid motion at the core Surface*, *Phil. Trans. R. Soc. Lond. A* **306**, 1492, 235-246.
- Willis, D.M., A. Hewish, H. Rishbeth and M.J. Rycroft, 1994, *Synoptic data for solar-terrestrial physics: The U.K. contribution to long-term monitoring*, *J. Atmos. Terr. Phys.* **56**, 7, 871-886.

Accepted February 21, 2007

A Search for Users of Magnetic Observatory Data

Larry NEWITT

Canadian Hazards Information Service, Natural Resources Canada
7 Observatory Crescent, Ottawa, Canada K1A 0Y3

Abstract

Statistics on the use of magnetic observatory data are not easy to come by. However, over three hundred day-files per month for each observatory are downloaded from the INTERMAGNET web site. Observatory data and derived products such as indices are widely used by researchers. An examination of eight widely read journals indicates that over 80% of the articles that deal in some way with geomagnetism use either data or products. Use by industry also appears to be extremely large.

1. Introduction

My oral presentation at the XXII IAGA Workshop was a rather unstructured talk entitled *A Personalized Account of Geomagnetism in Canada*. The talk had three themes: (1) what we do today in geomagnetism is very much connected to past events; (2) the nature of our science is such that we have been forced to find new ways of measuring and surveying the magnetic field; (3) we produce data so that science and society will use them. Because of the restrictions on the length of papers, I have decided to restrict this written version to the third theme. Do people use observatory data? What type of data do they use? What are the uses of the data? These are some of the questions I had in mind when I began the investigation. Answering them proved to be harder than expected.

2. Statistics on Observatory Data Usage

2.1 Sources and types of data

Magnetic observatories specialize in producing data that represent the true value for the magnetic field with a high degree of accuracy. Because of this, their traditional products are those that require accurate or stable data – mean values from annual to

hourly, indices and so on. There is certainly a group of users that need and want these data and data products. But there is a large group of users that is more interested in the resolution and sampling rate of data than its stability or absolute accuracy. Observatory one-minute data and data at faster sampling rates are of interest to this group.

It became apparent early on that it was going to be extremely difficult to come up with a complete picture of magnetic observatory data usage. This is due both to the numerous ways in which a user or researcher can obtain observatory data and to the numerous types of data that observatories produce. These are summarized in Table 1.

Table 1
Sources and types of observatory data

| Sources of observatory data | Types of observatory data | Derived products |
|-----------------------------|--|------------------------|
| INTERMAGNET web site | 1-minute data (preliminary or definitive) | Magnetic indices |
| Observatory web site | Hourly mean values (definitive) | Reference field models |
| Yearbooks and compilations | Monthly mean values | Magnetic forecasts |
| World data centers | Annual mean values (definitive) | |
| Third party | Fast-sample data (1-sec, 5-sec) | |

Third party refers to observatory data that are redistributed as part of another data set. The inclusion of some Canadian observatory data with the MACCS data set is an example. Preliminary data refer to data that have not had baseline corrections applied. After the application of baseline corrections the data are considered definitive. The table also lists three derived products. Reference field models and forecasts obviously use non-observatory data as well, but observatory data are an essential component.

2.2 Requests for INTERMAGNET data

Of the five sources listed in Table 1, reliable statistics are available for only one, the INTERMAGNET web site and then only for one type of data, 1-minute. I was also able to obtain comparable numbers for requests that came to the Geological Survey of Canada Geomagnetism web site; this is a single example of data distributed by an observatory site. Data are downloaded from the INTERMAGNET site in day-files. Table 2 shows the number of day-files loaded on a month-by-month basis from January 2005 to October 2006. I have also given the most-requested observatory for each month. The table also gives the number of Canadian data downloaded from the INTERMAGNET site for comparison with the Canadian data downloaded from our own web site.

Table 2
Number of day-files requested from INTERMAGNET site

| Month | Preliminary data | | | | Definitive data |
|--------------|-------------------|----------------|------------------------|-------------------|-------------------|
| | All observatories | Most-requested | Canadian observatories | Canadian web site | All observatories |
| Jan 2005 | 9903 | STJ (650) | 1651 | 745 | 7009 |
| Feb 2005 | 6477 | RES (413) | 1280 | 56 | 6356 |
| Mar 2005 | 7125 | BMT (834) | 75 | 739 | 8721 |
| Apr 2005 | 11116 | VSS (1086) | 1242 | 60 | 45453 |
| May 2005 | 2660 | KAK (951) | 75 | 117 | 1098 |
| Jun 2005 | 4279 | ASP (488) | 243 | 180 | 17444 |
| Jul 2005 | 14381 | EYR (577) | 1339 | 91 | 18524 |
| Aug 2005 | 6407 | STJ (919) | 1134 | 23 | 11290 |
| Sep 2005 | 3631 | BOU (394) | 914 | 2216 | 2702 |
| Oct 2005 | 12963 | BNG (296) | 1546 | 50 | 29185 |
| Nov 2005 | 2759 | KOU (277) | 149 | 50 | 2534 |
| Dec 2005 | 2441 | STJ (746) | 809 | 58 | 1741 |
| Jan 2006 | 4543 | BNG (669) | 509 | 276 | 9411 |
| Feb 2006 | 8148 | FUR (223) | 493 | 105 | 24721 |
| Mar 2006 | 3334 | SPT (293) | 257 | 162 | 77139 |
| Apr 2006 | 5875 | FRD (493) | 464 | 346 | 136685 |
| May 2006 | 2163 | RES (256) | 500 | 225 | 9689 |
| Jun 2006 | 4333 | CLF (744) | 1012 | 263 | – |
| Jul 2006 | 5514 | QSB (468) | 604 | 263 | – |
| Aug 2006 | 11476 | STJ (1277) | 1768 | 1129 | – |
| Sep 2006 | 1982 | PHU (366) | 339 | 261 | – |
| Oct 2006 | 10620 | AAE (1012) | 1659 | 294 | |
| Total | 142130 | | 18062 | 7709 | 409702 |

Data from approximately 100 observatories are available from the INTERMAGNET site. An average of approximately 65 day-files of preliminary data per observatory per month is downloaded. Data from the 12 Canadian observatories are obtained from the INTERMAGNET site at approximately the same rate. However, an additional 29 station-days per observatory per month are obtained from the GSC Geomagnetism web site. Canadian data are also supplied in quasi-real-time to the Ottawa Forecast Centre, adding another 30 day-files per observatory month.

The number of requests for definitive data is even larger – 241 day-files per observatory per year. Note that definitive data are also distributed as binary month files. To make comparisons easier I have converted these to dayfiles. Combining requests for preliminary and definitive data gives an average of 306 day-files per observatory per month. This is a large amount of data but it is probably an extreme underestimate since it does not include data requested from the WDCs or any other institute. Nor does it include requests for anything other than one-minute data, such as annual, monthly and hourly means, or one-second and 5-second data.

Neither the INTERMAGNET web site nor the GSC site request identification from users beyond an e-mail address. Therefore, it is difficult to determine in detail who is requesting the data. However, through an examination of all e-mail addresses associated with downloads of Canadian data I was able to garner institutional information for about one half of the users. These were roughly divided among academia, industry and government/military.

2.3 Use of observatory data in journals

Observatory data can be used both operationally and for research purposes. Again, obtaining complete statistics on who uses the data and for what purposes is virtually impossible but I was able to obtain some information through limited studies. To start, I looked at the publications and reports produced by our own group, most of which are preserved in bound volumes as the Contributions from the Dominion Observatory and the Contributions from the Earth Physics Branch. These span the period from 1950 to 1982, the year the Earth Physics Branch became part of the Geological Survey of Canada. The compilation undoubtedly missed some publications, but it is fairly complete and should give a reasonable picture of our internal usage.

Table 3 shows the number of publications broken down by topic, and the percentage that actually used observatory data. The major research interest of the organization was paleomagnetism which does not depend on or even use observatory data. But nevertheless over that 30 year period an average eight papers were published per year, two of which made use of observatory data. The present situation is also reflected in the table in the four columns which give statistics on the number of reports, papers and presentations produced by the group during the period 2000 to 2005.

The shift in our research interests is obvious, the main topic of research now being geomagnetic hazards. It is also interesting that we still produce eight papers per year on average, but now 70% of them use observatory data. We also give a large number of presentations at conferences and elsewhere, most of which make use of our data.

2.4 Use of observatory data in publications

Papers using observatory data are published in numerous international journals and in numerous institutional publications. I chose to restrict my examination of the literature to 8 widely recognized journals. I further restricted the search to the time interval 2000 to 2005. I then used the search facility of SCOPUS™, an extensive database of research literature, to search for articles in these journals on the basis of

Table 3
Usage of observatory data by GSC

| Category | 1950 to 1982 | | 2000 to 2005 | | | |
|-----------------------------|--------------|-------------------|--------------|-------------------|----------------|-------------------|
| | Number pubs. | % using obs. data | Number pubs. | % using obs. data | Number present | % using obs. data |
| Variations | 59 | 80 | 7 | 86 | 10 | 100 |
| Induction/MT | 40 | 20 | 0 | 0 | 0 | 0 |
| Internal/Crustal/main field | 35 | 26 | 5 | 80 | 8 | 50 |
| Instrumentation | 22 | 0 | 0 | 0 | 0 | 0 |
| Hazards | 0 | 0 | 27 | 67 | 39 | 87 |
| Forecasts | 0 | 0 | 4 | 100 | 7 | 86 |
| Paleomagnetism | 85 | 0 | 0 | 0 | 0 | 0 |
| Other | 14 | 0 | 5 | 20 | 3 | 67 |
| | 255 | 25 | 48 | 69 | 67 | 82 |

Table 4
Number of articles retrieved by SCOPUS™ literature search

| Search terms | GJI | GRL | AG | JGR (all) | EPS | PEPI | EPSL | Nature | |
|--|--------|---------|--------|-----------|--------|------|------|--------|-----|
| Magnetometer data | 0 | 12 (2) | 43 (3) | 41 (3) | 5 | 1 | 0 | 0 | 102 |
| (Geo)magnetic indices | 3 | 20 (2) | 29 (3) | 5 | 6 | 0 | 3 | 0 | 66 |
| (Geo)magnetic (sub)storm | 4 | 103 (8) | 97 (8) | 128 (10) | 15 (1) | 0 | 0 | 3 | 350 |
| (Geo)magnetic field model | 12 (1) | 11 (1) | 0 | 2 (10) | 21 | 2 | 2 | 0 | 50 |
| (Geo)magnetic secular variation (change) | 21 (2) | 6 | 1 | 1 | 7 | 7 | 12 | 3 | 58 |
| | 40 | 152 | 170 | 177 | 54 | 10 | 17 | 6 | 626 |
| GJI = Geophysical Journal International EPS = Earth, Planets and Space GRL = Geophysical Research Letters PEPI = Physics of the Earth and Planetary Interiors AG = Annales Geophysicae EPSL = Earth and Planetary Science Letters JGR = Journal of Geophysical Research (all editions) | | | | | | | | | |

several search terms that I had chosen. Table 4 shows the number of articles selected by SCOPUS for each set of search terms for each journal. In actual fact, the number of articles selected by SCOPUS was considerably larger than the number given in the table; I rejected many others (35%) as being off the topic on the basis of their titles. For example, using the search terms (geo)magnetic AND secular AND variation OR change retrieved numerous articles on paleosecular variation. Table 4 gives the number of articles retrieved for each journal and for each search term.

To determine whether these papers actually used observatory data, derived products or other forms of magnetic data would have required reading the abstract of each and possibly the entire article. Since there were 626 articles, this was too great a task. I therefore chose 50 articles semi-randomly; that is, the distribution of articles chosen roughly matched the distribution in the above table. The bracketed values in Table 4 indicate the number of articles chosen for that subject and for that journal. Table 5 gives the percentage of papers that use magnetic data or derived products (indices, reference field models). Although only 36% of papers use observatory data directly, a full 82% use either observatory data or derived products.

Table 5

Data usage in geomagnetism research papers

| Type of data | Usage [%] |
|----------------------------|-----------|
| Magnetic observatory | 36 |
| Other ground magnetic data | 30 |
| Satellite data | 42 |
| Indices | 50 |
| Models | 8 |
| None | 10 |

2.5 Derived products and other data

Table 5 indicates that researchers make great use of magnetic indices. In fact, indices are used in 50% of the papers. Researchers also make use of models for a variety of purposes. However, models, indices (to a lesser extent), and magnetic forecasts are widely used outside the research community. Again, with one exception, I have only draw on the statistics from the GSC Geomagnetism web site, which are given in Table 6 for various data products.

Two numbers are given under on-line declination calculator: the number of accesses for our own site and the number of accesses to the calculator on the WDC-A site, supplied by Susan McLean (private communication).

Table 6
Usage of derived products

| Product | Daily access |
|---|--------------|
| Magnetic forecasts | 3200 |
| Forecast related products | 250 |
| On-line declination calculator (GSC) (WDC) | 200 800 |
| On-the-fly plots | 80 |
| Local indices and ranges | 60 |

3. Discussion

Despite the very limited scope of this study it appears that magnetic observatory data and derived products are widely used. Of fifty papers selected for examination more than 80% use either data or derived products. If the same ratio applies to the whole sample of 626 papers then more than 100 papers per year that use data or products are published in the eight selected journals. The total usage of data or products by the academic research community is likely several times this number. Industry also uses data. My own experience indicates that major industrial users include the aeromagnetic survey community and the directional drilling community, among many others.

The use of derived products is also extremely large. Indices were used in fully half the research papers. We also know that indices, in particular Kp, are used by industries that are affected by disturbances, such as the GPS survey industry and electrical power industry. Accesses to our forecasts exceed 3000 per day. We do not track user profiles but experiential evidence indicates that the user base is extremely broad. Both our own statistics and those of WDC-A indicate the continued need for magnetic reference field models.

Despite the wide use of observatory data and products it is my opinion that the importance of our data is generally underappreciated. Better tracking and publication of user statistics by all institutes that disseminate data or derived products would enable a much more complete analysis to be carried out. This would be a valuable service to the magnetic observatory community.

Acknowledgements. I wish to acknowledge the following for their help in the research and preparation of this report. Jennifer Parmelee for supplying the INTERMAGNET and other statistics; the staff of the Earth Sciences Sector library for help with the journal searches; Susan McLean for supplying information on reference field model use at WDC-A.

Accepted February 15, 2007

On the Use of Fast Registrations of Observatories as a Reference for Magnetotelluric Measurements

Anne NESKA

Institute of Geophysics of the Polish Academy of Sciences
ul. Księcia Janusza 64, 01-452 Warszawa, Poland
e-mail: anne@igf.edu.pl

A b s t r a c t

Surprisingly, some records of geomagnetic variations measured in observatories are able to support magnetotellurics, a geophysical branch relatively far away from investigations of the magnetic field itself. Magnetotellurics is an electromagnetic induction method to study the solid Earth. The way it can benefit from geomagnetic observatories is outlined here.

1. Variation Measurements at Observatories

The continuous measurement and recording of variations of the Earth's magnetic field is a fundamental task of geomagnetic observatories. The data obtained thereby serve, on the one hand, to investigate the external field itself, and on the other hand, they are taken into account during the evaluation of absolute measurements.

The international standard of the INTERMAGNET network (St.-Louis 2004) demands a registration of the components X, Y, and Z carried out with a sampling interval of not less than 10 seconds to cover these variations. Interestingly, some observatories are able to provide a more densely sampled registration. E.g. Niemegk and Belsk carry out continuous variation measurements in the framework of their daily work that result in a steadily available one-second registration. In special cases, a still much higher sampling rate of 100 Hz is reached, i.e. if the observatory performs a monitoring of the Schumann Resonance phenomenon, as it is done in Nagycenk, Hornsund, and Belsk, (see Neska *et al.* 2007, this volume).

Now it turned out that such variation data can serve another purpose beside the ones they are designed for. They are able to support magnetotelluric measurements in a situation that is fatal for them. This possibility will be illustrated below.

2. Magnetotellurics

A broad introduction of this field is beyond the scope of this paper. It can be found in textbooks like (Zhdanov *et al.* 1994). However, features that are essential to our topic will be described in the following.

2.1 Some basics

Magnetotellurics is a geophysical method targeted on the investigation of the electric conductivity of the Earth's crust and mantle. Thereby it contributes to solid Earth studies, since different electric conductivities allow to draw conclusions about different underlying rocks and their state. E.g., sediments saturated with saline water are better conductors than not-weathered, not-porous crystalline rocks like granite. Other examples for good conductors in terms of geology are partially or completely molten rocks and some minerals like graphite and sulfides. Furthermore, the conductivity of a rock depends highly on its temperature. Hence, a model of the conductivity distribution in the subsurface (which magnetotellurics intends to find by numerical modeling) gives answers on geological, tectonic, and petrophysical questions about the region of interest.

Such a conductivity model is based on information obtained from variations of the natural electromagnetic field via the induction equation. This works as follows: The given region is covered by a network of magnetotelluric stations. Each of them measures field variation of five components, the horizontal electric ones in north and east direction (E_x and E_y) and three magnetic ones in north, east, and vertical direction (B_x , B_y , B_z). See Fig. 1 for an example record demonstrating the similarity, i.e. correlation or coherency, between certain components caused by electromagnetic induction. The registration can have rather varying parameters and instrumentation depending on the depth range one is interested in. So shallow studies use fast sampling rates in the Hz to kHz range, short recording durations of several hours, and induction coils to measure the magnetic channels. In contrast, deep studies work with a sampling interval in the second range, they last several weeks, and they use, in general, fluxgate magnetometers to measure B_x , B_y , and B_z .

During the data processing, all time series are Fourier-transformed to the frequency domain, and the so-called transfer functions between several field components are calculated. So the impedance tensor \mathbf{Z} transforms (B_x, B_y) into (E_x, E_y)

$$\begin{pmatrix} E_x \\ E_y \end{pmatrix} = \begin{pmatrix} Z_{xx} & Z_{xy} \\ Z_{yx} & Z_{yy} \end{pmatrix} \begin{pmatrix} B_x \\ B_y \end{pmatrix}, \quad (1)$$

and the induction arrow (A, B) connects (B_x, B_y) with B_z :

$$(B_z) = (A \ B) \begin{pmatrix} B_x \\ B_y \end{pmatrix}. \quad (2)$$

Both transfer functions are complex functions of frequency or, which is equivalent, of period T . Usually, the impedance at a certain station is plotted in form of apparent

resistivity and phase and the induction arrow in form of a vector with components A in North and B in East direction (see Fig. 3).

The above-mentioned transfer functions contain the desired conductivity information under the condition that the underlying mechanism of their generation is electromagnetic induction, indeed. This includes that the so-called far-field condition is fulfilled, i.e. the source of the magnetic variations must be so far away that the latter comes as a plane wave to the study area. For natural variations this is generally met in mid latitudes.

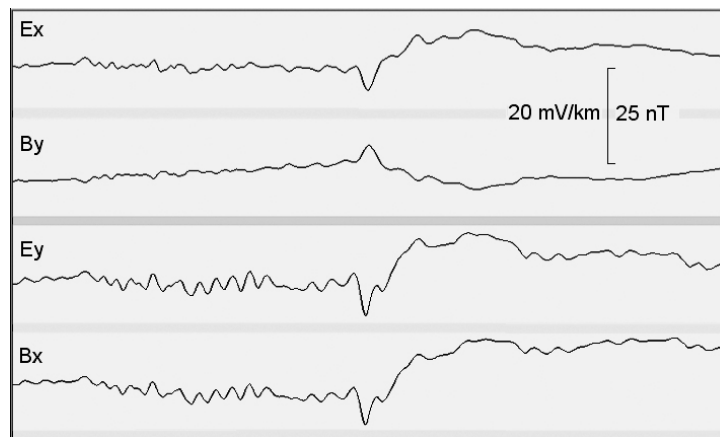


Fig. 1. Horizontal electric and magnetic channels recorded by a magnetotelluric station with a 2 s sampling interval. The length of time series is 25 min, the visible pulsations are mainly pc2 and pc3. The induction-caused similarity between perpendicular E and B components is significant.

2.2 The correlated noise problem

However, if there is registered an artificial electromagnetic signal from a near-by source, this basic requirement of magnetotellurics is not accomplished. When doing magnetotelluric measurements in Poland, one faces such a situation in the proximity of electrified railways, which are run with direct current (DC) here. The start-up peaks of the moving trains are clearly visible in the time series in Fig. 2, destroying the harmony of the pc2 and pc3 pulsations expected in the given time range. Nevertheless, these peaks are correlated between different field components. This fact leads to the term “correlated noise” for such a kind of disturbances. Correlated noise is a big problem for the magnetotelluric method, because such features will enter the transfer functions due to their coherent nature, if affected time series are processed. This means, that a part of the impedances and induction arrows will be dominated by the railway disturbances which do not fulfill the far-field condition. Thereby, the latter will distort the conductivity information obtained at the given station. Figure 3, left-hand side, shows such distorted transfer functions of a station at a distance of 25 km from a DC railway. The distortions are always characteristic: they misleadingly suggest the presence of a bad conductor beneath the railway.

Fortunately, there is a method rescuing the magnetotelluric approach in such a correlated-noise situation.

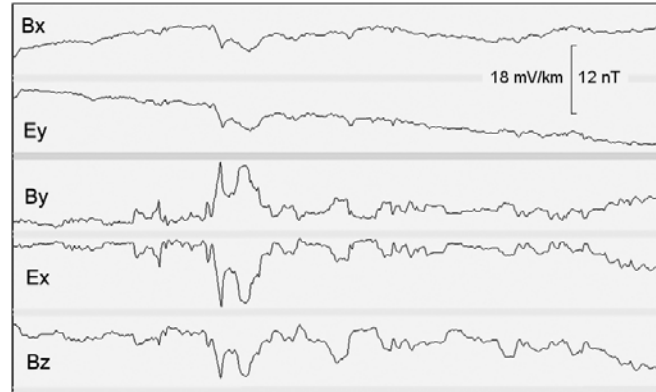


Fig. 2. Time series (34 min) recorded by a station 7 km off a DC railway. The peaked, angular structures are not natural, but due to the railway. Note the coherency between channels.

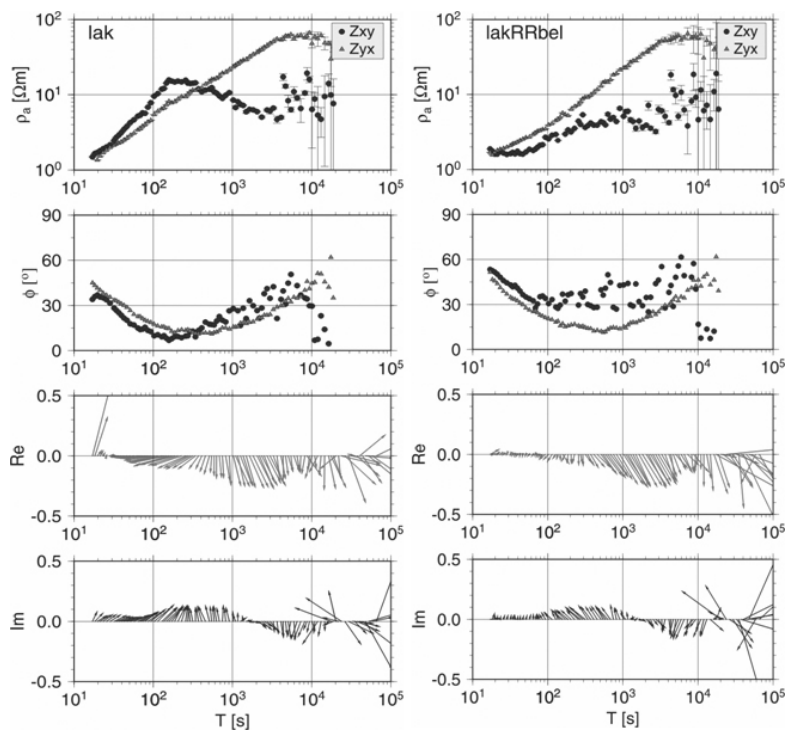


Fig. 3. Magnetotelluric transfer functions of a station affected by correlated noise 25 km off a railway. Left-hand side processed without, right-hand side with Belsk observatory records as reference data. The upper two panels show apparent resistivity and phase of the off-diagonal elements of the impedance tensor, the lower ones real and imaginary induction arrows. Note that there are artificial features (enhanced resistivity and decreased phase in Z_{xy} , too long induction arrows) in the transfer functions without Remote Reference at periods below 1000 s.

2.3 The Remote Reference technique

The method to suppress the influence of correlated noise on transfer functions is called Remote Reference technique, introduced by Gamble *et al.* (1979). The most important task of this processing approach, the distinction between natural signal and artificial noise, is solved by means of a simple fact: The artificial noise decays within a relatively short distance to its source; in my experience with the Polish sedimentary basin, it is not traceable much farther than 100 km from the railway. In contrast, the natural magnetic variations are correlated over several hundred kilometers in mid latitudes, as can be seen in Fig. 4.

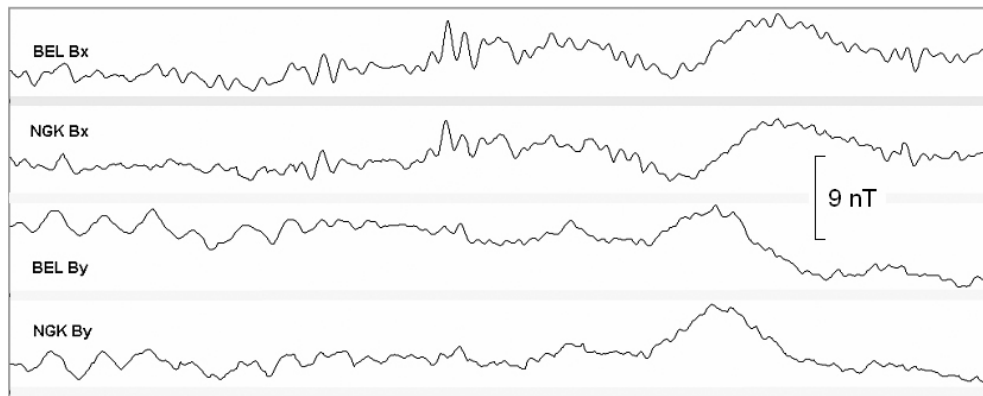


Fig. 4. Natural magnetic pulsations are correlated over several hundred kilometers: In spite of the distance of 560 km between Niemegk and Belsk, their horizontal records look similarly. Length of time series 25 min.

So, when comparing time series of a local station affected by railway disturbances and a some hundred kilometers remote reference station, the natural variations will be correlated between both sites and the railway noise will not. Hence, synchronously recorded horizontal magnetic time series of a remote reference station are included into the processing in the following way: To obtain, e.g., Z_{xy} in general, one must take a number of spectral values of the field components E_x , B_x , and B_y at the same frequency and apply the least-square solution:

$$Z_{xy} = \frac{[E_x^* B_x][B_y^* B_y] - [E_x^* B_y][B_x^* B_y]}{[B_x^* B_x][B_y^* B_y] - [B_x^* B_y][B_y^* B_x]}, \quad (3)$$

where $[\]$ indicates the average of the spectra in between and A^* the complex conjugate of A . The solution for the Remote Reference technique looks as follows

$$Z_{xy}^R = \frac{[E_x^* B_x^R][B_y^* B_y^R] - [E_x^* B_y^R][B_x^* B_y^R]}{[B_x^* B_x^R][B_y^* B_y^R] - [B_x^* B_y^R][B_y^* B_x^R]}, \quad (4)$$

where a superscript R indicates spectra of the reference station.

Due to the cross spectra between local and remote data it is provided that only features correlated between both sites, i.e. natural variations, can enter the result, whereas the railway noise is suppressed. Let it be noted that features in the reference data caused via induction by the subsurface of the remote site do not enter the local transfer functions, since the remote spectra appear quasi in the numerator and the denominator of Eq. (4) and are thereby cancelled down. It remains just the benefit from the averaged cross spectra which removes the influence of correlated noise in the local time series. Figure 3, right-hand side, shows transfer functions of a railway-affected station, which have been corrected by the Remote Reference technique.

A more detailed discussion of magnetotelluric data processing including the Remote Reference technique can be found in (Neska 2006).

3. Observatories as Remote Reference Stations

From the above description, it becomes clear that under certain conditions, observatory records can play the role of reference data for magnetotelluric measurements. These conditions are mainly connected with the sampling rate of both observatory and magnetotelluric registration, and with the distance between observatory and magnetotelluric sites. The sampling rates should not be very different from each other; in the ideal case they are equal. If the observatory samples faster, it is also easy to deal with: the data must be just low-pass filtered and resampled to the magnetotelluric rate. If conversely the observatory samples slower, the magnetotelluric data have to be adapted in the same way to the observatory rate, which would, however, lead to a loss of information from the highest frequencies. For the example shown in Fig. 3, the one-second registration of Belsk Observatory has been adapted to the two-second sampling of the field measurement.

Figure 5 demonstrates that even more “exotic” measurements carried out in observatories can have an application that supports other geophysical fields. In this case, a relatively high-frequency magnetotelluric record was concerned by correlated noise. Amongst others, it contains a band sampled with 64 Hz. It could be subjected to a Remote Reference processing using horizontal magnetic variation data which have been measured with a 100 Hz sampling rate in Belsk. The reason for recording such data steadily is the observation of the Schumann Resonance phenomenon at the observatory, cf. (Neska *et al.* 2007). The comparison of Z_{xy} results processed with and without Remote Reference in Fig. 5 shows that the former leads to vanishing correlated-noise features which are visible in the first.

Concerning the question of distance, it has to be stated that observatory and station network must be remote enough to avoid being within the reach of the same emitter of correlated noise, e.g. the same DC railway. It is on the other hand intuitively clear that the possible distance is not unlimited for the coherency of the natural magnetic variations is a condition *sine qua non*. However, in my experiments I did not reach that limit, I can only confirm that a distance of about 500 km did not cause any problems in Remote Reference processing. The statement that natural variations are correlated over several hundred kilometers in mid-latitudes stems from Schmucker (1984).

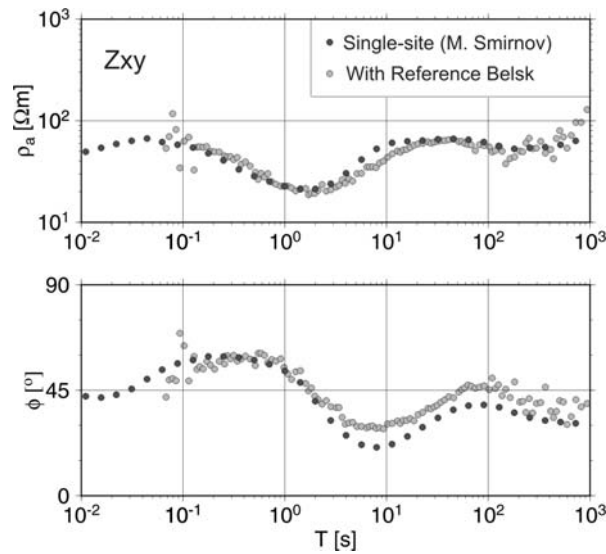


Fig. 5. An application of Remote Reference at higher frequencies with data from Belsk. Local data has been measured by V. Červ, the observatory-station distance is 350 km. Apparent resistivity and phase of impedance tensor element Z_{xy} show correlated-noise features around 10 s, when processed without reference (single-site, done by M. Smirnov).

It has to be emphasized that the absence of uncorrelated (i.e. local) noise in the remote reference data is not demanded for the success of processing. Such a noise (which can hardly be kept away from Mid-European observatories) does not endanger the ability of the Remote Reference technique to compensate for correlated noise in the local site. However, if such a remote noise is strong compared to the natural signal, it can lead to somewhat scattered sounding curves, as it can be seen in Fig. 3, right-hand side.

Concluding, I would like to illustrate what meaning the availability of observatory data can have for people carrying out a magnetotelluric field campaign. When measuring in areas affected by correlated noise like Poland, it is absolutely necessary to have a Remote Reference station. If not counting on observatories, the magnetotelluric worker has to provide this station on his own. This means that one instrument is blocked for this role during the entire campaign. Furthermore, it costs a notable effort regarding staff and transportation to install and maintain such a station, since it must be in a certain distance from the rest of the network as mentioned above. Finally, field stations are less secure than observatories; they are endangered by bad weather, animals, and in worst case, by vandalism and theft, so one cannot be sure to get uninterrupted data from it. In contrast, using observatory records guarantees continuous, steadily available data from a sufficient distance without additional measurement effort for the magnetotelluric worker.

From this point of view it would be desirable that magnetic observatories provide also variation records sampled faster than with a ten-second interval.

Acknowledgments. I gratefully acknowledge contributions from H.-J. Linthe, K. Nowożyński, J. Reda, and J. Pek. All field data presented here have been measured in the framework of the large-scale magnetotelluric project EMTESZ introduced in Brasse *et al.* (2006).

References

- Brasse, H., and EMTESZ-WG, 2006, *Probing Electrical Conductivity of the Trans-European Suture Zone*, EOS, 2006ES001383, **87(29)**.
- Gamble, T.D., W.M. Goubeau and J. Clarke, 1979, *Magnetotellurics with a remote reference*, Geophysics **44**, 53-68.
- Neska, A., 2006, *Remote Reference versus Signal-Noise Separation: A least-square based comparison between magnetotelluric processing techniques*, PhD thesis, Freie Universität Berlin, Fachbereich Geowissenschaften, available at <http://www.diss.fu-berlin.de/2006/349>
- Neska, M., G. Sători, J. Szendroi, J. Marianiuk, K. Nowożyński and S. Tomczyk, 2007, *Schumann resonance observation in Polish Polar Station at Spitsbergen and Central Geophysical Observatory in Belsk*, *Publs. Inst. Geophys. Pol. Acad. Sc. C-99* (398) (this issue).
- Schmucker, U., 1984, *EM Übertragungsfunktionen aus Beobachtungen mit mehreren gleichzeitig registrierenden Stationen*. **In:** 10. Kolloquium Elektromagnetische Tiefenforschung, Grafrath in Oberbayern, 35-36 (in German).
- St-Louis, B.J. (ed.), 2004, *INTERMAGNET Technical Reference Manual, Version 4.2*, available at www.intermagnet.org
- Zhdanov, M.S., and G.V. Keller, 1994, *The Geoelectrical Methods in Geophysical Exploration*, Elsevier, Amsterdam.

Accepted February 12, 2007

Experience with New Geomagnetic Activity Index E Based on Power Spectra

Jan REDA

Institute of Geophysics, Polish Academy of Sciences
ul. Księcia Janusza 64, 01-452 Warszawa, Poland
e-mail: jreda@igf.edu.pl

Abstract

Properties of classical magnetic activity indices K and new indices E based on power spectra are described. Relation between the two indices and magnetic activity is discussed. A comparison of correlation of planetary indices Ep and Kp with solar wind parameters is made.

Key words: geomagnetic activity, geomagnetic indices.

1. Introduction

The magnetic activity indices are used to characterize the magnetic activity in local, regional and global scales. The most widely used measure of magnetic activity is the 10-digit K scale. The K index was designed by Bartels *et al.* (1939). The K index determination consists in finding the maximum amplitude of irregular changes of horizontal components X(H) or Y(D) of geomagnetic field variations in the three-hour time interval and in ascribing to these amplitudes an integer between 0 and 9. The K index is a local index, characterizing the field activity in a specified place. In order to describe the state of activity of the whole Earth, there were introduced planetary indices Kp. The Kp index is an arithmetic mean of standardized indices Ks from the selected thirteen observatories in middle geomagnetic latitudes. The Kp indices provide information on global energy supplied to the magnetosphere (Menvielle *et al.* 1991)

The K indices have many advantages and therefore are widely used. First of all, they can be very easily determined from analog recording that is still in use in some observatories. However, they also have very serious drawbacks, the major being the following:

1. The K index is determined from the maximum amplitude of one component, which is not precise, since the K index depends not only on amplitude of irregular variations but also on polarization direction. The K index determined from components X and Y may differ from that determined from H and D.
2. The K index does not depend on the number of occurrences of irregular disturbances in the three-hour interval. The K index is the same if the disturbance of a certain amplitude occurred once or more often.
3. The K index is determined from the maximum amplitude of irregular variations of just one horizontal component. When, for instance, $K_x = 3$ and $K_y = 0$, the K index will be the same as for $K_x = 3$ and $K_y = 3$.

It seems that the main idea of those who invented the K-indices was the simplicity of determination. The physical sense of the definition was taken into account to a lesser extent.

2. The E Index Based on Power Spectra

Because of various shortcomings of the K-indices, postulates for developing new indices, whose physical meaning would be more fit to the present knowledge of the mechanisms that produce magnetic disturbances, have already been put forward in the past (Pirjola *et al.* 1991). Even earlier, Lanzerotti and Surkan (1974) had proven that there exists a statistical dependence between the K indices and the power spectrum of irregular magnetic variations. They also stated that further exploration of the possible use of an index based on the actual geomagnetic power seems to be required.

Reda and Jankowski (2004) proposed a definition of a new index E, based on the calculation of energy contained in irregular variations of the horizontal geomagnetic field components. The definition is the following:

The E index is a digit from the interval 0-9 proportional to the logarithm of energy of two horizontal components variations in the interval of 3 hr. The number is normalized so that the observatories situated in moderate geomagnetic latitudes have similar activity indices and the new indices are similar to the K indices.

The E indices, like the K indices, can be calculated by a computer from the digital recording of a given observatory. The first step in the E index determination procedure is to eliminate the regular variations S_R . For this purpose, the adaptive smoothing method (ASm) (Nowożyński *et al.* 1991) was applied.

3. Relation of the E and K Indices to the Geomagnetic Activity

The E indices determined according to the above definition do not depend on the choice of components (X and Y or H and D). In both cases the indices are identical, since the energy used for the E index determination is calculated as a sum of energies of both horizontal components. As we know, the energy is additive, so the energy-derived indices must in both cases be the same. Needless to say, the geomagnetic energy is one, regardless of the choice of coordinate system in which the geomagnetic

field is observed. The definition of K indices contradicts this obvious fact, and the differences in magnetic indices determined in XY or HD systems may be considerable, notably in observatories in which the declination value is large (e.g., in excess of 10 deg).

At the beginning, the K indices were determined from three components, i.e., the vertical component Z was used too. Such an approach turned out to be improper since changes of this component, in particular at moderate geomagnetic latitudes, are mainly a result of induced electric currents flowing in upper layers of the Earth's crust. The error was corrected in 1963, when IAGA decided that the Z component should not be used for K index determination (IAGA Bulletin 19, 1963, p. 359, resolution 4). In practice, this change does not much affected the K index determination since the irregular disturbances of the Z component are, as a rule, much smaller than the horizontal component disturbances.

The notion of magnetic activity is a collective notion, referring to many geomagnetic phenomena. Therefore, it should take into account various phenomena to a possibly equal degree (Krański 1968). It is worth to realize that the K index somewhat discriminates in favor of bay-type disturbances. Such disturbances attain large amplitudes and therefore bring the main contribution to the K index estimation, while the Pc3, Pc4 and Pi pulsations have small amplitudes and their share in the K index determination is almost negligible. Instead, the E indices take into account not only the large-amplitude disturbances, but all disturbances whatsoever, since these indices are calculated on the basis of the energy of all irregular variations.

The procedure proposed by Reda and Jankowski (2004) for calibration of the E indices on the basis of the K indices makes it possible to treat the former as a continuation of the latter. The differences between the K and E indices were shown to be not large (only in about 0.1% of cases did they exceed 1), but clearly noticeable.

In the above paper it was also demonstrated, on the basis of ample statistical material, that the E indices for a given observatory better correlate with the solar wind parameters than the classical K indices. The analysis concerned the following parameters: (a) vertical component B_z , i.e., the component Z of the interplanetary magnetic field (IMF) in the geocentric solar magnetospheric coordinates, (b) plasma temperature T_p , and (c) solar wind speed V . However, scientists and people solving practical tasks prefer to use the planetary index K_p . Therefore, of utmost interest was to examine whether the E_p indices derived from the E indices would better correlate with the solar wind parameters than the K_p indices. Such an analysis is one of the objectives of the present study. Prior to statistical analyses, we converted the K_p and E_p indices to the equivalent amplitudes a_K expressed in nanoteslas. Such an approach is justified by the fact that the K_p and E_p indices are just the codes (Mayaud 1980). An analysis was made for the whole year 1999 except of the periods when the E_p indices could not be calculated because of gaps of data in some observatories or the lack of magnetospheric indices B_z , T_p or V . The planetary indices E_p were calculated from data of the same 13 observatories whose data were used to calculate the planetary indices K_p . For the needs of the present study, the E_p indices were calculated in a simplified manner, omitting the stage of E index standardization; while in the case of

the K_p indices calculation the standardization was applied. The correlation analysis was made in two variants:

- for cases when the K_p indices differed from the E_p indices; the results are shown in Fig. 1
- and for all cases ($K_p = E_p$ and $K_p < E_p$); the results are in Fig. 2.

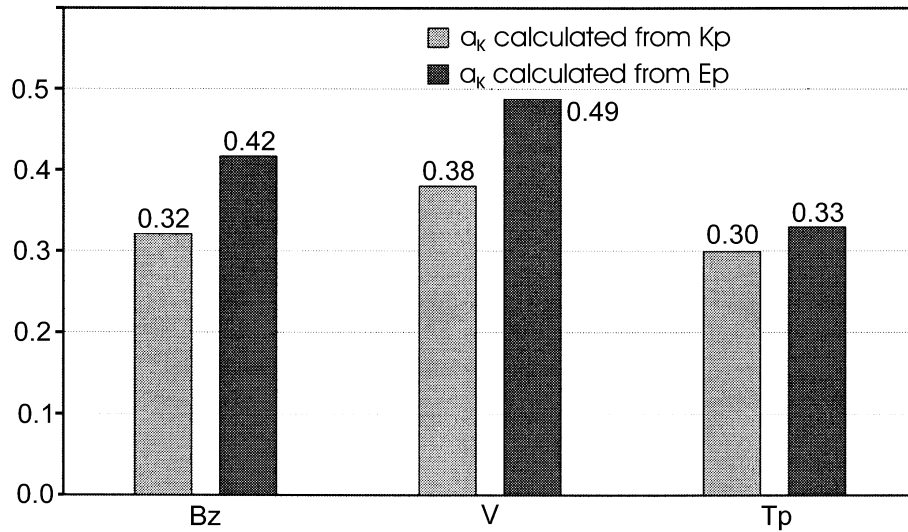


Fig. 1. Correlations of the K_p and E_p indices with the solar wind parameters for cases when $K_p > E_p$.

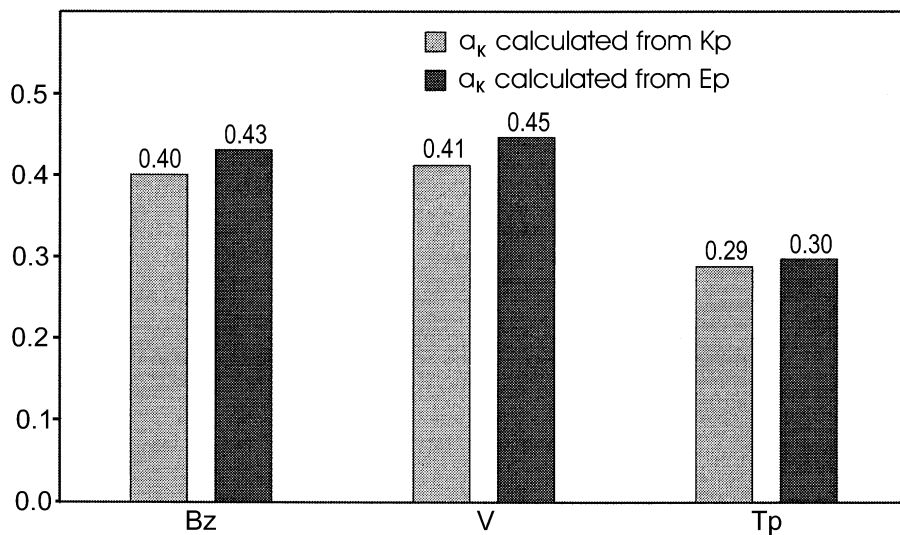


Fig. 2. Correlations of K_p and E_p with the solar wind parameters for all cases ($K_p = E_p$ and $K_p < E_p$).

We see from the above figures that the E_p indices correlate with the solar wind parameters better than the K_p indices. An improvement of correlation is more distinctive than that reported by Reda and Jankowski (2004) for a single observatory. For parameters B_z , V and T_p , the improvement of correlation for the calculations according to the second variant (e.g., for all the cases) is 8%, 9% and 3.5%, respectively.

4. Fourier Analysis of K and E Indices

The Fourier analysis is a method widely applied in different fields of science. In the present work, it has been used to investigate phenomena of periodic occurrence in geomagnetic activity. To compare the spectral characteristics of K indices with those of newly proposed E indices, there has been carried out a Fourier analysis of amplitude equivalents of both types of indices. For this comparison, there has been selected a 10-years-long period from 1 January 1990 until 31 December 1999 from Belsk data. The results are presented in Figs. 3 and 4. This analysis allows to state that the spectra in both cases are almost identical. This means, amongst other things, that the new E indices are just as sensitive to periodic phenomena of geomagnetic activity as the K indices are. Hence also from this point of view it follows that the E indices can be regarded as a continuation of the actually applied K indices.

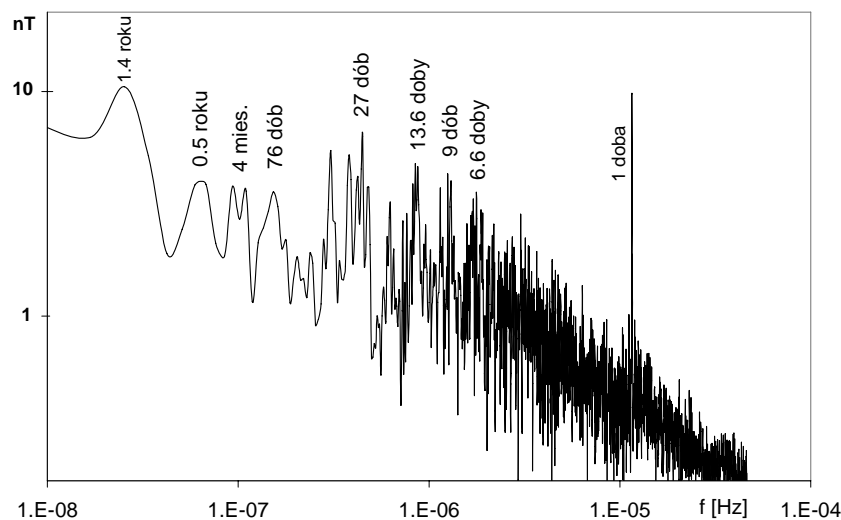


Fig. 3. Spectrum of amplitude equivalents of K indices from Belsk for 1990-1999; indices calculated with the ASm method.

5. Conclusions

The main advantage of the E indices is the fact that they are calculated on the basis of energy contained in irregular geomagnetic field variations. Therefore, the planetary indices E_p calculated from them better correlate with solar wind parameters B_z , V and T_p than the K_p indices. This is in accordance with expectations since it is the solar

wind energy transfer to the magnetosphere that decides upon the intensity of irregular variations observed at the Earth's surface. Furthermore, the E indices can be regarded as a continuation of the actually applied K indices from a spectral analysis point of view as well.

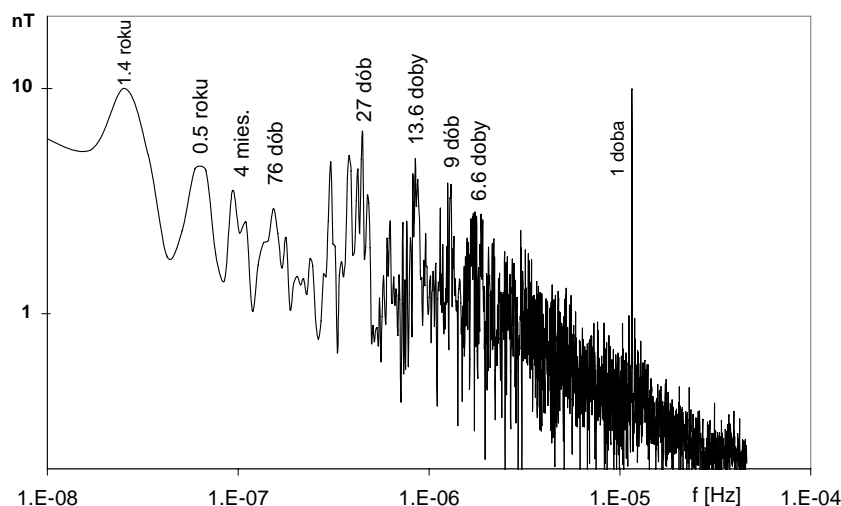


Fig. 4. Spectrum of amplitude equivalents of E indices from Belsk for 1990-1999.

Acknowledgments. The geomagnetic data from the Canberra, Lerwick, Wingst and Belsk observatories were taken from the CD-ROM 1999 issued by Inter-magnet. The magnetospheric data were taken from the http Server NSSDC (National Space Science Data Center, [ftp://nssdcftp.gsfc.nasa.gov/spacecraft data/omni/](ftp://nssdcftp.gsfc.nasa.gov/spacecraft_data/omni/)).

The author wishes to thank Professor Jerzy Jankowski for valuable comments and suggestions and Mrs Anna Dziembowska for translating the text.

References

- Bartels, J., N.H. Heck and H.F. Johnston, 1939, *The three-hour range index measuring geomagnetic activity*, Geophys. Res. **44**, 411-454.
- Kraiński, W., 1968, *O aktywnosci gemagnetycznej i wskaźnikach K*, Acta Geophys. Pol. **16**, 1, 57-69.
- Lanzerotti, L.J., and A.J. Surkan, 1974, *ULF Geomagnetic Power. Near L= 4. Relation to Fredericksburg K index*, J. Geophys. Res. **79**, 2413-2419.
- Mayaud, P.N., 1980, *Derivation, meaning and use of geomagnetic indices*, Geophys. Monogr. **22**, 154.

- Menvielle, M., and A. Berthelier, 1991, *K-derived planetary indices description and availability*, Reviews Geophys. Space phys. **29**, 3, 415-432.
- Nowożyński, K., T. Ernst and J. Jankowski, 1991, *Adaptive smoothing method for computer derivation of K-indices*, Geophys. J. Int. **104**, 85-93.
- Pirjola, R., C. Sucksdorff and L. Hakkinen, 1991, *On machine production of K-indices*, HHI-Report No. 22, Berlin.
- Reda, J., and J. Jankowski, 2004, *Three hour activity index based on power spectra estimation*, Geophys. J. Int. **157**, 141-146.

Accepted February 8, 2007

Installation of a High Resolution Potassium Magnetometer in the Coast of Oaxaca, Mexico

Gerardo CIFUENTES-NAVA¹, Enrique CABRAL-CANO¹, Esteban HERNÁNDEZ
-QUINTERO¹, Ivan HRVOIC², Francisco LÓPEZ² and Mike WILSON²

¹ Instituto de Geofísica, Universidad Nacional Autónoma de México
Ciudad Universitaria., Del Coyoacán, México D.F, C.P. 04510

² GEM Advanced Magnetometers
52 West Beaver Creek Road, 14, Richmond Hill, ON, Canada L4B 1L9
e-mail: info@gemsys.ca

A b s t r a c t

In the up-to-date significant investments in earthquake studies and especially in detection of earthquake precursors there is a lot of emotional and in general non-critical measurements of precursors. We are trying to establish some kind of reference conditions for detection of precursors. A brief analysis of the number of measurements and especially Loma Prieta precursor is given. Based on Loma Prieta precursor and in general confirmed by a series of other precursors, a spatial distribution of expected magnetic anomalies for a given magnitude of earthquake was calculated. Different methods of measurement are assessed and a short base gradient method explained. Supersensitive (50 fT) potassium 3 sensor gradiometer is described and some initial field data presented.

1. Introduction and General Overview

Attempts to foresee earthquakes, and to measure or assess precursors goes far back in history and includes such impractical things as unusual behavior of animals etc. Magnetic measurements started more than 100 years ago and reported anomalies of several hundred nT were common (Fig. 1). However, after discovery of proton magnetometer when measurements could be done more accurately, the “anomalies” suddenly decreased close to few nT or even fractions of nT. Obviously, previously reported hundreds of nT anomalies could be assigned to anything but earthquakes. This kind of approach to measurement (“better to measure something than not to measure at all”) finally discredited the method entirely.

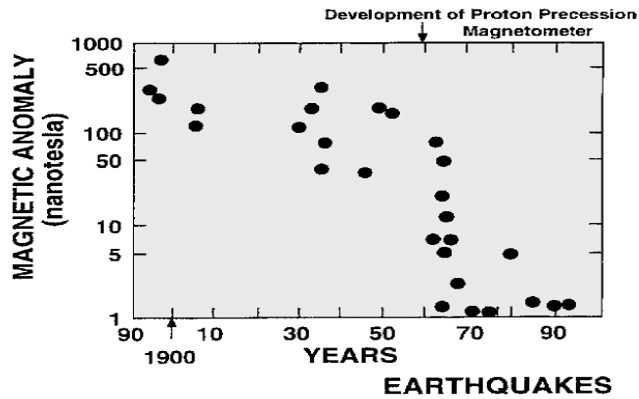


Fig. 1. Reported tectonomagnetic anomalies as a function of time. Sufficient drop of anomaly intensities happened when absolute proton precession magnetometers and noise reduction techniques were introduced (Johnston 1997).

Magnetic precursors to seismic activity can be expected as a result of gradual build up of strain in the rocks (confirmed in the laboratory tests) that induce a temporal change in its magnetic properties, i.e., create small magnetic anomalies. A number of other phenomena, such as (ionized) water flow, or microcracks with charge separation may exist and cause magnetic precursors.

Natural disasters caused by earthquakes can be better mitigated if these emotional/romantic and non-critical approaches were replaced by a rigorous engineering approach. So far there are quite few reported precursors that could be used to establish a reference, a background for detection of precursors for given earthquake magnitude.

Most spectacular Loma Prieta precursor (Ms 7.1 Central California earthquake happened on Oct. 17, 1989, near Loma Prieta), shown in Fig. 2 (Fraser-Smith 1990, disputed by some) offers us a possibility to calculate spatial distribution of magnetic field anomalies due to earthquakes so we can assess what can be expected in future earthquakes.

Loma Prieta 1989 Precursor

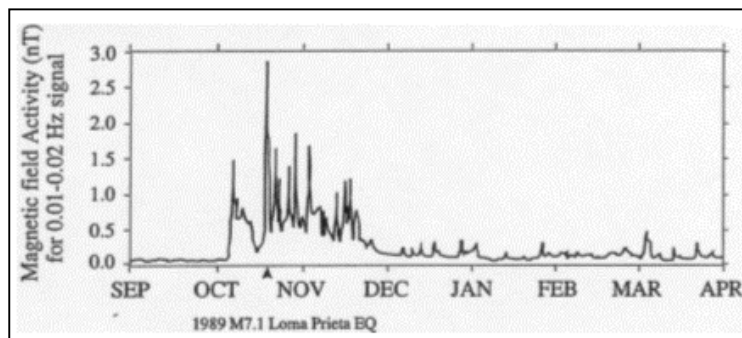


Fig. 2. Loma Prieta (M7.1) \rightarrow $B = 5$ nT anomaly at 17 km distance to hypocenter and 1.7×10^{11} Am² magnetic moment (Fraser-Smith 1990).

Assuming the “anomaly” is dipolar and knowing geometry of measurement and magnitude of the earthquake we can calculate total fields and gradients produced by the dipole. Also, assuming the anomalies are proportional to earthquake energy we can calculate expected magnetic fields for all earthquake magnitudes. Dipolar fields decrease with a cube of distance, gradients of magnetic field with a fourth potential of distance.

From Table 1 it is evident that smaller magnitude earthquakes (M4 or M5) are virtually undetectable except for immediate vicinity of the hypocenter. Detectable anomalies even for magnitude 6 are situated very close to the hypocenter.

Table 1
Dipolar magnetic fields/gradients as per Loma Prieta

| Estimated Magnetic Moment Am^2 | Earthquake Magnitude | Magnetic Fields & Gradients Distance from Hypocenter | | | | | | | |
|---|----------------------|---|-------------------------------|--------------------|-----------------|-------------------|--------------------|--------------------|----------------|
| | | 10km | 20km | 40km | 80km | 160km | 320km | 640km | 1280km |
| 2.26×10^{14} | 9 | 22.6 μT 6.78nT/m | 2.82 μT 420pT/m | 350nT 26.5pT/m | 44nT 1.7pT/m | 5.5nT 0.1pT/m | 0.69nT 6.5fT/m | 86pT 0.4fT/m | 11pT 25aT/m |
| 7.15×10^{12} | 8 | 714nT 214pT/m | 89nT 13.4pT/m | 11.2nT 0.84pT/m | 1.4nT 52fT/m | 0.17nT 3.3fT/m | 22pT 0.2fT/m | 2.75pT 12.5aT/m | |
| 2.26×10^{11} | 7 | 22.6nT 6.78pT/m | 2.82nT 0.42pT/m | 0.35nT 26.5fT/m | 44pT 1.7fT/m | 5.5pT 0.1fT/m | 0.69pT 6.5aT/m | | |
| 7.15×10^9 | 6 | 0.714nT 214fT/m | 89pT 13.4fT/m | 11.2pT 0.84fT/m | 1.4pT 52aT/m | 0.17pT 3.3aT/m | 22fT 0.2aT/m | | |
| 2.26×10^8 | 5 | 22.6pT 6.78fT/m | 2.82pT 0.4fT/m | 0.35pT 26.5aT/m | 44fT 1.7aT/m | 5.5fT 0.1aT/m | 0.7fT 0.006aT/m | | |
| 7.15×10^6 | 4 | 0.714pT 0.2fT/m | 89fT 13aT/m | 11fT 0.8aT/m | 1.4fT | 0.17fT | 22aT | | |

Now it is clear why we have so few precursors detected. Smaller, more common earthquakes may be undetectable, larger are very rare. Few precursors in the past were detected by sheer luck only when sensors happened to be very close to epicenter/hypocenter.

For example, according to Table 1 to ensure detectability of say M7 in certain area we would have to have a network of gradiometers sensitive better than 1.7 fT/m spaced at less than 2×80 km. More realistic is 2×40 km = 80 km so the anomaly can be detected with relatively high signal to noise ratio. By the same token, M6 event could only be detected at one half of this distance with good S/N ratio.

On top of the above dipolar limitations, deep anomalies will be further attenuated due to skin-effect caused by conductivity of soil. Practically, measurements should be done at frequencies below 10 mHz to avoid severe attenuation due to skin-effect.

However there is a general fair agreement of reported precursors with the calculated fields according to the Loma Prieta precursor (Table 2).

Table 2
Case histories

| Place and Reporter | Magnitudes | Sensor Distance / Sensitivity at Frequency | Signal Reported | Signal as per Loma Prieta |
|---|------------|--|---------------------------|--|
| Hector Mines Klemperer et al 1999 | 7.1 | 132km / 25 – 50pT/0.01Hz | No signal | 14pT without Skin effect 0.3fT/m |
| San Juan Bautista Karakehian et al 2000 | 5.1 | 9.4km / 20pT/0.01Hz | 20pT | 20pT 6fT/m |
| Spitak Molchanov et al 1992 | 6.9 | 129 / 20pT / 0.1 – 1.0Hz | 50 – 200pT | 7pT 0.17fT/m |
| Italy, a swarm Villante et al 1997 | < 5.8 | 65 – 85km / ? | No signal | 1.3pT 0.06fT/m |
| Loma Prieta Park et al 1993 | 7.1 | 30km / ? / 10Hz | No signal | No signal; skin effect attenuation over 1,000 times |
| GUAM Hayakawa 1996 | 7.1 | 88km | 0.1nT | 47pT without skin effect $\Delta = 2.9\text{km} @ 0.01\text{Hz}$ at sea $2\Delta \rightarrow 6.5\text{pT}/0.17\text{fT/m}$ |
| GUAM Hayakawa 1999 | 8.2 | 88km | Positive Fractal analysis | 2.1nT / 71fT/m without skin effect $2\Delta = 7.4$ times attenuation 0.28nT / 9.6fT/m |

2. Magnetic Methods of Measurement

Sensitivity of magnetometer/gradiometer must not be compromised by other non-earthquake sources of magnetic anomalies.

Traditionally, magnetic measurements must be done in gradiometric form to avoid daily (diurnal) variations of the magnetic field. Long base differential measurement with the reference magnetometer far away allows for only partial reduction of diurnal influences and final sensitivities are of nT range. Short base allows for better elimination of diurnal and other far-away influences but it requires much more sensitive magnetometers.

One limitation of short base gradiometers is the difference in inclination/declination between the sensor points. This difference will result in reduced diurnal variations invading gradient measurements. The effect was discovered by B. Ginzburg and B. Shirman of Soreq and Survey of Israel, respectively, when analyzing data from the supergradiometer installation in Amram tunnel near Eilat in Israel. The effect can be compensated by addition/subtraction of reduced amplitude of diurnal variations.

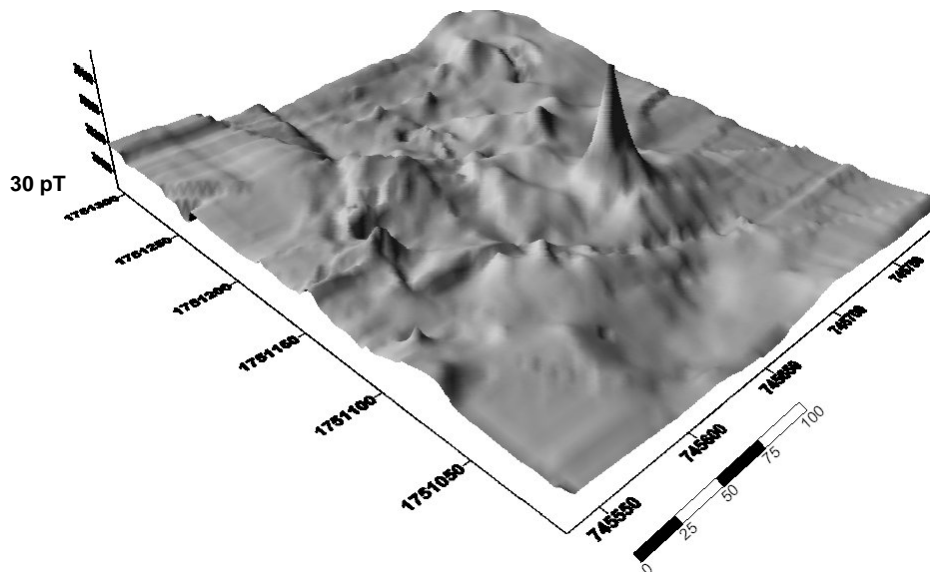
Another source of unwanted interference comes from the ionosphere that generates its own gradients at the place of measurement.

3. Supergrad in Mexico

Potassium SuperGradiometer developed by GEM Systems in cooperation with Acad. E. Alexandrov and his group and Dr. A. Green of USGS shows extraordinary sensitivity of 50 fT for one reading per second. This sensitivity opens the door to short base gradiometric measurement in earthquake studies. At 50 m spacing of sensors the gradient sensitivity of this instrument reaches 1 fT/m. From Table 1 one can see this sensitivity to be better (detectability reaches farther) than a fraction of nT sensitivity achieved in long base measurement.

The SuperGradiometer consists of three large potassium sensors operating at a single, very narrow (0.15 nT) potassium valence electron spin resonance spectral line. Sensors are attached to 100 m long cables to avoid magnetic influence of a console. Mutual sensor spacing can be selected from 1-200 m.

The installation location on the Pacific coast in Oaxaca, Mexico, was carefully selected considering several site characteristics that include relatively flat topography away from local villages and large main roads. The selected installation site was surveyed using an Overhauser vertical gradiometer to produce magnetic and gradiometric maps (Figs. 3 and 4). This survey allowed us to select three orthogonal locations for the three sensors in low gradient areas with a baseline of 140 m (NS) and “height” of 70 m (West). Gradients $S_3 - S_2$ and $S_2 - S_1$ are routinely recorded and $S_3 - S_1$ is of course also available as well as all 3 total fields. Directions of magnetic fields at the 3 sensors have been measured as shown on Table 3.



tion corrections obtained from potassium dIdD. At this point the dIdD has not yet been deployed in El Trapiche Cozoaltepec in Oaxaca, Mexico.

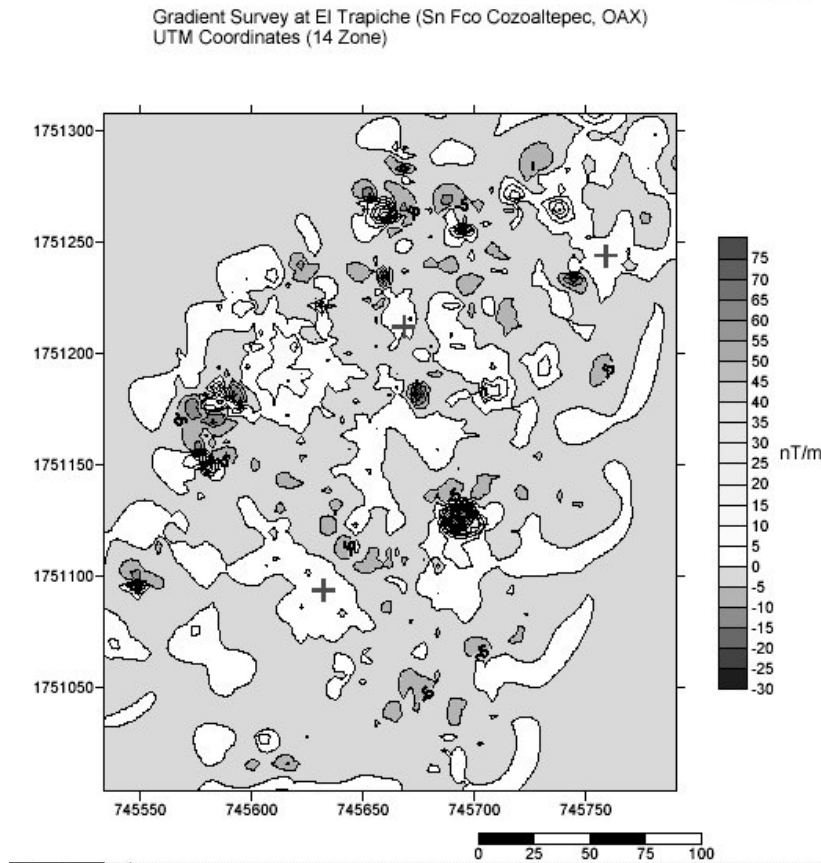


Fig. 4. Site selection: sensor location.

Table 3

Inclinations and declinations at sensor positions

| | Inclination | Inclination difference | Declination | Declination difference |
|-----------|-------------|------------------------|-------------|------------------------|
| Sensor 1: | 43.16° | | 5.11° | |
| | | 2.4' | | 2.4' |
| Sensor 2: | 43.12° | | 5.05° | |
| | | 4.2' | | 1.2' |
| Sensor 3: | 43.19° | | 5.27° | |

The system is away from power lines so the energy for the instrument is derived from a solar panel array and lead-acid. Data is organized in hourly files in a local

computer and transmitted via an Internet satellite link for further archiving and processing at Instituto de Geofísica-UNAM in Mexico City. Several graphs of total field and gradients are shown in Figs. 5, 6 and 7.

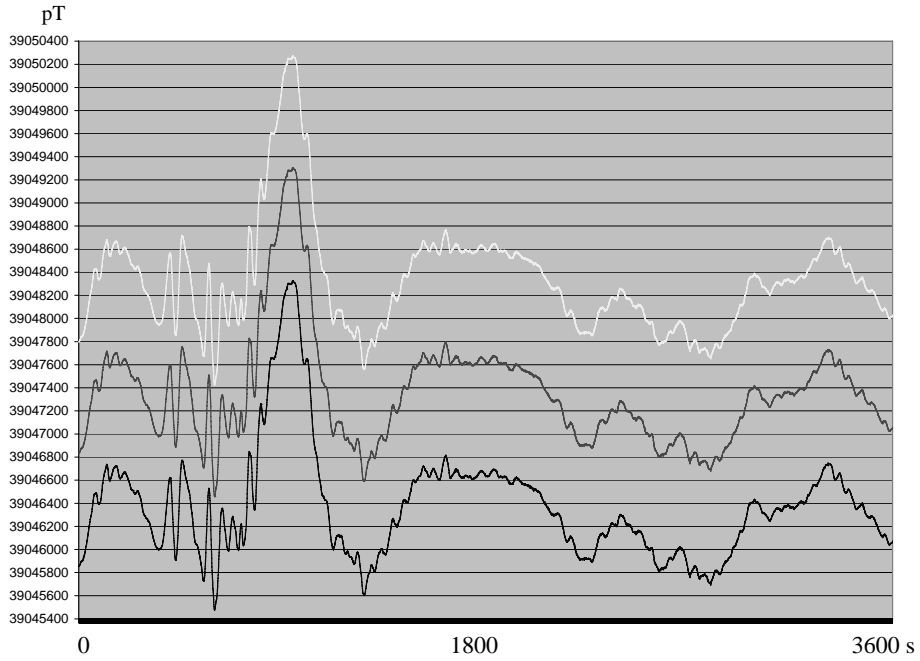


Fig. 5. Sample of SuperGrad total field record.

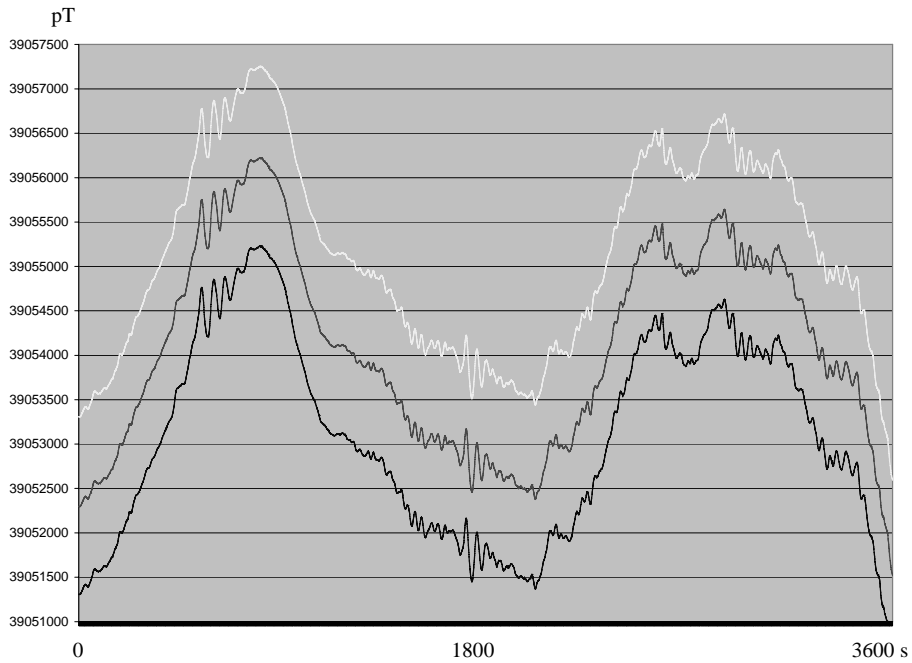


Fig. 6. Sample of SuperGrad total field record.

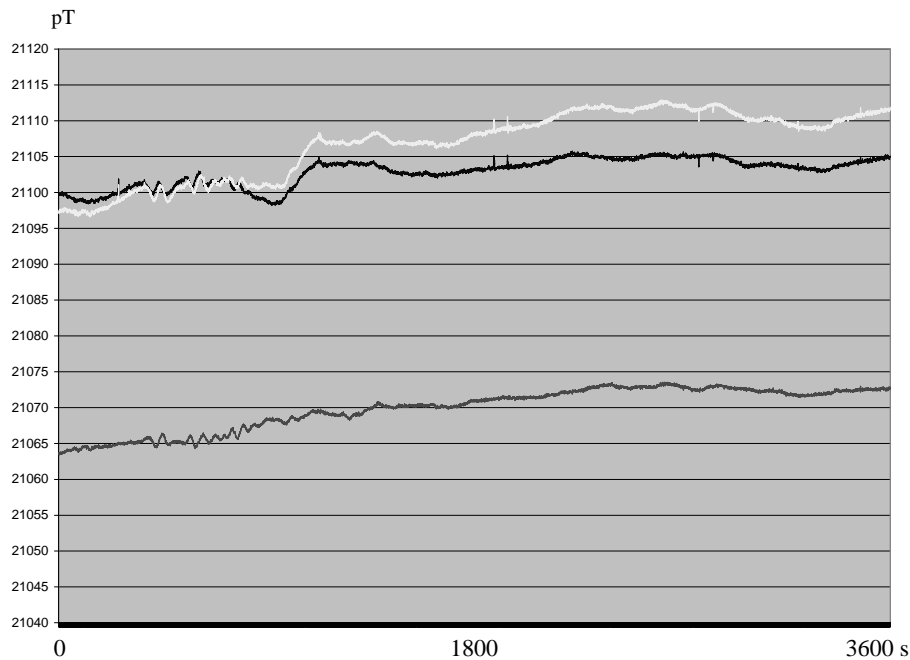


Fig. 7. Sample of SuperGrad total field record.

4. Conclusion

Installation of a SuperGradiometer in the Oaxaca, Mexico segment of the Middle America trench, in close proximity to the seismogenic zone, besides performing as a supersensitive magnetic observatory (once the installation of Potassium dID magnetometer is completed) offers an excellent possibility to detect precursors from large earthquakes. The field deployment of a SuperGradiometer under harsh conditions has gained sufficient ruggedness to operate reliably in a tropical environment.

References

- Fraser-Smith, A.C., A. Bernardi, P.R. McGill, M.E. Ladd, R.A. Helliwell and O.G. Jr. Villard, 1990, *Low-frequency magnetic field measurements near the epicenter of the M_s 7.1 Loma Prieta earthquake*, Geophys. Res. Letts. **17**, 9 1465-1468.
- Hayakawa, M., R. Kawate, O.A. Molchanov and K. Yumoto, 1996, *Results of ultra-low-frequency magnetic field measurements during the Guam earthquake of 8 August, 1993*, Geophys. Res. Letts. **23**, 3, 241-244.
- Hayakawa, M., T. Ito and N. Smirnova, 1999, *Fractal analysis of ULF geomagnetic data associated with the Guam earthquake on August 8, 1993*, Geophys. Res. Letts. **26**, 18, 2797-2800.
- Johnston, M.J.S., 1997, *Review of electric and magnetic fields accompanying seismic and volcanic activity*, Surveys Geophys. **18**, 441-475.

- Karakelian, D., S.L. Klemperer, G.C. Beroza and A.C. Fraser-Smith, 2000, *Eos Trans. AGU* **81**, 48.
- Karakelian, D., S.L. Klemperer, G.A. Thompson and A.C. Fraser-Smith, 2000, *Results from electromagnetic monitoring of the Mw 5.1 San Juan Bautista, California earthquake of 12 August 1998*. In: G. Bokelman and R.L. Kovach (eds.), "Tectonic problems of the San Andreas Fault System", Stanford University Publication, Geological Sciences **21**, 334-345.
- Molchanov, O.A., Iu.A. Kopytenko, P.M. Voronov, E.A. Kopytenko, T.G. Matiashvili, A.C. Fraser-Smith and A. Bernardi, 1992, *Results of ULF magnetic field measurements near the epicenters of the Spitak ($M_S = 6.9$) and Loma Prieta ($M_S = 7.1$) earthquakes: comparative analysis*, *Geophys. Res. Letts.* **19**, 14, 1495-1498.
- Park, S.K., M.J.S. Johnston, T.R. Madden, F.D. Morgan and H.F. Morrison, 1993, *Electromagnetic precursors to earthquakes in the ULF band: A review of observations and mechanisms*, *Reviews Geophys.* **31**, 2, 117-132.
- Villante, U., M. Villante and A. Pincatelli, 2001, *Ultra low frequency geomagnetic field measurements during earthquake activity in Italy (September-October 1997)*, *Annali di Geofisica* **44**, 2, 229-237.

Accepted March 7, 2007

Upstream Wave Related Pc3 Pulsations Observed by the MM100 Meridional Magnetometer Array

B. HEILIG¹, A. CSONTOS¹, L. PANKRATZ², K. PAJUNPÄÄ³, J. KULTIMA⁴,
T. RAITA⁴, J. REDA⁵ and M. VÁCZYOVÁ⁶

¹ Eötvös Loránd Geophysical Institute, Tihany Geophysical Observatory
Kossuth u. 91, H-8237 Tihany, Hungary
e-mail: heilig.elgi.hu

² USGS Geomagnetism Group
1711 Illinois street, Golden CO 80401-1865, USA
e-mail: pankratz@usgs.gov

³ Finnish Meteorological Institute, Nurmijärvi Geophysical Observatory
FIM-05100 Röykkä, Finland
e-mail: kari.pajunpaa@fmi.fi

⁴ Oulu University, Sodankylä Geophysical Observatory
FIN-99600 Sodankylä, Finland
e-mail: johannes.kultima@sgo.fi

⁵ Polish Academy of Sciences, Belsk Geophysical Observatory
ul. Ks. Janusza 64, 01452 Warsaw, Poland
e-mail: jreda@igf.edu.pl

⁶ Slovak Academy of Sciences, Hurbanovo Geophysical Observatory
Komarnanska 108, 947 01 Hurbanovo, Slovak Republic
e-mail: magdi@geomag.sk

A b s t r a c t

The upstream waves (UWs) are typically 20-30 s magnetosonic waves generated in the Earth's foreshock region. Under appropriate interplanetary conditions the UWs are able to enter the magnetosphere, propagate across field lines down to the ionosphere and reach the ground as Pc3 geomagnetic pulsations. In the past years, a semi-automated method was developed to monitor UW-related geomagnetic pulsation activity. The method was based on cross spectral density estimation of signals recorded at meridionally distributed stations or by satellites at LEO (CHAMP). The MM100 meridional array, including Finnish, Polish, Slovak and Hungarian observatories, was established in 2001. In the present pa-

per we review the first results of the analysis of UW-related ground pulsations observed by the MM100 network. We demonstrate the relation of these pulsations to upstream phenomena and consequently, to the state of the interplanetary medium.

1. Introduction

Modern history of pulsation study in Tihany Geophysical Observatory started in 1996, when on the initiation of A.W. Green (USGS Geomagnetism Group) two identical magnetometers were installed in Tihany (Hungary) and in Srobarovo (Slovak Republic) with the support of the US-Hungarian Joint Fund. The Srobarovo-Tihany magnetometer pair was planned to be a part of a global network of gradient stations to identify field line resonances and upstream waves (Green *et al.* 1999). Although this network was never completed, two further stations were later installed in Hungary, one in Nagycenk and another in Farkasfa in 1999 and 2000, respectively.

The need for a mid-latitude high resolution magnetometer array emerged again in 1999 on preparing a measuring campaign organised for the observation of the possible geomagnetic effects of the total solar eclipse of August 11, 1999. In addition to one minute mean, normal observatory records, our aim was to observe one second data, as well, in as many stations in Europe as possible, for Pc3 (22-100 mHz) pulsation studies. At that time, our initiation was supported by the Sodankylä, Nurmijärvi, Belsk and Hurbanovo observatories. The results of this eclipse campaign were published recently (Heilig *et al.* 2001, Bencze *et al.* 2007).

The analysis of most pulsation phenomena requires magnetic networks rather than single stations. The reliable identification of field line resonances can be realized with meridional pairs of closely (100-250 km) spaced stations according to the gradient method (Green *et al.* 1993). On the other hand, monitoring the upstream wave related pulsations claims several stations from different latitude zones (Heilig *et al.* 2007). Meridional array consisting of gradient pairs, or a properly dense meridional magnetometer chain can fulfil both criteria.

There are only a few meridians in the Earth with sufficient land coverage suitable for establishing a meridional array connecting both polar regions. Beside the circum-Pacific region and the American continent, Europe and Africa form a natural basis for global meridional arrays. The Circum pan-Pacific Magnetometer Network (70°N – 65°S mag. lat.) have been operating since 1995, its predecessor, the MM210 was started in 1990 (Yumoto *et al.* 2001). A meridional network, McMAC is currently being formed in the American continent, but a similar array is still missing in Europe. Existing European regional networks (IMAGE and SAMNET in Scandinavia and North-Western-Europe, and low-latitude SEGMA in Southern-Europe) are not connected with each other. MM100 is the first initiative to fill the gap between high and low latitude European networks.

2. The MM100 Meridional Magnetometer Array

MM100 is the acronym for a quasi-meridional magnetometer array established for pulsation study, in September 2001. The array consists of Finnish, Estonian, Polish, Slovak and Hungarian stations from high to mid latitudes ($L = 6.09$ to 1.84). The

Finnish and Estonian sites belong to the IMAGE (Lühr *et al.* 1998) array. The Polish and Slovak observatories are maintained by the national Academies of Sciences. Tihany, Farkasfa and Nagycenk stations in Hungary were installed in 1996, 1999 and 2000, respectively, as a result of a joint project of the USGS Geomagnetism Group and ELGI (Hungary). Nagycenk station is operated by the Geodetic and Geophysical Institute (GGRI) of the Hungarian Academy of Sciences.

Below we list the AACGM coordinates and L-shell values of MM100 stations in the order: **Station name**, **IGA code**, operating institute, AACGM-2001 latitude (North) and longitude (East), L-shell-value; **Kilpisjärvi**, **KIL**, *op*: FMI, *aacgm*: 66.10°, 104.00°, *L*: 6.09; **Sodankylä**, **SOD**, *op*: Oulu University SGO, *aacgm*: 64.16°, 107.46°, *L*: 5.26; **Hankasalmi**, **HAN**, *op*: FMI, *aacgm*: 59.01°, 104.78°, *L*: 3.77; **Nurmijärvi**, **NUR**, *op*: FMI, *aacgm*: 57.23°, 102.34°, *L*: 3.41; **Tartu**, **TAR**, *op*: FMI, *aacgm*: 54.48°, 103.04°, *L*: 3.01; **Belsk**, **BEL**, *op*: PAS, *aacgm*: 48.01°, 96.15°, *L*: 2.23; **Hurbanovo**, **HRB**, *op*: SAS, *aacgm*: 43.56°, 92.86°, *L*: 1.90; **Nagycenk**, **NCK**, *op*: ELGI-GGRI-USGS, *aacgm*: 43.27°, 91.53°, *L*: 1.89; **Farkasfa**, **FKF**, *op*: ELGI-USGS, *aacgm*: 42.43°, 91.00°, *L*: 1.84; **Tihany**, **THY**, *op*: ELGI-USGS, *aacgm*: 42.44°, 92.39°, *L*: 1.84.

The instrumentation at these stations is not identical. However, high resolution, low noise fluxgate or torsion photoelectric magnetometers are used in each station with GPS synchronized timing and sampled at least at 1 Hz. The most important technical parameters of current MM100 stations are given in Table 1. All MM100 data are transformed into the magnetic field oriented HDZ system and archived in uniform format, in ELGI.

3. Upstream Waves

Upstream waves (UWs) are typically 20-30 s magnetosonic waves generated in the Earth's foreshock. These waves are driven by a wave-particle interaction, i.e. the ion-cyclotron instability. The resulting waves are swept back to the magnetosphere by the super-Alfvénic solar wind. The frequency of the generated UW is directly proportional to the interplanetary magnetic field (IMF) strength. Their amplitude is controlled by the solar wind speed and the so-called cone angle, i.e. the angle between the Sun-Earth line and the direction of the IMF. Under appropriate conditions the UWs are able to enter the magnetosphere, travel down to the ionosphere and finally reach the ground as Pc3 (22-100 mHz) geomagnetic pulsations (e.g. Yumoto *et al.* 1984).

4. Data Processing

In the past years we developed a semi-automated method to monitor UW-related geomagnetic pulsation activity based on the comparison of spectral energy densities of signals recorded at meridionally distributed locations or in low-Earth-orbit satellites (CHAMP). In a single station magnetic record, the UW pulsations are usually masked by local field line resonances (FLR). For this reason the UW frequency can be determined only from the records of a set of meridionally distributed magnetometers. Supposing that the UW related pulsations are coherent over large areas extending up to

Table 1
Instrumentation at MM100 stations

| IAGA code | Magnetometer | | f_{sampling} | Bandwidth DC – | Resolution | rms noise (0.01-0.1 Hz) | Timing |
|-----------|--------------|------------------------|-----------------------|----------------|------------|-------------------------|--------|
| | model | type | | | | | |
| KIL | LEMI 004 | fluxgate | 1 Hz | 1 Hz | 10 pT | 20 pT | GPS |
| SOD | PSM | torsion photo-electric | 2 Hz | 0.3 Hz | 3 pT | 20 pT | GPS |
| HAN | FGE | fluxgate | 1 Hz | 1 Hz | 10 pT | 50 pT | GPS |
| NUR | FGE | fluxgate | 1 Hz | 1 Hz | 10 pT | 50 pT | GPS |
| TAR | FGE | suspended fluxgate | 1 Hz | 1 Hz | 10 pT | 50 pT | GPS |
| BEL | PSM 8511-01P | torsion photo-electric | 1 Hz | 0.3 Hz | 3 pT | 10 pT | GPS |
| HRB | Magson | fluxgate | 1 Hz | n/a | 100 pT | 50 pT | GPS |
| NCK | Narod S-100 | fluxgate | 1 Hz (16 Hz*) | 5 Hz* | 1 pT* | 20 pT | GPS |
| FKF | Narod S-100 | fluxgate | 1 Hz (16 Hz*) | 5 Hz* | 1 pT* | 20 pT | GPS |
| THY | Narod S-100 | fluxgate | 1 Hz (16 Hz*) | 5 Hz* | 1 pT* | 20 pT | GPS |

* In January of 2004, band-pass (3-200 mHz) filter cards and DAQ system were replaced, sampling rate was increased to 16 Hz. In this study we use 1 Hz means.

thousands of kilometres on the ground, this UW-related activity can be emphasised by calculating the cross spectral densities of the signals recorded at MM100 stations on different geomagnetic latitudes. The averaging at the same time suppresses the latitude dependent FLRs. The method is described in details in Heilig *et al.* (2007). In the current paper, the peak frequencies estimated from time series recorded in January of 2003 are analysed.

Hourly pulsation activity indices are routinely calculated for all MM100 stations. The local activity index is the rms amplitude of the Pc3-band-pass filtered H-component signal expressed in pT. The value of this index depends on both UW and FLR activity. In this paper we used the 2003 activity indices for all stations (except for SOD, where only the first six months data were considered).

5. Results

5.1 Distribution of Pc3 power

The MM100 activity indices yield a possibility to map the distribution of Pc3 power in a zone bounded by the 42° and 66° magnetic latitudes (Fig. 1). At lower than 60° latitude this distribution can be characterised by a gradual increase after sunrise

followed by a decrease after the local noon till sunset. This behaviour is typical for mid-latitude Pc3s and thought to be related to the upstream origin of this activity. Along the MM100 array, two activity maxima can be established. The first one is located near the latitude of 48° (BEL). The average UW frequency estimated from the IMF magnitude was in the range of 30-40 mHz in the considered period. Since the local FLR frequency at BEL is usually within this range, the coupling of the incoming fast mode and Alfvén mode waves is the strongest near the latitude of the BEL (Heilig *et al.* 2007), the resulting FLRs may be responsible for the observed peak. The enhanced power poleward from the 60° magnetic latitude is considered to be caused by processes taking place at the magnetopause.

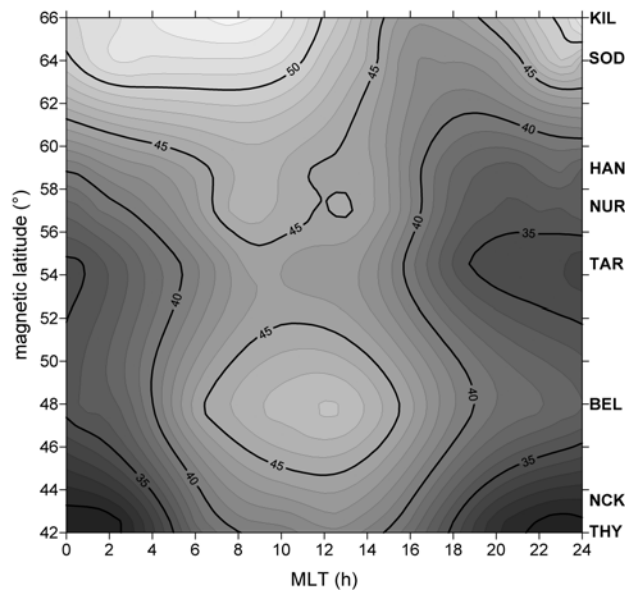


Fig. 1. Average distribution of Pc3 power as $20 \cdot \log_{10}(\text{Pc3ind})$ vs. magnetic local time and magnetic latitude (KIL, SOD, HAN, NUR, TAR, BEL, NCK, THY, January 1 to December 31, 2003).

The relation between the daily (solar zenith angle $< 60^\circ$) activity levels at different latitudes can be well approximated by linear formulae, as

$$\text{Pc3ind}_{\text{STA}} = a \cdot \text{Pc3ind}_{\text{STA_ref}} + b,$$

where STA and STA_ref stands for the code of the investigated and an arbitrary reference stations, respectively. Taking THY as a reference station and limiting the THY activity within the 20-300 pT range, the linear regression yields the following parameters for 2003: for NCK $a = 1.191$, $b = 15$ pT; for BEL $a = 1.762$, $b = 48$ pT; for TAR $a = 1.225$, $b = 23$ pT; for NUR $a = 1.575$, $b = 26$ pT; for HAN $a = 1.358$, $b = 38$ pT; for SOD $a = 1.993$, $b = 70$ pT; and for KIL $a = 2.497$ and $b = 71$ pT. The high correlations with THY at stations located at magnetic latitudes lower than 60° (0.99, 0.85, 0.69, 0.71, 0.72, 0.50 and 0.48 for the case of NCK, BEL, TAR, NUR, HAN, SOD,

KIL, respectively) suggest the common source of Pc3s in this latitude range, at least partially.

5.2 The relation of Pc3 pulsations to interplanetary conditions

The Pc3 activity at all stations correlates with radial solar wind speed and anti-correlates with interplanetary cone angle (Fig. 2). The former property of Pc3 pulsations can be explained by different source mechanisms including the upstream wave theory. The dependence on the cone angle, however, unambiguously indicates the role of upstream waves in the generation of ground Pc3s. Nevertheless, the most widely accepted test for the verification of upstream origin of selected pulsation events is the comparison of the dominant Pc3 frequency with the magnitude of the IMF. Based on the ion-cyclotron origin, there exist several theoretical, as well as empirical evidences (e.g. Yumoto *et al.* 1984) that confirm the following relation between the frequency of UWs and the IMF strength: f_{UW} (mHz) = $(6 \pm 1.5) \cdot B_{IMF}$ (nT). The UW candidate events selected by our algorithm behave exactly the expected way (Fig. 3). We argue then, that this result unambiguously validates the efficiency of our automated event selecting algorithm.

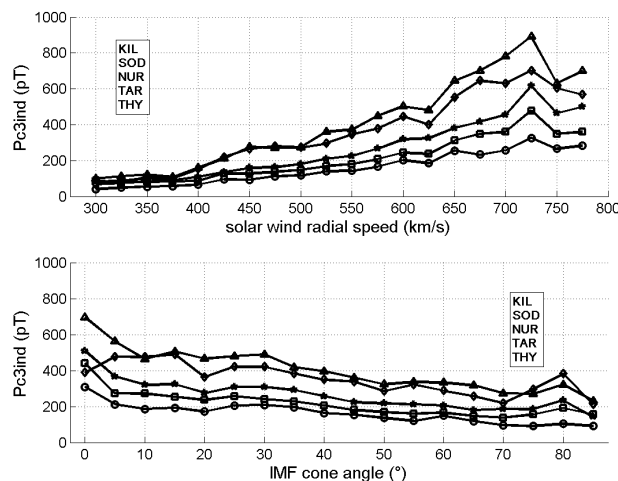


Fig. 2(a) The relation of Pc3 activity index to ACE solar wind speed at KIL (triangles), SOD (diamonds), NUR (stars), TAR (squares) and THY (circles) MM100 stations in 2003, (b) relation of Pc3 activity index to ACE IMF cone angle, format is the same as in the case of (a).

The most important advantage of the automated algorithm is that it makes possible a comprehensive statistical analysis of UW related pulsations. Most of the questions still open in this area could have not been answered so far because of the lack of large enough reliable datasets. Using the automatically selected UW events, our first important result was the confirmation of the existence of the Doppler-shift of UWs in the solar wind (Heilig *et al.* 2007). The dependence of pulsation activity on the subsolar distance of the magnetopause and on upstream Alfvén Mach number was also demonstrated for the first time (Heilig 2007).

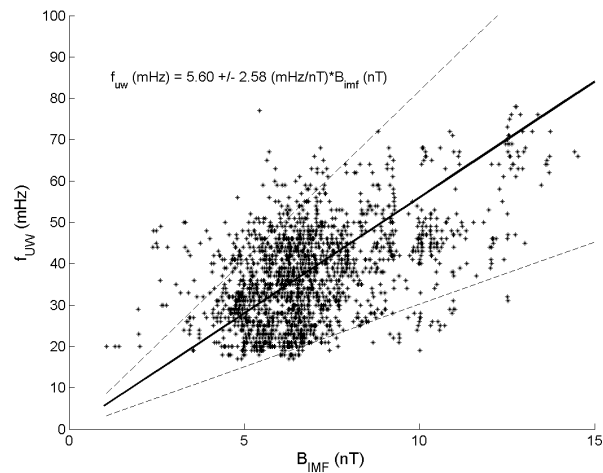


Fig. 3. Relationship between peak frequency and IMF strength, January 2003. The solid line and the equation in the left upper corner represent the result of the linear regression; the dashed lines limit the range containing 90% of all 2171 cases.

5.3 Interstation and space-ground coherence

In Bencze *et al.* (2007) it was demonstrated that interstation coherence calculated between stations located far away from each other can also be used to estimate the UW frequency. The coherence spectra have a peak at the dominant frequency of UWs. However, if the UW frequency is close to the local field line resonance at one of the considered stations, the coherence drops to a lower level near the resonant frequency.

The first results of our space-ground coherence analysis (Heilig *et al.* 2007) verified both the direct propagation of UW related waves from the subsolar magnetopause (CHAMP-THY case) and the existence of a field guided propagation of Alfvén mode waves coupled to the incident fast mode waves (CHAMP-NUR case).

6. Summary

The MM100 magnetometer array established in 2001 is maintained by institutes of 5 EU countries. As it was shown, the MM100 network can give an important contribution to the study of magnetospheric ULF pulsations. In this paper, some preliminary results of our multistation approach have been presented. Our results indicate that UW related pulsations can be traced using the MM100 array. Based on the large amount of events selected by our method, it is planned to carry out a comprehensive statistical analysis on UW related pulsation events in the near future.

The MM100 project is a registered Coordinated Investigation Program of IHY2007 under the nr. CIP 39 (ULF waves in the magnetosphere). Monitoring of plasmaspheric mass density is also targeted by this project, this topic was not discussed here.

Acknowledgments. The authors are grateful to J. Veró for helpful discussions. We thank H. Lühr and the CHAMP team for providing the CHAMP magne-

tometer data. The provision of the ACE data by the ACE MAG and SWEPAM instrument teams and the ACE Science Center is greatly acknowledged. This study is supported by the Hungarian Space Office (TP 153) and by the Hungarian Scientific Research Fund (NI 61013).

References

- Bencze, P., B. Heilig, B. Zieger, J. Szendrői, J. Verő, H. Lühr, K. Yumoto, Y. Tanaka and J. Střeščík, 2007, *Effect of the August 11, 1999 total solar eclipse on geomagnetic pulsations*, Acta Geod. Geoph. Hung. **42**, 23-58.
- Green, A.W., E.W. Worthington, L.N. Baransky, E.N. Fedorov, N.A. Kurneva, V.A. Pilipenko, D.N. Shvetzov, A.A. Bektemirov and G.V. Philipov, 1993, *Alfven field line resonances at low latitudes ($L = 1.5$)*, J. Geophys. Res. **98**, 15693-15699.
- Green, A.W., E.W. Worthington, T.A. Plyasova-Bakounina, A. Körmendi, L. Hegymegi, W. Goedecke and Z. Vörös, 1999, *Field line resonance studies in North America and Central Europe*, Geophys. Trans. **42**, 3-4, 181-193.
- Heilig, B., 2007, *The behaviour of Pc3 pulsations during low-density solar wind events. Revisiting the problem: how the Pc3 pulsation activity relates to solar wind conditions?*, Geophysical Research Abstracts 9, 10521.
- Heilig, B., A. Csontos and P. Kovács, 2001, *The geomagnetic effect of the solar eclipse of 11 August, 1999*, Contrib. Geophys. Geod. **31**, 1, 83-89.
- Heilig, B., H. Lühr and M. Rother, 2007, *Comprehensive study of ULF upstream waves observed in the topside ionosphere by CHAMP and on ground*, Annales Geophys. **25**, 737-754.
- Lühr, H., A. Aylward, S.C. Buchert, A. Pajunpää, K. Pajunpää, T. Holmboe and S.M. Zalewski, 1998, *Westward moving dynamic substorm features observed with the IMAGE magnetometer network and other ground-based instruments*, Annales Geophysicae **16**, 425-440.
- Yumoto, K., T. Saito, B.T. Tsurutani, E.J. Smith and S.-I. Akasofu, 1984, *Relationship between the IMF magnitude and Pc 3 magnetic pulsations in the magnetosphere*, J. Geophys. Res. **89**, 9731-9740.
- Yumoto, K., and the CPMN Group, 2001, *Characteristics of Pi 2 magnetic pulsations observed at the CPMN stations: A review of the STEP results*, Earth Planets Space **53**, 981-992.

Accepted February 15, 2007

Study of Geomagnetically Induced Current from Time Derivative of the Earth's Magnetic Field

V.V. VODJANNIKOV¹, G.I. GORDIENKO¹, S.A. NECHAEV²,
O.I. SOKOLOVA¹, S.J. HOMUTOV³ and A.F. YAKOVETS¹

¹Institute of Ionosphere MES RK
050020, Almaty, Kamenskoe plato, Kazakhstan
e-mail: olgsokolova@yandex.ru

²Magnetic Observatory "Irkutsk" ISZF RAN
664033, Irkutsk, Russia
e-mail: san@irlan.ru

³Geophysical Observatory "Klyuchi", Altai-Saian Branch of Geophysical Service
of the Siberian Branch of the Russian Academy of Science
630090, Koptyug av., 3, Novosibirsk, Russia
e-mail: khomutov@gs.nsc.ru

Abstract

One of negative impacts of space weather on technological systems is the occurrence in conducting ground systems (electric power systems, pipelines) of geomagnetically induced current (GICs) caused by variations of the geomagnetic field during large magnetic storms. Analysis of variations of the horizontal component (H) of the geomagnetic field and its time derivative (dH/dt) for seven periods of high magnetic activity in 2003-2005 is carried out using data from magnetic observatories Alma-Ata, Novosibirsk and Irkutsk. Distributions of directions of H and dH/dt are derived. It is shown that the large dH/dt determining significant GICs are caused by variations of a magnetic field of three types: a sudden pulse (SI) observed in the beginning of a magnetic storm, pulsations, and casual variations of the field during a magnetic storm.

1. Introduction

During large magnetic storms, variations of geomagnetic field induce currents in the Earth's surface called geomagnetically induced currents. Different regions of the Earth have different conductivity. Igneous rocks do not conduct electricity very well so the currents tend to take the path of least resistance and flow through man-made

conductors that are present on the surface. During large magnetic storms, these GICs can cause serious problems for the operation of the power systems, disrupting the operation of transformers and other facilities. Greatest GICs problems occurred at power systems located at high latitudes due to their proximity to dynamic auroral electrojets; therefore, the majority of studies were carried out in the high latitudes. However, recently Koen and Gaunt (2002) showed that GICs are present even at the mid-latitudes during strong geomagnetic storms. Moreover, Kappenman (2003) showed that global burst in intensity of the geomagnetic field (the sudden beginning of a magnetic storm) can be a reason of significant GICs at all geomagnetic latitudes including equatorial ones.

Therefore, the GICs problem is actual for Kazakhstan where a network of high-voltage (220–1150 kV) power electric lines of general extent of 27 000 km operates. The aim of the present work is studying a possibility of occurrence of significant GICs in this region using measurements of variations of the horizontal component of the geomagnetic field at magnetic observatories of Alma-Ata, Novosibirsk and Irkutsk whose geomagnetic latitudes are close to geomagnetic latitudes of southern and northern borders of Kazakhstan.

2. Method of Data Analysis

There are several methods of GICs study. The most common method is based on linear dependence between GIC and time derivative of the horizontal component of the magnetic field (dH/dt) as Faraday's law states. Validity of the method has been confirmed by Bolduc *et al.* (2000) where results of simultaneous measurements of variations of the geoelectric field and dH/dt of the magnetic field orthogonal to the electric field were compared. The further acknowledgement of reliability of this method has been obtained by Viljanen (1998). Here, direct measurements of GICs at high-voltage transformers in power electric lines were carried out. Changes of the northern component of the geomagnetic field (H_x) generate the east component (E_y) of an electric field; therefore, measurements of dH_x/dt give E_y , and measurements of dH_y/dt are used for calculation of E_x . The current generally induced in a power system is expected to be:

$$GIC = c(aE_x + bE_y), \quad (1)$$

where a and b depend on the geometry of the power line and its resistance. The coefficient c is used to equalize theoretical and observed GICs. For the Finnish power grid whose extent is not so large, the values of a and b have been 10 and 94 A·km/V, respectively, (strength of electric field in expression (1) is given in V/km). It is obvious that for Kazakhstan with its extended electric power lines, the values of multipliers a and b should exceed Finnish ones.

In order to estimate the rate of change of the horizontal component of the geomagnetic field we used the data of three magnetic observatories. The southern part of Kazakhstan was provided with the data of the observatory Alma-Ata (code AAA, geographical coordinates: 43.25N, 76.92E, geomagnetic coordinates: 34.13N, 152.62E).

Northern part of Kazakhstan was provided with the data of the observatory Novosibirsk (NVS, geographical coordinates: 54.85N, 83.23E, geomagnetic coordinates: 45.39N, 159.41E) and the observatory Irkutsk (IRK, geographical coordinates: 52.17N, 104.45E, geomagnetic coordinates: 41.73N, 176.73E). For the present study we used one-minute data of the northern (H_x) and eastern (H_y) components of the geomagnetic field of observatories Alma-Ata and Novosibirsk and the horizontal component (H) and declinations D of the observatory Irkutsk. To provide the field components variations their base-lines were subtracted from the primary data. Further, under H we shall understand variations of the horizontal component. The time derivative (dH/dt) was calculated as $(H_{t+1 \text{ min}} - H_t)/1 \text{ min}$. Variations of northern and eastern components are designated as X and Y , respectively.

3. Variations of the Geomagnetic Field and its Derivative

Present analysis includes seven periods of the high magnetic activity occurred in 2003-2005. In Fig. 1 variations of the northern component and its derivative (dX/dt) for three observatories at magnetoactive periods are presented.

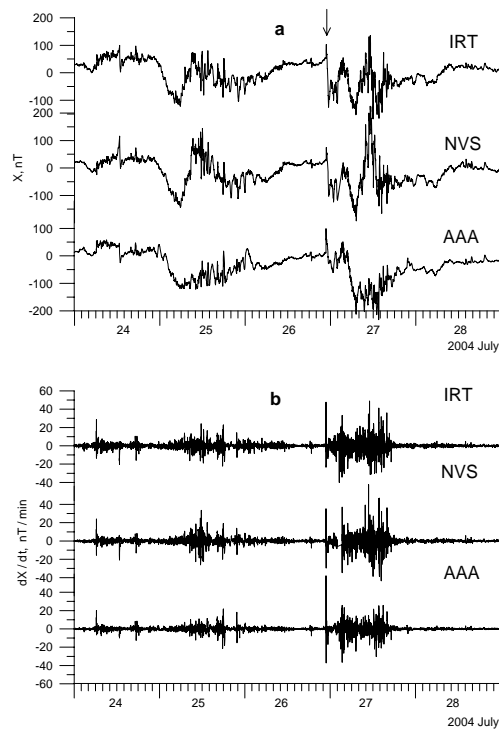


Fig. 1. Variations of the northern component (a) and its derivative (dX/dt) (b) for two successive large magnetic storms.

The analyzed period includes two successive large magnetic storms during which substantial intensification of the dX/dt was observed. It is evident that dX/dt for Irkutsk

and Novosibirsk is larger in comparison with Alma-Ata. The second storm began from a strong sudden pulse (SI) at all three stations at 22:28 UT (pointed by the arrow). The burst in dX/dt occurred practically simultaneously at all three observatories and its amplitude was maximal at the southern station. Dates, time and amplitudes of dX/dt bursts occurred synchronously at observatories Alma-Ata and Novosibirsk are presented in Table 1. Three of the bursts (26.07.04, 07.11.04 and 09.11.04) are connected with SI which preceded the beginning of large magnetic storms. In all these cases the dX/dt magnitude in Alma-Ata exceeded the values observed in Novosibirsk. Several successive significant dX/dt bursts not connected with SI were observed on the recovery phase of very large storm occurred on 31.10.03 at 02:24 UT. Amplitudes of the biggest bursts are presented in the table. These bursts have been caused by periodic pulsations of the geomagnetic field with the average period of 7.2 minutes. In this case, amplitudes of bursts in Novosibirsk exceeded amplitudes of Alma-Ata. Detailed global pattern of Pc5 geomagnetic pulsation for this storm was presented by Kleimenova and Kozyreva (2005).

Table 1
Time and amplitudes of dX/dt bursts

| Date | UT | dX/dt [nT/min] | | Type of disturbances |
|----------|---------------|------------------|-------------|----------------------|
| | | Alma-Ata | Novosibirsk | |
| 31.10.03 | 02.10 – 02.30 | 105 | 252 | Pulsations |
| 31.10.03 | 05.30 – 05.55 | 75 | 155 | Pulsations |
| 31.10.03 | 10.25 – 10.55 | 85 | 80 | Pulsations |
| 26.07.04 | 22.28 | 59 | 37 | SI |
| 07.11.04 | 18.31 | 65 | 60 | SI |
| 09.11.04 | 18.52 | 78 | 54 | SI |

It is known that rotation of $d\mathbf{H}/dt$ by 90° anticlockwise gives the direction of the horizontal electric field at the Earth's surface. In order to estimate the possible strength and direction of GICs, we calculated $|d\mathbf{H}/dt|$ distributions and direction distributions of \mathbf{H} and $d\mathbf{H}/dt$ for the cases considered with the condition $|d\mathbf{H}/dt| > 5$ nT/min. In Fig. 2 these values are plotted for storms presented in Fig. 1. For better presentation the \mathbf{H} and $d\mathbf{H}/dt$ distributions are normalized at each subplot. The condition $|d\mathbf{H}/dt| > 5$ nT/min was used by Koen and Gaunt (2002) as a threshold determining the occurrence GICs in power systems. The most interesting features of plots in Fig. 2 are the narrow \mathbf{H} distributions for all observatories and the narrow $d\mathbf{H}/dt$ distribution for Alma-Ata, extended in the geomagnetic north–south direction and scattered $d\mathbf{H}/dt$ distributions for Novosibirsk and Irkutsk.

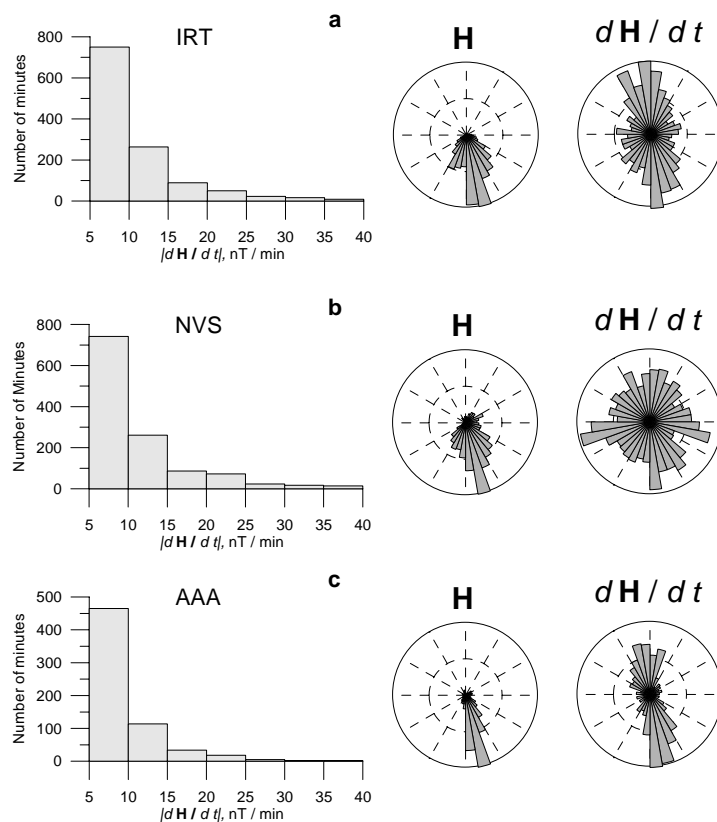


Fig. 2. $|d\mathbf{H}/dt|$ distributions and direction distributions of \mathbf{H} and $d\mathbf{H}/dt$ for the cases considered under the condition $|d\mathbf{H}/dt| > 5$ nT/min.

Table 2

Total time when $|d\mathbf{H}/dt| > 30$ nT/min

| Date | K_p | Total time with $ d\mathbf{H}/dt > 30$ nT/min | |
|--------------------|-------|--|-------------|
| | | Alma-Ata | Novosibirsk |
| 29-31 October 2003 | 9 | 148 | 445 |
| 22-23 January 2004 | 7+ | 0 | 0 |
| 24-28 July 2004 | 8 | 5 | 56 |
| 7-10 November 2004 | 9- | 8 | 78 |
| 7-8 January 2005 | 8- | 0 | 0 |
| 16-19 January 2005 | 8- | 3 | 6 |
| 21-22 January 2005 | 8 | 12 | 26 |

Koen and Gaunt (2002) carried out $d\mathbf{H}/dt$ measurements simultaneously with GICs records in the South African power grid. Comparison of the GICs and $d\mathbf{H}/dt$ values has shown that when $|d\mathbf{H}/dt| > 30$ nT/min, the induced current causing undesirable consequences in power grids has arisen. We have taken the same value as a threshold for definition of total time of existence in power grids of Kazakhstan of the appreciable induced currents. Table 2 presents total time (minutes) when $|d\mathbf{H}/dt| > 30$ nT/min. The data show that during strong storms (on October, 29-31, 2003, on July, 25-27, 2004, on November, 7-10, 2004, on January, 21-22, 2005) power grids, in particular at the north of Kazakhstan, can undergo to the appreciable overloads caused by GICs.

4. Conclusion

Variations of the geomagnetic field during large magnetic storms induce an electric field which induces electric current (GICs) in the high voltage transmission lines. Basically, GICs are a problem of auroral latitudes but during large magnetic storms GICs can appear at all latitudes. In the present work, the analysis of variations of \mathbf{H} and $d\mathbf{H}/dt$ for seven periods of the high magnetic activity in 2003-2005 is carried out. Distributions of directions \mathbf{H} and $d\mathbf{H}/dt$ are calculated; the most interesting property of distributions was narrow distributions \mathbf{H} and $d\mathbf{H}/dt$ for Alma-Ata, extended in the geomagnetic north-south direction and scattered $d\mathbf{H}/dt$ distributions for Novosibirsk and Irkutsk. It is shown that the large $d\mathbf{H}/dt$ are caused by the geomagnetic field variations of three types: a sudden pulse (SI) observed in the beginning of a magnetic storm, pulsations of the magnetic field at the phase of recovery, and casual variations of the field during a magnetic storm. It is shown that during strong storms, power grids, in particular in the north of Kazakhstan, can be subjected to the appreciable overloads caused by GICs.

References

- Bolduc, L., P. Langlois, D. Boteier and R. Pirjola, 2000, *A study of geoelectromagnetic disturbances in Quebec 2. Detailed analysis of a large event*, IEEE Trans. Power Delivery **15**, 272-285.
- Kappenman, J.G., 2003, *Storm sudden commencement events and associated geomagnetically induced current risks to ground-based systems at low-latitude and mid-latitude locations*, Space weather **1**, 3, 1016, doi:10.1029/2003SW000009.
- Kleimenova, N.G., and O.V. Kozyreva, 2005, *Large geomagnetic pulsation Pc5 at the recovery phase of great storms of October and November 2003*, Geomagnetism and Aeronomy **45**, 597-612.
- Koen, J., and C.T. Gaunt, 2002, *Geomagnetically induced currents at mid-latitudes*, Abs. The 27 General Assembly of URSI, 17-24 August, Netherlands, Maastrich, 177.
- Viljanen, A., 1998, *Relation of geomagnetically induced currents and local geomagnetic variations*, IEEE Trans. Power Delivery **13**, 1285-1290.

Accepted February 15, 2007

Long-Term Variation of the Geoelectric Activity Index T

Árpád KIS, András KOPPÁN, István LEMPERGER, Tímea PRODÁN,
Judit SZENDRŐI, József VERŐ and Viktor WESZTERGOM

Geodetic and Geophysical Research Institute of the Hungarian Academy of Sciences
9400 Sopron, Csatkai u. 6-8. Hungary
e-mails: lempi@ggki.hu; wv@ggki.hu

Abstract

We study the long-time behavior and variability of the Earth geomagnetic activity based on the uniquely long geoelectric field observations recorded at the Nagycenk Geophysical Observatory for the past five decades. According to our results there is no clear correlation between the solar activity (expressed in sunspot number) and the daily T index. On the other hand, we found an almost linear relation between the Ap and T indices.

1. Introduction

From the ground based magnetometer measurements, different activity indices are obtained. Some of them cover many solar cycles: The K index was introduced by Bartels in 1939, the Ap index is available since 1932. In the middle of 1800's Rudolph Wolf devised a daily method of estimating the solar activity by counting the number of individual sunspots and groups of spots on the solar disk. Geomagnetic activity is generated by the interaction between the solar wind and the magnetosphere. Many features of the geomagnetic and solar activity have been discovered by spectral and statistical analysis of the uninterrupted time series of indices. Besides the well known 11 year and annual cycle and the coronal holes related 27 days recurrence period, a 13.5 day period was found recently. The semi-annual and annual variabilities are related to the tilt of the Earth's orbit to the Sun's rotation axis. The 11 year variability of the geomagnetic activity is more or less correlated with the solar activity cycles, but in the geomagnetic activity three major peaks appear according to the dominance of different sources (solar eruptions and coronal holes). The largest one occurs 2-3 years after the solar maximum (Vennerstrom and Friis-Chistensen 1996).

The Nagycenk Observatory (IAGA code: NCK, $L = 1.9$, $\varphi = 47^{\circ}38'$, $\lambda = 16^{\circ}43'$, altitude = 153.70 m) has been providing a special activity index called T, hand-scaled

from continuous telluric (geoelectric) recording. The telluric field is generated by the time variation of the geomagnetic field ($\text{curl } \mathbf{E} = -\partial\mathbf{B}/\partial t$), therefore T characterises the higher frequencies in comparison with the magnetic range indices (since \mathbf{E} is proportional to the angular frequency of the geomagnetic variation). Statistical analysis of T confirms the main characteristics of geomagnetic activity known from numerous former studies (e.g. Schreiber 1998), but slight differences are found due to the dominating higher frequency variations like giant pulsations.

2. T Index Data Series at Nagycenk Geophysical Observatory

The high time resolution Earth current measurements started in 1957 at the Nagycenk Geophysical Observatory (NGO). From the beginning it was decided to focus on certain spectral indices from the records, like the hourly averaged amplitude in the time periods of 0-2, 2-6, 6-12, 12-24, and 24-60 minutes and the value of the T index. The 3 hour T index is scaled from 0 to 9 characterizing the geoelectric activity during 3 hour intervals corresponding to the largest range covered by the variation of E_x and E_y . The (daily) T index is the sum of the corresponding three hour T index values. The ten classes of the range are scaled with a linear step of 1.8 mV/km. Before the digital recording, i.e. from 1957 to the early nineties, the data series of the T index were obtained from the so-called normal run Earth current recordings (25 mm/hour). To ensure continuous digital data for almost five decades, the earlier data has been carefully transformed to digital format by hand. This way we obtained a uniform (digital) data series for the past 48 years. The daily variations were eliminated from the T indices for the whole available time period. A 3-hour interval proved to be adequate to indicate any geomagnetic transient event and to provide a suitable time resolution as well.

Like any other geoelectric and geomagnetic indices, the T index also has its limitations. The activity level is strongly affected by the local time, by the geomagnetic latitude and by the local geological structure (i.e., the spatial distribution of the conductivity); the latter can strongly influence the electric field. From the point of view of the geological structure, the location of the observatory is optimal. According to earlier investigations (Ádám and Verő 1967, 1981), the observatory lies on the slope of a local crystalline basement. The thickness of the conductive sediment is about 1500 m. This fact implies that the periods of the variations shorter than 8 min lie in the magnetotelluric (MT) S-interval, i.e. in the increasing branch of MT sounding curves, which represent the high-resistivity basement. This means that the phase shift between the electric and the magnetic field is close to zero and the surface impedance is nearly constant.

Corresponding to the outlined conditions, the magnetic and electric variations expressed in nT and mV/km, respectively, have the same numerical value during normal (i.e. quiet) daily variations. The numerical values of electric variations are about 2-5 times larger than the corresponding magnetic ones in the period range of substorms and about 100 times larger in the scale frequency of pulsations. Slight anisotropy is caused by regional effects. The transfer function between the magnetic and electric field components is routinely determined in order to check the scale value of the measurements in the observatory.

The thick conductive sediment prevents the observation site from the man-made disturbances. In addition, the NGO is situated in a natural park, as far as possible from settlements. General analysis of the man-made ULF noise was carried out by Villante et al. (2004) at NGO and other observatories. From this analysis it was concluded that the man-made noise amplitude at NGO is orders of magnitude lower than the variations caused by natural effects, however the spectral analysis of long time data series might be influenced by working days of stronger effects and reduced weekend noise levels. To conclude, the T index determined from records at NGO is minimally distorted and it can be regarded as a valuable and representative indicator of geomagnetic induction.

Statistical and Spectral Analysis of the T Index

For some reasons the geoelectric field is seldom measured continuously and its nature is much less known than the characteristics of the geomagnetic field. However, this tendency is about to change. The knowledge of the long term characteristics of the geoelectric field is of increasing importance in several space weather applications, especially in geomagnetic risk assessments (see Boteler and Pirjola 1998, Pirjola and Viljanen 1998). This fact also increases the value of the T index data series.

In our study we present a statistical analysis of the T index for the recent 47 years and its correlation with solar activity and the Ap index.

Figure 1 presents, from top to bottom, the T index and the sunspot number versus time for the time period under investigation. Both the T index and the sunspot number data series were smoothed with a 1-year running average in order to filter out the high-frequency fluctuations and to be able to study the long-term variations. The sunspot number variation, which reflects the changes in solar activity, seems to have minimal effect on the T index variation, i.e on the geoelectric activity.

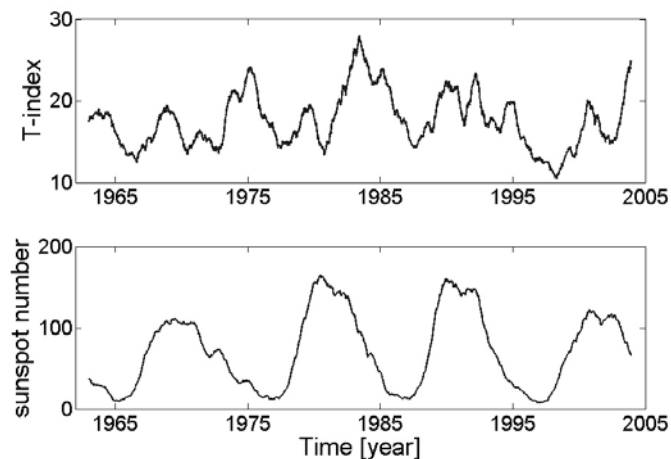


Fig. 1. Fifty years of T index (top) and sunspot number (bottom) data smoothed with one year running average.

Figure 2 presents the unbiased covariance value between the T index and the total sunspot number. As it can be seen, the unbiased covariance does not have a maximum value at year 0, instead it has a local maximum at ~ 2.7 years.

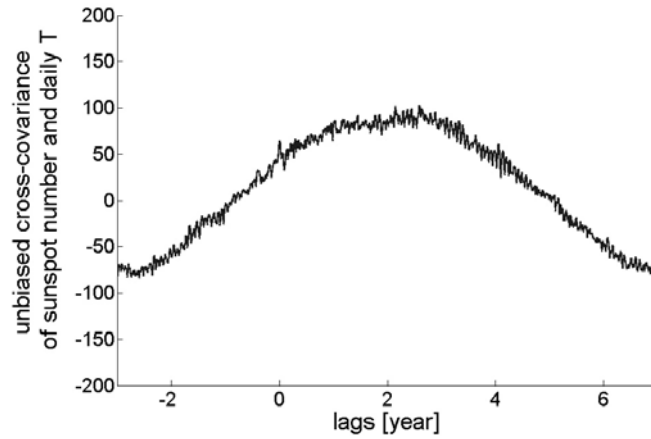


Fig. 2. Unbiased cross-covariance between sunspot number and T index.

Figure 3 presents the Ap index versus the T index. Both the Ap and the T indices were one year averaged. It can be seen that the Ap and the T indices are almost linearly correlated. This is clearly demonstrated on the upper panel of Fig. 4, where the unbiased covariance between the 27 day averaged T and the Ap indices is shown. The lower panel in Fig. 4 presents the T index versus the Ap index. The occurrence of high geomagnetic activity and its coincidence with a high value of the induced electric fields shows that the Ap and the T indices reflect essentially the same geoelectromagnetic activity. The almost linear relation between the Ap and the T indices suggests that the Ap indices can be calculated from the T indices. However, some differences might result between the observed and the calculated Ap indices, since the T index is influenced by the pulsation activity.

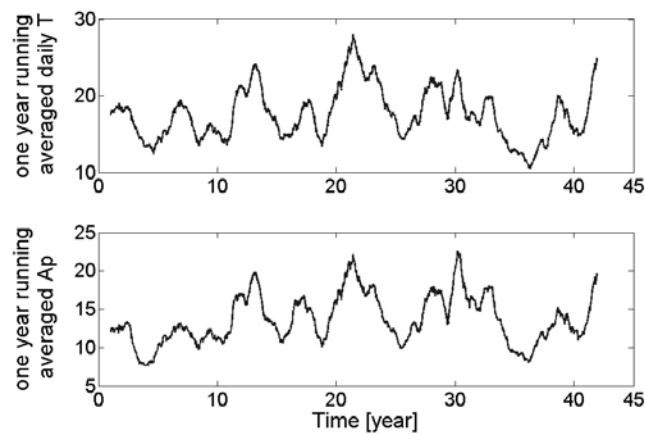


Fig. 3. One year running average smoothed T (top) and Ap (bottom) indices.

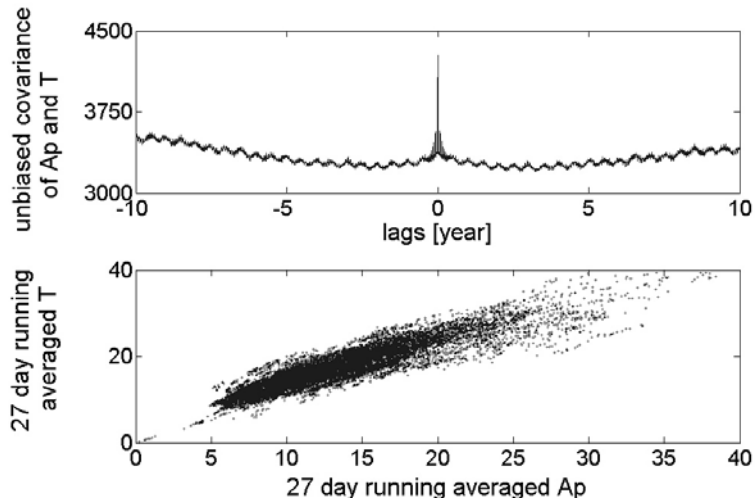


Fig. 4. Unbiased covariance of Ap and T indices (top), 27 day running average smoothed T versus Ap (bottom).

In order to study the average variation of the T index, we superposed and normalized the T index values for each year beginning with the year 1957 up to 2005. As it can be observed in Fig. 5, the yearly averaged T index presents two maxima during one year time period. This yearly average wave has a clear six-month periodicity. Both equinoctial maxima are roughly of the same level, however the summer values are slightly higher than the winter ones. This deeper winter activity in our opinion might be connected to the winter anomaly, which is a decrease of the pulsation activity in high solar activity years.

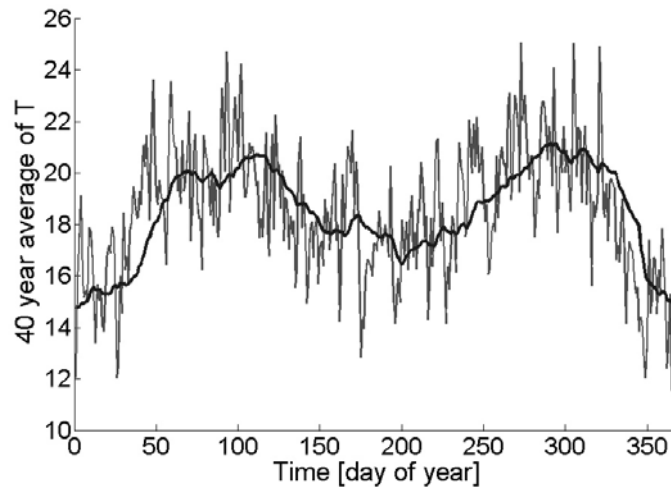


Fig. 5. Forty year average of daily T index at each day of year and its 27-day running average curve.

In the power spectrum of daily T sums shown in Fig. 6, a significant peak occurs at 11 years which can be related to the solar cycle. At shorter periods there is a lot of peaks between 1 and 11 years, possibly resulting from the irregular form of the solar cycle wave. The well known half-year wave of geoelectromagnetic activity is the strongest in its period range but there is also a yearly wave which can be due to a change in the direction of the geomagnetic disturbance vectors as the resistivity tensor of the Nagycenk Observatory is slightly elongated towards E-W (or ENE-WSW).

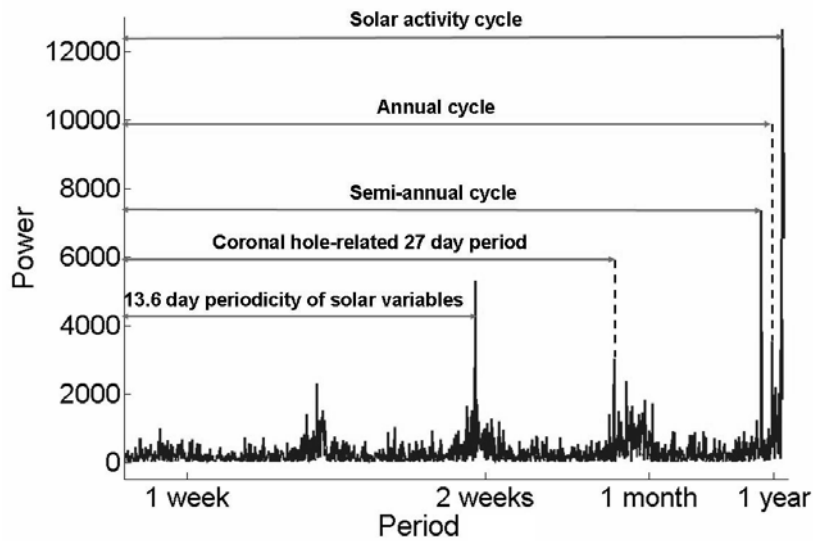


Fig. 6. The well known spectral peaks are indicated on the spectra of the T index. (The 11 year solar cycle is the outside right peak.)

The next higher frequency group of peaks belongs to the 27-day rotation of the Sun together with its second and third harmonics; moreover, a rather small peak at about 28 days might be due to the influence of the Moon. The 13.5 day quasi-periodicity peak also clearly appears on the spectra produced by two-stream structures (Mursula and Zieger 1996).

3. Conclusions

Nearly fifty years long time series of the NCK observatory is a representative, homogeneous and unique data set for statistical analysis of the long-term variation of the geomagnetic induction effect.

The present study compared the earth-current (telluric) activity index T with sunspot number and geomagnetic Ap indices. The occurrence of high geomagnetically induced electric fields and their coincidence with the phases of solar activity is less clear than that of maximum magnetic activity but it was shown that Ap and T indices reflect essentially the same geoelectromagnetic activity which is, in turn, correlated

with the sunspot number. As the weights of variations with different periods are rather different in geomagnetic and earth-current indices, there are also differences between the two kinds of activities. An attempt was made to identify such differences between the two time series and also in connection with solar activity time series. Several kinds of differences result from the influence of the pulsation activity on the T index. With the help of a polynomial connection between Kp and T indices, expected values can be computed from Kp for T. The difference of the observed and computed T indices may contain information about the effect of changing spectrum of geoelectromagnetic activity on these indices.

Several features of the geomagnetic activity have been confirmed and some further information has been obtained which we believe to be of importance.

References

- Ádám, A., and J. Verő, 1967, *Latest results of electromagnetic measurements in Hungary* (in Hungarian), *Geofizikai Közlemények* **16**, 25-52.
- Ádám, A., and J. Verő, 1981, *The geophysical observatory near Nagycenk, Electromagnetic measurements and processing of data*, *Acta Geod., Geoph. Mont. Hung.* **16**, 331-351.
- Boteler, D.H., and R. Pirjola, 1998, *Modelling geomagnetically induced currents produced by realistic and uniform electric fields*, *IEEE Trans. Power Delivery* **13**, 17-27.
- Mursula, K., and B. Zieger, 1996, *The 13.5-day periodicity in the Sun, solar wind, and geomagnetic activity: The last three solar cycles*, *J. Geophys. Res.* **101**, 27077-27090.
- Pirjola, R., and A. Viljanen, 1998, *Complex image method for calculating electric and magnetic fields produced by an auroral electrojet of finite length*, *Ann. Geophys.* **16**, 1434-1444.
- Schreiber, H., 1998, *On the periodic variations of geomagnetic activity indices Ap and ap*, *Ann. Geophys.* **16**, 510-517.
- Vennerstrom, S.M., and E. Friis-Chistensen, 1996, *Long term and solar cycle variation of the ring current*, *J. Geophys. Res.* **101**, 24727-24735.
- Viljanen, A., H. Nevanlinna, K. Pajumpää and A. Pulkkinen, 2001, *Time derivative of the horizontal geomagnetic field as an indicator*, *Ann. Geophys.* **19**, 1107-1118.
- Villante, U., M. Vellante, A. Piancatelli, A. Di Cienzo, T.L. Zhang, W. Magnes, V. Wetztergom and A. Meloni, 2004, *Some aspects of man made contamination on ULF measurements*, *Ann. Geophys.* **22**, 1335-1345.

Accepted February 26, 2007

ULF Geomagnetic Pulsations at High Latitudes: the Italian Contribution

Lili CAFARELLA¹, Marcello DE LAURETIS², Domenico DI MAURO¹,
Patrizia FRANZIA², Stefania LEPIDI¹, Antonio MELONI¹, Paolo PALANGIO¹,
Andrea PIANCATELLI², Lucia SANTARELLI¹, Massimo VELLANTE²
and Umberto VILLANTE²

¹Istituto Nazionale di Geofisica e Vulcanologia
Via di Vigna Murata 605, 00143 Roma (Italy)
e-mail: cafarella@ingv.it

²Dipartimento di Fisica – Università dell'Aquila
Via Vetoio, 67010 Coppito-L'Aquila (Italy)
e-mail: marcello.delaretis@aquila.infn.it

Abstract

The study of geomagnetic field variations in Antarctica is important in that local field lines are close to extreme magnetospheric regions, such as the polar cusp, where several generation mechanisms for ULF waves are active.

Since the eighties, the Italian scientific community developed a research activity in Antarctica at Mario Zucchelli Station (TNB, CGM latitude 80°S), where magnetic facilities are continuously operating. In this review we present the experimental results obtained by a number of investigations conducted in the last years on geomagnetic pulsations in the Pc3-Pc5 frequency range. We also show compared analyses with measurements from other Antarctic and low latitude stations, and, in particular, a statistical analysis of propagation characteristics of low frequency geomagnetic field fluctuations between the two Antarctic stations, TNB and Scott Base.

1. Introduction

Geomagnetic field measurements at very high latitudes are important for the understanding of several dynamical processes which control the energy transfer from the solar wind (SW) to the Earth's magnetosphere. Indeed, local field lines reach magnetospheric regions close to the extreme magnetosphere boundary, the magnetopause,

and to the polar cusp, which separates sunward, closed magnetospheric field lines from tailward, open field lines.

The Antarctic Italian geomagnetic observatory Mario Zucchelli Station (formerly Terra Nova Bay, international geomagnetic observatory code TNB, geomagnetic latitude 80°S , magnetic local time $\text{MLT} = \text{UT} - 8$ hours) was installed in the austral summer 1986-87. Due to the Earth's rotation, through the day TNB has a variable distance from the cusp. Around magnetic midnight and during the major part of the day, it is in the polar cap at the footpoint of open field lines, while at noon it approaches the cusp. Taking into account that the cusp latitude depends on interplanetary parameters (Zhou *et al.* 2000), in particular, conditions TNB can be located at the footprints of closed field lines.

The ULF geomagnetic pulsations are magnetic field fluctuations with periods ranging from seconds to minutes, which obtain their energy from the SW. We show the results obtained in the last few years in the mid (Pc3-Pc4, $f = 7\text{-}100$ mHz) and low frequency range (Pc5, $f = 2\text{-}7$ mHz).

Generation mechanisms of Pc3-5 pulsations can be basically related to: (a) Kelvin-Helmholtz instability along the flanks of the magnetopause (Atkinson and Watanabe 1966), (b) upstream waves generated by SW ions in the foreshock region through a ion-cyclotron instability mechanism (Greenstadt *et al.* 1981) (schematically shown in Fig. 1) and (c) local phenomena in the cusp region (Engebretson *et al.* 1986).

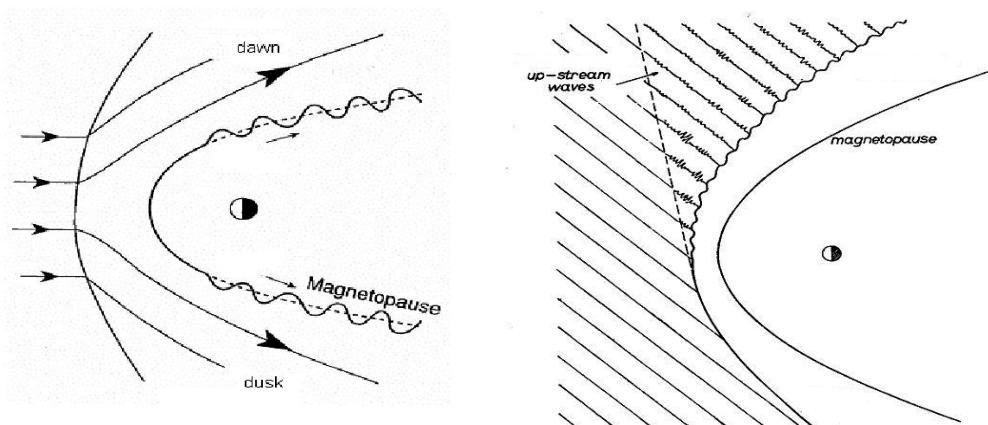


Fig. 1. Schematic view, in the equatorial plane, of the Kelvin-Helmholtz instability (left side) generated on the magnetopause by the SW flux, indicated by arrows, and of upstream waves (right side) generated along the interplanetary magnetic field lines, indicated by the 45° inclined lines.

Interplanetary shocks impacting on the magnetopause can be an additional source of low frequency pulsations in that they may generate magnetospheric cavity/waveguide modes (Kivelson and Southwood 1985) between an outer boundary, such as the magnetopause, and an inner turning point (Fig. 2). Such modes at discrete frequencies have a global character in the magnetosphere and have been observed at

auroral (Walker *et al.* 1992), low latitudes (Francia and Villante 1997) and even in the polar cap (Villante *et al.* 1997).

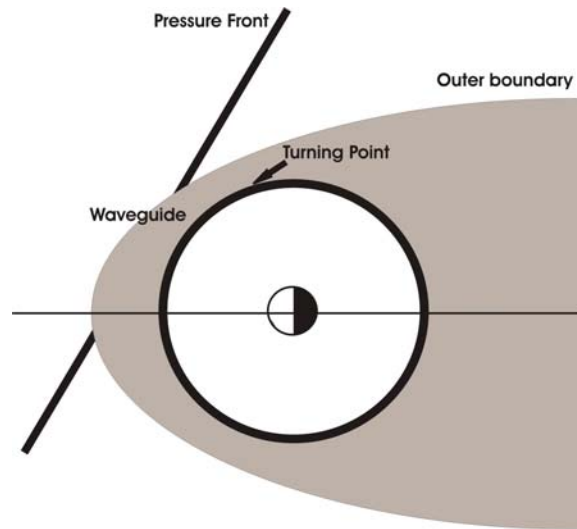


Fig. 2. Schematic view in the equatorial plane of the impact of a shock front on the magnetopause.

2. Experimental Results

In Fig. 3 we show the MLT dependence of Pc3 and Pc4 pulsation power. It is evident that power maximizes at noon, when TNB approaches the cusp; this result suggests that a main source related to local phenomena can be active.

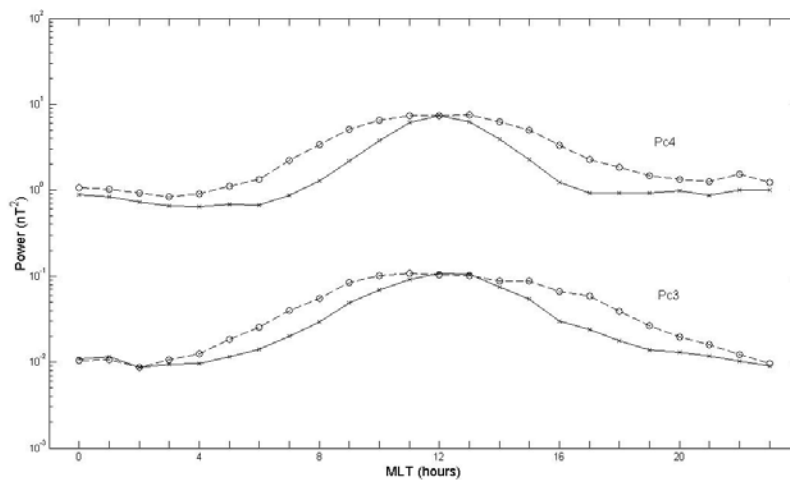


Fig. 3. The diurnal variation of Pc3 and Pc4 pulsation power for the north-south H (solid line) and east-west D (dashed line) horizontal components (from Villante *et al.* 2000).

We also show in Fig. 4 the MLT dependence of the correlation coefficient r between the pulsation power and the SW speed. It can be seen that for Pc3 pulsations r is higher in the morning indicating an upstream wave source while for Pc4 pulsations r is higher in morning and afternoon as expected for pulsations generated by the Kelvin-Helmholtz instability.

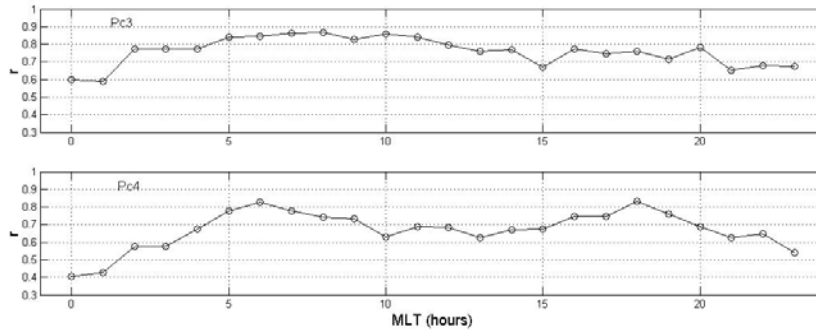


Fig. 4. Daily variation of the correlation coefficient r between Pc3 and Pc4 power and SW speed (from Villante *et al.* 2000).

The analysis of selected Pc3 wave packets observed during a period of variable interplanetary magnetic field (IMF) conditions has shown a linear relation between the pulsation frequency and the IMF strength clearly indicating an upstream waves source (Fig. 5).

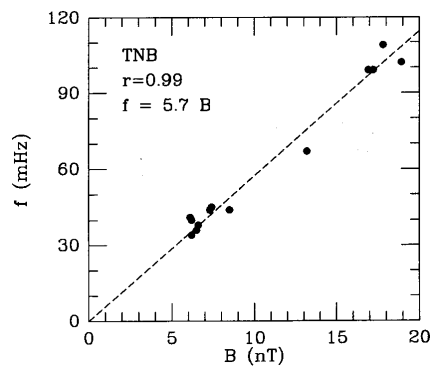


Fig. 5. Dependence of the frequency of Pc3 waves on the IMF strength B (from Villante *et al.* 1999).

The arrival of interplanetary structures characterized by SW pressure pulses can trigger quasi monochromatic pulsations in the Pc5 frequency range. In Fig. 6 it is shown the pulsation event during the Earth's passage of the April 11, 1997 magnetic cloud. In order to ascertain the global character of the observed pulsations, the analysis was extended also to a low latitude station (AQ, corrected geomagnetic latitude 36.2°N) and to geosynchronous spacecraft (GOES 8 and 9). It can be seen that the

power spectra are characterized by common peaks, in particular at 3.6 mHz, and the filtered data by simultaneous wave packets, suggesting a common SW source.

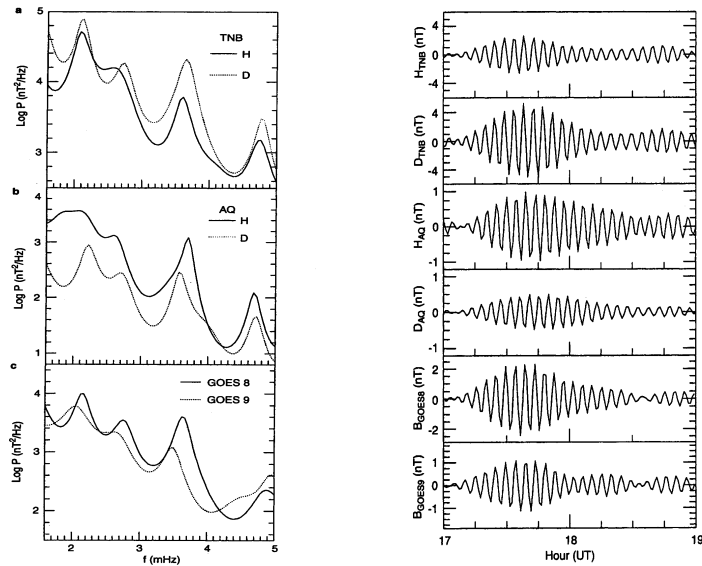


Fig. 6. Left panels: power spectra of the H and D components at TNB and AQ and of the total field from GOES spacecraft in the time interval 17-19 UT on April 11, 1997. Right panels: 3.6 mHz filtered data (from Lepidi *et al.* 1999).

In order to investigate the propagation characteristics of Pc5 pulsations we statistically analyzed the phase difference between coherent pulsations at TNB and Scott Base (SBA) during 2001-2002. The two Antarctic stations are at the same geomagnetic latitude but with one hour difference in MLT. Then, the phase difference indicates an azimuthal propagation: it is positive (negative) for SBA (TNB) leading, i.e. for signals propagating westward (eastward). We can see in Fig. 7 a phase difference

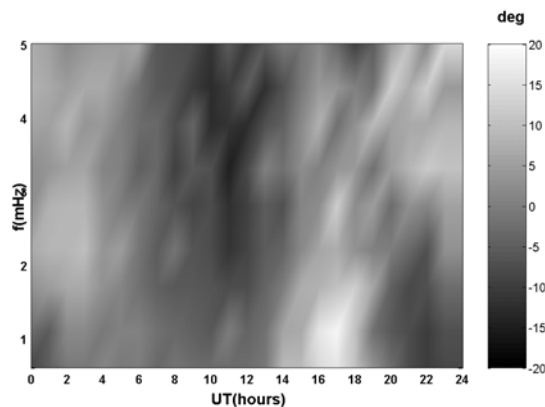


Fig. 7. Phase difference between coherent pulsations at TNB and SBA during 2001-2002.

reversal at ~19 UT for $f < \sim 2.5$ mHz, indicating a longitudinal propagation away from noon, and a second reversal at ~7 UT for $f > \sim 2$ mHz, indicating a longitudinal propagation away from midnight.

Acknowledgment. This research activity at TNB was supported by Italian PNRA (Programma Nazionale di Ricerche in Antartide) and MIUR.

References

- Atkinson, G., and T. Watanabe, 1966, *Surface waves in the magnetospheric boundary as a possible origin of long period geomagnetic micropulsations*, Earth Planet. Sci. Lett. **1**, 89-91.
- Engbretson, M.J., C.-I. Meng, R.L. Arnoldy and L.J. Cahill Jr., 1986, *Pc3 pulsations observed near the south polar cusp*, J. Geophys. Res. **91**, 8909-8918.
- Francia, P., and U. Villante, 1997, *Some evidence for ground power enhancements at frequencies of global magnetospheric modes at low latitude*, Ann. Geophysicae **15**, 17-23.
- Greenstadt, E.W., R.L. McPherron and K. Takahashi, 1981, *Solar wind control of daytime, midperiod geomagnetic pulsations, ULF pulsations in the magnetosphere*, Tokyo, Center for Academic Publications Japan, Dordrecht, D. Reidel Publishing Co., 89-110.
- Kivelson, M., and D. Southwood, 1985, *Resonant ULF waves: a new interpretation*, Geophys. Res. Lett. **12**, 49-52.
- Lepidi, S., P. Francia, U. Villante, A. Meloni, A.J. Lazarus and R.P. Lepping, 1999, *The Earth's passage of the April 11, 1997 coronal ejecta: geomagnetic field fluctuations at high and low latitude during northward interplanetary magnetic field conditions*, Ann. Geophysicae **17**, 1245-1250.
- Villante, U., S. Lepidi, P. Francia, A. Meloni and P. Palangio, 1997, *Long period geomagnetic field fluctuations at Terra Nova Bay*, Geophys. Res. Lett. **24**, 1443-1446.
- Villante, U., S. Lepidi, P. Francia, M. Vellante, A. Meloni, R.P. Lepping and F. Mariani, 1999, *Pc3 pulsations during variable IMF conditions*, Ann. Geophysicae **17**, 490-496.
- Villante, U., M. Vellante and G. De Sanctis, 2000, *An analysis of Pc3 and Pc4 pulsations at Terra Nova Bay (Antarctica)*, Ann. Geophysicae **18**, 1412-1421.
- Walker, A.D.M., J.M. Ruohoniemi, K.B. Baker, R.A. Greenwald and J.C. Samson, 1992, *Spatial and temporal behavior of ULF pulsations observed by the Goose Bay HF radar*, J. Geophys. Res. **97**, 12187-12202.
- Zhou, X.W., C.T. Russell, G. Le, S.A. Fuselier and J.D. Scudder, 2000, *Solar wind control of the polar cusp at high altitude*, J. Geophys. Res. **105**, 245-251.

Accepted February 12, 2007

Morphological Features in the Structure of Geomagnetic Variations in Relation to Earthquakes in Vrancea

Vladimir BAKHMUTOV, Frina SEDOVA and Tamara MOZGOVAYA

Institute of Geophysics, National Academy of Science of Ukraine
Palladin av.32, 03680 Kiev-142, Ukraine
e-mail: bakhm@igph.kiev.ua

A b s t r a c t

On example of the Vrancea seismic zone, the correlation between geomagnetic field disturbances and earthquakes is shown. The geomagnetic situation was studied for more than 200 earthquakes during the period 1988-1996. The significant statistical material has demonstrated that the polar sub-storms and their middle-latitudinal manifestation is a trigger mechanism for realization of the seismic energy in Vrancea. The release of seismic energy is related to abrupt changes (gradients) in H-component of geomagnetic field. The energy class of the earthquake is connected with the amplitude of the change in H-component. The differences between durations of near-midnight polar sub-storms preceding earthquakes on various depths have been determined. Taking into account the temporal interval from maximum of sub-storm up to the shock, the connection between geomagnetic disturbances and earthquakes is always positive. The time interval between maximum of polar sub-storm and earthquake is correlated with the depth of the earthquake.

1. Introduction

The Sun – interplanetary space – magnetosphere – ionosphere – atmosphere – Earth's tectonosphere chain is a complicated open dynamic nonlinear system wherein high-energy effects cause a complex of processes. In this context, the seismicity phenomena of the Earth should be considered as a part of the whole Sun-Earth system. The relation between seismicity and processes in the Sun-Earth chain is still ambiguous, but most of the researchers tend to their positive correlation. The studies of regional seismicity with the solar activity, the amplitude of the Earth tides, the Earth's rotation rate, etc. show the influence of these processes on the stressed state of the Earth's crust with subsequent activation of seismic activity. Some authors show that the changes in the underground water level, the ionosphere parameters, the electro-

magnetic and the geomagnetic field, the electrical conductivity of rocks, the radon emanation, etc. should be considered as precursors of seismic events (Rikitaky 1979, Sidorin 1992, Sobolev 1993).

The problem of relationship between seismicity and geomagnetic activity is under discussion as well. Many scientists searched for a relationship between geomagnetic storms and tectonic events. But the processes of transformation of solar flare energy into the energy of tectonic processes are still not clear. The influences of magnetic storm with sudden commencements on seismicity have been discussed in (Sobolev *et al.* 2001). The studies of technogenic impulse electrical signals when the number of the seismic events tended to increase 3-4 days after the impulse passing were the premise to the above said (Tarasov *et al.* 1999). The duration of activation was several days and its area reached some hundreds km. As far as the energy pumped into the Earth is by several orders smaller than the released seismic energy, the trigger mechanism of the influence has been taken into consideration.

An assumption on the trigger mechanism of the effect of the magnetic disturbance (magnetic storms) on the seismicity in Kirghizia, Kazakhstan and Caucasus (with the maximum effect in 2-7 days after disturbance) was discussed by Sobolev *et al.* (2001) and Zakrzhevskaya and Sobolev (2002). However, the correlation was not evident that the magnetic storm could be considered as the cause of tectonic events. The positive or negative effects were explained by different geological structures of the regions.

One of the mechanisms of the effect of magnetic storms on seismicity may be electro-osmotic phenomena in the rock massif (Kormiltsev *et al.* 2002). The electro-osmotic fluid flow induced by magnetic storms generates anomalous porous pressure which could be the triggering of the tectonic event. As this effect is small, the correlation between the magnetic field variations and tectonic processes will be weak.

In this paper we consider that most of the earthquakes are a result of stress discharge which slowly accumulated in different parts of the crust and upper mantle. We study the correlation between geomagnetic field disturbances and earthquakes on the example of the concentrated seismicity zone (Vrancea, South Carpathian region). The aim of this article is to show how the reaction of the stress-strained medium responds to geomagnetic disturbances (morphological features in the geomagnetic variation structure).

2. Initial Data

The geomagnetic situation was studied for more than 200 earthquakes with intermediate-depth hypocenters beneath Vrancea zone during the period of 1988-1996. The Vrancea zone is considered as one of the classical examples of concentrated seismicity (Martin *et al.* 2005). The deep-foci earthquakes zone is elongated as a narrow band of 90 km length and 25 km width. The earthquake foci are placed both in the Earth's crust and in the upper mantle in 100-180 km depth. The deep-foci shocks characterized by high seismic energy reach a magnitude $M > 7$.

The seismicity of the Carpathian region has been described in detail by Kutas *et al.* (2001). For the Vrancea zone the total seismic energy was determined from year to year, with maxima due to the greatest earthquakes in 1977, 1986 and 1990. We examined the geomagnetic situation during the period 1988-1996, but did it separately for deep-foci earthquakes (sub-crust) and crust ones (shallow) in conformity with Seismological Bulletins of Ukraine. We have analyzed more than 150 deep-foci and ca 60 crust shocks in Vrancea zone. The energy class of the shocks (K) and the foci depth (h , km) were taken as the seismic characteristics.

The analyses of geomagnetic variations in relation to earthquakes were carried out from Yastrebovka (45.5°N; 34.1°E) and Korets (50.6°N; 27.2°E) magnetic observatories data. The morphological features of the variations were studied by the changes of the amplitude of the H-component of the geomagnetic field.

3. Results

Earlier analysis of one of the strongest earthquakes in Vrancea (30.05.1990) showed that the release of seismic energy was related to abrupt changes (“gradients”) in H-component of geomagnetic field (Sedova *et al.* 2001). The concept of the “main gradient” – the greatest change in the horizontal H-component which may precede the shock in the interval from several days or more, and the “gradients” – changes in the horizontal H-component 1-2 days before the shock – were described by Sedova *et al.* (2001) and Bakhmutov *et al.* (2006). The connection between deep-foci earthquakes in Vrancea and preceding geomagnetic disturbances was determined, while the seismic events themselves occur mainly on weakly disturbed and quiet days (85%), and only 15% of the events took place on geomagnetic disturbed days ($\sum Kp > 30$). The crust shocks are related to sudden commencement storms. The geomagnetic activity determined by Kp -indices in relation to seismicity in the Vrancea zone is always positive when considering the time intervals from the “gradient” to the shock (Bakhmutov *et al.* 2006). The time interval τ from the “main gradients” in the geomagnetic field to the deep-foci earthquakes varies from several days to one month and more (Fig. 1a) while τ from “gradients” to the shallow shocks is most often several hours, and rarely exceeds two days (Fig. 1b).

An analysis of the geomagnetic situation in 1988-1996 showed that the release of seismic energy is connected with definite morphological features in the magnetic field variation spectrum rather than with the geomagnetic activity as a whole. For the Vrancea zone, about 90% of shocks are associated with the near-midnight polar substorms and their middle-latitudinal manifestation. Figure 2 presents the distribution of substorms (H-component of the geomagnetic field) depending on the time before shallow and sub-crust earthquakes. The maximum of substorms is 20-24UT (22-02LT).

An example of the mid-latitudinal manifestation of polar substorms during the quiet background of the geomagnetic field is given in Fig. 3. The shock of 18.04.1993 at 02:03 UT ($K = 9.9$, $h = 150$ km) is preceded by the substorm of 17.04 with the maximum in the H-component at about 18:00 UT. The amplitude of the substorm was digitized from a base line, conventionally taken as a normal field (zero level).

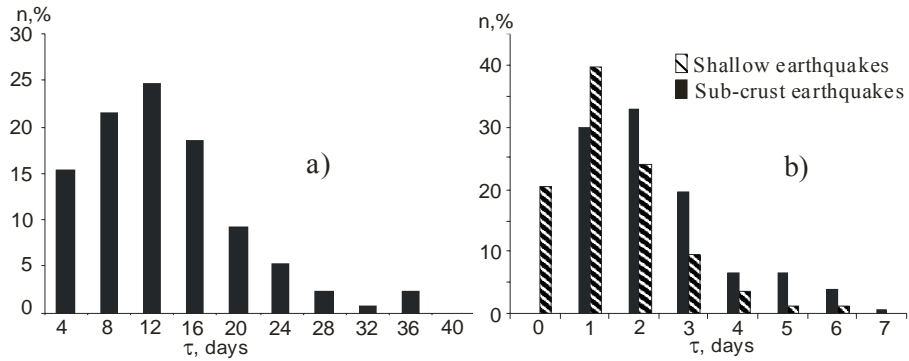


Fig. 1. The time interval τ from "main gradients" to sub-crust earthquakes (a); from the "gradients" preceding the sub-crust and shallow shocks in Vrancea (b).

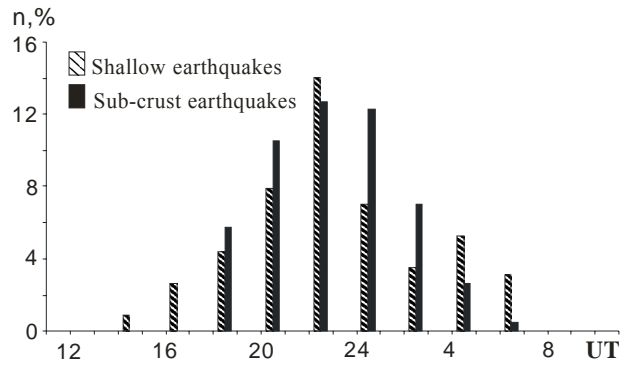


Fig. 2. Daily substorms distribution before the shallow and sub-crust earthquakes in the Vrancea zone for the period 1988-1996.

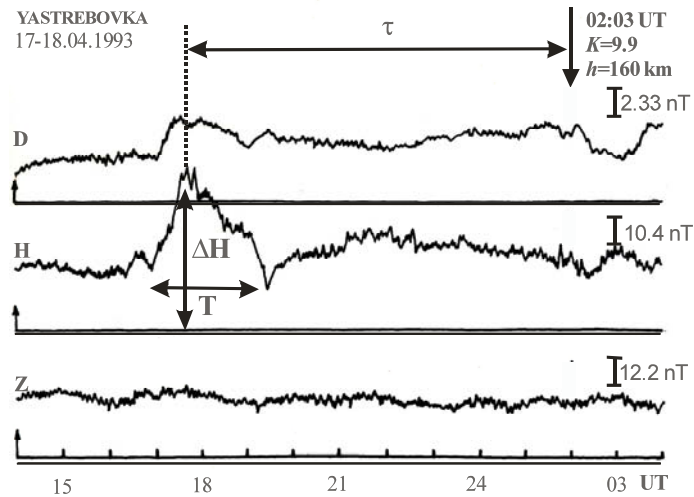


Fig. 3. A copy of the magnetograms from 17-18.04.1993, magnetic observatory Yastrebovka.

For the whole period of studies the earthquakes intensity in Vrancea is rather stable within the range of $K = 9 - 11$ both for the deep-foci earthquakes and for the crust shocks. The weaker shocks ($K < 9$) were 5.3%, and the shocks with $K > 11$ attain 7.6%. The main distribution of the energy class K of sub-crust earthquakes for 1988-1996 and the mean statistical values of the amplitudes of the H-component at the maximum of magnetic polar substorm's development preceding the shock are shown in Fig. 4. In spite of the rather narrow limits of the earthquake's intensity changes, their linear dependence on the substorm amplitude ΔH is clear, particularly if the main seismic events of 04.03.1997 ($K = 15.8$) and 30.05.1990 ($K = 16$) are included in the diagram.

Before the shallow earthquakes, the ΔH amplitudes are 50-80 nT which are comparable with amplitudes of substorms occurring before the deep-foci earthquakes (Fig. 5a). Before the deep-foci shocks the amplitude range is wider and $\Delta H = 90 - 110$ nT in 10% of events. An analysis of the duration (T , min) of the midnight polar substorms preceding the shallow and sub-crust earthquakes shows that they are different (Fig. 5b). In most cases sub-crust earthquakes were preceded by substorms with $T > 60$ min while before shallow shocks $T \leq 60$ min.

We obtained a common linear dependence of the foci depth and the duration T of the midnight polar substorms both for the deep-foci and for the crust shocks (Fig. 6a). This result agrees with the geodynamic model of the Vrancea zone which is a localized downwards narrowing crater-shaped structure for which the notion of crust-mantle discontinuity (estimated depth of 50-60 km) may be considered as a conventional one (Chekunov 1980, Martin *et al.* 2005).

The time interval between the maximum of polar sub-storm and the earthquake is correlated with the depth of earthquake foci (Fig. 6b). The deeper the earthquake focus h , the longer the delay time τ . As shown in (Bakhmutov *et al.* 2006) the time interval τ depends both on the geomagnetic field disturbance and on the mean annual level of geomagnetic activity. The abrupt changes in the geomagnetic field during the magnetic storm may notably shorten the time interval τ (to 4-7 hours) which affects the linearity between τ and foci depth h .

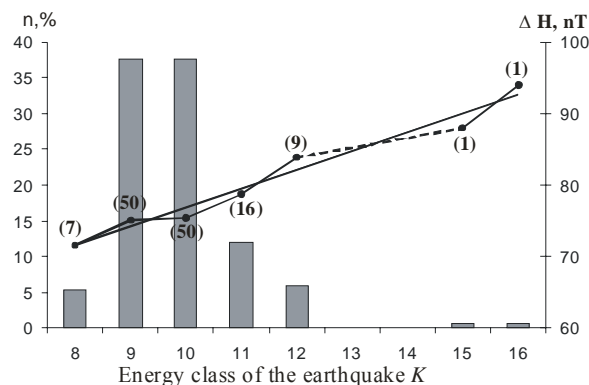


Fig. 4. The distribution of the energy class K of sub-crust earthquakes for 1988-1996 and the mean values of the amplitudes of the H-component at the maximum of the polar substorm's development. The amount of earthquakes is given in parentheses.

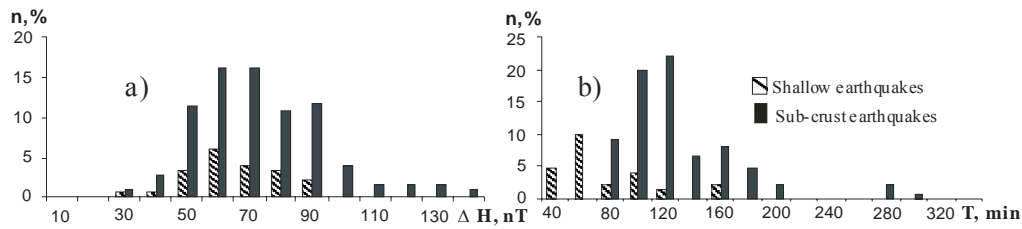


Fig. 5. The amplitudes (a) and the duration (b) of the magnetic polar substorm preceding the shallow and sub-crust earthquakes.

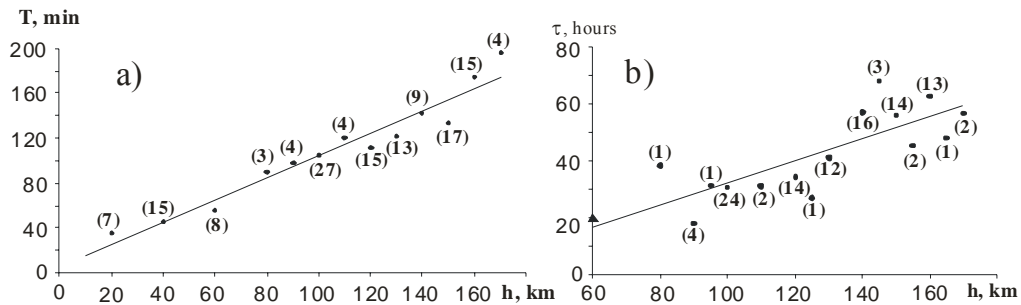


Fig. 6. The dependence of the earthquakes foci depths on the substorms duration (a) and the time interval τ for sub-crust earthquakes (b). Triangles denote the average time interval τ for the shallow shocks. The amount of earthquakes is given in parentheses.

4. Discussion and conclusion

As noted above, more than 90% of shocks recorded in the Vrancea zone are associated with the mid-latitude manifestation of the near-midnight polar substorms. The substorms manifested themselves both against the quiet geomagnetic field background and during magnetic storms. As a substorm reflects a complex of magnetospheric and ionospheric phenomena where the main factor is an increase of the auroral electrojet, each substorm has individual features due to the high dynamics of electrojet currents. On the other hand, the geomagnetic storm is the sum of the Dst variation, the disturbed diurnal variation and the irregular variation. The last one specifies the various character of the storm. There are relatively slow changes of the magnetic field lasting from several minutes to several hours which are superposed by faster fluctuations. The irregular variation spectrum is independent of the geomagnetic storm intensity (Afanasyeva *et al.* 1972).

A storm is featured by a decrease of the H-component in middle and low latitudes related to the ring current development. The relation between the processes responsible for the geomagnetic storms and substorms cannot be explained unambiguously (Gelberg *et al.* 2000). We are not discussing the mechanism of these processes.

Taking into account the temporal interval from maximum of sub-storm up to the shocks, the connection between geomagnetic disturbances and earthquakes is always

positive. We systematized the changes (“gradient”) in the magnetic field related with polar substorm by three main types (groups): (1) the isolated near-midnight polar substorm occurs against a quiet background of the geomagnetic field; (2) the substorm precedes the main phase of the magnetic storm; (3) the substorm is manifested during the attenuation of the *Dst* variation.

The second and third types of changes of the H-component are called the “direct” and the “inverse” ones, respectively. The sudden commencement storms should be separated against the polar substorms into another group.

The other “gradients” in the magnetic field are rare and not related to the substorms, e.g. a recurrent storm with a sudden commencement, an anomalous behavior of the diurnal H-component changes when the *Sq* variation is not expressed (the field level is very high or low) but there are no substorms, etc. All of these events do not exceed 10%.

In accordance with this classification for each deep-focus Vrancea earthquake, the geomagnetic field behavior preceding the shock was determined. The three distinguished types correspond to 90% of shocks. When there are no substorms we have no records of deep-foci earthquakes in Vrancea at all.

The processes may be presumed as a triggering mechanism by Sobolev *et al.* (2001), when “pumping in” of energy into the Earth’s crust occurs during the magnetic storm and it is subsequently released at the earthquake. In addition, the detected regularities of substorms at their midlatitudinal manifestation should be considered as estimations of the “pumped in” energy.

In summary, we emphasize that the seismicity in the Vrancea zone is connected with a definite type of geomagnetic disturbances, such as midlatitudinal manifestation of a near-midnight polar substorm. The abrupt changes (“gradient”) in geomagnetic field (H-component) related to the maximum of the polar substorm precedes the seismic energy discharge – the seismic event occurs at a definite time interval τ after the substorm. The time interval τ from the maximum in the substorm development to the shock is associated with the earthquake focal depth. The energy class of the earthquake is connected with the amplitude of the H-component changes (during near-midnight polar substorm manifestation). Definite morphological signs preceding realization of seismic energy have been detected in the geomagnetic variation spectrum. They are systematized for different types, three of which correspond to 90% of seismic events. The effect of the magnetic disturbance on the seismic energy release is always positive taking into consideration the temporal interval from sub-storm up to the shocks. The results do not contradict the assumption of a triggering mechanism of the magnetic storm effect on the seismicity but suggest a definite contribution of the substorms which are manifested at middle latitudes.

References

- Afanasyeva, V.I., V.M. Litinsky and F.I. Sedova, 1972, *Irregular part of geomagnetic storms in the mid latitudes*, *Geomagnetism and Aeronomy* **5**, 953-955 (in Russian).

- Bakhmutov, V.G., F.I. Sedova and T.A. Mozgovaya, 2006, *Morphological features in the structure of geomagnetic variations in relation to earthquake in Vrancea zone*, Geophys. J. **28**, 1, 42-50 (in Russian).
- Chekunov, A.V., 1980, *Evolutionary changes of crust-mantle boundary*, Geophys. J. **2**, 6, 18-24 (in Russian).
- Gelberg, M.G., S.Z. Kartengolts, L.P. Shadrina and S.V. Sharayeva, 2000, *Relationship between classes of geomagnetic storms and auroral geomagnetic disturbances*, Geomagnetism and Aeronomy **40**, 1, 26-32 (in Russian).
- Kormiltsev, V.V., N.P. Kostrov, A.N. Ratushnyak and V.A. Shapiro, 2002, *The influence of electro-osmotic pressure generating by geomagnetic disturbances on the evolution of seismotectonic process*. In: M. Nayakawa and O.A. Molchanov (eds.), "Electromagnetic: Lithosphere-Atmosphere-Ionosphere Coupling", Terrapub, Tokyo, 203-207.
- Kutas, V.V., I.M. Rudenskaia and I.A. Kalitova, 2001, *Recurrence of the Carpathian earthquakes*, Geophys. J. **23**, 4, 46-54 (in Russian).
- Martin, M., F. Wenzel and the CALIXTO working group, 2005, *High-resolution teleseismic body wave tomography beneath SE Romania – II. Imaging of a slab detachment scenario*, Geophys. J. Int. **164**, 3, 579-595.
- Rikitaky, T., 1979, *Earthquakes Prediction*, Mir Press, Moscow, 388 pp. (in Russian).
- Sedova, F.I., T.A. Mozgovaya and V.G. Bakhmutov, 2001, *On morphological signs in the structure of geomagnetic variations on the eve and at the moment of earthquake in the Crimea-Black Sea and the Carpathian regions*, Geophys. J. **23**, 4, 61-68 (in Russian).
- Sidorin, A.Y., 1992, *Earthquakes Precursors*, Nauka Press, Moscow, 191 pp. (in Russian).
- Sobolev, G.A., 1993, *Bases of the Forecast of the Earthquakes*, Nauka Press, Moscow, 313 pp. (in Russian).
- Sobolev, G.A., N.A. Zakrzhevskaya and E.P. Kharin, 2001, *On the relation between seismicity and magnetic storms*, Phys. Solid Earth, Russian Acad. Sc. **11**, 62-72 (in Russian).
- Tarasov, N.T., N.V. Tarasova, A.A. Avagimov and V.A. Zeigarnik, 1999, *The effect of high-power electromagnetic pulses on the seismicity of the Central Asia and Kazakhstan*, Volcan. Seismol., Russian Acad. Sc. **4/5**, 152-160 (in Russian).
- Zakrzhevskaya, N.A., and G.A. Sobolev, 2002, *On the seismicity effect of magnetic storms*, Phys. Solid Earth, Russian Acad. Sc. **4**, 3-15 (in Russian).

Accepted February 26, 2007

The New Index of Geomagnetic Activity

Taras SUMARUK and Yuri SUMARUK

Institute of Geophysics NASU
Lviv Magnetic Observatory, Ukraine
e-mail: sumar@mail.lviv.ua

Abstract

Up-to-date indices of geomagnetic activity are widely used for scientific purposes. The indices D_{st} , K_p and AE characterize activity of geomagnetic field at low, middle and high latitudes, respectively. However, these indices do not characterize the energy injected into the magnetosphere by the solar wind, although the change of energy has an influence on the meteorological and biological Earth's processes. The AE index is the most suitable for this aim, but it is set too low for disturbed periods. We propose index $\Sigma(H-S_q)$. This index may be effectively calculated on middle latitude magnetic observatories data.

The index is determined as a daily sum of differences between mean hourly values of horizontal (H) component and corresponding mean hourly values of H on five international quiet days of the preceding month.

The new index corresponds to the standard AE index for quiet day periods and is better than AE' for disturbed periods.

Key words: geomagnetic activity indices, internationally quiet days, magnetic storms.

The flow of charged particles from the Sun interacts with the Earth's magnetic field and creates several magnetospheric and ionospheric current systems. These systems disturb the main geomagnetic field by about 1-2%. To compare the intensity of the disturbances, several indices were adopted. The D_{st} , K_p and AE are the most often used indices for scientific and practical purposes.

Index D_{st} characterizes intensity of the magnetospheric ring current and currents of the magnetopause. The index is a deviation of the horizontal component (H) from its quiet time value, averaged over four low latitude observatories: Honolulu, San Juan, Hermanus and Kakioka. The D_{st} -index shows the value of geomagnetic field variations at low latitudes and do not express the variations induced by auroral zones ionospheric currents.

Index K_p is a mean standardized K-index from 12 observatories at middle and sub-auroral latitudes. The K_p -index has the longest row of meanings. But K_p and its equivalent ranges a_p and daily index A_p do not take into consideration full variation induced by magnetospheric ring currents.

A new definition of the K-index was proposed by Polish scientists (Reda, Jankowski 2004, Nowożyński 2006). The definition is based on the calculations of energy contained in irregular changes of components X and Y.

The AE-index was introduced by Davis and Sugiura in 1966 to measure global electrojets activity in the auroral zone. The AE-index derives from the horizontal component of geomagnetic variations observed at 12 observatories along the auroral zone (geomagnetic latitudes 60° - 71°). Table 1 shows a list of these observatories.

Table 1
List of AE index observatories

| No | Observatory | Geographical coordinates | | Geomagnetic coordinates | |
|----|-----------------|--------------------------|-----------|-------------------------|-----------|
| | | φ | λ | Φ | Λ |
| 1 | Cape Chelyuskin | 77.43 | 104.17 | 66.4 | 177.2 |
| 2 | Dixon Island | 73.32 | 080.33 | 63.1 | 162.3 |
| 3 | Tixie Bay | 71.35 | 129.00 | 60.7 | 192.4 |
| 4 | Barrow | 71.18 | 156.45 | 68.8 | 242.6 |
| 5 | Abisko | 68.21 | 018.49 | 65.8 | 115.7 |
| 6 | Cape Wellen | 66.10 | 180.50 | 62.1 | 238.5 |
| 7 | College | 64.51 | 147.52 | 65.0 | 258.1 |
| 8 | Baker Lake | 64.20 | 096.02 | 73.8 | 317.7 |
| 9 | Reykjavik | 64.11 | 021.41 | 80.9 | 072.2 |
| 10 | Narsarsuaq | 61.10 | 314.80 | 70.8 | 038.7 |
| 11 | Fort Churchill | 58.44 | 096.15 | 68.7 | 325.0 |
| 12 | Sitka | 57.03 | 135.20 | 60.2 | 277.1 |

The AE-indices allow to evaluate the values of energy injected from solar wind into the magnetosphere (Spiro *et al.* 1982, Feldstein 1992). The AE-indices have very essential drawback. They are underestimated during magnetic storms. It is so because the auroral electrojets (both westward and eastward) shift to the sub-auroral latitudes (Feldstein *et al.* 1999).

Figure 1 shows the position of the auroral westward electrojet during the magnetic storm at different universal times. The horizontal axis is the geomagnetic latitude and the vertical axis is disturbance of horizontal and vertical components. Position of

electrojet is above the observatory where ΔX is maximal, and ΔZ is zero. One may see that the position of electrojet changes from latitude 65° to 56° .

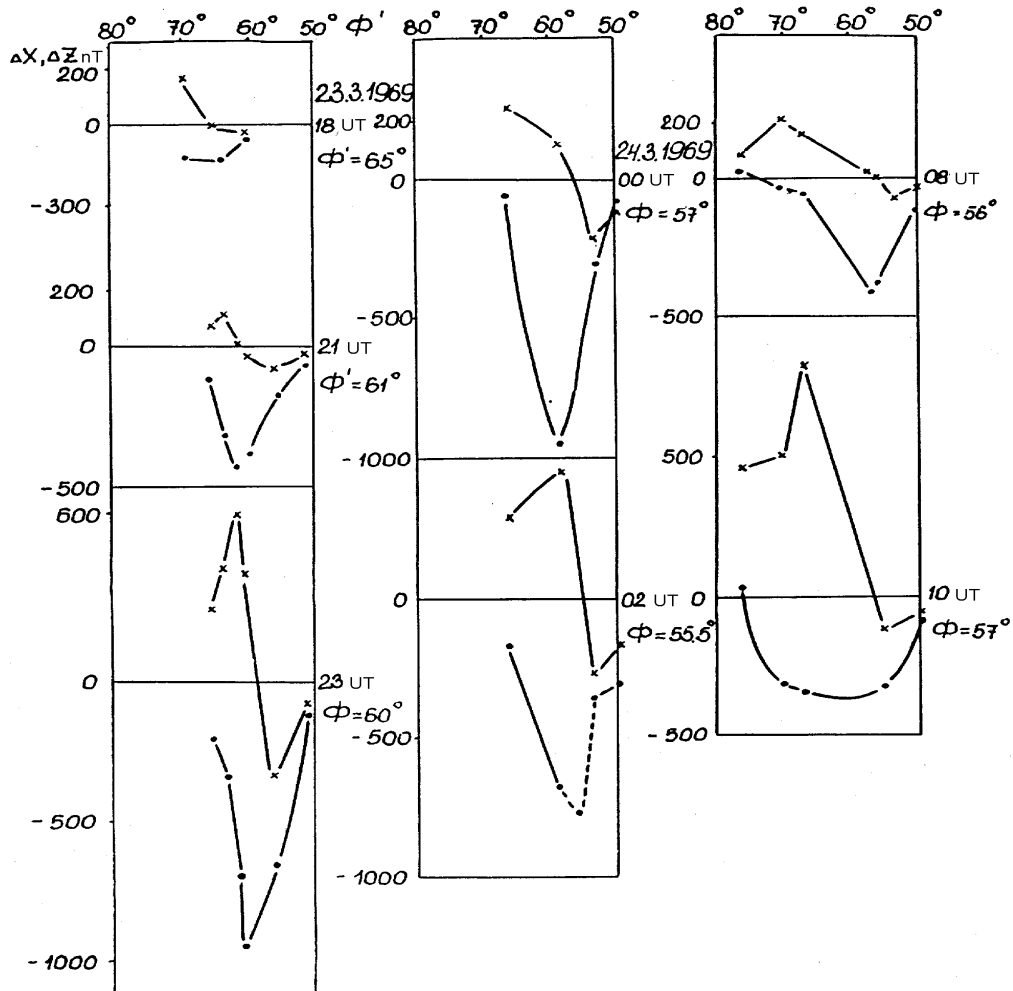


Fig. 1. Position of the auroral westward electrojet during the magnetic storm.

Thus, the chain auroral zone magnetic observatories do not register the maximal variations created by auroral electrojets. It is necessary to use data of sub-auroral observatories to correct AE. Figure 2 shows the understated AE and corrected AE' for 22-23 March 1969 magnetic storm (the corrected AE' are marked by the dotted line). To correct AE it is necessary to use data of sub-auroral observatories. Table 2 shows the list of these observatories. Correction of AE is a difficult job.

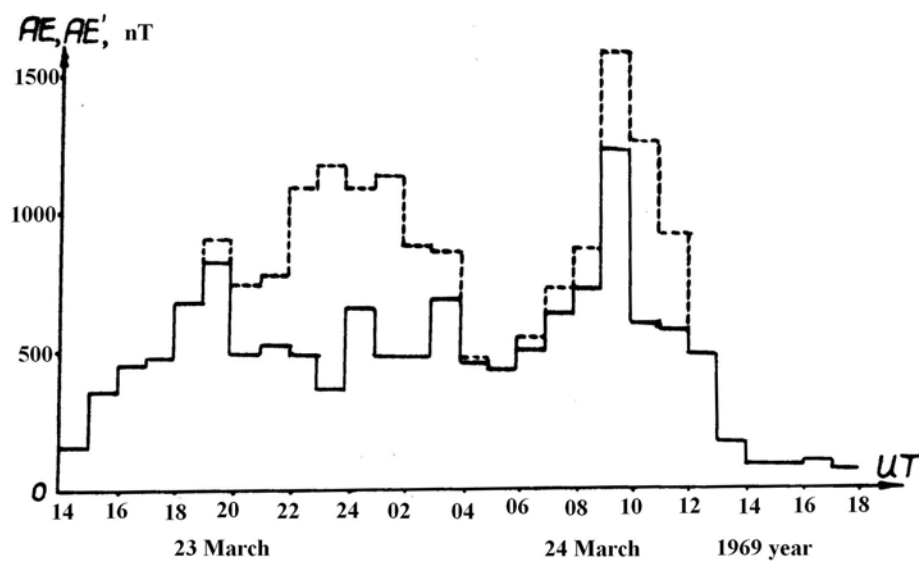


Fig. 2. Underestimated AE (solid line) and corrected AE' (dotted line) during magnetic storm.

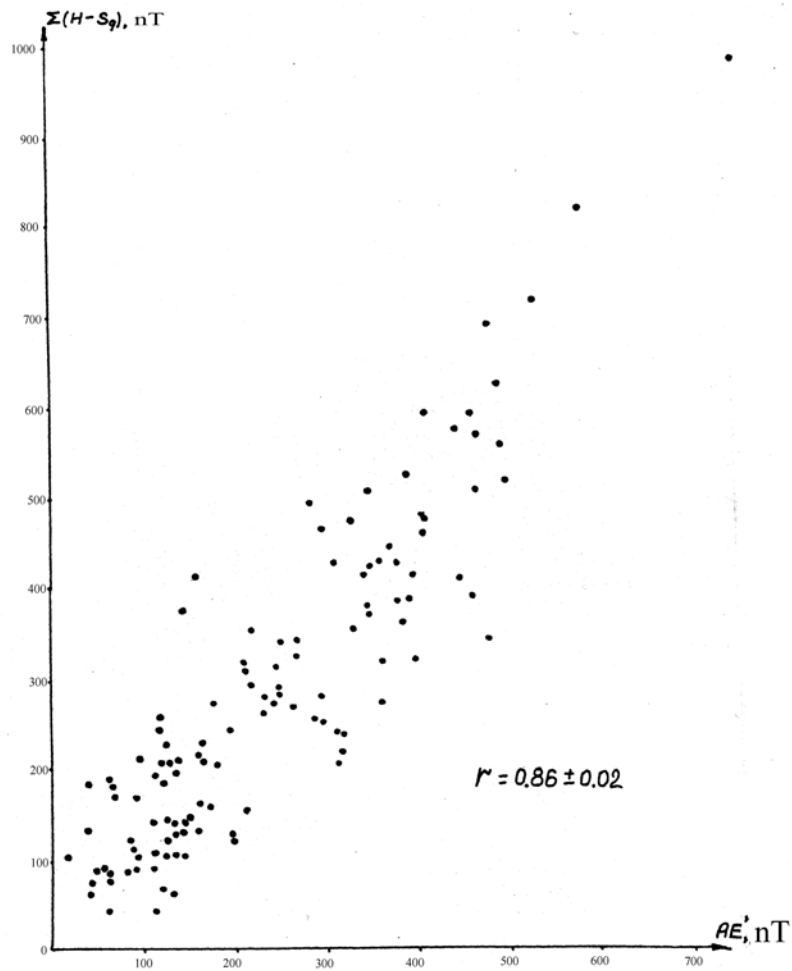
Table 2

List of AE' index observatories

| No | Observatory | Geographical coordinates | | Geomagnetic coordinates | |
|----|-----------------|--------------------------|-----------|-------------------------|-----------|
| | | φ | λ | Φ | Λ |
| 1 | Cape Chelyuskin | 77.43 | 104.17 | 66.4 | 177.2 |
| 2 | Dixon Island | 73.32 | 080.33 | 63.1 | 162.3 |
| 3 | Tixie Bay | 71.35 | 129.00 | 60.7 | 192.4 |
| 4 | Barrow | 71.18 | 156.45 | 68.8 | 242.6 |
| 5 | Abisko | 68.21 | 018.49 | 65.8 | 115.7 |
| 6 | Cape Wellen | 66.10 | 180.50 | 62.1 | 238.5 |
| 7 | College | 64.51 | 147.52 | 65.0 | 258.1 |
| 8 | Baker Lake | 64.20 | 096.02 | 73.8 | 317.7 |
| 9 | Reykjavik | 64.11 | 021.41 | 80.9 | 072.2 |
| 10 | Narsarsuaq | 61.10 | 314.80 | 70.8 | 038.7 |
| 11 | Fort Churchill | 58.44 | 096.15 | 68.7 | 325.0 |
| 12 | Sitka | 57.03 | 135.20 | 60.2 | 277.1 |
| 13 | Yakutsk | 62.01 | 129.40 | 51.2 | 194.9 |

Table 2 (continuation)

| No | Observatory | Geographical coordinates | | Geomagnetic coordinates | |
|----|-------------|--------------------------|-----------|-------------------------|-----------|
| | | φ | λ | Φ | Λ |
| 14 | Nurmijarvi | 60.30 | 024.39 | 57.7 | 113.5 |
| 15 | Lerwick | 60.08 | 001.11 | 62.2 | 089.6 |
| 16 | Meanook | 54.37 | 113.20 | 62.0 | 303.0 |
| 17 | Ottawa | 45.24 | 075.45 | 56.7 | 353.4 |
| 18 | Agincourt | 43.47 | 079.16 | 55.0 | 348.8 |
| 19 | St. Johns | 47.36 | 052.41 | 58.2 | 023.0 |

Fig. 3. Correlation between $\Sigma(H-S_q)$ and AE' for 1980 at the magnetic observatory Lviv.

We propose a new index $\Sigma(H-S_q)$, i.e., a daily sum of differences between the mean hourly values of horizontal component at middle latitude observatory and the corresponding mean month values of the same component on five international quiet days of the preceding month. Coefficients of correlation between these values and corrected AE-indexes are high for disturbed and quiet time intervals.

The correlation coefficient is 0.86 and its dispersion is 0.02 (see Fig. 3). That is to say that the dependence is almost functional. Figure 3 shows dependence of $\Sigma(H-S_q)$ at the Lviv Magnetic Observatory on corrected AE' index for 1980 year of high solar activity.

Thus, it is possible to use $\Sigma(H-S_q)$ as a geomagnetic activity index. The advantage of the index is that it may be calculated immediately. It may be used to evaluate the quantity of energy injected into the magnetosphere. The drawback of our index is that it has only daily interval values. The proposed index may be operatively calculated on the data of any middle latitude observatory.

Conclusions

A new geomagnetic activity index $\Sigma(H-S_q)$, is presented. The index is a daily sum of differences between the mean hourly values of horizontal component at middle latitude observatory and the corresponding mean monthly values of the same component on five international quiet days of the preceding month.

The index has only day interval time values. The correlation between $\Sigma(H-S_q)$ and corrected AE' indices is high.

References

- Feldstein, Y.I., 1992, *Modeling of the magnetic field of magnetospheric ring current as a function of interplanetary medium parameters*, Space Sci. Rev. **59**, 83-165.
- Feldstein, Y.I., L.I. Gromova, A. Grafe, C.-I. Meng, V.V. Kalegaev, I.I. Alexeev and Yu.P. Sumaruk, 1999, *Auroral electrojet dynamics during magnetic storm, connection with plasma precipitation and large-scale structure of magnetospheric magnetic field*, Ann. Geophys. **17**, 497-507.
- Nowozyński, K., 2006, *On regularities in long-term solar quiet geomagnetic variation*, Earth Planet. Sc. Lett. **241** (3-4), 85-93.
- Reda, J., and J. Jankowski, 2004, *Three hour activity index based on power spectra estimation*, Geophys. J. Int. **157**, 141-146.
- Spiro, R.W., P.H. Reiff and L.J. Maher, 1982, *Precipitation electron energy flux and auroral zone conductance: an empirical model*, Geophys. J. Int. **87**, 10, 8215-8227.

Accepted February 22, 2007

On Geomagnetic Activity Forecasting

Taras SUMARUK and Petro SUMARUK

Institute of Geophysics NASU
Lviv Magnetic Observatory, Ukraine
e-mail: sumar@mail.lviv.ua

Abstract

The mean-term forecasting of geomagnetic activity has been carried out at the geomagnetic observatory "Lviv" during 2001-2005. The forecasts are based on 27-day recurrence of solar and geomagnetic activity, their changes during the solar cycles and existence of the so-called "active longitudes on the Sun".

The existence of the "active longitudes on the Sun", especially during the decay phase of solar cycle, allows to improve the forecasting. The successful forecast of geomagnetic storms was in about 65% of cases. An accuracy of the forecast increases with decreasing geomagnetic activity.

Key words: geomagnetic activity, Wolf number, solar cycle.

The magnetic activity forecasting has been performed in the USA (Joselyn 1995). The forecasting was correct at 45%. The qualitative mean-term and long-term forecasting of geomagnetic activity is carried out at magnetic observatory "Lviv" (LVV). The magnetic activity strongly depends on solar activity modulated by daily, seasonal and yearly events in the magnetosphere and ionosphere, i.e., by the daily Earth rotation, the inclination of the Earth to the ecliptic plane and the Earth's rotation around the Sun. The eleven-year solar activity cycle is well known. The duration of solar cycles may change from nine to fourteenth years.

The main characteristics of all experimentally used solar cycles are shown in Table 1, where T is the duration of the cycle, T_1 the duration of the cycle growth phase, T_2 the duration of the cycle decay phase and ΔW the amplitude of Wolf numbers in cycles. A shorter growth phase corresponds to a greater amplitude of Wolf numbers in cycle and a longer decay phase, as shown in Table 1.

Table 1
The main characteristics of solar activity cycles

| Cycle No. | T | T ₁ | T ₂ | ΔW |
|-----------|----|----------------|----------------|------------|
| 0 | 11 | 6 | 5 | 78 |
| 1 | 11 | 6 | 5 | 76 |
| 2 | 9 | 3 | 6 | 95 |
| 3 | 9 | 3 | 6 | 147 |
| 4 | 14 | 3 | 11 | 122 |
| 5 | 12 | 6 | 6 | 44 |
| 6 | 13 | 6 | 7 | 46 |
| 7 | 10 | 5 | 5 | 58 |
| 8 | 10 | 4 | 6 | 130 |
| 9 | 13 | 5 | 8 | 113 |
| 10 | 11 | 4 | 7 | 92 |
| 11 | 11 | 3 | 8 | 132 |
| 12 | 11 | 5 | 6 | 61 |
| 13 | 12 | 4 | 8 | 79 |
| 14 | 12 | 4 | 8 | 61 |
| 15 | 10 | 4 | 6 | 92 |
| 16 | 10 | 5 | 5 | 72 |
| 17 | 11 | 4 | 7 | 108 |
| 18 | 10 | 3 | 7 | 141 |
| 19 | 10 | 3 | 7 | 186 |
| 20 | 12 | 3 | 8 | 96 |
| 21 | 10 | 3 | 7 | 140 |
| 22 | 10 | 5 | 7 | 146 |
| 23 | | 5 | | |

Figure 1 shows the dependence of amplitudes ΔW on the ratio T_1/T_2 ; figures mean numbers of cycles. The correlation coefficient between these values is $r(\Delta W, T_1/T_2) = 0.83$ and its dispersion $\sigma_r = 0.06$. The high correlation between the amplitudes of Wolf number in cycles and ratios of duration the growth and decays phases allows to perform forecasting of decay phase duration when we know the growth phase duration and the amplitude. The twenty third solar cycle has the duration of growth phase of five years and its amplitude is $\Delta W = 102$. We have found the duration of decay phase T_2 equal to 6 years, as it seen from Fig. 1. It means that the minimum of 23 solar cycle will be in 2007.

The mean-term activity forecasting is based on 27-days reiteration of magnetic storms because of solar rotation round its axis. Such a forecasting is effective on the decay phase of solar cycles. Forecasting of storms with SSC by such a method is not successful. The storms with SSC may be forecast on solar bursts.

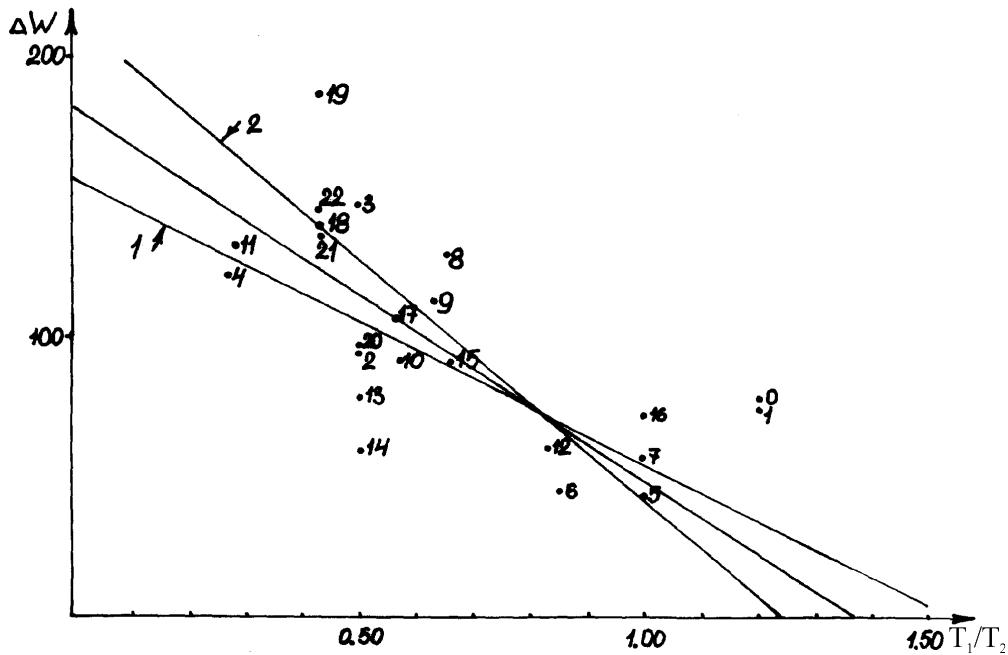


Fig. 1. Dependence of solar cycles amplitudes on relation T_1/T_2 .

The mean-term forecasting is fulfilled from January 2001 till December 2004 at magnetic observatory "Lviv" (LVV). The time interval was 1461 days. The forecast was for 426 disturbed days. In reality we observed 428 disturbed days. The forecasting was correct at sixty five percent of all days, because some days forecast as quiet were disturbed, and vice versa. The quality of forecasting for 2005 year was correct at 89%. This means that for the quietest interval, the forecasting is more successful. The forecasting is most successful if there exist the so-called active longitudes on the Sun. Two such areas existed during 2003-2004.

Conclusion

Long-term and mean-term forecasting of magnetic activity was performed. The minimum activity will be observed in 2007. Forecasting of the magnetic storms was successful at 65% for the observatory LVV.

References

- Joselyn, A., 1995, *Geomagnetic activity forecasting: the state of the art*, Rev. Geophys. **33**, 3, 383-401.

Accepted March 23, 2007

Fast Analysis of the Solar Wind Energy

Yuri SUMARUK and Taras SUMARUK

Institute of Geophysics NASU
Lviv Magnetic Observatory, Ukraine
e-mail: sumar@mail.lviv.ua

Abstract

The solar wind energy injected into the magnetosphere may be evaluated by means of the AE-index of the geomagnetic activity. However, these indexes are underestimated for the disturbed periods and available too late to be efficiently used. For a fast analysis, daily sums of the differences between the mean hourly values of horizontal component and the corresponding mean hourly values of H on five international quiet days have been used instead of the AE-index.

These sums were calculated from the data of mid-latitude observatories. They have a high correlation with the corrected AE-indexes for the quiet and disturbed periods. Using these sums, the solar wind energy injected into the magnetosphere was estimated for the years 1953-2001 as the daily, monthly and yearly values. It is shown that the energy increased with increasing solar and magnetic activity. At some cycles of the solar activity, the increase of the injected energy continued for several years on the descending phases of cycles and at some cycles the injected energy and solar activity have changed their phase.

Key words: solar wind, magnetic activity indices, injected energy, magnetosphere.

Solar wind carries the energy of 10^{13} joule per second on the disk of magnetosphere with radius $15R_E$ (R_E is the Earth's radius). The main part of the energy is the kinetic energy of plasma. The heat, electric and magnetic energies are ten times smaller (or even more). The main mechanisms of the solar wind energy access into the magnetosphere are the penetration of plasma through the cusps and side surfaces of the magnetosphere, and also the hydromagnetic mechanisms such as viscous interaction and reconnection of the magnetic field lines on the magnetopause.

The above-mentioned mechanisms inject into the magnetosphere the energy of 10^{11} – 10^{12} J/sec and it is enough to generate magnetic storms and sub-storms. How-

ever, one cannot judge which mechanism prevails because the experimental materials are not sufficient for making final conclusion. Most probably, all the mechanisms act, but their effectiveness changes with changing solar wind parameters and state of the magnetosphere.

The value of the energy injected into the magnetosphere is controlled by interplanetary medium parameters (Atkinson 1978). The main flow down of injected energy is Joule heating of high latitude atmosphere (Banks 1981, Stern 1984). The Joule heating is connected with the existence of electric current systems in the ionosphere. Some part of injected energy is piled up into the magnetosphere and another one penetrated to the ionosphere and generates electric current systems. Akasofu (1982) distinguished three kinds of the expenditure of solar wind energy in the magnetosphere: energization of auroral particles (U_A), energy of dissipation in the ionosphere (U_J), and energization of the ring current ions (U_{DR}). According to Spiro *et al.* (1982) and Feldstein (1992):

$$U_A = (1.75 \text{ AE}/100 + 1.6) \cdot 10^{10};$$

$$U_J = 0.32 \text{ AE} \cdot 10^9;$$

$$U_{DR} = 0.74 [\partial R / \partial t + DR(\tau)] \cdot 10^{10}.$$

Here τ is in hours, AE and DR in nT, and U in J/sec. Thus, the value of the energy stored in the magnetosphere and ionosphere can may be estimated by means of AE indices.

It is well known that during magnetic storms, when D_{st} -index is smaller than 150 nT, auroral electrojets move down to the sub-auroral latitudes. It means that standard AE-index is underestimated. To obtain the correct AE indices one must use also data of sub-auroral latitude observatories. To avoid it, we have used data of middle latitude observatories Lviv (LVV) and Fredericksburg (FRD) to receive an index adequate to AE.

Figure 1 shows dependence of the corrected mean daily indices AE on the daily sum of $(H - S_q)$ values for the year 1980 at magnetic observatory LVV. Here H is mean hourly value of horizontal component at observatory Lviv, and S_q are the mean hourly values the same component on five international quiet days for the same month. The correlation coefficient between the values is $r = 0.86 \pm 0.02$. A similar high correlation coefficient was received for observatory Fredericksburg. This means that it is possible to use daily sum $\Sigma(H - S_q)$ instead of AE. By substituting in the above formulas AE by $\Sigma(H - S_q)$ and taking into account the transition coefficient, we calculated the energy injected to the magnetosphere. Daily, monthly, yearly values of energy were determined.

Figure 2 shows the monthly total energy (E) and its dispersion for the years 1953-2001. The line without bars shows the mean yearly Wolf numbers. It is seen that the increase of solar activity leads to an increase in the stored energy in the magnetosphere. In the nineteenth solar cycle, such an increase started in 1954 and continued till 1959, although the solar maximum passed in 1957. The maximum mean monthly value of energy for 1959 is $7549 \cdot 10^{14}$ J. Since this year, a sudden decrease of energy

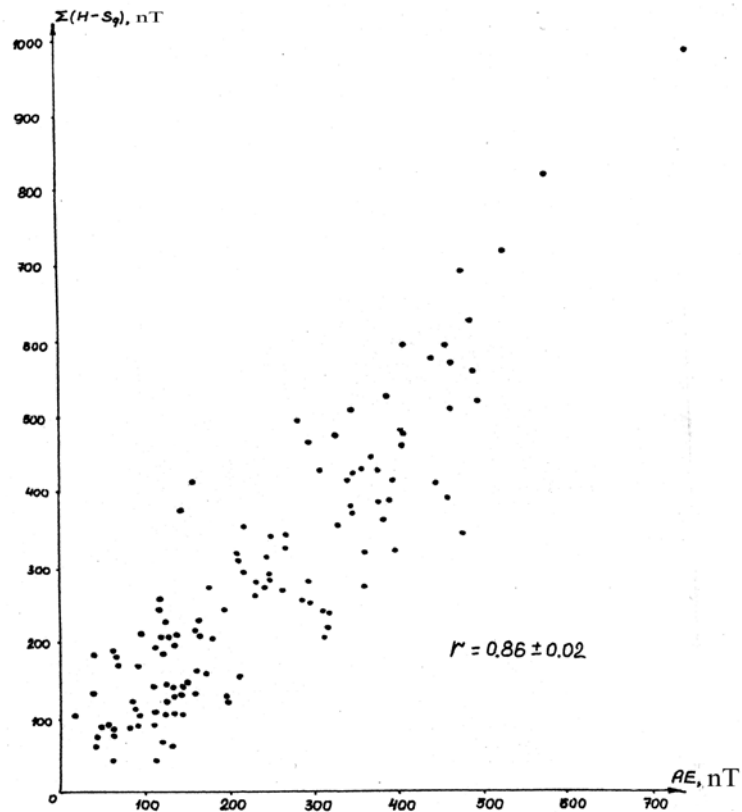


Fig. 1. Dependence between $\Sigma(H-Sq)$ and ΣAE for the year 1980 at magnetic observatory LVV.

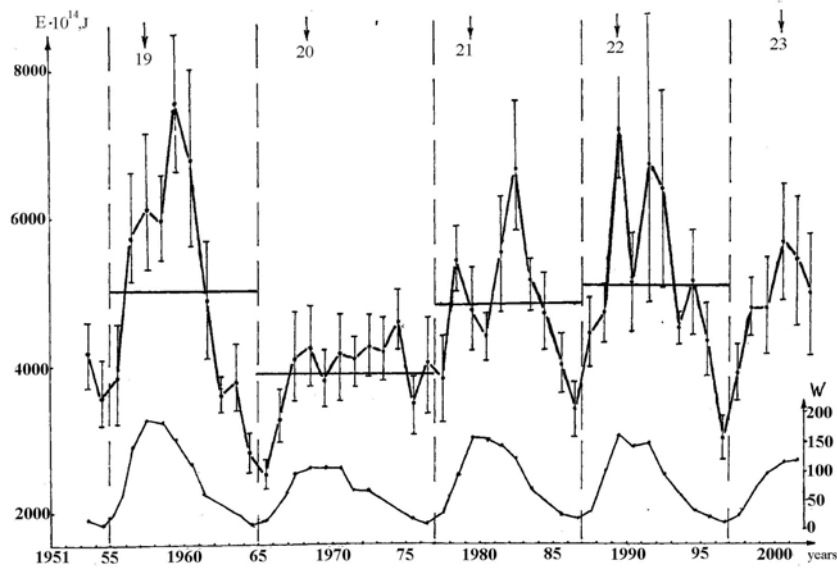


Fig. 2. The monthly total energy injected into the magnetosphere for the years 1953-2001. The lower curve is the year Wolf number.

was observed. A particularly deep decrease was observed in 1961. The deep minimum of energy at the end of nineteenth cycle is the deepest one for examined time interval ($E = 2576 \cdot 10^{14} \text{J}$). The twentieth cycle (1964-1976) was unusual. First of all, the solar maximum was low and blurred. The difference between maximum and minimum was small. The changes of injected energy were also small. The ratio of the maxima of injected energy in nineteenth and twentieth cycles was one and a half. Characteristic features of the twenty-first and twenty-second cycles were the two maxima of energy. In the twenty-first cycle, the second maximum appeared at the decreasing stage of solar cycle, but in the twenty-second cycle both maxima of energy appeared correspondently to the maxima of Wolf number. The mean-per-cycle energy values are shown in Fig. 2 by thick horizontal lines.

Figure 3 shows dispersion of energy, i.e., the deviation of the monthly energy from its mean value. It is seen that the dispersion increased with the growth of the injected energy. This means that an increase of solar activity leads to growth of the seasonal amplitude of the magnetic activity and, consequently, the injected energy.

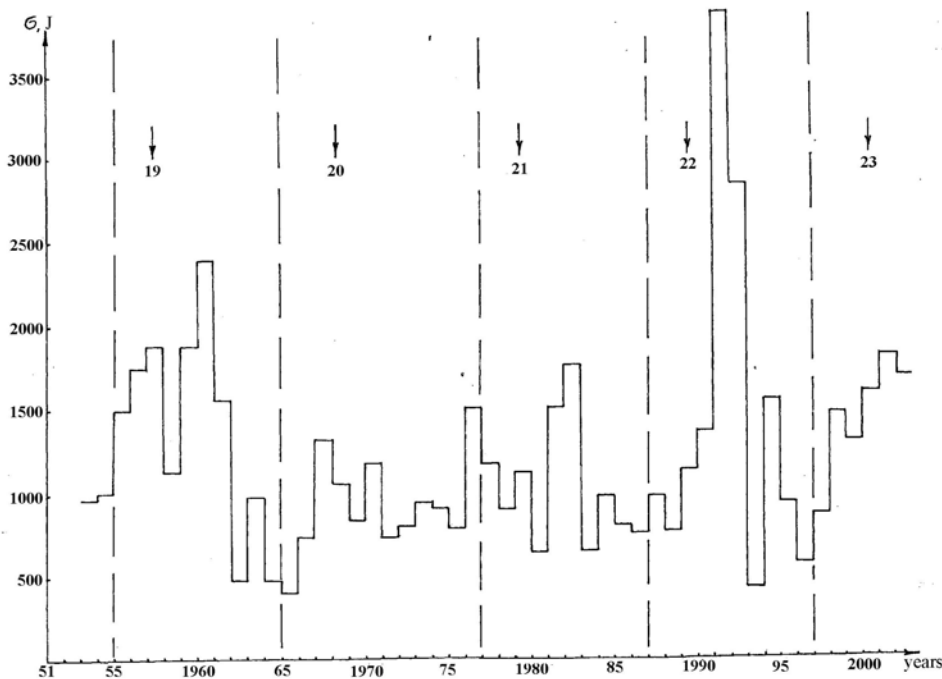


Fig. 3. The dispersion of the energy injected into the magnetosphere in 1953-2001.

Conclusions

The value of the solar wind energy injected into the magnetosphere is increasing (decreasing) along with increasing (decreasing) solar and magnetic activities. In 19-21 solar cycles, the increase of the injected energy continues through the next several years further, on the decreasing phase of solar activity. The solar activity and values of

the injected energy change their phase in 22 and 23 solar cycles. Seasonal changes of the amplitude of injected energy and its yearly dispersion have been increasing with growth of the solar and magnetic activities.

References

- Akasofu, S.I., 1982, *Energy coupling between solar wind and magnetosphere*, Space Sci. Rev. **28**, 121-190.
- Atkinson, G., 1978, *Energy flow and closure of current systems in the magnetosphere*, J. Geophys. Res. **83**, 1089-1103.
- Banks, P.M., 1981, *Energy sources of the high latitude upper atmosphere*. In: C.S. Deer and J.A. Holtet (ed.), "Exploration of the polar upper atmosphere", D. Reidel Publishing Co., Dordrecht, 113-128.
- Feldstein, Ya.I., 1992, *Modeling of the magnetic field of magnetospheric ring current as a function of interplanetary medium parameters*, Space Sci. Rev. **59**, 83-165.
- Spiro, R.W., P.H. Reiff and L.J. Maher, 1982, *Precipitation electro energy flux and auroral zone conductance: an empirical model*, IbiD. **87**, 10, 8215-8227.
- Stern, D.P., 1984, *Energetics of the magnetosphere*, Space Sci. Rev. **39**, 193-213.

Accepted March 23, 2007

Proceedings of XII IAGA Workshop on Geomagnetic Observatory Instruments, Data Acquisition and Processing

Contents

| | |
|---|----|
| Preface | 3 |
| Measurement Session During the XII IAGA Workshop at Belsk <i>J. Reda and M. Neska</i> | 7 |
| I. History of Observatories/Present Activity of Observatories | |
| 1. Past and Present of Polish Geomagnetic Observatories – <i>J. Jankowski and J. Marianiuk</i> | 20 |
| 2. 50 Years of History of the Tihany Geophysical Observatory – <i>A. Csontos, L. Hegymegi, B. Heilig, P. Kovács, L. Merényi and Z. Szabó</i> | 32 |
| 3. Keetmanshoop – A New Observatory in Namibia – <i>H.J. Linthe, P. Kotze, M. Manda and H. Theron</i> | 38 |
| 4. Replacement of Gnangara (GNA) with a New Observatory at Gingin – <i>P. Crosthwaite, P. Hopgood and A. Lewis</i> | 46 |
| II. Observatory Instruments and Measurement Technology | |
| 1. GAUSS: <u>G</u> geomagnetic <u>A</u> utomated <u>S</u> ystem – <i>H.U. Auster, M. Manda, A. Hemshorn, M. Korte and E. Pulz</i> | 49 |
| 2. Advanced Proton Magnetometer Design and its Application for Absolute Measurement – <i>V. Auster, O. Hillenmaier, R. Kroth and M. Wiedemann</i> | 60 |
| 3. New Concepts in Geomagnetic Observatories Operation – <i>J.L. Rasson and S. van Loo</i> | 69 |
| 4. Presentation of the Prototype of an Automated DIFlux – <i>S. van Loo and J.L. Rasson</i> | 77 |
| 5. Underwater Magnetometer MG-01/2003 for Geomagnetic Offshore Soundings – <i>J. Marianiuk, W. Jóźwiak, A. Neska and M. Neska</i> | 87 |

| | |
|--|-----|
| 6. Schumann Resonance Observation in Polish Polar Station at Spitsbergen and Central Geophysical Observatory in Belsk – <i>M. Neska, G. Sători, J. Szendrői, J. Marianiuk, K. Nowożyński and S. Tomczyk</i> | 93 |
| 7. A New Model of Telluric Amplifier for Magnetotelluric Soundings – <i>S. Tomczyk</i> | 99 |
| 8. Project of Absolute Three-Component Vector Magnetometer Based on Quantum Scalar Sensor – <i>A. Vershovskiy</i> | 105 |
| 9. Fast 3-Component Variometer Based on a Cesium Sensor – <i>A. Vershovskiy, M. Balabas, A. Ivanov, V. Kulyasov, A. Pazgalev and E. Alexandrov</i> | 110 |
| 10. Extending Magnetic Observations to Seafloor: the Case of GEOSTAR and ORION Missions in the Adriatic and Tyrrhenian Seas – <i>A. De Santis, D. Di Mauro, L. Cafarella, P. Palangio, L. Beranzoli, P. Favali and S. Vitale</i> | 114 |

III. Observatory Praxis/Data Acquisition/Data Processing

| | |
|---|-----|
| 1. Comparison of Observatory Data in Quasi-Real Time – <i>K. Nowożyński and J. Reda</i> | 123 |
| 2. The New BCMT Magnetic Database – <i>D. Fouassier and A. Chulliat</i> | 128 |
| 3. The Hourly Mean Computation Problem Revisited – <i>J.-J. Schott and H.J. Linthe</i> | 135 |
| 4. Intercalibration of dIdD and Fluxgate Magnetometers – <i>B. Heilig</i> | 144 |
| 5. On the Various Published Formulas to Determine Sensor Offset and Sensor Misalignment for the Di-flux – <i>J. Matzka and T.L. Hansen</i> | 152 |
| 6. An Assessment of the BGS $\delta D\delta I$ Vector Magnetometer – <i>S. Marsal, J.M. Torta and J.C. Riddick</i> | 158 |
| 7. Quality Assurance Project for the Magnetic Calibration and Test Laboratory of the Nurmijärvi Geophysical Observatory – <i>K. Pajunpää, M. Genzer, P. Posio, H. Nevanlinna and W. Schmidt</i> | 166 |
| 8. Temperature Tests on Modern Magnetometers – <i>A. Csontos, L. Hegymegi and B. Heilig</i> | 171 |
| 9. Temperature Influence over the Magnetic Declination Measurements – <i>I. Cholakov and B. Srebrov</i> | 178 |
| 10. Development of Artificial Geomagnetic Disturbances Monitoring System – <i>T. Okawa, T. Tokumoto, S. Nakajima, T. Owada, T. Toya, F. Muromatsu, N. Kumasaka and T. Koike</i> | 183 |
| 11. Intercomparison of Momentary Values: an Application to Check the Reliability of Ebre Observatory Data – <i>S. Marsal and J.J. Curto</i> | 189 |

IV. Secular Variation/Surveys

1. Survey of Magnetic Observatory Charging Practices – *L. Newitt* 196
2. A New Geomagnetic Field Model for Southern Africa Based on 2005 Ground Survey Data – *P.B. Kotzé, M. Manda and M. Korte* 201
3. Systematic Magnetic Observations in Italy – *A. Meloni, L. Cafarella, P. De Michelis, A. De Santis, D. Di Mauro, G. Dominici, S. Lepidi, P. Palangio, R. Tozzi and A. Zirizzotti* 209
4. The Newest Measurements of the Total Magnetic Field Strength in Croatia – *A. Marki, G. Verbanac, E. Vujić and V. Vujnović* 217
5. Correlation Between IGRF2000 Model and Measured Geomagnetic Data on the Territory of the Republic of Macedonia from 2003 and 2004 Measurements – *S. Panovska, T. Delipetrov, B. Delipetrov and M. Delipetrov* 227
6. Geomagnetic Data of the Republic of Macedonia Obtained in 2004 – *M. Delipetrov, T. Delipetrov, B. Delipetrov and S. Panovska* 234
7. Repeat Station Data Reduction Using the CM4 Model – *Z. Andriambahoaka, J.-J. Schott and F. Ranaivonomenjanahary*..... 242
8. Report on Activities and Plans of MagNetE – the Group for European Repeat Station Surveys – *G. Duma* 250
9. On Separation of the Secular Variations from Different Origins – *Yu. Sumaruk*..... 252
10. Experimental Modeling of the Impact Effects on the Magnetic Susceptibility of Geological Materials – *A. Lamali, P. Rochette, J. Gattacceca and M. Boustie* 260

V. Global Networks

1. World Monthly Means Database Project – *A. Chulliat and K. Telali* 268
2. Worldwide Observatory Hourly Means from 1995 to 2003: Investigation of Their Quality – *M. Korte, M. Manda and N. Olsen* 275
3. Panagjurishte Observatory Upgrade for INTERMAGNET – *H.J. Linthe, I. Cholakov and M. Manda* 284
4. New INTERMAGNET Fluxgate Magnetometr – *V. Korepanov, Ye. Klymovich, O. Kuznetsov, A. Pristay, A. Marusenkov and J. Rasson*..... 291

VI. Application of Observatory Data/Magnetic Indices

1. Magnetic Observatories in the 21st Century: an Endangered Species? – *D. Kerridge*..... 299

| | |
|---|-----|
| 2. A Search for Users of Magnetic Observatory Data – <i>L. Newitt</i> | 308 |
| 3. On the Use of Fast Registrations of Observatories as a Reference for Magnetotelluric Measurements – <i>A. Neska</i> | 315 |
| 4. Experience with New Geomagnetic Activity Index E Based on Power Spectra – <i>J. Reda</i> | 323 |
| 5. Installation of a High Resolution Potassium Magnetometer in the Coast of Oaxaca, Mexico – <i>G. Cifuentes-Nava, E. Cabral-Cano, E. Hernández-Quintero, I. Hrvoic, F. López and M. Wilson</i> | 330 |
| 6. Upstream Wave related Pc3 Pulsations Observed by the MM100 Meridional Magnetometer Array – <i>B. Heilig, A. Csontos, L. Pankratz, K. Pajunpää, J. Kultima, T. Raita, J. Reda and M. Váczyová</i> | 339 |
| 7. Study of Geomagnetically Induced Current from Time Derivative of the Earth's Magnetic Field – <i>V.V. Vodjannikov, G.I. Gordienko, S.A. Nechaev, O.I. Sokolova, S.J. Homutov and A.F. Yakovets</i> | 347 |
| 8. Long-Term Variation of the Geoelectric Activity Index T – <i>Á. Kis, A. Koppán, I. Lempurger, T. Prodán, J. Szendrői, J. Verö and V. Wesztergom</i> | 353 |
| 9. ULF Geomagnetic Pulsations at High Latitudes: the Italian Contribution – <i>L. Cafarella, M. De Lauretis, D. Di Mauro, P. Francia, S. Lepidi, A. Meloni, P. Palangio, A. Piancatelli, L. Santarelli, M. Vellante and U. Villante</i> | 360 |
| 10. Morphological Features in the Structure of Geomagnetic Variations in Relation to Earthquakes in Vrancea – <i>V. Bakhmutov, F. Sedova and T. Mozgovaya</i> | 366 |
| 11. The New Index of Geomagnetic Activity – <i>T. Sumaruk and Yu. Sumaruk</i> | 374 |
| 12. On Geomagnetic Activity Forecasting – <i>T. Sumaruk and P. Sumaruk</i> | 380 |
| 13. Fast Analysis of the Solar Wind Energy – <i>Yu. Sumaruk and T. Sumaruk</i> | 383 |
| List of Participants | 388 |

**PUBLICATIONS OF THE INSTITUTE OF GEOPHYSICS
POLISH ACADEMY OF SCIENCES**

C. EARTH MAGNETISM

List of our publications since 2000 dealing with the Earth magnetism; the full list is published on the cover of our former issues.

- C-85 (356)** Results of geomagnetic observations, Belsk 2002.
- C-86 (357)** Results of geomagnetic observations, Polish Polar Station, Hornsund, Spitsbergen 2002.
- C-87 (358)** Results of geomagnetic observations, Hel Geophysical Observatory 2002.
- C-88 (364)** New methods for parametrization and determination of transfer function and impulse response, by K. Nowożyński.
- C-89 (368)** Results of geomagnetic observations, Belsk 2003.
- C-90 (369)** Results of geomagnetic observations, Polish Polar Station, Hornsund, Spitsbergen, 2003.
- C-91 (370)** Results of geomagnetic observations, Hel Geophysical Observatory 2003.
- C-92 (379)** Results of geomagnetic observations, Belsk 2004.
- C-93 (380)** Results of geomagnetic observations, Polish Polar Station, Hornsund, Spitsbergen, 2004.
- C-94 (381)** Results of geomagnetic observations, Hel Geophysical Observatory 2004.
- C-95 (386)** Monographic Volume: Study of geological structures containing well-conductive complex in Poland
- C-96 (392)** Results of geomagnetic observations, Belsk Geophysical Observatory 2005.
- C-97 (393)** Results of geomagnetic observations, Polish Polar Station, Hornsund, Spitsbergen, 2005.
- C-98 (394)** Results of geomagnetic observations, Hel Geophysical Observatory 2005.

ISBN-83-88765-70-1